JSC-23184

Mission Report on the Orbiter Camera Payload System (OCPS) Large Format Camera (LFC) and Attitude Reference System (ARS)

December 1988

Prepared under

Contract NAS 9-17900
Job Order K4-427

By

Lockheed Engineering & Sciences Company
Engineering and Science Program Office
Houston, Texas

For

Flight Systems Branch
Man-Systems Division
Space and Life Sciences Directorate

National Aeronautics and
Space Administration

Lyndon B. Johnson Space Center
Houston, Texas

LESC-23799

JSC-23184

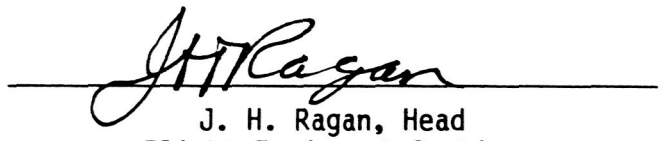
MISSION REPORT ON THE ORBITER CAMERA PAYLOAD SYSTEM (OCPS) LARGE FORMAT CAMERA (LFC) AND ATTITUDE REFERENCE SYSTEM (ARS)

Job Order K4-427

PREPARED BY

Bernard H. Mollberg and Bruton B. Schardt

APPROVED BY



J. H. Ragan, Head
Flight Equipment Section
Flight Systems Branch

Prepared By

Lockheed Engineering & Sciences Company

For

Man-Systems Division

Space and Life Sciences Directorate

NATIONAL AERONAUTICS AND SPACE ADMINISTRATION
LYNDON B. JOHNSON SPACE CENTER
HOUSTON, TEXAS

December 1988

LESC-23799

ABSTRACT

The Orbiter Camera Payload System (OCPS) is an integrated photographic system which is carried into earth orbit as a payload in the Space Transportation System (STS) Orbiter vehicle's cargo bay. The major component of the OCPS is a Large Format Camera (LFC), a precision wide-angle cartographic instrument that is capable of producing high resolution stereo photography of great geometric fidelity in multiple base-to-height (B/H) ratios. A secondary, supporting system to the LFC is the Attitude Reference System (ARS), which is a dual lens Stellar Camera Array (SCA) and camera support structure. The SCA is a 70-mm film system which is rigidly mounted to the LFC lens support structure and which, through the simultaneous acquisition of two star fields with each earth-viewing LFC frame, makes it possible to determine precisely the pointing of the LFC optical axis with reference to the earth nadir point. Other components complete the current OCPS configuration as a high precision cartographic data acquisition system. The primary design objective for the OCPS was to maximize system performance characteristics while maintaining a high level of reliability compatible with Shuttle launch conditions and the on-orbit environment. The full-up OCPS configuration was launched on a highly successful maiden voyage aboard the National Aeronautics and Space Administration (NASA) STS Orbiter vehicle Challenger on October 5, 1984, as a major payload aboard mission STS 41-G. This report documents the system design, the ground testing, the flight configuration, and an analysis of the results obtained during the Challenger mission STS 41-G.

ACKNOWLEDGMENTS

Interests in and recognition by the National Aeronautics and Space Administration (NASA) of the need for a precision cartographic system for deployment in space within the coming decades dates back to the mid 1960's. In-depth NASA studies (1965 and 1967) defined these requirements, which were endorsed by the National Academy of Science (1969 and 1970). The 1972 report by the Federal Mapping Task Force of the Office of Management and Budget (OMB) further endorsed the spaceborne cartographic system concept. As the progress in spacecraft and their payload weight accommodations continued, so did the definition in the system requirements and potential configuration continue. A successful concept proposal for a "Large Format Camera" (LFC) was presented to the NASA Office of Space Sciences and Applications (OSSA) by the NASA Lyndon B. Johnson Space Center (JSC) on November 29, 1976. The LFC's maiden voyage aboard the Challenger vehicle's mission STS 41-G (STS-17) was flown October 5 through 13, 1984. Since then much time has been spent by a host of researchers worldwide in the analysis and applications of the recorded imagery.

In reflecting on the evolution and consummation of the LFC as a highly reliable spaceborne cartographic system, one cannot help but think of those dedicated colleagues at the Litton Itek Optical Systems in Lexington, Massachusetts, who developed, designed, and crafted the LFC. Though many excellent people at Itek contributed their energies and talents to the evolution of the LFC, special recognition is given to J. R. (Rick) Manent, E. W. (Ernie) Pigeon, R. J. (Bob) Heath, D. A. (Dave) Womble, and Lloyd Ralls.

Then there is that very special group of individuals who were the "LFC Team" from Lockheed Engineering & Sciences Company (LESC) who dedicated nearly a decade of their lives to the program from its inception through testing, field deployment, integration, mission planning, and manning their stations in mission control's mission payload support room. This dedicated team of engineers consisted of Ray S. Hall, David K. Mains, Ronald F. Merkel, John J. Salmon, and Brent A. Sims.

Invaluable help was received from other agencies of the Federal government during the course of the LFC program when, in 1978, NASA chartered the LFC Interagency Working Group (LFCIWG). This group included representatives from the following agencies and organizations:

- The U.S. Department of Agriculture (USDA), Forestry Service and Soil Conservation Service
- The Department of Commerce, National Oceanic and Atmospheric Administration (NOAA) National Ocean Service
- The Department of Defense, Defense Mapping Agency and Corps of Engineers
- The Department of Energy, Research and Development Coordination Council
- The Department of the Interior, Geological Survey, National Mapping Division

And then there are those such as Barbara Nowakowski, who did the geography and plotting of more than 2,200 LFC footprints for the LFC Mission Ephemeris; Carol Laurence, whose professionalism in technical editing contributed significantly to this document; and by no means least, Johnny Salinas and Bill Miller and their team in JSC's Metric Photographic Laboratory, who supported the effort from concept illustrations to precision reproduction of the flight imagery for exhibit, analysis, and publication. All are masters in their specialties.

To these, and many, many more dedicated individuals, the authors are humbly indebted.

Bernard H. Mollberg[1]
Bruton B. Schardt[1]

---

[1] Throughout the development of the LFC, from proposal submission through space flight and subsequent image analysis and data distribution, Mr. Bernard H. Mollberg was the Project Manager/Scientist and Principal Investigator at the NASA Lyndon B. Johnson Space Center, and Mr. Bruton B. Schardt was the Program Manager at NASA Headquarters.

CONTENTS

Section		Page
ACRONYMS AND ABBREVIATIONS		xxi
1.	SYSTEM DESCRIPTION	1-1
	1.1 INTRODUCTION	1-1
	1.2 LARGE FORMAT CAMERA	1-3
	1.2.1 LFC LENS ASSEMBLY	1-5
	1.2.1.1 LFC Shutter Description	1-7
	1.2.1.2 Shutter Speeds	1-8
	1.2.1.3 LFC Optical Filters	1-8
	1.2.1.4 Lens Focal Frame	1-10
	1.2.2 FILM MAGAZINE ASSEMBLY	1-11
	1.2.2.1 Forward Motion Compensation	1-14
	1.2.3 AUXILIARY DATA	1-15
	1.3 ATTITUDE REFERENCE SYSTEM	1-17
	1.4 PRESSURIZATION SYSTEM	1-20
	1.5 THERMAL STABILIZATION	1-23
	1.6 DATA ACQUISITION	1-25
2.	FLIGHT PERFORMANCE	2-1
	2.1 INTRODUCTION	2-1
	2.1.1 BACKGROUND	2-1
	2.1.2 OBJECTIVES	2-1
	2.1.2.1 Orbital Altitudes	2-2
	2.1.2.2 Film Emulsion Evaluation	2-2
	2.1.2.3 Mechanical and Electrical Design Verification	2-2
	2.1.2.4 System Command and Control	2-3

Section Page

2.1.2.5 Thermal Design 2-3

2.1.2.6 Optical Performance 2-3

2.1.2.7 Data Acquisition Techniques 2-3

2.1.3 SUMMARY EVALUATION 2-4

2.2 MISSION PLANNING 2-4

2.2.1 SYSTEM INTEGRATION 2-5

2.2.2 SYSTEM COMMAND AND CONTROL 2-6

2.2.3 FLIGHT FILM EMULSIONS 2-9

2.3 PLANNED/ACTUAL DATA PASSES 2-13

2.4 GLOBAL WEATHER IMPACT 2-19

2.5 MISSION ALTITUDE SUMMARY 2-22

2.6 ATTITUDE RATES 2-25

3. MISSION ANALYSIS 3-1

3.1 DESIGN VERIFICATION 3-1

3.1.1 SOFTWARE APPLICATION 3-4

3.1.2 COMMAND GENERATION 3-6

3.1.3 COMMAND SEQUENCING 3-10

3.1.4 THERMAL PERFORMANCE 3-11

3.1.5 ATTITUDE CONTROL 3-12

3.2 PERFORMANCE VERIFICATION 3-13

3.2.1 ALTITUDE COMPARISON 3-14

3.2.2 FILM COMPARISON 3-17

3.2.3 PHOTO RESOLUTION 3-18

3.2.4 SYSTEM COMPARISON 3-20

3.2.4.1 Aircraft Systems 3-23

Section Page

3.2.4.2 Cartographic Systems 3-26

3.2.4.3 Crew Camera Systems 3-27

3.3 ACQUIRED DATA CATEGORIES 3-29

3.3.1 SYNOPTIC ORBITAL STEREOSCOPY 3-30

3.3.2 USER DISCIPLINE SATISFACTION 3-33

3.3.2.1 Cartography 3-34

3.3.2.2 Geomorphology 3-35

3.3.2.3 Demography 3-38

3.3.2.4 Oceanography 3-39

3.3.2.5 Volcanology 3-40

3.3.2.6 Geography 3-41

3.3.2.7 Hydrology 3-41

3.3.2.8 Archaeology 3-42

3.3.2.9 Meteorology 3-43

3.3.2.10 Paleolithology 3-44

3.4 DISCREPANCIES 3-44

3.4.1 MISSION ANOMALIES 3-45

3.4.2 SYSTEM ANOMALIES 3-46

3.4.2.1 Discrete Exposure Setting 3-47

3.4.2.2 Excessively Long Exposure 3-49

3.4.2.3 Miscellaneous Discrepancies 3-51

4. FILM SENSITOMETRY 4-1

5. LFC BIBLIOGRAPHY AND APPLICABLE DOCUMENTATION 5-1

5.1 LFC BIBLIOGRAPHY 5-1

5.2 LFC APPLICABLE DOCUMENTATION 5-7

Appendix Page

A. SYSTEM PERFORMANCE TESTING..... A-1

A.1 LENS RESOLUTION AND DISTORTION TESTING..... A-1

A.2 LENS/FOCAL PLANE CHARACTERISTICS TESTING..... A-3

A.3 LFC FLIGHT SIMULATION TEST..... A-4

A.4 LFC LABORATORY PERFORMANCE RESULTS..... A-5

A.4.1 FOCUS SETTING..... A-5

A.4.2 VEILING GLARE..... A-5

A.4.3 RELATIVE ILLUMINATION..... A-6

A.4.4 LENS T-NUMBER..... A-6

A.4.5 SPECTRAL TRANSMITTANCE..... A-6

A.4.6 SYSTEM RESOLUTION - STATIC..... A-6

A.4.7 SYSTEM RESOLUTION - DYNAMIC..... A-8

A.4.8 PRINCIPAL POINT OF AUTOCOLLIMATION..... A-8

A.4.9 GEOMETRIC DISTORTION..... A-9

A.5 FOCUS VERIFICATION..... A-9

A.6 LENS DISTORTION VERIFICATION..... A-10

B. LFC GROUND COVERAGE MAPS..... B-1

TABLES

Table		Page
1-1	LFC OPERATIONAL PARAMETERS	1-2
1-2	WEIGHTS OF THE MAJOR COMPONENTS OF THE OCPS	1-4
1-3	LFC STORED PROGRAM COMMANDS FOR ROTARY SHUTTER SPEEDS AND BUILDABLE COMMANDS	1-9
1-4	GAS CONSUMPTION DATA FOR LFC/GSA, STS 41-G	1-21
1-5	HEATER/HEATER CONTROLLER POWER SUMMARY	1-25
1-6	THE RELATIONSHIP OF FORWARD O/L OF SUCCESSIVE LFC FRAMES TO B/H RATIO AND VE FACTORS AS AN ADJUNCT TO TERRAIN DATA EXTRACTION AND ANALYSIS	1-28
2-1	SUMMARY OF UPLINK COMMANDS ISSUED TO THE LFC	2-8
2-2	OCPS TM MEASUREMENTS WHICH WERE MONITORED DURING THE STS 41-G MISSION	2-9
2-3	CHARACTERISTICS OF AERIAL FILMS FLOWN WITHIN THE LFC ON STS 41-G	2-10
2-4	FILM TYPES FLOWN IN THE LFC AND THE SCA ON STS 41-G	2-11
2-5	HISTORICAL DOCUMENTATION OF THE OCPS FILMS FLOWN ON STS 41-G	2-12
2-6	OCPS FLIGHT FILM HANDLING MILESTONES	2-14
2-7	LFCIWG CO-INVESTIGATOR TARGET SUMMARY	2-16
2-8	LFC CO-INVESTIGATOR FILM PREFERENCE	2-17
2-9	PLANNED AND ACTUAL LFC DATA PASSES DURING STS 41-G	2-19
2-10	SUMMARY OF THE CLOUD COVER CONTENT OF LFC IMAGERY ACQUIRED ON STS 41-G	2-21
2-11	THREE TARGET ALTITUDES ACHIEVED DURING THE STS 41-G MISSION	2-22
2-12	STS 41-G ALTITUDES AND THE AMOUNT OF FILM EXPOSED AT EACH	2-24
2-13	LFC DATA PASSES AND FRAMES OF PHOTOGRAPHY AT THREE ALTITUDES	2-24

Table		Page
3-1	LIFETIME OPERATING TIMES (CLOCKS) AND EVENTS (COUNTERS) OF THE LFC LENS CONE AND FILM MAGAZINE ASSEMBLIES	3-4
3-2	LFC AND ARS THERMAL VACUUM EXPOSURE SUMMARY	3-5
3-3	LFC/AERIAL CARTOGRAPHIC GROUND COVERAGE	3-15
3-4	CHARACTERISTICS OF PHOTOGRAPHIC FILM EMULSIONS USED IN SHUTTLE FLIGHTS	3-22
3-5	AREA DATA FOR MAGNIFIED LFC SCENES OF BOSTON, MASSACHUSETTS	3-24
3-6	FOV CHARACTERISTICS OF STS 41-G TERRAIN RECORDING CAMERAS	3-28
3-7	EXPOSURE THRESHOLDS FOR THE FIVE LFC DISCRETE REGISTER SHIFTS FOR FMC DELAY COMMANDS	3-48
4-1	LFC FILM SENSITOMETRY DATA SUMMARY, STS 41-G	
	(a) B&W Film	4-2
	(b) Color Film	4-3
4-2	LFC FLIGHT FILM PROCESSING SENSITOMETRY, STS 41-G	4-4
A-1	LFC TEST AND FLIGHT FILMS	A-2
A-2	SEMIDIAGONAL AND TARGET PLACEMENT	A-3
A-3	RELATIVE ILLUMINATION	A-6
A-4	CALCULATED T-NUMBER	A-7
A-5	SPECTRAL TRANSMITTANCE	A-7
A-6	LFC AVERAGE RADIAL AND TANGENTIAL RESOLUTION (lp/mm)	A-8

FIGURES

Figure		Page
1-1	The OCPS, showing the components	1-29
1-2	The OCPS LFC, shown in a same-scale comparison to a standard aerial survey camera	1-30
1-3	The film magazine (upper) and the lens cone assembly (lower)	1-31
1-4	Schematic of the LFC cartographic lens assembly	1-32
1-5	Finished LFC lens components prior to assembly	1-32
1-6	The LFC thermal door assembly shown in the open (picture-taking) position	1-33
1-7	The aft end of the LFC lens assembly	1-34
1-8	Schematic layout for the LFC rotary shutter blades	1-35
1-9	Schematic presentation of the LFC capping shutter action	1-35
1-10	Measured lens/antivignetting filter relative transmittance	1-36
1-11	The filter holder and drive mechanism	1-36
1-12	The LFC focal frame	1-37
1-13	The under side of the LFC focal frame prior to assembly	1-38
1-14	Schematic of the LFC film magazine assembly	1-39
1-15	The film magazine	1-40
1-16	The LFC focal plane and format mask layout with auxiliary data imprints	1-41
1-17	SCA optical path and film transport schematic	1-42
1-18	Schematic of the placement of the SCA image pairs on the 70 mm film web	1-43
1-19	The reseau plate mask for the SCA	1-43
1-20	Schematic of the OCPS pressurization system	1-44
1-21	Image point drift	1-45

Figure		Page
1-22	LFC data acquisition concept for the 80-percent forward O/L mode	1-46
1-23	Presentation of the LFC gross stereo model area available in the 80-percent (and less) forward O/L mode	1-47
1-24	The effect of B/H ratioed imagery on the VE factor effect	1-48
2-1	The OCPS, shown in full flight configuration status on the MSFC MPESS	2-28
2-2	The LFC/SCA, shown being placed on the MPESS by KSC integration personnel	2-29
2-3	Final fit check of the LFC/SCA into the LFC support structure mounted to the MPESS	2-30
2-4	The OCPS (right) and companion ORS payload (left)	2-31
2-5	Inflight photo of Orbiter cargo bay, showing OCPS payload installed in aft end	2-32
2-6	Planned and actual film consumption by the LFC during STS 41-G	2-33
2-7	Photograph of the LFC at the completion of the oblique data pass to acquire imagery of Hurricane Josephine off the U.S. eastern seaboard	2-34
2-8	Orbiter vehicle reference axes	2-35
2-9	Mounting options for attachment of the SCA to a constant LOF of the LFC	2-36
2-10	Roll, pitch, and yaw deadband with the crew awake and performing onboard activities - data pass 125.0	2-37
2-11	Roll, pitch, and yaw deadband maintenance during crew sleep period - data pass 38.0	2-37
2-12	Roll, pitch, and yaw deadband maintenance during crew sleep period, both passes made on orbit 62	2-38
3-1	LFC computer-generated map for all land masses between latitudes 60° N and 60° S	3-53
3-2	Example of an actual LFC frame count software output	3-54
3-3	Revised LFC land and water boundary interface map	3-55

Figure		Page
3-4	Revised LFC multiple albedo map series	3-56
3-5	An actual LFC command set	3-58
3-6	Thermal history for the LFC film platen	3-59
3-7	Thermal history for the LFC lens cell	3-60
3-8	Thermal history for the LFC lens support structure	3-61
3-9	LFC footprints (area of ground coverage) at various altitudes	3-62
3-10	Tubruq, Libya	3-63
3-11	Port aux Poules, Algeria	3-64
3-12	Port aux Poules, Algeria	3-65
3-13	Two sites in Turkey and Armenia	3-66
3-14	Toyama, Japan	3-67
3-15	Flin Flon, Manitoba, Canada	3-68
3-16	Flin Flon, Manitoba, Canada	3-69
3-17	Flin Flon, Manitoba, Canada	3-70
3-18	Medicine Hat, Alberta, Canada	3-71
3-19	Medicine Hat, Alberta, Canada	3-72
3-20	Medicine Hat, Alberta, Canada	3-73
3-21	Medicine Hat, Alberta, Canada	3-74
3-22	Medicine Hat, Alberta, Canada	3-75
3-23	Medicine Hat, Alberta, Canada	3-76
3-24	Maryborough, Queensland, Australia	3-77
3-25	Maryborough, Queensland, Australia	3-78
3-26	Bundaberg, Queensland, Australia	3-79
3-27	Bundaberg, Queensland, Australia	3-80
3-28	Key West, Florida	3-81

Figure Page

3-29 Istanbul, Turkey..... 3-82

3-30 Beirut, Lebanon..... 3-83

3-31 Boston, Massachusetts..... 3-84

3-32 Venezia (Venice), Italy, on the Adriatic Sea at the upper end of the "boot."..... 3-85

3-33 High density agricultural development (plantations and irrigated cropland) in the Dubti-Tendaho region, Afar Depression, Ethiopia..... 3-86

3-34 Madrid, Spain..... 3-87

3-35 Walvis Bay..... 3-88

3-36 Rapid City, South Dakota..... 3-89

3-37 Ground distance covered during camera shutter "open" intervals at a nominal ground velocity of approximately 7.5 km/sec..... 3-90

3-38 Scene comparison of Boston, Massachusetts, as recorded by an NHAP aerial camera (left) and the NASA LFC..... 3-91

3-39 Boston, Massachusetts, area..... 3-92

3-40 Commercial aircraft on landing approach to Boston's Logan Airport..... 3-93

3-41 Inflight aircraft image quality as it is affected by flight direction of the aircraft and aircraft image-to-background contrast..... 3-94

3-42 Comparison of aerial photography (1952) and LFC photography (1984) of a hamlet in the Tug Wajale region of Somalia..... 3-95

3-43 Comparative frames of LFC and MC imagery..... 3-96

3-44 Comparative frames of LFC and MC imagery..... 3-97

3-45 Comparative frames of LFC and MC imagery..... 3-98

3-46 Comparative frames of LFC and MC imagery..... 3-99

3-47 Progressive magnification of the Ellsworth AFB site for evaluation of image structure integrity..... 3-100

3-48 Comparative frames of LFC and Hasselblad imagery..... 3-101

Figure Page

3-49 Comparative frames of LFC, Hasselblad, and Linhof imagery..... 3-102

3-50 Comparative frames of LFC, MC, and Hasselblad imagery..... 3-103

3-51 Comparative frames of LFC, MC, and Linhof imagery..... 3-104

3-52 The four basic acquisition modes of the LFC during photography of the earth..... 3-105

3-53 Stereo viewing..... 3-106

3-54 VE of terrain relief with the increase in the B/H ratio..... 3-107

3-55 Mt. Ararat stereogram demonstration..... 3-108

3-56 Cairns Reef area of the Great Barrier Reef on the Queensland, Australia, eastern seaboard..... 3-109

3-57 Contour line derivation combined with the orthophoto (facing page) of the White Mountain National Forest in New Hampshire..... 3-110

3-58 A 1:120,000 scale orthophotograph..... 3-111

3-59 Groundtrack map depicting area of coverage of uncontrolled photo mosaic of northwestern Australia (facing page)..... 3-112

3-60 Uncontrolled photo mosaic of northwestern Australia..... 3-113

3-61 Groundtrack map depicting area of coverage of uncontrolled photo mosaic of Afghanistan, Pakistan, and India region (facing page)..... 3-114

3-62 Uncontrolled photo mosaic of the Afghanistan, Pakistan, and India region..... 3-115

3-63 Two frames of LFC imagery combined as a constant scale mosaic of the Tibetan Plateau..... 3-116

3-64 Stream offset at the Kunlun Fault interface..... 3-117

3-65 Kunlun Fault in China (stereo)..... 3-118

3-66 Grand Erg Oriental, Algeria (stereo)..... 3-119

3-67 Erg Admer in Algeria (stereo)..... 3-120

3-68 Erg du Tenere in Niger (stereo)..... 3-121

3-69 Sechura Desert, Peru (stereo triplicate)..... 3-122

Figure Page

3-70 Durak Range in western Australia (stereo)..... 3-123

3-71 Bedford Station anomaly in western Australia (stereo)..... 3-124

3-72 Bedford Station anomaly in western Australia (stereo)..... 3-125

3-73 Complex folding in Tibetan Plateau (stereo triplicate)..... 3-126

3-74 Eroded folded zones in Tibetan Plateau (stereo)..... 3-127

3-75 Eroded folded zones in Tibetan Plateau (stereo)..... 3-128

3-76 Intrusive formation in Afghanistan (stereo)..... 3-129

3-77 Annular drainage, Tibetan Plateau (stereo)..... 3-130

3-78 Death Valley, California (stereo)..... 3-131

3-79 Samhan Range, Oman (stereo triplicate)..... 3-132

3-80 Farafra Oasis in Egypt..... 3-133

3-81 El Golea Oasis, Algeria, on the edge of the Grand Erg Occidental..... 3-134

3-82 Aggeneys, Republic of South Africa..... 3-135

3-83 Ocean surface detail in the Golfe d'Arzew at Port aux Poules, Algeria..... 3-136

3-84 A ship in the Ionian Sea completes an apparent collision avoidance maneuver by execution of a 1.5-km diameter circle..... 3-137

3-85 The island of Tahiti..... 3-138

3-86 Internal waves in the Indian Ocean off the northwest coast of western Australia..... 3-138

3-87 Plankton blooming in the Coral Sea off the eastern coast of Queensland, Australia..... 3-139

3-88 Erta Ale volcanic complex, Ethiopia (stereo)..... 3-140

3-89 Erta Ale volcanic complex, Ethiopia (stereo)..... 3-141

3-90 Volcanic vents, K'oboa, Ethiopia (stereo)..... 3-142

3-91 Active volcano at Gewane, Ethiopia (stereo)..... 3-143

3-92 Bola Selullse volcano, Ethiopia (stereo)..... 3-144

Figure		Page
3-93	Interface of the Mediterranean Sea and the African continent at the Libya and Egypt boundary	3-145
3-94	The world of Homer, with historic waterways and other geographic landmarks which have had many names during recorded history	3-145
3-95	The New England area	3-146
3-96	The Po River Valley, northern Italy	3-146
3-97	The Nile River Valley	3-147
3-98	The Po River Valley and Po River Delta, northern Italy	3-148
3-99	The Nile River Valley, Aswan Dam, and a portion of Lake Nasser in Egypt	3-148
3-100	Archer Bay on the Gulf of Carpentaria, Queensland, Australia	3-149
3-101	The western coast of Peru	3-149
3-102	Increasing magnification of the pampa floor, showing detail of the Nazca Lines	3-150
3-103	Hurricane Josephine, photographed off the eastern U.S. coast	3-151
3-104	Weather cells on the fringe of Hurricane Josephine	3-151
3-105	Cloud A as photographed from a slant range of approximately 930 km during orbit 117	3-152
3-106	Cloud B as photographed from a slant range of approximately 1,482 km during orbit 117	3-152
3-107	Cloud formations over the Bering Sea at about the Near Islands of the Aleutians	3-153
3-108	Imagery acquired over the Pacific Ocean just off the coast of southern Peru	3-153
3-109	A tropical disturbance developing in the area of the Sawu Sea	3-154
3-110	Major thunderstorms in the making over the southeastern coast of Africa at Quelimane, Mozambique	3-154
3-111	Glaciers and Paleolithic lakes in the Tibetan Plateau	3-155

Figure		Page
3-112	Paleolithic lake in the Tibetan Plateau	3-156
3-113	Karatax Shan glaciers in Tibet (stereo)	3-157
3-114	Glacial basins in Pamzal area, China (stereo)	3-158
3-115	Smeared and normal LFC imagery	3-159
3-116	AEC mode acquisitions	3-160
A-1	LFC image resolution and distortion test fixture	A-11
A-2	Collimator film target design for photo resolution and lens distortion testing	A-11
A-3	LFC resolution and distortion test fixture	A-12
A-4	LFC semidiagonal and target placement reference	A-13
A-5	Actual imagery from a resolution test sequence, showing relative target array placement	A-14
A-6	Coordinates for the geometric centers of the LFC cartographic lens assembly, serial number (S/N) 001	A-15
A-7	Thermal vacuum and dynamic resolution test chamber	A-15
A-8	Static resolution of the LFC lens assembly	A-16
A-9	Subassembly-level geometric distortion characteristics for the LFC lens cell, as performed on the laboratory collimator array	A-17
A-10	Nomograph for system focus shift as a function of pressure variations surrounding the lens cell	A-18
A-11	NOAA National Ocean Service's Metric Camera calibration facility located at Cloudcroft, New Mexico	A-19
A-12	LFC in position at the NOAA facility at Cloudcroft	A-19
A-13	LFC radial symmetric distortion	A-20
A-14	Total math model for LFC systematic distortion	A-21

ACRONYMS AND ABBREVIATIONS

AEC	automatic exposure control
AOS	acquisition of signal
ARS	Attitude Reference System
AWAR	area weighted average resolution
B	base
-B	minus blue
B&W	black and white
B/H	base to height
BIR	black and white infrared
CARR	customer acceptance readiness review
CDR	critical design review
CIR	color infrared
Co-I	co-investigator
Co-PI	co-principal investigator
COE	Corps of Engineers
COL	color
CRT	cathode-ray tube
DC	direct current
DMA	Defense Mapping Agency
DOA	Department of Agriculture
DOC	Department of Commerce
DOD	Department of Defense
DOE	Department of Energy
DOI	Department of the Interior
DRL	document requirements list

EDC	Earth Resource Observation System (EROS) Data Center
ERBE	Earth Radiation Budget Experiment
ERBES	Earth Radiation Budget Experiment Satellite
EROS	Earth Resource Observation Center
ESA	European Space Agency
EST	Eastern Standard Time
FILE	Feature Identification and Location Experiment
FMC	forward motion compensation
FMDM	flexible multiplexer/demultiplexer
FOV	field of view
GMS	geostationary meteorological satellite (Japanese)
GN_2	gaseous nitrogen
GOES	geostationary operation environmental satellite (U.S.)
GPC	general purpose computer
GPCA	gas pressurization control assembly
GRD	ground resolved distance (or ground resolved dimension)
GSA	gas supply assembly
GWC	Global Weather Central
-H	minus haze
H	height (i.e., altitude)
ICD	interface control document
IMC	image motion compensation (or image motion correction)
IR	infrared
IRIG-B	Interrange Instrumentation Group B
IVT	integration verification test
JSC	Lyndon B. Johnson Space Center

KSC	John F. Kennedy Space Center
l/mm	lines per millimeter
lp/mm	line pairs per millimeter
LED	light emitting diode
LESC	Lockheed Engineering & Sciences Company
LFC	Large Format Camera
LFCIWG	Large Format Camera Interagency Working Group
LOF	line of flight
LOS	loss of signal
Meteosat	meteorological satellite (European)
MAPS	Measurement of Air Pollution from Satellites
MC	Metric Camera
MCC	mission control center
MPESS	mission peculiar equipment support structure
MPSR	mission payload support room
MSFC	George C. Marshall Space Flight Center
MSS	multispectral scanner
MTF	modulation transfer function
NASA	National Aeronautics and Space Administration
NHAP	National High Altitude Photography (program)
NOAA	National Oceanic and Atmospheric Administration
NUSC	Naval Underwater Systems Center
O&C	operations and checkout
O/L	overlap
OCPS	Orbiter Camera Payload System
OMB	Office of Management and Budget

OPF	Orbiter Processing Facility
ORS	Orbital Refueling System
OSSA	Office of Space Sciences and Applications
OSTA-3	Office of Space and Terrestrial Applications 3
PCB	power control box
PCM	pulse code modulation
PCS	payload control supervisor
PDB	power distribution box
PDR	preliminary design review
PI	principal investigator
PIP	payload implementation plan
PPA	principal point of autocollimation
PPS	principal point of symmetry
PSU	power supply unit
RMS	root mean square
RTC	real-time command
S/N	serial number
SCA	Stellar Camera Array
SIMS	mission simulations
SIR-B	Shuttle Imaging Radar B
SOW	statement of work
SPC	stored program command
STS	Space Transportation System
trans.	transmittance
TDRSS-A	Tracking and Data Relay Satellite System A
TM	telemetry

TOC	target object contrast (or test object contrast)
USAF	U.S. Air Force
USDA	U.S. Department of Agriculture
V/H	velocity to height
VAB	Vertical Assembly Building
VIE	visual image evaluation
VE	vertical exaggeration

1. SYSTEM DESCRIPTION

1.1 INTRODUCTION

The Orbiter Camera Payload System (OCPS) is a major STS cargo bay payload. The current and "as flown" configuration for the OCPS is shown in figure 1-1. The primary component is the Large Format Camera (LFC), shown mounted on its maintenance dolly and with its thermal (protective) door open in the acquisition mode. Performing a secondary and supporting function to the LFC operations in flight is the Attitude Reference System (ARS). The ARS is composed of a dual lens ballistic camera called the Stellar Camera Array (SCA); the SCA flight support structure, an annular ring structure, which rigidly mounts the SCA to the LFC; and the remotely mounted ARS electronics assembly. Other flight items comprising the OCPS include the LFC electronic assembly, also remotely located; a high pressure gas supply assembly (GSA); a gas pressurization control assembly (GPCA); and pneumatic and electrical lines and cabling. The GPCA is, incidentally, mounted to the LFC lens support structure. The OCPS ground checkout station is shown in the background. Table 1-1 provides a summary of some of the design and operational parameters of the LFC and the ARS.

The LFC is, of course, used for making very high resolution photographs of the earth surfaces with great inherent geometric fidelity. The SCA is used to make simultaneous photographs of two star fields at the precise instant of the midpoint of exposure (time) of each LFC terrain photograph. By execution of an inflight stellar calibration sequence, whereby three star fields are photographed simultaneously by each of the three lenses, a precise relationship (lock angle) of the LFC optical axis to the two SCA optical axes is obtained. Such information is later used during postflight data analysis to determine the absolute pointing attitude of the LFC with reference to the center of the referenced geoid, the Earth.

Because of the enormous payload weight-carrying capability of the STS (32 tons), a severe weight reduction program was not exercised during the design phases of the LFC project. Additionally, the underlying and basic

TABLE 1-1.- LFC OPERATIONAL PARAMETERS

Parameter	LFC	ARS / SCA
Lens		
• Focal length	30.5 cm (12 in.)	15.2 cm (6 in.)
• Aperture	f/6.0 (T/16)	f/2.8 (T/3.5)
• Spectral range	400 to 900 nm	400 to 900 nm
• Distortion	<10 μm (average)	<5 μm (average)
Shutter		
• Type	3 disk rotary intralens with capping blade	"Barn doors" in front of each lens
• Speed range	4 to 32 msec	200 msec (only)
• Speed select	External command or automatic exposure control (AEC)	None
Forward motion, type	Translation of platen	None
Compensation, range	11 to 41 mrad/sec	None
Camera internal pressure	2 psig	Vacuum
Film flattening	Vacuum	Platen press
Image format	22.9 x 45.7 cm (9 x 18 in.)	6.48 x 6.18 cm
Forward overlap modes	10, 60, 70, and 80%	None
B/H ratios	0.3 to 1.2	None
Filters		
• Antivignetting	Front of lens	None
• Minus-haze	Intralens	None
• Minus-blue	Intralens	Lens front
Minimum cycle time	7.5 sec	7.5 sec
Field of view (FOV)		
• Along track	73.7° (1.5 x altitude)	24.0°
• Across track	41.1° (0.75 x altitude)	22.9°
Film		
• Width	24.1 cm (9.5 in.)	7.0 cm (2.75 in.)
• Roll length	1,220 m (4,000 ft)	670 m (2,200 ft)
• Exposures/roll	2,500	2,450
Electrical		
• Voltage	28 ± 4 Vdc	28 ± 4 Vdc
• Power	273 W, average	131 W, average
Total flight weight	434.76 kg (954.2 lb)	186.02 kg (410.1 lb)
Total OCPS LFC/ARS flight weight[a]	618.78 kg (1,364.3 lb)	

[a] Fully integrated for flight, the OCPS has a total flight weight of 1,617.14 kg (3,565.3 lb), including the mission peculiar equipment support structure (MPESS) and other peripherals. See table 1-2 for weight of components.

requirement for a cartographic system is dimensional stability to enhance the geometric integrity of the system; this is reflected in the system's structure and, quite often, in weight. For this reason, construction materials were not selected purely on the basis of their weight characteristics, but more for the appropriateness of their application.

Many times, weight reduction objectives force the designer into the selection of rather exotic materials whose availability and production processes (casting, shaping, and machining) can greatly increase complexity and costs of the hardware items. An example of the avoidance of this extra complexity and expense is the selection of a ferrous material for the lens cell housings as opposed to materials much lighter in weight, such as beryllium or aluminum and magnesium alloys. Based on their mechanical and thermal properties, the ferrous materials selected for the LFC lens cell housing have an acceptability equal to that of a beryllium material, yet entail only a fraction of the procurement and fabrication costs and complexities.

The weight breakdown of the major OCPS components has been summarized in table 1-2. This breakdown serves to identify what one might encounter in the planning of a sophisticated geometrically stabilized imagery acquisition system. Again, the design objectives were based on intended application and not necessarily on weight reduction goals.

1.2 LARGE FORMAT CAMERA

The LFC is a cartographic camera system used for precision acquisition of earth imagery of great geometric fidelity. It is, in many respects, a scaled-up version of the standard aerial survey cameras (figure 1-2) used throughout the world to photomap the natural and manmade features of the earth. It is, by the nature of its intended application, unique in many respects in order to accommodate the extreme altitudes (low earth orbit) at which it is used. Like the aerial systems, the LFC lens is designed to reduce geometric distortion to an absolute minimum without compromising the much greater spatial resolution required of it. Since the LFC is deployed in an unusual single-flight application over an extended period of time, it has

TABLE 1-2.- WEIGHTS OF THE MAJOR COMPONENTS OF THE OCPS

System and component	Weight	
	kg	lb
LFC	(405.69)	(890.0)
• Lens cone assembly	277.19	611.1
• Film magazine assembly[a]	91.00	200.6
• Camera electronics assembly	34.47	76.0
• Thermal blankets	1.04	2.3
ARS	(186.02)	(410.1)
• SCA	69.12	152.4
• Film cassette assemblies[b]	32.94	72.6
• Camera electronics assembly	30.84	68.0
• SCA flight support structure	56.58	111.5
• Thermal blankets	2.54	5.6
Gas (GN_2) Pressurization System	(29.07)	(64.2)
• GSA[c]	21.95	48.5
• GPCA	7.12	15.7
Total OCPS	618.78	1,364.3
Carrier structure, etc.[d]	998.36	2,201.0
Total flight weight	1,617.14	3,565.3

[a] Includes 38.1 kg (70.0 lb) of film.

[b] Includes 5.5 kg (12.2 lb) of film.

[c] Includes 4.5 kg (10.0 lb) of gaseous nitrogen (GN_2).

[d] Includes MPESS, flex multiplexer/demultiplexer (FMDM), power control box (PCB), power distribution box (PDB), and cables.

a great capacity for film supply and number of frames of imagery. In order to retain the same acquisition geometry (wide angle FOV), it is of greater lens focal length and greater image area (or larger format).

But, most of all, its greatest variance from its air breathing progenitors lies in the fact that it is used in what many might consider the hostile environment of space, and the ascending powered flight phase does have great dynamic loads (acceleration and vibration) imposed upon it. The on-orbit flight environment does subject the instrument to great extremes of temperature excursions, and there is a near total absence of air molecules to provide a sensible operating pressure. In order to survive and perform its intended functions, the LFC is a closed loop environmental system (figure 1-3) which is, in itself, a pressure vessel providing its own pressure and thermally conditioned environment.

1.2.1 LFC LENS ASSEMBLY

The LFC cartographic lens assembly (see figures 1-3, 1-4, and 1-5) is a nine-element aspheric design with an effective focal length of 30.5 cm (12 in.), an aperture of f/6, and a T-number of less than 14. Including the front thermal (glass) window, the total glass weight of the lens is 54.25 kg (119.59 lb). The upper and lower machined lens cell castings (see figures 1-4 and 1-5) are of type G30 Meehanite™, a type of cast iron. The total weight of these two finished castings is 71.44 kg (157.5 lb). The lens element retaining rings are also of machined cast Meehanite. To avoid a prolonged aging process required for curing of cast iron, an accelerated thermal curing process was employed.

The lens design includes a cemented doublet (elements 2 and 3) with the aspheric surface figured on the inboard side of element 3 and a cemented triplet (elements 4, 5, and 6). All exposed transmitting surfaces are magnesium fluoride coated. The thermal window also serves as the substrate for the antivignetting filter and as the pressure barrier for maintaining the required internal operating pressure within the LFC. The rotary shutter and two spectral filters are mounted within the space separating the doublet and the triplet lens subassemblies. These two filters are mounted within a sector disc in such a manner that upon receipt of the filter select command, one filter will swing out of the optical path as the other swings into position.

Surrounding the assembled lens cell is an aluminum cylinder (see figure 1-3) that serves as a pressure vessel to maintain the required internal operating pressure at 2 psig. This tank is constructed of sheet aluminum rolled into a large diameter cylinder. Eight 2.75-W strip heaters are bonded to the exterior surface of this structure. A second (unpressurized) vessel, large enough to contain the lens pressure vessel, is constructed of fiberglass and fitted with a remotely operated thermal door. The exterior of this vessel is painted with a white Lord Corp. polyurethane (Chemglaze II™) thermal paint. The interior is lined internally with a multilayer thermal insulating blanket composed of aluminized Mylar™ and Kapton™ films with a fibrous filler. These two cylinders constitute the thermal/vacuum environmental enclosure for the LFC lens cone assembly. The antivignetting filter in front of the lens serves three barrier functions: an illumination equalizing barrier for the image formation, a thermal barrier for heat rejection, and a pressure barrier which completes the forward closure of the vessel.

Completing the closure of the external envelope is the LFC thermal door assembly. This door (see figure 1-6) serves three purposes: it provides a mechanical barrier to prevent contamination of the optics during ascending flight and attitude control motor firings, and throughout all quiescent periods; it provides a barrier to the thermal environment, preventing gain of heat from sunlight and loss of heat to deep space or earth's dark side; and its contained strip heater thermally conditions the forward end of the lens assembly. This door automatically opens when the LFC is issued an "operate" command and closes upon receipt of a "standby" command; it can also be opened or closed through issue of thermal door override commands.

Thermal stability of the lens assembly and focal plane is critical to maintaining the exact plane of focus and preserving the calibrated lens distortion characteristics. The aft lens cell casting is permanently affixed to the camera support structure, which is a thick machined cast aluminum plate (see figure 1-7). The LFC film magazine assembly also attaches to this plate and, through use of an O-ring in the rectangular channel, seals the aft end of the lens, completing closure of the pressure vessel. Additionally, this plate serves as a mounting surface for hermetically sealed cable connectors.

Notice in particular the two rectangular quick connect/disconnect electrical connectors through which all power and electrical signals enter and exit the film magazine assembly. To ensure maximum thermal stabilization of this plate, six strip heaters are mounted, producing a total of 91 W of energy.

The focal frame assembly is rigidly mounted to this plate also. This is a metal mask which defines the limits of the image area and also contains projectors for the 12 edge fiducials and the lens serial number.

1.2.1.1 LFC Shutter Description

The LFC has a rotary intralens-type shutter (located between lens elements 3 and 4). The LFC's two spectral filters are also located at the same general area (see figure 1-3). The housing for both the shutter drives and the filter drive mechanism is of cast aluminum.

The rotary shutter is composed of three rotating circular blades (discs) and a capping blade (figure 1-8). Apertures within the discs are fixed, the duration of the exposure being controlled by their angular velocity. Two of the blades are referred to as the "high speed" blades. One rotates in a clockwise direction and the other in a counterclockwise direction, and the two have diametrically opposed apertures. The third blade rotates in a clockwise direction, has a single aperture, and is described as the "low speed" blade. The high speed blades are geared in a 1:1 ratio to the shutter drive motor, whereas the low speed blade is geared in a 0.4:1 ratio, such that the rotation velocity ratio between the high and low speed blades is 2.5:1. Apertures of all three blades come into alignment in the optical path at each complete revolution of the low speed blade.

Depending on the angular velocity commanded, the frequency of alignment of the three apertures varies. At each alignment of these apertures, an exposure opportunity presents itself. However, an exposure to the film is prevented by the positioning of the capping blade (see figure 1-9), which is normally closed. When a command for capping blade open is issued, the capper does not immediately open, but its electrical logic is primed to look for a

feedback signal of pending alignment of the three rotary disc apertures. When this signal is received, the capper will open and will remain open until all three apertures have come into alignment and closed. The capper will then revert to closed position awaiting the next open command.

1.2.1.2 Shutter Speeds

The angular velocity of the rotary shutters is controlled by a remote electrical command. This command is an analog (variable voltage) signal and may be selected for any level over the desired range to produce film exposure durations of 4 to 32 msec (or, expressed fractionally, 1/250 to 1/31 sec). During a mission, stored program commands (SPC's) for shutter speeds (see table 1-3) were built to command the shutter in increments of 1/4 f/stop. Since the LFC exposures have been made intentionally long, the higher resolution (and slower speed) film materials can be used. The forward motion compensation (FMC) incorporated into the film platen eliminates the image smear which would be encountered at these relatively long exposure times.

1.2.1.3 LFC Optical Filters

The LFC is fitted with a permanent "in-front-of-the-lens" filter (see figure 1-4) which provides two distinct functions. First, this filter (1.3 cm or 0.5 in. thick) forms the pressure retention barrier for the LFC, also functioning, to some degree, as a thermal protection window for the interior lens elements. Thus, it could be described as an environmental (pressure and heat) protection window. Second, this optically flat glass plate serves as the substrate for a readily variable neutral density filter. The density is greatest in the center and diminishes to zero at the outboard reaches of its aperture.

The purpose of this filter is to balance the amount of light energy falling over the entire area of the format. As is true with wide angle lenses, their transmittance is greatest on axis and falls off with increasing field angle (essentially the cosine of the angle), as shown in figure 1-10. The LFC lens is considered to be a wide angle lens (e.g., diagonal FOV of 79.9°, or 39.9° half-angle). The amount of light energy reaching the focal plane film falls

TABLE 1-3.- LFC STORED PROGRAM COMMANDS FOR ROTARY SHUTTER SPEEDS AND BUILDABLE COMMANDS

LFC shutter speeds, sec						Pulse code modulation (PCM) count
Full f/stop, sec		Half f/stop, sec		Quarter f/stop, sec		
Decimal	Fraction	Decimal	Fraction	Decimal	Fraction	
0.032	1/31					53
				0.028	1/36	61
		0.024	1/42			71
				0.020	1/50	85
0.016	1/63					107
				0.014	1/71	121
		0.012	1/83			141
				0.010	1/100	170
0.008	1/125					212
				0.007	1/143	243
		0.006	1/167			284
				0.005	1/200	340
0.004	1/250					425

off dramatically from the center of the format to the corners of the format, producing the effect of image density vignetting at the image plane. This filter attempts to equalize the amount of energy throughout the image area, producing a relatively uniform exposure throughout. For this reason, this filter is called an "antivignetting" filter.

In addition, the LFC has two intralens spectral filters which can be selected on an "either/or" basis, meaning that one or the other filter is in position within the optical path at all times. One of the filters is a "minus haze" (-H) filter and the other is a "minus blue" (-B) filter. Both provide sharp cutoff of the short wavelength end. The -H filter absorbs much of the very

short wavelength blue energy which is scattered in the upper atmosphere; it is used with true color positive film and, when light levels are low, with panchromatic negative films. The cutoff point for this filter is 425 nm. The -B filter absorbs all blue energy and shorter wavelengths, eliminating all atmospheric scattering; this filter, equivalent to a Wratten™ G, is used with color infrared positive films and black and white (B&W) panchromatic negative films. The -B filter has a cutoff at 525 nm. Transmittance of both filters is approximately 92 percent of the energy in the band pass region. Selection of the desired spectral filter is via an electrical command. The filters are mounted in a sector wheel (figure 1-11) which is driven to stop positions at either end of travel by reversal of a direct current (DC). Transition time between the two filter positions is approximately 4 sec, and such selection is made as part of the prepass command formatting. Filters are not normally changed during a data acquisition period, though there is no reason that this could not be done.

1.2.1.4 Lens Focal Frame

As noted in the narrative describing the aft lens assembly (see figure 1-7), the lens focal frame is the aft end of the lens assembly. This component provides a mask to define the image format area of 22.86 by 45.72 cm (9 by 18 in.) and to provide the absolute reference for any point within the image area relative to the lens calibration. All points of key location are referenced to the intersection of the primary fiducials and, to a lesser degree, the intersection of the secondary fiducials. This is a precision machined metal frame which is rigidly affixed to the camera support structure along with the lens cone and which becomes an integral part of the lens assembly. The validity of all lens geometric calibrations is based on the integrity of the frame position. Though registration pins and post installation pinning are provided, the removal, reinstallation, or any other type of disturbance of this frame places all referenced geometric calibrations in doubt.

Figure 1-12 shows the lens focal frame attached to the camera support structure, revealing the proximity of the frame to the aft lens elements. It will be observed on closer inspection that there is a black opaque

rectangular mask which has been painted onto the aft surface of lens element 7. This serves to baffle internal light reflections and thus reduce veiling glare. A similar light baffling mask is found behind lens element 1 in the forward end of the lens cell (see figure 1-6), though this one is of sheet metal.

Prior to installation (see figure 1-13), the under side of the format mask shows the 12 fiducial projector housings and the 2 lens serial number projector housings. Light emitting diodes (LED's) provide the radiant energy to illuminate the bull's-eye reticle containing the 50-μm-diameter dot used for all reference measurements. (Details of the format area are shown in diagrams found in section 1.2.3, Auxiliary Data.)

1.2.2 FILM MAGAZINE ASSEMBLY

The LFC film magazine assembly (see figure 1-14) utilizes a roll of film which is 24.13 cm (9.5 in.) in width and 1,220 m (4,000 ft) in length. The films normally used are the thin base material, which is 0.06 mm (2.5 mils) thick. When spooled to maximum capacity, the LFC film roll provides approximately 2,500 image frames and weighs 31.75 kg (70 lb). The LFC can also use standard base film which is 0.10 mm (4.0 mils) thick, but in this case the spool would contain a significantly lesser length of film.

The LFC film magazine assembly, designed as a pressure vessel, completes the rear closure to the assembled camera. All electrical connectors providing copper paths between the lens cone and film magazine are the quick connect/ disconnect type on the camera support structure (rectangular connectors) as shown in figure 1-7. The keying of these two connectors, in addition to the use of guide pins, ensures proper mating of the magazine with regard to flight direction orientation. The film magazine attaches to the camera support structure, as shown in figure 1-15.

The film magazine assembly was fitted with internal strip heaters to stabilize the temperature of the film platen. In addition, this assembly was provided with a soft, encasement-type thermal blanket composed of multiple

layers of aluminized Mylar™ and contained by a durable cover of beta (glass fiber) cloth.

The LFC film magazine utilizes the displacement design concept whereby the initial film load finds the supply film spool diameter encroaching into the volume allowed for the takeup spool. With this technique, the takeup spool diameter increases as the supply spool decreases in diameter. Eventually, the takeup spool diameter becomes large enough that it then encroaches into the volume originally allocated to the supply roll of film which, by this time, has been reduced significantly in diameter. In order to accomplish this feat and maintain a reasonable compactness to the total volume of the film magazine, unique flanging of the film spools is required.

During the factory spooling of the film, the film spool is equipped with two identical machined flanges, each with a diameter of 14.25 in. During the actual film loading process prior to final integration of the LFC, one of the large flanges is removed and replaced with a small flange whose diameter is 6.49 in. Similarly, the empty takeup spool is fitted with a large- and a small-diameter spool flange so that, when the spools are installed in the film magazine, the matching ends are large to small and small to large, thus allowing the spool cores to be positioned much closer to each other.

Shortly after the roll diameter of the takeup spool exceeds the diameter of the small flange, the now-vacant area of the supply spool's large flange serves as a guide to film spooling buildup on the takeup roll. The same principle applies to the film supply in that, early on, the vacant region of the takeup's large spool flange also keeps the open end of the supply film roll from slipping in the direction of its small flange. This ensures proper tracking of the film throughout the entire film path from supply to takeup.

Another feature of the film transport system is that once a data take sequence is initiated, torque motors on both the film spools (supply and takeup) start the spools into a state of continuous, though slow, rotation that continues until the data sequence is completed, be it 10 frames or 100 frames.

Initiation of a data sequence first sees the supply spool slowly drive to meter out film, but since the film is still stationary in the vicinity of the magazine's vacuum film platen, this freshly despooled film enters a dancer assembly, which slowly fills by looping the film between rollers. Concurrent with this, a similar dancer assembly on the takeup side is empty, and the takeup spool has not yet started to drive.

Immediately after completion of the first frame of the sequence, a film metering/framing roller drive assembly pulls the film from the platen area, delivering it to the empty takeup dancer, and empties the supply dancer of film. At this time, the takeup spool starts turning to empty its full dancer assembly. From this point on, both film spools remain in continuous rotation, the supply film slack being taken up by the supply dancer and the takeup removing freshly exposed film from the takeup dancer.

Upon completion of the final frame in a data sequence, the LFC begins to reach a standby mode condition. During this shutdown the film magazine transport does two things. First, the takeup spool continues rotation until it empties the takeup dancer, after which a brake engages to stop and hold the spool at its final position. Second, sensing no further need to supply fresh film, the supply spool drive motor stops and drives in the opposite direction, returning fresh film to the supply spool until such time as the supply dancer becomes empty. At this point a brake engages, holding the supply spool in its stowed (standby) position. This keeps the film taut during all quiescent periods.

Most aerial framing type cameras have intermittent spool rotations corresponding to each exposure cycle. This starting and stopping of the spools is permissible on aircraft and certainly simplifies transport mechanism design. However, on spacecraft, and certainly on satellite applications, the sudden starting and stopping of a 34.5-kg (70-lb) spool of film induces unreasonable torque which must be compensated for by the vehicle's attitude control system. Since the initial design concepts derived for the LFC considered its potential application as a free flyer, this type of transport was considered mandatory.

The film magazine also contains the auxiliary data printer head, which is a single alphanumeric LED. This printer prints stored data pertaining to the last frame exposed as the film is being transported past the printer head. The film platen also has fixed data printers which give the serial number of the film magazine (currently only one) and arrows that indicate the direction of flight.

The LFC utilizes a vacuum film platen to ensure precise flattening of the film in the focal plane and intimate contact with the reseau references during the scene exposure. The makeup gas is provided to the LFC from a remote storage vessel, the GSA, to maintain internal pressure during the intermittent venting of gas to flatten film. This gas, GN_2, is preconditioned (heated) prior to entering the LFC. (For a detailed sequence of events for film flattening and for transport sequence, please refer to section 1.4, Pressurization System.)

1.2.2.1 Forward Motion Compensation

The forward orbital velocity of the spacecraft is approximately 7.7 km/sec (25,400 ft/sec) at an altitude of 300 km (162 n. mi.). The velocity over the ground track is slightly less than this (7.4 km/sec) since the circumference of the earth is slightly less than the orbital circumference traversed during the same time interval. At the 300 km altitude during the minimum camera exposure of 4 msec (1/250 sec), the image would have ground targets elongated by 30 m. Since this is greater than a resolution element, the resulting image would be "smeared" to a detectable level. At the longest exposure of 32 msec (1/31 sec), the smear would be approximately 240 m.

To avoid this type of image degradation, a means of moving the film along with the image during the exposure cycle must be implemented to compensate or offset this forward motion of the image. There are various ways to accomplish this, but in the LFC film magazine, FMC is accomplished by translation of the vacuum film platen in the positive velocity vector (into the direction of flight), which is the line-of-flight (LOF) axis. In effect, the image, as it is being formed on the emulsion surface, is carried along

with the film at a translation velocity which is scaled to the ground velocity of the spacecraft.

The film platen is suspended from two flexural points at both ends of the platen. These flexural devices are kept in constant tension by the application of pressure from four vernier screws which have Teflon™ covered pads to allow smooth sliding action when the platen is driven to motion. The FMC motor-driven lead screw drive assembly is mounted on the platen housing and connected to the platen.

When the FMC drive is actuated, just prior to the initiation of an exposure, the lead screw rotates and pushes the platen in the flight direction at the velocity for the current orbital altitude. After completion of the exposure, the lead screw returns the platen to start position. This action is controlled by a velocity servo, consisting of a servo preamplifier, power amplifier, drive motor, and tachometer. A potentiometer signal is substituted, and the drive acts as a position servo during the return to start position to be in readiness for the next exposure. The range of the FMC drive is from 11 to 41 mrad/sec.

1.2.3 AUXILIARY DATA

The focal plane of the LFC's cartographic lens assembly (figure 1-12) is defined by a metal frame with an opening which is 22.86 by 45.72 cm (9 by 18 in.). As a key to image point location and mensuration, two types of fixed references are provided. The first type is provided by a total of 12 fiducial projectors, 5 on either side of the format long dimension (LOF axis) and 1 each at center on the forward and aft edges of the focal frame. The four primary fiducials (see figure 1-16) are positioned precisely midway on each of the rectangle sides. The four secondary fiducials are used to define the central 22.9- by 22.9-cm (9- by 9-in.) square of the format. The remaining four fiducials are positioned at the four corners of the focal frame. All fiducial projectors are flashed for 1 msec at the exact midpoint of the LFC scene exposure.

In addition to the focal frame fiducials, 45 reseau projectors are mounted within the 1-in.-thick machined cast aluminum vacuum film platen. These projectors are deployed in five rows of nine each, with each row and member positioned at 5-cm intervals. They are flashed through the film base just prior to initiation of the FMC drive. Their sole purpose is to serve as reference points for the determination of residual errors in the processed imagery (original or duplicate) due to film shrinkage or stretching.

Thus, the fiducials and reseaus are auxiliary benchmarks for use as "hardpoints" in the recovery of image positional data during the analytical process. Both of these are recorded on the film and are used with system calibration record information when work is being done with various generations of imagery. By their nature, this type of data is nonvolatile, it is fixed and, hopefully, is quite firm in nature.

There is other auxiliary information which is recorded on the film imagery, some of which is updated with each frame of photography. Those items which remain fixed for the entire mission include direction of flight arrow indicators, current mission identification, and lens and film platen serial numbers.

Those data items which are updated for each film exposure are sampled at the midpoint of the actual exposure, stored within the LFC electronic storage bank, and then sequentially printed out on both halves of the frame (see figure 1-16) on the edge of the film as the related exposed imagery frame is transported past the data printer (alphanumeric LED) assembly. The spacecraft puts out a modified Interrange Instrumentation Group B (IRIG-B) time code which is updated each second. This time signal is received constantly by the LFC electronics assembly, and each update starts a 1-kHz clock running. When the exposure midpoint signal is received, this clock data is frozen and stored. This information is expressed in current GMT time (day, hour, minute, second, and millisecond) and the current individual frame number. This information is most important for postmission recovery of flight vector data (altitude, geographic coordinates, roll, pitch, and yaw) for use in both preparation of the LFC mission ephemeris and for data analysis.

The GMT date is the number of the day in the year, with January 1 being day number 1 and the launch day, October 5, 1984, being day number 279. Thus, the time string of 279 17 52 23.675 would indicate the 17th hour, the 52nd minute, the 23rd second, and the 675th part of the following second of October 5, 1984 (day 279).

The mission number displayed on all frames is set prior to launch and reads 4107 for STS 41-G. By protocol, the first numeral "4" indicates the year 1984, and the "1" identifies the launch site as John F. Kennedy Space Center (KSC). The last two numerals are for the mission number (up to 99) for the year, which in this case was "G," the 7th letter of the alphabet.

The frame number is four numerics and is updated one count for each frame. When the flight film was loaded into the LFC film magazine in preparation for integration into the spacecraft, the counter was set at 0000. Integration verification testing and prelaunch checkouts consumed 53 frames, such that the first frame shot in orbit was recorded as 0054. The final frame on orbit was 2300, indicating a net of 2,247 frames on orbit. STS 41-G photographs throughout this document are referenced by the four-digit frame number only.

1.3 ATTITUDE REFERENCE SYSTEM

The OCPS ARS is a major adjunct to the LFC, providing attitude data to establish the degree of nonverticality of the LFC imagery. The ARS is composed of the SCA, a dual lens ballistic camera; the SCA support structure, which rigidly attaches the SCA to the LFC; and the ARS electronics assembly. The ARS has no autonomy; it receives commands only from the LFC electronics and sends all housekeeping telemetry (TM) through the LFC electronics assembly for signal conditioning and transmission.

The SCA (see figure 1-1), whose dual lens system images on a single roll of film, makes a stellar pair of images for each LFC image. The SCA lenses are orthogonal to each other, making simultaneous placement of the image pairs side by side on the film quite convenient, as shown in figure 1-17.

The SCA uses film which is 7.0 cm (2.52 in.) in width and 685 m (2,250 ft) in length and uses thin base films with a base thickness of 0.06 mm (2.5 mils). The SCA film roll (685 m) provides approximately 2,500 pairs (5,000 frames) of stellar imagery.

The SCA film transport concept is similar to that of the LFC (e.g., continuous spool motion) with the exception that a single dancer assembly is used. The dancer assembly is, however, free to travel in two directions along a single axis such that when it moves into the direction of the supply spool it empties fresh film into the two film platen areas and simultaneously loads up with freshly exposed film. Once the film becomes motionless and is clamped into the exposing gates, the dancer reverses its direction, pulling fresh film from the supply and emptying exposed film into the takeup spool. The film is held firmly in the exposing gates by the foam-surfaced platen press devices, driving the film into intimate contact with the SCA rear lens element surfaces.

Unlike the LFC stowing procedure, once the final frame of a sequence is completed, the dancer fills with fresh film and empties the exposed film that had filled it after the final exposure. As with the LFC, the film is held taut throughout all quiescent (standby) periods. This allows the SCA to be ready to make an exposure immediately upon receipt of the first exposure command from the LFC electronics logic.

Film flattening in both the LFC and the SCA is accomplished by two totally diverse but positive means. The LFC utilizes a vacuum film platen and the SCA employs a mechanical press type platen. Both means ensure precise flattening of the film in the focal plane and intimate contact with the reseau references.

Since the SCA imagery supports the LFC image analysis function, two key items of transient ancillary information (see figure 1-18) are recorded directly onto the SCA film: (1) the number of the LFC frame to which the SCA imagery is paired and (2) the time delta of the midpoint of stellar exposure for each SCA frame to the reference LFC frame midpoint of exposure.

The SCA image format, masking, and content of the reseau plate are illustrated in figure 1-19. This information is deposited on the outer surface of the rear element of the SCA lenses. The blocking material used for the mask, the reseau crosses, the reader flags, the reseau plate serial number, and the station annotation (e.g., left or right) is an alloy of Inconel and chrome. A total of 152 reseau crosses is incorporated into the reference grid, whose vertical and horizontal intersections are on 0.5-cm centers. As with the LFC reseau grid, the SCA reseau is used for the correction of residual film errors during postflight analysis.

The SCA has a "barn door" type shutter in front of each lens assembly. This type of shutter was used for two reasons. First, the exposure time for capture of star images is relatively long, 200 msec (1/5 sec), making it unnecessary to design a high velocity actuating system. Second, the exposure scheme requires flooding the SCA lens with light in order to record the reseau plate data.

During the SCA image exposure, the film is held in contact with the reseau plate by the cushioned platen press. To cause the reseau crosses to be detectable and to give some background density to the image area, louvered electroluminescent panels on the interior surface of the SCA shutter doors are strobed - just prior to the start of the stellar exposure - to flood light into the lens and to produce shadow graphs of the reseau and the other fixed auxiliary data points. The desired background density on the film is approximately 0.2. When this exposure is imparted to the film, the effective film speed is also increased, making it possible to extend the capture range of stars by at least 1 visual magnitude.

The sequence of the star exposure requires approximately 100 msec (1/10 sec) for each of the two doors to reach fully open position and another 100 msec to reached fully closed position. The doors remain in the fixed open position for 100 msec. Effective exposure of the image begins when the doors are half open (e.g., 50 msec or 1/20 sec) and ends when the doors have reached the half-closed position. Thus 50 + 100 + 50 msec gives a total stellar exposure time of 200 msec (1/5 sec).

Each SCA lens has a -B filter mounted in front of the lens. The function of this filter is to reduce the point spread function of the point image of a star. Use of this filter limits the use of stars to those of higher red saturation than blue, but it also produces smaller (less than 25 μm width) and more dense star images. The smaller the star image, the greater the mensuration accuracy in determining its position.

1.4 PRESSURIZATION SYSTEM

Design feasibility studies for the LFC were based on its complete and constant immersion in the space environment by virtue of being mounted in the Orbiter vehicle's cargo bay. The LFC uses photographic film as the detector, and such films do contain a surprising amount of moisture (a single roll of LFC film has 295 sq m of emulsion surface and contains approximately 1.65 kg of water). Placing such film in a vacuum environment without adequate protection would soon cause loss of this moisture, with subsequent embrittlement and cracking of the emulsion during transport through the system. Additionally, a positive pressure is required to hold the film flat against the film platen during the image exposure event.

These facts, combined with experimental testing, established the need for the LFC to be a pressure vessel in itself, and a minimum internal pressure of 138 mbars (2 psig) was required to flatten the film against the film platen. GN_2 was selected as the pressurizing gas. The film platen was to be vented to a sufficiently lower pressure to "suck" the film flat against the platen. In an air breathing system, this would require a vacuum pump. On the LFC, however, solenoids venting first to space and then to a pressure supply created the desired effect. Thus, the "harsh" vacuum environment of space worked for the LFC by providing a never-fail vacuum source.

Thus the pressurization system (see figure 1-20) was composed of a vessel to be pressurized, the LFC, supplied by the GSA, a regulation/conditioning GPCA, plumbing, electrical power, and signal cabling.

The GSA provides the LFC with GN_2 during the mission to maintain the LFC internal operating pressure at 2 psig. This unit is composed of three high pressure spheres (see figure 1-1) joined to a central plenum conditioning unit which preheats and regulates the delivery pressure (30 psig). The unit also has a temperature and pressure transducer whose output is used for TM to the ground to allow calculation of leakage and consumption rates throughout the mission. The GSA is mounted in proximity to the LFC but remote to it.

The GSA was designed for a safe operating pressure of 3,000 psig and has been proof tested to a burst pressure of approximately 8,000 psig. For the first sortie mission of 8 to 10 days, the unit was pressurized to 2,600 psig prior to launch. In terms of weight, this is equivalent to 4.91 kg (10.8 lb) of GN_2. Actual GN_2 consumption data results from the STS 41-G mission are summarized in table 1-4. This computes to a launch pad (at sea level and 21° C) leakage rate of 3 g (0.006 lb) per hour and a combined gas consumption and leakage rate (at altitude, and essentially 0° C) of 0.2 g (0.0004 lb) per frame.

TABLE 1-4.- GAS CONSUMPTION DATA FOR LFC/GSA, STS 41-G

Date	Operation	Pressure (psig)	Gas Weight	
			kg	lb
09/27/84	GSA load at launch pad	2,600	4.912	10.83
	Leakage for 8 days	-	0.558	1.23
	Leakage rate per hr	-	0.003	0.006
10/05/84	TM first frame	2,304	4.344	9.60
10/13/84	TM final frame	2,059	3.900	8.60
	consumption/frame	-	0.0002	0.0004
10/23/84	GSA demate	2,000	3.778	8.33

The GSA delivers GN_2 to the GPCA, which is mounted on the LFC camera support structure. The supply pressure is 30 psig, and the GPCA regulates the LFC internal gas pressure to 1.8 psig during periods of "standby" and 2.0 psig

during periods of "operation." During those periods preceding each film transport cycle, a film "blow-off" pressure of 4.0 psig through a needle valve for 4 sec is provided. A plenum within the GPCA is used to thermally condition the gas to 21° C prior to its entry into LFC.

During ascent and descent and with power off, the GPCA has a network of relief valves to relieve a pressure differential - across the LFC vessel to outside - of greater than 3 psi at a rate of change of 11 psi/min. At lift-off from the pad through ascending flight, the overpressure relief valve vents gas overboard until the LFC internal pressure reaches 1.8 psig. Once on orbit, this pressure is maintained through resupply of gas from the GSA. At completion of the mission and throughout the deorbit, descent, and landing phases, the underpressure relief valve opens and allows ambient air to enter the LFC in order to maintain an internal pressure of 2 psig.

The LFC vacuum film platen contains a gas plenum on its back side. Holes drilled through the platen connect the plenum to a raceway grid on the platen front surface. This grid is somewhat less than the film web width and frame length. During operation, the LFC vessel pressure is maintained at 2 psig through bidirectional flow of GN_2 into and out of the platen plenum through two solenoid-controlled valves which govern the direction in which the gas flows.

Upon receipt of a command to initiate an exposure sequence, the venting solenoid opens and provides a direct path from the platen plenum to the LFC's external environment (in orbit, this is essentially 0 psig, and in the laboratory this is whatever the ambient atmospheric pressure might be). As the plenum drops in pressure, this causes a sudden rush of gas into the raceways and holes, pulling the film base into intimate contact with the front side of the platen, "clamping" it in place.

Shortly after completion of the exposure event, the vent solenoid closes and the gas supply solenoid opens, allowing an inrush of gas into the platen plenum at 4 psig. With the LFC internal volume at 2 psig, the incoming gas vents through the platen; "blows" - or strips - the film from the platen; and

closes 4 sec later. When this sequence is completed, the film transport actuates and meters 48.25 cm (19 in.) of fresh film into the platen area in anticipation of the next exposure event.

1.5 THERMAL STABILIZATION

The two extremes of the Orbiter cargo bay orbital thermal models, the hot case and the cold case, were used to determine the means and the optimum temperature at which to control and stabilize the optical assemblies. Paramount to determination of this thermal "set point" for stabilizing these masses were the following considerations:

- Survivability of the photographic emulsion(s), both mechanical and base fog, over a relatively long period of exposure (45 days prelaunch, 10 to 15 days on-orbit, and 30 days postlaunch).
- Optics stability. With temperature changes, a lens grows or shrinks, resulting in a change in both the effective focal length and the geometric characteristics.
- Limited electrical power for heat generation.

After the OCPS thermal models were created and played against the STS mission thermal models, a thermal set point of 21° ± 1° C (69.8° ± 1.8° F) was established as being slightly warmer than the projected LFC internal temperature after exposure to direct sunlight for a duration of 1 hr. Since the LFC and SCA employ active heating and passive cooling techniques (i.e., heating with electrical heaters and cooling by radiating heat to the environment), minimum power would be required during periods of standby or nonoperations, assuming the setpoint is slightly higher than the anticipated worst case. To avoid introduction of unnecessary heat, 95 percent of the LFC and SCA electronics were mounted at remote locations.

Thermal stability of the lens assemblies and focal planes is extremely critical in maintaining an exact plane of focus and preserving the calibrated lens distortion characteristics. Should the temperature of any part or all of the glass and metal of the optical assembly increase or decrease from its

desired thermal set point, a change in the focal length of the lens would result in a shift from critical image focus to varying degrees of defocus. Similarly, distortion characteristics of the lens internal geometry would change significantly.

During an actual mission, or during certain system checkout and optical testing in the laboratory, the OCPS component systems are stabilized at their thermal set points. To accomplish this, passive cooling (thermal dumping) and active heating techniques are employed.

The scheme for controlling and stabilizing the temperature of the LFC, SCA, SCA support structure, and other peripherals requires a total of 52 strip heaters and 19 temperature controllers to maintain thermal balance in the 19 thermal zones of the system. Capacities of these heater strips range from 1.1 to 55 W, delivering a total of 354 W. An additional 18 W of power is required for circuit control logic and monitor of zone thermistors for downlist TM.

As noted in table 1-5, the LFC has a total of nine thermal zones located throughout the camera, magazine, and camera electronics assembly. These control 24 strip heaters delivering up to 191.8 W during periods of maximum heating demand. The ARS and its SCA, SCA support structure, and electronics assembly have 26 strip heaters and 8 thermal zone controllers, producing up to 88 W of active heating. Similarly, the Gas System has two thermal zone controllers (one each for the GSA and the GPCA) which have a total output of 74 W. Each controller controls one heater; these heaters are used to precondition the gas prior to delivery to the LFC internal volume.

Once on orbit, the OCPS is placed into the standby (heater) mode for the remainder of the mission. Depending on the thermal stress (cold) at each zone following launch, as much as 372 W and as little as 18 W of power could be required at this initial power up. Assuming the highest demand rate, as each zone is brought under control, the heaters will begin to cycle on and off until a thermal equilibrium is reached. From this point on, and for the

remainder of the mission, power consumption for thermal control will remain very low (e.g., 18 W plus short-duration maintenance surges).

TABLE 1-5.- HEATER/HEATER CONTROLLER POWER SUMMARY

System component	Heater controllers	Total heaters	Total power, W	Set point, °C
LFC	(9)	(24)	(191.80)	
• Lens assembly	6	16	144.5	21
• Film magazine	1	6	7.3	21
• Electronics assembly	2	2	40	-15
ARS	(8)	(26)	(88.22)	
• SCA (lenses/body)	4	10	32.62	21
• SCA support structure	2	14	15.6	21
• Electronics assembly	2	2	40	-15
Gas System	(2)	(2)	(74.00)	
• GSA	1	1	55	21
• GPCA	1	1	19	21
Subtotal	19	52	354.02	
Control electronics	-	-	18	
Total	19	52	372.02	

1.6 DATA ACQUISITION

The acquisition of photography by the LFC in orbit is not unlike the acquisition by its air-breathing counterpart being flown on a mapping flight line in an aircraft. Unlike the aircraft, however, the Orbiter has to fly upside down in order to let the LFC (and the cargo bay) look at the earth. True, the forward velocities are much greater in the Orbiter than in, say, a Lear jet - by more than 2 orders of magnitude, in fact (e.g., 215,000 km/hr, or 116,000 kn, as opposed to 741 km/hr or 400 kn, respectively).

Also, one often sees a skew offset in photographic frame overlap (O/L) which is due to either drift or crab in aircraft photography. In orbital mapping flight lines one will see target offset from one frame to the next and confuse this with the aircraft drift or crab. This is due to the fact that

while the Orbiter flies a straight (though circular) flight line, the earth is rotating beneath it (see figure 1-21). This offset is variable, depending on latitude, such that with a 10-sec interval between exposures the offset will be 2.99 km at 50° latitude and up to 4.65 km at the equator. This is not a new awakening, and those who have used uncorrected Landsat imagery will remember seeing the skewed or rhomboid shape of those images, which is typical of line scanners.

The LFC has four acquisition modes in operational sequences, and these produce frame-to-frame O/L's of 10, 60, 70, or 80 percent in the forward direction. Figure 1-22 illustrates the sequence of acquisition in the 80-percent forward O/L mode, and figure 1-23 demonstrates how the frames create a gross stereo model area so useful to the photogeologist, the interpreter, and the cartographer. One might question why the 10-, 70-, or 80-percent forward O/L modes are even provided when the 50- to 60-percent range is normal to aircraft acquisition. There is a great advantage in orbital stereoscopy (as with aircraft) to have the greatest parallax possible in order to increase the accuracy of the data reduction product. This is accomplished by increasing the air base, or distance (B) between photos or by a lower percentage of overlap. However, when a large variation in terrain slopes exists within a single stereo model area, it is a great advantage to have the same general localized areas available in more than two frames of imagery.

Realize that the LFC has an extremely wide FOV, such that the area covered by a single frame at any given altitude, or height, (H) is 1.5 x H along the velocity vector (flight path or along track) and 0.75 x H across the velocity vector (across track). In the case of a typical altitude of 250 km, the area covered is 375 km by 187.5 km, or 70,300 sq km. Within an area this vast one might expect to see large sized areas with slopes as little as a few degrees (plains, deserts, savannahs, plateaus, etc.) or as steep as 50° to 60° or more (mountains, valleys, gorges, etc.).

The lower the relief (flatness), the greater the base-to-height (B/H) ratio required to discern the subtle changes in elevation. In those areas of great terrain relief (steepness), only a relatively low B/H ratio is required in

the imagery. In high B/H ratio imagery of great elevation changes, it is possible to see side A of Z-big mountain and not side B in one frame and then not see side A but see side B of the same Z-big mountain in an adjoining frame. Viewed stereoscopically, the Z-big mountain's upper elevations appear to float above the local terrain of lesser slopes. The heart of the matter is that it is necessary to cause greater vertical exaggeration (VE) in low terrain features (figure 1-24) to make them appear with greater relief in order to detect (and measure) their subtleties. Those of greater terrain differentials require less VE.

In the case of orbital applications of the LFC, operating the unit in the 80-percent forward O/L mode (see table 1-6) gives the user 100-percent coverage of the groundtrack with B/H ratios of 0.3, 0.6, 0.9, and 1.2 with VE factors of 1.4, 2.8, 4.2, and 5.5. Though this would consume film at a more rapid pace, the versatility of such data is immense. For the other O/L modes, table 1-6 presents similar values derived from their application. It should be noted that the 10-percent O/L mode has been provided where stereoscopy is not required and contiguous coverage of the ground track is sufficient (e.g., ocean surfaces, cloud cover sampling, surveying for terrain, crop, land use, and cultural changes).

Determination of the time interval between individual exposures is computed by the LFC electronics based on ground calculated values for the velocity to height (V/H) ratio from the current flight vector projections. This value and the command for desired mode for forward O/L is uplinked from the mission control center (MCC) at JSC to the spacecraft, which in turn routes it to the LFC electronics. Upon receipt, the LFC electronics computes and sets the required time interval. This same uplinked V/H value is processed by the LFC electronics to compute and set the FMC for the data pass. One should realize that the command string for any data pass or group of data passes is built several minutes to several hours prior to the actual pass accomplishment, and the fewer calculations to be made at the ground station the better. (See section 3.1.2 for detailed command generation descriptions.)

TABLE 1-6.- THE RELATIONSHIP OF FORWARD O/L OF SUCCESSIVE LFC FRAMES TO B/H RATIO AND VE FACTORS AS AN ADJUNCT TO TERRAIN DATA EXTRACTION AND ANALYSIS

Parameters				Gross stereo model area				Groundtrack covered, %
				Model area factor, times H		250 km (135 n. mi.) altitude (H)[a]		
Fwd. O/L mode, %	Fwd. unit access, %	B/H ratio	VE factor	Length	Width	n. mi.^{2}	km^2	
80	80	0.30	1.38	1.20	0.75	16,402	56,250	100
	60	0.60	2.77	0.90	0.75	12,302	42,188	100
	40	0.90	4.15	0.60	0.75	8,201	28,125	100
	20	1.20	5.54	0.30	0.75	4,101	14,062	100
70	70	0.45	2.08	1.05	0.75	14,352	49,219	100
	40	0.90	4.15	0.60	0.75	8,201	28,125	100
	10	1.35	6.23	0.15	0.75	2,050	7,031	33.3
60	60	0.60	2.77	0.90	0.75	12,302	42,188	100
	20	1.20	5.54	0.30	0.75	4,101	14,062	50
10	10	1.35	6.23	0.15	0.75	2,050	7,031	20

[a] Typical STS orbital altitude.

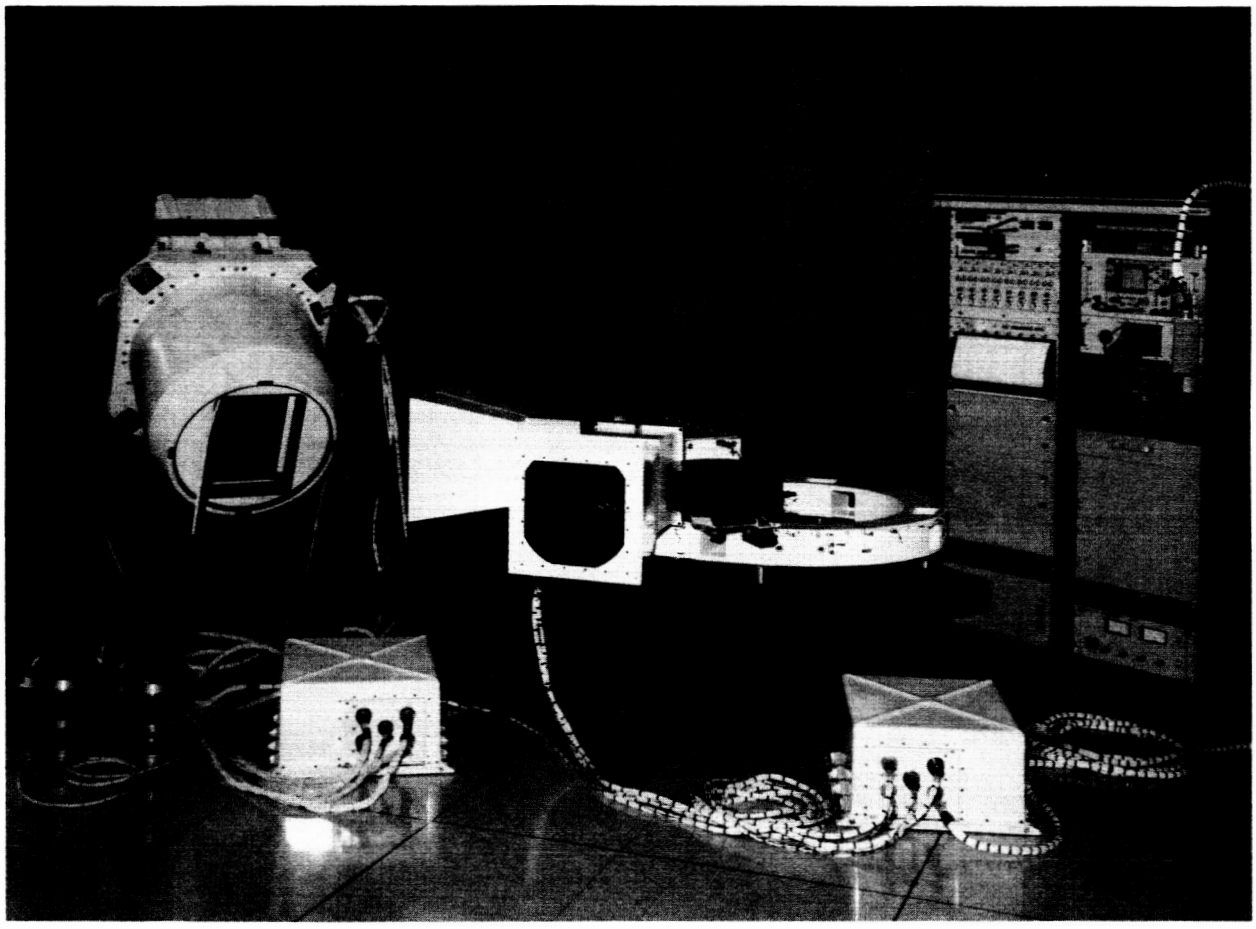
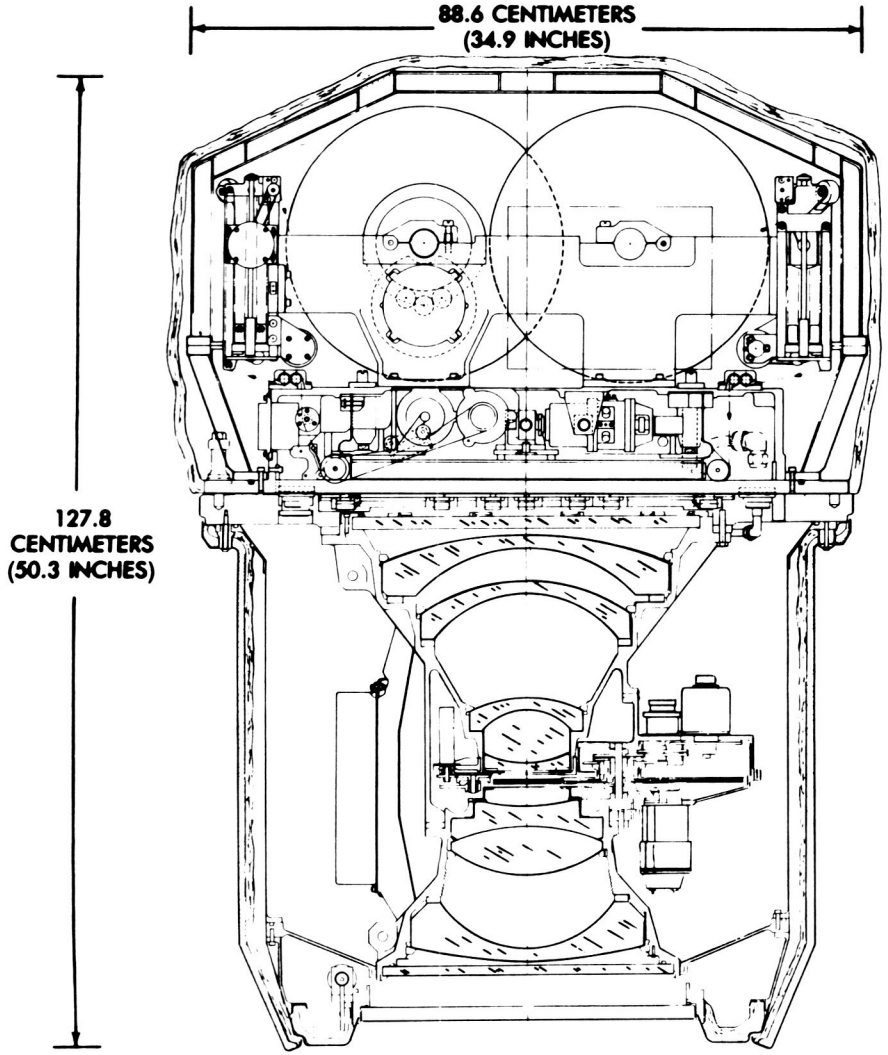


Figure 1-1.- The OCPS, showing the components. From left to right: GSA; LFC; LFC electronics assembly; SCA, shown mounted to the SCA support structure (ring); ARS electronics assembly; and the electrical test and checkout console (NASA photo S83-41587).



OCPS LARGE FORMAT CAMERA

FILM CAPACITY = 1220 METERS (4000 FEET) - 2500 FRAMES

WEIGHT:		
	LENS CONE ASSY.	284.1 Kgs.
	FILM MAGAZINE ASSY.	91.2
	CAMERA ELECTRONICS ASSY.	31.1
		406.4 Kgs.
		(896 Lbs.)

NOTE: DIMENSIONS ARE HARDPOINTS.

STANDARD AERIAL SURVEY CAMERA

FILM CAPACITY = 150 METERS (500 FEET) - 600 FRAMES
TOTAL WEIGHT: 85.5 KILOGRAMS (188.5 POUNDS)

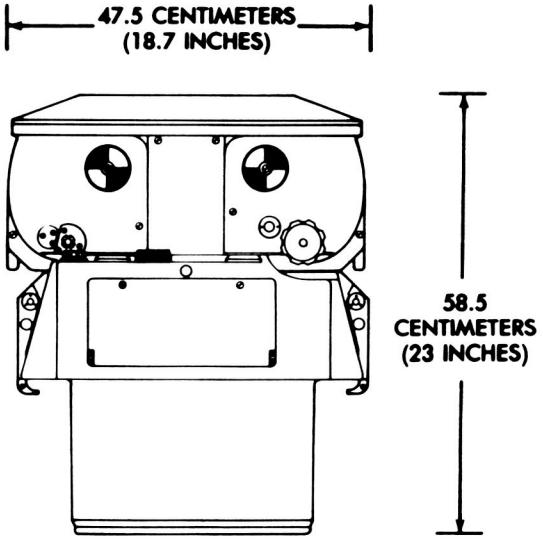


Figure 1-2.- The OCPS LFC, shown in a same-scale comparison to a standard aerial survey camera.

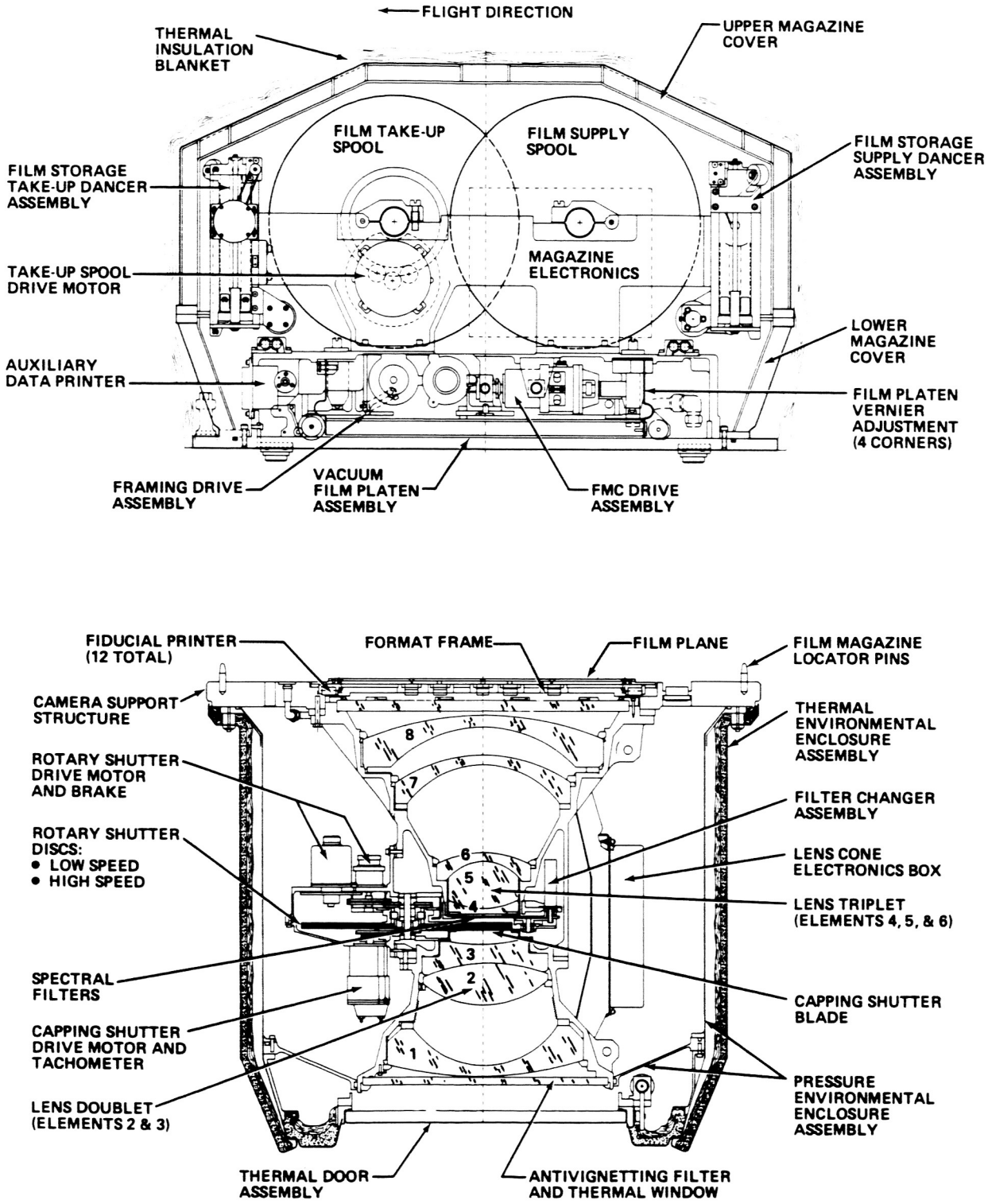


Figure 1-3.- The film magazine (upper) and the lens cone assembly (lower). When mated, these two components form an environmentally controlled pressure vessel.

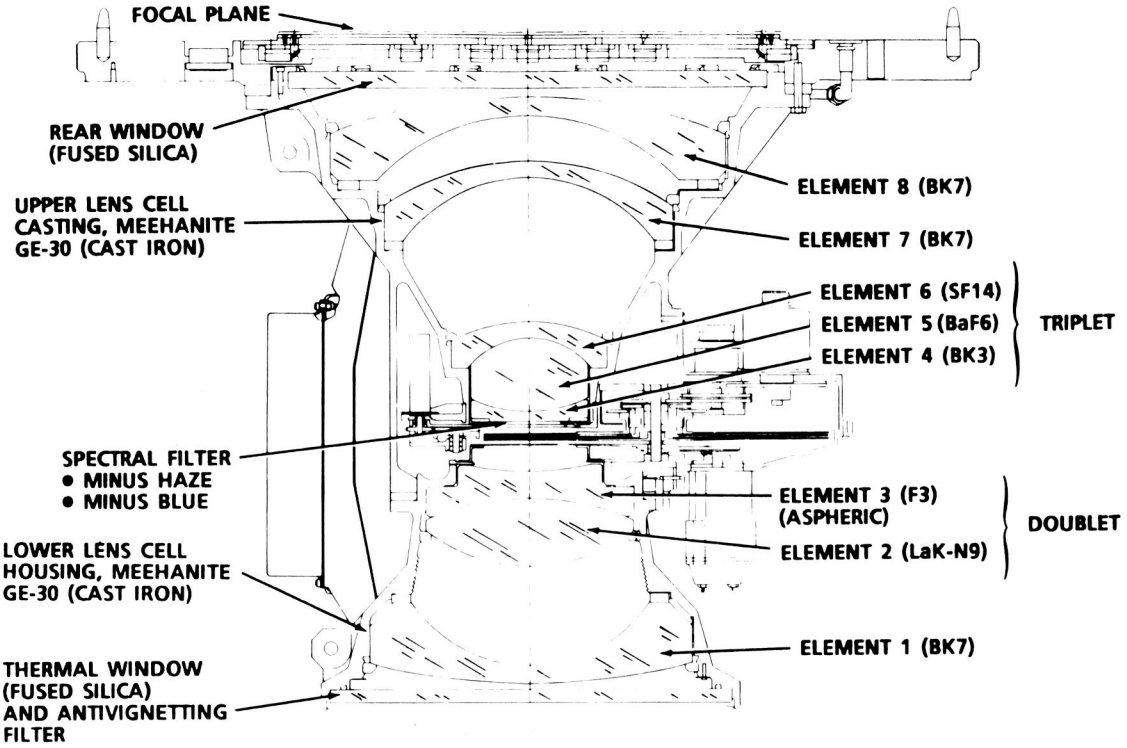


Figure 1-4.- Schematic of the LFC cartographic lens assembly. This schematic shows the types of glass used for manufacture of the individual lens elements.

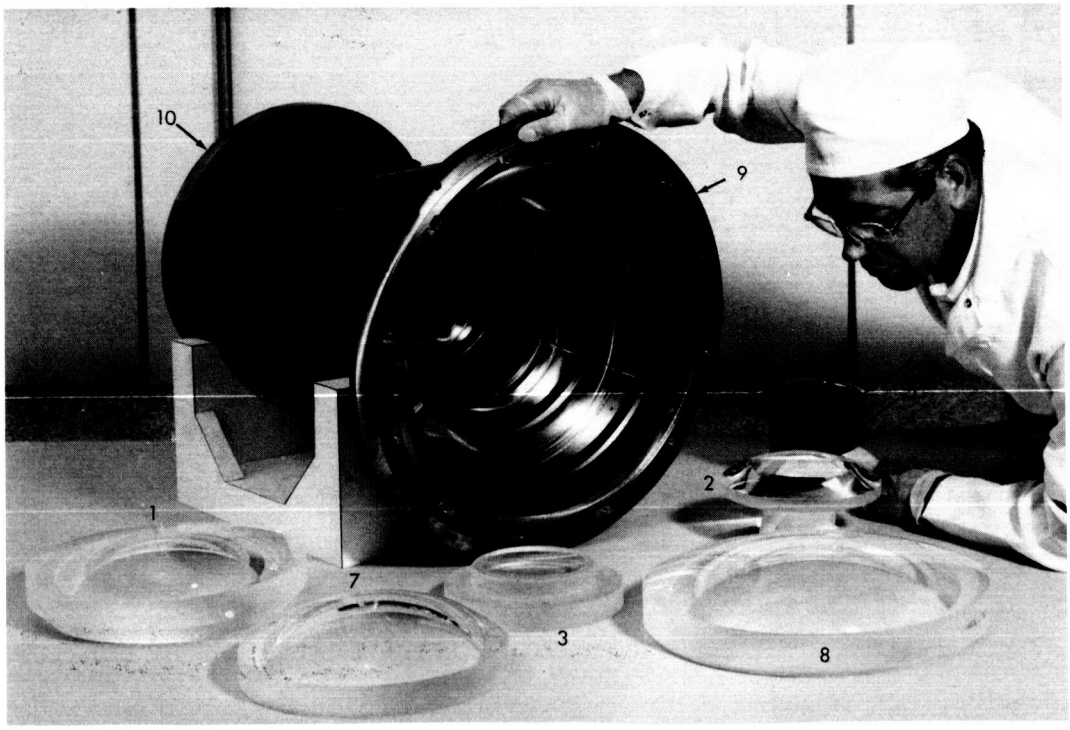


Figure 1-5.- Finished LFC lens components prior to assembly. Shown are the front lens (element 1), the doublet (elements 2 and 3), the triplet (elements 4, 5, and 6), the rear lens (element 8), and the machined lens cell castings (9 and 10). (NASA photo S79-35862.)



Figure 1-6.- The LFC thermal door assembly shown in the open (picture taking) position. Behind the interior surface of the open door is a strip heater which is used to maintain proper temperature of the forward lens elements (NASA photo S81-29612).

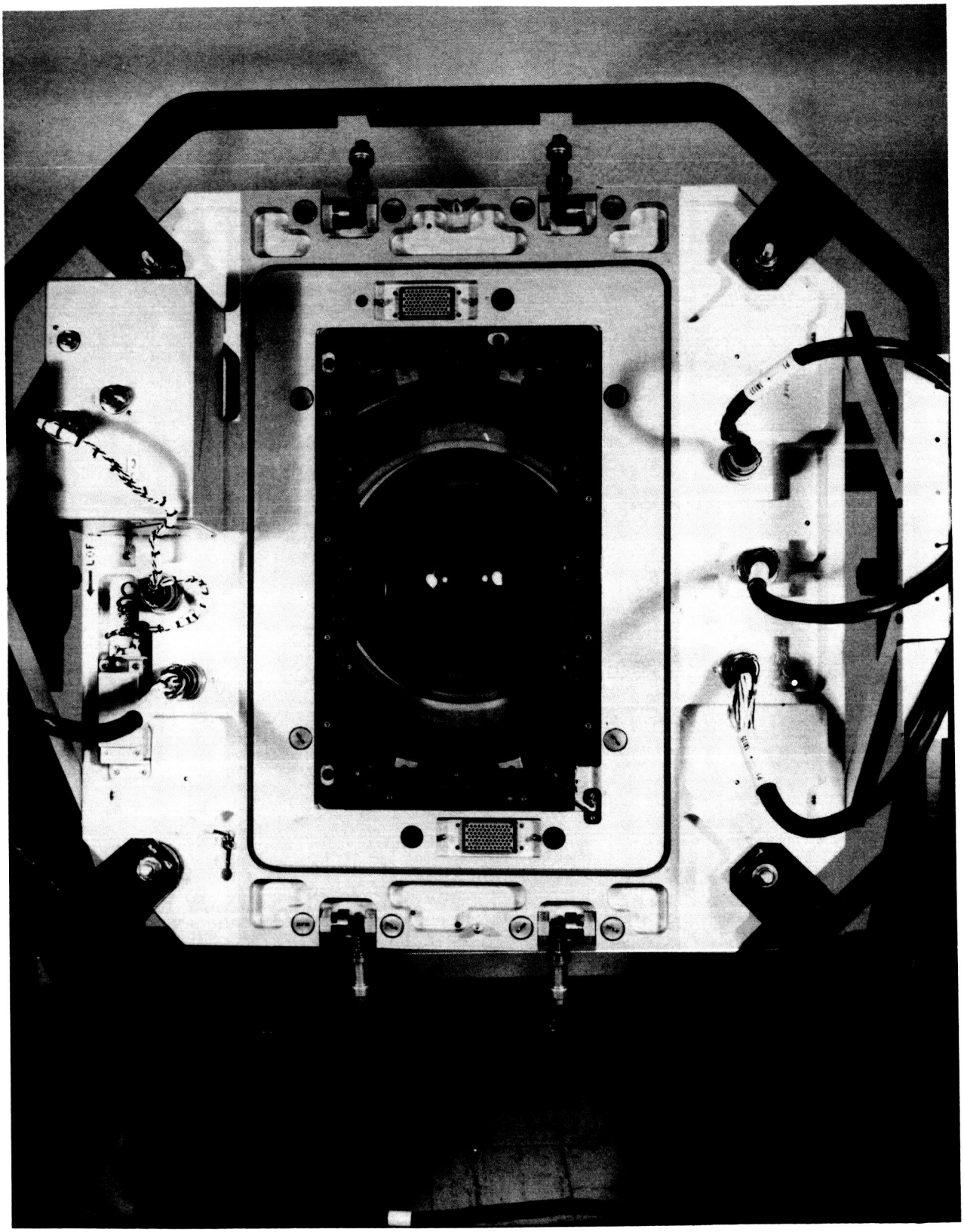


Figure 1-7.- The aft end of the LFC lens assembly. Shown are the format mask, the rear lens elements, the film magazine attach points, and the electrical connector interfaces (NASA photo S81-31664).

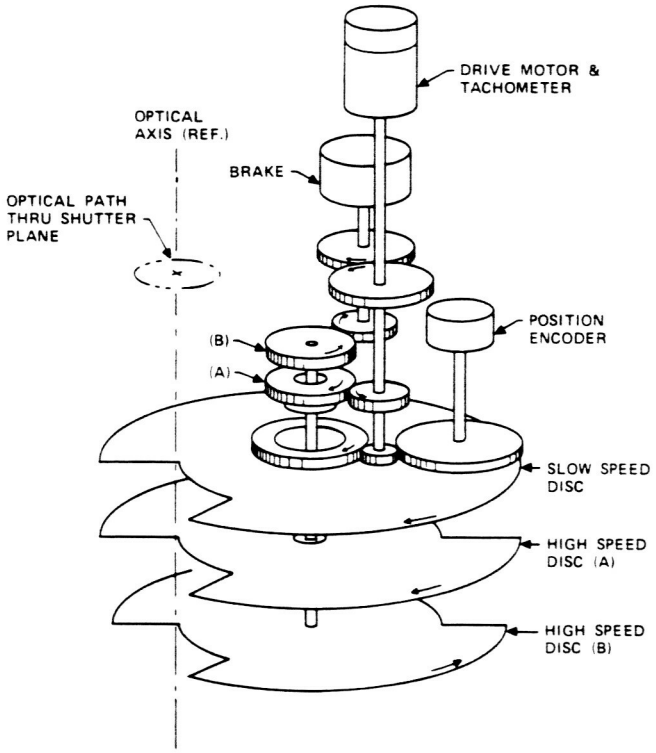


Figure 1-8.- Schematic layout for the LFC rotary shutter blades.

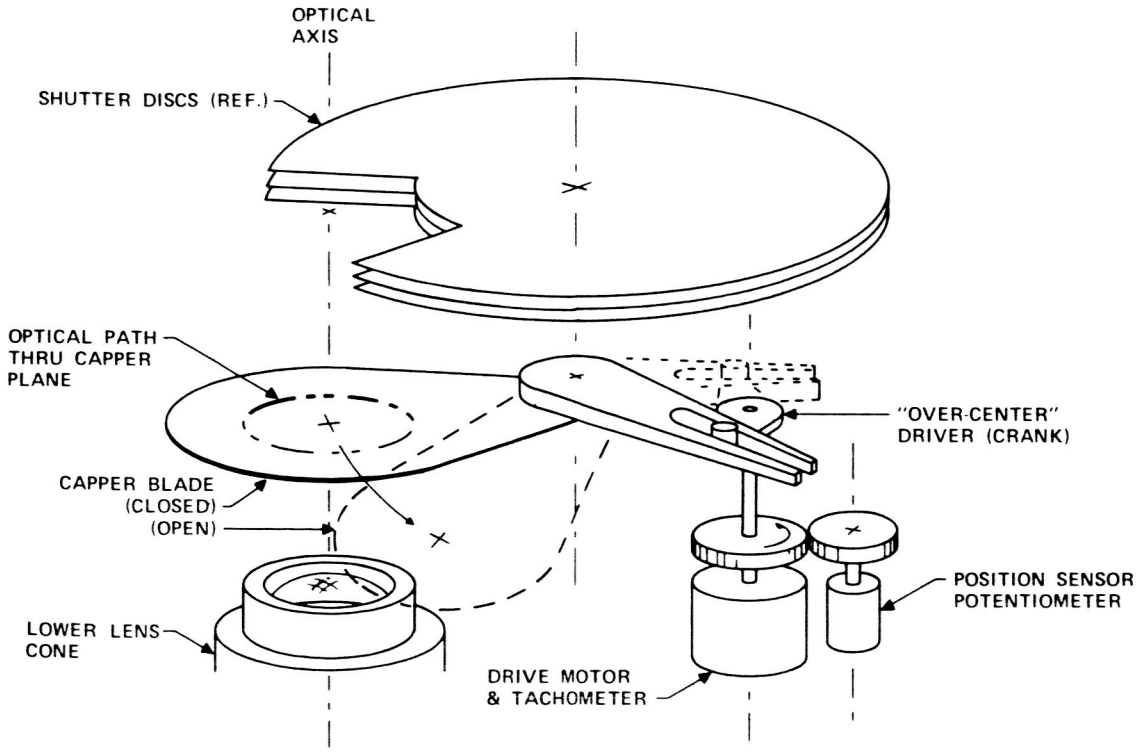
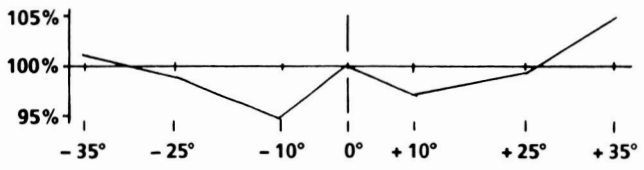


Figure 1-9.- Schematic presentation of the LFC capping shutter action.



Field angle	Wavelength		
	580 nm	650 nm	720 nm
– 35°	103%	100%	101%
– 25°	99	98	100
– 10°	94	93	94
0°	100	100	100
+ 10°	97	97	97
+ 25°	100	98	100
+ 35°	106	102	106

Figure 1-10.- Measured lens/antivignetting filter relative transmittance.

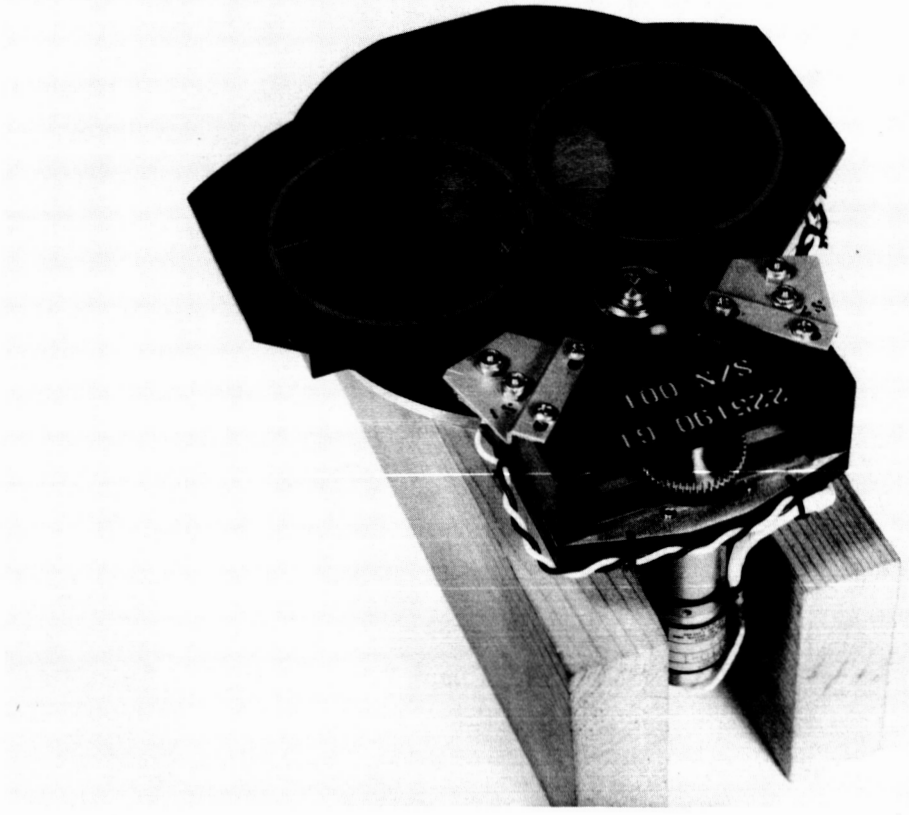


Figure 1-11.- The filter holder and drive mechanism. Shown stopped at a point halfway between the two select positions; view is prior to installation of the two spectral filters (NASA photo 80-26243).

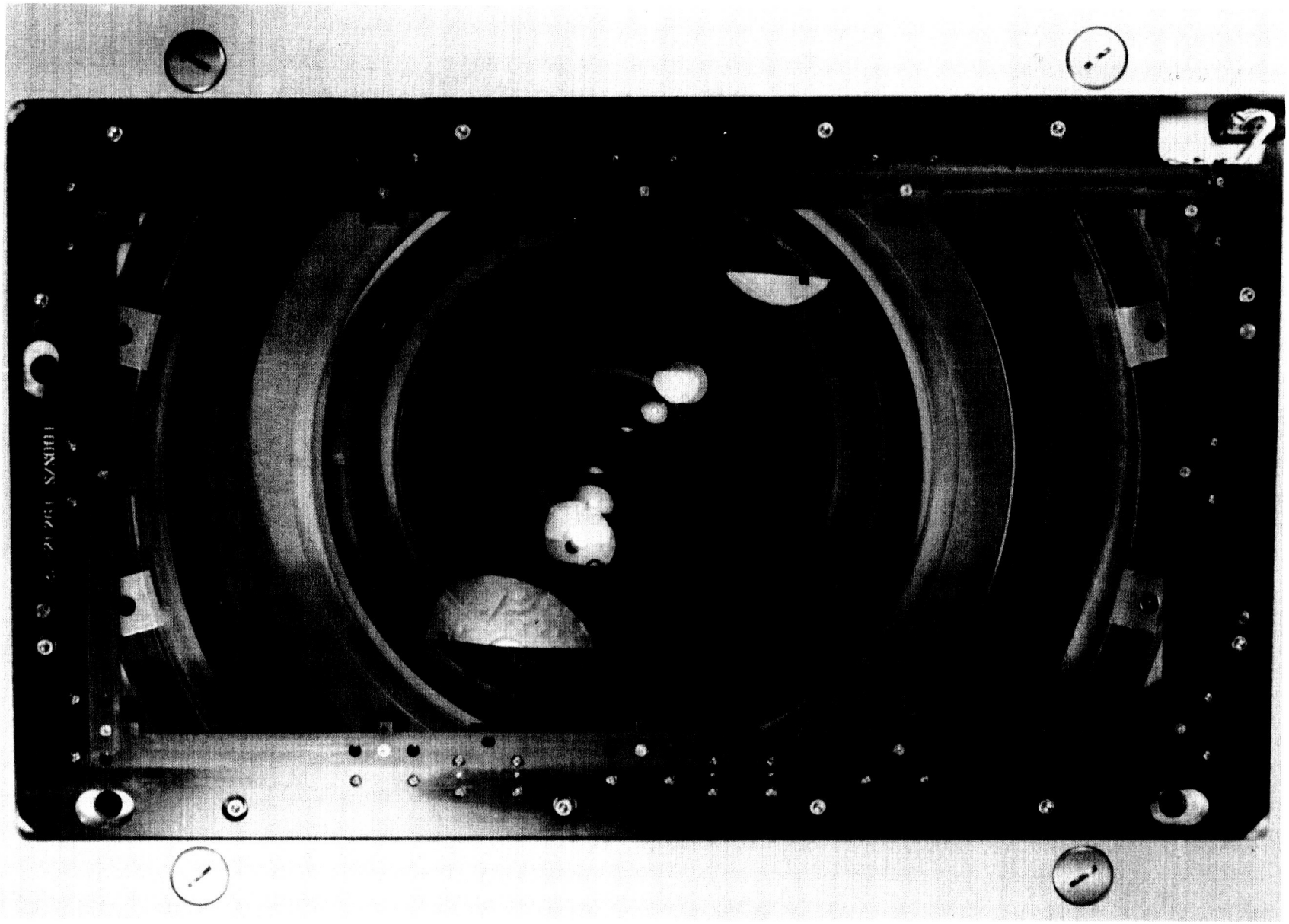


Figure 1-12.- The LFC focal frame. Shown attached to the camera support structure (NASA photo S81-31659).

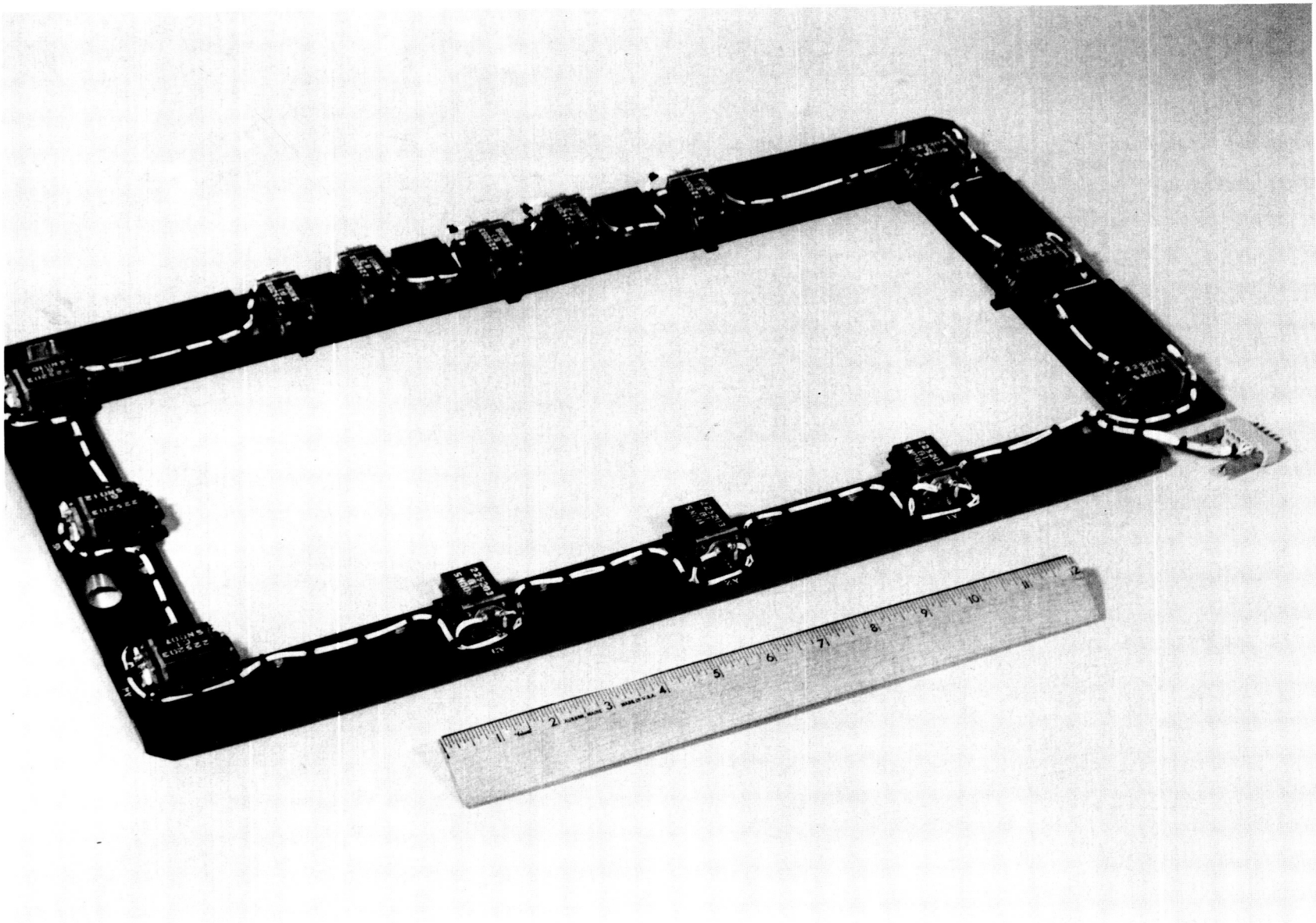


Figure 1-13.- The under side of the LFC focal frame prior to assembly. Shown are the 12 fiducial projectors (A), the 2 lens serial number projectors (B), and the film magazine serial number illuminations (C). (NASA photo S80-26270.)

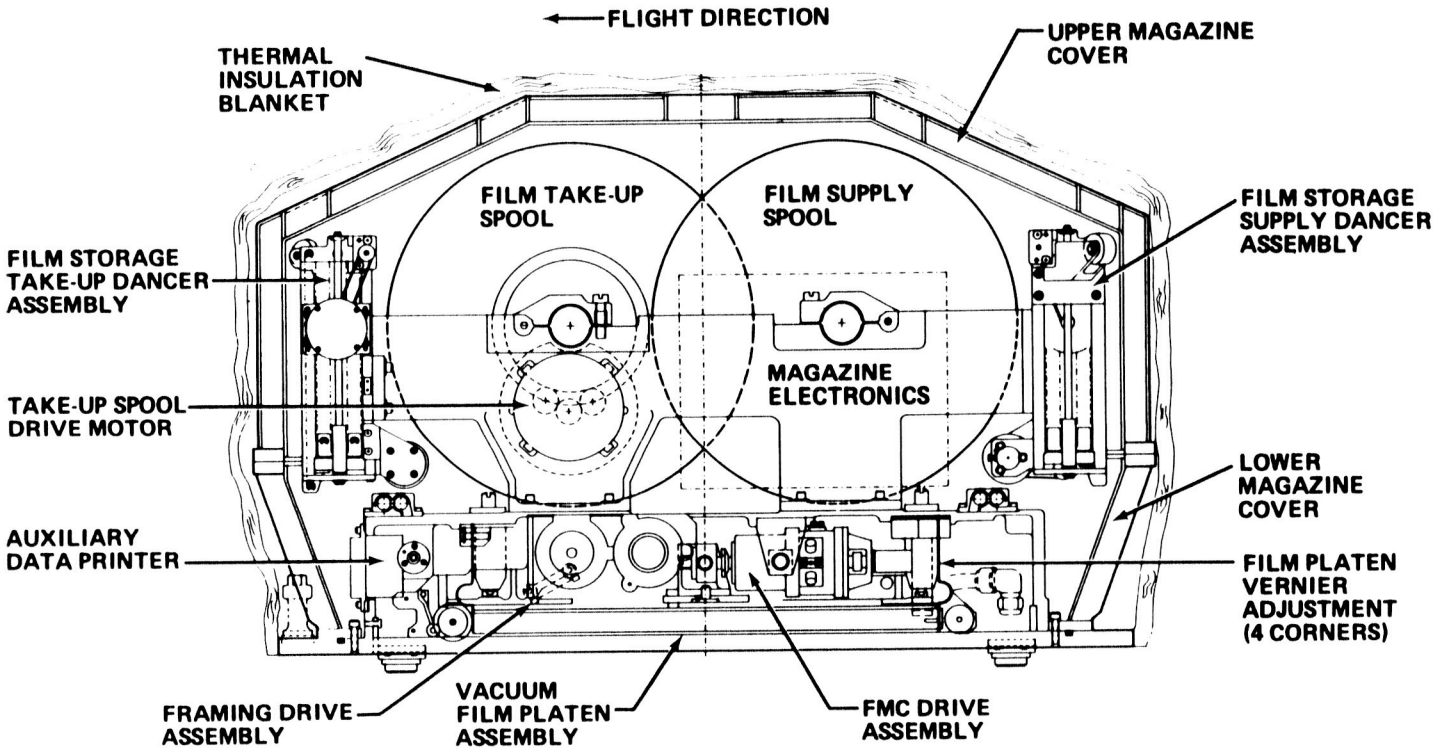


Figure 1-14.- Schematic of the LFC film magazine assembly. When it is mated to the lens cone assembly, the two assemblies form a pressure vessel which is pressurized to 2 psig from liftoff through landing.

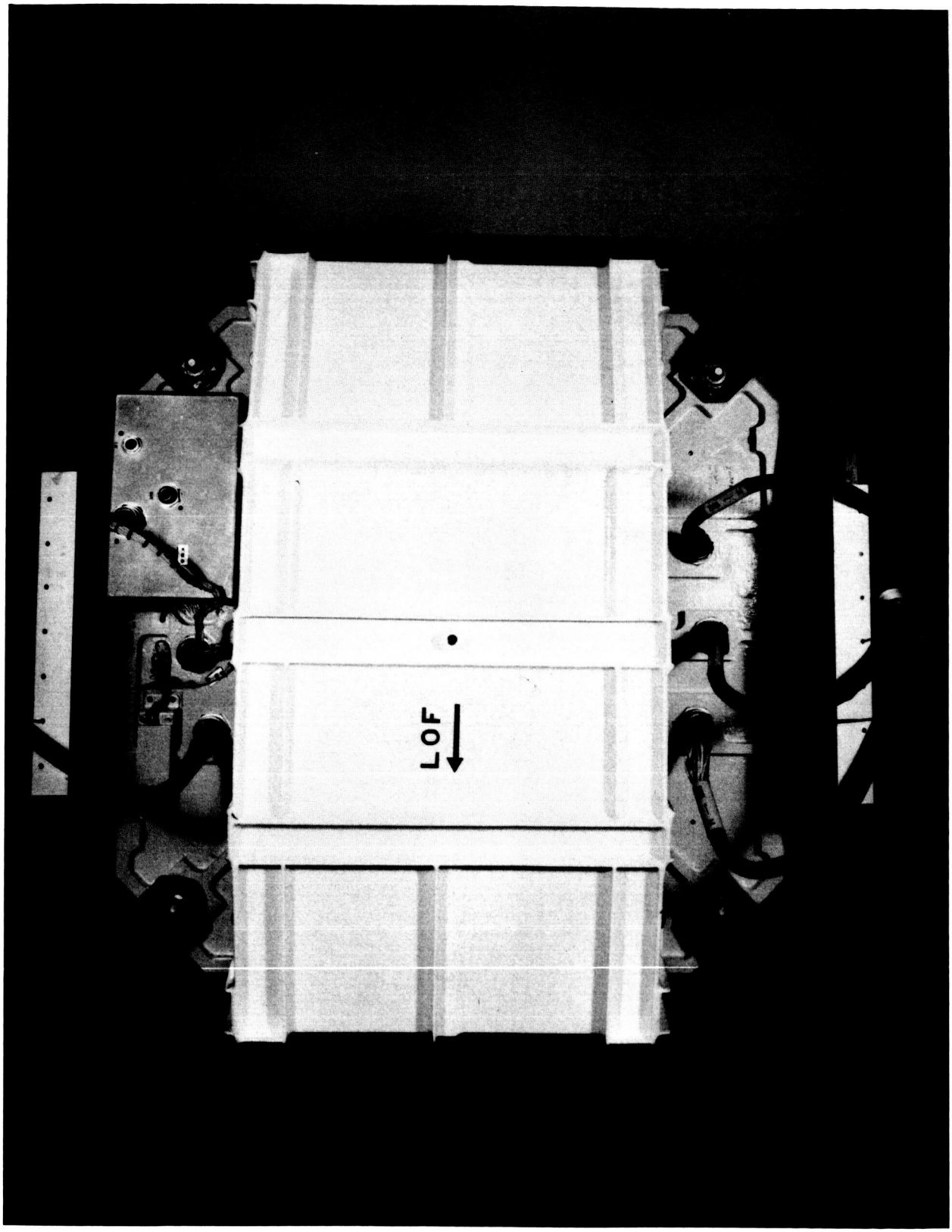


Figure 1-15.- The film magazine. Shown mounted to the camera support structure (NASA photo S81-31654). Compare this view with figure 1-7.

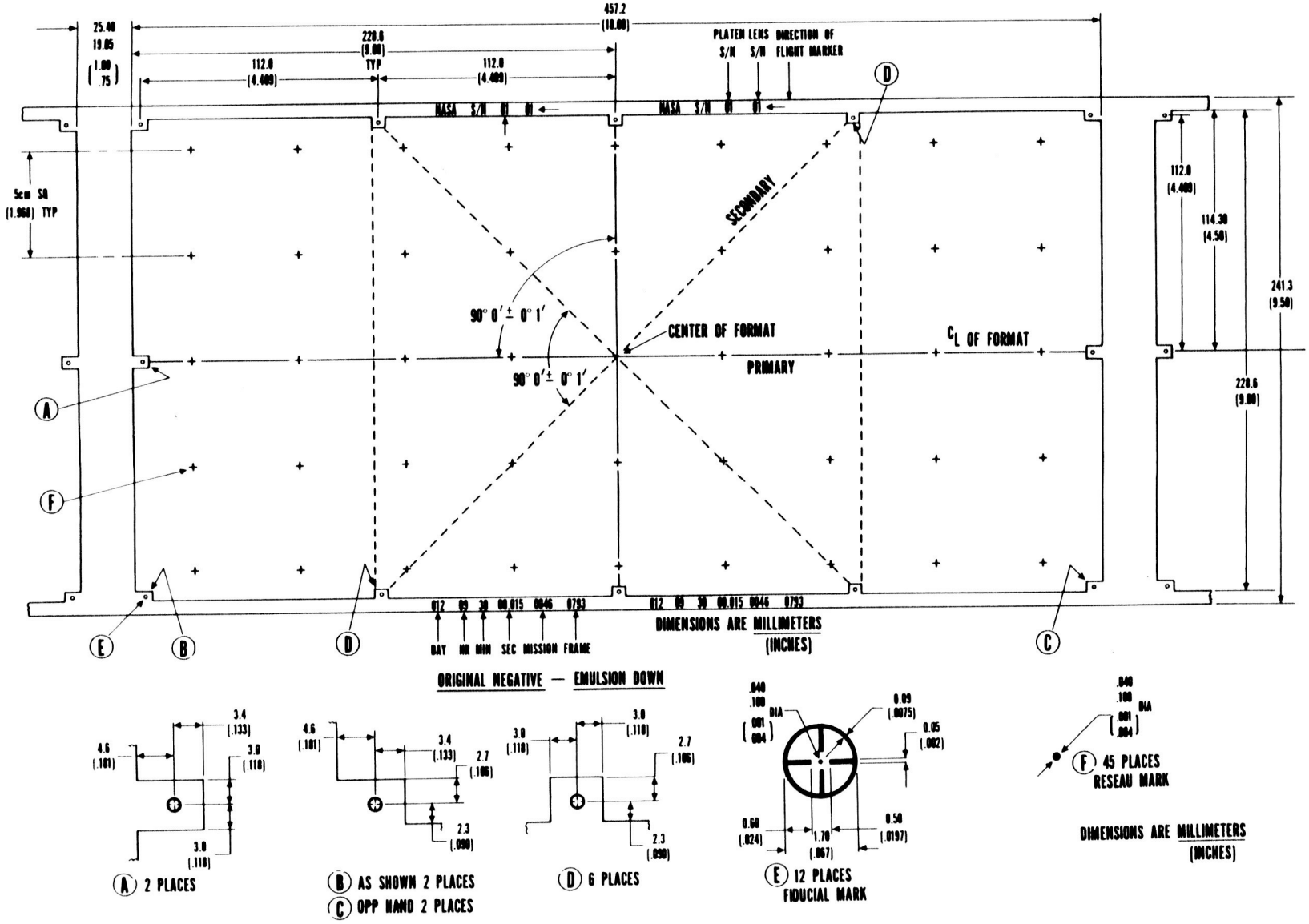


Figure 1-16.- The LFC focal plane and format mask layout with auxiliary data imprints.

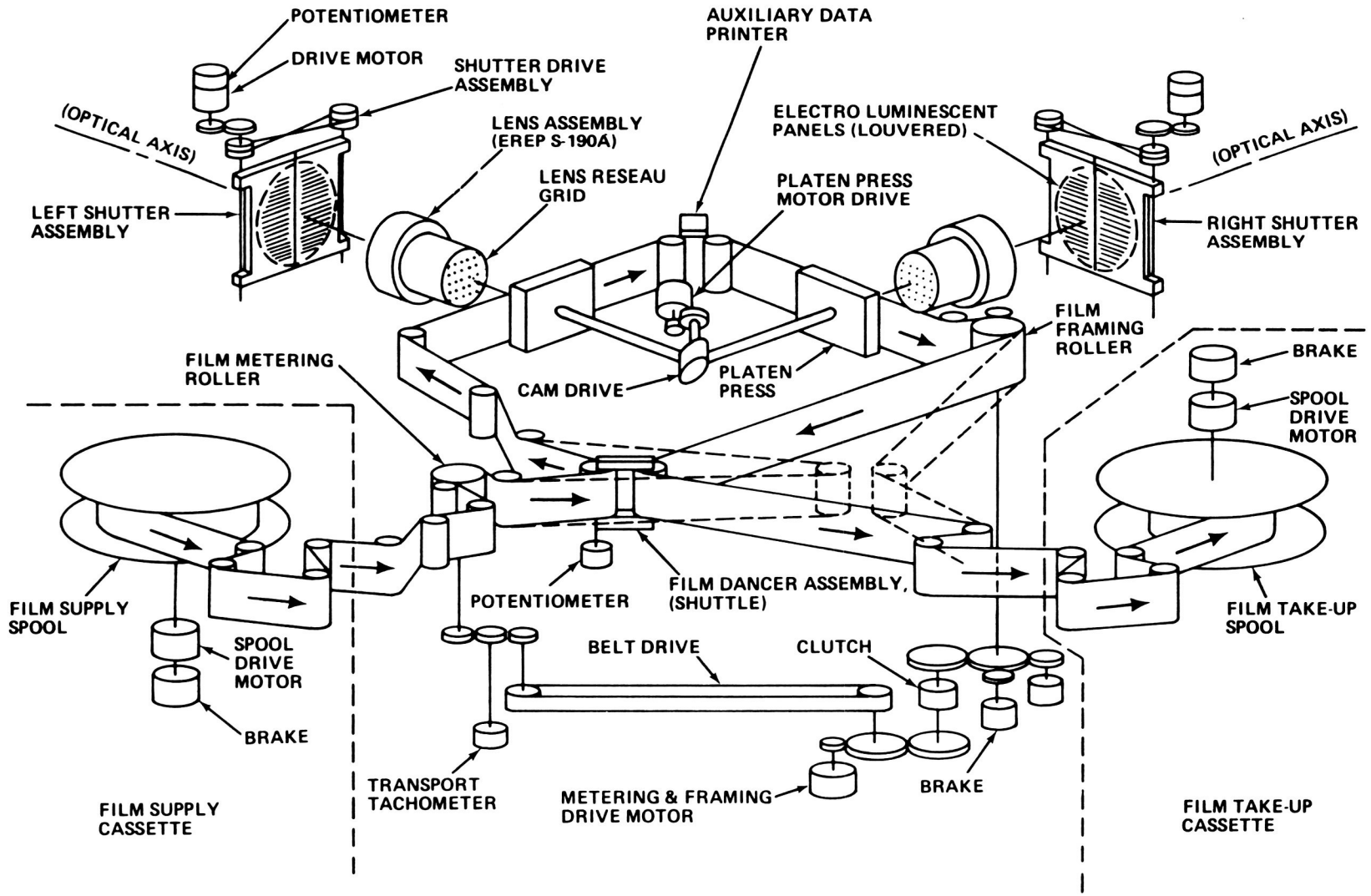


Figure 1-17.- SCA optical path and film transport schematic.

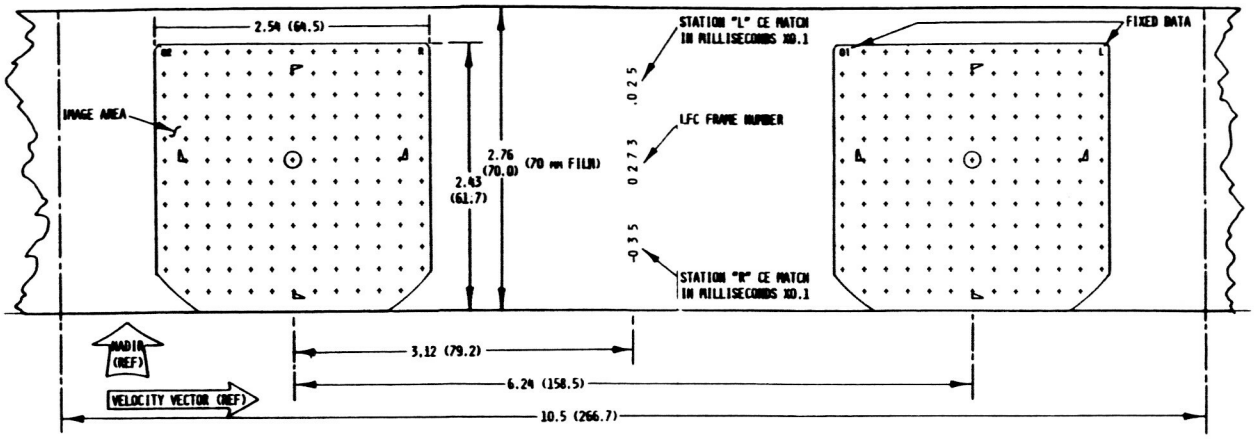


Figure 1-18.- Schematic of the placement of the SCA image pairs on the 70 mm film web.

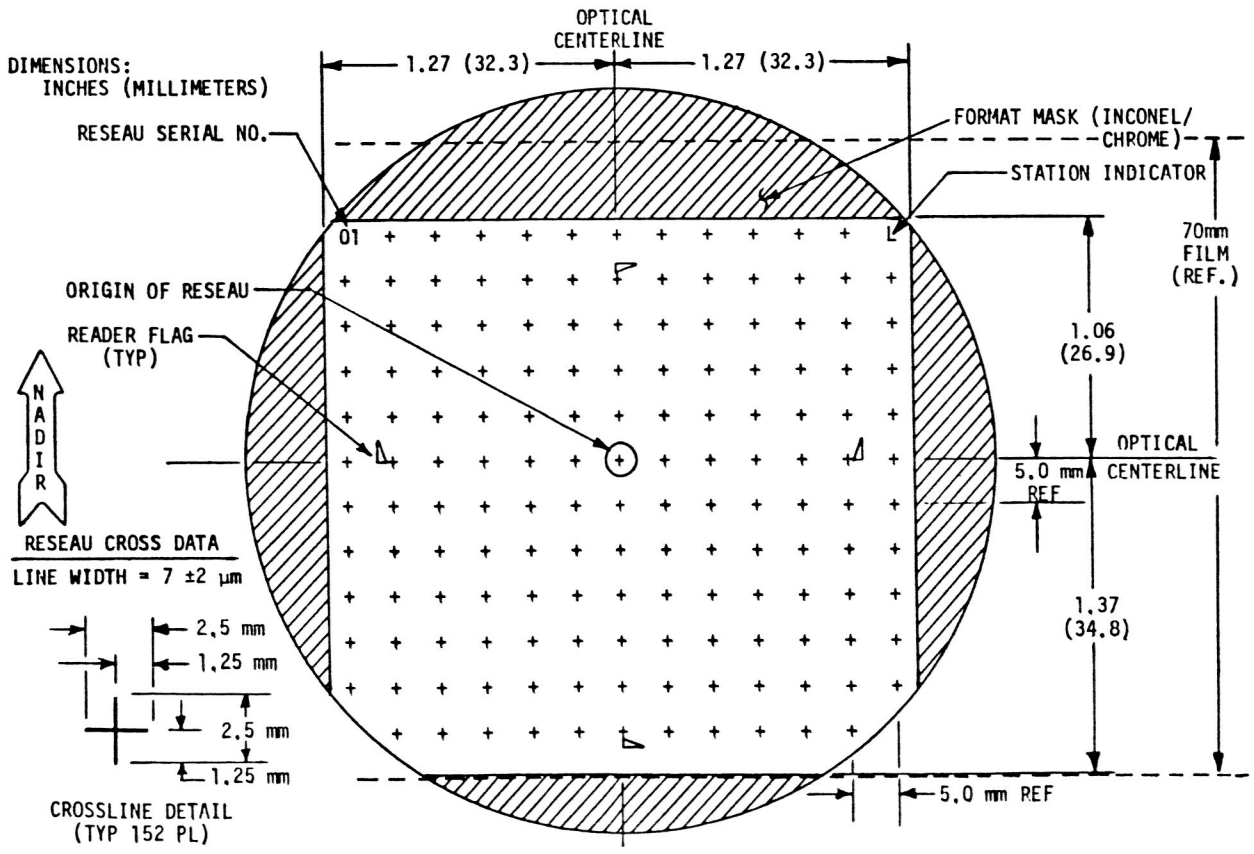


Figure 1-19.- The reseau plate mask for the SCA.

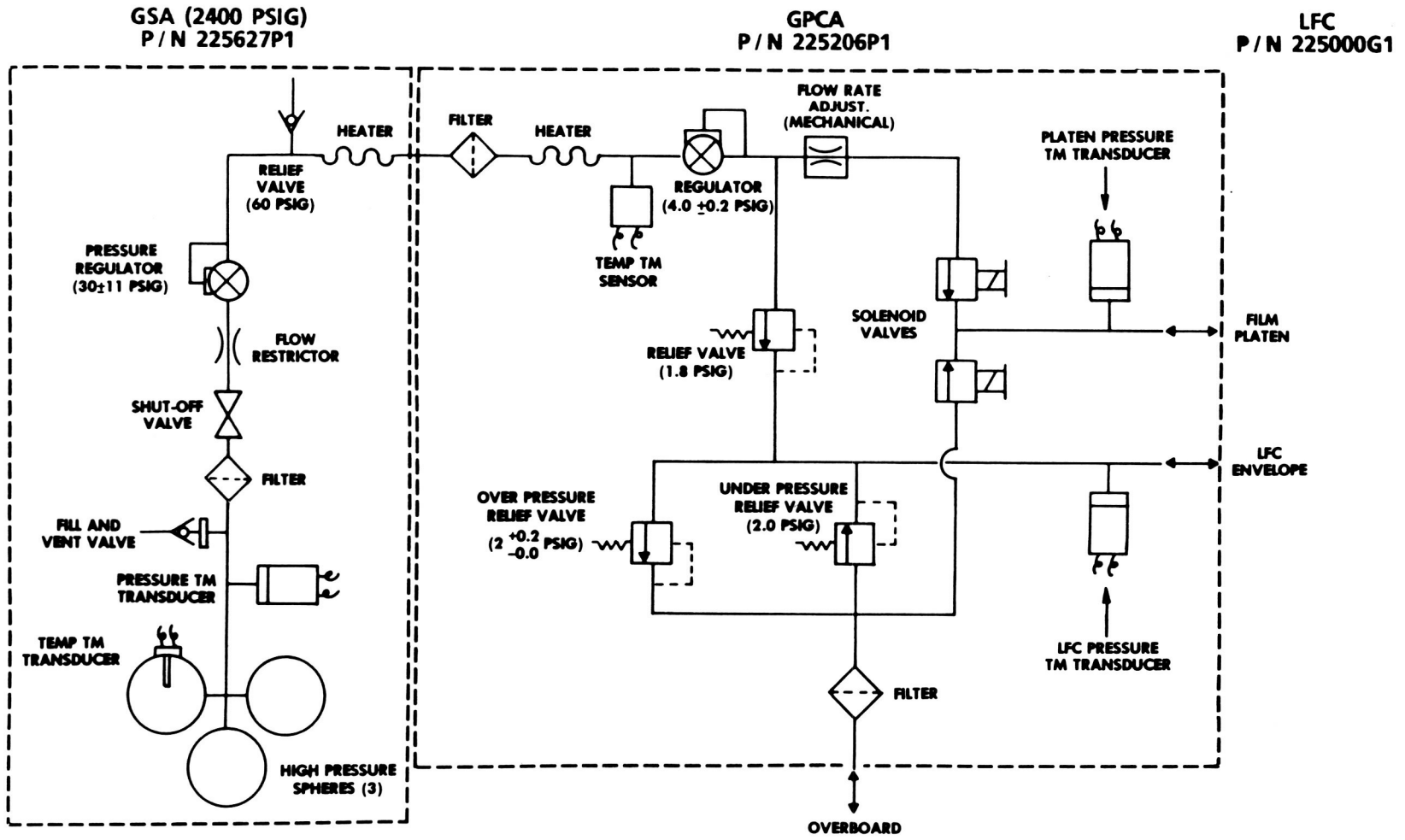
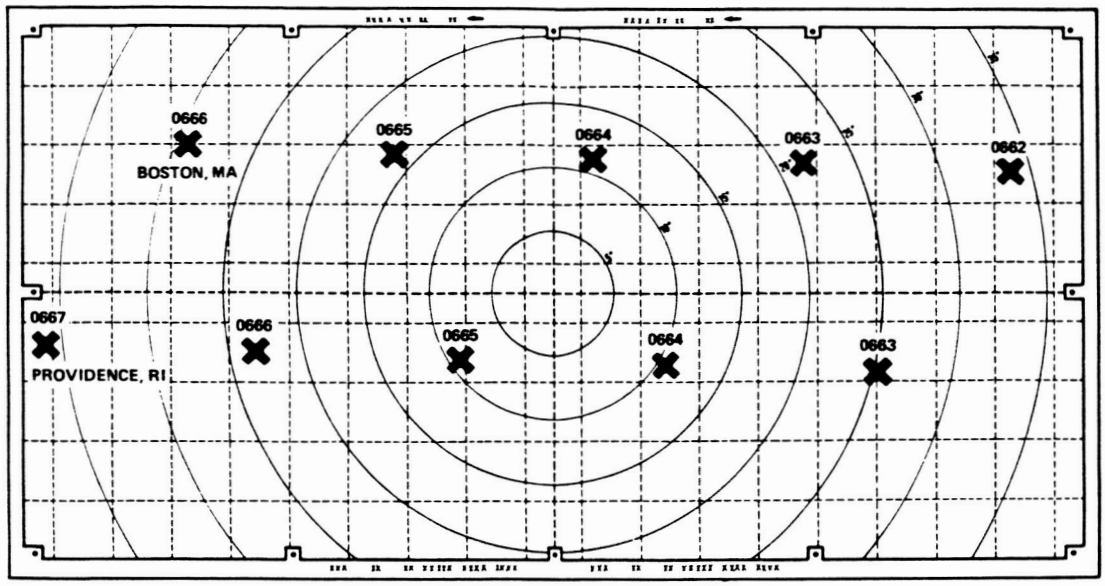


Figure 1-20.- Schematic of the OCPS pressurization system.



DISPLACEMENT OF THE TARGET POSITION IN SUCCESSIVE FRAMES DUE TO EARTH ROTATION.

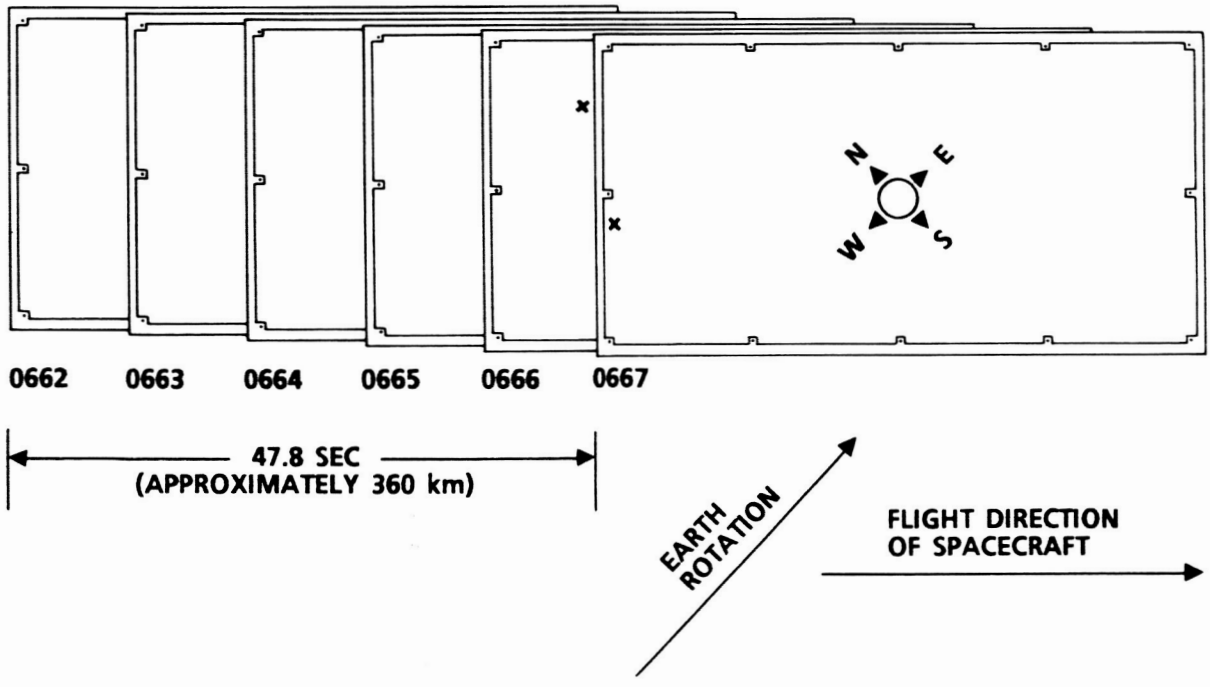
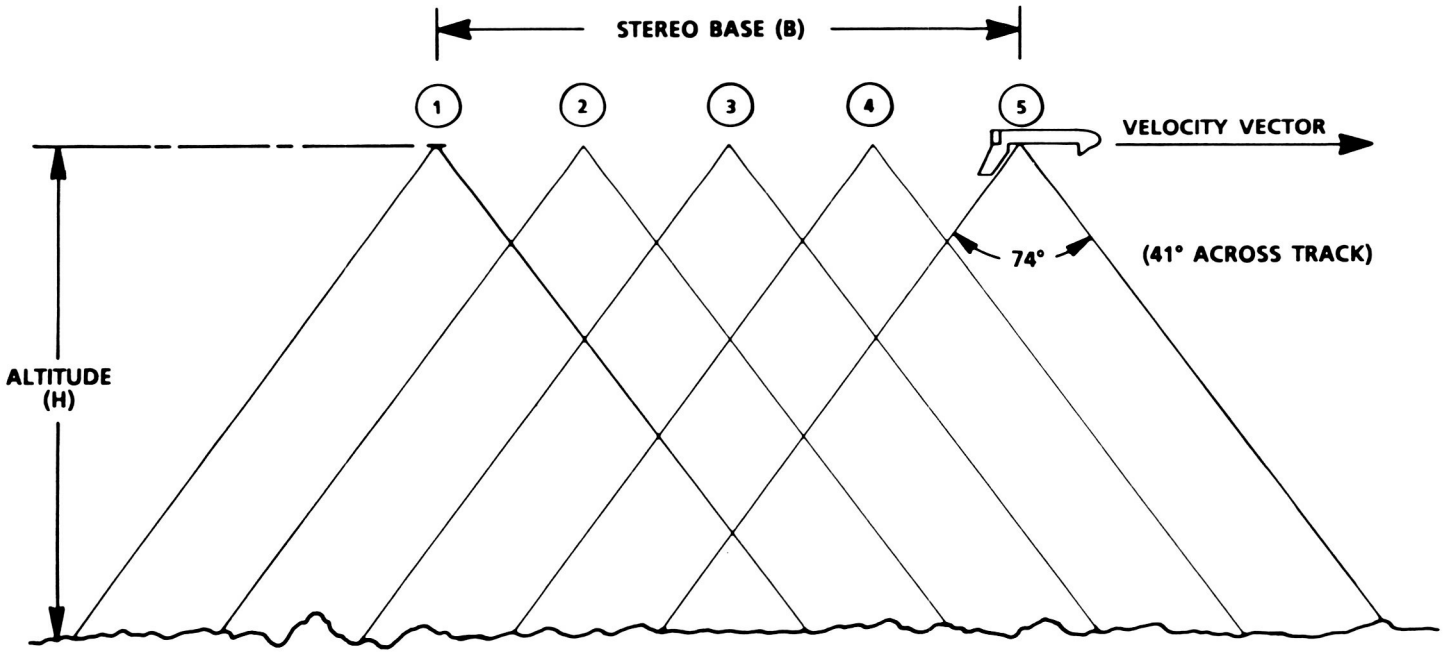


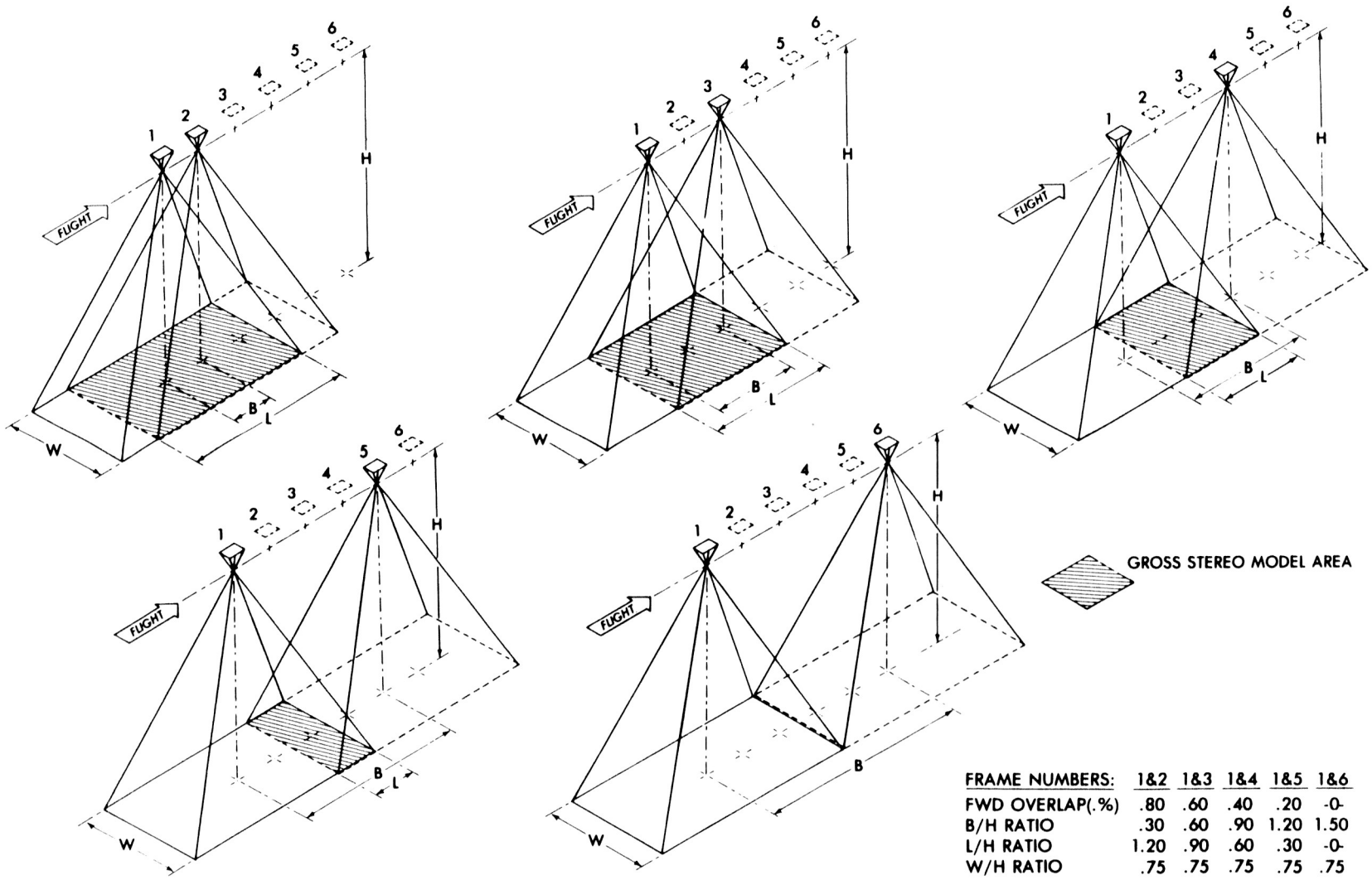
Figure 1-21.- Image point drift. Figure shows drift across a format area on successive frames, at 80-percent forward O/L, due to the easterly rotation of the earth (top), and the effect of successive frame offset due to this rotation (bottom).



TYPICAL ALTITUDE	: 278 kilometers (150 nautical miles)		
PHOTOGRAPHIC SCALE	: 1:912,000		
GROUND FOOTPRINT	: ALONG TRACK (1.50H)	= 417.0 km	(225 n.mi.)
	ACROSS TRACK (0.75H)	= 208.5 km	(112.5 n.mi.)
	AREA COVERED	= 86,945.0 km^2	(25,312 n.mi.^{2})

	1&2	1&3	1&4	1&5
: SELECTED FRAMES				
FORWARD OVERLAP (percent)	80	60	40	20
BASE/HEIGHT (B/H) RATIO	0.3	0.6	0.9	1.2
VERTICAL EXAGGERATION FACTOR	1.4	2.8	4.2	5.5
RELATIVE POSITION ACCURACY (± meters)	14	14	14	14
RELATIVE HEIGHTING ACCURACY (± meters)	28	15	9	7

Figure 1-22.- LFC data acquisition concept for the 80-percent forward O/L mode.



FRAME NUMBERS:	1&2	1&3	1&4	1&5	1&6
FWD OVERLAP(.%)	.80	.60	.40	.20	-0-
B/H RATIO	.30	.60	.90	1.20	1.50
L/H RATIO	1.20	.90	.60	.30	-0-
W/H RATIO	.75	.75	.75	.75	.75

Figure 1-23.- Presentation of the LFC gross stereo model area available in the 80-percent (and less) forward O/L mode. (Note that this illustration does not depict the footprint offset due to the earth's rotation. See figure 1-21.)

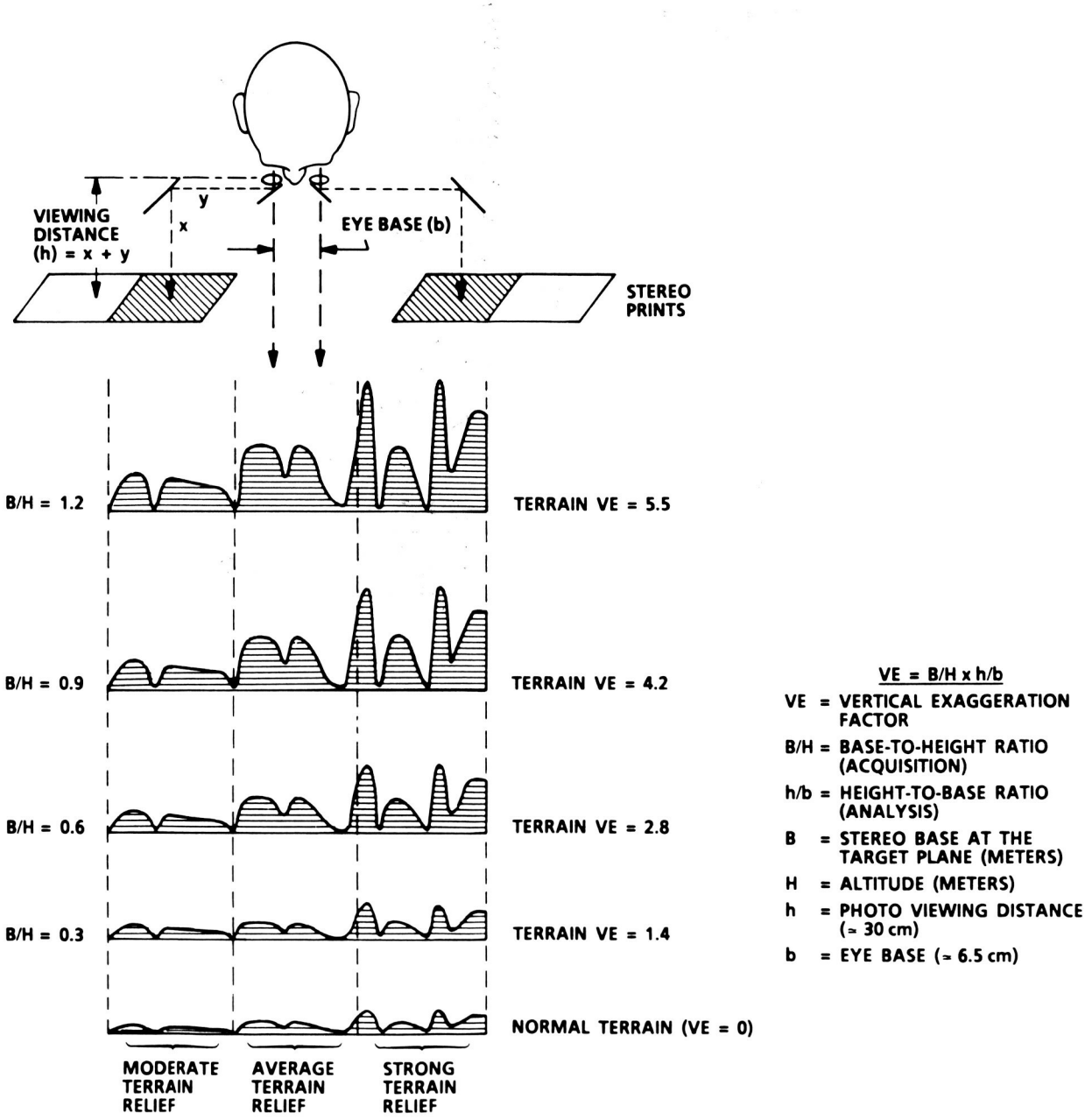


Figure 1-24.- The effect of B/H ratioed imagery on the VE factor effect.

2. FLIGHT PERFORMANCE

2.1 INTRODUCTION

2.1.1 BACKGROUND

At 0703 hours, Eastern Standard Time (EST), on the morning of October 5, 1984, NASA's OCPS was lifted from the launch pad at KSC, on the eastern coast of Florida, and carried into an initial low earth orbit some 370 km (200 n. mi.) above the earth by the Orbiter vehicle Challenger. The mission, designated STS 41-G, was identified as the Office of Space and Terrestrial Applications 3 (OSTA-3)/LFC mission by virtue of the major payloads aboard. The OSTA-3 payload included the Feature Identification and Location Experiment (FILE), the Measurement of Air Pollution from Space (MAPS), and the Shuttle Imaging Radar B (SIR-B). In addition to the OSTA-3 and LFC payloads, STS 41-G also carried the Earth Radiation Budget Experiment (ERBE) satellite, which was released into independent orbit early in the mission, and the Orbital Refueling System (ORS), which was a demonstration of the feasibility to refuel satellites in orbit. The inclination for the STS 41-G mission was 57°. Landing was 1222 hours, EST, at KSC on October 13, 1984, after 133 orbits of the earth. This maiden voyage of the OCPS payload lasted 8 days, 5 hours, and 19 minutes.

During these 8 days in orbit, the LFC was commanded into operation a total of 79 times with successful operation each time, acquiring a total of 2,247 high resolution frames of imagery (photographs) of the earth and heavens. Of these 79 data passes, 72 were of the sunlit earth and 7 were of either the stars (2), for calibration, or the dark side of the earth (5), for geodesy and lightning.

2.1.2 OBJECTIVES

Since this was the maiden voyage of the LFC, the mission was classified as an engineering mission. The two major goals of the mission were to proof the system on high performance photographic film emulsions in the space environment and to acquire high resolution stereoscopic imagery of great geometric fidelity for development of photo interpretive and analysis techniques.

Specific objective categories were established to allow detailed assessment of the system for future orbital applications. The OSTA-3 Post Launch Mission Operations Report (E 420-41-G-09), dated June 10, 1985, judged the LFC mission as successful, based on the prelaunch objectives.

2.1.2.1 Orbital Altitudes

Orbital altitudes achieved during the STS 41-G mission provided opportunities for LFC imagery acquisition at three discrete altitude ranges: 361 km, or 195 n. mi. (224 statute miles); 264 km, or 142 n. mi. (164 statute miles); and 230 km, or 124 n. mi. (143 statute miles). This provided an assessment of wide field synoptic applications, as well as analysis of spatial resolution and photo scale utility to map product generation.

2.1.2.2 Film Emulsion Evaluation

Five types of photographic film emulsions were flown in the LFC, and two types were flown in the LFC's supporting ARS. For LFC imagery, samples were collected on two B&W negative films and two color positive films, using true color (COL) and color infrared (CIR) film in the visible and visible/near infrared, respectively. The fifth film, high speed B&W negative, was used for imaging the stars and dark-side earth surface phenomena. Two types of B&W negative films were used with the ARS SCA to evaluate their suitability for stellar imaging.

2.1.2.3 Mechanical and Electrical Design Verification

Though the total system had undergone extensive laboratory testing in the simulated space environments and mission applications, this mission was to verify to its operation when fully integrated into a spacecraft with various mechanical linkages and electrical services provided by the host vehicle. Thus, it provided a full end-to-end assessment of the overall hardware design concept and interface/supporting services design - the compatibility to the host vehicle and the environment.

2.1.2.4 System Command and Control

A major objective was to evaluate the system command and control in three specific areas: (1) an evaluation of the command software system for uplink of commands and downlink of TM; (2) an evaluation of the LFC response to these commands; and (3) a verification of the utility of the ground command team. With the exception of the inflight stellar calibration sequence during orbit 23, which was commanded by the onboard Mission Specialist, all LFC/ARS commands were generated and issued by the LFC team in MCC at JSC either as real-time commands (RTC's) or as SPC's.

2.1.2.5 Thermal Design

Maintenance of a predetermined thermal "setpoint" is extremely critical with high performance optical systems. Stability of the LFC optics and film platen and the ARS SCA at an internal temperature of 21° ±1° C was paramount. Exposure of the system to intermittent long periods of sunlight and extreme cold (dark side) dictated an extensive design effort to maintain the items within a 2° C temperature envelope through use of active heating and passive cooling (heat loss) techniques.

2.1.2.6 Optical Performance

How well the system would perform optically is more than a function of the design of the optical system, the mechanical and electrical elements, and the thermal stabilization techniques. How well it performs in the flight environment also includes the stability (roll, pitch, and yaw) of the spacecraft, the skill of the crew members as pilots, and the accuracy of the ground control team and their computational software programs. The end product to be evaluated is a result of the sum total of all these factors.

2.1.2.7 Data Acquisition Techniques

The actual acquisition concepts employed by the LFC in earth orbit is not unlike that employed by air breathing (aircraft-borne) cartographic camera systems. The two greatest differences are (1) the inherently greater stability of the spacecraft over the aircraft (both altitude and attitude)

and (2) the vastly different scale of the resulting imagery because of the deployment altitudes. At the maximum altitude (361 km) of STS 41-G, the photographic scale (lens focal length/altitude) of the LFC imagery is a ratio of 1:1,184,000 as opposed to 1:60,000 for a standard (152 mm focal length) cartographic camera at an altitude of 9.1 km (30,000 ft). This places the aircraft imagery at a scale nearly 20 times larger than the LFC imagery.

2.1.3 SUMMARY EVALUATION

System performance during the mission is summarized by the key performance factors listed below:

- System thermal stability (21° ±1° C) - Excellent
- LFC response to uplink commands - Excellent
- Downlink of telemetry - Excellent
- Mechanical and electrical functions - Excellent
- Ground software program - Outstanding
- Automatic exposure control - Mostly adequate
- Optical Performance - Outstanding
- Post flight inspection and test - No degradation

2.2 MISSION PLANNING

Planning for a space flight actually begins years before the actual flight. In the NASA hierarchy of event milestones after project approval, it actually begins as early as the preparation of the statement of work (SOW), which is the technical specification for the instrument to be designed and built. In the SOW are defined the purpose(s) to be satisfied; the results or end products desired; and the means of their optical, electrical, mechanical, and structural accomplishment. The SOW also defines those environments which must be survived and accommodated. It continues through the preliminary design review (PDR); the critical design review (CDR); the qualification and acceptance testing and verification; the document requirements list (DRL); and finally the "buy-off," or customer acceptance readiness review (CARR).

While all of this is in process, interface negotiations are begun with the integration organization to consummate agreements on the interface control documents (ICD's) which define how the experiment will be integrated into the spacecraft, the services the experiment will require, and the compatibility of any new instrument with the spacecraft. Lines of communication with the spacecraft organization must be established to generate the definitive payload implementation plan (PIP) and its various annexes (subdocuments). The documents define in detail both parties' physical (mechanical and electrical) interfaces with the spacecraft, the spacecraft services, the mission control support services, and the specific mission participation.

2.2.1 SYSTEM INTEGRATION

The OCPS is a cargo bay instrument. As such, it requires a substantial carrier structure to mount it into an acceptable position and position it in an acceptable pointing attitude. Economy dictates that if a suitable structure is available somewhere in the system, it should be used. This eliminates much of the very costly reinvention process and simplifies standardization of support hardware and proper utilization of existing costly hardware items.

For the OCPS maiden voyage, the carrier structure used was one developed by the George C. Marshall Space Flight Center (MSFC) to be a universal structure for comparatively small payloads. In fact, it is capable of carrying numerous payloads and payload components on a single central core structure. This structure, the MPESS, has flown many times and has carried an extremely wide range of payload items, some singly and others in clusters.

The OCPS components, as integrated onto the MPESS and flown on STS 41-G, are shown in figure 2-1. The payload integrator provided the unique cantilevered LFC support structure. The FMDM was used for signal receipt, sending, and conditioning as the command interface with the Orbiter. The FMDM is also a standard component which is easily reconfigured for different payload requirements. In addition, the payload integrator provided a junction box (electrical cable interconnect box), a power supply unit (PSU)

for electrical power distribution, a PCB for power surge protection, and electrical interface wiring harnesses and pneumatic lines. Without the OCPS components, the MPESS and these supporting items weigh 998.4 kg (2,201 lb). The total payload weight, with the OCPS components (618.8 kg) fully integrated, is 1,617.2 kg (3,565.3 lb).

Integration of the OCPS configuration at the launch site is a carefully planned and orchestrated operation to ensure that the fit is proper and that no damage results to either the payload or the carrier structure. Figures 2-2, 2-3, and 2-4 show the actual operation of installing the flight hardware onto the MPESS in the high bay of the KSC operations and checkout (O&C) building in preparation for final test and checkout prior to integration into the Orbiter cargo bay at the pad. Normally, it is much preferred to integrate payloads into the cargo bay while the Orbiter is in a horizontal position. However, because of the uniqueness of the OCPS companion payload on the MPESS, the ORS, this activity was delayed until the spacecraft had been moved to the pad and was in the vertical or flight mode.

The acquisition of earth imagery by the LFC is much the same as acquisition by aerial mapping cameras, with the exception that the STS flies upside down so that the cargo bay points to the earth. Figure 2-5 shows the OCPS payload on orbit as it was mounted in the aft portion of the STS Orbiter cargo bay. In this illustration, it will be noted that the LFC thermal door is in the open position, indicating that when the crew member took this photo, the LFC was also in the process of taking photography.

2.2.2 SYSTEM COMMAND AND CONTROL

A major objective of this first mission was to verify the command links and the command computational software programs developed for building the OCPS commands. Though these commands are built many weeks before the mission, it is a certainty that they will be modified or changed in real time as the mission progresses, because of changes in the attitude timelines. Though this scenario was rehearsed many times during the mission simulations (SIMS), such an operation is always subject to real-time changes.

With the exception of the inflight stellar calibration sequence during orbit 23, which was commanded by the onboard payload specialist, all OCPS LFC/ARS commands were issued from the OCPS team in MCC at JSC as real-time commands (RTC's) or as stored program commands (SPC's). These commands (see table 2-1) were uplinked from ground direct to the spacecraft or relayed from ground stations to the Tracking and Data Relay Satellite System A (TDRSS-A) and thence to the Orbiter vehicle.

A reverse of this routing was employed for downlink of OCPS TM. In the event a scheduled data pass was during a period of loss of signal (LOS) - i.e., out of range of ground stations or TDRSS, SPC's were received by the Orbiter during acquisition of signal (AOS) periods and stored in buffers within the onboard payload control supervisor (PCS) or the onboard general purpose computer (GPC); these commands were later called up on an automatic time tag schedule for issue to the payload. If the scheduled data pass was during a period of AOS, the RTC's were issued to the OCPS via the Orbiter the instant they were received.

During periods of AOS, TM from an instrument is downlisted via the Orbiter to mission control to provide a real-time assessment of how a system's operation is proceeding. This data falls into three general categories: diagnostic data for problem solving, data for postmission analysis, and health data for monitoring normal functions in process. On STS 41-G the OCPS downlist TM required 27 discrete and 25 analog functions covering levels, rates, movements, events, and flags (warnings) as shown in table 2-2.

In the event there had been a failure on STS 41-G whereby commands could not be built by ground personnel and uplinked to the LFC, a contingency capability existed whereby the Challenger crew could call up a cathode-ray tube (CRT) display which emulates the LFC command station. With this at hand, the crew could then issue individual commands in real time and cause the LFC to execute these commands. This capability was solely for an emergency situation and was not required during the mission. Had it been necessary, the amount of LFC coverage would have been significantly less,

TABLE 2-1.- SUMMARY OF UPLINK COMMANDS ISSUED TO THE LFC

Command[a]	Parameter	Type	Comments
Power	ON/OFF	Discrete	Activation/deactivation
Mode	Standby Operate Test Calibrate	Discrete Discrete Discrete Discrete	Heaters active only Data acquisition Auto 5-frame advance Single frame time exposure of 2.4 sec
Forward O/L	80% 70% 60% 10%	Discrete Discrete Discrete Discrete	(Percentage of O/L of imagery with next frame of imagery)
Exposure time	Time range 4.0 msec (1/250 sec) 32.0 msec (1/32 sec) Automatic exposure control (AEC)	 Analog Analog Analog	 Minimum exposure time Maximum exposure time Automatic
Exposure bias	+ 1/2 stop Normal - 1/2 stop	Discrete Discrete Discrete	Minor adjustment to exposure when under control of the AEC
FMC	11 mrad/sec 41 mrad/sec	Analog Analog	Minimum rate Maximum rate
Filter select	-H -B	Discrete Discrete	Cutoff at 400 nm Cutoff at 500 nm
Film select	3 film types	Discrete	Three film speeds
Thermal door		Discrete	Opens or closes door
Capping shutter		Discrete	Opens or closes capping shutter (calibrate mode only)
FMC inhibit		Discrete	Inhibits FMC if required

[a] All commands for the ARS/SCA are generated by the LFC logic.

TABLE 2-2.- OCPS TM MEASUREMENTS WHICH WERE MONITORED DURING THE STS 41-G MISSION

Parameter	LFC	ARS	Type
Position	2	-	Analog
Rate	1	-	Analog
Pressure	2	-	Analog
Temperature	13	1	Analog
Current	1	-	Analog
Voltage	1	-	Analog
Velocity	1	-	Analog
Radius	1	-	Analog
Count	2	-	Analog
Event	13	8	Discrete
Flag	3	3	Discrete
Total	40	12	

because of other demands on crew member time. The method used allowed the crew to perform other experiment functions, and it also allowed the LFC to be operated throughout the crew eat and sleep periods.

2.2.3 FLIGHT FILM EMULSIONS

A major objective of this first flight was to evaluate the optical performance and usefulness of the four film emulsions contained in the LFC and two film emulsions contained in the SCA. Though three altitudes were flown during this voyage, it was not possible to do photography at each altitude with each type of film. It was possible, however, to acquire identical ground targets on two or more film types, and this will be discussed later. Table 2-3 lists the film emulsions flown in the LFC and those flown in the SCA. Both rolls were manufactured at the Eastman Kodak facilities in Rochester, New York.

Those rolls were manufactured to a specification which required mixing the film types into a single roll by splicing the sections together using a 12-in. section of clear film base between each film type. This clear section had a 1-in.-wide piece of aluminized Mylar™ tape running across the web from one edge of the film to the other edge. This tape was used to interrupt

TABLE 2-3.- CHARACTERISTICS OF AERIAL FILMS FLOWN WITHIN THE LFC ON STS 41-G

Type of film (Kodak)		Resolution lp/mm at TOC[a]		Root mean square (RMS) granularity
Number	Description	1000:1	1.6:1	
2402	Plus-X Aerographic[b], B&W negative	160	50	20
3411	Plus-X Aerocon[b], B&W negative	160	50	28
3412	Panatomic-X Aerocon II, B&W negative	400	125	9
3414	High definition aerial, B&W negative	800	250	8
SO-131	High definition, Aerochrome infrared, COL positive	160	50	9
SO-242	Aerial color, COL positive	200	100	9

[a] TOC - target object contrast.

[b] For stellar calibration and nighttime geodesy only.

light from an infrared (IR) emitting diode being sensed by a photo detector within the LFC film splice detection unit mounted within the film magazine. Each time the light output was interrupted (e.g., at each change of film types), the output signal from the detector would change state (e.g., high or low). This signal was processed by the LFC TM package for downlink to mission control, alerting the LFC team that a film change had, in fact, taken place, so that exposure commands (e.g., shutter speed) could be changed to accommodate the speed rating of the new film. Knowing the exact amount of film in each film segment allowed the command team to monitor and manage film consumption quite accurately and anticipate an upcoming film change. This scenario worked quite successfully throughout the mission, and the ground team was never more than 1 frame off at any change.

The order in which the film rolls were assembled at Kodak are shown in table 2-4. Table 2-5 presents a record of the actual film coating manufacturing batch number and expiration dates should any future investigations be desired.

TABLE 2-4.- FILM TYPES FLOWN IN THE LFC AND THE SCA ON STS 41-G

[Films types listed in the order of appearance in the film roll]

Roll pos. no.	Type of film (Kodak)		Total length		Approx. no. of frames
	Number	Description	m	ft	
	LFC				
1	3414	High definition aerial	198	650	410
2	3411	Plus-X Aerocon[a]	23	75	47
3	3414	High definition aerial	62	200	126
4	3412	Panatomic-X Aerocon II	152	500	315
5	SO-242	Aerial color	152	500	315
6	3414	High definition aerial	152	500	315
7	SO-131	High definition Aerochrome infrared	152	500	315
8	3414	High definition aerial	152	500	315
9	3411	Plus-X Aerocon[a]	16	50	31
10	3414	High definition aerial	>43	>140	88
		Total LFC	1,102[b]	3,615	2,277[b]
	SCA				
1	3411	Plus-X Aerocon	457	1,500	1,674[d]
2	2402	Plux-X Aerographic	152	500	558[d]
		Total SCA	609[c]	2,000	2,232[d]

[a] Used for stellar calibration and nighttime photography only.

[b] LFC maximum film capacity with 3414 film is 1,220 m (4,000 ft) and 2,500 frames.

[c] SCA maximum film capacity with 3411 film is 670 m (2,200 ft) and 2,450 frame pairs.

[d] An SCA frame pair is composed of a left viewing frame and a right viewing frame; the actual number of frames is twice that shown.

TABLE 2-5.- HISTORICAL DOCUMENTATION OF THE OCPS FILMS FLOWN ON STS 41-G

[Flight roll 9.5 in. by 3,640 ft, spool 980]

Roll position number	Film type	Emulsion batch number	Expiration date
Head out			
1	3414	198-14-4-4	Jun 1986
2	3411	172-17/1-4-4	Nov 1985
3	3414	198-14-4-4	Jun 1986
4	3412	65-25-4-4	May 1986
5	SO-242	72-12-4-4	May 1985
6	3414	198-14-4-4	Jun 1986
7	SO-131	225-13-4-4	May 1985
8	3414	198-14-4-4	Jun 1986
9	3411	172-17/1-4-4	Nov 1985
10	3414	198-14-4-4	Jun 1986
Tail (film core)			

As a means of verifying the effect of both the ground process flow (preflight preparation and postflight demate) and the on-orbit flight environments on the films, preexposed sensitometric strips, with latent images of a step wedge for each film type, were flown within a special canister (a metal tube) mounted within the LFC film magazine. In addition, identical sample strips were retained at the film processing (developing) facility as controls, others were stored in a freezer, and still others were stored at ambient laboratory temperature. All of these samples had a reserved area for exposing additional sensitometry just prior to film development.

At the time of flight film and sensitometric strip receipt at this facility, these strips and the retained control strips were given identical

sensitometric exposures on each strip's reserved area. This later set of exposures satisfied an evaluation of latent image decay and a mark on film desensitization. As an added control, refrigerated, reserved bulk film of each type was also given identical sensitometric exposures. All samples of each film type were then processed to the processing standards established months prior to the mission.

Even though the flight film was in the LFC and SCA for 62 days, there was no indication of latent image failure or any meaningful change in photographic response as a result of the handling and flight environments. The film remained in refrigerated storage up to the point of magazine loading and immediately following recovery from the spacecraft. The environment at the launch pad was tightly controlled such that the cargo bay inlet purge air temperature was maintained at less than 24° C (less than 75° F). Since the landing was at KSC, there were no extremes of temperature that might be associated with a landing and loiter at Dryden Flight Research Facility (in the Mojave Desert) and then a ferry flight to KSC.

Another advantage to using slower speed films, in addition to that of greater spatial resolution, is their much lower sensitivity to adverse environments (primarily higher temperatures) and radiation sources. Early in the OCPS development effort, thoughts were given to using a dosimeter in the film compartments, but because of earlier favorable experience on extended low earth orbit missions (Skylab) and Apollo lunar flights, this idea was abandoned.

For record and for someone planning a similar operation involving photographic film at a launch site in the future, table 2-6 gives a reasonable guide to those milestones which one might anticipate.

2.3 PLANNED/ACTUAL DATA PASSES

A considerable amount of effort must be expended in the planning of coverage by the LFC on a Shuttle mission. This planning is a complete package of

TABLE 2-6.- OCPS FLIGHT FILM HANDLING MILESTONES

Event	Date	Condition
Kodak ships film	5/2/84	Air express
Film arrives KSC	5/3/84	Refrigerated
Flight film loaded, LFC	8/21/84	Ambient
Flight film loaded, SCA	8/22/84	Ambient
Functional test complete	8/29/84	Ambient
OCPS to OPF[a]	9/4/84	Ambient
OCPS to pad	9/9/84	Ambient
Challenger to pad[b]	9/13/84	Ambient
Install in Challenger	9/15/84	Ambient
IVT at pad[c]	9/19/84	Ambient
Launch (07:30 EST)	10/5/84	Ambient
Landing (12:22 EST)	10/13/84	Ambient
Demate from Challenger	10/16/84	Ambient
Unload LFC/SCA	10/22/84	Refrigerated
Film shipped to processor	10/25/84	Air express
Film storage	10/25/84	Refrigerated
Film processing, start	10/29/84	
Film processing complete	10/30/84	

[a] The Orbiter Processing Facility (OPF) is KSC's former Vertical Assembly Building (VAB).

[b] Challenger was not transported to the pad until fueling of the OCPS companion payload, the ORS, was complete. This is a hazardous operation requiring "clear the pad" procedures.

[c] The integration verification test (IVT) is the final operational test (and film advance) of the OCPS before launch.

uplink commands (shutter speed, percent of forward O/L, and V/H command) which is specifically keyed to a portion of a desired orbit and is time tagged for the precise moment in the orbit for execution of the commands to be issued. This is done many months before the mission event. This document, referred to as the "command plan," is prepared electronically so it can be sent to the mission planners for integration into the overall uplink command package. It must be formatted to be compatible with the STS command link.

The LFC was originally scheduled to fly on STS 41-D (Discovery vehicle) in June 1984, and then reflown some 3 months later on STS 41-G (Challenger vehicle) in October 1984. STS 41-D was to be an inclination of 28.5°, and STS 41-G was to be a 57° inclination. As such, there was absolutely no similarity to the ground tracks nor to the command sequences, and the effort for STS 41-D could not be transferred to the STS 41-G mission. Both were planned as unique work packages, and work continued on both missions as parallel efforts.

The STS 41-D mission experienced a pad abort on June 25 and again on June 26. Because of projected delays required to execute corrective actions on the Discovery vehicle, this mission was combined with the next mission and payloads were prioritized. On July 11, 1984, the LFC was deleted from the manifest and upon completion of demating of payloads, the LFC was returned to the KSC O&C laboratory on July 19 for preflight preparation for the STS 41-G mission.

Months before the fact, a precise forecast of launch data and time of day is received along with the target mission altitudes. Using this information, other state vector data, and plots of the ground track, it is possible to generate the command sequences for all candidate data passes.

Target site selection for LFC coverage was in process for several years. The LFC principal investigator (PI) led a team of co-principal investigators (Co-PI's) who were supported by their co-investigator (Co-I) groups and individuals. This team, the LFCIWG, was composed of representatives of

several U.S. Government agencies. Each Co-PI represented his agency personnel, foreign governments, individuals, and both academic and industrial communities. The list of worldwide sites identified by this group was published as the LFCIWG Co-Investigator Target Summary, JSC-19957, June 1, 1984, coinciding with efforts for the STS 41-D and following STS 41-G missions. By the time of the STS 41-G mission, both the number of Co-I's and the number of targets had increased significantly. A summary of these Co-PI groups and their supporting sites is given in table 2-7.

TABLE 2-7.- LFCIWG CO-INVESTIGATOR TARGET SUMMARY

LFCIWG sponsor[a]	Circa June 1, 1984		Circa Oct. 1, 1984	
	No. of Co-I's	No. of targets	No. of Co-I's	No. of targets
NASA	7	18	33	77
DOA	-	-	3	27
DOC	21	42	22	47
DOD/DMA	98	59	98	59
COE	4	11	4	11
DOE	-	-	2	4
DOI	80	238	83	268
Totals	210	368	245	494

[a] NOTES:

DOA Department of Agriculture (higher inclination of desired domestic sites covered by STS 41-G)

DOC Department of Commerce

DOD Department of Defense

DMA Defense Mapping Agency (cooperative mapping programs with developing nations)

COE Corps of Engineers (domestic waterways and flood control projects)

DOE Department of Energy

DOI Department of the Interior

Since the LFC is a high spatial resolution, high geometric control instrument, it is not surprising that high resolution panchromatic B&W film materials were most requested. Surprisingly, for those requesting a color medium, the European Co-I's preferred "true" color (i.e., COL) film rather than the CIR material preferred by the U.S. Co-I's. In all cases, Co-I's were requested to give desired film types and acceptable alternate films. A very brief summation of both the number of sites requested and their area (based on square degrees of earth coordinates) is given in table 2-8.

TABLE 2-8.- LFC CO-INVESTIGATOR FILM PREFERENCE

Film type	Desired film type, percent		Alternate film type, percent	
	Sites	Area	Sites	Area
B&W	41.3	64.8	30.5	24.4
COL	20.7	10.2	19.0	26.0
CIR	35.3	23.4	30.4	28.9
BIR[a]	0.3	-	2.7	1.4
(any)	2.4	1.6	17.4	19.3
	100.0	100.0	100.0	100.0

[a] BIR - black and white infrared.

Post-STS 41-G mission planning saw the list of Co-I's swell to over 300 in number and their sites to almost 600, since this follow-on mission had a potential polar inclination.

The only real unknown in the planning exercise is the condition of weather over the desired sites. Since the commands are finalized and generated 5 to 6 months before the fact, only statistical data can be used to project weather conditions at various world sites. On this basis, it is prudent for the planning to include prime data passes and alternate or backup data passes. The LFC planning group did this to the extent that it generated command packages for approximately 100 percent more coverage than the amount of film available.

As is often the case, mission anomalies and time line changes caused a nearly complete revision of all command functions each day of the mission. The largest impact on the STS 41-G LFC plans was the extremely high percentage of cloud cover seen over the northern hemisphere, both in the Americas and in Europe. Additional non-LFC related changes to the time line did occur for various reasons, however, and these problems can be summarized as follows:

- Delay in ERBE Satellite deployment
- Steering problems with STS Ku-band tracking antenna
- TDRSS tracking station problem
- SIR-B antenna stowage

In many cases, both the planned LFC prime and backup passes were aborted because of weather conditions and the problems listed above. These other problems did, however, make it possible for the LFC team to add additional new or unplanned data passes which had not been scheduled because of priorities of other instruments. Such new coverage ended up as 19.1 percent (14 of 73 passes) of the actual LFC sunlit passes during this mission. A summation of the planned and actual data passes (table 2-9) demonstrates the flexibility of the LFC command software programs to accommodate real-time changes.

Planned data pass loading was essentially uniform for the first 7 days of the mission, with the 8th and final day being heavily scheduled. The reason for this was to plan a relatively uniform rate of film consumption to ensure that all of the four types of film loaded into the LFC were utilized over certain target sites. On the 8th day, all other major payloads were to be powered down and inoperative, allowing the STS to remain in proper attitude for LFC applications. On these final orbits, several data passes were planned for each orbit.

The only other day with more actual data pass acquisitions was day 2, during which 15 data passes were acquired. Day 2 was heavily loaded because of problems being experienced by factors which allowed STS to remain in the proper velocity vector and attitude for LFC photography. The steering

TABLE 2-9.- PLANNED AND ACTUAL LFC DATA PASSES DURING STS 41-G

Flight day	Mission plan	Mission actuals				Percent of plan
		Plan	Abort	New	Total	
1	17	5	12	-	5	29.4
2	18	10	8	5	15	55.6
3	17	9	8	-	9	52.9
4	18	11	7	-	11	61.1
5	17	8	9	-	8	47.1
6	18	7	11	2	9	38.9
7	18	5	13	3	8	27.8
8	28	10	8	4	14	35.7
	151	65	86	14	[a]79	43.0

[a] Includes six passes where film was exposed on the dark side of the orbit for calibration and geodesy experiments.

(pointing) problem with the onboard Ku-band antenna likewise caused the aborting of all LFC data passes over central and eastern South America. In these areas the STS had to be maneuvered to point the Ku-band antenna at the TDRSS in order to downlink onboard data tapes of stored high-bit-rate Shuttle Imaging Radar B (SIR-B) data. Even so, the rate of LFC film consumption was not too different from that planned premission, as illustrated in figure 2-6.

2.4 GLOBAL WEATHER IMPACT

During the maiden voyage of the OCPS LFC, an inordinate number of broad weather systems were encountered throughout the northern hemisphere, particularly in North America and Europe. The U.S. Navy oceanographer aboard the Challenger, P. D. Scully-Power, commented at postmission crew debriefing ". . . look at the total earth and you would expect about 30 percent cloud cover. . . . we were looking at more like 60 or 70 percent cloud cover." Many of the primary LFC test sites for this mission were at the latitudes above 28° N and below 28° S and located mostly in Canada, the United States,

and Europe. Because of excessive cloud cover, it became necessary to abort 80 to 90 percent of the planned data passes over these two continents and to resort to secondary test sites falling between latitudes 28.5° N and 28.5° S.

Premission ground rules were established whereby scheduled data passes with weather predictions of 35 percent or less cloud cover would be considered acceptable and would be executed. Marginal weather conditions, 35 to 70 percent cloud cover, would be considered in near real time, and decision to execute would be based on the need to deplete film in order to maintain the scheduled rate of film consumption. Unacceptable conditions included those ground tracks with greater than 70 percent cloud cover.

Approximately 50 percent of all aborted passes were due to the inclement world weather conditions, and the remainder were for various non-LFC problems. Many world sites were totally or relatively cloud free, but many of the most highly desired northern hemisphere sites were experiencing cloud cover ranging from 70 to 100 percent.

As part of the plan to run or abort a pass, each day of the mission, the LFC team provided the U.S. Air Force (USAF) Global Weather Central (GWC) with the next day's replanned ground tracks, listing the geographic coordinates for LFC operation start and stop. During the afternoon and early evening, GWC would analyze all sources of weather information for these ground tracks and report their predictions for these passes prior to midnight. Their predictions were reported as one of three prearranged classifications: acceptable (0 to 35 percent clouds); marginal (35 to 70 percent clouds); and unacceptable (more than 70 percent clouds). Additionally, if part of an intended pass was relatively cloud free, they would flag these sections, making it possible to at least acquire those portions of the pass.

At JSC mission control in Houston, the NOAA Spaceflight Meteorology Station is staffed 24 hours each mission day and has access to real-time satellite imagery from the geostationary weather satellites on equatorial stations. The NOAA facility used the U.S. geostationary operation environmental satellite (GOES) to cover the eastern Pacific, the Americas, and the western

Atlantic; the European meteorological satellite (Meteosat) to cover the eastern Atlantic, Europe, and Africa; and Japan's geostationary meteorological satellite (GMS) to cover Asia and the Pacific area. By using imagery from these weather satellites, it was then possible to make near real-time modifications of certain go/no-go decisions in order to maintain a reasonable rate of scheduled film consumption. Table 2-10 reports the cloud cover experienced during photography on STS 41-G.

TABLE 2-10.- SUMMARY OF THE CLOUD COVER CONTENT OF LFC IMAGERY ACQUIRED ON STS 41-G

[During this mission 2,143 frames of photography were made during daylight passes]

Acceptable			Marginal			Unacceptable[a]		
Cloud cover, %	No. of frames	Percent of total	Cloud cover, %	No. of frames	Percent of total	Cloud cover, %	No. of frames	Percent of total
0	476	22.2	40	161	7.6	80	125	5.8
5	137	6.4	50	148	6.9	90	83	3.9
10	229	10.7	60	114	5.4	95	11	0.5
20	252	11.7	70	142	6.5	100	71	3.3
30	194	9.1						
	1,288	60.1		565	26.4		290	13.5

[a] Many of these are proving to be very useful to the oceanographic and atmospheric science communities.

Capture of transient weather phenomena by the LFC was one objective of the LFC mission, and many Pacific ocean hurricanes and tropical depressions were tracked in an attempt to intercept them on upcoming ground tracks. Unfortunately, such a collision course never presented itself, and since such passes were during crew sleep periods, rolling the Challenger to acquire oblique photography was not possible. However, one sequence of oblique LFC imagery was acquired of Hurricane Josephine off the U.S. eastern seaboard (see figure 2-7).

2.5 MISSION ALTITUDE SUMMARY

The STS 41-G mission was an extremely good engineering mission for the LFC, since it provided three widely separated near-circular orbital altitudes for image collection at significant photographic scale changes. There was some variance within the three discrete altitudes and a little more elipticity, perhaps, than was desired. The goal had been to maintain the spherical path with an error of less that 2 percent in order to avoid too frequent an update of the LFC FMC commands during any given data pass. Such an avoidance would provide a more reliable assessment of command execution and image smear due to forward motion of the Orbiter, which is nominally 7.5 km/sec in the velocity vector.

The three altitudes attained during the mission are summarized in table 2-11. It will be noted that the minimum-to-maximum range in altitude at any one of the three discrete altitudes is given with a mean average for the stay at that general altitude. The maximum altitude represents the apogee (the high

TABLE 2-11.- THREE TARGET ALTITUDES ACHIEVED DURING THE STS 41-G MISSION

No. of frames acquired	Orbital altitude				Photo scale
	Range	km	n. mi.	Statute miles	
228	Maximum	367	198	228	1:1,204,000
	Average	361	194	224	1:1,184,000
	Minimum	355	191	220	1:1,164,000
335	Maximum	271	146	168	1:889,000
	Average	264	142	164	1:868,000
	Minimum	258	139	160	1:846,000
1684	Maximum	239	129	148	1:784,000
	Average	230	124	143	1:755,000
	Minimum	222	120	138	1:728,000

point), and the minimum represents the perigee (the low point) of that orbital altitude. Generally, the time lapse between these two points is approximately 45 min (nominal 90 min per orbit).

The objective of the high altitude orbit was twofold: (1) to deploy the ERBE satellite and (2) to acquire LFC imagery of as many urban areas as possible for system performance analysis. The stay (approximately 32 hr) at this altitude was somewhat longer than anticipated because of the extra caution being taken with the deployment of the ERBE. This longer period of time allowed the LFC, though severely weather restricted in the northern hemisphere, to expose 228 frames of imagery on eight data passes between orbits 2 and 22. The altitude excursion at the high altitude was 13 km, or roughly 1.8 percent about a nominal 361-km altitude.

As a result of the schedule change, a short stay (approximately 16 hr) was spent at the medium altitude for purposes of collecting LFC imagery and executing stellar calibration exposures with both the LFC and the SCA. Additionally, this gave the SIR-B radar experiment an opportunity to activate and collect sample imagery. The altitude excursion at the medium altitude was 13 km, amounting to approximately 2.5 percent about a nominal of 264-km altitude.

The balance of the mission was spent at the low altitude where most of the various experiments had planned to collect the bulk of their data. Though there was not a severe shortage of propellants for circularizing and maintaining a target altitude, fewer trim burns were executed because of the large number of unscheduled attitude maneuvers (Ku-band pointing) which were executed. Even so, the altitude was maintained within a range of 17 km, or 3.7 percent of a nominal 230-km altitude.

An additional objective of the mission was to compare the relative merits of four photographic film emulsions for high performance space applications. Because of the way the roll had been manufactured, there had been no plan to try each emulsion at all three altitudes, and to do so would have severely complicated the roll manufacture. As it was assembled, there was a total of

18 film splices within the roll in order to incorporate the film change detector sections separating each of the 10 sections (five film types, including the nighttime film, 3411) of film emulsion. Table 2-12 summarizes the film types exposed at the three target altitudes.

TABLE 2-12.- STS 41-G ALTITUDES AND THE AMOUNT OF FILM EXPOSED AT EACH

[Does not include passes on type 3411 film]

Altitude (Average)	Flight film type 3412		Flight film type 3414		Flight film type SO-131		Flight film type SO-242	
	Passes	Frames	Passes	Frames	Passes	Frames	Passes	Frames
361 km (195 n. mi.)	-	-	9	228	-	-	-	-
264 km (142 n. mi.)	[a]1	23	11	263	-	-	-	-
230 km (124 n. mi.)	9	293	26	688	11	321	10	308

[a] One data pass only over areas of little or no cultural content.

Table 2-13 summarizes the orbital altitudes achieved during STS 41-G and the number of LFC data acquisition passes and frames of photography made at these altitudes.

TABLE 2-13.- LFC DATA PASSES AND FRAMES OF PHOTOGRAPHY AT THREE ALTITUDES

Orbit number	Nominal altitude	Total data passes	Total frames
1 - 22	370 km (200 n. mi.)	9	228
23 - 36	272 km (147 n. mi.)	12	333
37 - 128	239 km (129 n. mi.)	56	1,675
		[a]77	[b]2,236

[a] Does not include two stellar photography passes.

[b] An additional 54 frames were expended during prelaunch testing at KSC.

2.6 ATTITUDE RATES

The attitude of the spacecraft vehicle is defined in a coordinate system such that the +X axis is out of the nose of vehicle; the +Z axis is out of the belly of the spacecraft (-Z is out of the payload bay and coincident with the optical axis of the LFC); and the +Y axis is out of the starboard (right hand) wing, completing a right handed coordinate system (see figure 2-8). Positive (+) yaw, pitch, and roll are clockwise looking from the point of origin out the appropriate positive axis. The sequence associated with these values is roll, pitch, and yaw around the X, Y, and Z axes, respectively. The initial or reference attitude (0,0,0) is defined as +X in the appropriate velocity vector (nose forward), +Y normal to the orbital plane, and -Z through the center of the earth (along the geocentric radius vector).

During data acquisition by the LFC during the STS 41-G mission, the vehicle was maintained in a -ZLV mode (-Z axis pointed at the local vertical) with the +X axis ("little end" or nose) forward in the velocity vector. This attitude aligns the optical axis of the LFC lens on the nadir point and places the LFC LOF, or the long axis of the image format, along the ground track with the FMC driving in the +X direction (forward velocity vector) to correct for image motion. (Note that the LFC coordinate system does not have the same polarity as the spacecraft, such that the LFC -X axis must always be into the velocity vector as shown in figure 2-9.)

Were one to rotate the LFC 180° about the LFC optical axis at the time of installation, the spacecraft would then be flown with the "big end" (tail) forward but still in the -ZLV mode. In fact, the design of the LFC interface was such that integration into the cargo bay can be in any one of four positions which are 90° to each other; either the nose or tail (+X or -X) is into the velocity vector, or the vehicle could be either starboard or port wing (+Y or -Y) forward. Similarly, the SCA support structure which holds the SCA can also be positioned at four 90° positions about the LFC optical axis (figure 2-9).

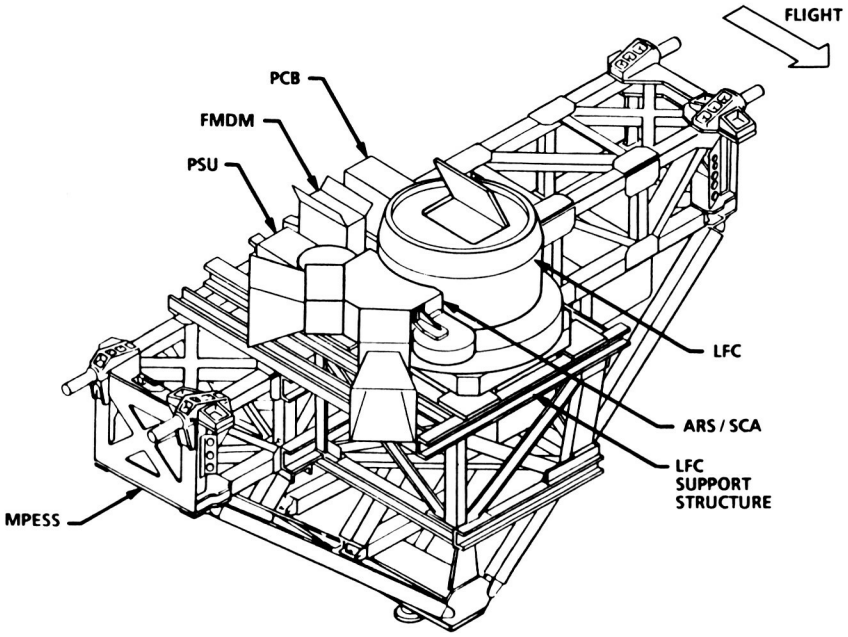
Detailed inspection of suspect frames during periods of high spacecraft roll rates has revealed very little image degradation in the cross-track direction, and certainly no more than that experienced due to the rotation of the earth. Using 40,074 km as the mean equatorial circumference of the earth, the earth rotational velocity at the equator is approximately 464 m/sec. STS 41-G had an inclination of 57°, such that the rotational velocity at 57° N or 57° S is 252 m/sec based on a nominal circumference of 21,608 km at 57°.

All launches out of KSC are in an easterly direction, imparting some degree of correction in the cross-track smear. At the equator the relative cross-track smear is approximately 65 m, assuming an LFC shutter speed of 15 msec as an example, but the moderator of the spacecraft going in the same direction reduces this effect to a very few meters.

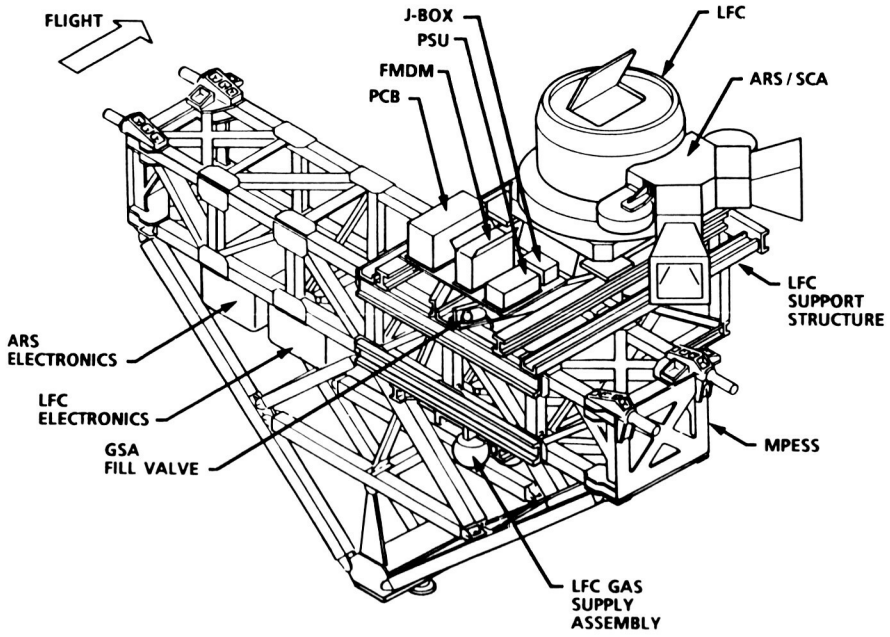
Vehicle roll, pitch, and yaw rates pose the greatest potential input to image smear with roll, of course, being the most significant. Maintenance of a deadband of ±2 degrees about the pointing axis is all that the spacecraft organizations will agree to, but the rates within this deadband could be very significant. In practice, however, a significantly tighter deadband is maintained, and the rates within this deadband are kept at an extremely low value while instruments are operating.

Downlist TM allows one to determine both the drift within the deadband and the rate of this drift. Figure 2-10 illustrates one of the more significant roll rates in which the roll was from +1° to -1° in 190 sec, or 0.0105°/sec. Within this period, there were rates as high as 0.0413°/sec. This was during a crew awake period during which crew members moving about do cause some perturbation to spacecraft attitude. This instance can be contrasted to two crew sleep periods shown in figure 2-11 (data pass 38.0) and figure 2-12 (data passes 62.0 and 62.2), in which the deadband for all three axes of pass 38.0 is extremely tight (±0.136°). During passes 62.0 and 62.2, the rates are extremely small, also; however, the pitch was biased to a 1.127 ± 0.11 degree nose-up attitude with very low rates within the biased pitch.

Less than half a dozen isolated frames of LFC imagery showed any significant cross-track smear due to momentary high roll rates, but even these frames suffered less than 50 to 60-percent loss of resolution. In all such instances, the frame immediately preceding or following the affected frame was of good resolution, and the affected frames were not seriously degraded.



(a) Forward end.



(b) Aft end.

Figure 2-1.- The OCPS, shown in full flight configuration status on the MSFC MPESS.

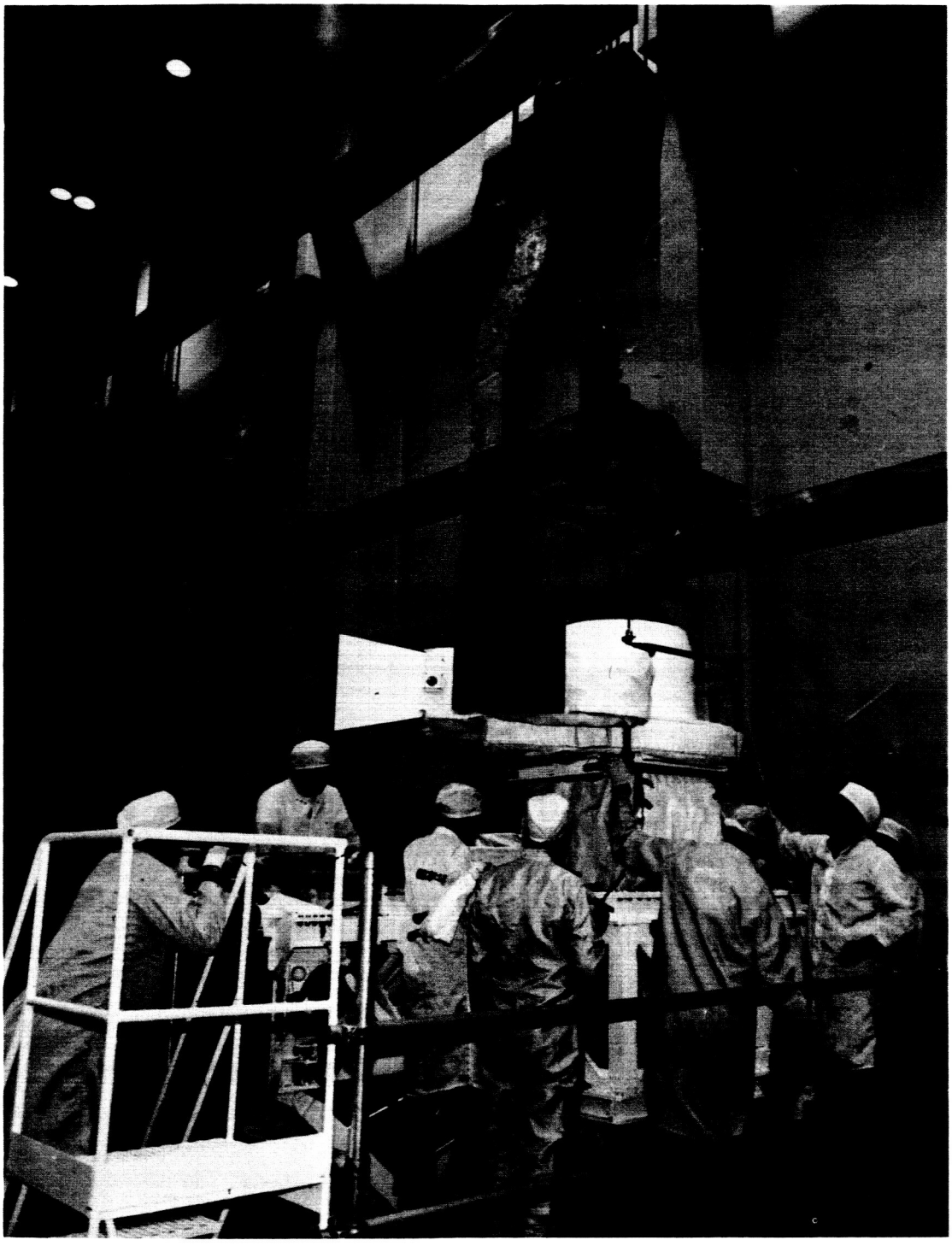


Figure 2-2.- The LFC/SCA, shown being placed on the MPESS by KSC integration personnel. (NASA photo S85-26826.)

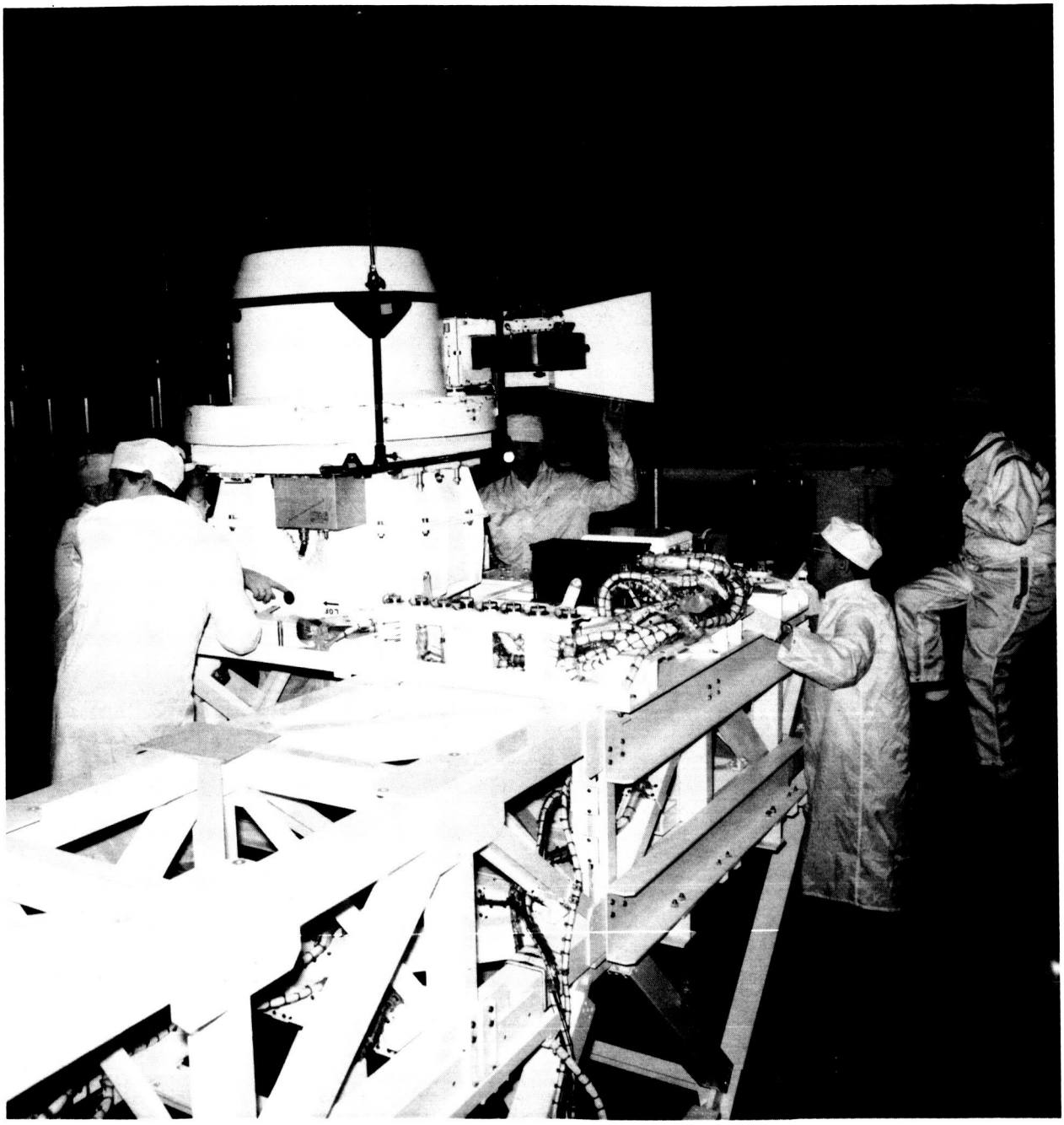


Figure 2-3.- Final fit check of the LFC/SCA into the LFC support structure mounted to the MPESS. The PCB, FMDM, PSU, junction box, and electrical interface cabling are shown in the foreground (NASA photo 108-KSC-384C-932/3).

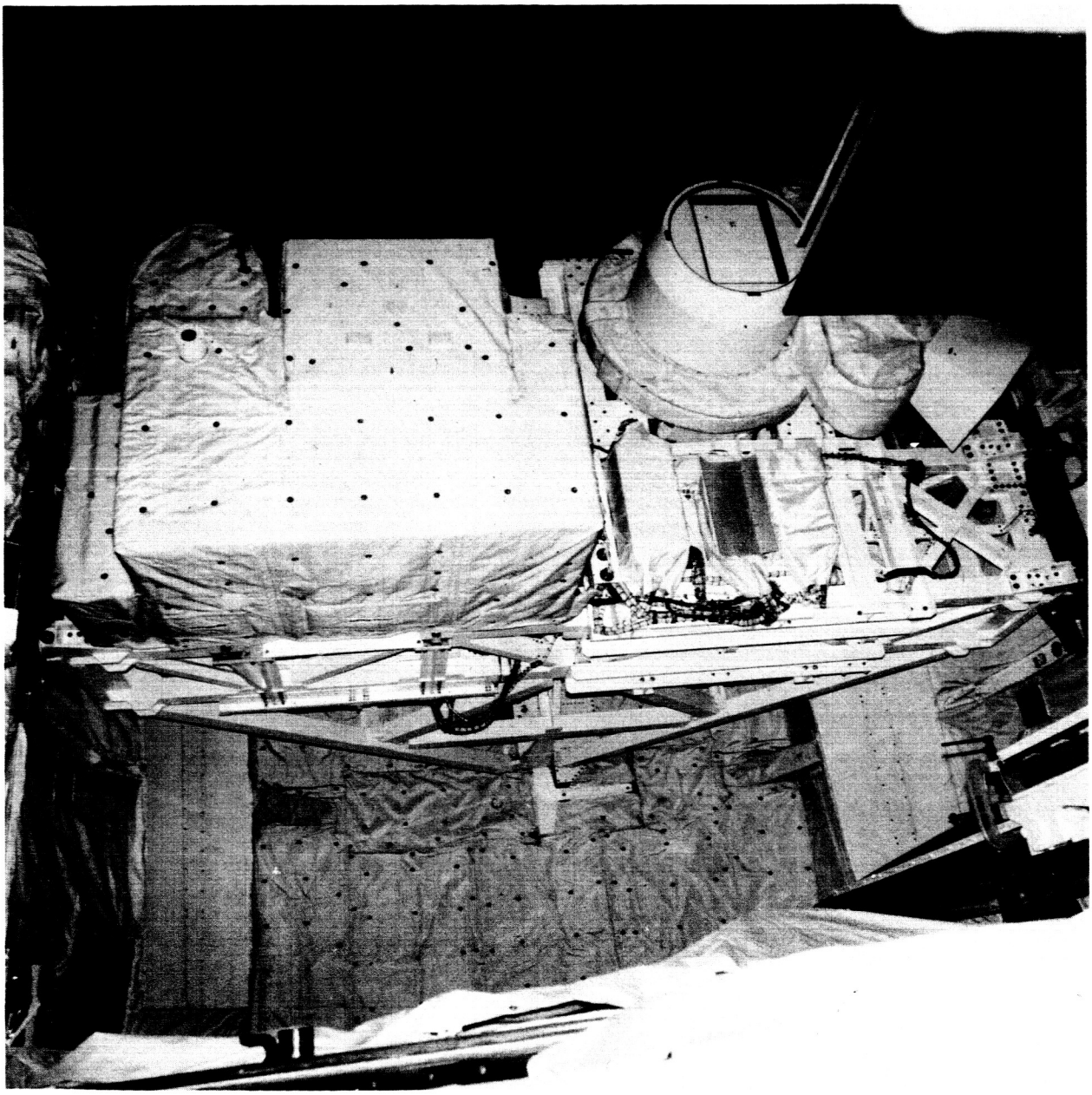


Figure 2-4.- The OCPS (right) and companion ORS payload (left). Payloads are shown fully integrated into the Orbiter cargo bay at the launch pad, with all thermal protective blankets in place. KSC closeout photo prior to launch (NASA photo S85-26824).

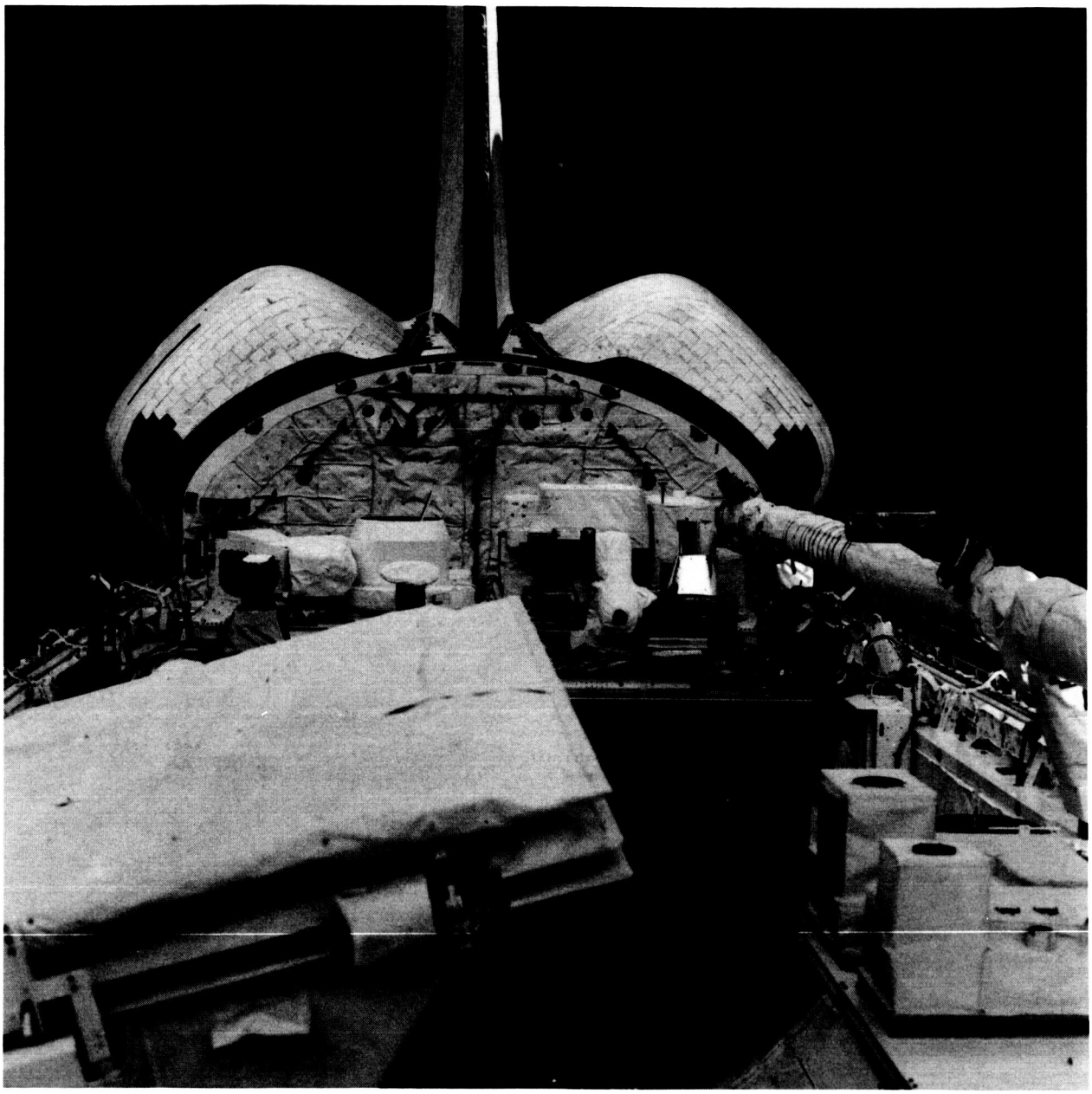


Figure 2-5.- Inflight photo of Orbiter cargo bay, showing OCPS payload installed in aft end. The ERBE satellite is immediately in front of the OCPS/ORS/MPESS. The folded SIR-B antenna (left foreground) and FILE and MAPS (lower right) comprise the OSTA-3 payload (NASA photo S17-32004).

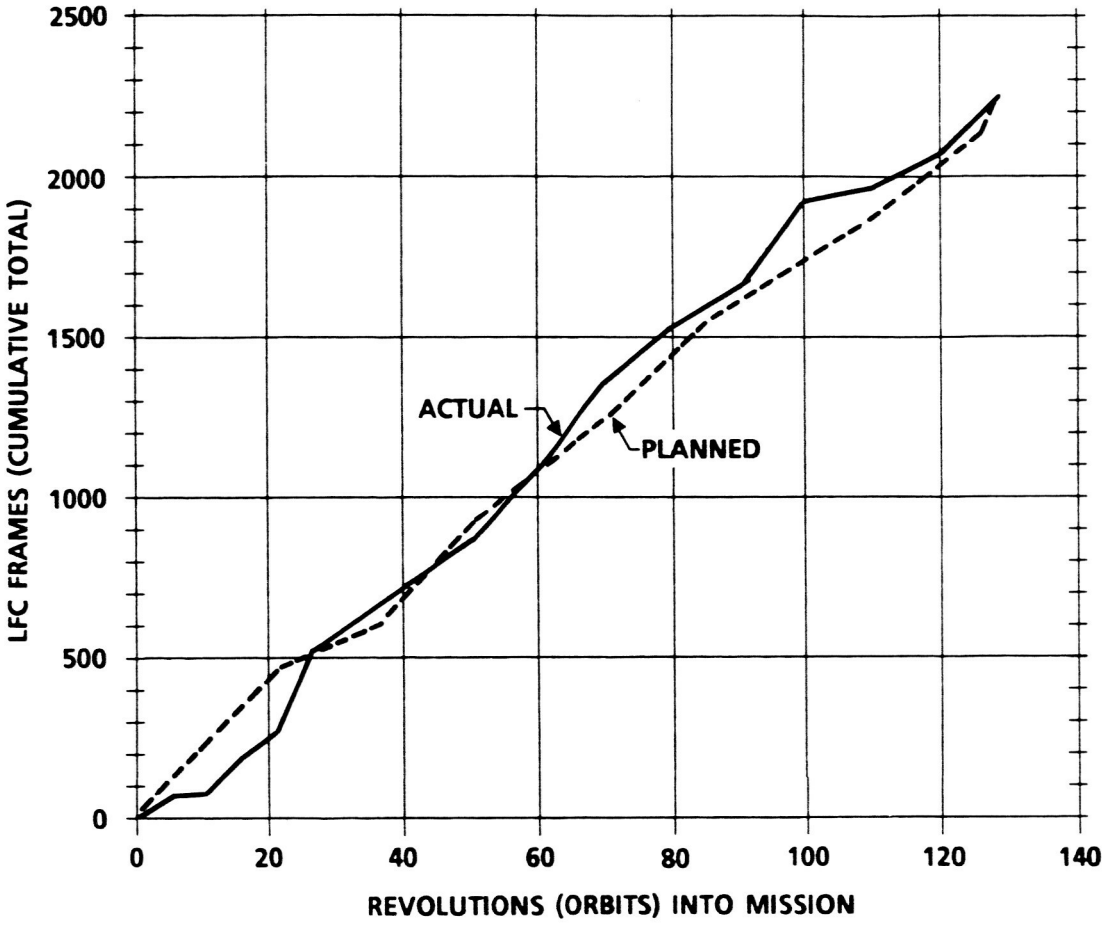


Figure 2-6.- Planned and actual film consumption by the LFC during STS 41-G.

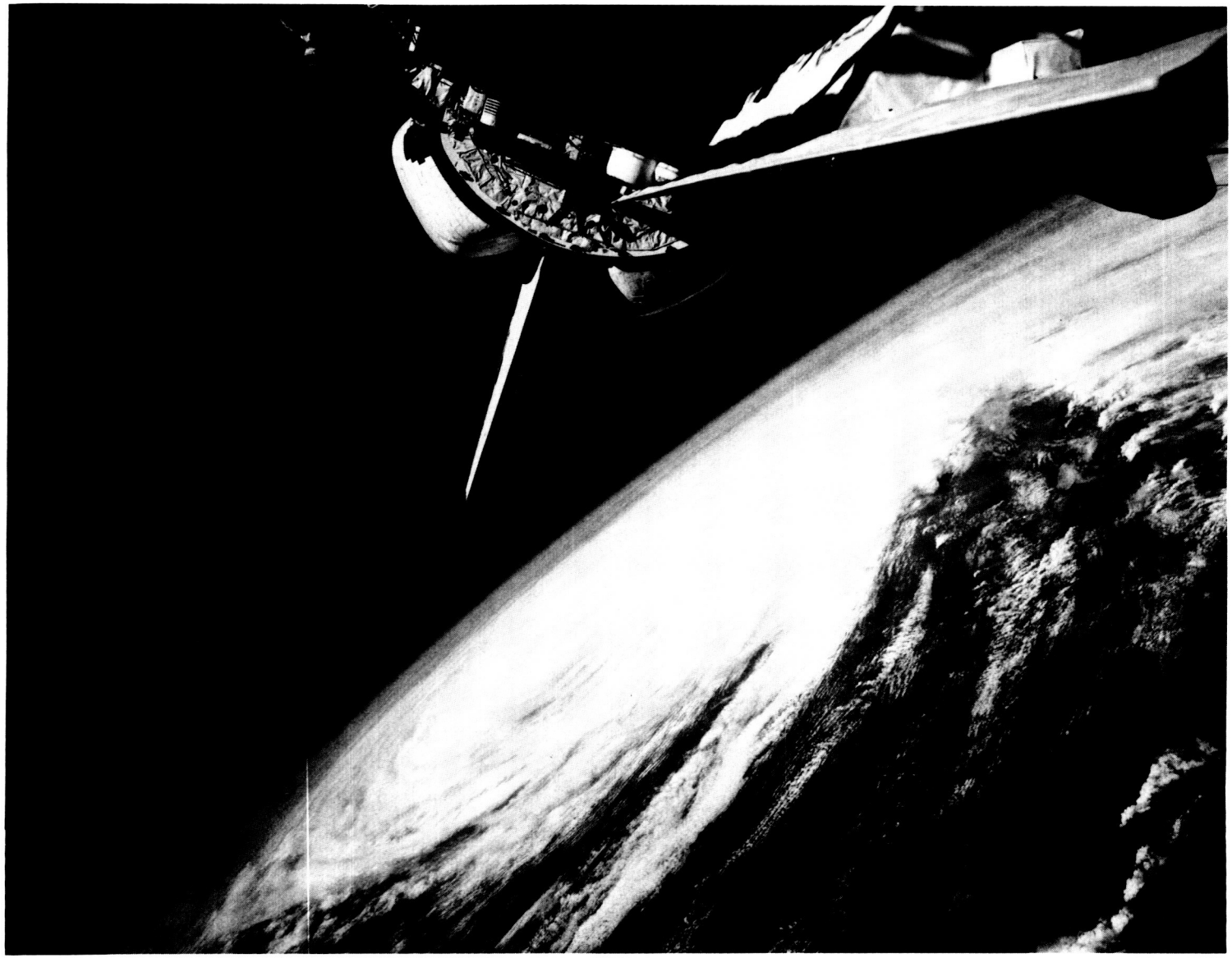
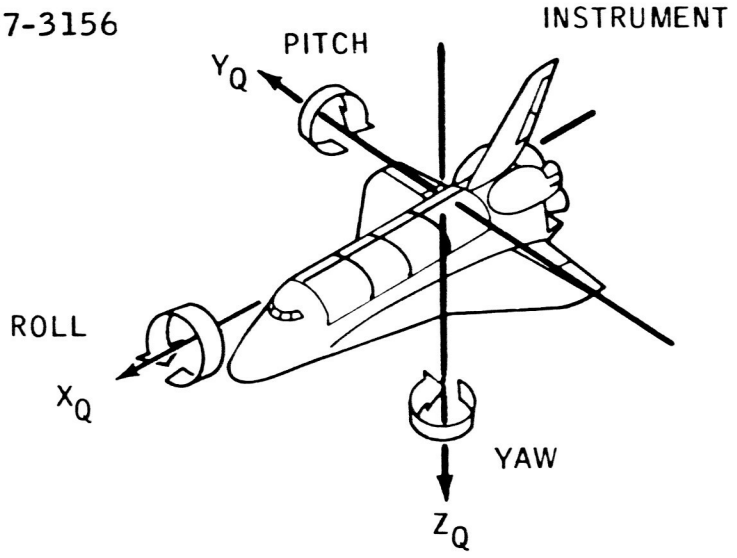


Figure 2-7.- Photograph of the LFC at the completion of the oblique data pass to acquire imagery of Hurricane Josephine off the U.S. eastern seaboard. (NASA photo S17-121-099.)

NASA-S-77-3156



NAME:	INSTRUMENT POINTING COORDINATE SYSTEM
ORIGIN:	INSTRUMENT CENTER LOCATION
ORIENTATION:	THE X_Q AXIS IS PARALLEL TO THE CENTERLINE OF THE **CARGO** BAY, POSITIVE IN THE DIRECTION OF THE NOSE OF THE ORBITER THE Z_Q AXIS LIES IN A PLANE PARALLEL TO THE PLANE OF SYMMETRY AND IS PERPENDICULAR TO THE X_Q AXIS AND IS POSITIVE DOWN IN THE LANDING ATTITUDE THE Y_Q AXIS COMPLETES THE RIGHT-HANDED SYSTEM
CHARACTERISTICS:	ROTATING RIGHT-HANDED SYSTEM

Figure 2-8.- Orbiter vehicle reference axes.

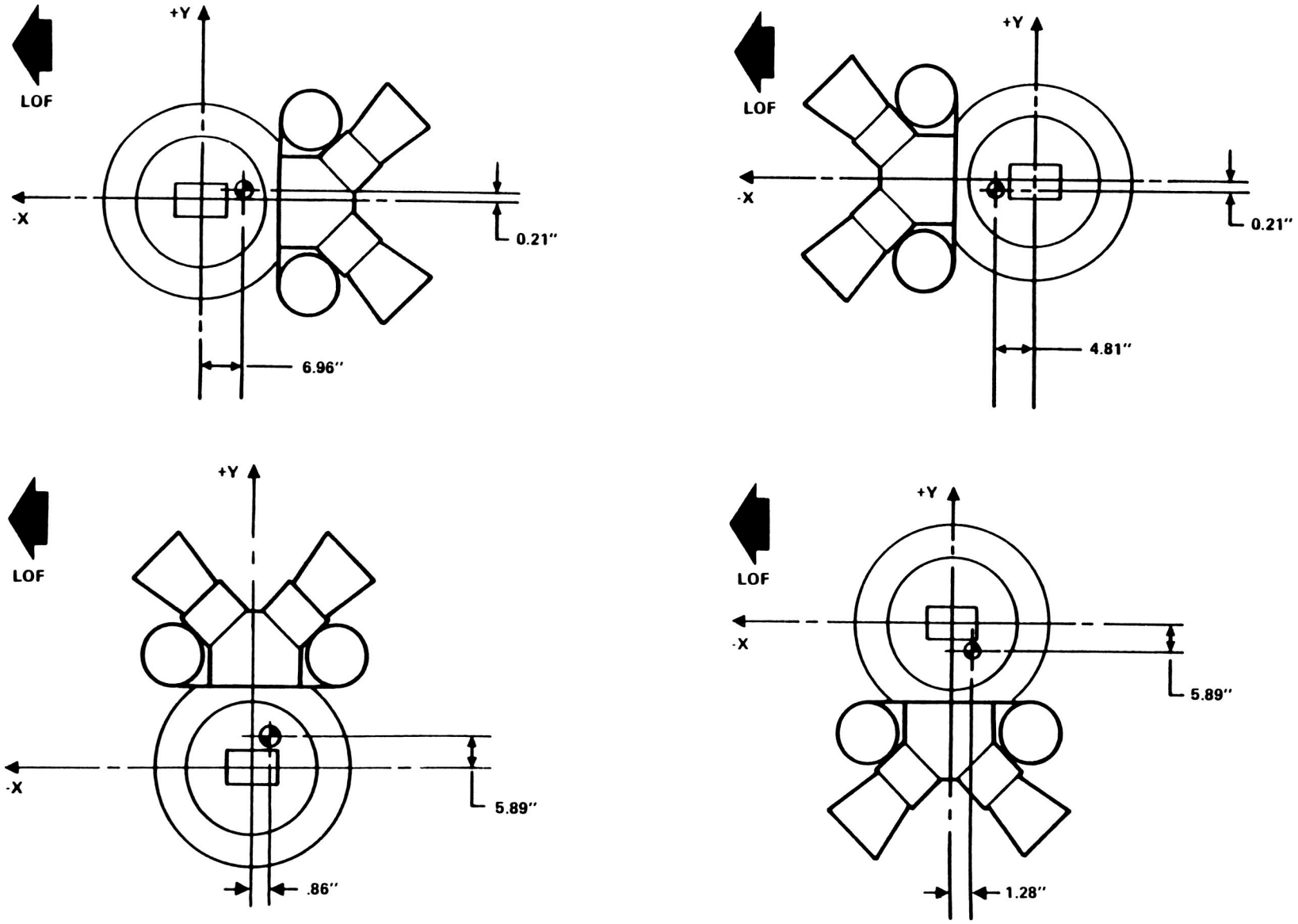


Figure 2-9.- Mounting options for attachment of the SCA to a constant LOF of the LFC.

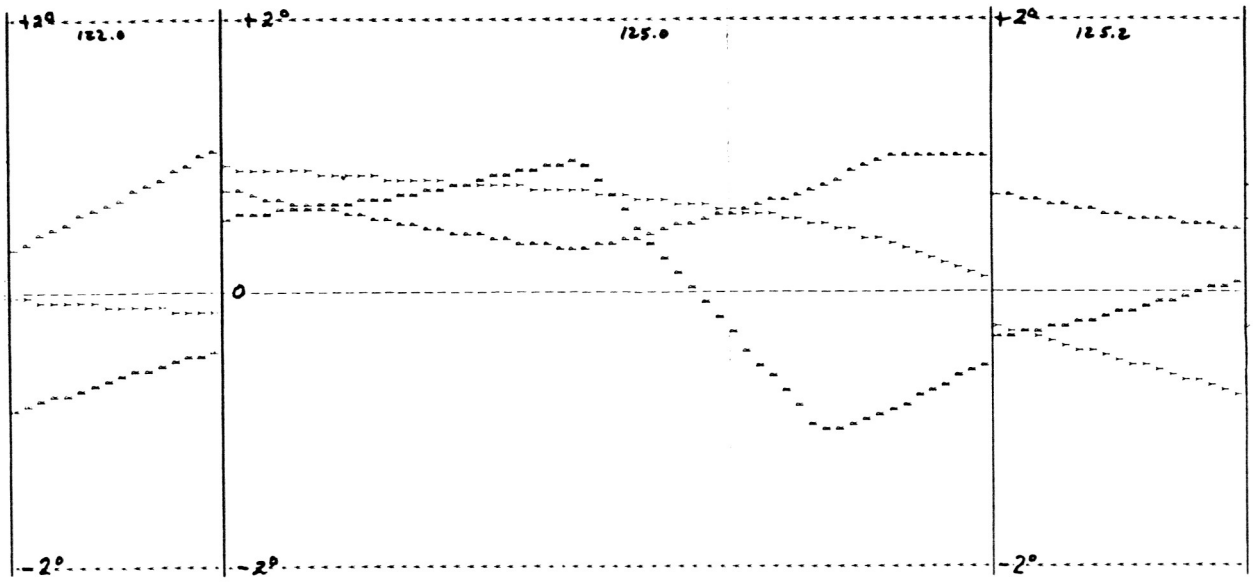


Figure 2-10.- Roll, pitch, and yaw deadband with the crew awake and performing onboard activities – data pass 125.0. (Sampled at 10-sec intervals.)

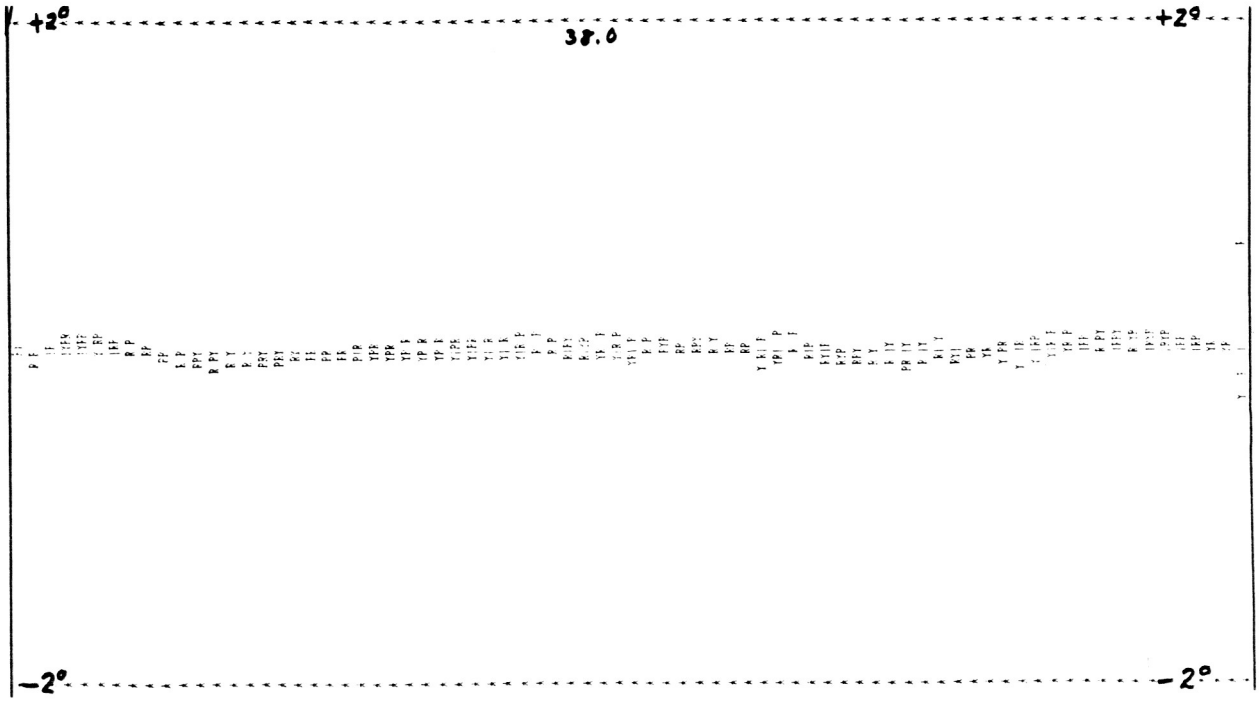


Figure 2-11.- Roll, pitch, and yaw deadband maintenance during crew sleep period – data pass 38.0. (Sampled at 10-sec intervals.)

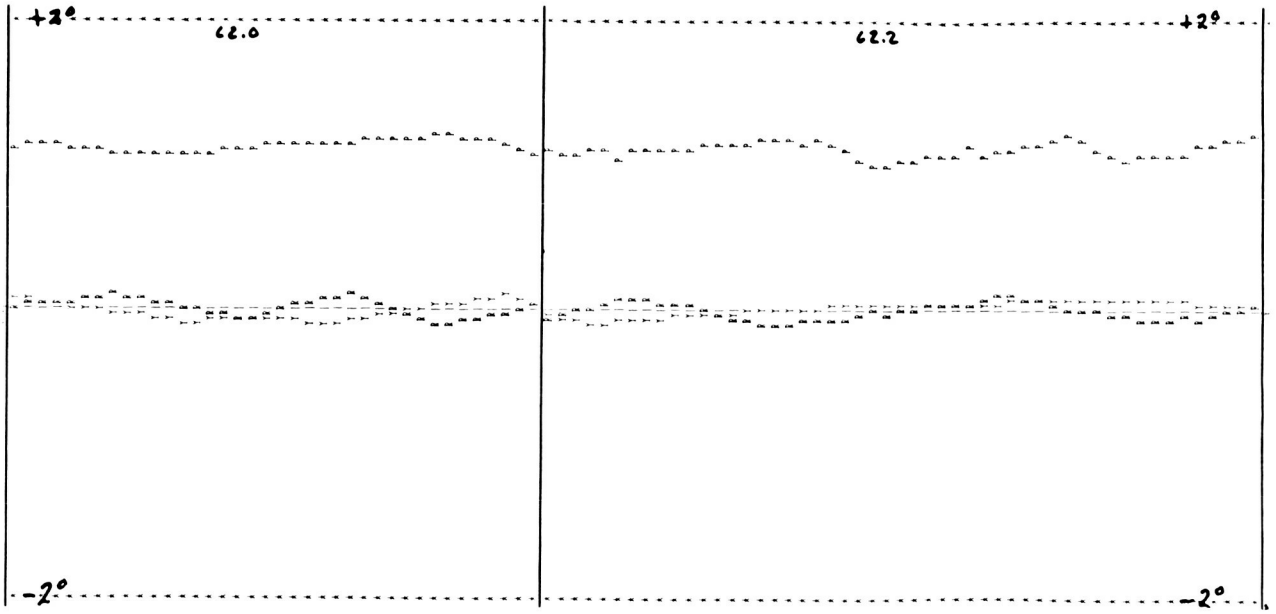


Figure 2-12.- Roll, pitch, and yaw deadband maintenance during crew sleep period, both passes made on orbit 62. During this orbit a continuous 1.127° nose-up pitch attitude was inadvertently maintained. (Sampled at 10-sec intervals.)

3. MISSION ANALYSIS

The obvious statement of any analysis is the quality of the end product. However, there are many other facets which contribute to both the end product and those elements required to produce that end product. All of these elements, which must perform in concert, include the various design disciplines (mechanical, electrical, optical, environmental, etc.); mathematical computations and solutions; empirical and statistical data (orbital mechanics, geographic reference points, terrain characteristics, etc.); software design/generation and planning programs; and people with the ability to integrate these elements.

Therefore, prior to a discussion of the imagery and its uses, let us first consider some of the system elements - how well they performed their functions and their adequacy to complement the overall system design. We obviously want to verify that the design met and satisfied the anticipated and experienced mission parameters.

3.1 DESIGN VERIFICATION

Challenger's flight as STS 41-G offered the opportunity to deploy and verify the various design and operational elements of the OCPS in the precise environment for which it had been specified. Though there were several changes to the timelines (scheduled operations), this mission was a "nominal" mission that satisfied all of the anticipated factors. It was a good mission for use as verification of those design and operational benchmarks required for follow-on mission deployments. Though the flight system had been "flown" on simulated missions in the laboratory in the anticipated thermal and vacuum environments, it had never seen the spacecraft's mechanical, electrical, and command interfaces.

Once the OCPS System had been integrated into the host carrier structure, the MPESS, and simulated spacecraft electrical and command functions at the KSC launch site, several preflight discrepancies were detected. In fact, this is precisely why this sort of testing is so important to major payload systems.

This is where threshold voltage and signal-level discrepancies will show up; mechanical attach point discrepancies will become evident; connector mismatches will be readily apparent; and a host of minor malfunctions, problems, and annoyances may occur.

It was no different with the OCPS, and there is no gauge whereby one could say this experience was above or below the norm. The LFC had one mismatched connector, as did some of the OSTA-3 instruments, and the problem areas were found to involve identical connectors from the same manufacturer. This error was a keying error at the connector manufacturer's facility whereby the pins on the instruments were to design but the sockets on the mating harnesses were offset less than a full pin when the key was set.

Several design errors in the OCPS threshold signal detection levels were isolated for the extreme low levels of the interface. A few operational anomalies within the OCPS components were also detected during this phase of testing that were not obvious during earlier simulations, and some were not detected until after flight. Fortunately, there was time to effect modifications at KSC on most of these. For those which could not be fixed in the field or for the one which had no immediate resolution, workarounds in the flight operational procedures resolved the problem until a fix could be developed and effected postflight. In all respects, the OCPS components lived up to their expectations, and postmission inspection revealed a clean and healthy group of instruments. There was absolutely no degradation or contamination of any component as a result of the 8 days and 5 hours exposure to the orbital environment or the launch and landing environments.

The durability of the OCPS components in withstanding the rigors of both the laboratory and the space environments is certainly evidence of design verification; but before we further examine the OCPS and its STS 41-G performance, let us review some historical facts of interest.

When running time is considered, it must be pointed out that the LFC lens cone assembly has both clocks (for time) and counters (for events); the same is true for the film magazine assembly. The clocks start running when the

system is in an operate mode and motors are operating, and they stop when the system is returned to the standby mode or powered down. The counters record events: for the lens cone assembly, this is a capping shutter actuation (an exposure for a photograph); and for the film magazine assembly, this event is the transport of a frame of photography.

In the laboratory, these two assemblies are capable of being operated independently of each other for specific test objectives; or the combined assemblies can operate as an integrated unit. For this reason, it would never be expected that either the two clocks or the two counters would read the same. A final reading of these devices was made on May 19, 1986, after their final power down and preparation for storage. A summary of running times and events is given in table 3-1. (Similar recording devices were not included within the SCA.) This would appear to present a rather stable picture of the level of design, manufacturing, and maintenance quality of the LFC when one considers periods of operation covering a time span of approximately 7 years (1979 through 1986) without a major malfunction.

When looking at the environmental acceptability of the LFC as a design verification checkpoint, the cumulative laboratory and flight thermal vacuum environmental exposure times must be taken into account. Prolonged exposure to the laboratory vacuum environment provides many checkpoints to the suitability of system design. This exposure provides, for example, an excellent verification of the integrity of sealing techniques and their materials for systems designed to be pressure vessels, such as the LFC. Further, it allows for the verification of complex electrical circuit designs and their various components when these must operate in unpressurized containers (such as the LFC and ARS electronic assembly packages). It also provides a check on both components and materials susceptible to outgassing. In addition, it provides a thermal shock exposure when the vacuum chamber walls are super cooled with liquid nitrogen or helium and then heated to create the thermal cycling one anticipates in the space environment; this allows for evaluation of both the thermal protective devices and the heating methods required to maintain thermal stability within the system.

TABLE 3-1.- LIFETIME OPERATING TIMES (CLOCKS) AND EVENTS (COUNTERS) OF THE LFC LENS CONE AND FILM MAGAZINE ASSEMBLIES

Milestone/assembly	Time, hr	Events	Equivalents
Lifetime (5/19/86 - Preparation for Storage)			
• Lens Cone Assembly	530.08	76,723	22.09 days[a] 32 rolls[b]
• Film Magazine Assembly	368.50	80,943	15.35 days[a] 33.7 rolls[b]
Demate From Challenger (10/24/84)			
• Lens Cone Assembly	506.20	73,812	-
• Film Magazine Assembly	343.15	77,614	-
Delta for Postmission Testing			
• Lens Cone Assembly	23.88	2,911	-
• Film Magazine Assembly	25.35	3,329	-

[a] 1 day = 24 hr.

[b] 1 roll of film = 2,400 frames (4,000 ft thin-base film).

It must be kept in mind that the LFC was the first component of the OCPS to be built and that the ARS was added some 3 years later. As such, the LFC and LFC subsystem components were subjected to the full series of thermal vacuum exposures during laboratory verification (1980). These components then underwent this same series of tests when the ARS and ARS subsystem components were integrated and similarly tested (1983). These subsystem components included the LFC and ARS electronic assemblies and the LFC's two gas assemblies, the GSA and GPCA. The exposure time accumulation for these environmental sequences is summarized in table 3-2.

3.1.1 SOFTWARE APPLICATION

During the development portion of the LFC program, certain members of the LFC team devoted much of their time to the preparation of unique software

TABLE 3-2.- LFC AND ARS THERMAL VACUUM EXPOSURE SUMMARY

Test dates	Test objective	Test duration, hr	
		LFC	ARS
Laboratory Phase			
May-June 1980	ATV-1[a], Preliminary evaluation	36.5	-
June-July 1980	ATV-2	260.5	-
July 1980	Photo resolution testing	6.5	-
Aug.-Sept. 1980	(Void)[b]	-	-
Oct. 1980	ATV-3	87.0	-
Oct.-Nov. 1980	Photo resolution testing	101.5	-
	Subtotal-1980	**492.0**	-
	(days)	(20.5)	(-)
Mar. 1983	ATV-1	134.0	134.0
Mar. 1983	Static search testing	121.5	121.5
	Subtotal-1983	**255.5**	**255.5**
	(days)	(10.6)	(10.6)
	Total laboratory testing	**747.5**	**255.5**
	(days)	(31.1)	(10.6)
Flight Phase			
Oct. 5, 1984	Launch STS 41-G, GMT 1103		
Oct. 13, 1984	Landing STS 41-G, GMT 1622	197.5	197.5
	Total thermal vacuum exposure	**945.0**	**453.0**
	(days)	(39.4)	(18.9)

[a] ATV = Acceptance thermal vacuum (test).

[b] (Void) = Awaiting availability of vacuum chamber.

programs to assist in the building of command sequences which were to be utilized during the premission planning and command generation phases. These programs were designed to perform major calculations to establish the variables in each film exposure (e.g., shutter speed and FMC for each frame) and to execute precise timing for the data sequence to start and then to cease operation.

During a mission, spacecraft state vectors (groundtrack, altitude, velocities, etc.) are recomputed daily for the upcoming mission day. These are issued during the early evening hours in order to allow command teams to make changes and modifications to an experiment's premission command plan. These changes are necessary to accommodate any timeline discrepancies, trim burns, altitude variations, and other orbit perturbations during the immediate 24-hour period. Using these corrected state vectors allows the experiment command team to adjust for minor variations in the timeline (landfall encounters, altitudes, spacecraft velocity, pointing attitude, solar elevation, etc.) and otherwise refine the chain of commands to be issued during the upcoming 24-hour period.

STS 41-G provided the LFC with an engineering flight to proof not only the hardware system but also the LFC command software programs and the ability of the LFC team members to employ them accurately and rapidly. This mission, because of the frequent timeline changes and altitude variations, provided ample opportunity to proof the software/people components. Without a doubt, the command software segment "came through with flying colors," as evidenced by the many successes in taking advantage of numerous new opportunities for incorporation of unplanned coverage - all on extremely short notice.

3.1.2 COMMAND GENERATION

Once orbit is achieved, the cargo bay doors are opened, and the cargo bay experiments are activated, the premission commands which were built weeks earlier are uplinked to the spacecraft for execution. In the case of the LFC, the first commands were executed some 20 min into the second revolution. The second period of LFC operation was some 20 min into the third revolution.

By this time, a good deal of the mission's orbital characteristics had been verified, and initial corrected flight vector data was released to payload experiment teams. At this point in time it became necessary to make decisions regarding the acceptability of upcoming commands - if they were acceptable "as is" or if they needed to be rebuilt to accommodate any mandatory changes. This is not as severe as it might sound, but it was a serious milestone early on in the mission.

The LFC planning software is composed of a number of sections which, when combined into one program, provide GMT and MET time, altitude, sun angle, velocity of the Orbiter with respect to the earth, and position in degrees latitude and longitude. The software thus determines camera turn-on/turn-off times (based on when the Orbiter is over land), exposure settings for all film filter combinations in the camera, and velocity divided by altitude (V/H) values.

The first section of the program is an orbital mechanics program based on software used to track satellites. A model of the atmospheric drag is utilized along with a model of the earth's gravitational field and a simple oblate terrain elevation earth model. The output from this section provides time data in GMT and MET in increments of time defined by the user (the LFC utilized 10-sec increments) along with latitude and longitude, sun azimuth and elevation, altitude, and orbital velocity.

The second section of the software utilizes a computer-generated world map for landfalls and land loss (a map of all land and major water interfaces), which is stored in the memory with an accuracy of 1° of latitude/longitude. This section determines if the Orbiter is over land by comparing the latitude and longitude generated in the first section to the land/ocean map and subsequently generates 1 bit of data (land or water) for use in determining camera turn-on and turn-off times for photographing land areas. In order to conserve program run time, the map is made up of two data bases, one representing 5°-by-5° blocks and another with 1°-by-1° blocks. Where a 5°-by-5° block is not entirely land or ocean, reference is made to the 1°-by-1° block data for determining land or ocean. For the STS 41-G mission, this map

covered those areas falling between 60° N and 60° S latitudes, as shown in figure 3-1. (Map resolution is 1° of the earth's coordinate system.)

The third section calculates exposure time (shutter speed) using data based on a nomograph containing sensitivity curves for film, transmission of filters, camera parameters (lens T-number or aperture), sun angle, and target albedo. The albedo is stored in the computer as a map similar to the landfall/land loss map (see figure 3-1) and to the same spatial accuracy. The stored camera operational curves and operating points for film density are chosen by the user and are obviously camera and film unique. Output from this section is a list of exposure settings based on the above curves, albedo map, and sun angle for each of the film filter combinations required at the time intervals defined in section one of the software.

The fourth section of the software calculates V/H based on orbital velocity, Earth's rotational velocity, an oblate earth model, orbital altitude, and the orbital inclination. The computed value for V/H is uplinked to the LFC along with the other command parameters for a particular data pass. This command is used by the LFC to determine the required film platen velocity to compensate for forward image motion. The LFC also uses this information to calculate the time interval between successive exposures (frame rate) required to obtain the commanded percent of forward O/L between frames (e.g., 80, 70, 60, or 10 percent).

The final output from the combined sections is a file containing GMT, MET, orbit number, V/H, latitude, longitude, sun angle, film filter exposure settings, albedo value, and land/sea definition for 10-sec increments of time along the flight path. The information is provided for a duration of flight time specified by the user (typically 24 or 48 hr). Propagation errors due to the orbital mechanics software were within 1,500 m position after 16 consecutive orbits.

The output file is then utilized by additional software written in basic and is run on a PC to build a final command plan. This plan consists of initial setup commands (filter selection, exposure, automatic exposure selection,

exposure bias, V/H, film type, thermal door position, percent of O/L, and FMC inhibit selection), a turn-on command with associated time, and commands for V/H and exposure changes with associated times to be executed during the course of the data take.

The LFC turn-on time is determined by acquisition of land from the landfall/land loss map and is modified such that the leading edge of the first frame taken is at the land/water interface. The modification is a function of the footprint size at the orbital altitude and the time delay from turn-on to the time of first exposure (12 sec for the LFC). In a similar manner, LFC turn-off time is modified in order to have the trailing edge of the last frame be near the land/water interface.

Other software written for the PC calculates the number of frames to be expended during data takes, based on input from the command plan generated in the command planning software. Output from this program shows orbit number, pass number, and the number of frames used on each pass - as well as a running total - and is output to the printer. This data is used to plan desired locations of film changes and film utilization during the mission (see figure 3-2.)

The landfall map (figure 3-1) became the base for prompting the LFC to start and cease operation, allowing a sufficient time for the LFC to be removed from standby mode and placed into operate mode and to begin running just prior to land acquisition in the LFC FOV; it then continued to operate until land was lost from the FOV. Subroutines allowed for selective elimination of large areas of land masses when these areas contained no desired target areas. In such areas, the landfall map treated them as it did oceans; i.e., as an area of avoidance. However, when the need for coverage of oceans was required, simple changes in the command sequence allowed override of the land/water boundaries. Because of its highly successful application during the STS 41-G mission, and in anticipation of a near polar inclination in the future, the landfall map was revised to cover all land and water interfaces between the two poles. In addition, this mission demonstrated the feasibility to target the LFC for remote Pacific atolls and islands, and it was

decided to include all above water land masses in this map revision as shown in figure 3-3.

The albedo map employed the same geometry as did the landfall map, but reflectance values (albedo) were applied to all land surfaces. For the STS 41-G mission, this map contained only those areas falling between 60° N and 60° S; gross albedo change boundaries were employed, and the values were restricted to 3-, 12-, 20-, and 30-percent reflectance values. This map has now been expanded to cover land masses from pole to pole and to give finer resolution on albedo values over the extended range of 3 to 80 percent (see figure 3-4.) The use of landfall and albedo maps during STS 41-G made it possible to rapidly reformat and calculate the pass parameters at each daily update.

The LFC is a wide FOV instrument and from orbital altitudes will cover a vast area. This means that there are times when scene components will represent extreme ranges of albedo values, such as for barren deserts and lush river valleys (western and eastern deserts of Egypt and the Sudan and the Nile River Valley) or for coastal or inland rain forests adjoining inland or coastal desert regions (South America and Australia). For this reason the LFC albedo maps must be general in coverage, yet have sufficient small-area resolution (1° by 1°) to allow for smaller area targets of opportunity. However, the LFC used B&W emulsions (Kodak types 3412 and 3414) as the primary films because of their extreme tonal range and exposure latitude.

3.1.3 COMMAND SEQUENCING

Commands for a given pass are built in the order they are to be issued to the LFC and are "time tagged" for their callup for issue. This tagging is keyed to the mission elapsed time (MET) timer, which is directly calibrated to GMT used in LFC parameter calculations.

Each command set uplinked for each data pass establishes the initial startup configuration for the LFC (e.g., film type, filter, shutter speed, percent forward O/L, and V/H). As the data pass continues, commands for V/H and

shutter speed are updated to reflect a slight increase or decrease in altitude and an increase or decrease in the sun azimuth and elevation. The time at which these changes become effective is a product of the calculations resulting from the software programs just discussed. A typical LFC command set that was generated for the STS 41-G mission is shown in figure 3-5.

When the LFC operate periods occur during periods of Orbiter AOS, these commands can be uplinked for execution in real time or stored in the Orbiter GPC or the PCS for execution at the proper time. However, if the operate period is to be during periods of Orbiter LOS, the command set must be uplinked during a period of AOS and stored for issue at the proper time. Occasionally, a portion of a data pass was during a period of LOS, be it the start or end or in between. These portions must be in storage onboard before the LOS period is experienced.

As part of the LFC system proofing during the STS 41-G mission, the people, the command scheme, and the supporting software systems, it can be stated, worked perfectly with far fewer anomalies than would be expected for an initial flight. Though a follow-on mission could have been flown without making any alterations, those team members immediately involved with the system command function incorporated into the methods and sequences many improvements which are ready now for future use.

3.1.4 THERMAL PERFORMANCE

During both the design and development phase and the environmental testing of the OCPS flight hardware components, thermal stabilization of the optics network (glass, focal plane, supporting box, etc.) was paramount to ensuring maximum reliability, stability, and repeatability of the image. In ensuring this stability at a given thermal set point at which all optical laboratory procedures were accomplished, maximum sharpness of image (resolution) and stability of geometry (image distortion) are ensured.

The thermal responses of several critical areas were monitored throughout the mission as downlist telemetry of these temperature measurements. These

proved that the LFC thermal design and means of active heating and passive cooling were highly successful. Two critical temperature points, the film platen and the lens cell (see figures 3-6 and 3-7), show the stability of these two monitored points at three time intervals during the mission. The allowed thermal envelope was 21° ± 1° C.

There was one very critical point which did not stabilize at the desired thermal setpoint. This was the LFC lens support structure, which holds the lens cell assembly and supports the focal plane (mounted within the film magazine). This structure performs two major functions in addition to providing mechanical support. First, it maintains a fixed position of both the focal plane and the lens cell assembly, which is directly responsible for maintaining system focus. Secondly, it serves as a thermal path for removing heat from the lens cell and focal plane. Similarly, it serves also as a path for conducting heat into these two locations. In figure 3-8, the thermal history of the camera support is shown to be unstable when compared to those measurements shown in figures 3-6 and 3-7. A launch site modification to the LFC thermal enclosure by the integrating organization may have created this unstable condition.

3.1.5 ATTITUDE CONTROL

Pointing attitude of the spacecraft and stability at a given attitude are most important to an instrument such as the LFC. By the nature of its intent, the LFC's optical axis must be maintained in alignment with the earth nadir point while in operation. This is not a function under the LFC's control but is a reflection on the crew's ability and the spacecraft's guidance and control system.

When the crew are awake and active, there are natural minor disturbances in attitude stability of the spacecraft. These disturbances are due to the microgravity forces exerted on the structure through use of the structure itself as a means of in-cabin mobility. A force is exerted when a crew member uses the walls to push against in order to change location; an opposite force is exerted, of course, when his motion is arrested. However,

these "drifts" about the nominal are corrected by the Orbiter's Reaction Control System (RCS) low impulse jet. On the STS 41-G mission, this stability about a given pointing vector was much finer than the advertised deadband of ±2° in roll, pitch, and yaw. This should serve as a great testament to the crew's abilities as well as the Orbiter control system. A typical example of the Orbiter's pointing stability within a 2° deadband was shown earlier, for data pass 125, in figure 2-10.

Since the planning of LFC operation was based on a 24-hr day of access to targets, much of the LFC data acquisition was accomplished during crew sleep periods. With the crew asleep, these quiescent periods demonstrated very low-level changes in pointing attitude. This stability within a deadband was demonstrated in figure 2-11 (for sleep periods during orbits 38 and 62) and is typical of periods during which the crew were asleep. In regard to LFC operation, the Orbiter is a very stable platform for data acquisition, and the demonstrated deadbands and rates within these deadbands are more than acceptable.

3.2 PERFORMANCE VERIFICATION

The ultimate evaluation of a flight system is examination of the data product. One can look at a multitude of incoming telemetry data, evaluate how smooth or rough the flow of mission command functions went, note how well the "team" held up under pressure, and then make an immediate assessment of mission planning and execution. The final grade is on quality of the data produced and its usefulness to the user community. This is where the total people/system combination is measured as a single unit. The following sections will highlight those areas which were analyzed to render this final evaluation and to show some of the examples used during this analysis.

Throughout the remainder of section 3, a number of LFC imagery sets acquired during the STS 41-G mission have been included to demonstrate LFC operation

performance. The following comments should be kept in mind when viewing these images.

- Except where noted, the direction of Orbiter flight is from left to right.
- LFC images were reproduced from either a second generation duplicate negative made from the original flight film on Kodak type 2422 (direct duplicating) or from a Polaroid type 55 negative (4- by 5-in. positive/ negative film) made from a second generation film positive made from the original flight film on Kodak type SO-192 (aerial duplicating). In no case are any of the illustrations made directly from the first generation flight film.
- For reasons of space and economy, full LFC frames which have been included have been reduced to 36 percent of their original size (e.g., from 9 by 18 in. to 3.25 by 6.5 in.). Though unfortunate, this reduction was unavoidable.

Figure 3-9 illustrates the scope of LFC coverage at sample orbital altitudes, including the three nominal altitudes of the STS 41-G mission (i.e., 360, 260, and 222 km) and compares sizes of the area covered to those for a standard 6-in. cartographic camera and for the LFC if flown in aircraft at very high altitude (18.3 km. or 60,000 ft) and high altitude (9.1 km, or 30,000 ft). Table 3-3 is included to summarize the area coverage of the LFC and a standard aerial cartographic system (aircraft altitudes only) illustrated in figure 3-9.

3.2.1 ALTITUDE COMPARISON

During the very early planning phase for the LFC's initial flight, a request was formalized to allow the mission to be flown at a minimum of two discrete altitudes. Though the LFC is considered to be a major payload, the requirements of one payload must be weighted against the requirements of other payloads. At the time, the LFC's initial flight was scheduled for STS 41-D, which was to be the maiden voyage for the Discovery vehicle. Since this mission was to deploy and then retract a large solar panel, only a single predetermined altitude was possible. After the second pad abort, this

TABLE 3-3.- LFC/AERIAL CARTOGRAPHIC GROUND COVERAGE

Camera	Altitude (km)	Photo scale	Footprint (km)		Area coverage (sq km)
			Along track	Across track	
LFC (orbital)	[a]360	1:1,181,700	540.3	270.2	145,900
	296	1:972,800	444.8	222.4	98,900
	[a]259	1:851,000	389.3	194.6	75,800
	[a]222	1:729,600	333.6	166.8	55,600
	185	1:608,000	278.0	140.0	38,600
LFC (aircraft)	18.3	1:60,000	27.4	13.7	375
	9.1	1:30,000	13.7	6.9	94
Aerial cartographic camera	18.3	1:120,000	27.4	27.4	750
	9.1	1:60,000	13.7	13.7	187

[a] Nominal STS 41-G altitudes.

mission was combined with a later mission, the payload configuration was modified, and plans for the LFC were deleted.

The scheduled second flight of the LFC on STS 41-G then became the initial voyage. For this flight, a modified request for three discrete altitudes was granted, and the nominal altitudes of 365, 263, and 230 km were established. The plan was to fly the maximum altitude for the first day and deploy the Earth Radiation Budget Experiment Satellite (ERBES), descending to the intermediate altitude for a stay of approximately 17 hr and then descending to the lower altitude for the remainder of the mission.

Since it was impossible to intermix the four film types at a number of locations to provide sampling of each film type at the three altitudes, a large quantity of type 3414 film was positioned to be at the head of the roll and at frequent locations in the roll. This would, it was hoped, allow the acquisition of an identical target - or near identical target - at each of the three altitudes. Early on into the mission, however, the necessity for rapid changes to the timeline became apparent because of onboard problems and inclement weather at the earth level.

It was possible to get some representative targets with relatively dry air columns above and others with clear but moisture laden air columns. Though no single target was recorded at each of the three altitudes, several suitable urban targets were acquired at each altitude, and a relative analysis can be made of these as regards quality of image structure (edges of objects, primarily) and detection and identification of objects. A case in point is a pass over Tubruq, Libya (see figure 3-10), a major Mediterranean petro port, during the second STS 41-G orbit. This was at an altitude of 360.52 km and at a photo scale of 1:1,183,000 on the LFC negative. Though shipping activity is not evident in the imagery acquired on this pass, we can discern the dock facilities and identify the large oil storage tanks in the heights above the harbor.

A target area similar to the Tubruq site is shown in figures 3-11 and 3-12. This is also a Mediterranean petro port. This one, which is located at Port aux Poules, Algeria, was photographed for the first time on orbit 3 from an altitude of 361.5 km (photo scale of 1:1,186,000) and the second time during orbit 66 (94 hr later) from an altitude of 231.9 km (photo scale 1:760,700). As with the Tubruq site, there are oil storage tanks in the heights, but there is a large tanker moored to a loading terminal in both passes. This gives a graphic demonstration of the impact of orbital altitude on image quality.

It is not at all uncommon in orbital photography for the imaging system to record repetitive man-made objects which, with suitable ground truth information on their composure, can be used to augment the analysis effort. Such targets are usually of a higher contrast than desired, but they do appear much as the bar target arrays used in the laboratory. The LFC acquired numerous targets of these types during the STS 41-G mission; figure 3-13 shows two such sites - first in the vicinities of Bursa, Turkey, during orbit 17 from an altitude of 363 km and then during orbit 32 over Yerevan, Armenia, from an altitude of 266 km.

A pronounced bar target array sometimes presents itself, such as that shown in figure 3-14, imagery acquired during orbit 44 over Toyama, Japan, at an

altitude of 229 km. This large multiwinged building adjoining the seaport was acquired during a test of the LFC's FMC to evaluate the effectiveness of controlling image smear.

3.2.2 FILM COMPARISON

One major reason for carrying four film types in the LFC was the hope of acquiring the same ground target on each of the film samples flown. The three altitudes flown and the orbit ground track adjustments due to these altitude changes made this a rather reasonable plan. The great amount of sidelap of LFC footprints at the higher latitudes increased the probability of this happening should the weather over any given site permit. The probability of having this happen at nearly identical altitudes was, however, extremely remote.

A number of desirable sites were recorded on two types of film (Australia, North Africa, and Eurasia); one well-documented resource test site (Medicine Hat, Alberta, Canada) was recorded on three film types; and one site (Flin Flon, Manitoba, Canada) was recorded on all four film types.

The site at Flin Flon afforded fleeting opportunities because of the extremely poor weather in the northern hemisphere, but this local area was found open on 4 of the 5 successive days it was overflown. It was found relatively clear on orbits 21, 37, and 53 (days 280, 281 and 282); was closed in on orbit 69 (day 283); but was open on orbit 85 (day 284). Figure 3-15 shows progressive magnifications of this relatively isolated site; imagery was acquired on the first pass (orbit 21) from an altitude of 366.71 km at a film scale of 1:1,203,000. Reaching further into the industrial area (smokestack) and comparing the image structure quality on the four film types for this site, figure 3-16 reports all four at a magnification of 35X from the film size, and figure 3-17 repeats this coverage at a magnification of 100X.

Medicine Hat in Alberta, Canada, has long been an earth resource test site because of its rich agricultural content. Unfortunately, during the STS 41-G

overflights in early October, this site did not have the range of crops in production that are noticed during the spring and summer seasons. There are cultural features that can be used for landmarks in comparing the relative performance of film types used from the orbital vantage point. Photographs of the city of Medicine Hat show a golf course (figures 3-18 and 3-19) which had green grass at the time of the STS 41-G overflights; bridges over the river running through the center of the downtown area (figures 3-20 and 3-21); and the municipal airport (figures 3-22 and 3-23). All of these features can be used for both low contrast and high contrast performance comparison. Unlike Flin Flon, which is at approximately latitude 54.8° N, Medicine Hat is at approximately latitude 50.1° N. At this lower latitude, during the descending phase of the orbits, the sidelap in imagery begins to decrease, and this target site was imaged on only three orbits (54, 70, and 86) of the five for which imagery was acquired in this area of Canada. All three tracks were at approximately the same altitude, but three film types were sampled during these excursions.

Because of the comparatively poor spatial resolution performance of color film materials (SO-131 and SO-242) as compared to the much higher performance B&W materials (types 3412 and 3414), a cursory look was made, as a part of the film evaluation, to review the relative merits of recovering spatial data by tricolor separation of the color materials. This procedure would yield a B&W product, of course, but it does offer salvage potentials in some instances. Some of the preliminary results obtained are included for their curiosity value (see figures 3-24 through 3-28).

3.2.3 PHOTO RESOLUTION

Probably the greatest curiosity relating to any orbital imaging system eventually comes down to its relative ranking in terms of resolving power. Even the term "resolving power" is ambiguous, because resolving power requires definition in terms of units of something that can define a resolution element. Through the years, many treatises dealing with this subject have been expounded and expressed in terms of lines per millimeter (l/mm), line pairs per millimeter (lp/mm), and modulation transfer function (MTF, in

cycles per millimeter) - and then along came electronic imaging devices that used new terms such as "raster" and "pixel." All of these were to give a set of measuring units for a resolution element that could be used to calculate and express what size objects one could see from great distances. Arguments inevitably arise as to whether a line, cycle, or pixel makes up a "resolution element."

There are, of course, other qualifiers relating to the greater or lesser visual contrasts of objects being recorded, be they bar targets, Sieman stars, or whatever. These contrasts have been expressed in the form of ratios, and referred to as test object contrast, or target object contrast (TOC). These are designated as high contrast (1,000:1), medium contrast (5:1), or low contrast (2:1 or 1.6:1) - and various ratios in between - when, in actuality, there is little or no difference between a 1,000:1 TOC and a 10:1 TOC, considering photographic film emulsions.

A ship sitting on smooth, clear water in a harbor with no sun glint from the surfaces (assuming the ship is of some bright finish) will render probably one of the highest contrast targets one might experience from the space vantage point. Such a target might exceed a contrast ratio of 5:1, or even 7:1. Similarly, large buildings roofed with bright metal or white gravel might equal or even exceed these contrast ratios. On the whole, however, most of the target areas recorded from space are in the lower end of the contrast ratio range, seldom exceeding 3:1 or 4:1, unless it is a specular reflection of the sun from a bright metal roof or an aircraft flying over water.

So with all of these yardsticks and variables, one can calculate rather favorably what ground resolved distance, or ground resolved dimension (GRD), he might expect to see during a given space flight mission. This new unit of measure, GRD, needs some clarification. Is this the distance between two objects or the size of an object? And is resolution the detection of an object or is it the identification of the object? In order to make this determination, one must really go beyond these quantitative yardsticks and look at individual targets and evaluate their "edges." The edges of

individual target components may be rounded (oil storage tanks, sport stadiums, etc.) or straight (buildings, residences, etc.). One must use care not to select boulevards, highway interchanges, cloverleafs, highways, airport runways, or anything of great linear dimensions, for he will soon think he is seeing trucks and automobiles. Linear enhancement makes even a relatively poor system look like an outstanding performer.

With the sampling of magnified images shown so far, one may study the following examples (figures 3-29 through 3-36) selected from hundreds made of numerous LFC frames exposed during the STS 41-G mission. In many cases GRD's of less than 10 meters to as much as tens of meters within a single frame are seen at each of the three altitudes flown during this mission. Again, this is because of the amount of enhancement of a given target, due to both contrast and angularity. Some evaluators have reported GRD's of only a very few meters in photographs of areas with which they have great familiarity - detection or identification? A "blip" where something is supposed to be can put a real bias on objectivity.

3.2.4. SYSTEM COMPARISON

When a group makes an initial flight with a new hardware item, the compulsion is to place it against some other yardstick to see how it compares to other systems of comparable design or application. Members of the LFC analysis team were no different in this regard, because comparison gives such a group a point for satisfaction, or dissatisfaction, in the fruits of their labor. But most of all, a careful analysis gives a synopsis on the types of film imagery available from the current state-of-the-art Shuttle era camera technology.

In a system comparison, the obvious first point is to compare it to a generic progenitor - in the case of the LFC, the aerial cartographic camera. The LFC and its air breathing counterpart are both specific in that integrity of internal geometry is paramount. The application of cartographic quality systems in earth orbit is very limited at this point in time, but the European Space Agency (ESA) has flown one system, the Metric Camera (MC),

during their Spacelab mission in December 1983. This camera was a modified Zeiss RMK 30/23. In addition, NASA has flown several types of hand-held crew cameras in low earth orbit during the Shuttle era.

One must be extremely careful in this type of comparative analysis and maintain as much objectivity as possible, since both the variables and the unknowns of such a qualitative comparison could be boundless. In regard to the LFC and the other NASA camera systems, near equity was reached, in that comparative test imagery was a second generation film positive material [e.g., a film positive made from the original negative (or positive)]. At this point, the field began to widen, in that the LFC imagery was made on a very high spatial resolution B&W negative material (Kodak type 3414) and then printed on a very high film positive print material (Kodak type SO-192). Using this combination resulted in the best of all worlds, with a loss in spatial resolution of less than 10 percent in going from the original to the progeny.

It was a different case with the other NASA systems, in that they use a color positive material (Kodak type 5017) for the original, the second generation being duped on color positive reversal print stock (Kodak type 2447). In these instances, system spatial resolution is "film limited." In the case of the two aircraft imagery sets (Boston and Somalia), the original film, the generation of imagery, and the print material are all unknown. In the case of ESA MC, two types of film were used - a B&W negative material (Kodak type 2405) and a color positive infrared material (Kodak type 2443). It is safe to say that the imagery produced by the ESA MC is "film limited" in regard to spatial resolution. Table 3-4 demonstrates the manufacturers' ratings on the photographic film emulsions used by the systems in this comparison.

There is a commonality in the aircraft cameras, the NASA hand-held cameras, and the ESA MC in that high speed films had to be used to allow the use of higher shutter speeds since none of these cameras has means for correcting image smear caused by the extremely high in-track velocities of the Shuttle. The faster the shutter speed, the less smear of the resulting imagery; and the faster the shutter speed, the higher the "film speed" required to produce

TABLE 3-4.- CHARACTERISTICS OF PHOTOGRAPHIC FILM EMULSIONS USED IN SHUTTLE FLIGHTS

Film emulsion		ASA	Aerial film speed	Resolution, lp/mm	
Type/film description				TOC 1000:1	TOC 2:1
LFC					
3412	Panatomic-X Aerographic II	-	40	400	125
3414	High definition aerial	-	8	800	250
SO-131	High definition Aerochrome infrared	-	[a]6	160	50
SO-242	Aerial color	-	[a]6	200	100
2422	Aerographic direct duplicating (negative)	-	(NA)	500	200
SO-192	High resolution aerial duplicating (positive)	-	(NA)	800	250
NASA camera systems					
5017	Ektachrome commercial	64	--	125	50
2447	Aerochrome duplicating (reversal)	-	(NA)	100	50
ESA Metric Camera					
2405	Double-X Aerographic	-	500	125	50
2443	Aerochrome infrared	-	[a]40	63	32

[a] Effective aerial film speed.

[b] Duplicating film only (not flown).

an adequate exposure of the imagery. The LFC, on the other hand, has a means of correcting the image motion during the relatively long exposures (i.e., FMC), and thus little or no image smear exists throughout the full range of shutter speeds.

It is axiomatic that the higher the film speeds, the lower the spatial resolution capability of the material; and the lower the film speed, the

greater its spatial resolution capability. The systems compared to the LFC had no means of eliminating the forward motion smear; they were therefore forced to use high speed film emulsions to allow high camera shutter speeds. The LFC, on the other hand, had FMC capability, which allowed it to capitalize on the use of film materials with very low film speeds and the inherently high spatial resolution capability. It is for this reason that the LFC's spatial resolution performance is "system limited" rather than "film limited," since the B&W negative materials exceed the resolution capability of the LFC optical system. Figure 3-37 is a nomograph which shows the relationship of camera shutter exposure time and the expected image smear (in ground distances). Therefore, constraint should be used in the comparison of the images discussed in section 3.2.4.1, since they are included here for the sole purpose of depicting those data items currently being produced from space for the science and applications communities to use. No attempt has been made to quantify these comparisons, and no attempts should be made; for, indeed, the systems are only benchmarks for a given period in time, and their original objectives and applications differ widely.

3.2.4.1 Aircraft Systems

Since a major objective of the LFC was to produce orbital geometric fidelity to allow the production of 1:50,000 scale orthophoto maps, the first logical comparative approach seemed to be against aerial photography. A very limited search was made to find samples of aerial photos which covered the same areas that the LFC covered on STS 41-G. The LFC coverage of the continental United States was severely hampered by very restrictive weather conditions over North America during this mission, however, and comparative examples were few. With the help of the Earth Resource Observation System (EROS) Data Center (EDC) in Sioux Falls, South Dakota, one National High Altitude Photography (NHAP) program view of Boston, Massachusetts, was located. A contact print at a photo scale of 1:80,000 was used to compare to the enlarged LFC imagery (original scale 1:758,724) which was acquired at 1355:33 hours on a Sunday afternoon, October 7, 1984. This was from an altitude of 231.26 km, or 758,724 ft (124.8 n. mi., or 143.7 statute miles). By contrast, the NHAP photo was made from an altitude of 12.2 km (40,000 ft) on April 17, 1985,

some 6 months later. Figure 3-38 shows both of these photos at the same scale (e.g., 1:80,000).

If we study the LFC imagery from this frame (frame 0664) at magnifications up to 100 times enlargement (figure 3-39), we can realize the magnitude of the content in a full frame of LFC imagery. This is more apparent if one considers that portion of a full frame of LFC imagery used to make these target samples. Table 3-5 gives the relative areas of these samples. Remember that expression of photo scale at 1:758,725 is to say that 1 in. in the photo is equal to 758,725 in. on the ground (63,227 ft, or 11.97 statute miles), or that 1 cm in the photo is equal to 758,725 cm on the ground (7,587 m, or 7.587 km).

TABLE 3-5.- AREA DATA FOR MAGNIFIED LFC SCENES OF BOSTON, MASSACHUSETTS

[Full LFC frame is 9 by 18 in., or 162 in^2 of imagery]

Scene magnification	Area of original frame, in.	Percent of original frame	Equivalent photo scale
1X	3.0 x 3.0	5.56	1:758,725
4.5X	0.67 x 0.67	0.274	1:168,606
35X	0.09 x 0.09	0.0045	1:21,678
100X	0.03 x 0.03	0.00056	1:7,587

As a point of interest, this data pass over the New England area was unique in that a minimum of five inflight aircraft have been detected over water, over land, and on the final approach to Boston's Logan Airport (see figure 3-40). The aircraft approaching landing at Logan airport presents a rather graphic example of image smear. This commercial aircraft was on approach to Logan's NW to SE runway from the NW and is traveling in the same general direction as the spacecraft. The LFC's FMC is correcting for apparent ground motion in the opposite direction. Granted, the landing speed of the aircraft, possibly as much as 77 m/sec, gives only a slight variable to the spacecraft ground speed of approximately 7,500 m/sec, but it is enough to cause an elongation of the aircraft fuselage, loss of wing tips, and an

apparent absence of horizontal stabilizers. In the same sequence, two other commercial aircraft, one over water (Nantucket Sound) and the other over land (Needham, Massachusetts) but traveling across the Orbiter's ground track, remain intact, as shown in figure 3-41.

The preceding comparison between the LFC and an airbreathing counterpart uses a target of the same vintage (e.g., acquisition periods separated by 6 months). It would be interesting to compare the then-current LFC imagery to aircraft imagery of a somewhat older vintage to see how the demographics of an area can change. Such a comparison was made (see figure 3-42), and the imagery used for the comparison was from an agrarian location in relatively undeveloped countries currently in the news because of both a devastating drought and political uneasiness.

The case in point is the border between Ethiopia and Somalia in the Tug Wajale region, 140 miles due south of Djibouti. The area is devoid of so-called modern urbanization features such as expressways, overpasses, large buildings, and urban developments. The same basic ingredients are present but on a much lesser scale. What was strictly a farming area has suddenly become urbanized by fleeing hordes of starving refugees from the north moving south to escape the decade of drought. Here we can compare the demographics of February 1952 to October 1984, after more than 32 years of change, primarily in the past decade.

Figure 3-42 makes a graphic comparison of these changes within and without the circled area. The Royal Air Force aerial photo (top) was taken in December 1952 from an altitude of 6 km (20,000 ft) and LFC photo (bottom) was taken October 9, 1984, from an altitude of 225.7 km (740,000 ft). Both are printed at a scale of 1:40,000, representing an 18X magnification of the LFC image. As a point of interest, the arrow is approximately 800 m long. In 1952 the major agricultural and community development was on the Ethiopian side of the river. However, recent years have seen the spread of the Somalian development efforts in the area to the point where it would appear that the small town has also migrated across the river and assumed the characteristics of a somewhat modern urban community.

3.2.4.2 Cartographic Systems

The only direct comparison of the LFC to other space-borne cartographic camera systems is currently limited to ESA's MC flown on Spacelab I in December 1983. As mentioned earlier, the MC is a modified Zeiss aerial camera which was upgraded for space applications. The MC is a high performance system capable of great spatial resolution and of great geometric fidelity. Unlike the LFC, however, it had no means for correcting forward motion errors and had to rely on high shutter speeds and high speed film emulsions.

Groundtracks for both the LFC and the MC were studied to assess where common imagery had been obtained. All LFC acquisitions were obtained during the descending phase of the orbit (e.g., direction from north to south), while the MC acquisitions were obtained primarily on the ascending phase of the orbit (e.g., direction of the flight from south to north). This difference simplified the search by limiting it to where the groundtracks intersected, with the exception being that coverage of the Dakotas in the United States, where both tracks were descending. The search was also limited by the desire to have sites with cultural content to give some degree of quantitative comparison.

Several sites were identified, but many of these, upon inspection, had to be eliminated because of atmospheric conditions. When LFC imagery was clear, the comparable MC scene had heavy clouds, or else the LFC scene had clouds and the MC scene was clear. One good site was at Bandar Abbas, Iran, on the Strait of Hormuz (figures 3-43 and 3-44) and a second site at Rapid City, South Dakota (figures 3-45 and 3-46). The site at Rapid City was not an ideal site for the MC because of the low sun elevation and the fact that there was snow on the ground. Both sites were selected since there was also imagery from crew hand-held cameras which had been acquired simultaneously with LFC imagery on the STS 41-G mission.

Though it was not attempted on the MC imagery because of the grain size of the MC imagery, additional penetrations of the LFC imagery were done at

higher magnifications to ascertain the quality of the LFC image structure of the Ellsworth AFB target. The high contrast of the individual targets with linear structures enhances the apparent resolution in the features, as shown in figure 3-47.

3.2.4.3 Crew Camera Systems

On the STS 41-G mission two camera types were available to the crew for use in acquiring hand-held still photography of targets of opportunity using the nine Orbiter windows, located in the forward station (four), overhead (two), aft (two), and side hatch (one). Of these nine windows, only the side hatch window has optically flat glazings. The other windows are of good quality, but as the camera's line of site increases in obliquity to their surfaces, system spatial resolution performance decreases significantly.

The 70 mm Hasselblad 500 EL/M cameras have been a standard in the NASA manned space flight program for many years, being progressively upgraded through the years to incorporate new or improved features. The Hasselblad camera is equipped with interchangeable 50, 100, and 250 mm focal length lenses, and it uses Kodak Ektachrome 64 Professional (5017) film. Its image format size is 5.7 by 5.7 cm (2.25 by 2.25 in.) on 70-mm-wide roll film.

The Linhof Aero Technika 45 camera is a relatively new system which was added to support oceanography investigations for the U.S. Navy. It is an aerial reconnaissance camera which has been adapted for space flight applications; it is equipped with 90 and 250 mm focal length lenses and also uses the 5017 film. A larger format system, 7.6 by 11.4 cm (3 by 4.5 in.), it uses 5-in.-wide roll film. During STS 41-G, the Linhof utilized the 90 mm lens only.

With both systems, the shorter the lens focal length, the greater the FOV and the lower the GRD. With an increase in focal length, the Hasselblad camera shows marked increase in GRD. Both the NASA LFC and the ESA MC have 30.5 cm (12 in.) focal length lenses; their image formats are 22.9 by 45.7 cm (9 by 18 in.) and 22.9 by 22.9 cm (9 by 9 in.), respectively. Table 3-6 summarizes the FOV characteristics of all four camera systems. As a means of

TABLE 3-6.- FOV CHARACTERISTICS OF STS 41-G TERRAIN RECORDING CAMERAS

Camera system	Lens focal length	FOV width		FOV length		Square degrees
		x Ha	Deg.	x Ha	Deg.	
Hasselblad	50 mm 100 mm 250 mm	1.14 0.57 0.22	59.5 31.9 13.0	1.14 0.57 0.22	59.5 31.9 13.0	3,539 1,017 170
Linhof	90 mm 250 mm	0.99 0.36	52.6 20.2	1.27 0.46	64.8 25.8	3,408 519
ESA MC	305 mm	0.75	41.1	0.75	41.1	1,693
NASA LFC	305 mm	0.75	41.1	1.50	73.8	3,036

[a] The term "x H" = factor x altitude.

demonstrating the GRD which might be expected from these Shuttle camera systems on identical targets, a series of comparative target scenes have been selected and photographically enlarged to identical scales. One must remember that relative target resolution quality is a function of lens focal length, film emulsions used, motion correction capabilities, intervening windows, target contrast, sun elevation, and local climatic elements (e.g., snow, haze, etc.). None of the 50 mm focal length Hasselblad photography was selected because of its inherent GRD of no better than 250 m. In all cases, the Hasselblad and Linhof scenes selected were made within a few seconds of the LFC photography.

Figure 3-48 shows a comparison of LFC imagery (top) and nearly simultaneous Hasselblad imagery (bottom) of the community of Lee Vining, California, and surrounding volcanic forms on the western shores of Mono Lake. The LFC lens focal length (fl) is 304 mm, and the Hasselblad imagery was taken with the 100 mm fl lens. Both frames have been enlarged to identical scales for comparison of data content. Except for shorelines and lake surface, this scene is of low target contrast.

A rare example of near simultaneous photography by the LFC (304 mm fl), the Hasselblad (250 mm fl), and the Linhof (90 mm fl) - all acquired during STS 41-G - is shown in figure 3-49. These photos allow comparison of medium contrast imagery of the ocean surface texture which is created by polarization of sunlight at the air/sea interface. This is the strait between the active volcanic islands of Fernandina and Isabela in the Archipelago de Colon (Galapagos Islands) on the equator west of Ecuador in South America. These frames from the LFC (top), the Hasselblad (center), and the Linhof (bottom) have been enlarged to identical scales.

In a scene shown earlier in figure 3-46, figure 3-50 shows the Hasselblad (100 mm fl) imagery (bottom) obtained over Ellsworth AFB near Rapid City, South Dakota, in comparison to the two 304 mm fl systems - the LFC (top) and the ESA MC (center). All three frames have been enlarged to identical scales. A final scene comparison (in a scene also shown earlier, in figure 3-44) figure 3-51 shows the Linhof (90 mm fl) imagery (bottom) obtained over the Bandar Abbas - Dogerdan, Iran, region on the Strait of Hormuz in comparison to the two 304 mm fl systems - the LFC (top) and the ESA MC (center). Again, all three frames have been enlarged to identical scales.

3.3 ACQUIRED DATA CATEGORIES

When reviewing the data scenes acquired by the LFC during the STS 41-G mission and marveling at the multitude of landforms, sea states, and meteorological displays that were acquired during a single 8-day period, one can only use the single word "awesome" as a descriptive summary.

Though the mission was plagued by inclement weather over many of the prime target areas, no one can contest that the LFC imagery is truly a major benefit to user disciplines in the field of earth sciences. One who is familiar with the recent major compendium of earth resource imaging sensors, "Geomorphology From Space - A Global Overview of Regional Landforms"[1], will

[1] Short, N. M. (NASA/GSFC), and Blair, R. W., Jr. (Fort Lewis College), Editors, Geomorphology From Space - A Global Overview of Regional Landforms, NASA SP-486, 1986.

recognize that the LFC did record a multitude of "typical" landform examples of tectonic, volcanic, fluvial, deltaic, coastal, karst, eolian, and glacier/glacial structural embodiments. Though this compendium was being readied for the presses at the time the earliest LFC imagery releases were reaching the authors, several of the more notable LFC images were edited into the manuscript just prior to press time.

NASA is currently working on a companion Special Publication on this initial voyage of the LFC which will highlight the scientific utility of many of the acquired LFC data scenes relating to geomorphology, hydrology, oceanography, meteorology, agriculture, and other earth sciences.

3.3.1. SYNOPTIC ORBITAL STEREOSCOPY

One of the greatest tools in the use of LFC imagery for both the photo-interpreter and the cartographer is stereoscopy. Image acquisition during an LFC data pass ensures that succeeding frames overlap each other (see figure 3-52), producing similar images of "same" terrain features in these regions of overlap. The overlap regions comprise the stereo model area.

Viewing stereo (3-dimensional) photography requires that two nearly identical photo prints (a stereo pair) be viewed simultaneously, one eye looking at one print and the other eye looking at the other print. We will call these prints the "right" print and the "left" print. The only difference in the two photos is that they are, in fact, two separate and unique photographs of the same subject, object, or - in this case - terrain, which have been made with the camera located at two different locations or camera stations. Their difference is their perspective view of the same terrain at the instant the exposures are made.

If these two photographs are superimposed by some means and viewed under the proper conditions, the person viewing their contents perceives the illusion of depth, shapes, and contours. These conditions are derived when the left eye is allowed to view only the left print and the right eye is constrained to viewing only the right print. If we contrive a mechanical means or a self

discipline whereby each eye can simultaneously view only its designated print, we can enjoy and learn from this illusion. Fortunately, many means are available to accomplish this; these include equipment such as sophisticated analytical stereo plotters, table-top mirror stereoscopes, and simple "pocket" type stereoscopes (two lenses in a folding standoff support), or no equipment whatsoever. We will discuss this latter means.

To begin with, the photos must be properly positioned or mounted with "right" and "left" prints on the proper sides. In order to trick the brain into thinking that it is perceiving depth, we must first train the eyes to look at only one of the side-by-side photographs - the proper one. To do this, we can physically insert a blinder (a cardboard septa) on the seam where the two photographs are butted together and let it come up high enough or close enough that it almost touches the nose as shown in figure 3-53. Now, the left eye can see only the "left" photograph, and the right eye can see only the "right" photograph. Since each eye does not know what the other eye is doing, it can then focus on its individual image and the picture thus appears to have depth to it.

Once a person has done this frequently, he will find that the blinder can be discarded and he can cause the line of sight for each eye to become parallel to the other, as opposed to converging to a point. At first, a person will perceive three images; but he should ignore this and focus on only the middle image.

A person can train himself in this sort of eye control in this way: First, hold the index finger of each hand vertically in front of each eye, say 12 to 18 in. from the head. The fingers should be 1.5 to 2 in. apart. Then let a blank stare come into the eyes or, better yet, look at the wall beyond the fingers. When the eyes are focused for the distant surface, you will note that suddenly there appear to be three fingers in front of your eyes (if you see four fingers, never mind - just move the two fingers closer together). Slowly and carefully, bring only the center finger into focus. Actually, you are bringing each finger (right and left) into focus, but you have tricked

the brain into seeing the illusion of three but observing only the center nonexistent finger.

Referring back to figure 3-52, we should explain the advantage of stereo photography to exaggerate the offset in planes of interest. In the case of LFC data acquisition in the 80-percent forward O/L mode, five successive frames of imagery will produce four stereo pairs (i.e., frames 1 and 2, 1 and 3, 1 and 4, and 1 and 5), their difference being that the greater the stereo base (B) at constant altitude, or height (H), the greater the increase in ratio of base to height (B/H); e.g., B/H = 0.3, 0.6, 0.9, and 1.2, respectively. As the B/H ratio increases, the apparent relief in the terrain increases; or, more correctly, the greater is the VE of this relief (see figure 3-54).

Later in this document, certain stereoscopic LFC images are included to demonstrate geomorphological features. The reader may wish to return to this section as a refresher on the "how to's" of viewing these examples stereoscopically.

But a word of caution when one uses his own "left" and "right" prints - do not reverse their order! Figure 3-55 will demonstrate this cautionary flag. The proper "left" print is LFC frame 0592 and the "right" print is LFC frame 0596. These are shown in the left hand and center positions of figure 3-55. When frame 0592 is placed to the right of frame 0596, the viewer will be surprised to note that mighty Mt. Ararat (and its shroud of clouds) and surrounding lava flows no longer rise above the surrounding plane. Behold, the mighty volcano now sinks into the earth, as an inversion, and the viewer - it now appears - is now in a position inside the earth looking out. When properly positioned with frame 0592 on the left and frame 0596 on the right, the combination produces a normal stereogram. However, positioning frame 0592 to the right of frame 0596 produces a "false" stereogram, or what is better known as a "pseudo" stereogram.

3.3.2 USER DISCIPLINE SATISFACTION

Though cartography is the major application of the LFC imagery, ongoing analysis by earth science investigators continues to highlight an increasing awareness of the usefulness of LFC imagery in a wide range of disciplines.

In reviewing the overall applications of the LFC system, it becomes readily apparent that the key aspect is the synoptic view that each image provides. With the capability available to record, at high resolution, about 150,000 sq km (370 km altitude) of the earth's surface at a single instant, it is possible to place individual geologic features in their regional context. Only with the LFC can spatial distribution of such features as faults, sand dunes, and stream channels be viewed at high resolution in a single image. Several investigators have also found that, in detailed geomorphological studies, only with the stereo capability can they determine the true orientation and relative altitudes of different landforms.

A potential major contribution could be made by the LFC in the documentation of ground and atmospheric conditions at the time that other nadir-looking sensors are being flown onboard the Shuttle. Photography obtained during the STS 41-G mission demonstrated the utility of images to document snow cover, river flood stages, and ground characteristics in geographically remote areas when the LFC was operating simultaneously with FILE and MAPS and, to some extent, with SIR-B. More importantly, LFC images could provide regional overviews for data acquired by imaging spectrometer experiments to be flown by NASA in the early 1990's. These missions will obtain high spectral resolution data, but for only a very limited swath (approximately 12 km). The LFC would enable simultaneous determination of both the geographic setting of these data takes and the degree of cloud cover (the benefit being that both types of data would be acquired under the same lighting conditions).

Section 3.3.2 presents a rather broad description and pictorial synopsis of some of the typical applications of the LFC imagery acquired during the STS 41-G mission.

3.3.2.1 Cartography

Many aspects of geological research (and research within hydrology and ecosystems programs) depend on the knowledge of local topography for determining structural offsets, drainage basin area, and the elevation and local slopes of areas populated by different plant communities. For individual study areas, topographic maps derived from LFC images would significantly improve our knowledge of the more isolated parts of the world where comparative research (compared against U.S. and European test sites) would assist in the interpretation of these surface processes and phenomena.

A major objective of the LFC was to produce orbital imagery of sufficient clarity (spatial resolution) and geometric fidelity to allow the production of 1:50,000 scale orthophoto maps with topographic contour intervals appropriate for the scale. Work is now in progress at several locations in the United States, Canada, and Australia. Some results have been obtained, most notably by the USDA Forest Service and by Australia. Other cartographic applications are underway by NOAA's National Ocean Service, the Defense Mapping Agency, and the U.S. Geological Survey. Several sample maps produced from LFC imagery are shown in figures 3-56 through 3-62.

Figure 3-56 is a simple photomap produced of the Cairns, Queensland, Australia, area showing the rain forests of Australia's eastern seaboard and the Great Barrier reef in the Coral Sea. This map was produced by the Australian Department of Mapping and Surveying at a 1:373,000 scale from CIR LFC imagery.

Figure 3-57 presents a 1:120,000 scale orthophoto map (greatly reduced) of the White Mountain National Forest in New Hampshire. This map was produced by the Eastern Regional Office of the USDA Forest Service for experimental evaluation and demonstration purposes, using office methods for vertical and horizontal controls. Form line intervals are 200 ft. For clarity, these intervals are presented separately from the base map as figure 3-58. Data for this map was collected during a single orbit over the subject site.

Figure 3-59 is a locator map with projections of LFC ground footprints. Figure 3-60 is an uncontrolled photo mosaic of northwestern Australia, produced at a scale of approximately 1:733,000 from 55 LFC frames acquired during six adjacent orbits as a demonstration of the utility of LFC multipass data collection capabilities. Similarly, figures 3-61 and 3-62, showing the Afghanistan/Pakistan/India area, were produced at a scale of approximately 1:745,000 from 40 LFC frames acquired during four orbits. Both of these areas were selected for the vast and varied geomorphological content. They were prepared by the Metric Photography Laboratory at the Johnson Space Center.

3.3.2.2 Geomorphology

The planet Earth continuously displays its history in the forms displayed on its surface and below its surface. Except for fleeting and rapidly developing transient phenomena, precious little of the earth processes is recorded in written history. It is only man's curiosity in the recent past which has led to decryption of its geologically recorded history. The LFC has provided a tool to further the study and analysis of the earth's processes. A number of rather striking examples of the expansion of these analyses have emerged from early application of LFC imagery.

A major objective of NASA's geology program is to better understand the manner in which the continents have been assembled by the process of plate tectonics. Relative movement between the crustal plates (i.e., active fault line displacement) is occurring today (along the San Andreas fault line and in the Himalayas, for example). Recognition of the total displacement and the actual location of deformation is key to our understanding of earth structure (tectonics). High spatial resolution (greater than 10 m) is needed to identify recent offsets in small streams and agricultural features, since this displacement process operates slowly and is often masked by human activities.

A striking example of the usefulness of LFC imagery in fault detection is the 1-km left lateral offset of the Kunlun fault in the Tibetan Plateau. This

area is shown in a two-frame mosaic (figure 3-63) recorded by the LFC during orbit 30 (LFC frame 0502) on October 7, 1984, and during orbit 46 (LFC frame 0818) on October 8, 1984. The magnitude of this fault structure as it crosses the Tibetan Plateau is clearly evident in this high resolution wide-field mosaic. Evidence of this left lateral movement on the Kunlun fault, as detected in LFC imagery, was reported by G. Wells, K. Burke, and P. W. Francis of the Lunar and Planetary Institute in Houston, Texas, and presented to the American Geophysical Union Congress in Baltimore, Maryland, on May 27, 1985. A portion of the report is included here (see indented text which follows). Figure references (in brackets) and figures have been added to enhance understanding.

> The continuing collision between the Indian sub-continent and Asia has two consequences: the formation of (1) the Tibetan plateau and the Himalayan thrust structures and (2) major transcurrent faults (including Bolnai, Altyn Tagh, Kunlun, Kang Ting, and Red River) which facilitated the generally eastwards "tectonic escape" of the Chinese block. Evidence for the lateral movement on these faults has been furnished mostly from seismic studies and regional considerations; no direct geological evidence has been reported. Here we document for the first time direct evidence for left lateral movement on the Kunlun fault, obtained by the Space Shuttle Large Format Camera on October 8, 1984.
>
> Photographs acquired at 35.783 degrees N, 93.033 degrees E have a resolution of better than 10 m and show that over a 15 km segment of the fault north of the Ho Sai Hu Basin, nine streams flowing southward off the fault scarp have been offset by 1 km where they cross the fault trace [see figures 3-64 and 3-65]. Overall, the fault zone is about 1-2 km wide; the scarp formed by the most recent movements is about 100 m high. Although fresh scarps, sag ponds and other features related to recent fault movements can be traced for tens of kilometers along the fault, no other large offsets have been detected. The time span represented by the observed displacements is unknown, but the lack of paleostrandlines around the Ho Sai Hu indicates a postglacial age fan deposition and a possible rate of displacement of 5-10 cm/yr, a significant proportion of the total for the major fault systems.
>
> The fault offsets are not visible on Landsat MSS, Space Shuttle Metric Camera or 70 mm Hasselblad photography, emphasizing the importance of high resolution photography for many geological remote sensing applications.

It would be impossible to cover in this compendium all of those significant geomorphological structures recorded by the LFC during STS 41-G. A few

examples are included in the following pages to demonstrate eolian landforms typifying the many deserts of the world recorded by the LFC; volcanic landforms seen in major volcanic complexes recorder; and typical fluvial, coastal, deltaic, and glacial landforms.

Throughout the STS 41-G mission, the LFC recorded many of the earth's small and large deserts, sand seas, and desert systems. Though the topographic relief of these areas is small (e,g., 100 to several hundred meters), the use of LFC frame combinations with high B/H ratios reveals intimate facts of major dunes associated with their included smaller and smaller dunes on their surfaces. During the third orbit, passing over north Africa, the LFC recorded four major desert (erg) formations. Three of these are shown in figures 3-66 through 3-68. A continent away, the Sechura desert (see figure 3-69) was recorded on the west coast of South America, and the spacecraft followed the Peruvian coast during orbit 39.

The Australian continent contains a wealth of well-preserved surface geological features, including several impact craters where objects from outer space have penetrated the earth. It contains vast deserts and rain forests; because of its very arid interior, however, it contains few large flowing rivers. It is because of this lack of moisture and absence of severe water erosion forces that the geological history of hundreds of millions of years remains so visible. Figures 3-70 through 3-72, sample imagery of sites in western Australia, were selected to demonstrate LFC coverage in one relatively small location.

Through plate tectonics, the earth is constantly undergoing transformations whereby earlier continents have collided with other continental masses with such force as to cause the materials to undergo great upheavals, creating great mountain ranges. Through the sustained erosion by winds and water, much of the overburden has been removed, revealing the intricate structures created by these forces. Some of these more delicate structures exposed on the Tibetan Plateau are illustrated in figures 3-73 through 3-76.

With the rising and falling of parts of the earth's surface, the force and direction of drainage patterns are created and changed, giving a ready indication of the slopes and material content of the immediate area. Since the earth has an atmosphere with water content, all areas are subject to rainfall to greater and lesser degrees. Some interesting examples of drainage patterns are given in figures 3-77 through 3-79.

3.3.2.3 Demography

Elsewhere in this report, glimpses have been shown of metropolitan areas of the world which became target areas for LFC data acquisition. These views offer an insight into the applications of LFC imagery to demographic investigations. But as one analyzes and studies a single LFC frame and beholds the extent of human habitation in the most remote and inhospitable spots of the planet, one begins to grasp the meaning of the term habitability and begins to understand something of population distribution and population density.

Searching the stream beds fed by glaciers in the high altitudes of the Tibetan Plateau, we may not find cultivated fields, but we do find small groups of dwellings of the herdsman communities. If we search the dark spots in the great sand seas of the Sahara Desert, we find fertile fields belonging to yet other groups of humanity. As we look at environments ranging from oppressive cold to oppressive heat and from almost too little air to breathe to air heavily laden with suspended particles of all types, we can more clearly understand mankind's ability to adapt and survive.

If we can see a road or a trail in the LFC imagery, we know that it leads from one place to some other place. Searching the imagery of Australia's outback, we can trace a dirt road for scores of kilometers, and sooner or later we spot a population center of a half dozen or fewer habitats. We might even come to a crossroad or a fork in the road which, in turn, goes to other places, however remote they might be. A few typical examples of more remote human habitation sites have been included to contrast with the examples of the highly urbanized population centers illustrated elsewhere (see figures 3-80 through 3-82).

3.3.2.4 Oceanography

A major objective of STS 41-G was trained observation and study of the earth's seas and oceans. One of the two payload specialists onboard was Paul Scully-Power, an oceanographer with the Office of Research and Technology of the U.S. Naval Underwater Systems Center (NUSC), New London, Connecticut. With Comdr. John Hughes and James J. Gallagher, also of NUSC, he has published preliminary findings of his observations and their collective observations from detailed analysis of film imagery from the Hasselblad, the Linhof, and the LFC. The Hasselblad and Linhof produced a broad range of spectacular synoptic ocean surface displays which provided gross delineation of surface slicks, spiral eddies, whorls, internal waves, over-water frontal systems, and sediment patterns.

These researchers spent many hours looking at the LFC imagery and noted that which few others observed. The major objective of the LFC was the recording of landforms. In doing this, the LFC commenced operation prior to actual landfalls and continued to run momentarily after land loss. Additionally, oceans and seas covered briefly between major landforms or included along with landforms when shorelines paralleled the data pass were also recorded. They ignored the landforms and looked at the water surfaces. In particular, where even the most subtle sun glint was present, they could detect the presence of water surface detail.

During the duplicating process, involving imagery both with and without pronounced sun glint (and ignoring landforms), it was found that simple darkroom enhancement of the ocean surface brought out slicks within slicks, spirals within spirals, detail within ship wakes, minute plankton patterns, detailed bathymetric information, and patterns of complex internal waves. But most importantly, it brought a new dimension to study of the ocean surface texture. It revealed smaller waves within larger waves, and it also showed whitecaps on waves. Additionally, the great geometric fidelity of the LFC and verticality of mounting make it possible to mensurate crest-to-crest distances, wave train direction, and wave periodicities.

Figure 3-83 serves as a brief synopsis of the types of oceanographic data which can be recovered from the LFC imagery and the fine resolution of detail which is lost in lower performance camera systems; in it, one can observe the presence of intricate surface phenomena in the Golfe d'Arzew offshore oil shipping facility at Port aux Poules, Algeria. This is a demonstration of water surface enhancement at the expense of onshore detail.

Careful inspection of LFC ocean surface imagery may yield examples of seamanship protocol as demonstrated in figure 3-84, where a ship can be seen in the Ionian Sea executing a 360° maneuver, apparently to give right of way to a ship approaching from her left. Searching shorelines and offshore surface areas utilizes direct sun glint and water clarity to study shoreline wave diffraction patterns, such as can be observed in figure 3-85 (Tahiti), and both surface and internal wave directions, as in figure 3-86 (the Indian Ocean). Other surface phenomena do not require sun glint to reveal the content of the water or the surface when plankton blooms are present, as in imagery of the Coral Sea in figure 3-87.

3.3.2.5 Volcanology

The realization has grown that there exists a greater diversity of volcano types than has been observed during recorded history. In particular, very explosive eruptions of the same kind as Mt. St. Helens, but 20 to 50 times as explosive, have been recently identified in the Chilean Andes. Forty new volcanoes have been found with LFC data for this area, whereas until 1984 only 50 examples were known worldwide. The major advantage of the LFC in this instance has been the resolution needed to see small flow structures within these volcanic materials and the stereo capability required to estimate the volume of these deposits. Interestingly, U.S. geologists are now more willing to reassess their interpretations of deposits associated with some large U.S. volcanoes (e.g., Mt. Lassen and Mt. Shasta), which have been difficult to explain by conventional mapping.

A vast area within Ethiopia is punctuated with harsh terrain. This is, of course, associated with the African rift system and the collision boundary of

three massive plates, as seen in the active Erta Ale volcanic complex within the Afar (Danakil) depression (figures 3-88 and 3-89). Other areas within Ethiopia lend further credulity to this below-surface violent nature of the earth, where we find very active volcanic fields at K'oboa (figure 3-90), with hundreds of volcanic vents and recent lava outflows created by extensive fault features; Gewane (figure 3-91); and Bola Selullse (figure 3-92).

3.3.2.6 Geography

During STS 41-G the LFC acquired imagery at three altitudes; this allowed the evaluation of the wide-FOV imagery for the identification of continental land shapes, large and small bodies of water, waterways, transportation networks, and other features affecting the establishment of natural and surveyed international boundaries. Some of the acquired imagery is very appropriate to the demonstration of these geographic relationships. Very basic geographic annotation has been applied to some of this imagery as examples of both the scope and content in a single frame of LFC imagery and is presented in figures 3-93 through 3-97. The imagery in these figures has been reduced to approximately one-third of their original 9- by 18-in. full-frame size.

3.3.2.7 Hydrology

The redistribution of river sediment during different times of the year (as a consequence of seasonal rain or snow melt), the drainage patterns of major drainage basins, the entrapment of waters from rivers in major natural and manmade reservoirs, coastal estuary erosion, and the assessment of storm damage after storms and hurricanes create significant economic and land resource problems. Many of these coastal changes affect the distribution of fine sediments, coastal flooding, or the change in direction of small channels. Under traditional means of space imagery acquisition, these features typically have a scale of 5 million to 20 million and are poorly resolved and defined. However, the LFC makes it possible to provide greater breadth of coverage and superior definition of detail to enhance the study and understanding of many hydrologic disciplines.

A typical example of the value of high resolution wide-field photography provided by the LFC is shown in figure 3-98, imagery acquired over northern Italy. This photograph shows a large portion of the Po River Valley and the magnitude of the Po River delta as it empties into the Adriatic Sea carrying silt and sediments of a major drainage basin from the Italian Alps. Similarly, a scene showing a portion of the Nile River Valley, the Aswan Dam, and Lake Nasser (figure 3-99) illustrates an area of great economic importance amid a vast wasteland of arid desert. (Figures 3-98 and 3-99 are reduced to approximately one-third their original 9- by 18-in. full-frame size. Figure 3-100 is typical of hundreds of coastal estuaries which can be studied in detail with high resolution LFC imagery to analyze wetland processes both with and without the emphasis provided by sun glint.

3.3.2.8 Archaeology

Many archaeological sites have been discovered by noting obscure vegetation patterns on aerial photographs - patterns which turned out to be long-buried roadbeds, earthen embankments, or building foundations of cities long gone. One such site was recorded by the LFC during a data pass down the Peruvian coastline just outside Nazca, Peru, a few miles to the northwest. This site was well known and has been studied for decades, most notably by Dr. Maria Reiche, who has spent much of her life in charting these Nazca Lines and trying to find reason for their creation.

Figure 3-101 presents an overall scene of the location of these lines on the pampa and their relationship to the Pacific Ocean and the Andes Mountains. Though the patterns were created more than 2,000 years ago, the only weathering has been due to modern man and his conveyances. This area holds modern times records for least average annual precipitation (0.1 in.) and longest period without precipitation (13 yr). Such extremely dry climatic conditions contribute to the fact that these fragile and simple lines have withstood the ravages of time and that organic artifacts and human remains have been removed intact from the graves of these ancients. Figure 3-102 presents enlargements of the lines. Because of the smallness in size of the many associated animal effigies at this site, these could not be identified,

though their locations can be easily plotted in relation to the lines proper. Giant animal effigies further to the south were not recorded because of the heavy clouds obscuring these areas at the times of the STS 41-G overflights.

3.3.2.9 Meteorology

As mentioned, the STS 41-G mission was plagued with sustained inclement weather, not only in the tropical and ocean zones of the world, but in the northern hemisphere as well. Exposing film in order to get to film changes in the LFC on a predetermined schedule and to ensure using all of the film carried aloft, a considerable amount of imagery was obtained of vast cloud seas as well as isolated major storms.

Atlantic Hurricane Josephine, which was photographed during the mission by rolling the spacecraft 56° from nadir, is shown in figures 3-103 and 3-104. These two photograph are shown reduced to 36 percent of original size. Though there were several close passes to this hurricane, reconfiguring the attitude of the spacecraft and causing other sensors to lose scheduled data passes delayed its acquisition until late in the mission. While photographing transient weather phenomena is always a target objective on Shuttle missions, scheduling it months in advance of a mission is, of course, impossible. Though Hurricane Josephine had diminished considerably in intensity by the time LFC coverage could be instituted, the imagery acquired shows some of the outlying associated storm centers (see figure 3-104). The imagery provided significant insight into their magnitude, as well as a means for accurate mensuration of top altitude and anvil dimensions. Figures 3-105 and 3-106 show progressive enlargement of two such isolated thunderheads.

There were many outstanding meteorological displays during the STS 41-G mission, and just about every form of cloud and storm activity and distribution was photographed - not by intent but by circumstance. Much of this single-frame wide-field photography acquired on a global basis has, in fact, proven quite useful to the USAF, the U.S. Navy, and the civil communities. Figures 3-107 through 3-110 (all approximately one-third of original size) have been included as examples of the types of cloud coverage obtained.

3.3.2.10 Paleolithology

The solid earth preserves the record of climatic change over the time period since the last ice age (approximately 20,000 years ago). High resolution stereo photographic coverage is essential if space-acquired imagery is to be used for identifying former high stands of lakes, distribution of fossil sand dunes (for wind direction measurements), and glacial deposits.

During the STS 41-G mission, very good LFC imagery was obtained of the Tibetan Plateau, which contains one of the larger evaporative basins on the earth. Here we find scores of Paleolithic lakes (see figure 3-111) with terraces formed by massive sheets of ice on their surfaces thousands of years ago. Progressive evaporation, thaws, and refreezing as the lake levels dropped caused compression of each new shoreline, leaving a fossil record of its past (figure 3-112). Here we also see evidence of once extremely massive glaciers (figure 3-113) which pushed enormous terraces into place, leaving them high and dry as the glaciers receded through melting and evaporation. In the process of glacial runoff due to this melting process, massive alluvial fans were formed, filling the glacial valleys (see figure 3-114.) As a note, less than 2 months after the completion of the STS 41-G mission, a severe blizzard hit these portions of the Tibetan Plateau. Unconfirmed reports from China stated that 300,000 Tibetan herdsmen, it was estimated, were trapped with their herds and were feared dead. Though the region is hostile because of altitude and extreme climatic conditions, inspection of the paths of glacial streams reveals occasional small hamlets as minute population centers.

3.4 DISCREPANCIES

When it comes time to evaluate how well a system performs, both as a component of the whole (the mission) and as a subsystem of a group of payloads, the reviewer's attitudes always center on, first, how well his own instrument executed assignments and, second, how well his team members executed their tasks. If the assessment of these two factors is positive, then the evaluation of the mission itself is favorably influenced.

On any mission there will always be things that did not go exactly as expected, and these are then considered anomalous to the critical purview. In this respect, mission STS 41-G and the LFC were no different from any other system. But since the LFC did do an outstanding job and so very few real-time problems presented themselves, the assessment of the mission, therefore, is that it went well.

3.4.1 MISSION ANOMALIES

Having experienced two aborts and then removal of the system from the manifest on STS 41-D, the LFC team was extremely satisfied with the STS 41-G mission. The launch was right on schedule, and orbit insertion was perfect. The crew wasted no time in opening the cargo bay doors and activating the cargo bay payloads, and they made certain that the LFC's first data pass (unscheduled) on the second revolution would be possible.

The LFC started operation off the west coast of Ireland, continuing over southern England and into France, where it was placed into standby. The severe weather conditions were not at all conducive to system performance, but this gave the LFC mission control team an early opportunity to observe the LFC's vital signs.

With all systems "go," the LFC was restarted as the ground track approached the Libyan/Egyptian coastline and continued across Egypt's western desert, along the Nile, across the Sudan, Ethiopia, and Somalia, and into the Indian Ocean. Shortly thereafter, however, problems were encountered with the deployment and steering of the STS 41-G Ku-band antenna. This antenna is the critical link between the Orbiter and the TDRSS-A communications satellite. TDRSS handles all high data rate links between the spacecraft and the ground stations. The inability to point the Ku-band antenna at TDRSS-A while maintaining the Orbiter in -ZLV mode (for earth resource observations/imaging) was extremely critical to the onboard high data rate systems, primarily the SIR-B imaging radar experiment. This difficulty caused no impact on LFC operation until later in the mission, but it did cause immediate rescheduling for troubleshooting and study or workaround solutions. It necessitated a

somewhat longer stay at the maximum altitude and caused a delay in ERBES deployment and other scheduled onboard tasks.

In looking back, this was the single mission anomaly that impacted the cargo bay payloads. SIR-B utilized an onboard high data rate tape recorder and a dedicated optical (film) recorder to record its data. A means of dumping the tapes to ground stations was imperative for SIR-B, however, to allow for the reuse of the tapes to store new data. To provide this capability, all LFC passes over northern, central, and eastern South America were modified to allow use of the Orbiter vehicle as a platform for pointing the Ku-band antenna at TDRSS-A for data dumps. This caused the LFC to forfeit all scheduled data passes over this vast region of South America. Except for this problem, the STS 41-G mission was accomplished with ease and smoothness, and was truly a credit to the training and skills of the STS 41-G crew members.

3.4.2 SYSTEM ANOMALIES

During the course of the STS 41-G mission, the absence of any apparent LFC operational anomalies, as depicted on the incoming telemetry, gave the team in mission control a great deal of satisfaction. Though some potential problem areas had been identified preflight, the derived workarounds made it possible to avoid these. The only problem readily apparent during the mission was the problem of AEC response and the resulting impact on LFC real-time exposure variations.

The major design requirement for the LFC was to optimize image resolution performance during all stages of the hardware design and development cycle. It was to encompass every factor relating to image formation, ranging from the LFC's compatibility with the highest resolution aerial photographic film emulsions to the maintenance of maximum stability of the image point during the actual exposure event. The latter factor made it mandatory that means be provided for correcting image motion to compensate and correct the effects of the forward motion of the spacecraft. This is variously referred to as image motion compensation, or correction, (IMC) or forward motion compensation, or correction (FMC).

During orbit of the earth, the spacecraft is generating great ground speeds in the velocity vector that are in excess of 7.5 km/sec. Since the LFC exposure duration ranges from 4 msec to 32 msec (1/250th to 1/30th of a second), the relative image smear could result in a point elongation of 30 to 250 m, either of which could markedly degrade the quality of imagery. The design chosen was to incorporate a platen FMC technique in which the entire film platen assembly is moved, or translated, in the negative velocity vector during the entire exposure event (e.g., 4 to 32 msec) such that a ground image point is allowed to move with its reciprocal image point on the film surface.

The two significant LFC anomalies during the mission were both related to exposure increment/FMC deltas which resulted in the loss of significant quantities of data at various points during the mission. Neither of these anomalies was apparent until postmission film inspection.

3.4.2.1 Discrete Exposure Setting

Design of the shutter speed regulation method was planned with two goals in mind: to provide a nearly infinite range of shutter speeds between the minimum and maximum limits and to be compatible with the delays required for initiation of film platen translation (that is, for FMC). To do this, the design incorporated a speed shift register for five predetermined speed ranges (see table 3-7), and was shifted at four discrete points. The reason for this was to create delays in film platen actuation in order to synchronize platen motion with an open shutter.

The number of shutter speeds is essentially infinite between the shortest exposure (0.004 sec) and the longest exposure (0.032 sec). Shutter speed selection is an analog command voltage input which is processed by the LFC logic to set the voltage for rotary shutter velocity and then the delay for platen actuation. For each exposure, the drive mechanism for the platen must receive a statement directly from the speed shift register for the proper delay time.

TABLE 3-7.- EXPOSURE THRESHOLDS FOR THE FIVE LFC DISCRETE REGISTER SHIFTS FOR FMC DELAY COMMANDS

LFC exposure, msec	Exposure breakpoint, msec	Resulting FMC delay, msec
4 to 11	11	0
11 to 17	17	160
17 to 23	[a]23	310
23 to 28	28	453
28 to 32	-	588

[a] Intermittent register shift point failure at the 23-msec threshold.

This is a simple stairstep function up or down the scale, depending on where the last shutter velocity command was resting. However, as each of these thresholds is crossed, the delay command must be updated. During STS 41-G one of these threshold points (23 msec) was intermittently spurious in operation because its particular diode was relatively insensitive to low voltage inputs (5 Vdc). It could be described as "teter-tottering" on a fence, not being sure just which way to fall. If the exposure initiate command came at one of these times, it would not generate a delay signal and, though the rotary shutter velocity was correct, the FMC remained inhibited, awaiting an update for the amount of delay required.

On occasion, the command for 23.5 msec failed to generate any command for FMC delay values, either 310 or 453 msec. Because of microvolt variation in the 23.5 msec command level, it would sometimes inhibit the FMC command and sometimes issue the command. During the mission, there were 368 frames of photography (17 percent of all mission frames) commanded for 23.5 msec exposure duration. Of these, the FMC command was absent in 108 frames (29.3 percent of those commanded). The malfunction was random and certainly followed no predictable pattern for postflight malfunction search. The correction incorporated was to change the level from +5 Vdc to ±15 Vdc.

As an example, during orbit 31 a data pass began over Afghanistan and ended in the Bay of Bengal off India's east coast. This pass acquired a total of 40 frames and was run at two shutter speeds, 15.7 and 23.5 msec. At the 10th frame (LFC 5443) into the pass, 23.5 msec exposure was commanded with an immediate malfunction. On the 24th frame (LFC 0544) the problem cleared, still at the 23.5 msec command, and the commands continued in a normal manner throughout the pass to its conclusion. Figure 3-115 illustrates the effect of 176-m smear which is due to an inhibited FMC caused by the 23.5-msec command anomaly.

3.4.2.2 Excessively Long Exposure

The range of rotary shutter speeds is 4 to 32 msec. and, on input command, the maximum exposure time can range up to 38 msec, but not on a reliable basis. Shutter speed is controlled by selecting a discrete input voltage between +1.0 and +5.0 Vdc. To minimize command functions, no specific command was included to activate the LFC AEC. By setting the shutter speed command voltage level below +0.5 Vdc, the AEC sensor and control logic were activated, shifting shutter speed control from an operator-induced command to an AEC-induced command.

If the rotary shutter received a command voltage which would slow the shutter to less than the minimum speed (e.g., 32 or even 38 msec), the LFC would cease operation and issue a "no-go" flag. During the mission, however, if the AEC sensor's 1.9° FOV was completely covered by a very dark object (a lake or ocean) the voltage output command from the AEC would become quite small. In this case the rotary shutter velocity would slow down significantly, creating exposures which ranged from the normal maximum of 32 to 38 msec up to as much as 77 msec (which was at or very near the stalling point for the rotary shutter drive motor).

The mechanism of the smear generation is tied to the method for controlling the platen translation (that is, the FMC). As mentioned, the actuation of the platen drive is delayed depending on the upcoming shutter velocity. When FMC actuates, it first gets up to desired velocity in a very few milliseconds

and then maintains a constant velocity during the exposure event. However, it does not anticipate an exposure duration in excess of 38 msec, after which it decelerates and rapidly returns to the start position to await the next frame initiate command. If an excessively long exposure is initiated, FMC corrects for image motion during the first 38 msec and then returns to the start position. For exposure durations in excess of 38 msec, this erases the smear correction effort by then driving in the reverse direction while the shutter remains open. This negates the correction and then induces negative direction FMC correction. This gross image smear effect is illustrated in figure 3-116. On orbit 3, during a pass over the Mediterranean and into the Golfo d'Arzew and Port aux Poules, Algeria, the LFC was operated in AEC mode. Frame 0123 (figure 3-116, top frame) was exposed at 31.9 msec, the last scene brightness reading on the coast of Spain. However, by the next frame, 0124 (figure 3-116, bottom frame), the AEC sensor was reading brightness levels for the dark ocean surface and drove the shutter off lower limits for an exposure of 67.7 msec, far beyond the design capability of the FMC.

Dark holes such as these were encountered on several of the 14 data passes under active AEC control. These 14 data passes encompassed 615 frames of photography (slightly more than 25 percent of all mission imagery), and of these, perhaps 83 frames showed smear degradation of up to 580 m due to image motion correction during excessively long exposure. This amounts to 13.5 percent of the AEC controlled frames and 3.8 percent of all frames exposed during the mission. One of the mission objectives was to evaluate the utility of an AEC in this type of application. It has been decided that because of the extremely wide-angle FOV of the LFC, the great reliability of exposure calculation software, and the wide exposure latitude of high resolution B&W negative film materials, the AEC will not be used on future LFC missions.

In summary, the image smear which occurred was due to the 23.5 msec random anomaly (4.9 percent of all mission imagery) and AEC overexposure command anomaly (3.8 percent of all mission imagery). With these effects combined, the net result was seriously degraded imagery in 8.7 percent (191 frames) of the photography from the mission. Both problems have now been resolved by

hardware changes (23.5 msec anomaly) and procedural changes (delete use of AEC on future missions).

3.4.2.3 Miscellaneous Discrepancies

As one might expect from a first-time operation of a new system, little oversights and subtle variances become obvious. The LFC initial flight was no different, and a few small items became apparent on inspection of the final product. These are summarized briefly here.

- Double Imaging of the Reseau (and Fiducials)

  This double imaging has always been present, having first been noticed at the factory. It was analyzed many times and several fixes were instituted, but it kept coming back. This was present the final frame of each operate sequence when the shutdown sequence caused a second strobe of the LED's. It was an extra pulse that defied isolation and affected only one frame per pass when it did appear. It was always offset less than 0.5 cm. (Cause has been attributed to design error.)

- Internal Reflections

  These reflections appeared as very subtle fogging within the image format edges of both color and B&W films. This effect occurred on only a few isolated frames where the scene had very bright targets bordered by very dark targets (primarily oceans) at the edge of the format mask. The fogging was caused by internal reflections from the focal frame and the lens retaining rings, machined casting surfaces, and screw heads inadequately treated during manufacture. (This problem has been attributed to design/manufacturing oversight.)

- Film Density Blemishes

  There were a few isolated density streaks across the film web (lighter density in the color, heavier density in the B&W negative, and lighter in the B&W film positive). These are uneven linear single streaks about 0.5 to 1.5 cm in width with varied, very low density along their length.

This effect could have been caused by any one of many film rollers in the film transport. There were actually very few occurrences. (The cause is undetermined.)

- Frame Overlap

  There were three instances of partial frame overlapping where the film transport malfunctioned for a brief instant. This overlap effect has not been repeated in testing, and the cause has not been isolated.

- Forward Overlap Errors

  There were several instances of noticeable differences in the amount of forward overlap commanded as opposed to measured postflight (e.g., 86 percent measured versus 80 percent commanded). These have been traced to command procedural errors. More subtle differences (e.g., 81 to 81.5 percent measured versus 80 percent commanded) were also detected, and these have been traced to V/H command calculations. (This problem has been attributed to human error.)

- Miscellaneous Design Errors

  There have been a few design errors noted during postmission testing that were not encountered in flight. These differences seem due to the absence of humidity in the space environment as opposed to the high humidity encountered at JSC in the Texas coastal region; they relate to methods for locating and mounting certain transistors which are extremely sensitive to microvoltage leakage through only trace moisture paths. This was first noticed by audibly detecting an oscillation in rotary shutter speed - a speeding to coasting to speeding to coasting, etc. Where possible, all of these anomalies have been corrected by modifications to the printed circuit boards.

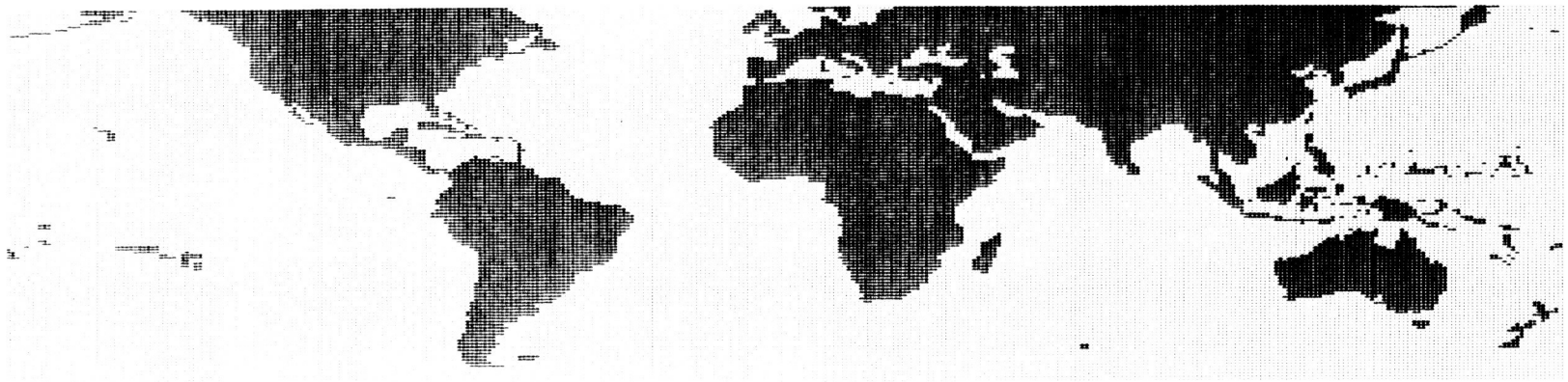


Figure 3-1.- LFC computer-generated map for all land masses between latitudes 60° N and 60° S. Used during the STS 41-G mission.

```
                FRAME COUNT   B:S41G.LST                PAGE 14 OF 14

            DESCRIPTION                          SUB-COUNT          TOTAL
=====================================   ====================   ======
PASS:   126.0   ORBIT:  126               OPER  1  69 FRAMES       4725
TARGET:  84.0E TO 106.5E
CMNT:   3414 - 41-G ON TIME 8/25
-------------------------------------------------------------------------
PASS:   126.2   ORBIT:  126               OPER  1  30 FRAMES       4755
TARGET: 109.5E TO 116.5E
CMNT:   3414 - 41-G ON TIME 8/25
-------------------------------------------------------------------------
PASS:   126.4   ORBIT:  126               OPER  1  47 FRAMES       4802
TARGET: 121.5E TO 137.0E
CMNT:   3414 - 41-G ON TIME 8/25
-------------------------------------------------------------------------
PASS:   127.0   ORBIT:  127               OPER  1  13 FRAMES       4815
TARGET:  45.5E TO  50.0E
CMNT:   3414 - 41-G ON TIME 8/25
-------------------------------------------------------------------------
PASS:   127.2   ORBIT:  127               OPER  1  53 FRAMES       4868
TARGET:  63.5E TO  80.5E
CMNT:   3414 - 41-G ON TIME 8/25
-------------------------------------------------------------------------
PASS:   127.8   ORBIT:  127               OPER  1  40 FRAMES       4908
TARGET:  83.0W TO  55.0W
CMNT:   3411 - NIGHT TIME US EAST COAST
-------------------------------------------------------------------------
PASS:   128.0   ORBIT:  128               OPER  1  23 FRAMES       4931
TARGET:  18.5E TO  29.5E
CMNT:   3414 - 41-G ON TIME 8/25
-------------------------------------------------------------------------
PASS:   128.2   ORBIT:  128               OPER  1  36 FRAMES       4967
TARGET:  41.0E TO  52.0E
CMNT:   3414 - 41-G ON TIME 8/25
-------------------------------------------------------------------------
```

Figure 3-2.- Example of an actual LFC frame count software output. (Final page output of printout of all sunlit overland and unique nighttime data opportunities and number of frames per opportunity for the STS 41-G mission. Note that exercise of all opportunities on the "shopping list" would result in more than twice the 2,300 LFC frames available.)

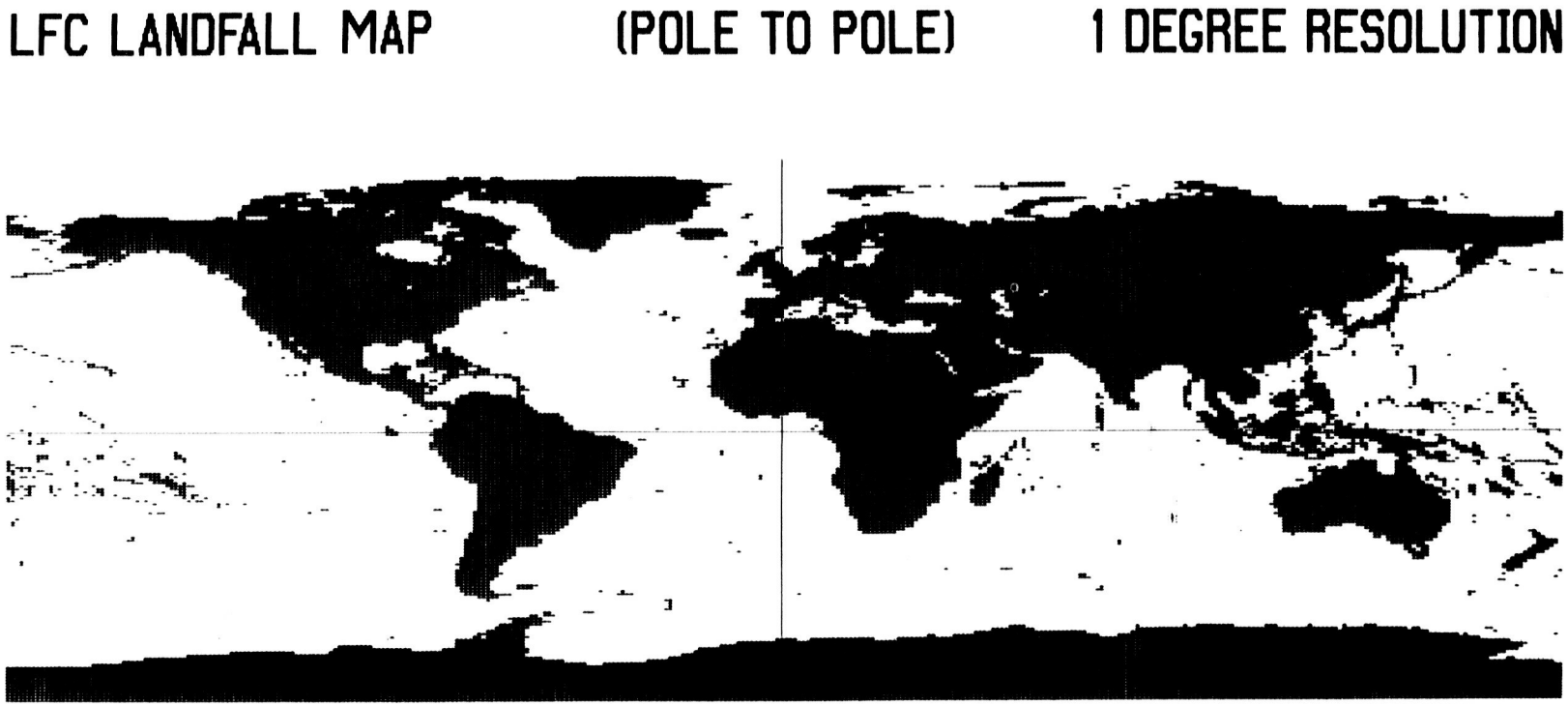


Figure 3-3.- Revised LFC land and water boundary interface map. This map may now be used for any orbit inclination, up to and including polar.

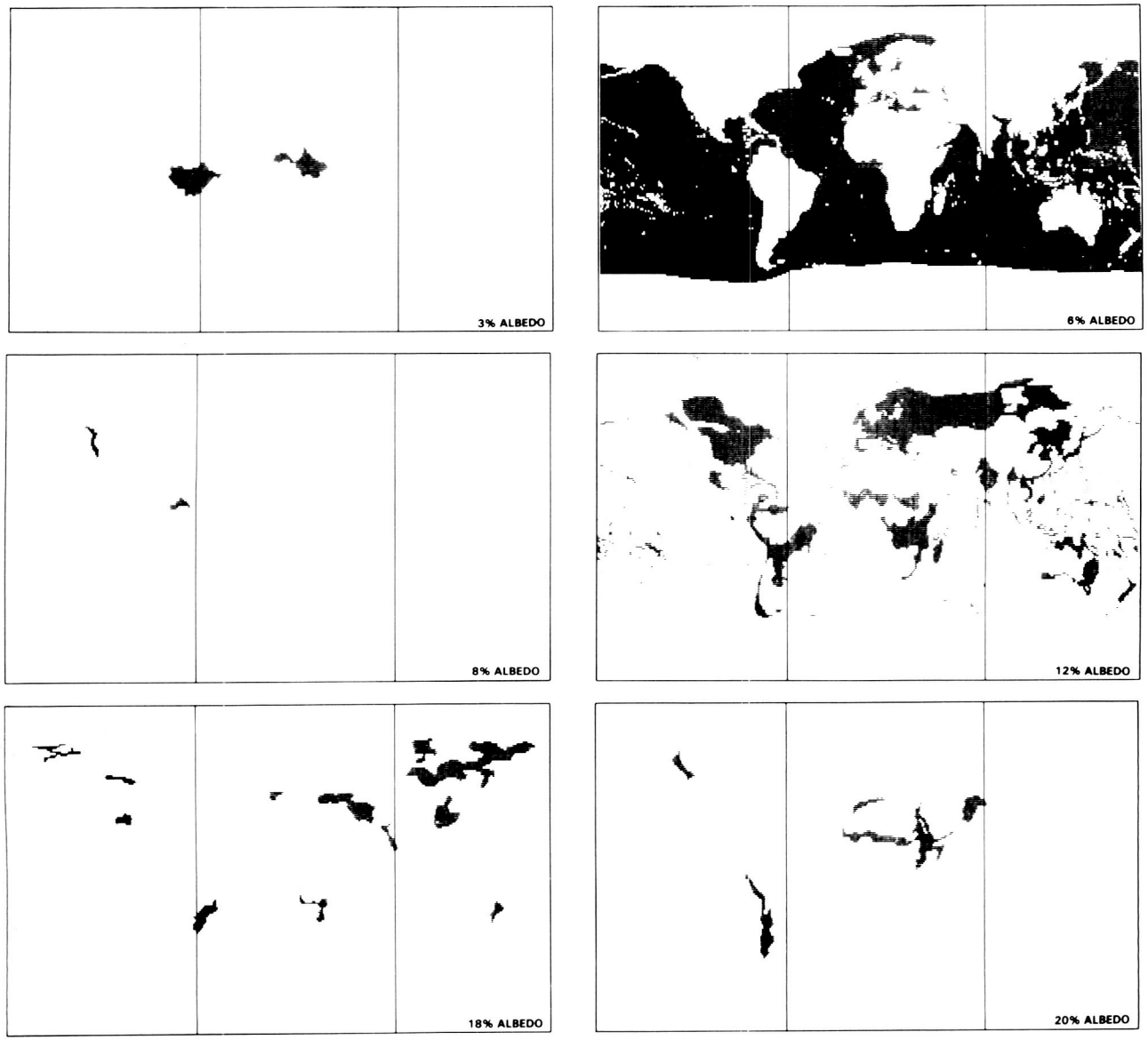


Figure 3-4.- Revised LFC multiple albedo map series. This series has been updated for higher inclination orbits such that it can now be used for any mission inclination, up to and including polar.

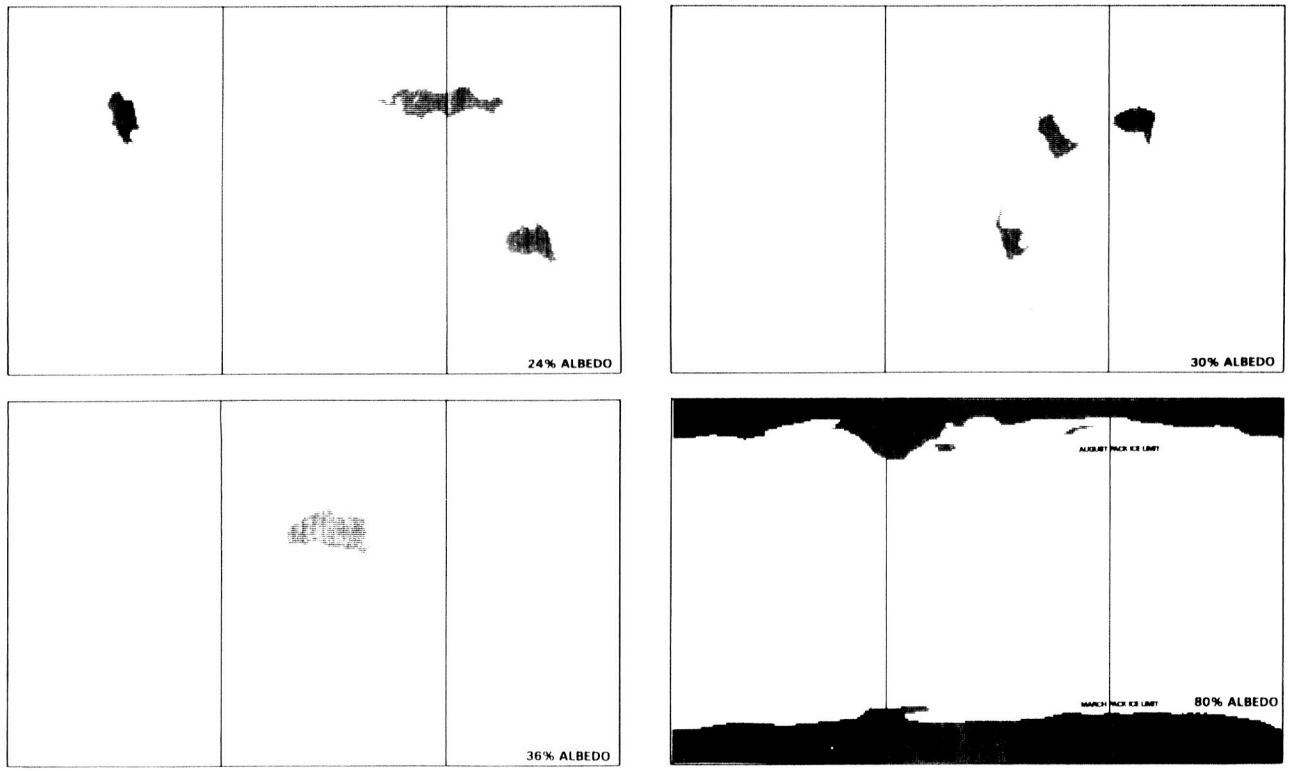


Figure 3-4.- Concluded.

41-G INTEGRATED PAYLOAD
COMMAND PLAN

281/00:00:00

	MET	DSM#	COMMAND	NOTES
	02/00:25:00	1532	MRTC - SETUP	LFC DT 33.00
		8320	LFC-80% OVERLAP CMD	EXECUTE MRTC 1532
		8323	LFC-FILM CMD (3414)	SETUP LFC DT 33.00
		8324	LFC-EXP BIAS CMD NORM	
		8327	LFC-FILT CMD (-HAZE)	
		8330	LFC-DOOR NORMAL CMD	
		8332	LFC-SHUTTER CLOSE CMD	
		8334	LFC-NORMAL FMC CMD	
		8175	LFC-V/H CMD=28.0	
		1047	LFC-EXP BC #2 36.0	
*	02/00;42:25	8315	LFC-OPERATE COMMAND	LFC DT 33.00
*	02/00:46:04	8180	LFC-V/H CMD=28.5	LFC DT 33.00
*	02/00:47:04	1048	LFC-EXP BC #3 42.0	LFC DT 33.00
*	02/00:50:14	8185	LFC-V/H CMD=29.0	LFC DT 33.00
*	02/00|52:54	1050	LFC-EXP BC #5 63.0	LFC DT 33.00
*	02/00:54:04	8198	LFC-V/H CMD=29.5	LFC DT 33.00
*	02/00:57:34	1049	LFC-EXP BC #4 50.0	LFC DT 33.00
*	02/00:59:24	1048	LFC-EXP BC #3 42.0	LFC DT 33.00
	02/00:59:54	1047	LFC-EXP BC #2 36.8	12144-LFC DT 33.00
	02/01:00:39	8313	LFC-STANDBY COMMAND	MSPC EXECUTION

Figure 3-5.- An actual LFC command set. This was the set used during STS 41-G for data pass 33.00 during orbit 33 on mission day 2. Note that GMT is converted to MET to be compatible with command uplink sequencing and execution time tags. Counting the initial pre-pass setup, this data pass called for 5 values for V/H and 6 values for shutter speed (exposure).

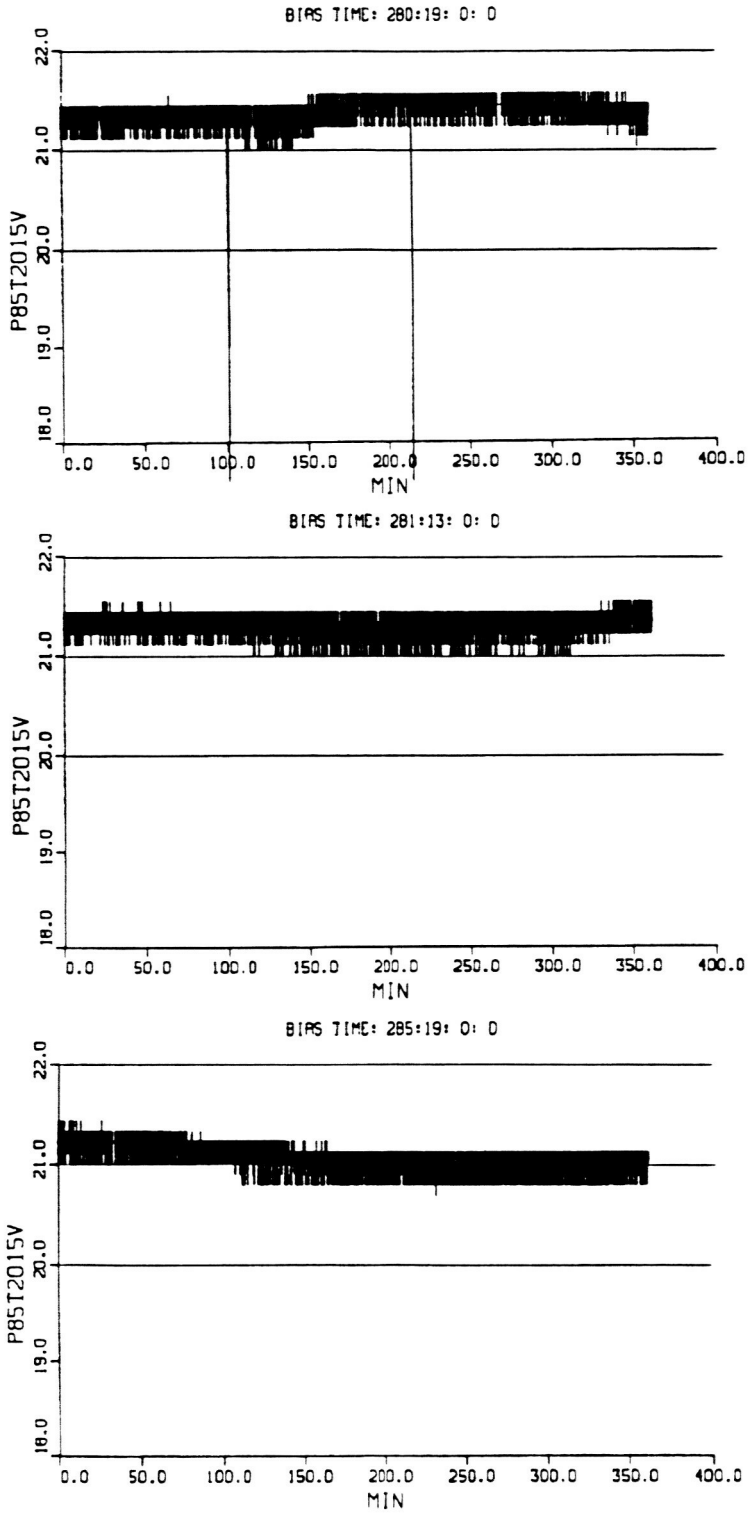


Figure 3-6.- Thermal history for the LFC film platen. (Measurement ID P85T2015.) Three discrete 6-hr intervals on days 280, 281, and 285.

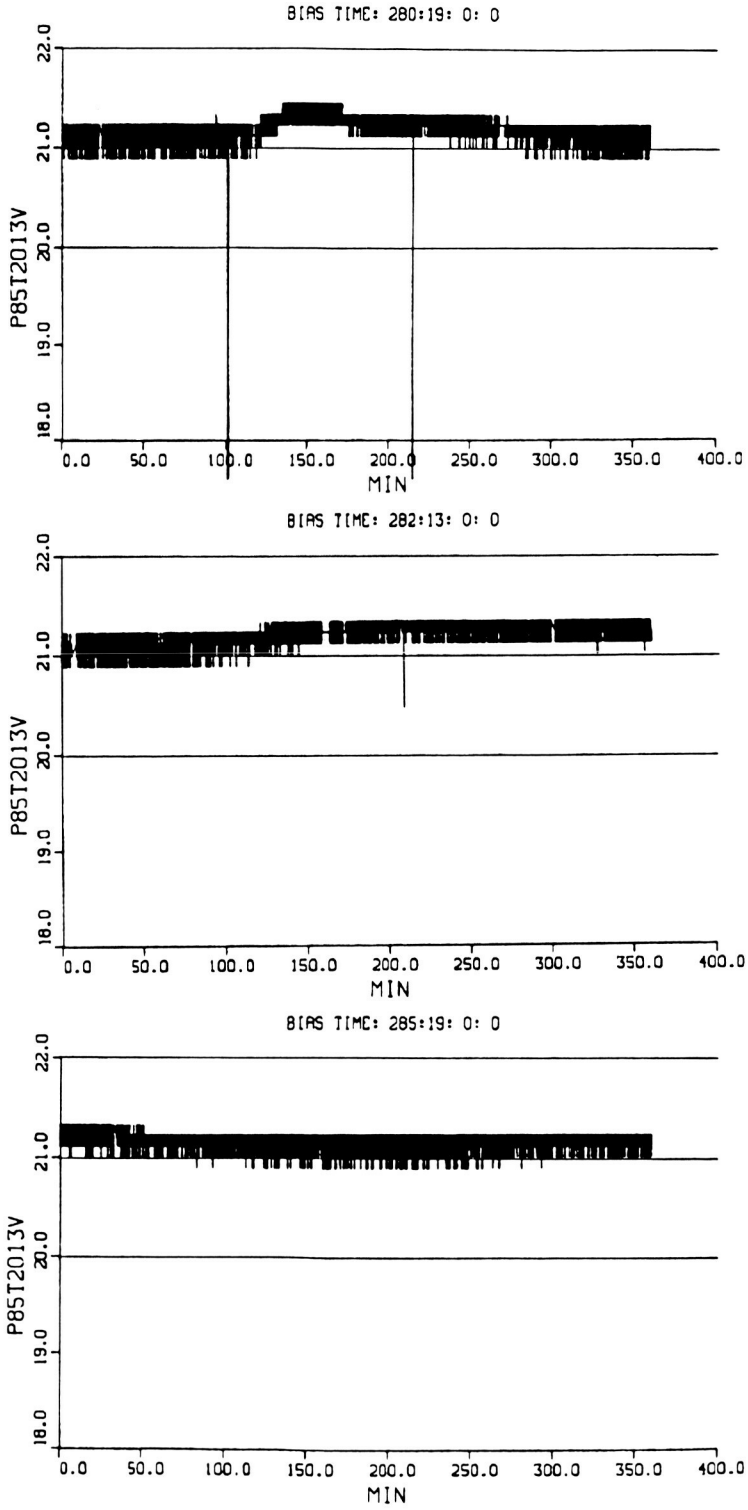


Figure 3-7.- Thermal history for the LFC lens cell. (Measurement ID P85T2013.) Three discrete 6-hr intervals on days 280, 281, and 285.

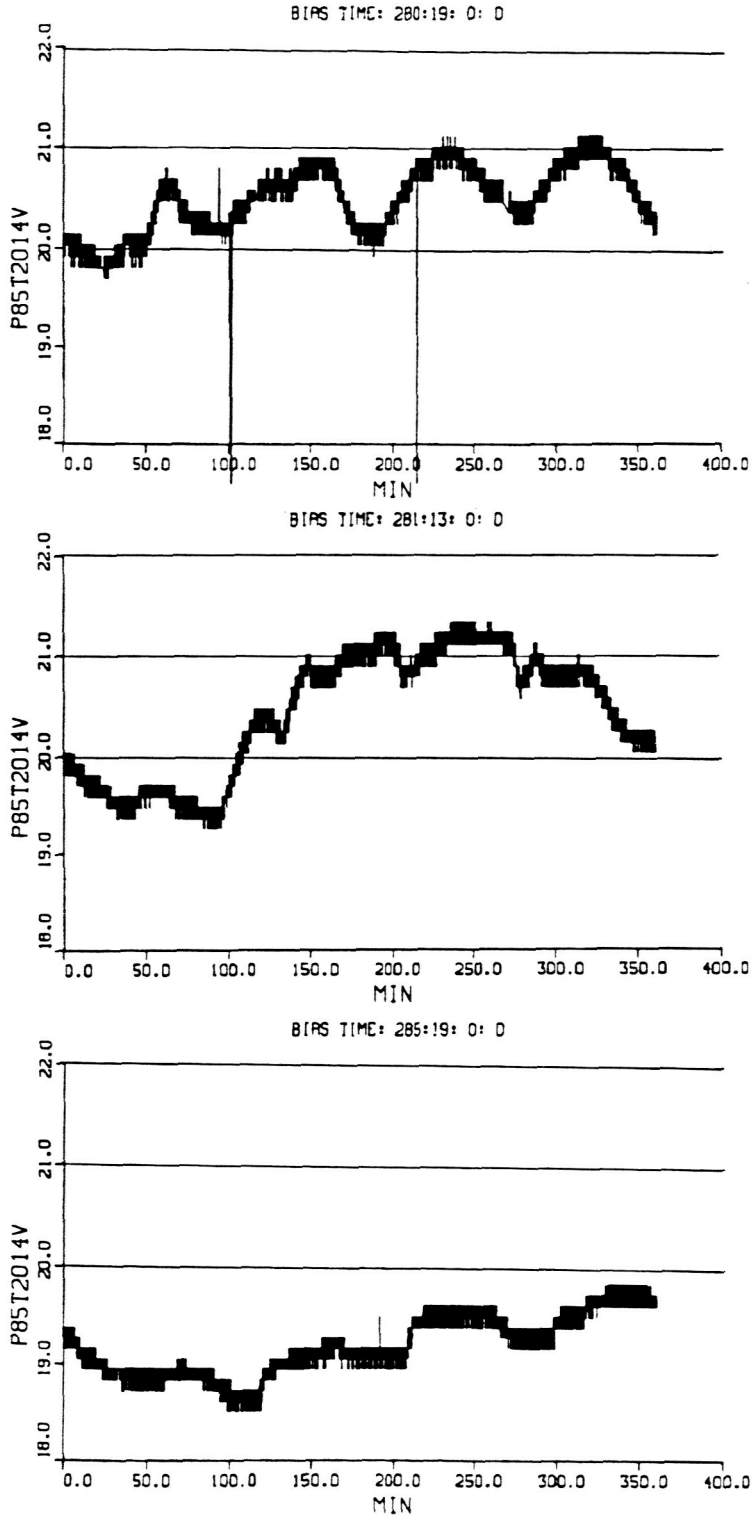


Figure 3-8.- Thermal history for the LFC lens support structure. (Measurement ID P85T2015.) Three discrete 6-hr intervals on days 280, 281, and 285.

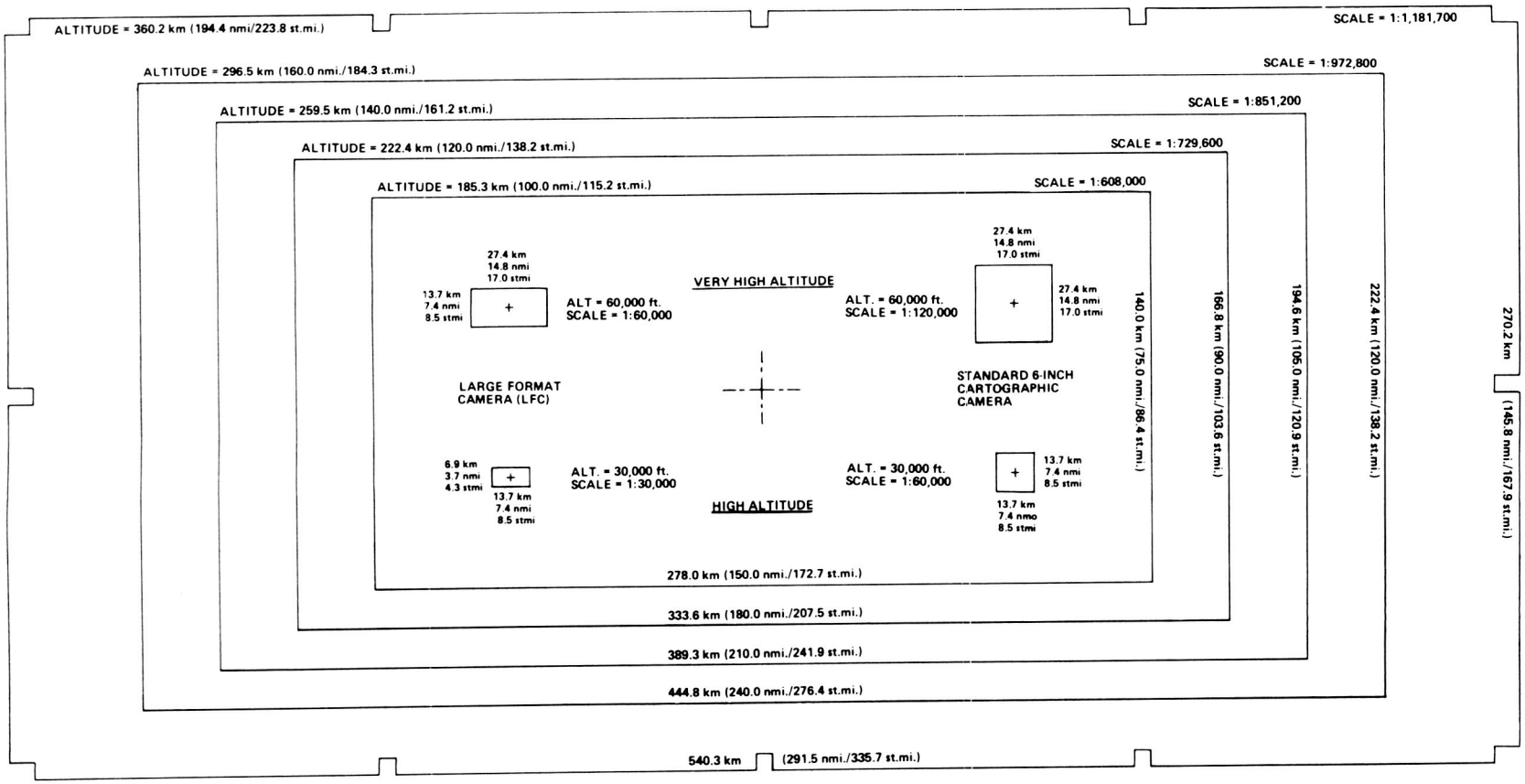
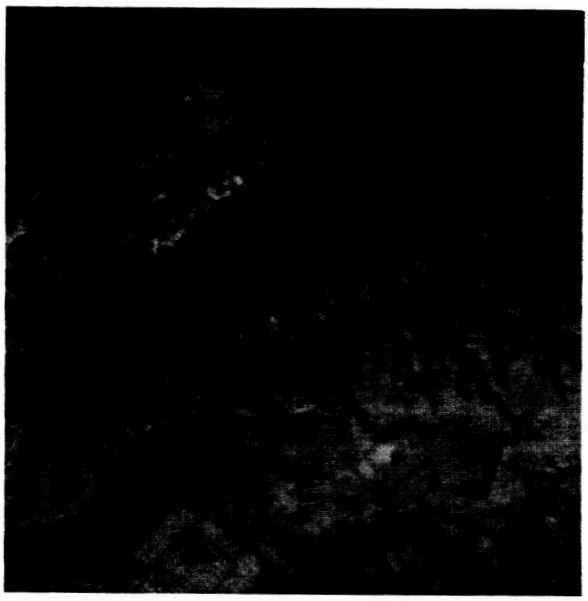


Figure 3-9.- LFC footprints (area of ground coverage) at various altitudes.



(a) Frame 0072, 10X, 1:118,300.



(b) Frame 0072, 35X, 1:33,800.

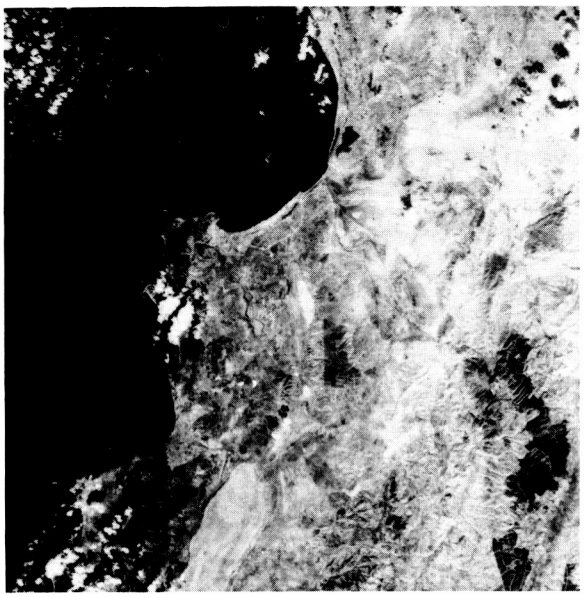


(c) Frame 0072, 35X, 1:33,800.

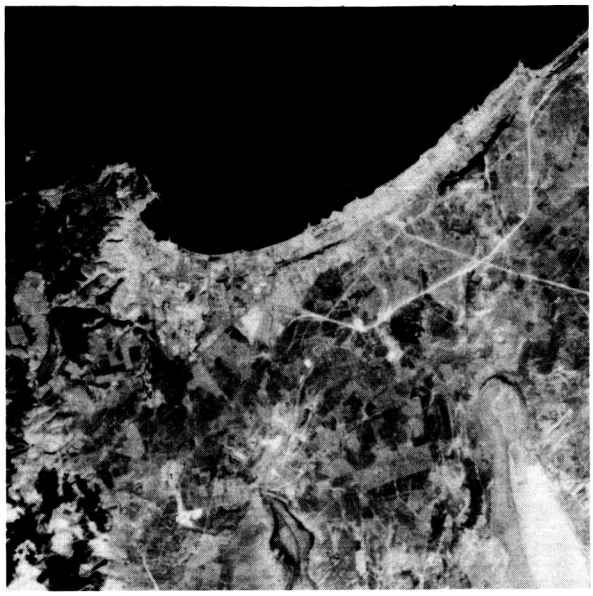


(d) Frame 0072, 100X, 1:11,800.

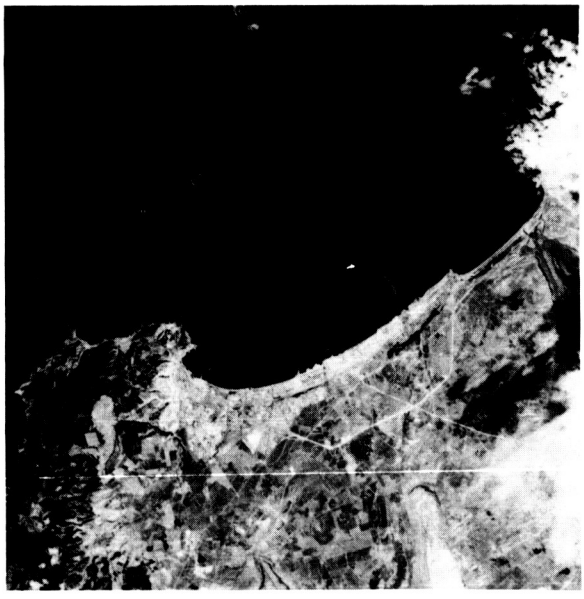
Figure 3-10.- Tubruq, Libya. Photos are from an altitude of 360.52 km, during orbit 2 (GMT 279:1305:52), with an original scale of 1:1,183,000, on type 3414 film.



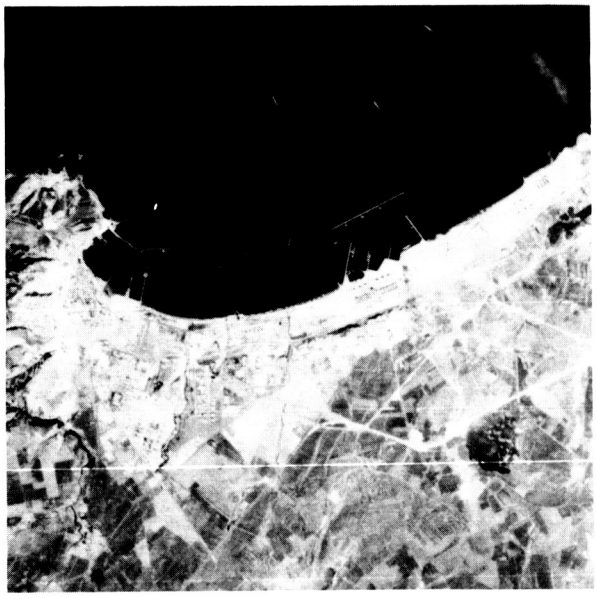
(a) Frame 0123, 1X, 1:1,186,000.



(b) Frame 0123, 4.5X, 1:264,000.



(c) Frame 1357, 1X, 1:761,000.



(d) Frame 1357, 4.5X, 1:169,000.

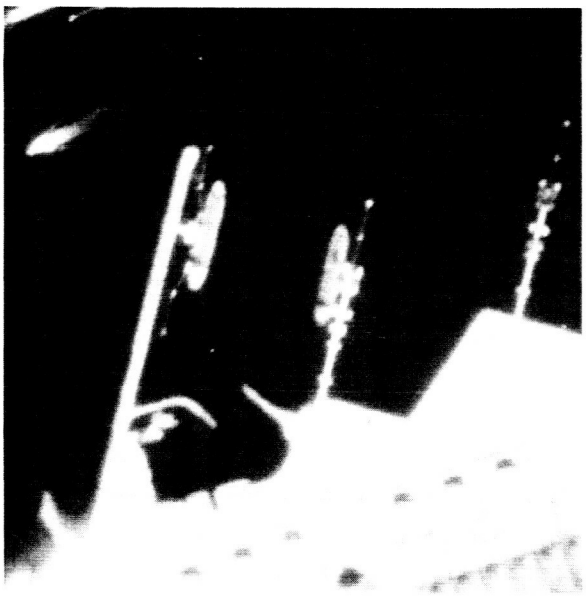
Figure 3-11.- Port aux Poules, Algeria. Photos a and b are from an altitude of 361.45 km during orbit 3 (GMT 279:1436:20), with an original scale of 1:1,186,000; c and d are from an altitude of 231.87 km during orbit 66 (GMT 283:1256:40), with an original scale of 1:761,000. Both are on type 3414 film.



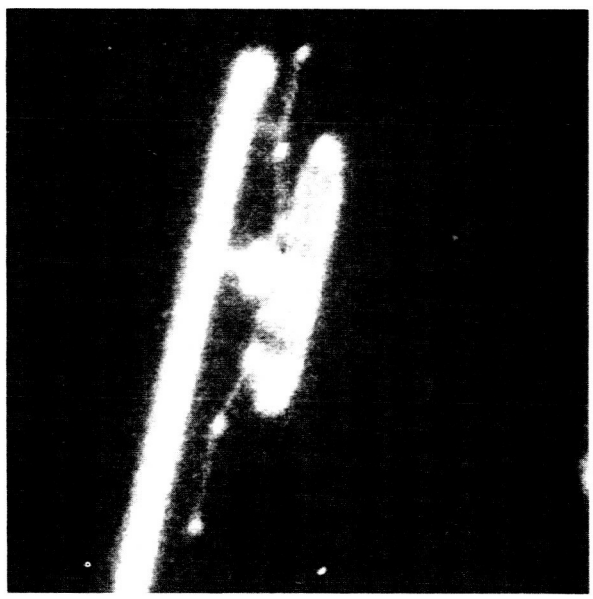
(a) Frame 0123, 35X, 1:34,000.



(b) Frame 0123, 100X, 1:11,860.

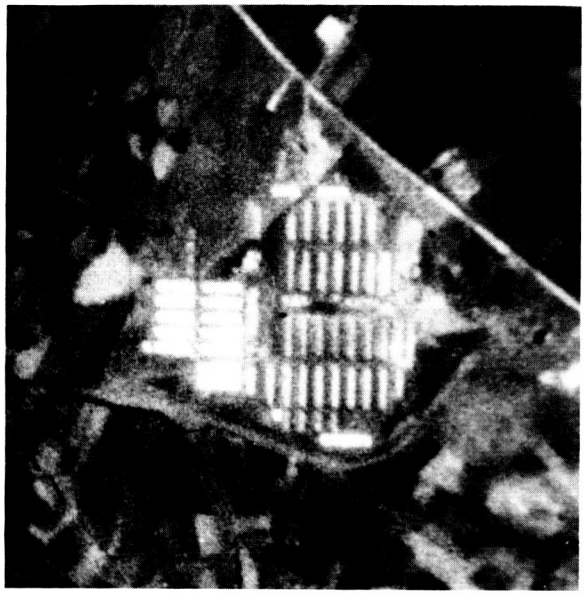


(c) Frame 1357, 35X, 1:21,700.

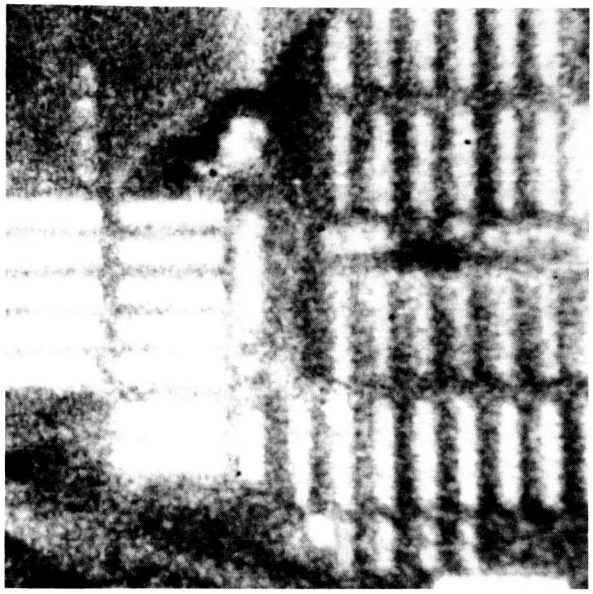


(d) Frame 1357, 100X, 1:7,600.

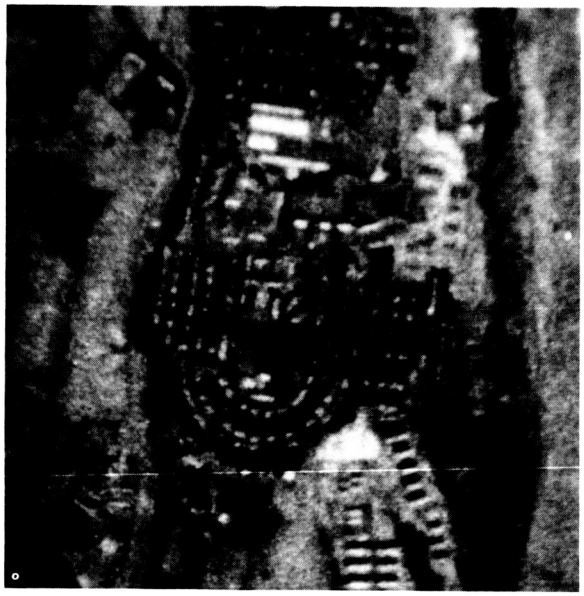
Figure 3-12.- Port aux Poules, Algeria. Photos a and b are from an altitude of 361.45 km during orbit 3 (GMT 279:1436:20), with an original scale of 1:1,186,000; c and d are from an altitude of 231.87 km during orbit 66 (GMT 283:1256:40), with an original scale of 1:761,000. Both are on type 3414 film.



(a) Frame 0217, 35X, 1:39,000.



(b) Frame 0217, 100X, 1:11,900.

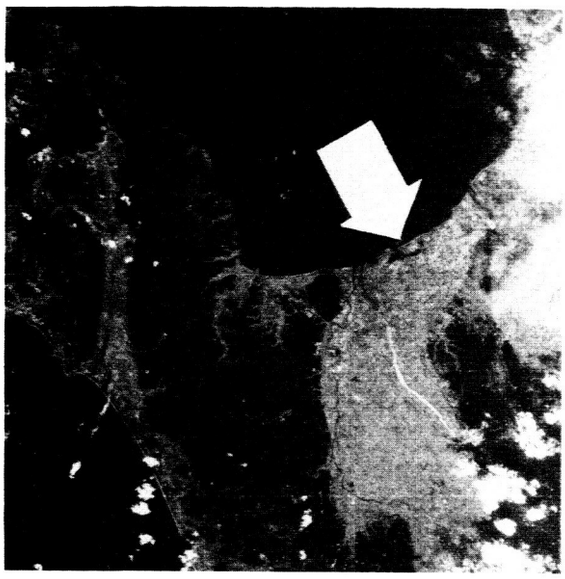


(c) Frame 0593, 35X, 1:25,000.



(d) Frame 0593, 100X, 1:8,720.

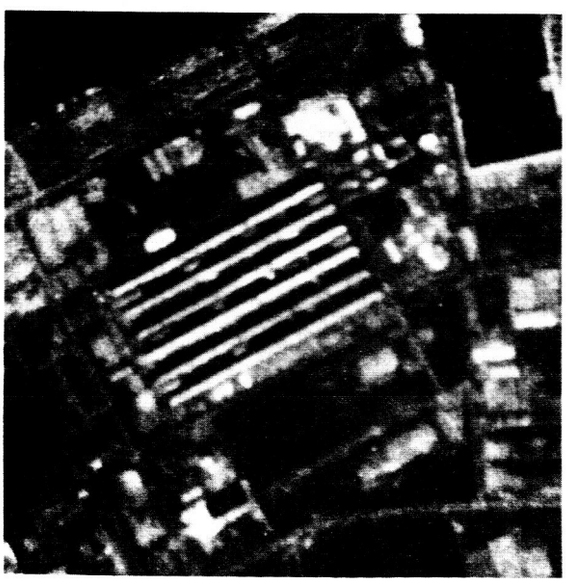
Figure 3-13.- Two sites in Turkey and Armenia. Photos a and b show Bursa, Turkey, from an altitude of 362.91 km during STS 41-G orbit 17 (GMT 280:1156:37), with an original scale of 1:1,190,000; c and d show Yerevan, Armenia, from an altitude of 265.88 km during orbit 32 (GMT 281:1030:56), with an original scale of 1:872,000. Both are on type 3414 film.



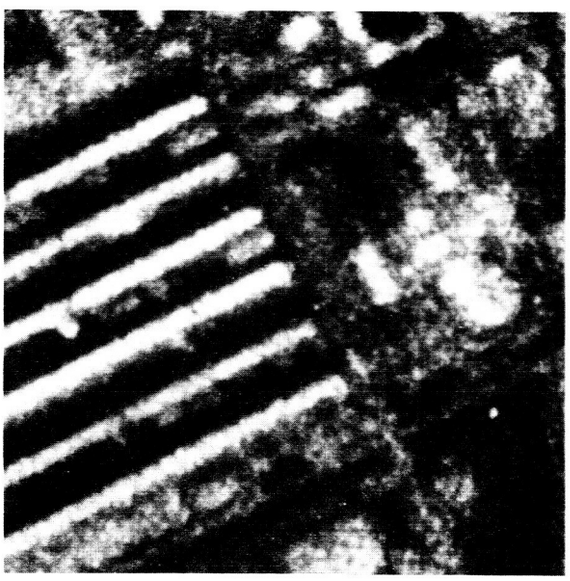
(a) Frame 0793, 1X, 1:752,000.



(b) Frame 0793, 10X, 1:75,200.

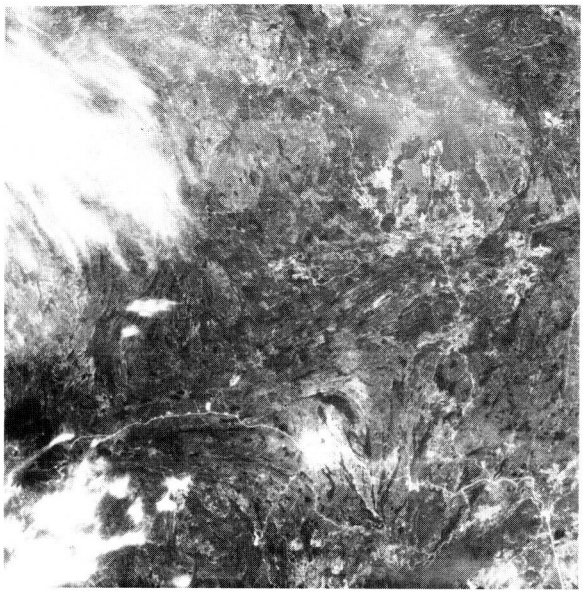


(c) Frame 0793, 35X, 1:21,500.

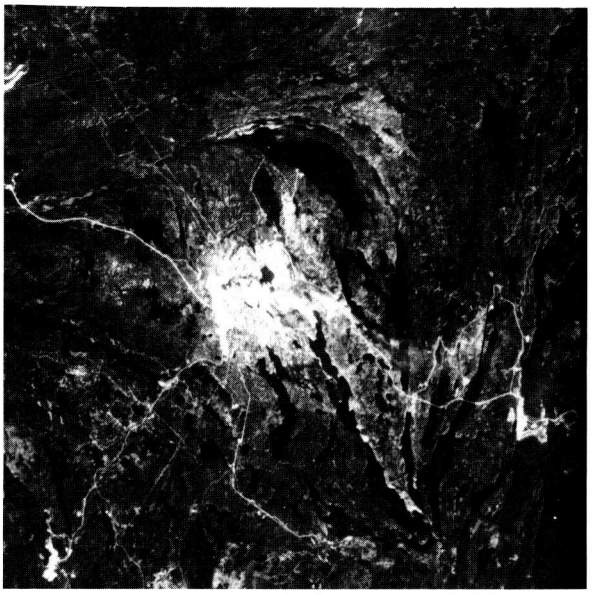


(d) Frame 0793, 100X, 1:7,520.

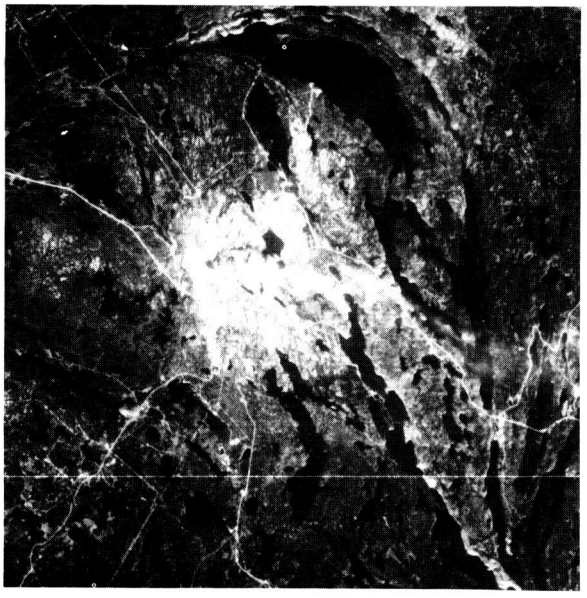
Figure 3-14.- Toyama, Japan. Photos are from an altitude of 229.28 km during orbit 44 (GMT 282:0420:01), with an original scale of 1:752,000 on type 3412 film.



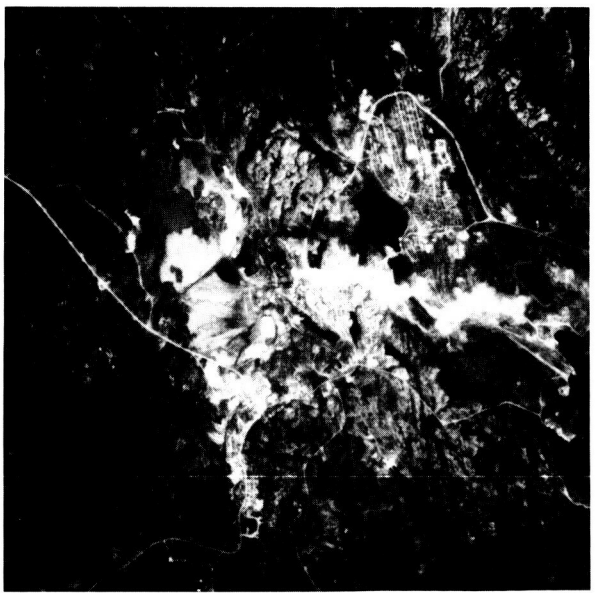
(a) Frame 0252, 1X, 1:1,203,000.



(b) Frame 0252, 3X, 1:401,000.



(c) Frame 0252, 4.5X, 1:267,000.



(d) Frame 0252, 10X, 1:120,000.

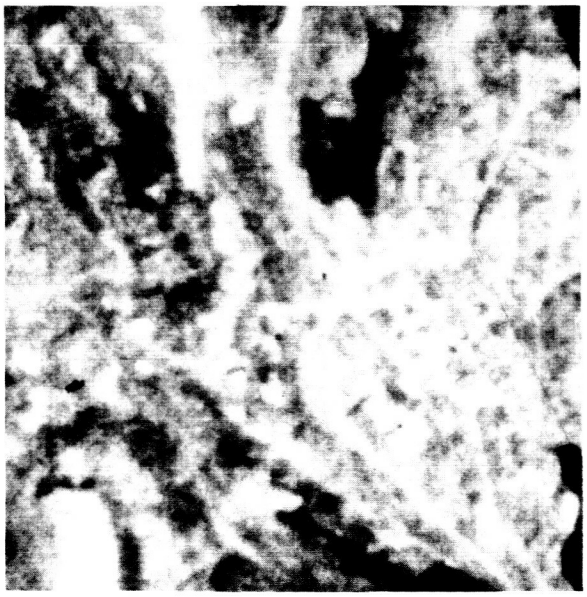
Figure 3-15.- Flin Flon, Manitoba, Canada. Photos are from an altitude of 366.71 km during orbit 21 (GMT 280:1754:56), with an original scale of 1:1,203,000 on type 3414 film.



(a) Frame 0252, 35X, 1:34,000.



(b) Frame 0626, 35X, 1:22,100.



(c) Frame 0946, 35X, 1:22,300.



(d) Frame 1608, 35X, 1:21,800.

Photo	LFC frame	Alt. (km)	Track nadir	GMT	Film type	Original scale
(a)	0252	366.71	56.2°N	280:1754:56	3414	1:1,203,000
(b)	0626	236.22	55.1°N	281:1749:29	3412	1:775,000
(c)	0946	237.88	54.9°N	282:1732:28	S0-242	1:780,000
(d)	1608	232.92	54.1°N	284:1659:08	S0-131	1:764,000

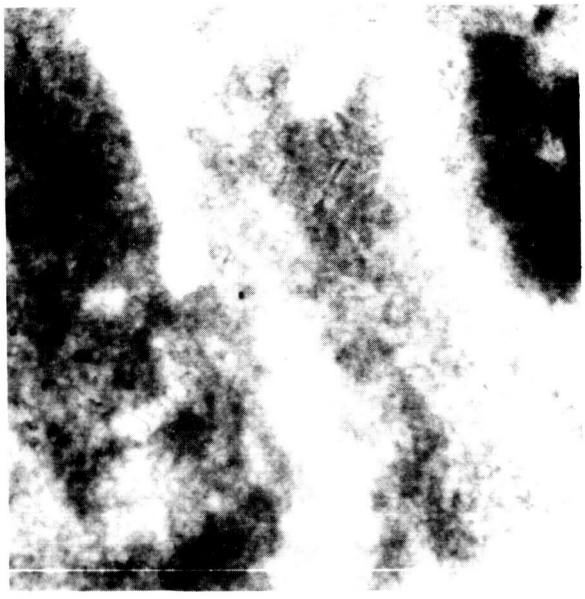
Figure 3-16.- Flin Flon, Manitoba, Canada. As recorded on four types of film by the LFC during STS 41-G (35X).



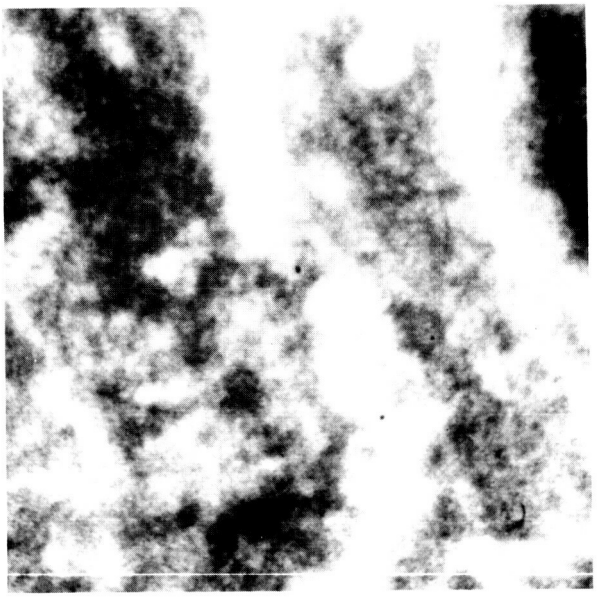
(a) Frame 0252, 100X, 1:12,000.



(b) Frame 0626, 100X, 1:7,750.



(c) Frame 0946, 100X, 1:7,800.



(d) Frame 1608, 100X, 1:7,640.

Photo	LFC frame	Alt. (km)	Track nadir	GMT	Film type	Original scale
(a)	0252	366.71	56.2°N	280:1754:56	3414	1:1,203,000
(b)	0626	236.22	55.1°N	281:1749:29	3412	1:775,000
(c)	0946	237.88	54.9°N	282:1732:28	S0-242	1:780,000
(d)	1608	232.92	54.1°N	284:1659:08	S0-131	1:764,000

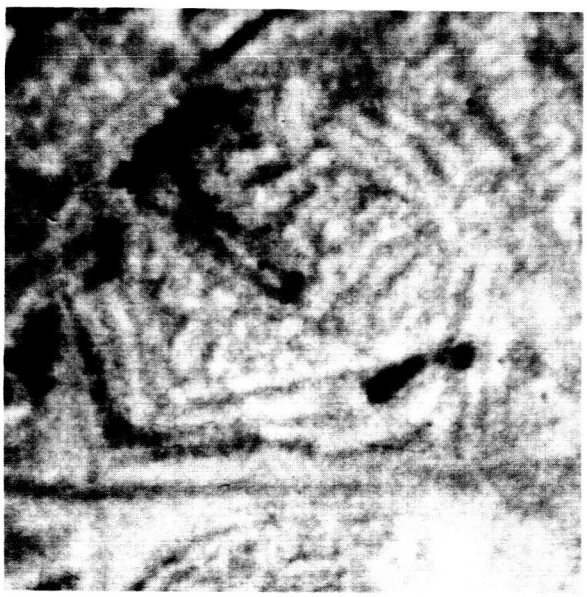
Figure 3-17.- Flin Flon, Manitoba, Canada. As recorded on four types of film by the LFC during the STS 41-G mission (100X).



(a) Frame 0982, 35X, 1:22,000.



(b) Frame 1452, 35X, 1:22,000.



(c) Frame 1631, 35X, 1:21,600.

Photo	LFC frame	Alt. (km)	Track nadir	GMT	Film type	Original scale
(a)	0982	236.12	50.3°N	282:1903:58	S0-242	1:774,000
(b)	1452	236.17	50.2°N	283:1847:21	3414	1:774,000
(c)	1631	231.40	49.3°N	284:1830:35	S0-131	1:759,000

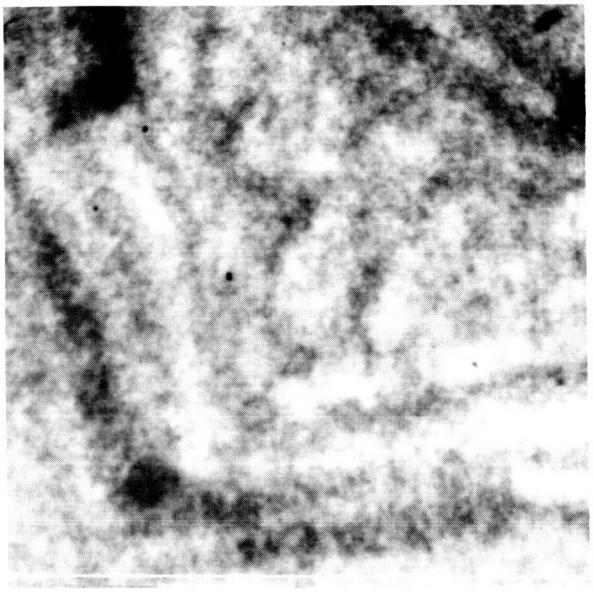
Figure 3-18.- Medicine Hat, Alberta, Canada. Municipal golf course, as recorded on three types of film by the LFC during STS 41-G (35X).



(a) Frame 0982, 100X, 1:7,700.



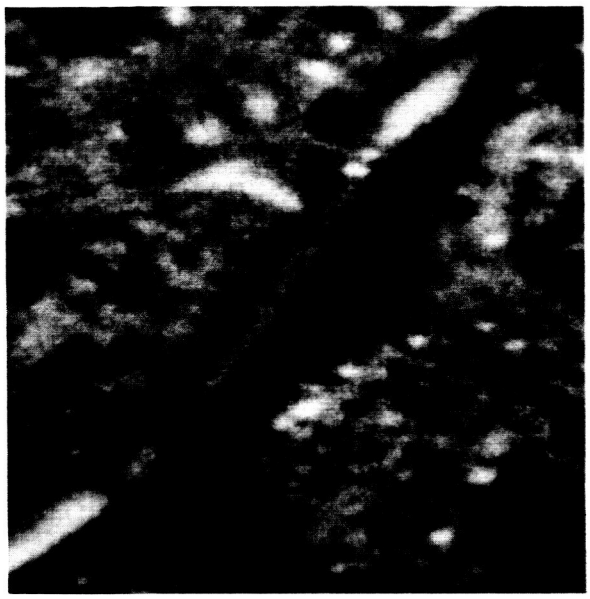
(b) Frame 1452, 100X, 1:7,700.



(c) Frame 1631, 100X, 1:7,500.

Photo	LFC frame	Alt. (km)	Track nadir	GMT	Film type	Original scale
(a)	0982	236.12	50.3°N	282:1903:58	S0-242	1:774,000
(b)	1452	236.17	50.2°N	283:1847:21	3414	1:774,000
(c)	1631	231.40	49.3°N	284:1830:35	S0-131	1:759,000

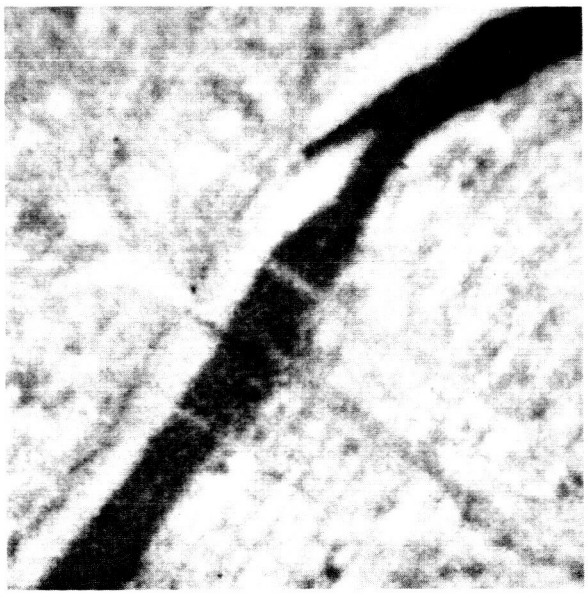
Figure 3-19.- Medicine Hat, Alberta, Canada. Municipal golf course, as recorded on three types of film by the LFC during STS 41-G (100X).



(a) Frame 0982, 35X, 1:22,000.



(b) Frame 1452, 35X, 1:22,000.



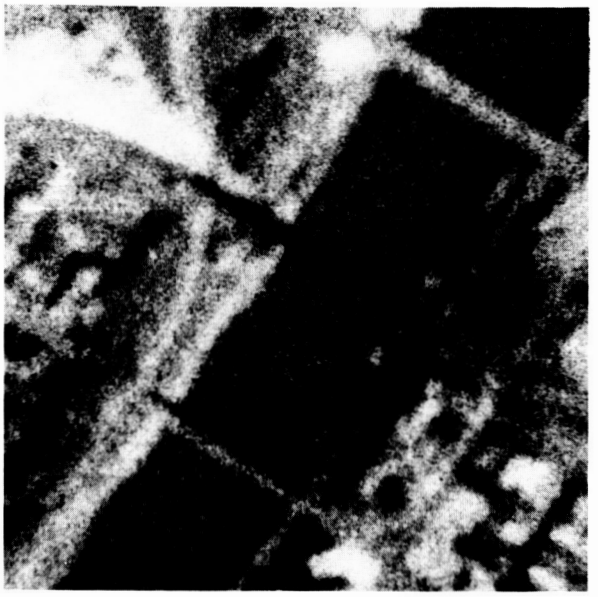
(c) Frame 1631, 35X, 1:21,600.

Photo	LFC frame	Alt. (km)	Track nadir	GMT	Film type	Original scale
(a)	0982	236.12	50.3°N	282:1903:58	S0-242	1:774,000
(b)	1452	236.17	50.2°N	283:1847:21	3414	1:774,000
(c)	1631	231.40	49.3°N	284:1830:35	S0-131	1:759,000

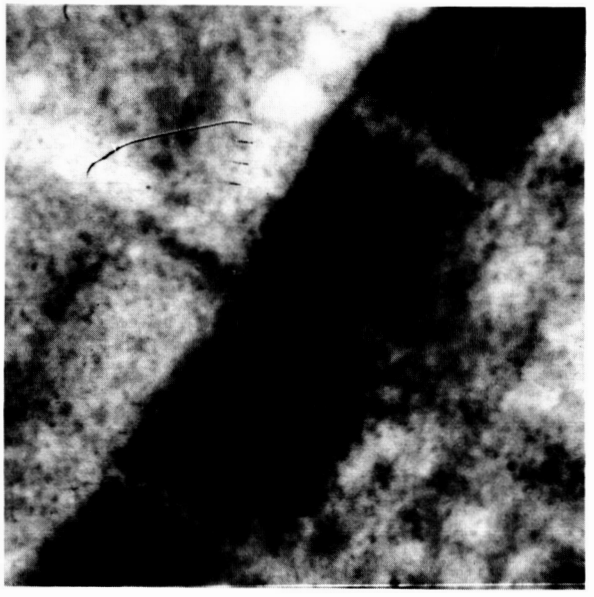
Figure 3-20.- Medicine Hat, Alberta, Canada. Downtown bridges, as recorded on three types of film by the LFC during STS 41-G (35X).



(a) Frame 0982, 100X, 1:7,700.



(b) Frame 1452, 100X, 1:7,700.



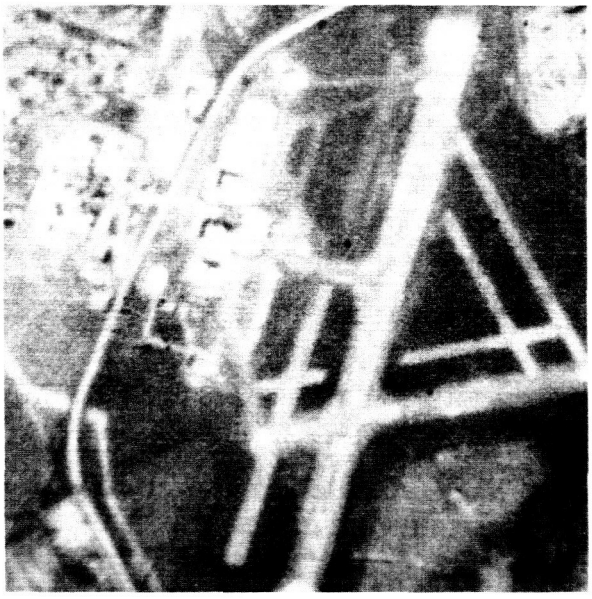
(c) Frame 1631, 100X, 1:7,500.

Photo	LFC frame	Alt. (km)	Track nadir	GMT	Film type	Original scale
(a)	0982	236.12	50.3°N	282:1903:58	S0-242	1:774,000
(b)	1452	236.17	50.2°N	283:1847:21	3414	1:774,000
(c)	1631	231.40	49.3°N	284:1830:35	S0-131	1:759,000

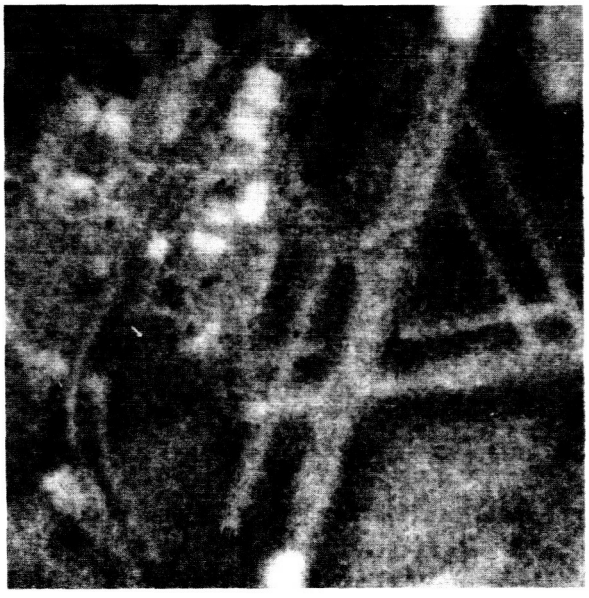
Figure 3-21.- Medicine Hat, Alberta, Canada. Downtown bridges, as recorded on three types of film by the LFC during STS 41-G (100X).



(a) Frame 0982, 35X, 1:22,000.



(b) Frame 1452, 35X, 1:22,000.



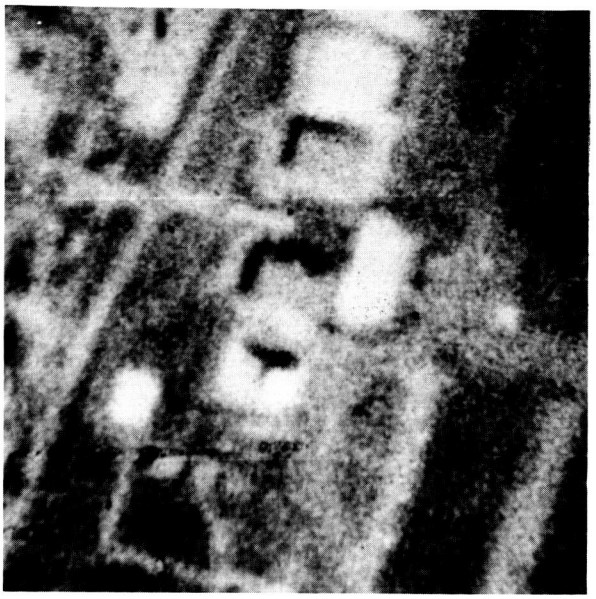
(c) Frame 1631, 35X, 1:21,600.

Photo	LFC frame	Alt. (km)	Track nadir	GMT	Film type	Original scale
(a)	0982	236.12	50.3°N	282:1903:58	S0-242	1:774,000
(b)	1452	236.17	50.2°N	283:1847:21	3414	1:774,000
(c)	1631	231.40	49.3°N	284:1830:35	S0-131	1:759,000

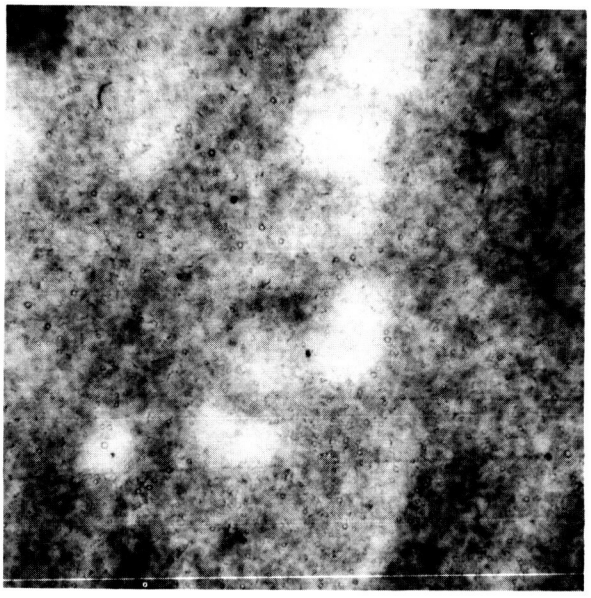
Figure 3-22.- Medicine Hat, Alberta, Canada. Municipal airport, as recorded on three types of film by the LFC during STS 41-G (35X).



(a) Frame 0982, 100X, 1:7,700.



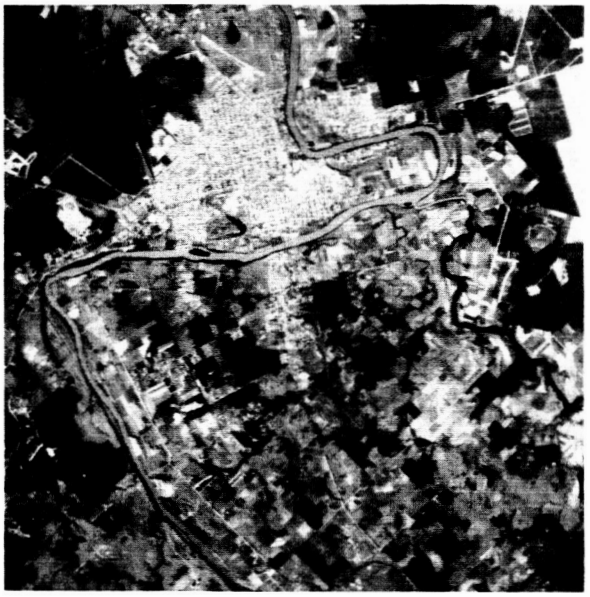
(b) Frame 1452, 100X, 1:7,700.



(c) Frame 1631, 100X, 1:7,500.

Photo	LFC frame	Alt. (km)	Track nadir	GMT	Film type	Original scale
(a)	0982	236.12	50.3°N	282:1903:58	S0-242	1:774,000
(b)	1452	236.17	50.2°N	283:1847:21	3414	1:774,000
(c)	1631	231.40	49.3°N	284:1830:35	S0-131	1:759,000

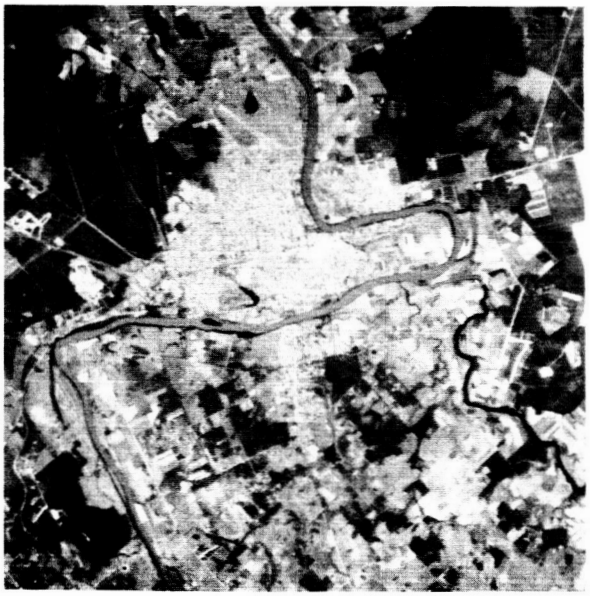
Figure 3-23.- Medicine Hat, Alberta, Canada. Municipal airport, as recorded on three types of film by the LFC during STS 41-G (100X).



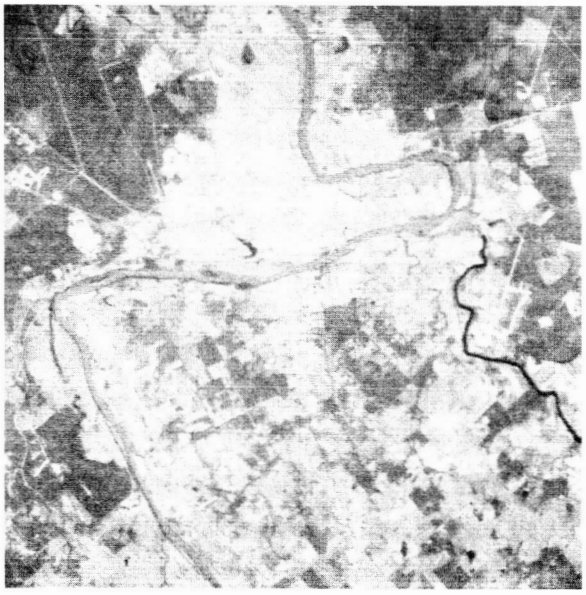
(a) Frame 1976, 4.5X, 1:164,000.



(b) Frame 1661, 4.5X, 1:164,000.



(c) Frame 1661, 4.5X, 1:164,000.



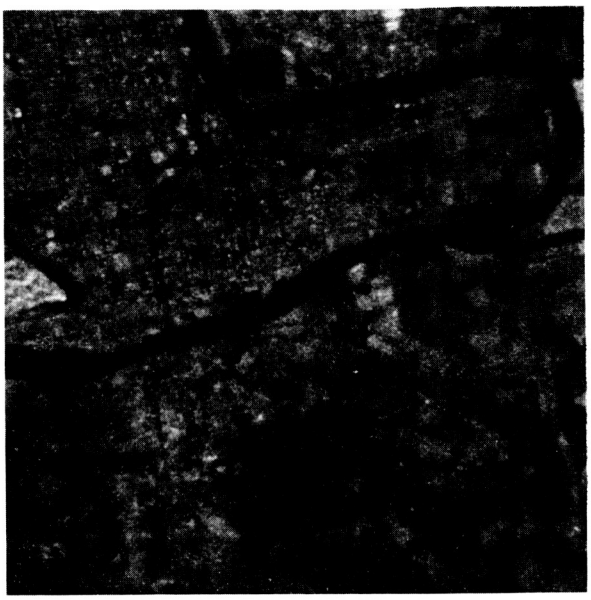
(d) Frame 1661, 4.5X, 1:164,000.

Photo	LFC frame	Alt. (km)	GMT	Film type	Original scale	Tricolor filter
(a)	1500	228.51	284:0533:39	3414	1:750,000	(None)
(b)	1705	227.66	285:0516:23	S0-131	1:747,000	Red
(c)	1705	227.66	285:0516:23	S0-131	1:747,000	Green
(d)	1705	227.66	285:0516:23	S0-131	1:747,000	Blue

Figure 3-24.- Maryborough, Queensland, Australia.



(a) Frame 1500, 10X, 1:167,000.



(b) Frame 1705, 10X, 1:166,000.



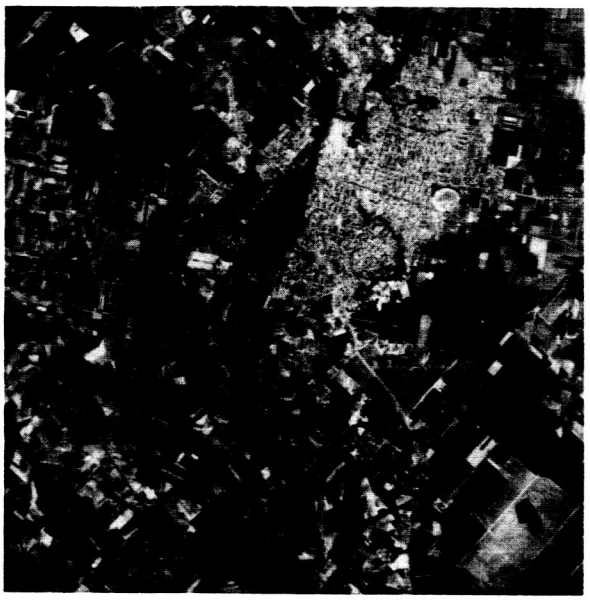
(c) Frame 1705, 10X, 1:166,000.



(d) Frame 1705, 10X, 1:166,000.

Photo	LFC frame	Alt. (km)	GMT	Film type	Original scale	Tricolor filter
(a)	1500	228.51	284:0533:39	3414	1:750,000	(None)
(b)	1705	227.66	285:0516:23	S0-131	1:747,000	Red
(c)	1705	227.66	285:0516:23	S0-131	1:747,000	Green
(d)	1705	227.66	285:0516:23	S0-131	1:747,000	Blue

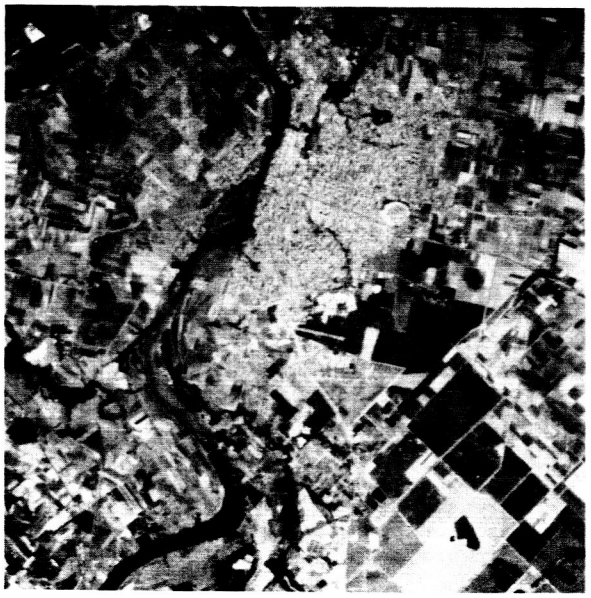
Figure 3-25.- Maryborough, Queensland, Australia.



(a) Frame 1500, 4.5X, 1:167,000.



(b) Frame 1705, 4.5X, 1:166,000.



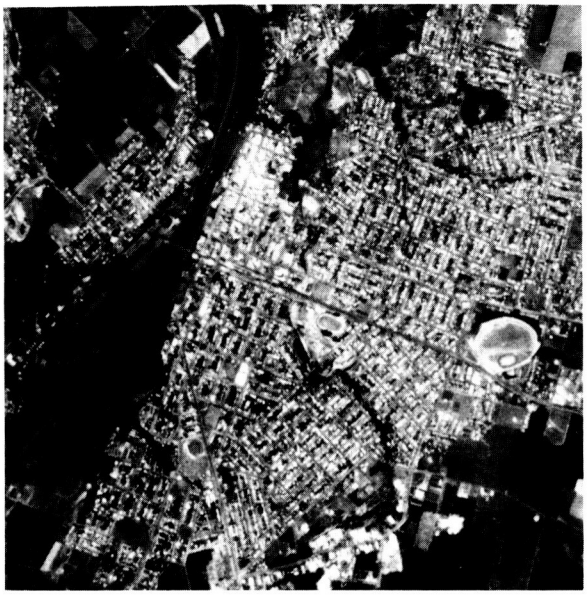
(c) Frame 1705, 4.5X, 1:166,000.



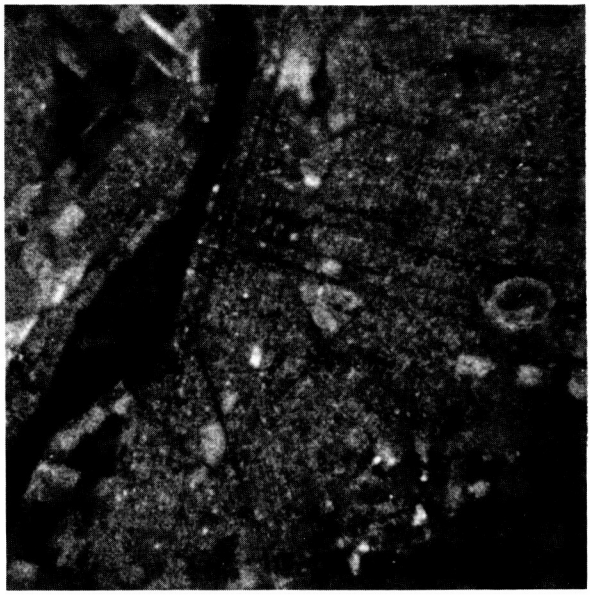
(d) Frame 1705, 4.5X, 1:166,000.

Photo	LFC frame	Alt. (km)	GMT	Film type	Original scale	Tricolor filter
(a)	1500	228.51	284:0533:39	3414	1:750,000	(None)
(b)	1705	227.66	285:0516:23	S0-131	1:747,000	Red
(c)	1705	227.66	285:0516:23	S0-131	1:747,000	Green
(d)	1705	227.66	285:0516:23	S0-131	1:747,000	Blue

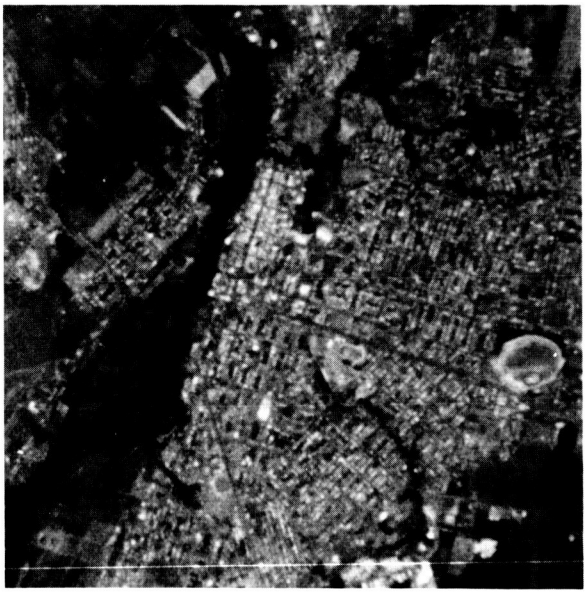
Figure 3-26.- Bundaberg, Queensland, Australia.



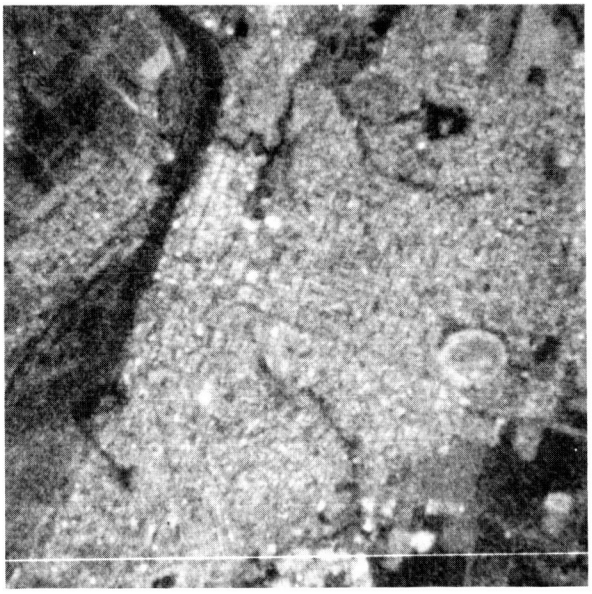
(a) Frame 1500, 10X, 1:167,000.



(b) Frame 1705, 10X, 1:166,000.



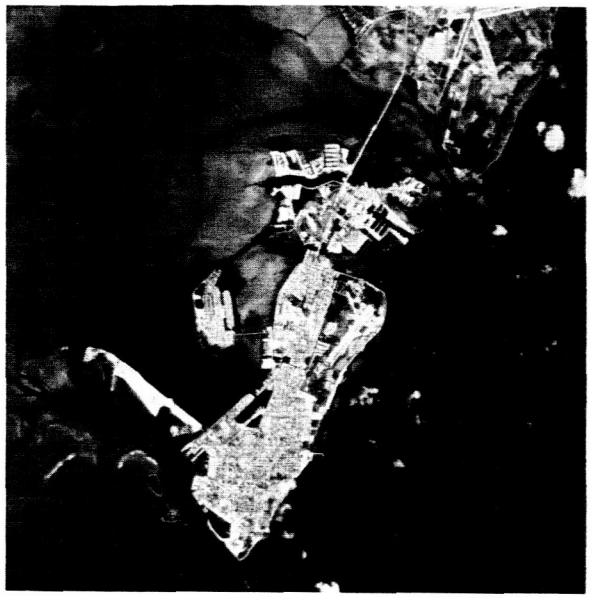
(c) Frame 1705, 10X, 1:166,000.



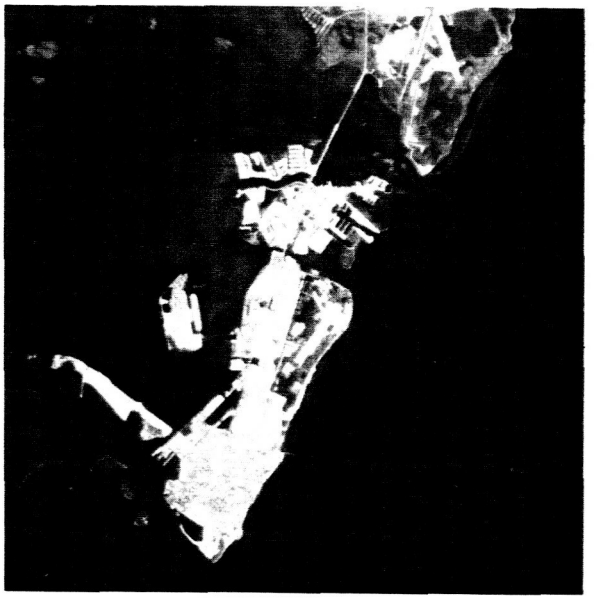
(d) Frame 1705, 10X, 1:166,000.

Photo	LFC frame	Alt. (km)	GMT	Film type	Original scale	Tricolor filter
(a)	1500	228.51	284:0533:39	3414	1:750,000	(None)
(b)	1705	227.66	285:0516:23	S0-131	1:747,000	Red
(c)	1705	227.66	285:0516:23	S0-131	1:747,000	Green
(d)	1705	227.66	285:0516:23	S0-131	1:747,000	Blue

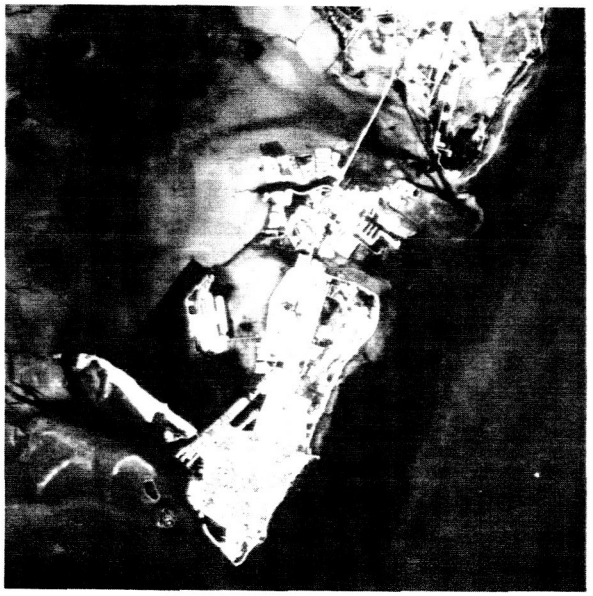
Figure 3-27.- Bundaberg, Queensland, Australia.



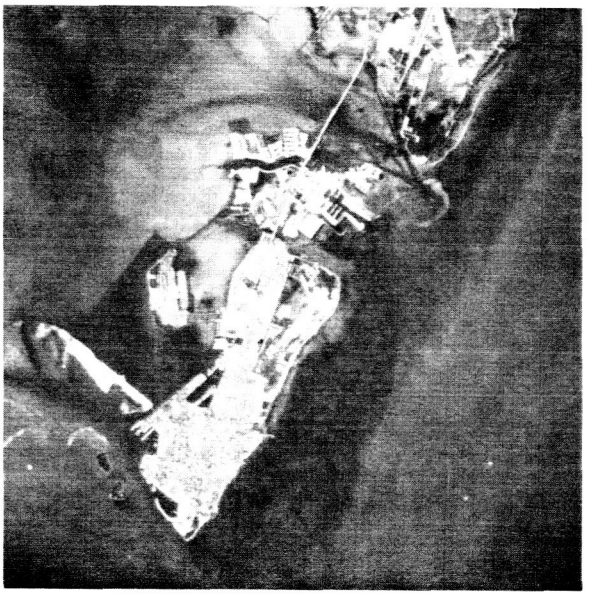
(a) Frame 1976, 4.5X, 1:164,000.



(b) Frame 1661, 4.5X, 1:164,000.



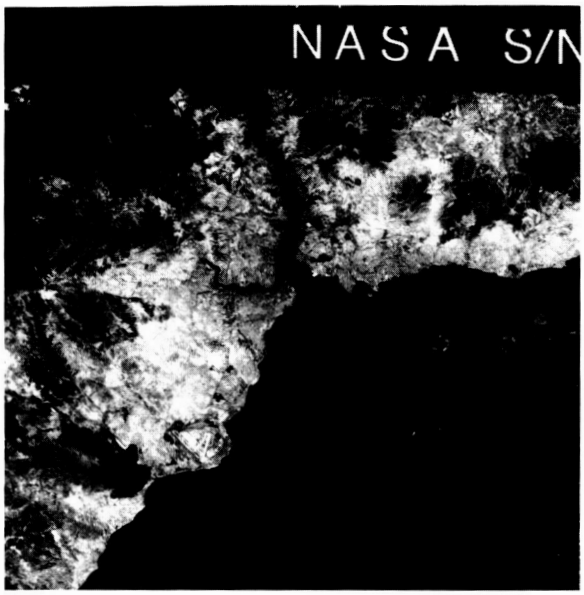
(c) Frame 1661, 4.5X, 1:164,000.



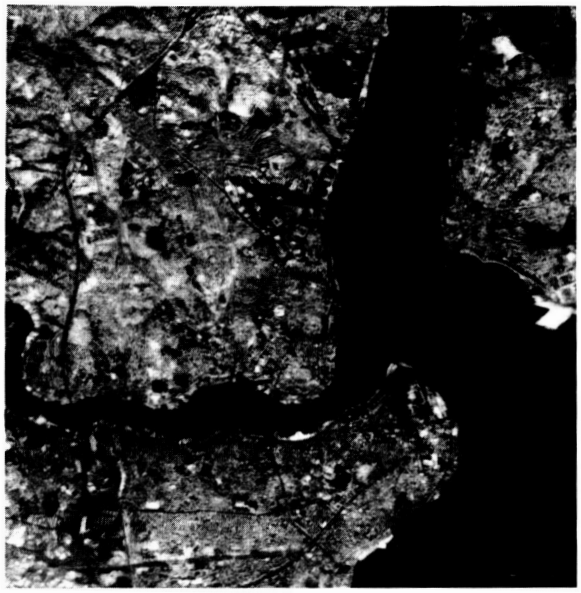
(d) Frame 1661, 4.5X, 1:164,000.

Photo	LFC frame	Alt. (km)	GMT	Film type	Original scale	Tricolor filter
(a)	1976	224.82	285:1821:32	3414	1:738,000	(None)
(b)	1661	225.06	284:1839:08	S0-131	1:738,000	Red
(c)	1661	225.06	284:1839:08	S0-131	1:738,000	Green
(d)	1661	225.06	284:1839:08	S0-131	1:738,000	Blue

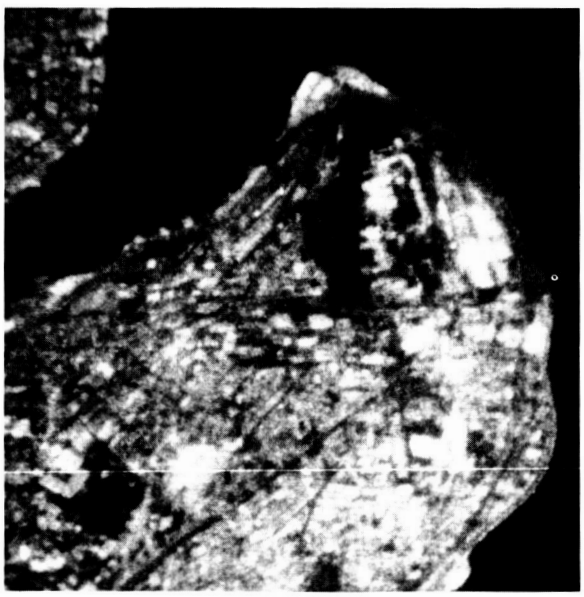
Figure 3-28.- Key West, Florida.



(a) Frame 0217, 2X, 1:595,000.



(b) Frame 0217, 10X, 1:119,000.

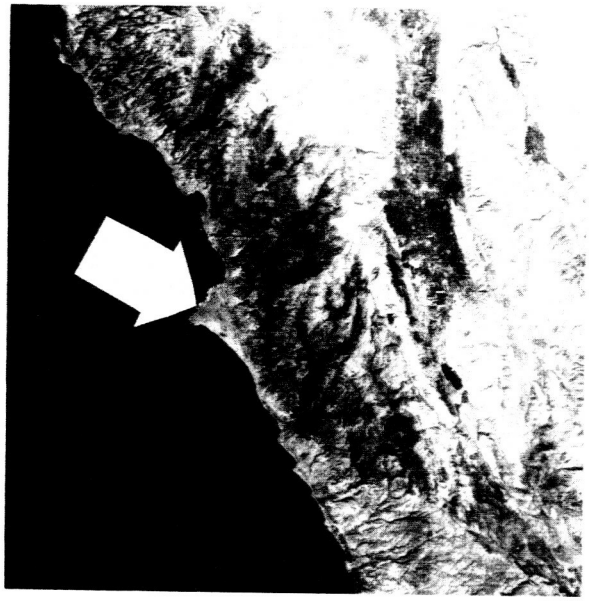


(c) Frame 0217, 35X, 1:34,000.

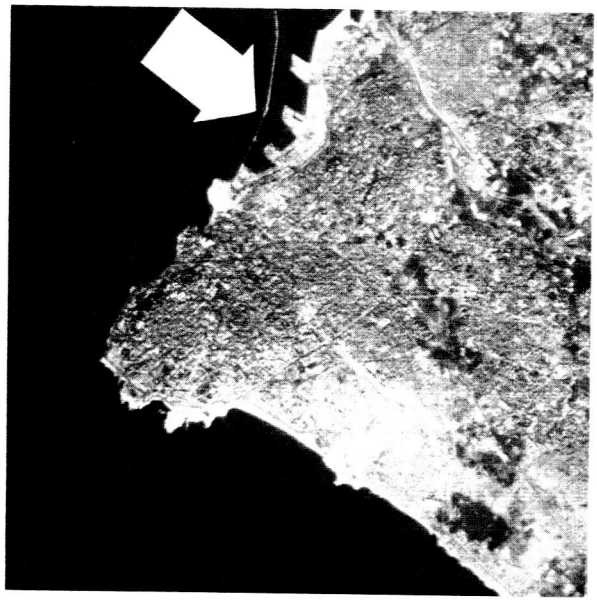


(d) Frame 0217, 100X, 1:11,900.

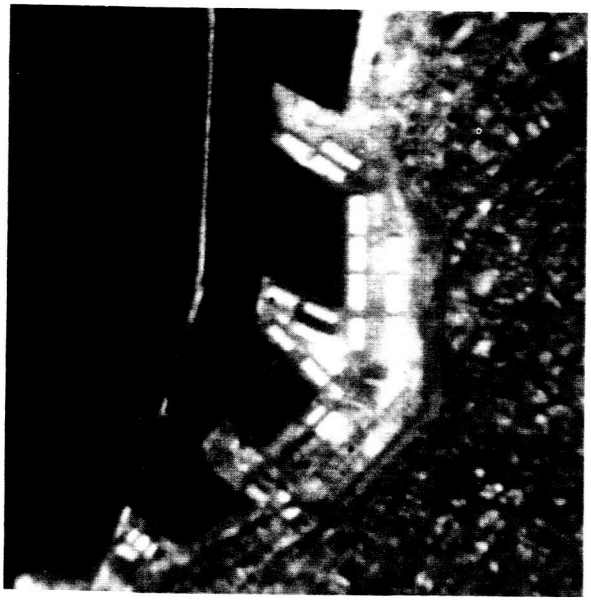
Figure 3-29.- Istanbul, Turkey. Lying between the Black Sea and the Marmara Denizi (sea), Istanbul is seen in this imagery acquired during orbit 17 from an altitude of 362.91 km (GMT 280:1156:37), on type 3414 film. Original scale was 1:1,190,000.



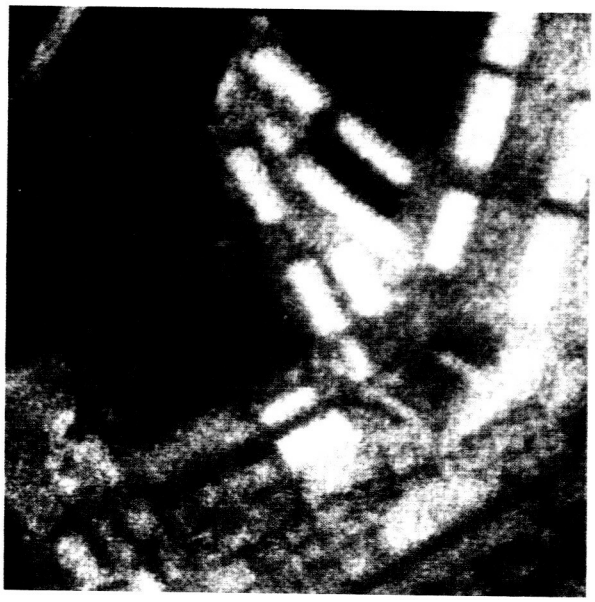
(a) Frame 0227, 1X, 1:1,185,000.



(b) Frame 0227, 10X, 1:118,500.

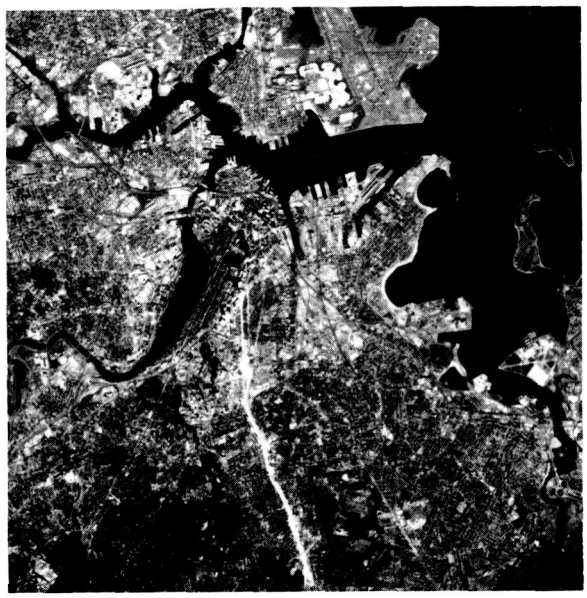


(c) Frame 0227, 35X, 1:33,800.



(d) Frame 0227, 100X, 1:11,800.

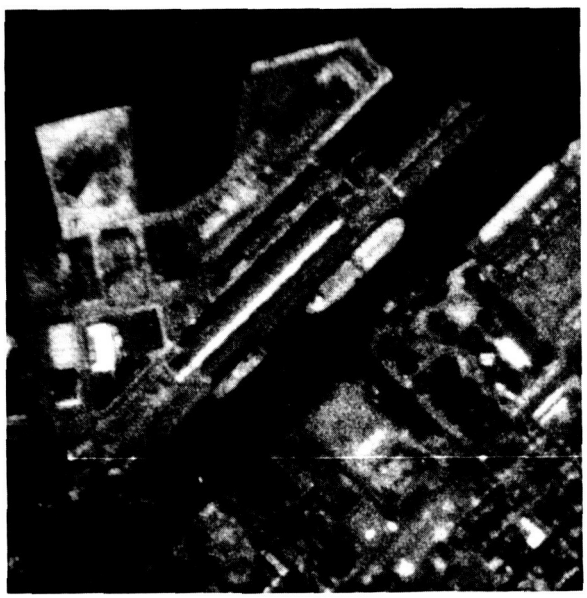
Figure 3-30.- Beirut, Lebanon. Beirut, situated at the eastern end of the Mediterranean Sea, is photographed during the continuation of orbit 17 from an altitude of 361.04 km (GMT 280:1159:03), approximately 2.5 min after Istanbul was photographed. Original scale photography is 1:1,185,000 on type 3414 film.



(a) Frame 0664, 4.5X, 1:168,000.



(b) Frame 0664, 10X, 1:75,900.

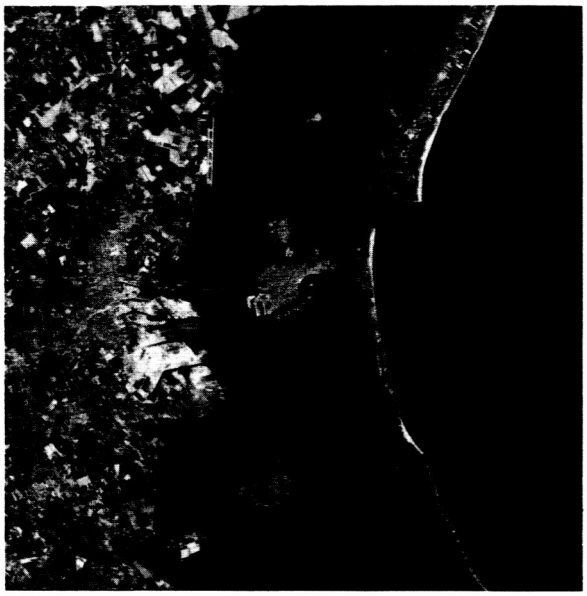


(c) Frame 0664, 35X, 1:21,600.



(d) Frame 0664, 100X, 1:7,590.

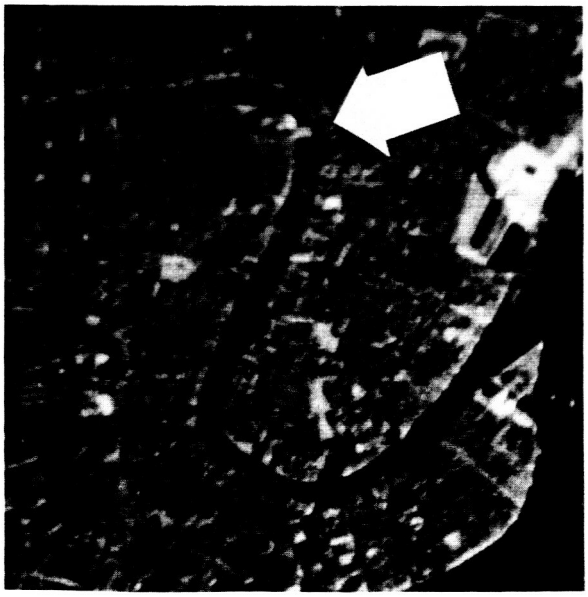
Figure 3-31.- Boston, Massachusetts. As covered during orbit 37 from an altitude of 231.26 km (GMT 281:1755:33). Original scale of photography is 1:759,000 on type 3412 film. Enhancement of resolution of pier side items is due to low albedo of harbor waters.



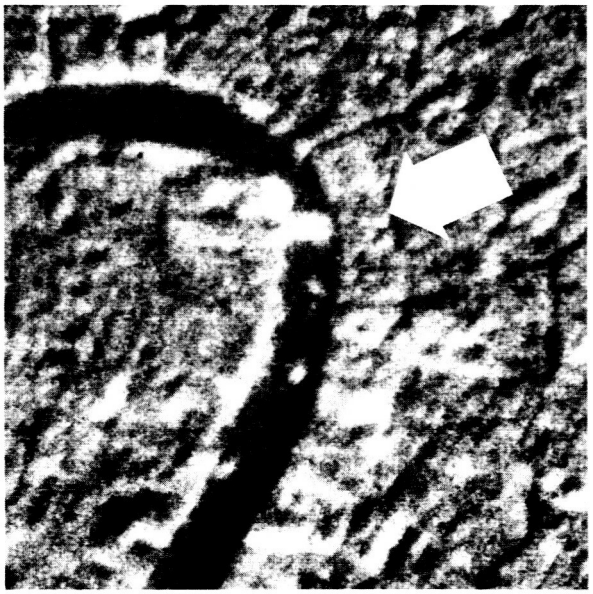
(a) Frame 1284, 2X, 1:385,000.



(b) Frame 1284, 10X, 1:77,000.



(c) Frame 1284, 35X, 1:22,000.



(d) Frame 1284, 100X, 1:7,700.

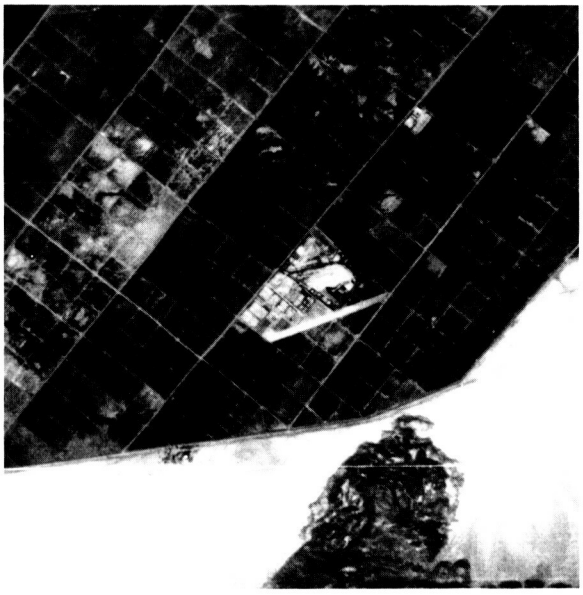
Figure 3-32.- Venezia (Venice), Italy, on the Adriatic Sea at the upper end of the "boot." As viewed on orbit 65 from an altitude of 234.67 km (GMT 283:1124:38). Original scale of photography is 1:770,000 on type 3414 film. As with the Boston scene, low albedo of harbor waters assists the enhancement of resolution.



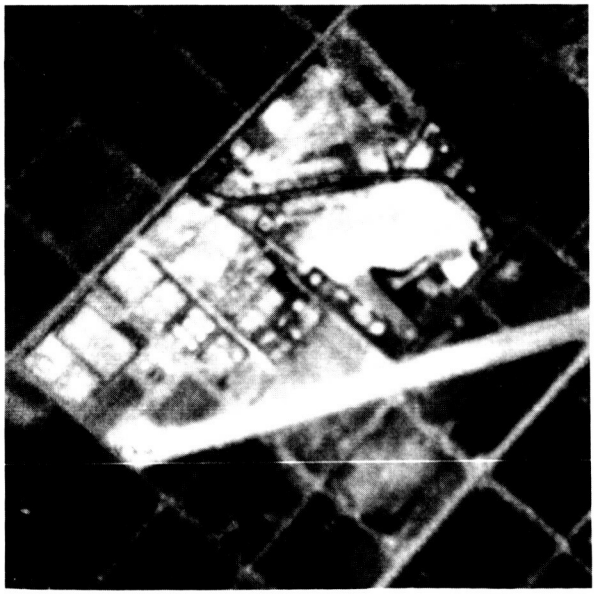
(a) Frame 1331, 2X, 1:370,000.



(b) Frame 1331, 4.5X, 1:165,000.

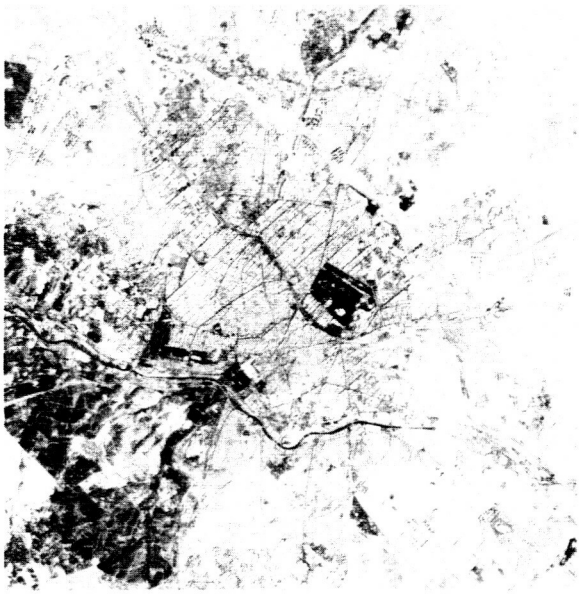


(c) Frame 1331, 10X, 1:165,000.

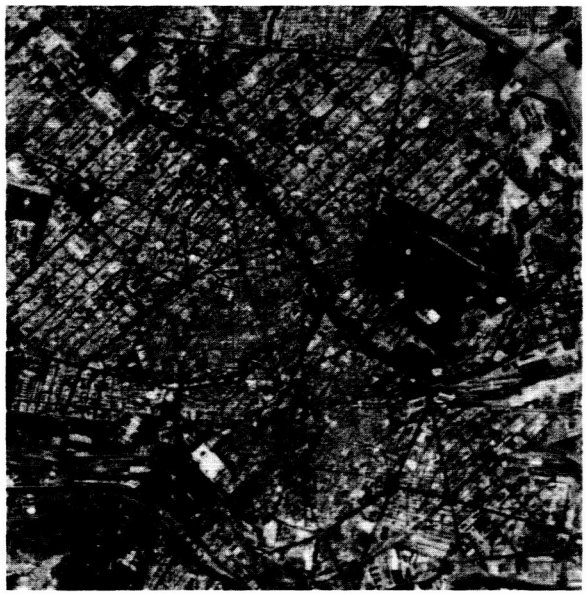


(d) Frame 1331, 35X, 1:74,000.

Figure 3-33.- High density agricultural development (plantations and irrigated cropland) in the Dubti-Tendaho region, Afar Depression, Ethiopia. Lack of other pronounced cultural features makes assessment of spatial resolution difficult. Acquired orbit 65, altitude 225.94 km (GMT 283:1135:24), original scale 1:741,000, on type 3414 film.



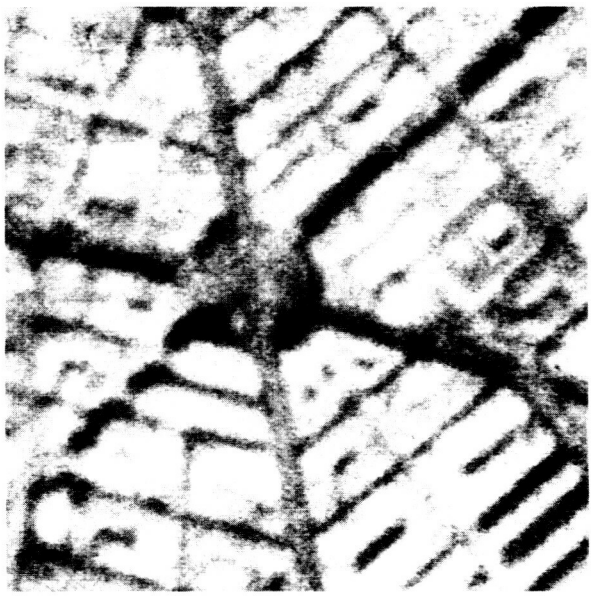
(a) Frame 1352, 4.5X, 1:170,000.



(b) Frame 1352, 10X, 1:76,400.

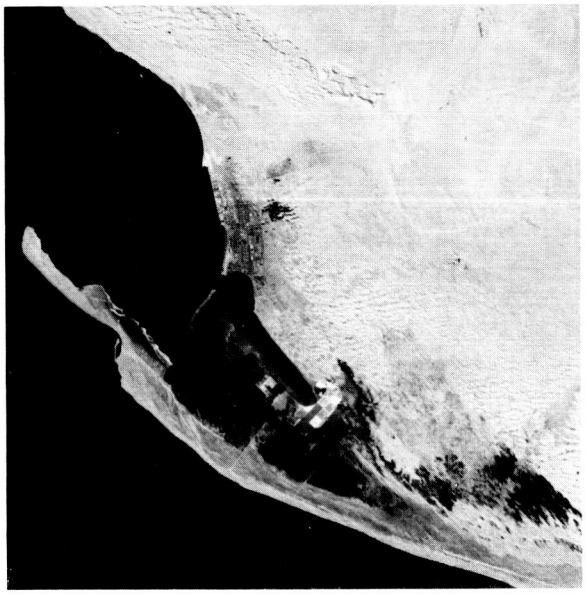


(c) Frame 1352, 35X, 1:21,800.



(d) Frame 1352, 100X, 1:7,600.

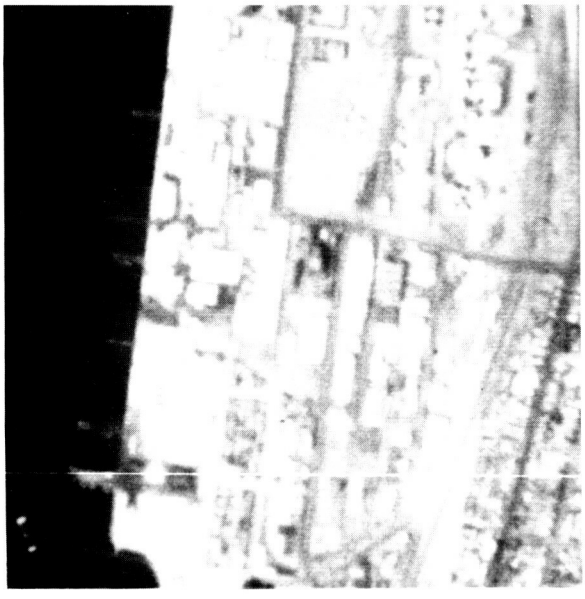
Figure 3-34.- Madrid, Spain. Imagery acquired during orbit 66 from an altitude of 232.94 km (GMT 283:1255:31). Original scale of photography is 1:764,000, on type 3414 film. The high degree of urban development provides many spectacular targets.



(a) Frame 1916, 2X, 1:371,000.



(b) Frame 1916, 10X, 1:74,300.



(c) Frame 1916, 35X, 1:21,200.

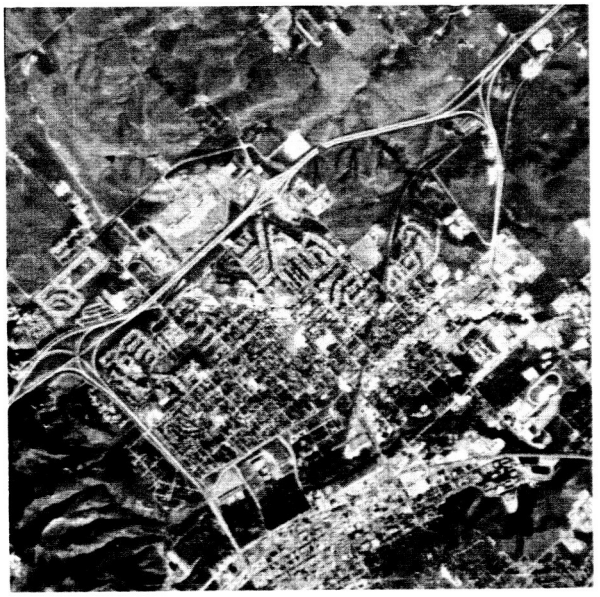


(d) Frame 1916, 100X, 1:7,600.

Figure 3-35.- Walvis Bay. A major urban center on the otherwise barren southeastern coast of Namibia and surrounded by the Namib Desert, as recorded during orbit 99 from an altitude of 226.34 km (GMT 285:1409:57). Original scale of photography is 1:743,000, on type 3414 film.



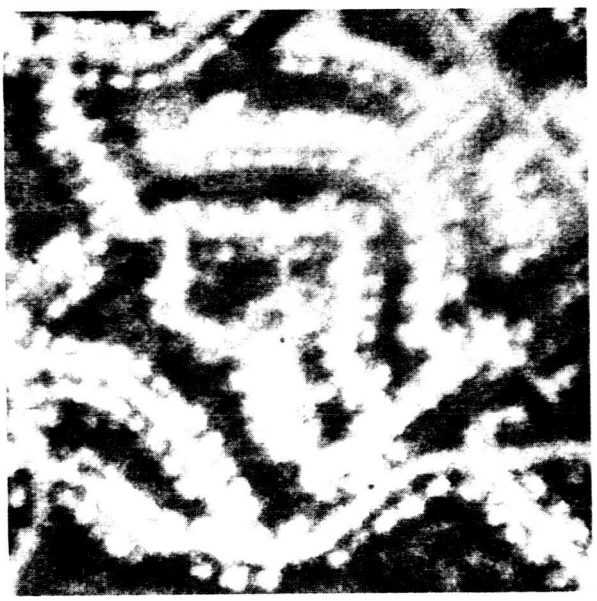
(a) Frame 1953, 2X, 1:377,000.



(b) Frame 1953, 10X, 1:75,400.

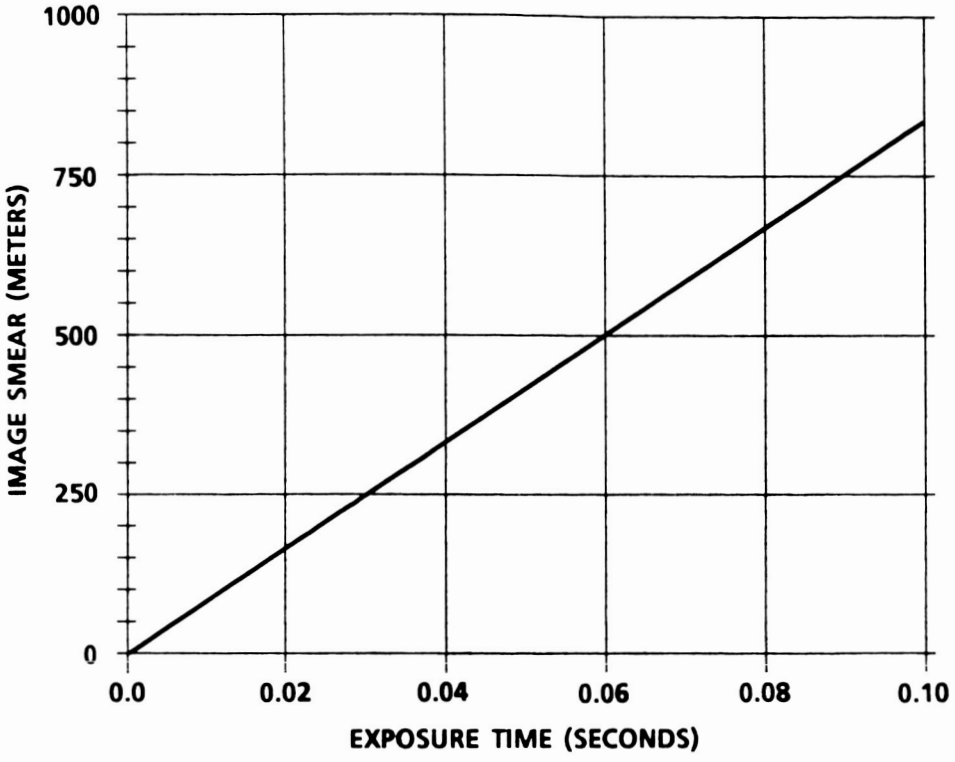


(c) Frame 1953, 35X, 1:21,500.



(d) Frame 1953, 100X, 1:7,500.

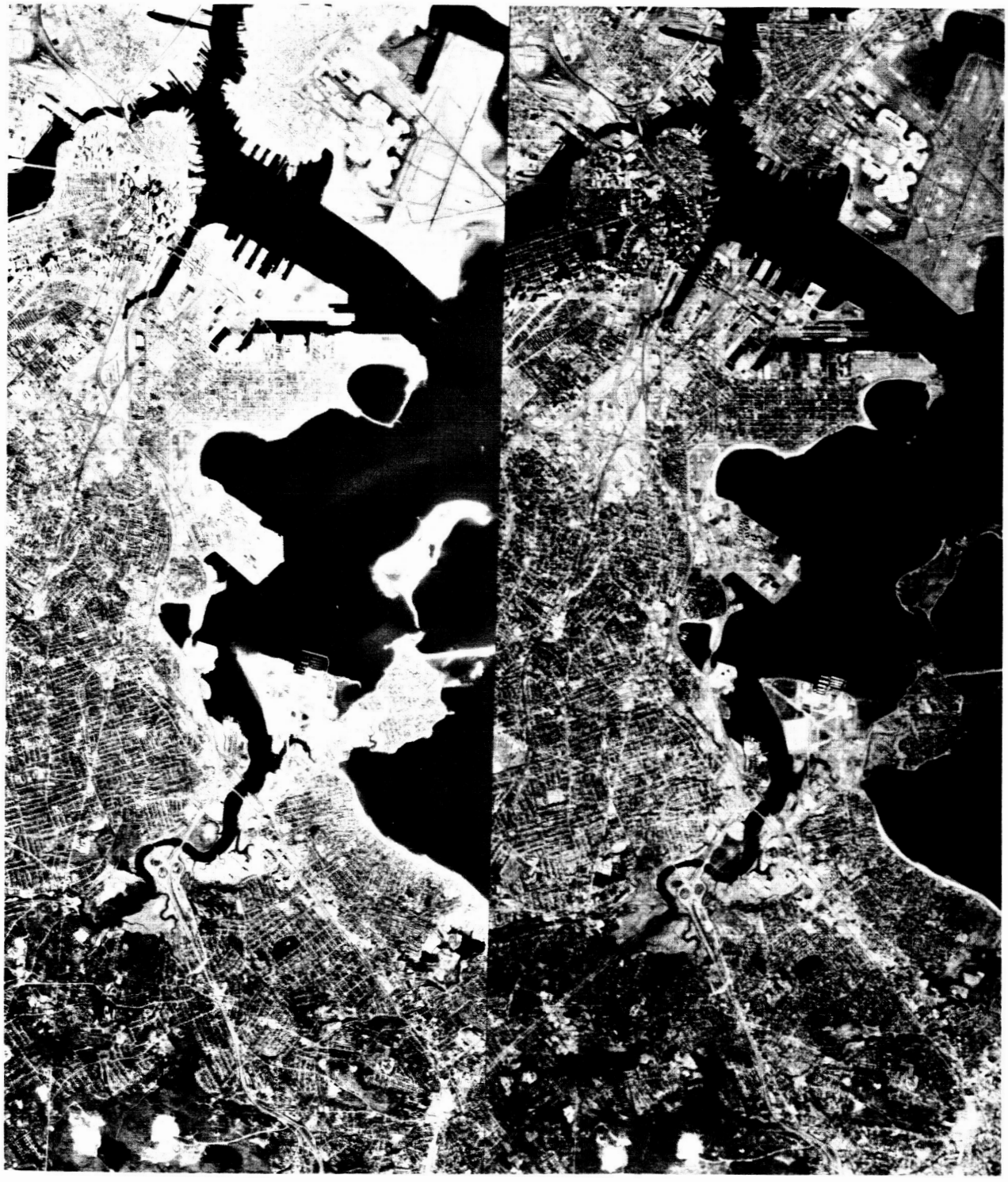
Figure 3-36.- Rapid City, South Dakota. The northeastern base of the Black Hills on one of the few clear crisp days found over the continental United States during STS 41-G. This frame contained numerous small urban targets, certainly with enough clarity for urban charting. Recorded orbit 102 from altitude 229.83 km (GMT 285:1814:52), on type 3414 film. Original scale was 1:754,000.



NOTE: Shutter speeds are as shown in the table below.

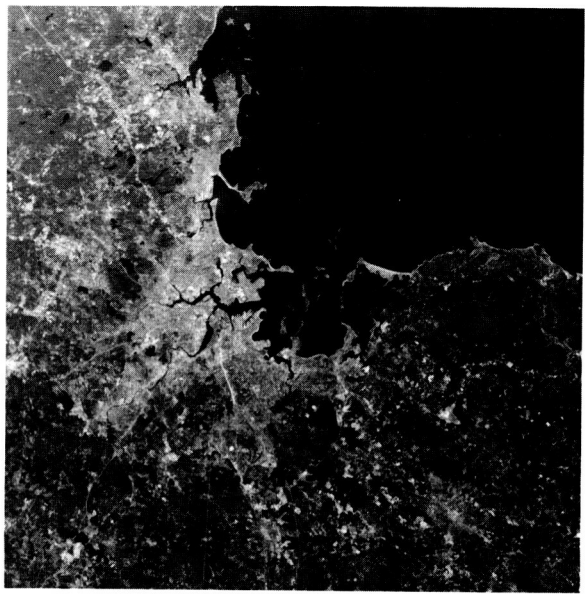
Camera	Range, sec	
	Decimal value	Fractional value
LFC	0.031 to 0.004	1/31 to 1/250
ESA MC	0.004 to 0.001	1/250 to 1/1000
NASA Linhof	0.067 to 0.002	1/15 to 1/500
NASA Hasselblad	0.040 to 0.002	1/25 to 1/500

Figure 3-37.- Ground distance covered during camera shutter "open" intervals at a nominal ground velocity of approximately 7.5 km/sec.

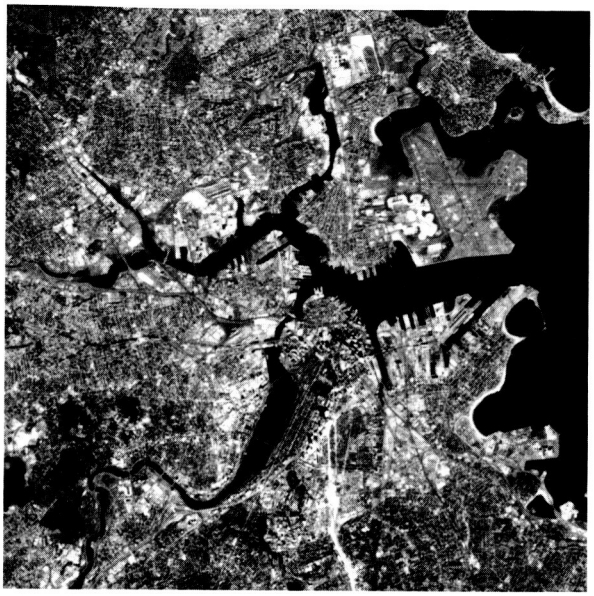


(a) NHAP photo 85-32256. *(b) LFC frame 0664.*

Figure 3-38.- Scene comparison of Boston, Massachusetts, as recorded by an NHAP aerial camera (left) and the NASA LFC. Both are presented at a photo scale of 1:80,000, the aerial view as a contact print and the LFC as an enlargement at a magnification of 9.48 times original size. (Note that the inherent contrast in the NHAP photo is a result of a light late season snowfall.)



(a) Frame 0664, photo scale = 1:758,725
(Original size - 1X)



(b) Frame 0664, photo scale = 1:75,872
(4.5X enlargement)



(c) Frame 0664, photo scale = 1:21,678
(35X enlargement)

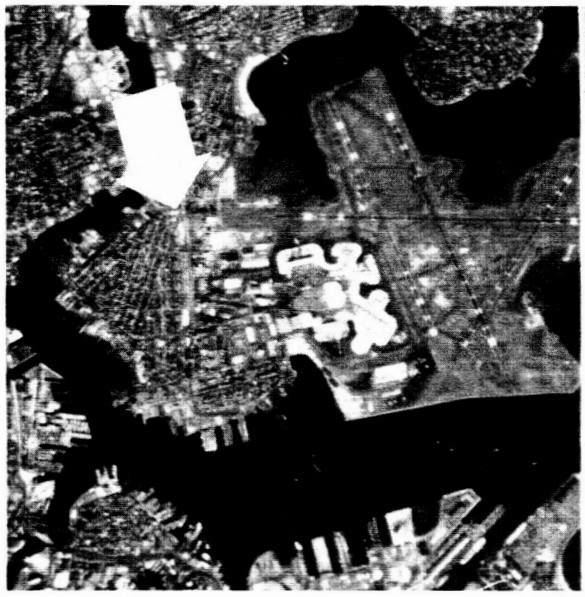


(d) Frame 0664, photo scale = 1:7,587
(100X enlargement)

Figure 3-39.- Boston, Massachusetts, area. Progressive enlargements of a small portion of LFC frame 0664. The LFC film is Kodak type 3412.



(a) Frame 0664, 10X.



(b) Frame 0665, 10 X.

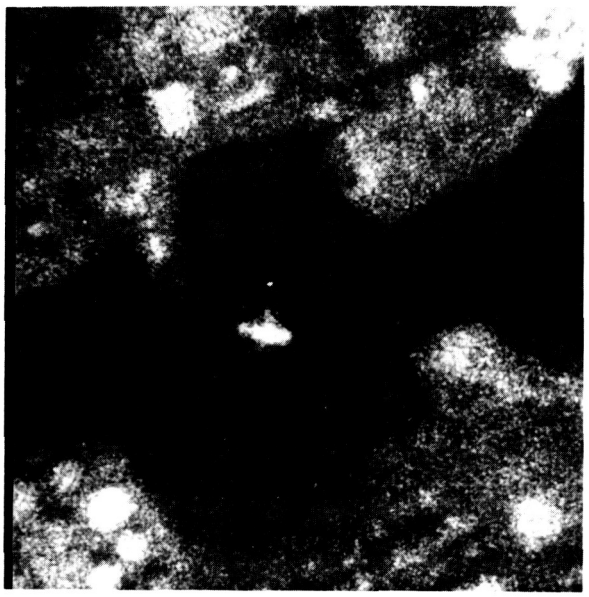


(c) Frame 0666, 10 X.



(d) Frame 0664, 35X.

Figure 3-40.- Commercial aircraft on landing approach to Boston's Logan Airport. Photographed by the LFC on October 7, 1984. LFC film is type 3412.



(a) Frame 0664, 10X.

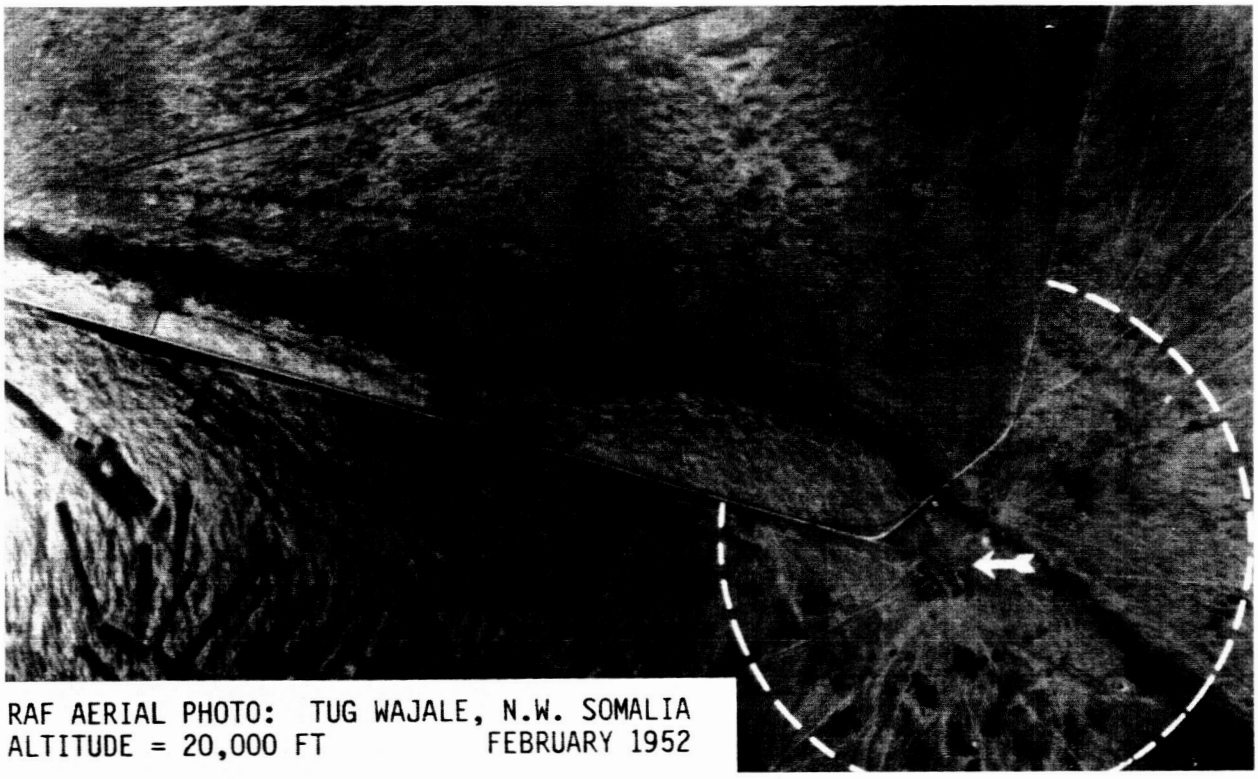


(b) Frame 0663, 10X.

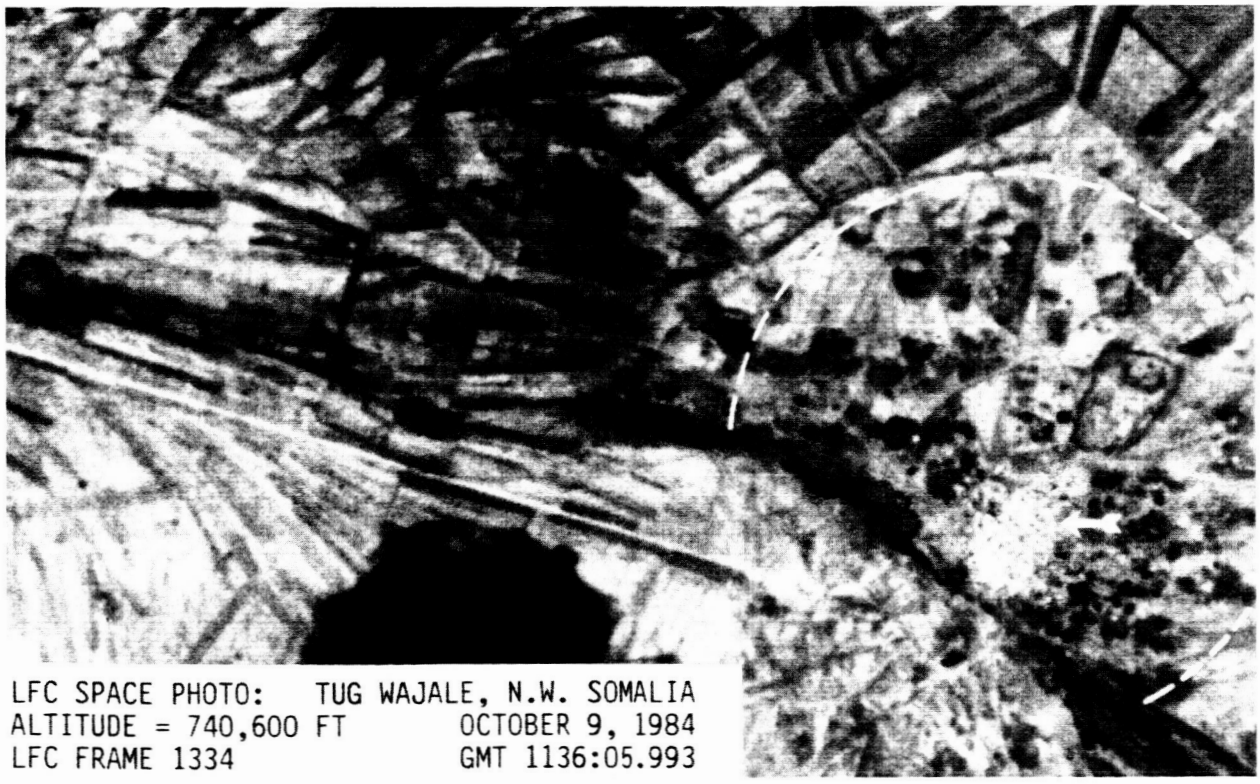


(c) Frame 0665, 100 X.

Figure 3-41.- Inflight aircraft image quality as it is affected by flight direction of the aircraft and aircraft image-to-background contrast. From left to right: aircraft approach to Logan airport; aircraft over Needham, Massachusetts; and aircraft over Nantucket Sound. Orbiter flight direction is from left to right. LFC film is Kodak type 3412.



RAF AERIAL PHOTO: TUG WAJALE, N.W. SOMALIA
ALTITUDE = 20,000 FT FEBRUARY 1952



LFC SPACE PHOTO: TUG WAJALE, N.W. SOMALIA
ALTITUDE = 740,600 FT OCTOBER 9, 1984
LFC FRAME 1334 GMT 1136:05.993

Figure 3-42.- Comparison of aerial photography (1952) and LFC photography (1984) of a hamlet in the Tug Wajale region of Somalia, showing demographic changes over a 32-yr period. (The dark blotch in the lower left center of the LFC photo is a shadow of a small cloud.)

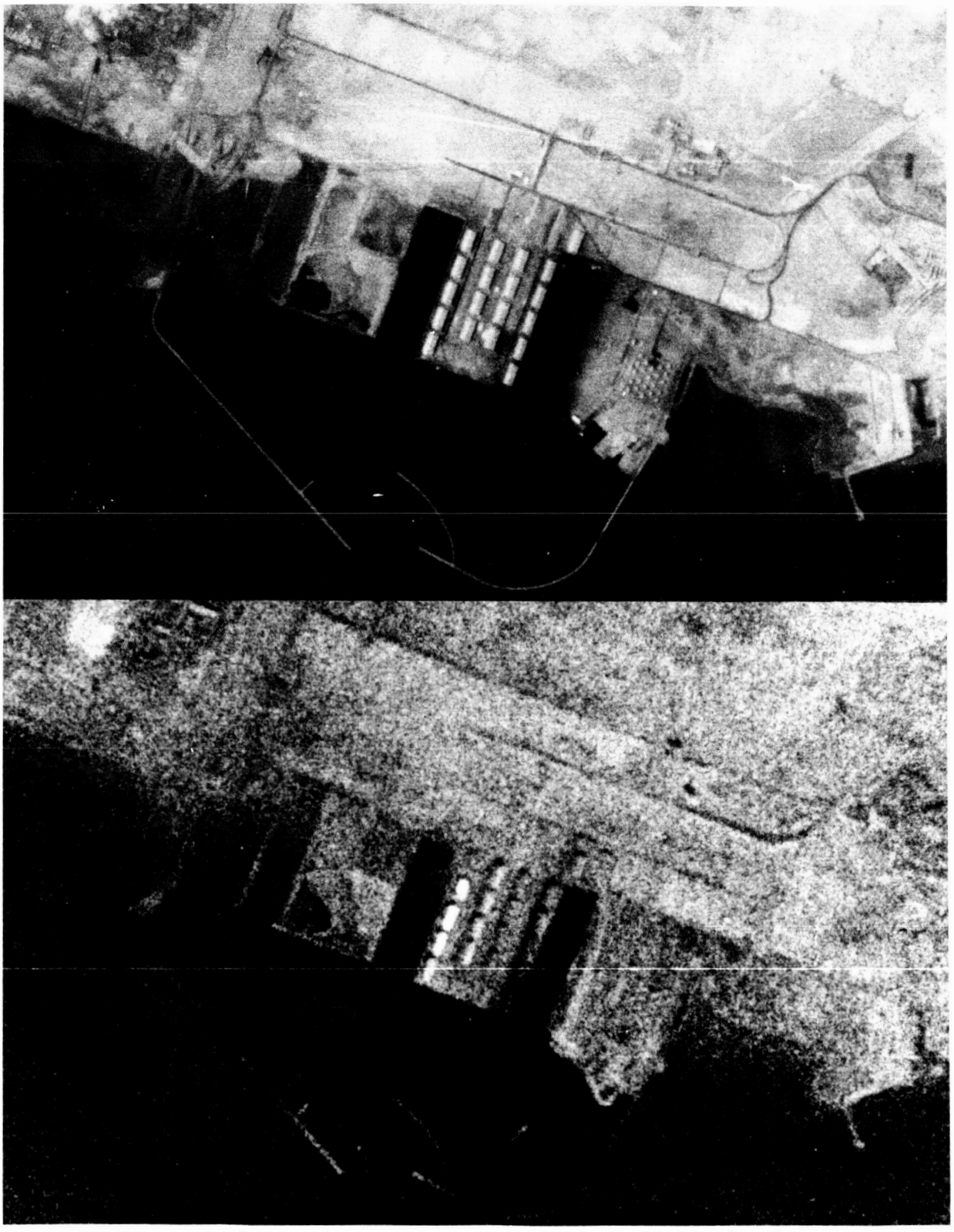


Figure 3-43.- Comparative frames of LFC and MC imagery. LFC frame 0616 (top) and MC 01-0601-22 (bottom) show the Bandar Abbas - Dogerdan, Iran, region on the Strait of Hormuz. Shown at same magnification, approximately 20X original size.

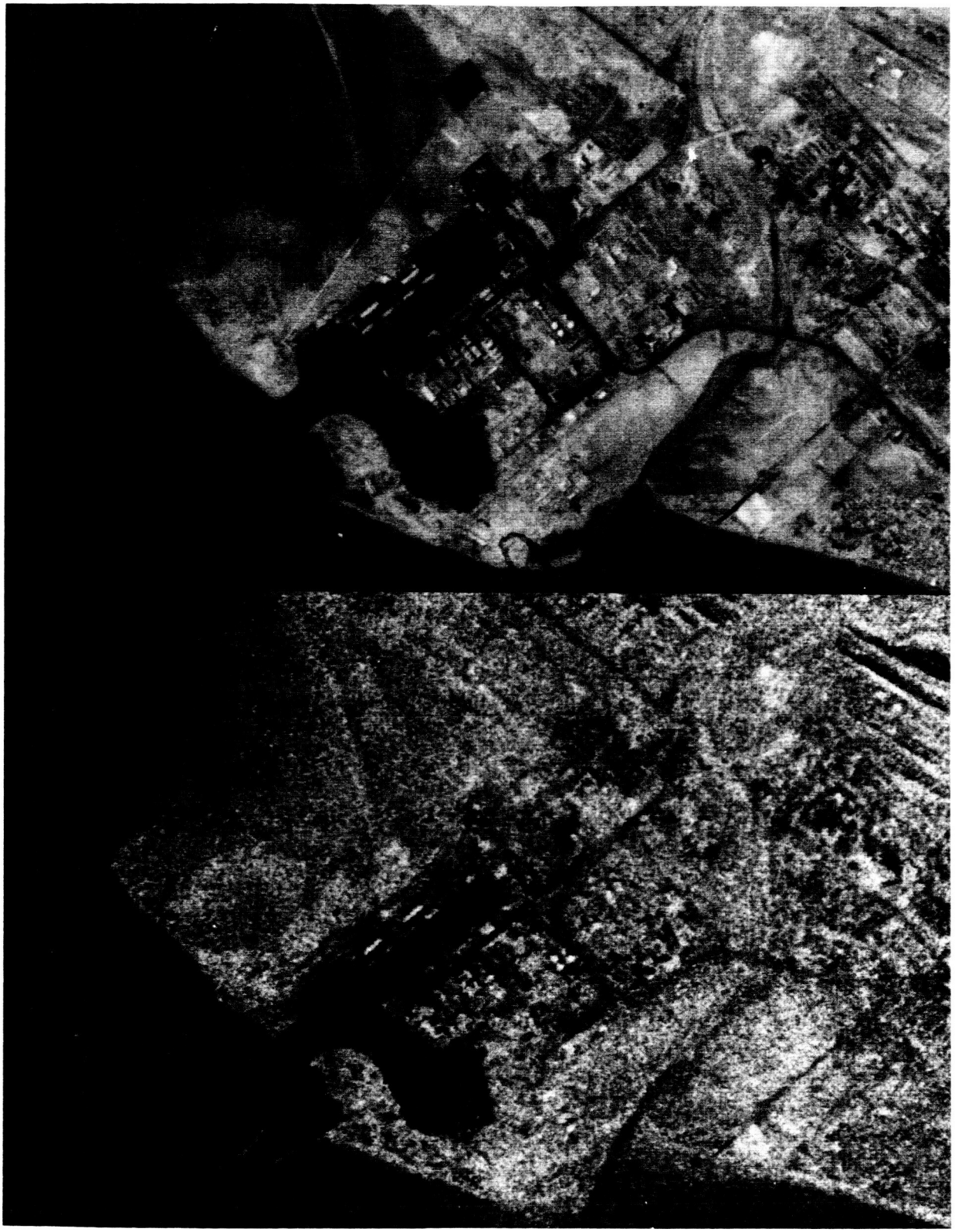


Figure 3-44.- Comparative frames of LFC and MC imagery. LFC frame 0616 (top) and MC 01-0601-22 (bottom) show the Bandar Abbas - Dogerdan, Iran, region on the Strait of Hormuz. Shown at same magnification, approximately 20X original size.



Figure 3-45.- Comparative frames of LFC and MC imagery. LFC frame 1953 (top) and MC 01-0929-32 (bottom) show Rapid City, South Dakota. Shown at same magnification, approximately 20X original size.

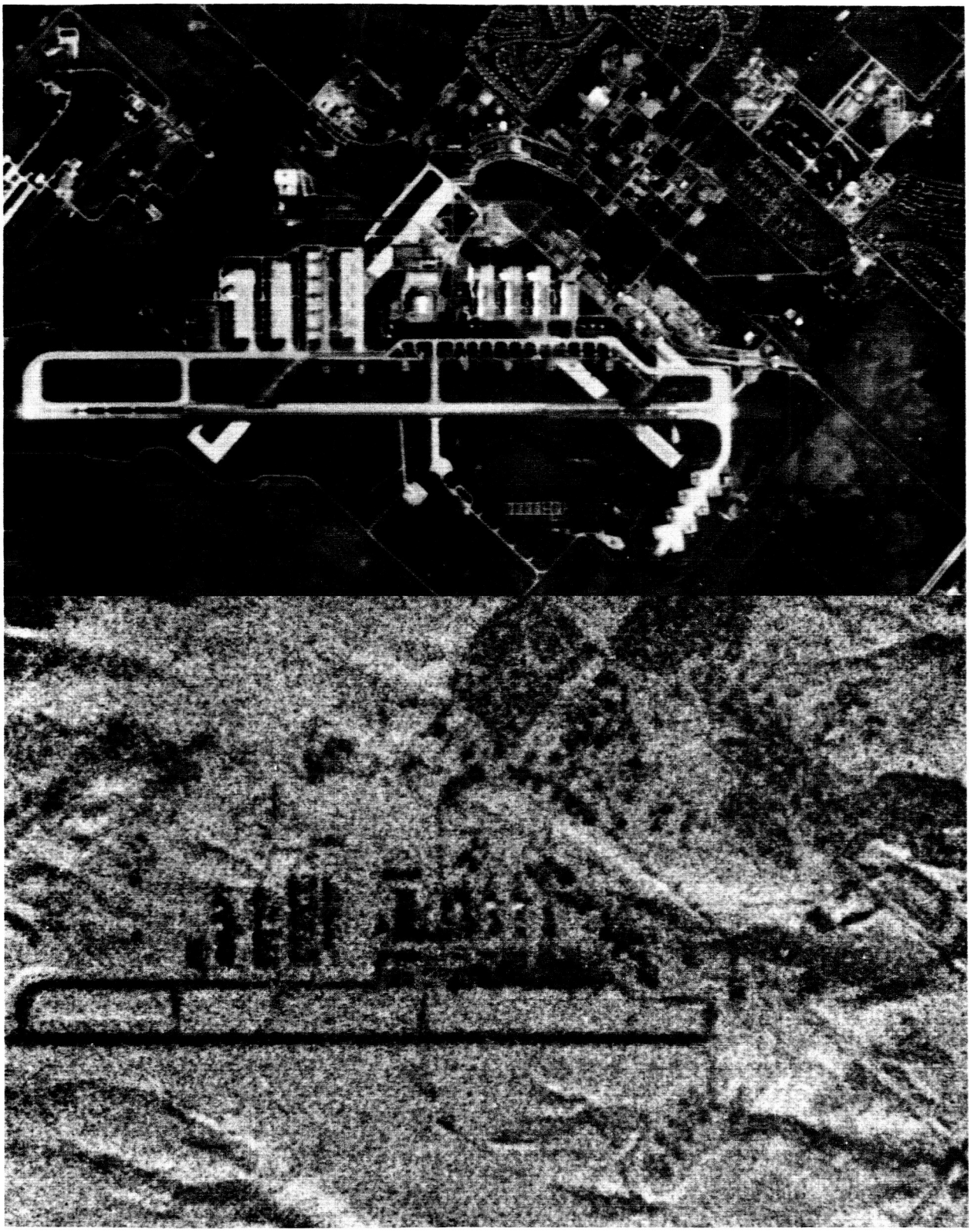
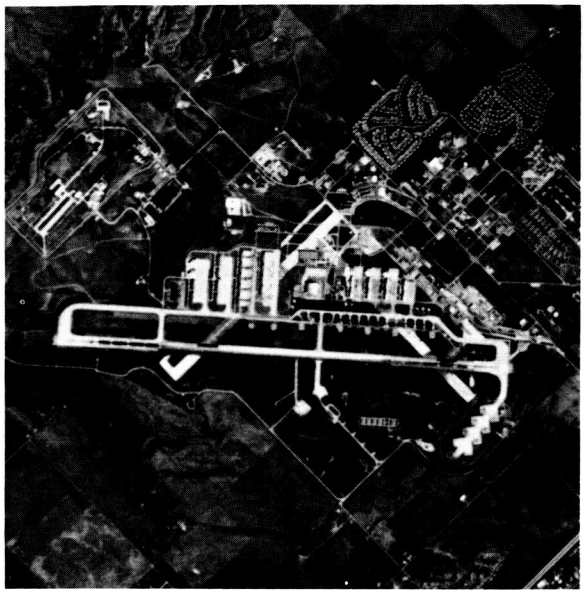
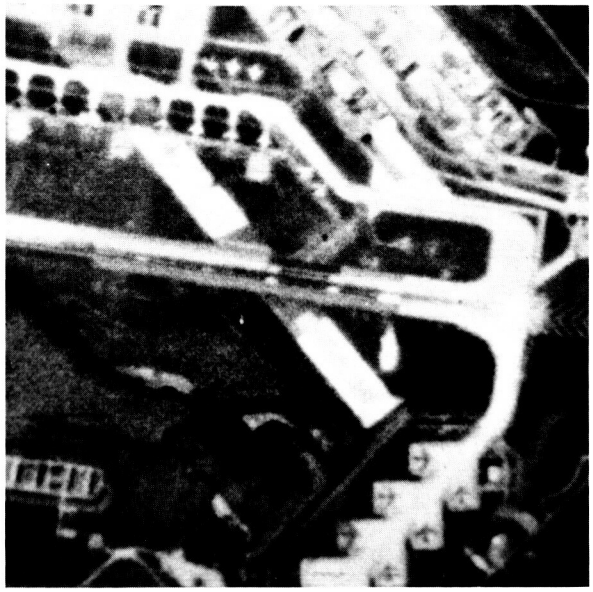


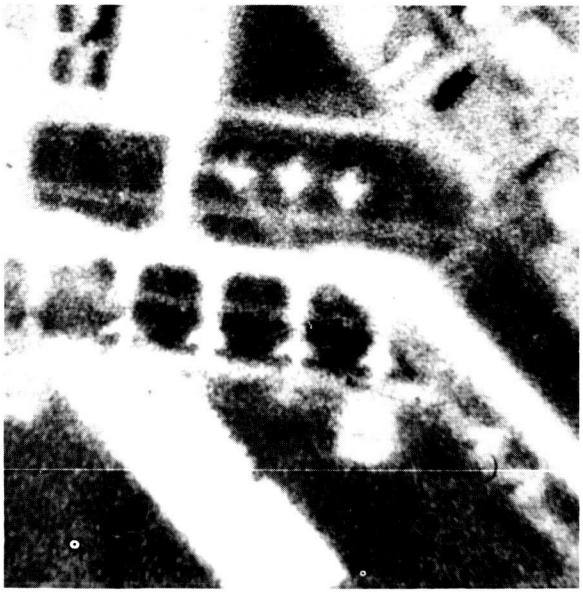
Figure 3-46.- Comparative frames of LFC and MC imagery. LFC frame 1953 (top) and MC 01-0929-32 (bottom) show Ellsworth AFB outside Rapid City, South Dakota. Shown at same magnification, approximately 20X original size.



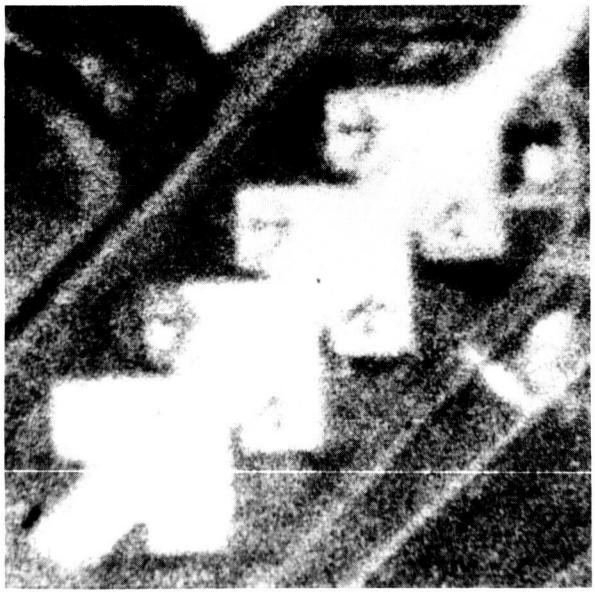
(a) LFC frame 1953, 10X
(scale 1:75,000)



(b) LFC frame 1953, 35X
(scale 1:21,400)



(c) LFC frame 1953, 100X
(scale 1:7,500)



(d) LFC frame 1953, 100X
(scale 1:7,500)

Figure 3-47.- Progressive magnification of the Ellsworth AFB site for evaluation of image structure integrity. Altitude of imagery is 229.83 km, and original scale is 1:750,000. LFC film is type 3414.



Figure 3-48.- Comparative frames of LFC and Hasselblad imagery. LFC frame 2059 (top) and Hasselblad 45-072 (bottom) show the volcanic region of Lee Vining, California, on Mono Lake's western shore. Projected at identical scales.

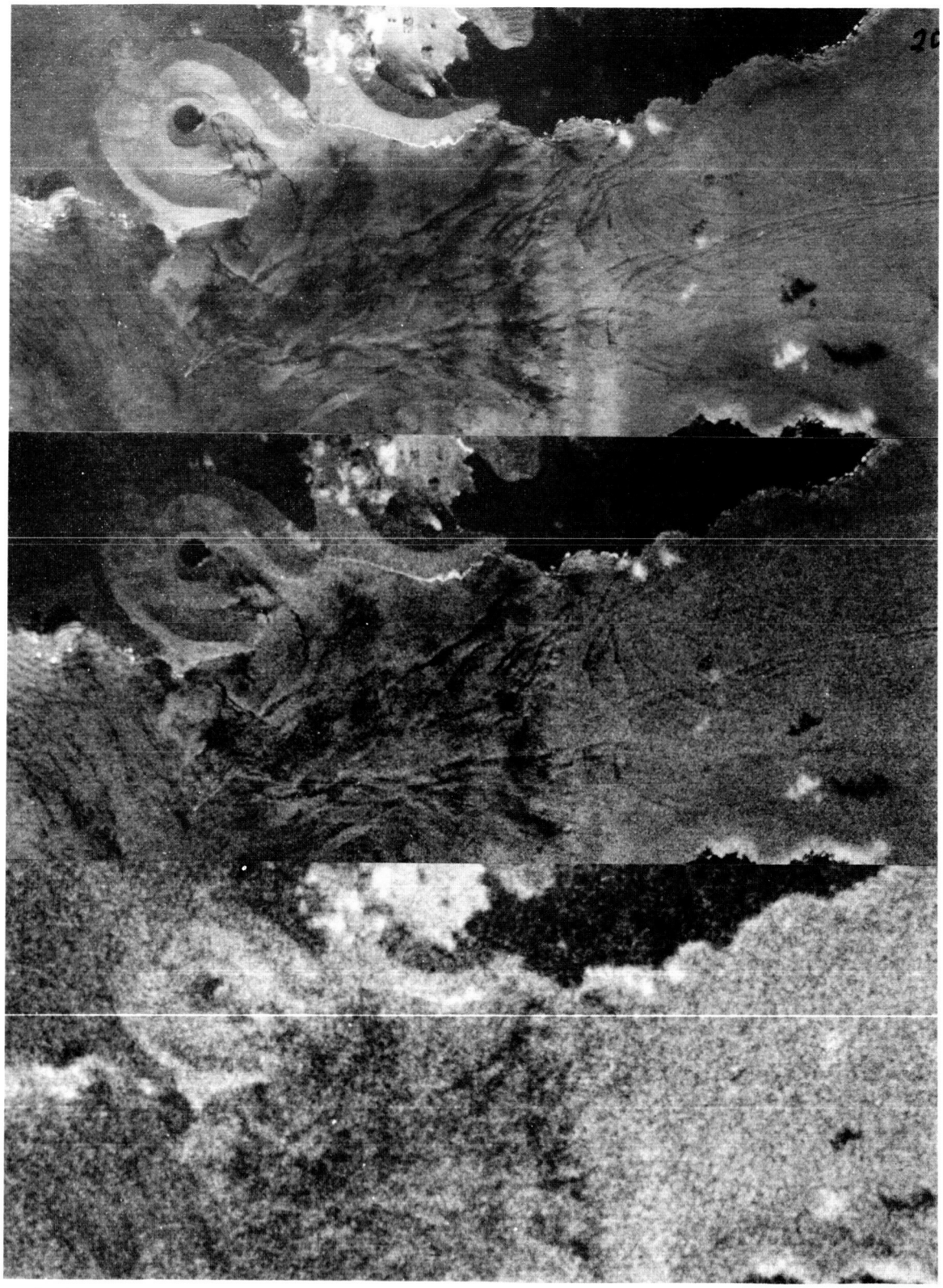


Figure 3-49.- Comparative frames of LFC, Hasselblad, and Linhof imagery. LFC frame 2086 (top), Hasselblad 44-037 (center), and Linhof 121-047 (bottom) show the ocean surface in the strait between the Galapagos islands of Fernandina and Isabela. Projected at identical scales.

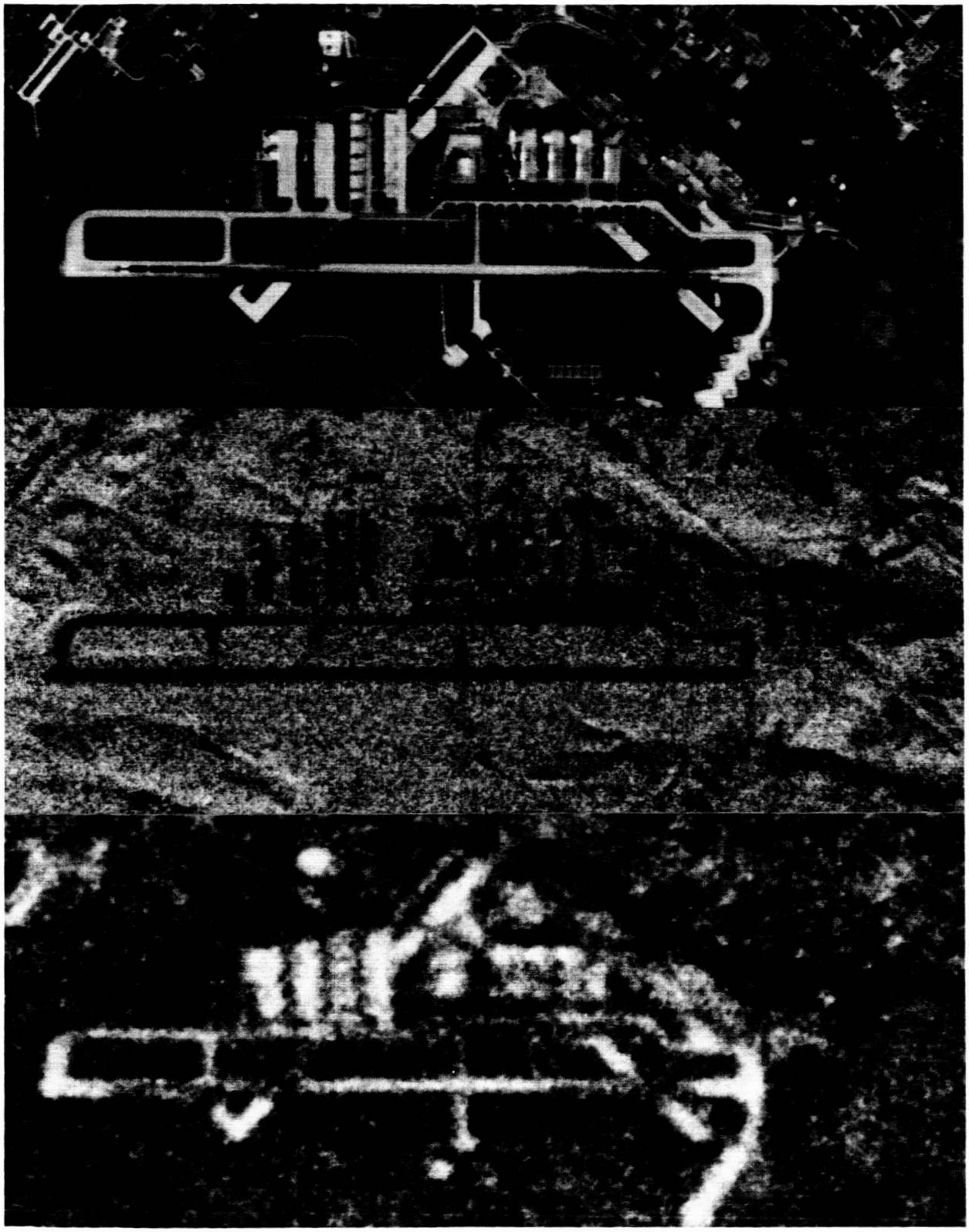


Figure 3-50.- Comparative frames of LFC, MC, and Hasselblad imagery. LFC frame 1952 (top), MC 01-0929-32 (center), and Hasselblad 45-046 (bottom) show Ellsworth AFB near Rapid City, South Dakota. Projected at identical scales.

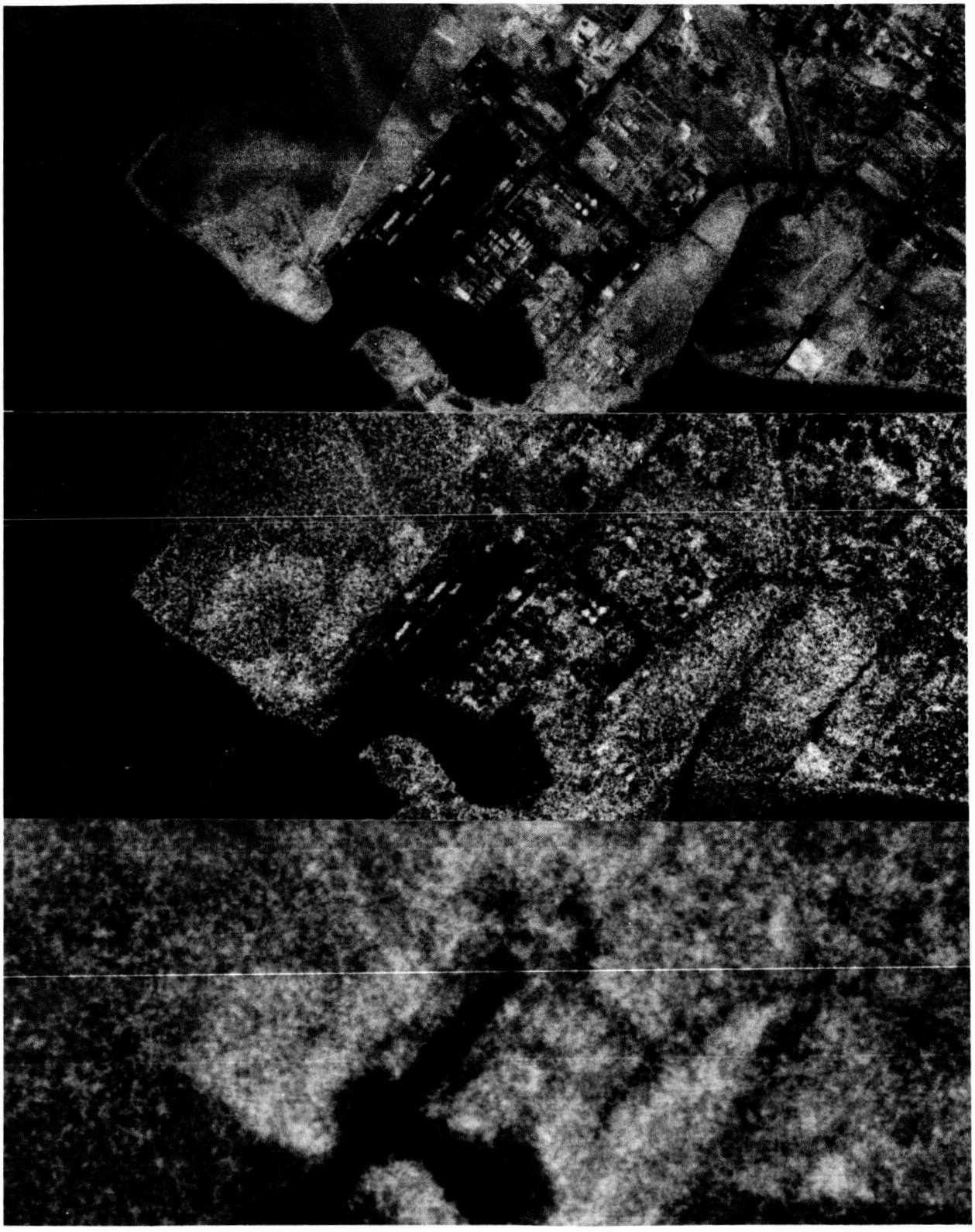


Figure 3-51.- Comparative frames of LFC, MC, and Linhof imagery. LFC frame 0616 (top), MC 01-0606-22 (center), and Linhof 121-163 (bottom) show the Bandar Abbas - Dogerdan, Iran, region on the strait of Hormuz. Projected at identical scales.

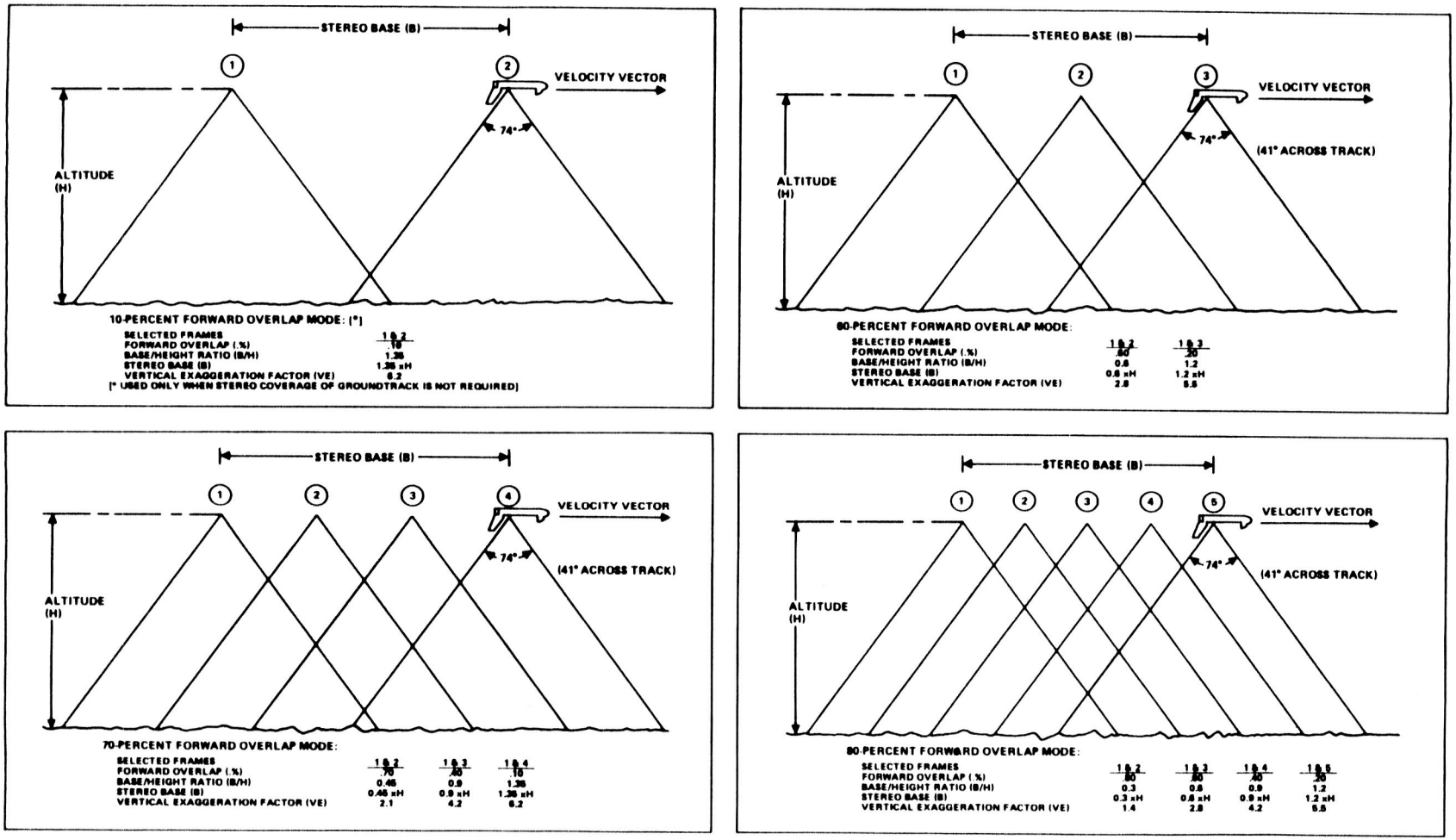


Figure 3-52.- The four basic acquisition modes of the LFC during photography of the earth. Illustrated are forward O/L modes of 10 and 60 percent (top) and 70 and 80 percent (bottom). Overlap of a frame with a succeeding frame(s) produces stereo imagery. Since the 10-percent mode produces such little overlap, it has very limited, specialized applications. (Also see figures 1-22 and 1-23.)

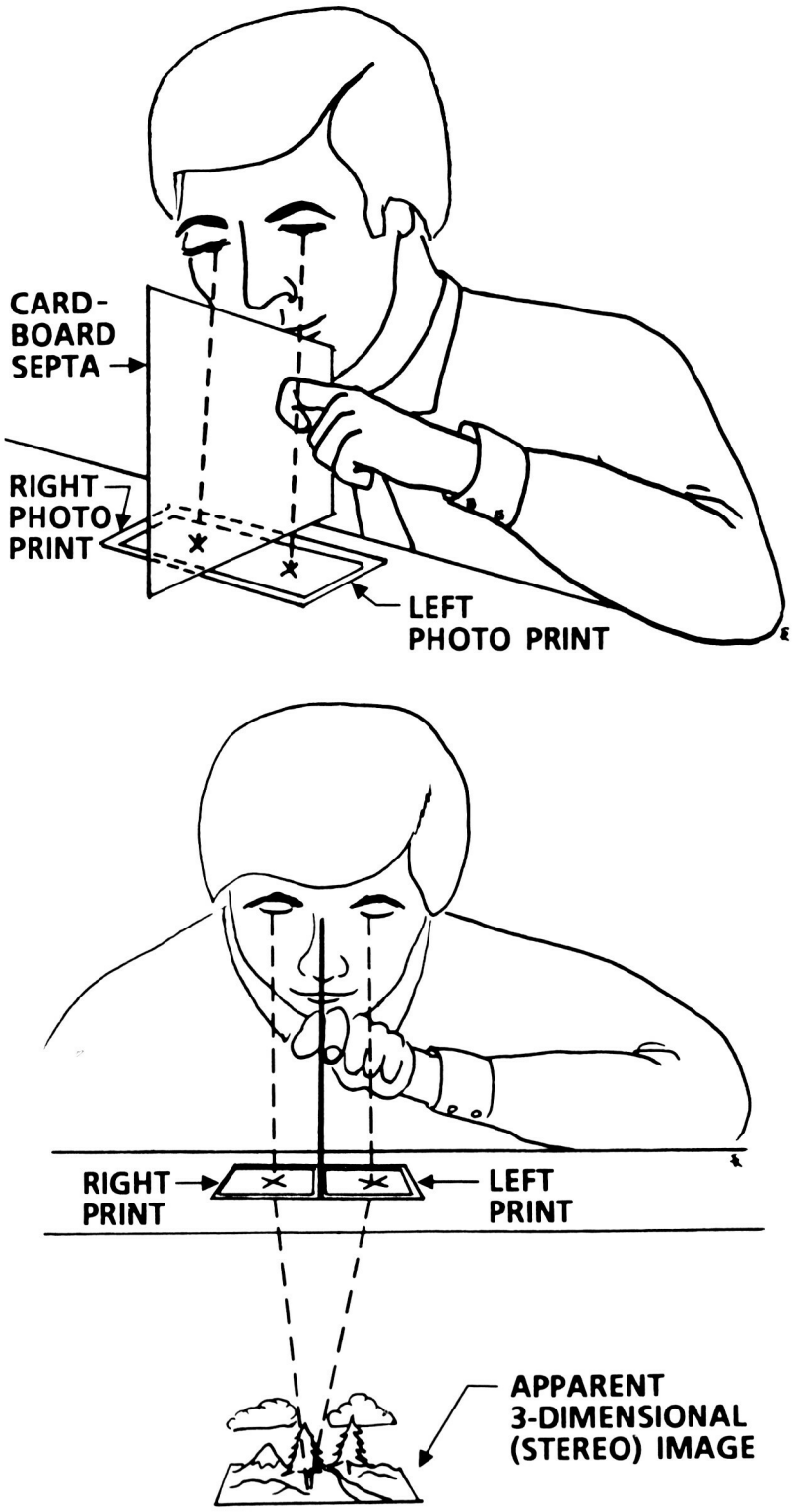


Figure 3-53.- Stereo viewing. Alignment of stereo prints and the use of a septa, or blinder, to aid in individual eye focus (top) in order to create the illusion of depth in the superimposed photos (bottom).

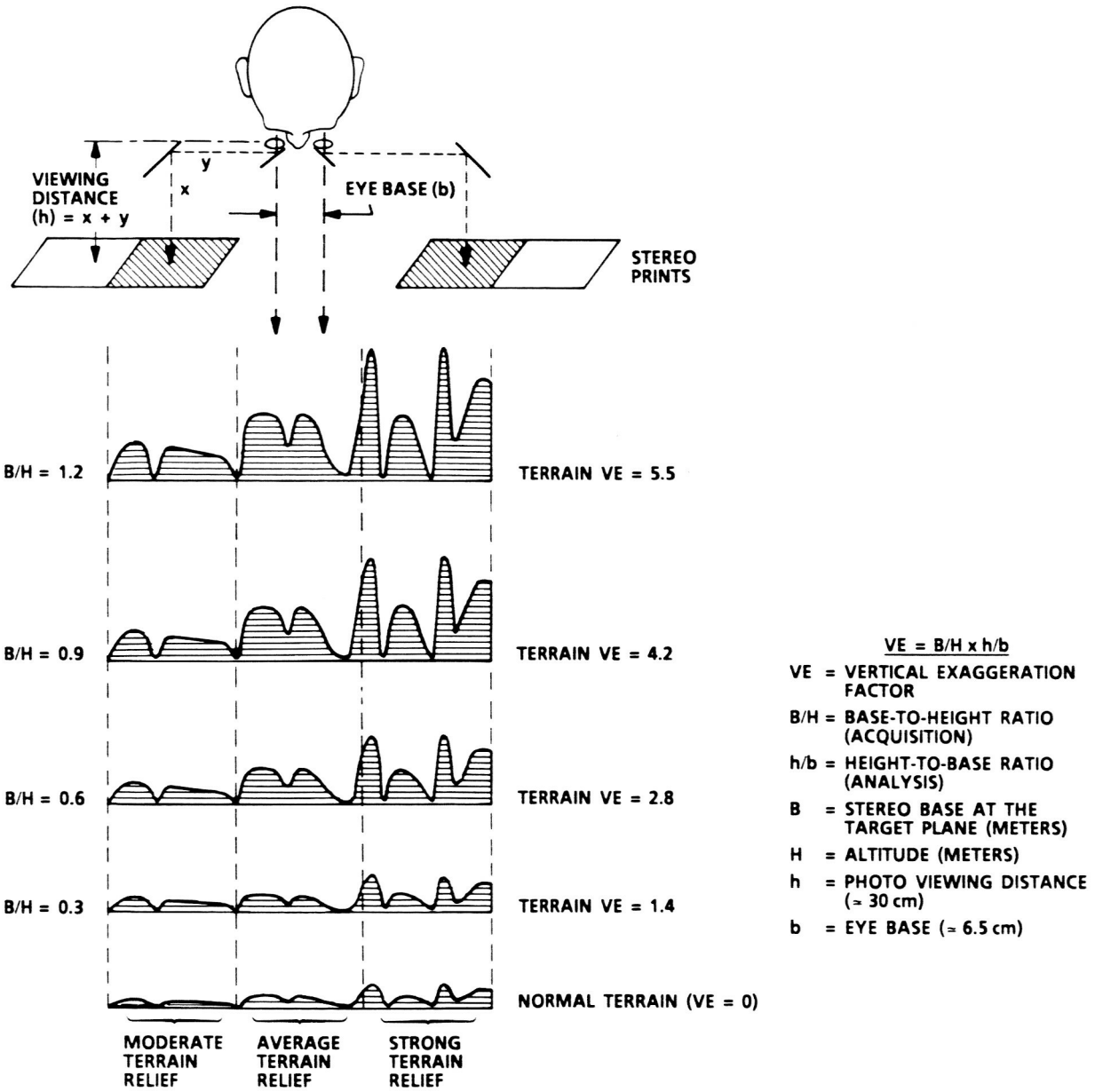
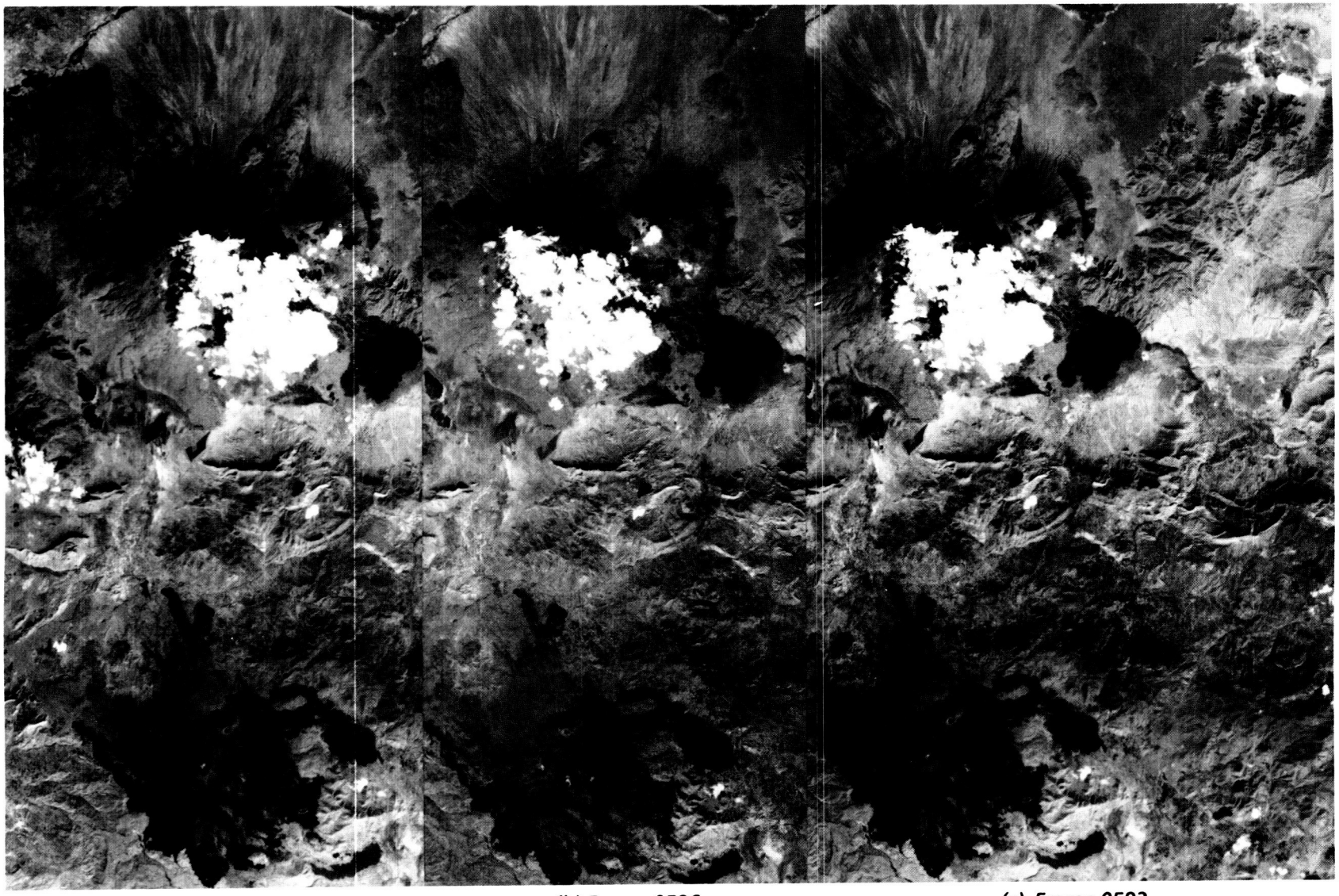


Figure 3-54.- VE of terrain relief with the increase in the B/H ratio.



(a) Frame 0592. (b) Frame 0596. (c) Frame 0592.

Figure 3-55.- Mt. Ararat stereogram demonstration. LFC frames 0592 and 0596 form a normal stereogram, but frames 0596 and 0592 produce a pseudo stereogram, or change of positive elevations to negative elevations, within the reference datum plane.

Figure 3-56.- Cairns Reef area of the Great Barrier Reef on the Queensland, Australia, eastern seaboard. Produced in a format measuring 34.5 by 17 in. (scale approximately 1:373,000) from a single LFC CIR frame. (Courtesy of the Department of Mapping and Surveying of the Australian Government, Brisbane.)

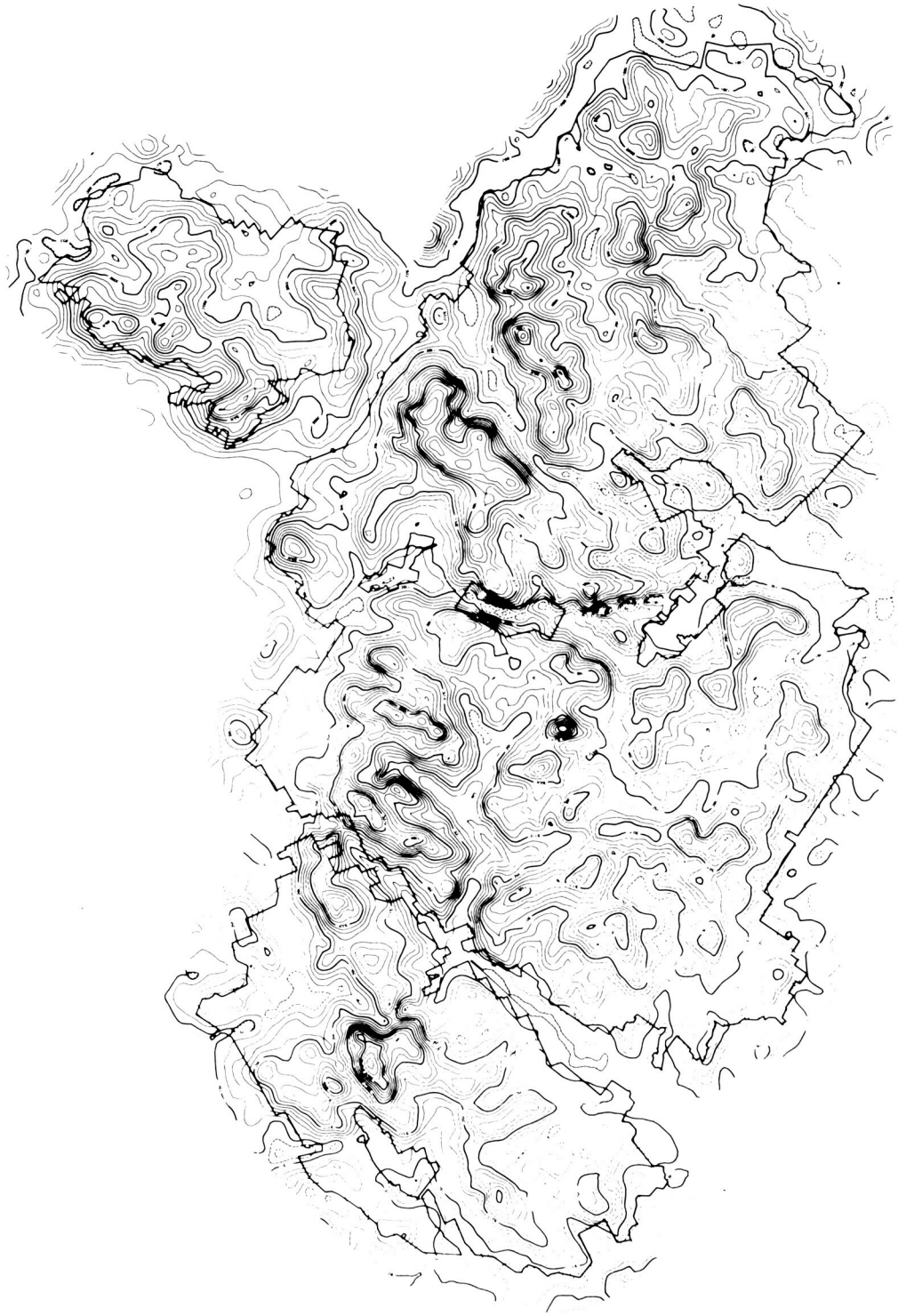


Figure 3-57.- Contour line derivation combined with the orthophoto (facing page) of the White Mountain National Forest in New Hampshire. Intervals are 200 ft, and horizontal and vertical controls were derived from office methods. (Courtesy of the Eastern Regional Office of the USDA Forest Service.)

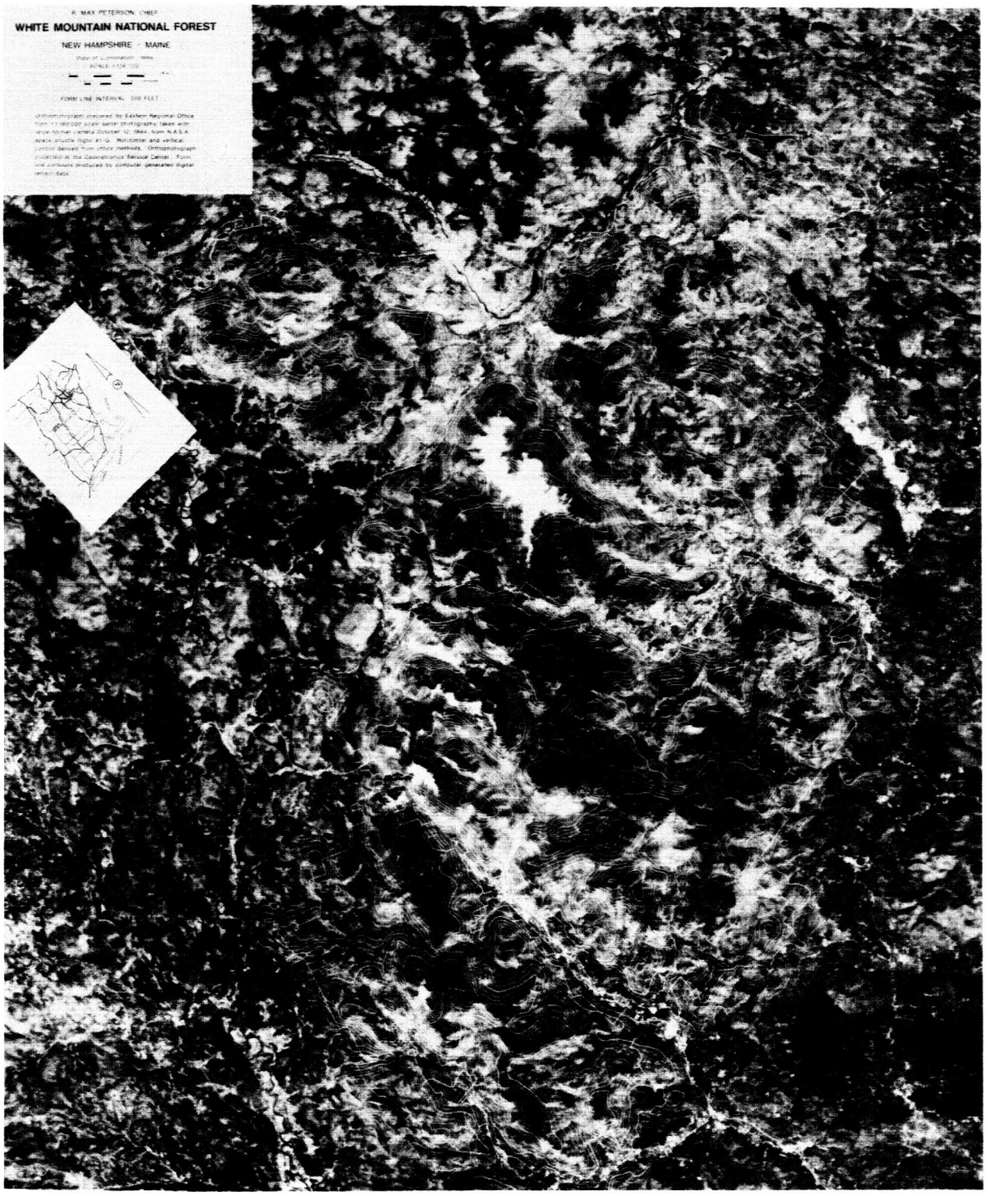
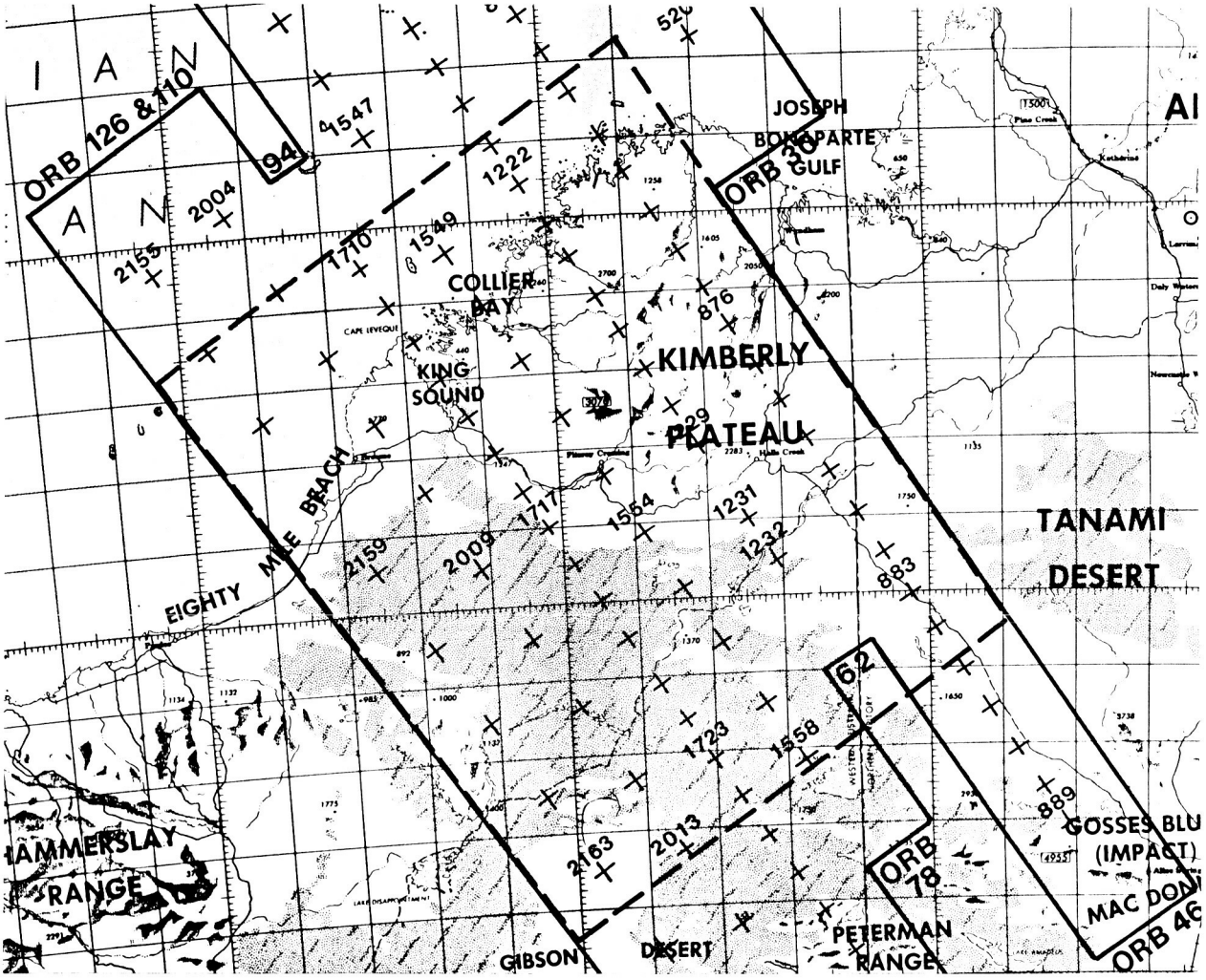


Figure 3-58.- A 1:120,000 scale orthophotograph. Prepared by the Eastern Regional Office, USDA Forest Service, White Mountain National Forest, New Hampshire, from 1:1,190,000 LFC imagery acquired on STS 41-G. Horizontal and vertical control derived from office methods; orthophotograph projected at the Geometronics Service Center; form and contours produced by computer-generated digital terrain data. (Courtesy of Eastern Regional Office of the USDA Forest Service.)



Orbit no.	Average altitude, km	Fwd O/L, %	Target time, sec[a]	Film type	LFC frames used			Average photo scale
					Start	Stop	Total	
46	223.5	80	103	3412	0871	0881	11	1:733,000
62	226.9	80	90	S0-242	1221	1232	12	[b]1:744,000
78	227.2	70	95	S0-131	1549	1556	8	[b]1:745,000
94	226.0	80	92	S0-131	1711	1721	11	[b]1:741,000
110	225.5	60	105	3414	2006	2012	7	[b]1:740,000
126	225.4	60	93	3414	2157	2162	6	[b]1:739,000
			577 (9.6 min)				55	

[a]Seconds over target.

[b]LFC frames projected to a scale of 1:733,000.

Figure 3-59.- Groundtrack map depicting area of coverage of uncontrolled photo mosaic of northwestern Australia (facing page).

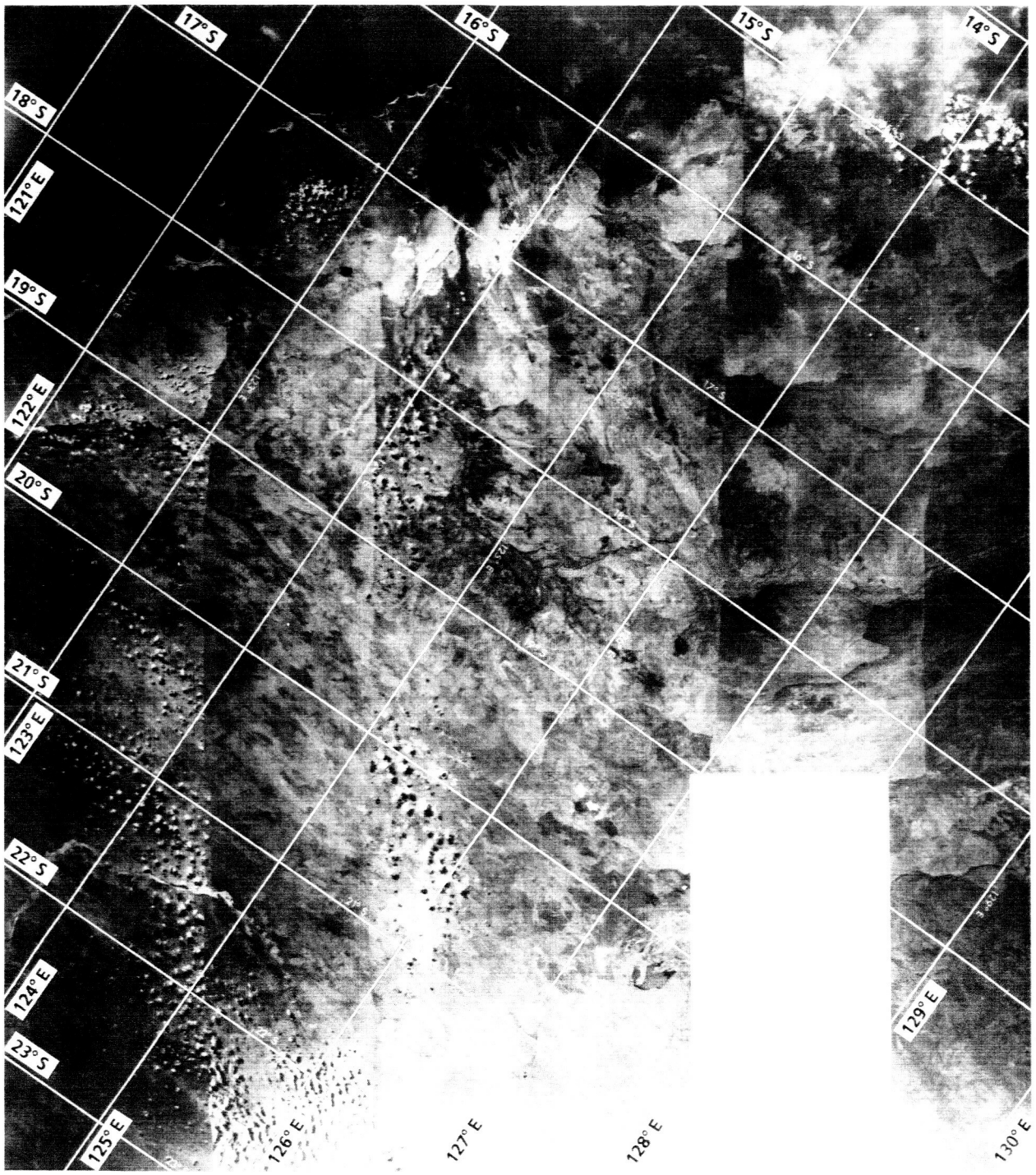
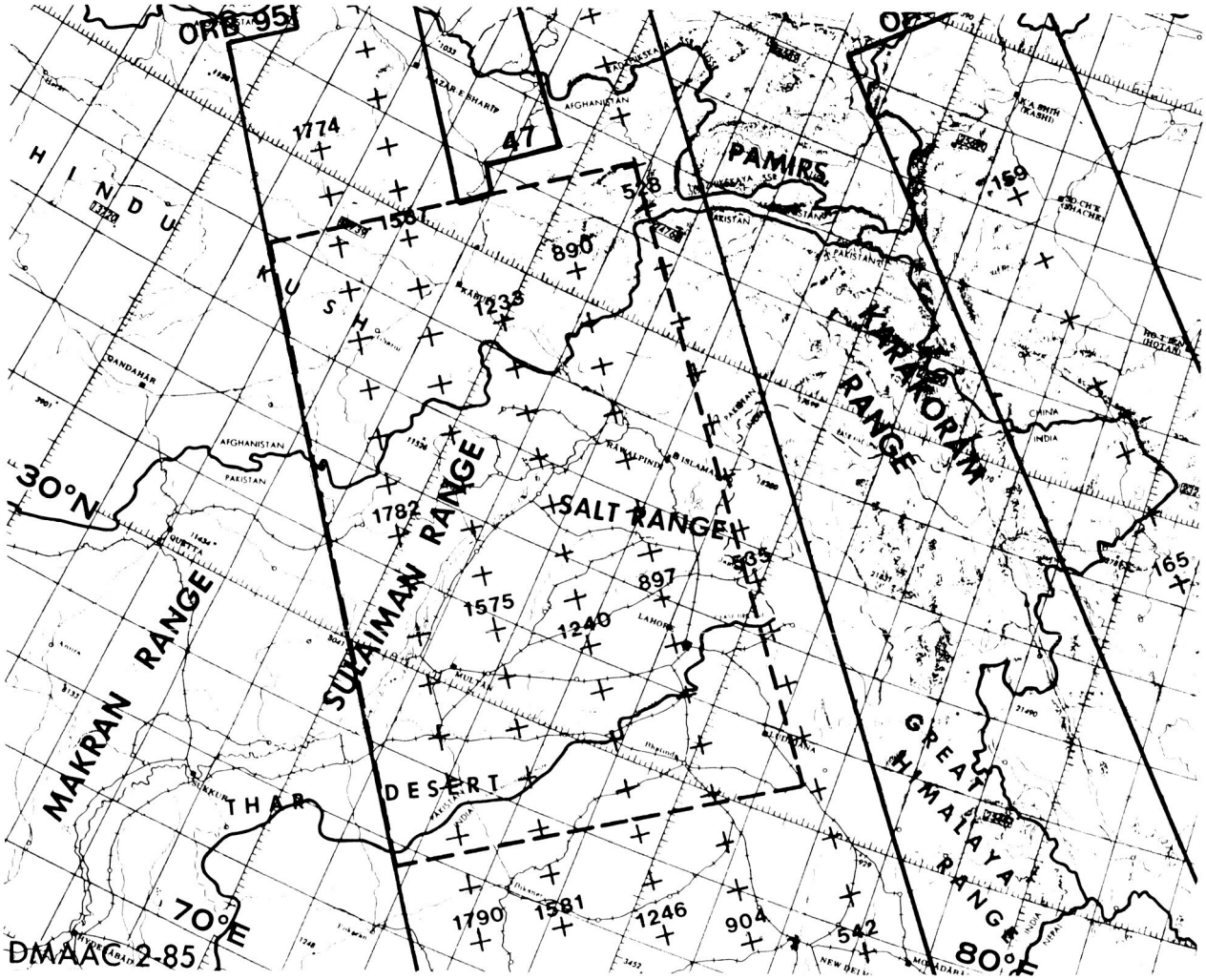


Figure 3-60.- Uncontrolled photo mosaic of northwestern Australia. Composed of four film types adjusted to a constant scale of 1:733,000 (NASA mosaic). A geographic coordinate grid has been applied to clarify map orientation.



Orbit no.	Average altitude, km	Fwd O/L, %	Target time, sec[a]	Film type	LFC frames used			Average photo scale
					Start	Stop	Total	
47	228.2	80	84	3412	0890	0899	10	[b]1:749,000
63	230.9	80	80	3414	1223	1242	10	[b]1:758,000
79	231.0	80	84	S0-131	1568	1577	10	[b]1:758,000
95	227.2	80	85	S0-131	1777	1786	10	1:745,000
			333 (5.6 min)				40	

[a]Seconds over target.

[b]LFC frames projected to a scale of 1:745,000.

Figure 3-61.- Groundtrack map depicting area of coverage of uncontrolled photo mosaic of Afghanistan, Pakistan, and India region (facing page).

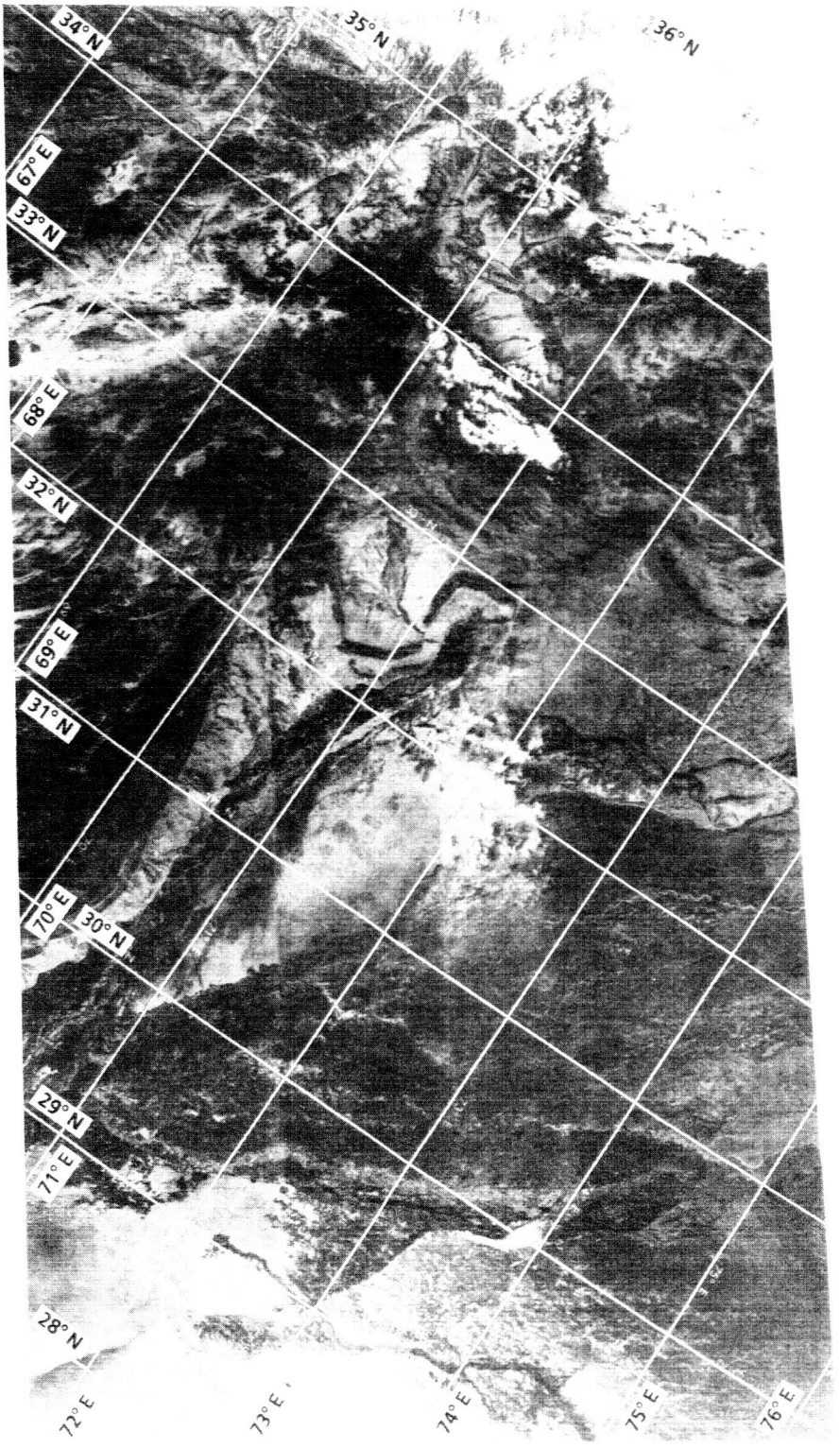


Figure 3-62.- Uncontrolled photo mosaic of the Afghanistan, Pakistan, and India region. Composed of three film types adjusted to a constant scale of 1:745,000 (NASA mosaic). A geographic coordinate grid has been applied to clarify map orientation.

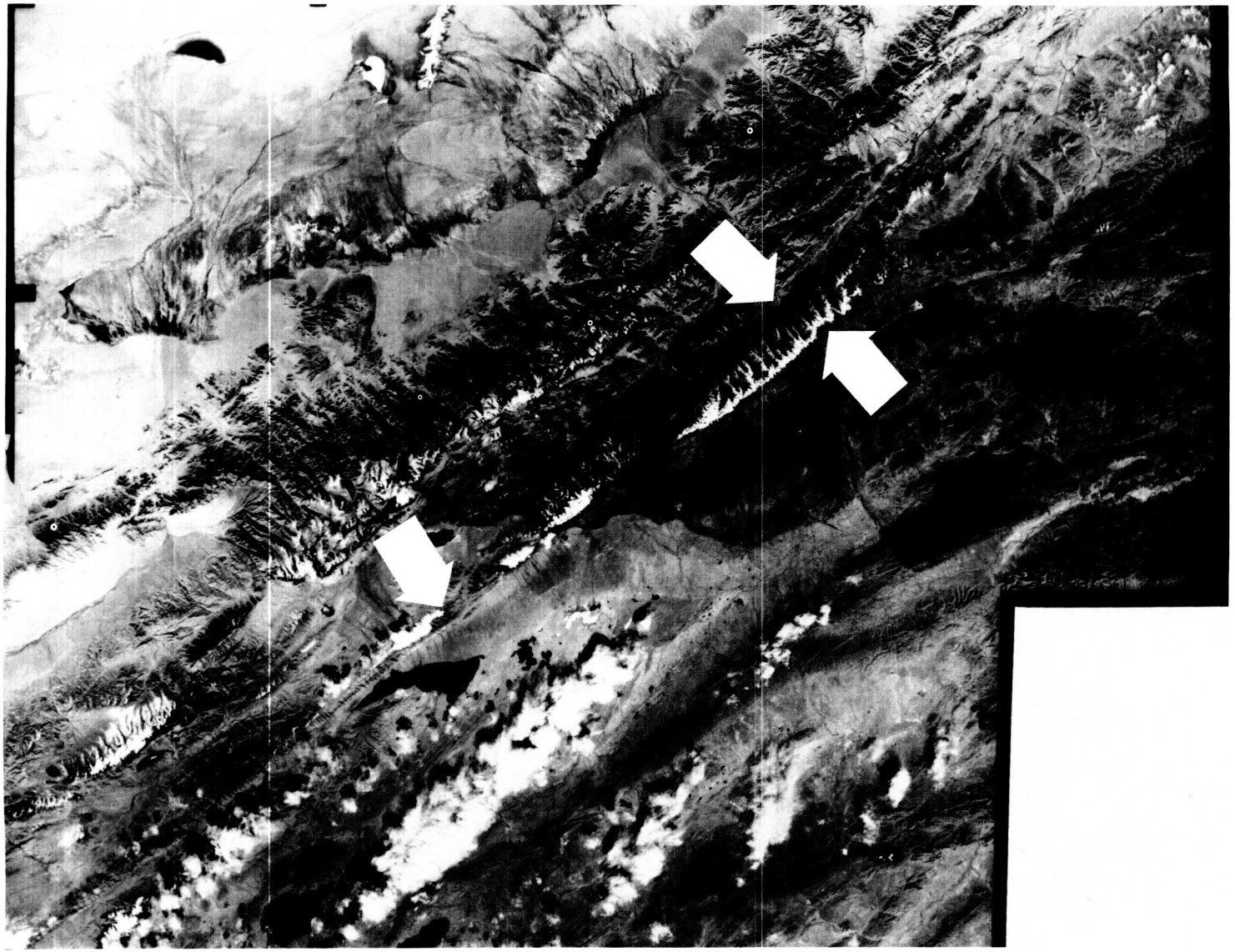
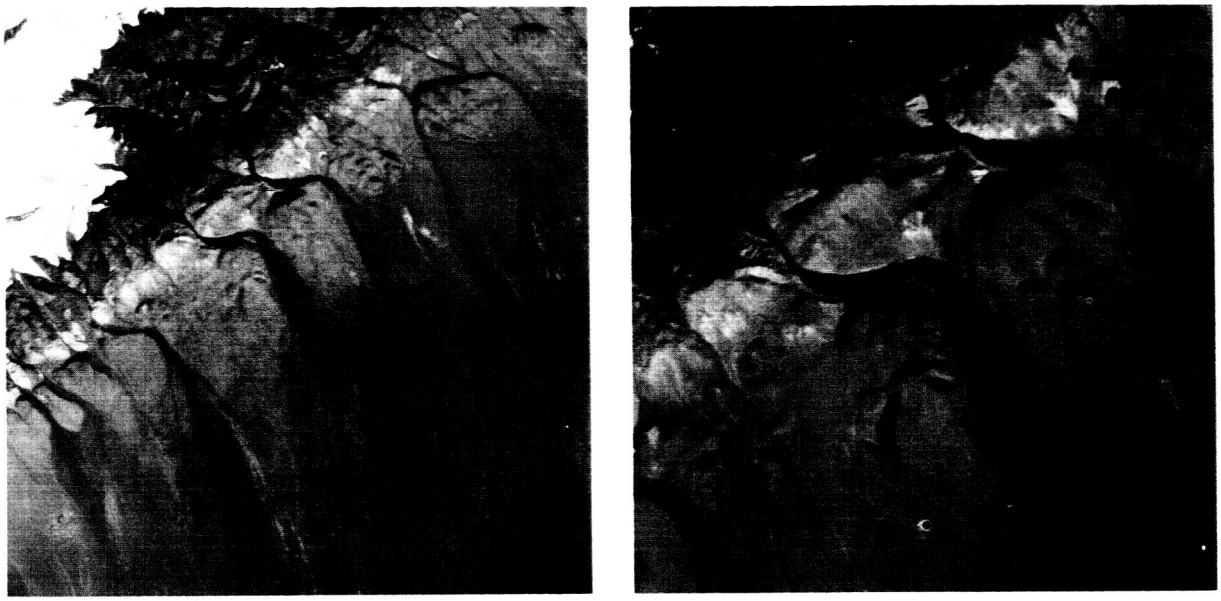


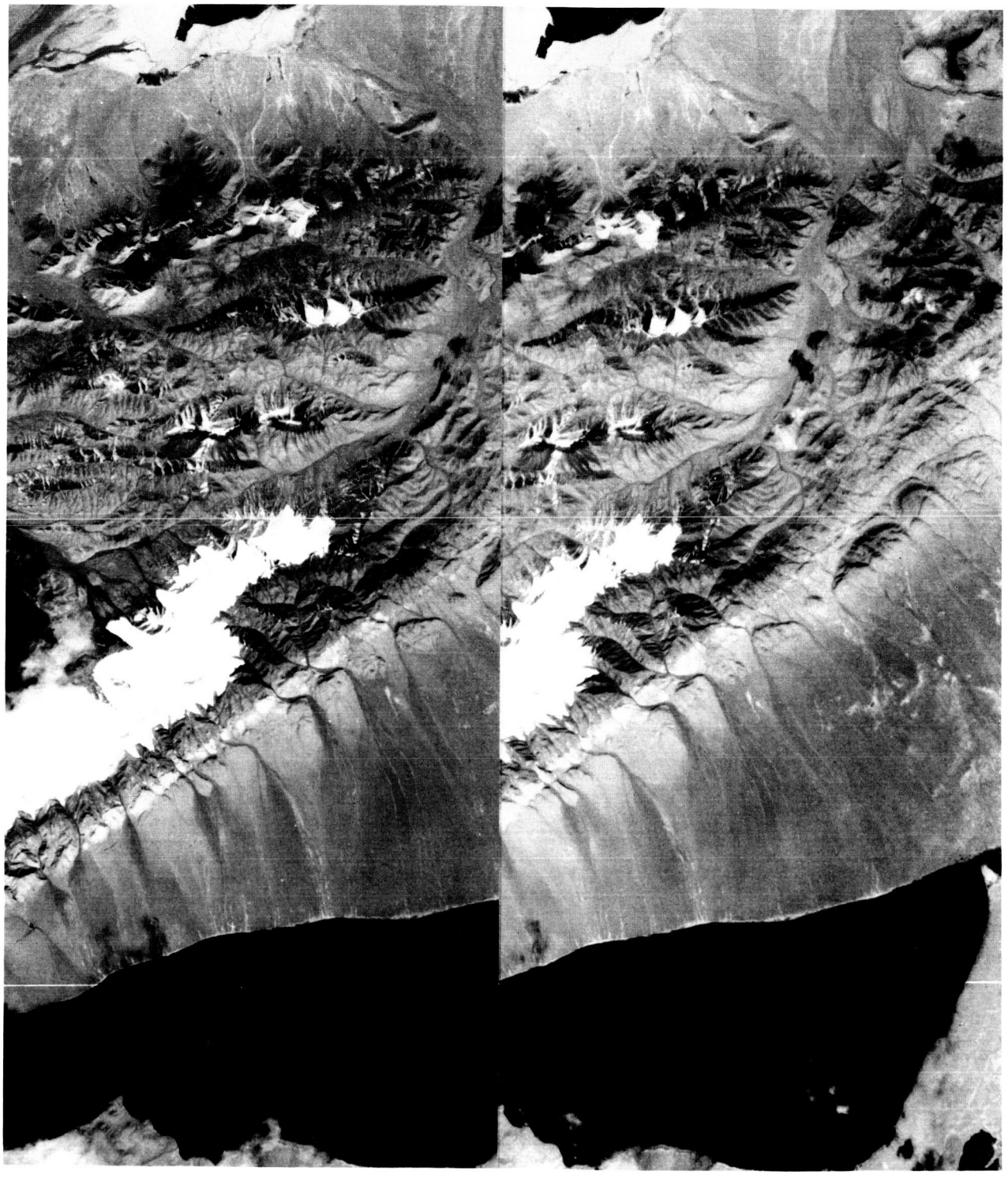
Figure 3-63.- Two frames of LFC imagery combined as a constant scale mosaic of the Tibetan Plateau. Note extent of Kunlun fault, which runs almost due east and west. Frame 0502 (top) acquired orbit 30 (GMT 0733:11), altitude 264.85 km, scale approximately 1:850,000. Frame 0818 (bottom) acquired orbit 46 (GMT 0718:07), at altitude 229.06 km, scale approximately 1:730,000.



(a) Frame 0818, 4.5X, 1:162,200.

(b) Frame 0818, 10X, 1:73,000.

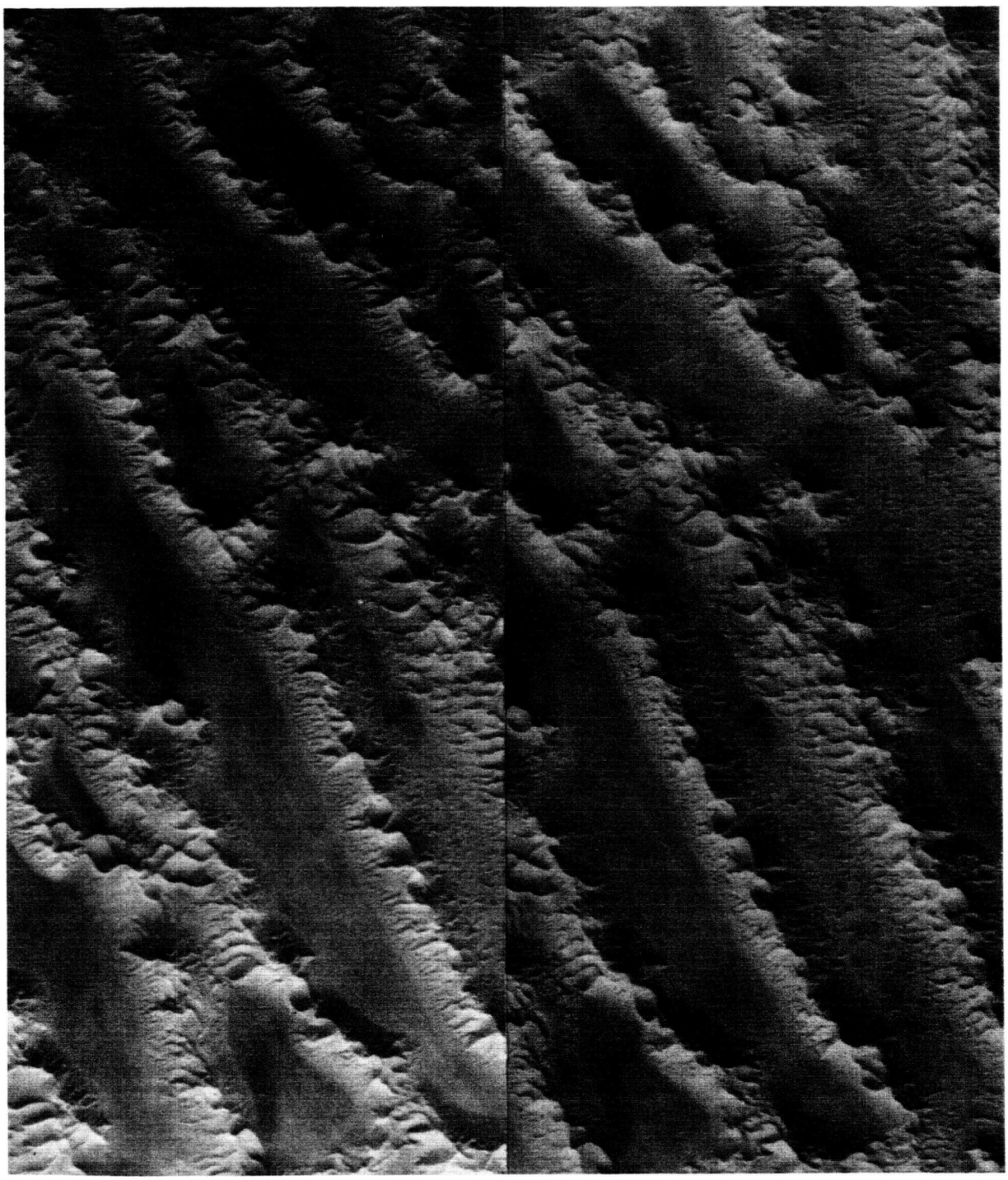
Figure 3-64.- Stream offset at the Kunlun fault interface.



(a) Frame 0817, 3X, 1:250,000.

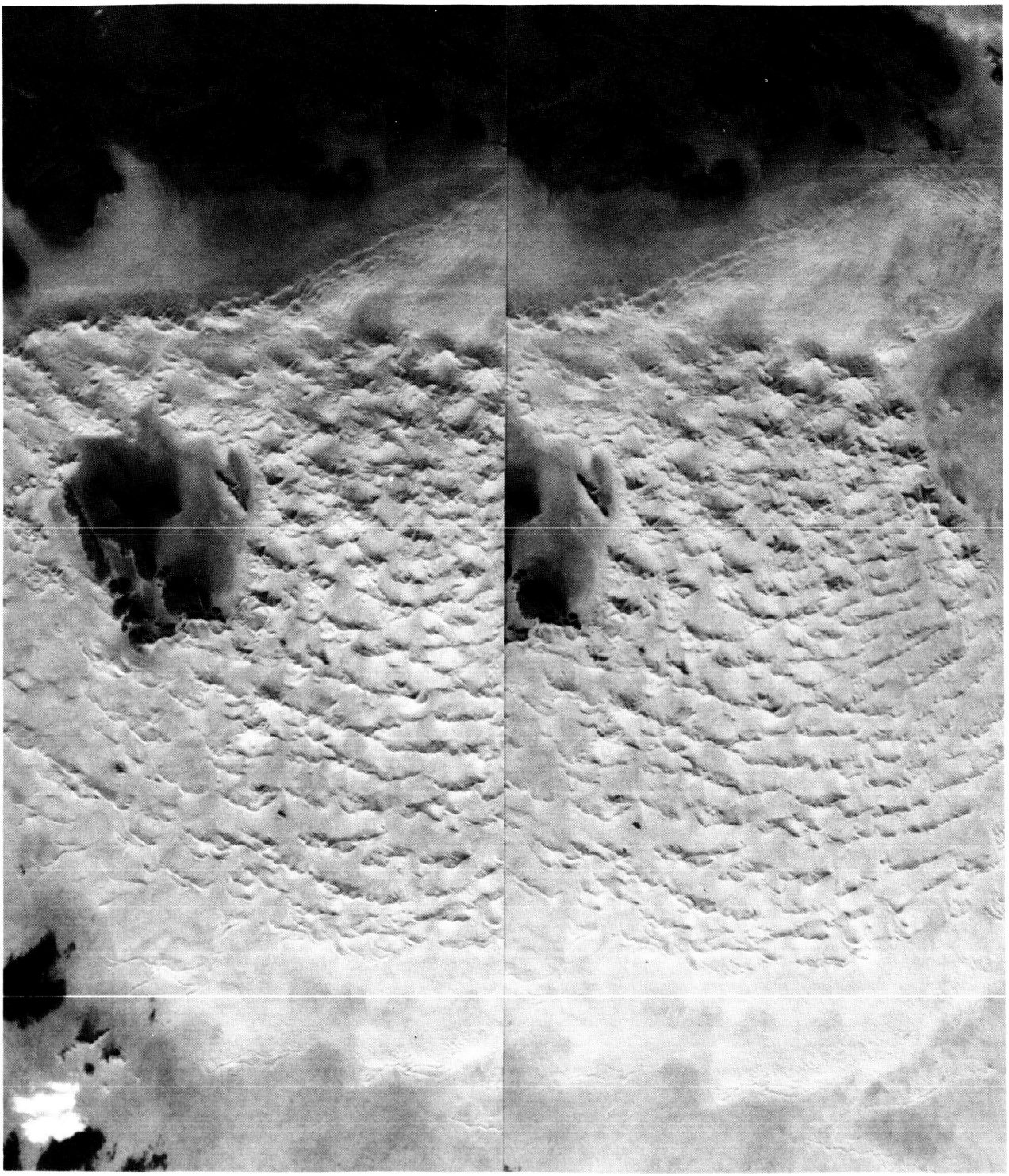
(b) Frame 0819, 3X, 1:250,000.

Figure 3-65.- Kunlun Fault in China (stereo). This well-defined fault structure associated with classical stream offset was recorded during orbit 46 (GMT 0718:07) from an altitude of 229 km, on type 3412 film. LFC was operating in 70-percent forward O/L mode, giving a B/H ratio of 0.90. Original scale was 1:750,000.



(a) Frame 0131, 10X, 1:117,000. *(b) Frame 0135, 10X, 1:117,000.*

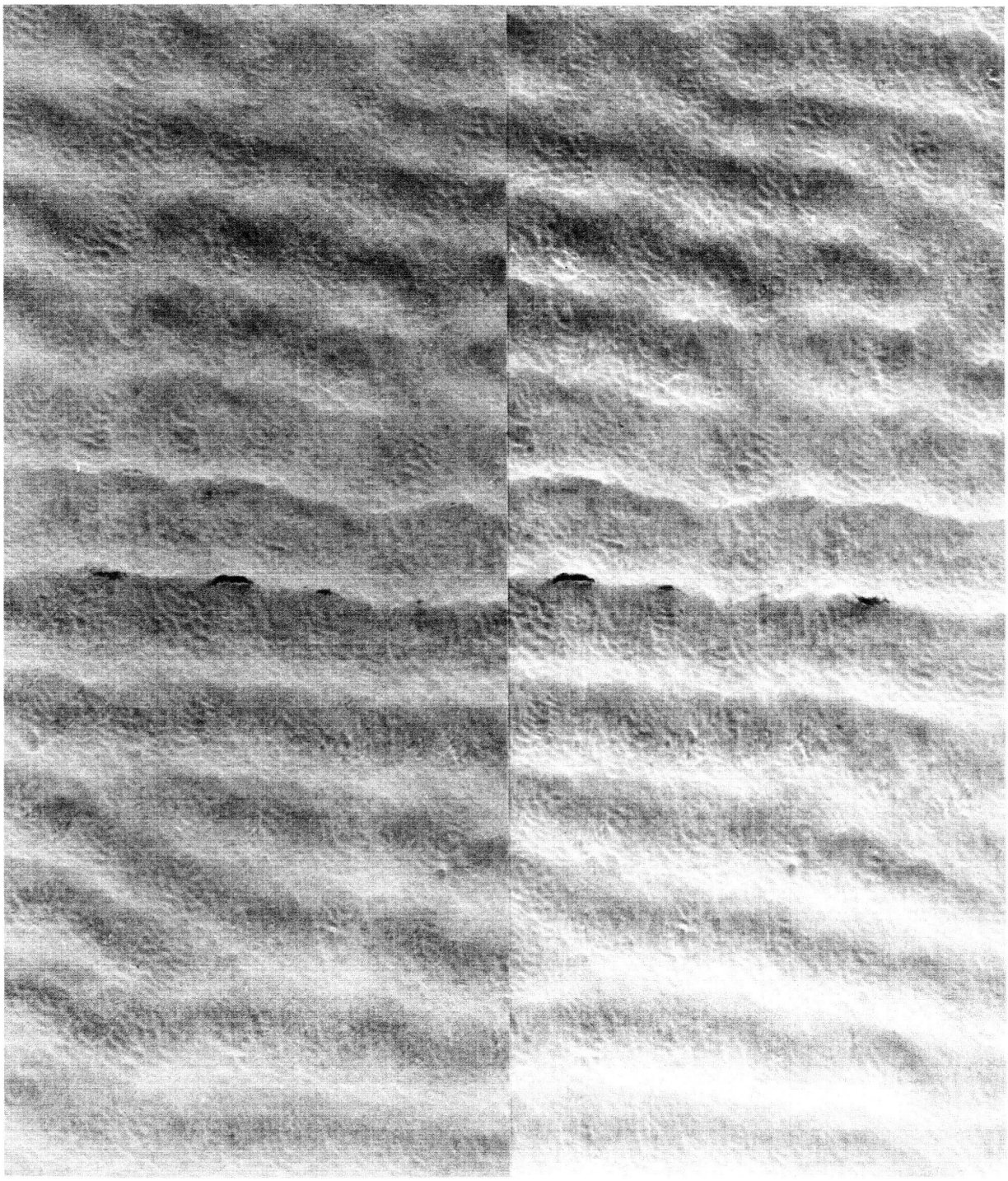
Figure 3-66.- Grand Erg Oriental, Algeria (stereo). This vast area of Medusa head dunes was recorded during orbit 3 (GMT 1438:41) from an altitude of 359 km, on type 3414 film. The LFC was operating in 80-percent forward O/L mode, giving a B/H ratio of 1.20. Original scale was 1:1,179,000.



(a) Frame 0136, 5X, 1:235,000.

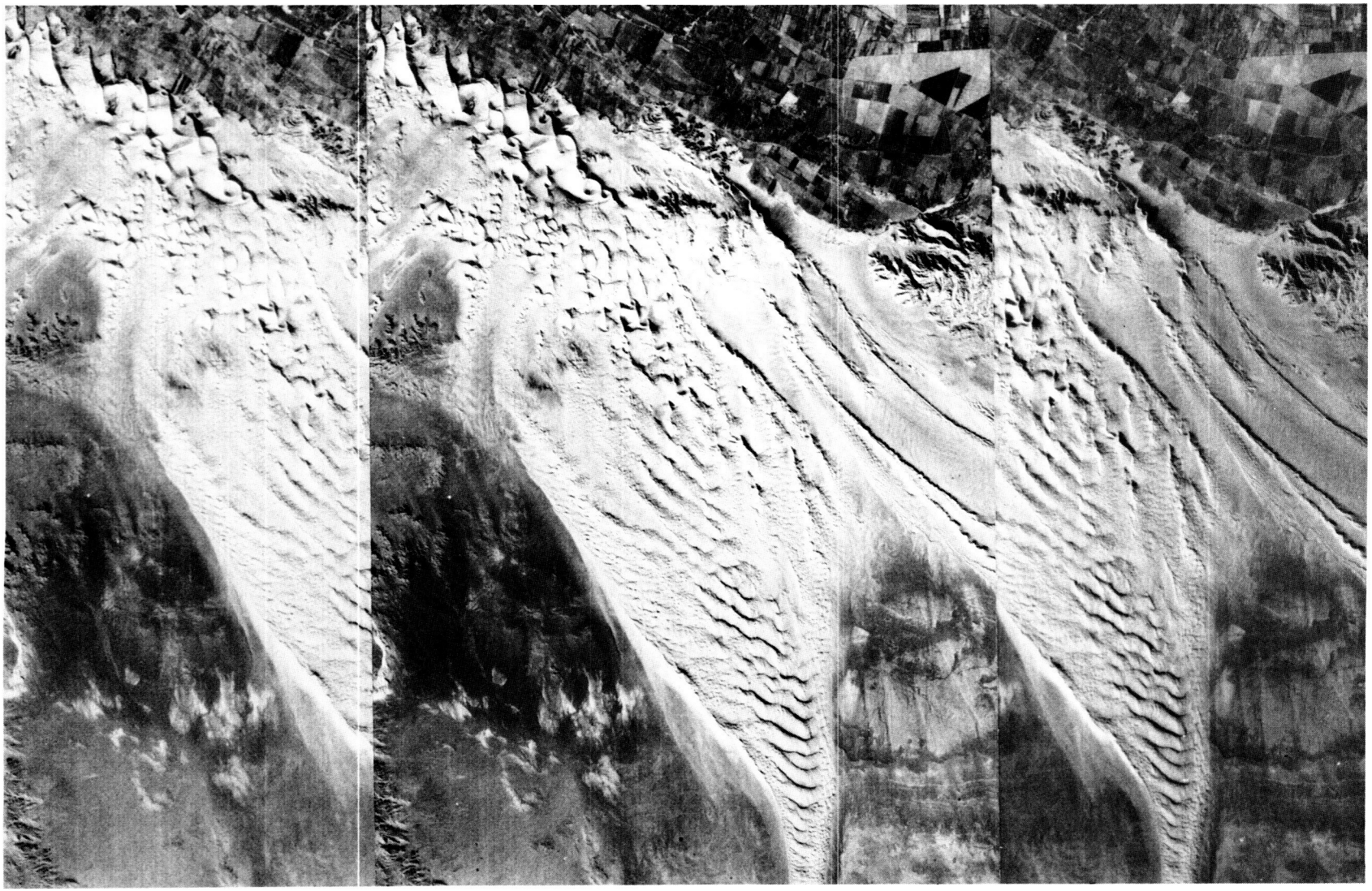
(b) Frame 0138, 5X, 1:235,000.

Figure 3-67.- Erg Admer in Algeria (stereo). This smaller involvement of well-defined dune formations was recorded during orbit 3 (GMT 1439:43) from an altitude of 358 km, on type 3414 film. The LFC was changing from 70- to 60-percent forward O/L mode, giving a B/H ratio of 0.80. Original scale was 1:1,177,000.



(a) Frame 0142, 10X, 1:117,000. *(b) Frame 0143, 10X, 1:117,000.*

Figure 3-68.- Erg du Tenere in Niger (stereo). These subtle dune formations were recorded during orbit 3 (GMT 1442:03) from an altitude of 357 km, on type 3414 film. The LFC was operating in 60-percent forward O/L mode, giving a B/H ratio of 0.60. Original scale was 1:1,172,000.



(a) Frame 0765, 4X. (b) Frame 0766, 4X. (c) Frame 0769, 4X.

Figure 3-69.- Sechura Desert, Peru (stereo triplicate). Recorded during orbit 39 (GMT 2109:53) from an altitude of 222 km, on type 3412 film. The LFC was operating in 80-percent forward OL mode with a B/H ratio of 0.30 for frames a and b and 0.90 for frames b and c. Original scale was 1:730,000, and above figure scale is 1:182,000.



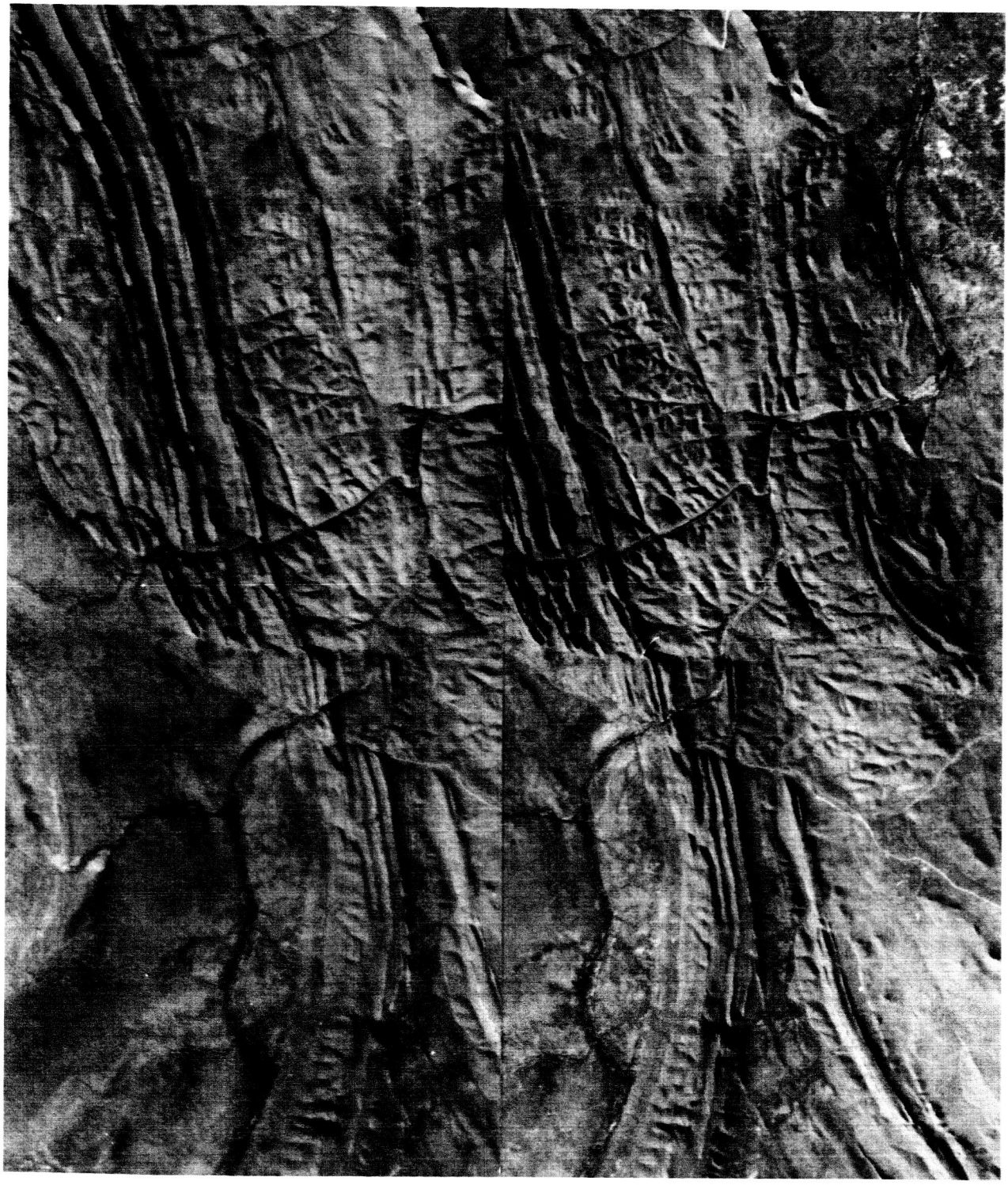
(a) Frame 0875, 2.5X, 1:293,000. (b) Frame 0878, 2.5X, 1:293,000.

Figure 3-70.- Durak Range in western Australia (stereo). The vast barren area associated with the Durak range contains great linear folds within a severely faulted zone. Imagery was recorded orbit 46 (GMT 0733:46) from an altitude of 223 km, on type 3412 film. The LFC was operating in 80-percent forward O/L mode, giving a B/H ratio of 0.90. Original scale was 1:734,000.



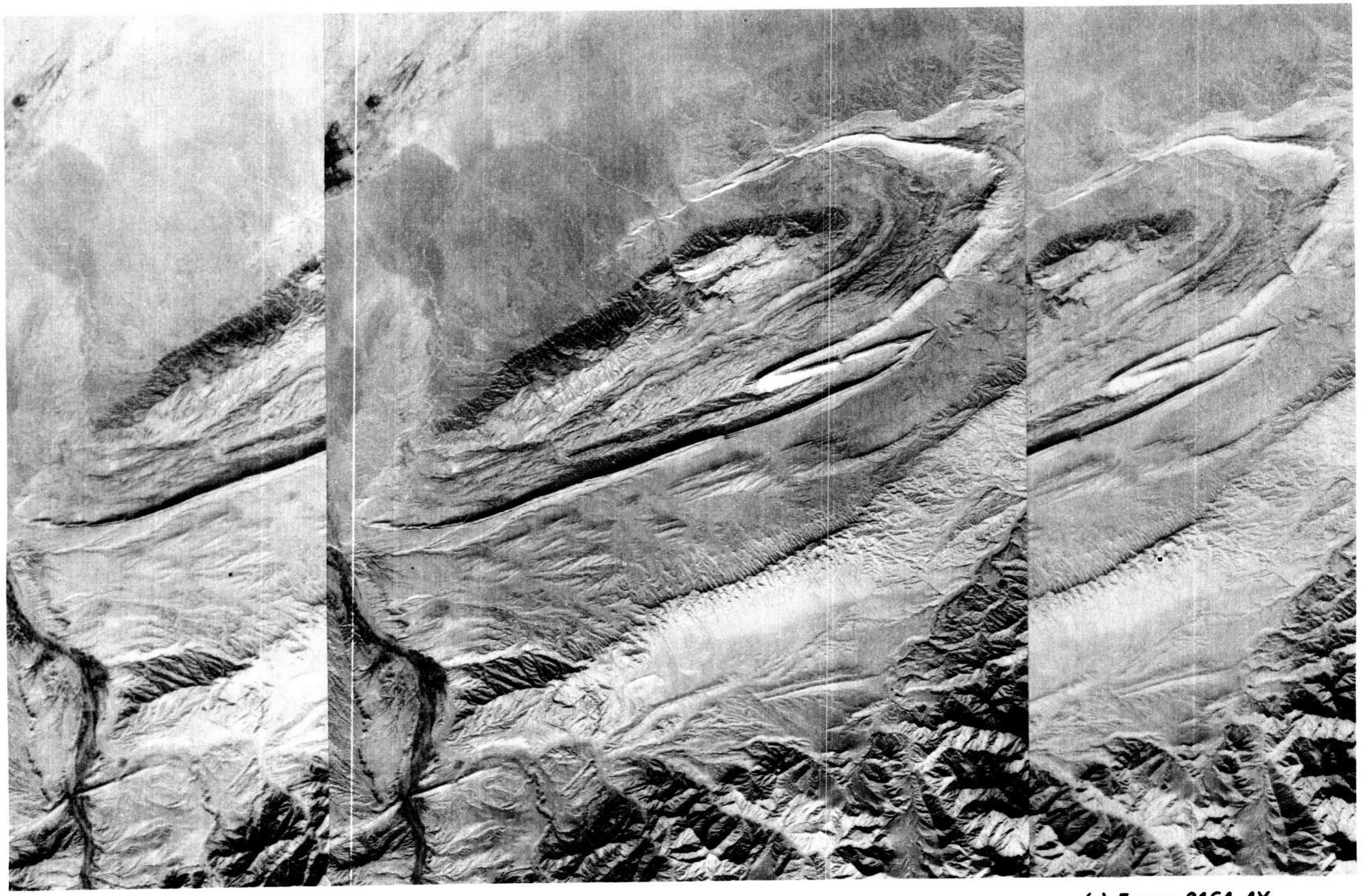
(a) Frame 0875, 4X, 1:183,000. *(b) Frame 0879, 4X, 1:183,000.*

Figure 3-71.- Bedford Station anomaly in western Australia (stereo). In this severely faulted area with circular folds appears a large crater of undetermined origin; imagery was recorded during orbit 46 (GMT 0734:12) from an altitude of 223 km, on type 3412 film. The LFC was operating in 80-percent forward O/L mode, giving a B/H ratio of 1.20. Original scale was 1:734,000.



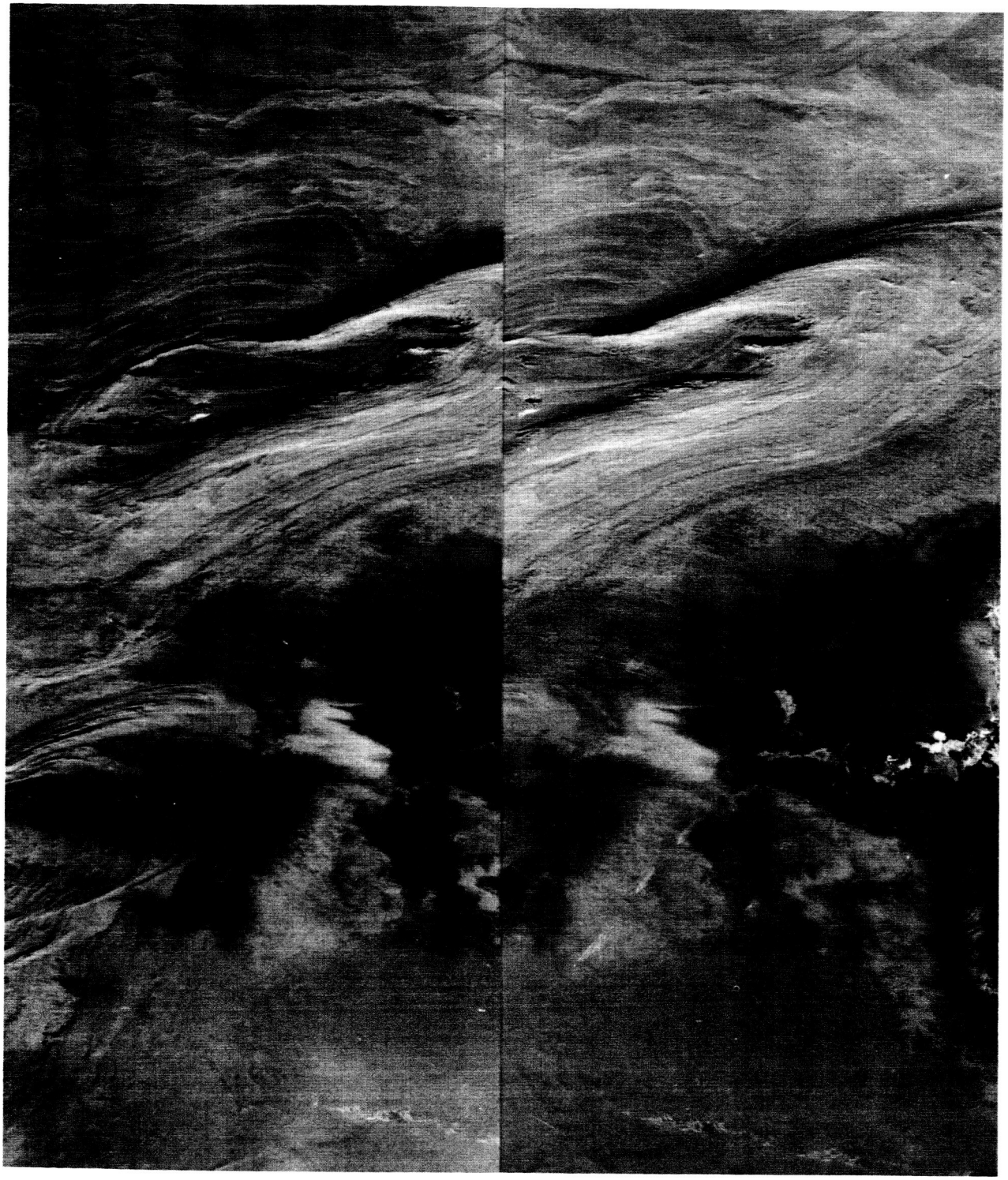
(a) Frame 0875, 10X, 1:73,000. *(b) Frame 0879, 10X, 1:73,000.*

Figure 3-72.- Bedford Station anomaly in western Australia (stereo). Greatly enlarged area of tremendous offsetting of ridges along multiple fault lines was recorded during orbit 46 (GMT 0734:12) from an altitude of 223 km, on type 3412 film. The LFC was operating in 80-percent forward O/L mode, giving a B/H ratio of 1.20. Original scale was 1:734,000.



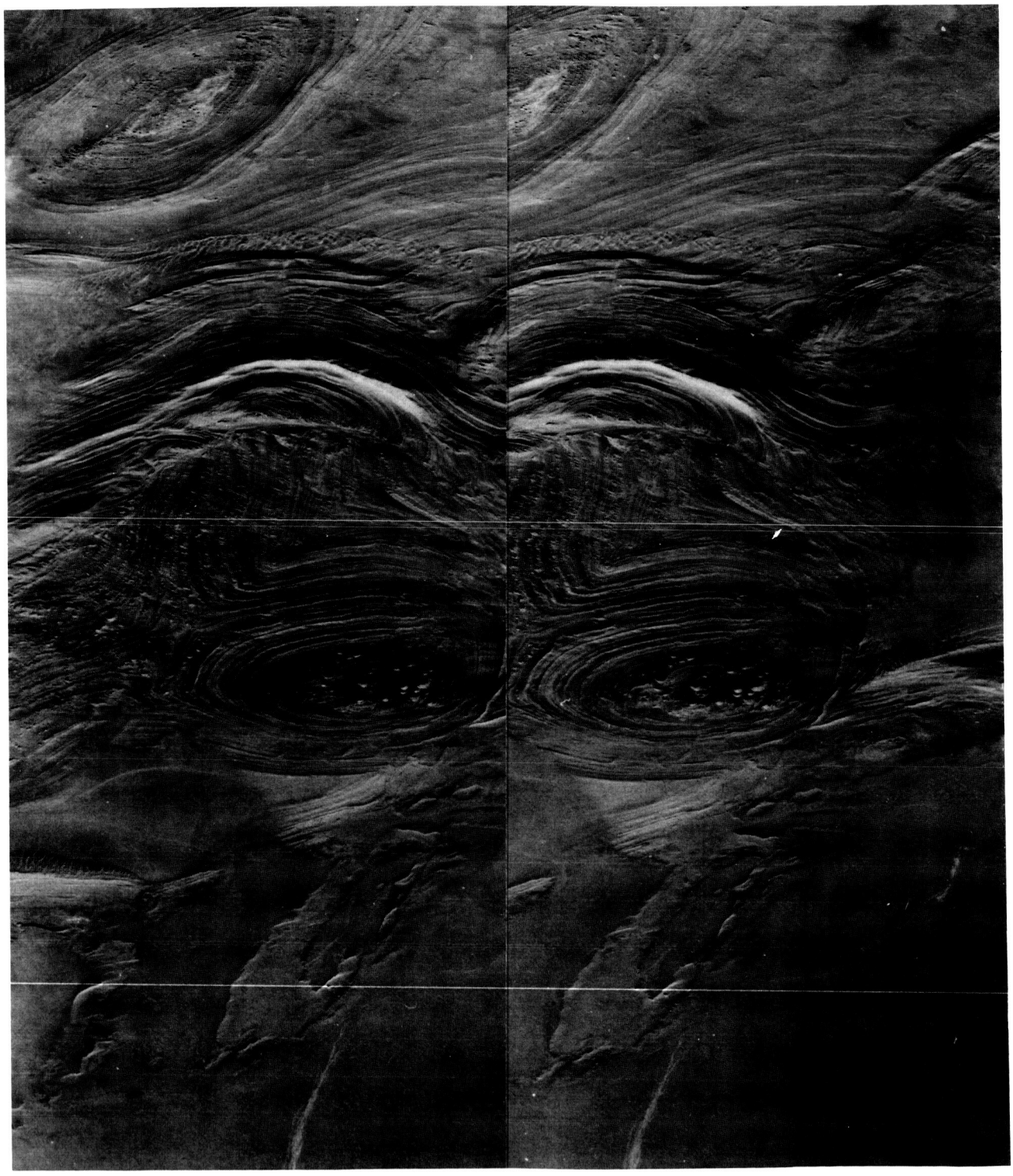
(a) Frame 0160, 4X. (b) Frame 0162, 4X. (c) Frame 0164, 4X.

Figure 3-73.- Complex folding in Tibetan Plateau (stereo triplicate). Recorded during orbit 15 (GMT 0854:52) from an altitude of 362 km, on type 3414 film. The LFC was operating in 80-percent forward O/L mode with a B/H ratio of 0.60 for frames a and b and 0.60 for frames b and c. Original scale was 1:1,187,000, and above figure scale is 1:296,000.



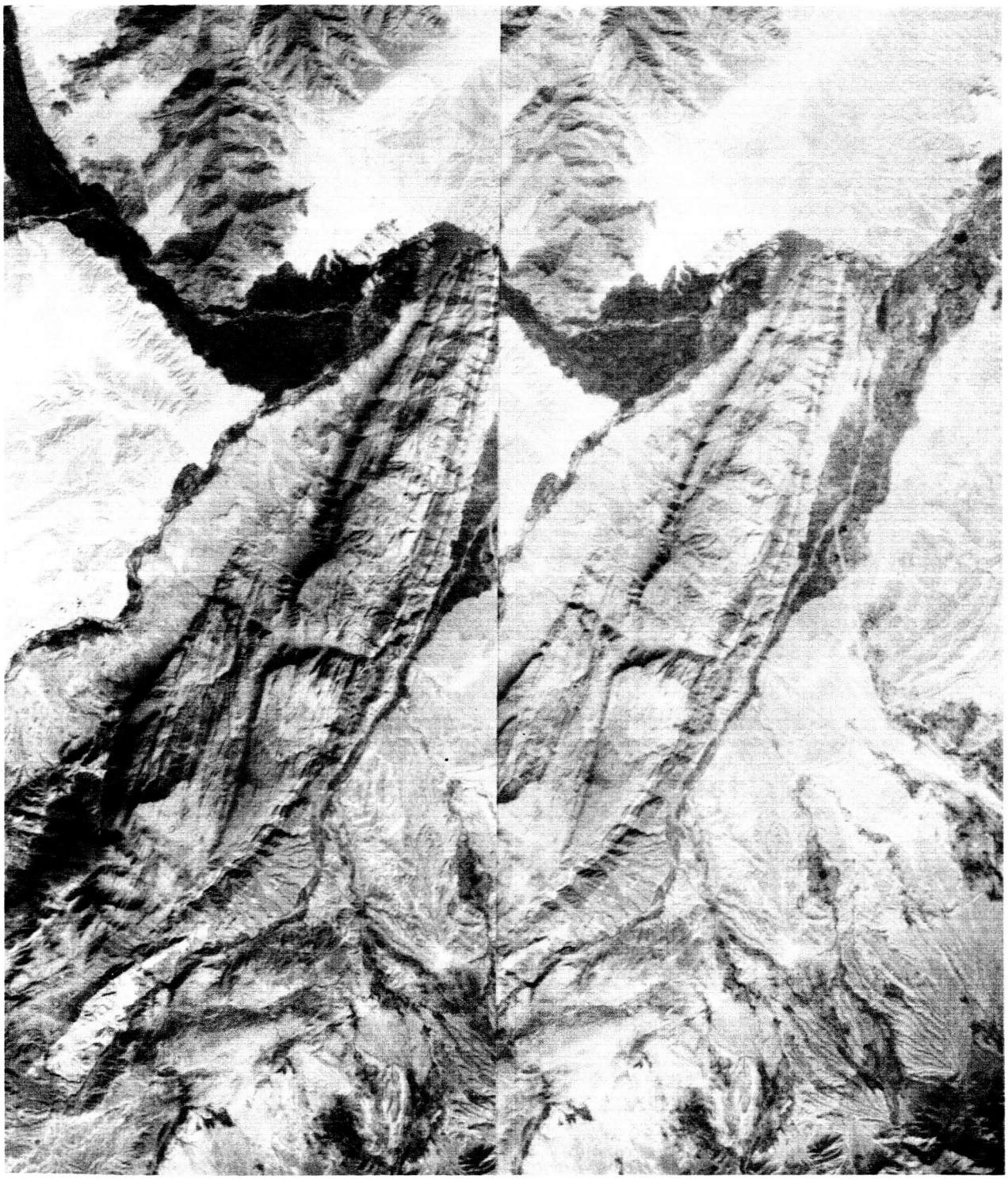
(a) Frame 0499, 4X, 1:217,000. *(b) Frame 0501, 4X, 1:217,000.*

Figure 3-74.- Eroded folded zones in Tibetan Plateau (stereo). Erosion over a large area in the Tibetan Plateau is due to arid conditions and high wind velocities. Recorded orbit 30 (GMT 0732:38) from altitude 265 km, on type 3414 film. The LFC was operating in 70-percent forward O/L mode, giving a B/H ratio of 0.90. Original scale 1:870,000. (See continuation in figure 3-75.)



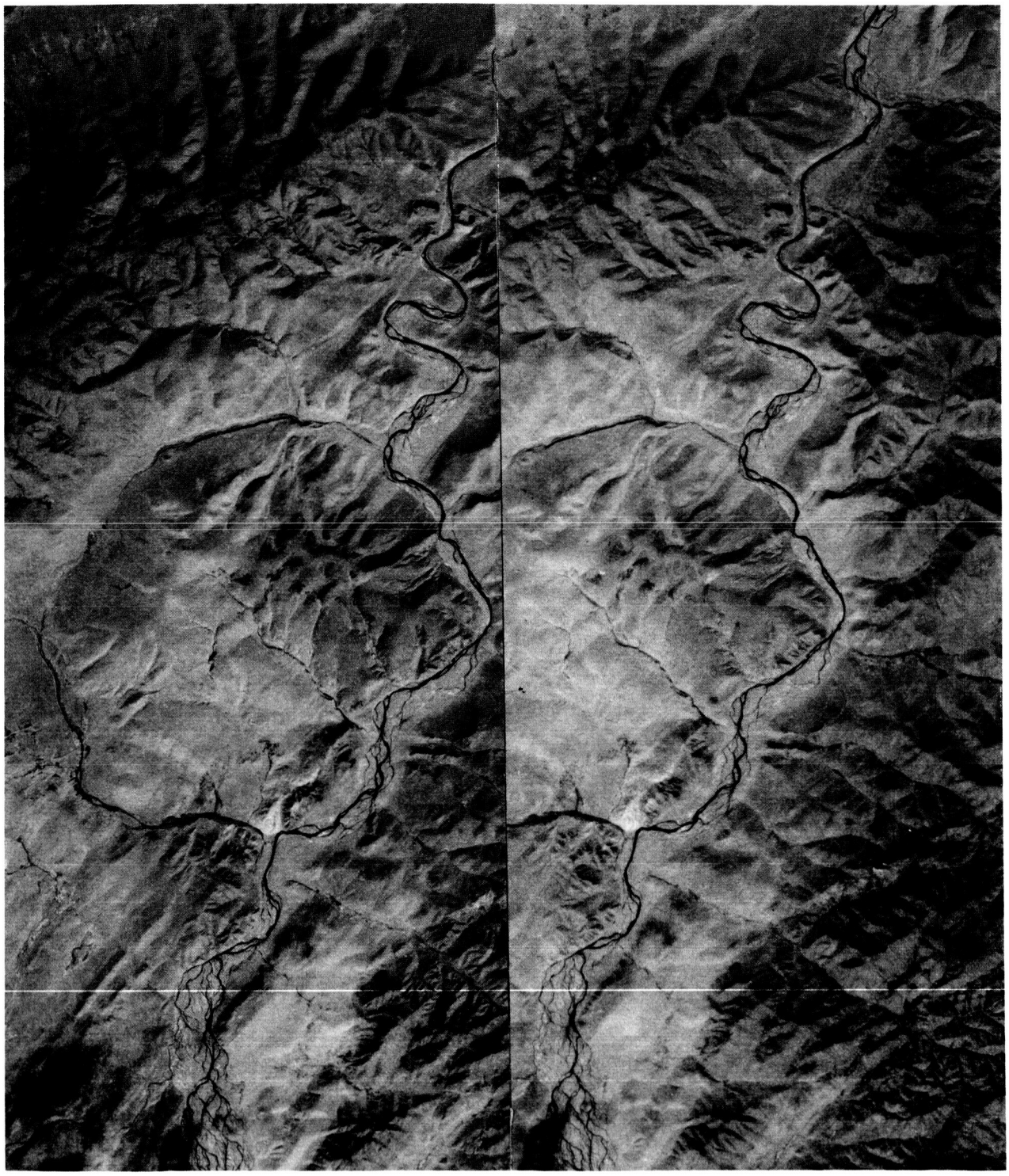
(a) Frame 0499, 4X, 1:217,000. *(b) Frame 0501, 4X, 1:217,000.*

Figure 3-75.- Eroded folded zones in Tibetan Plateau (stereo).



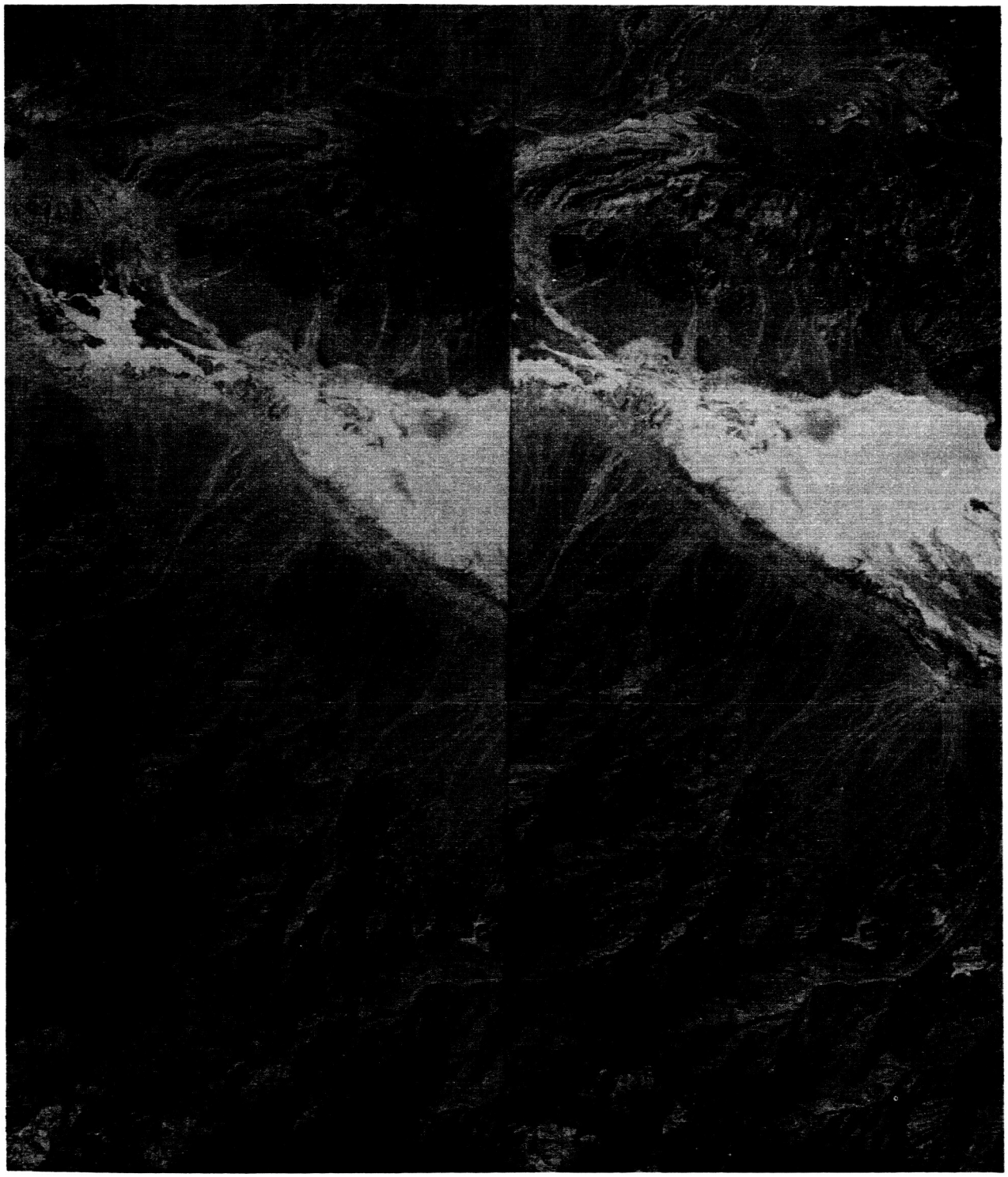
(a) Frame 1233, 2.5X, 1:303,000. *(b) Frame 1235, 2.5X, 1:303,000.*

Figure 3-76. *- Intrusive formation in Afghanistan (stereo). Prominent uplift feature recorded during orbit 63 (GMT 0830:42) from an altitude of 231 km, on type 3414 film. The LFC was operating in 80-percent forward O/L mode, giving a B/H ratio of 0.60. Original scale was 1:759,000.*



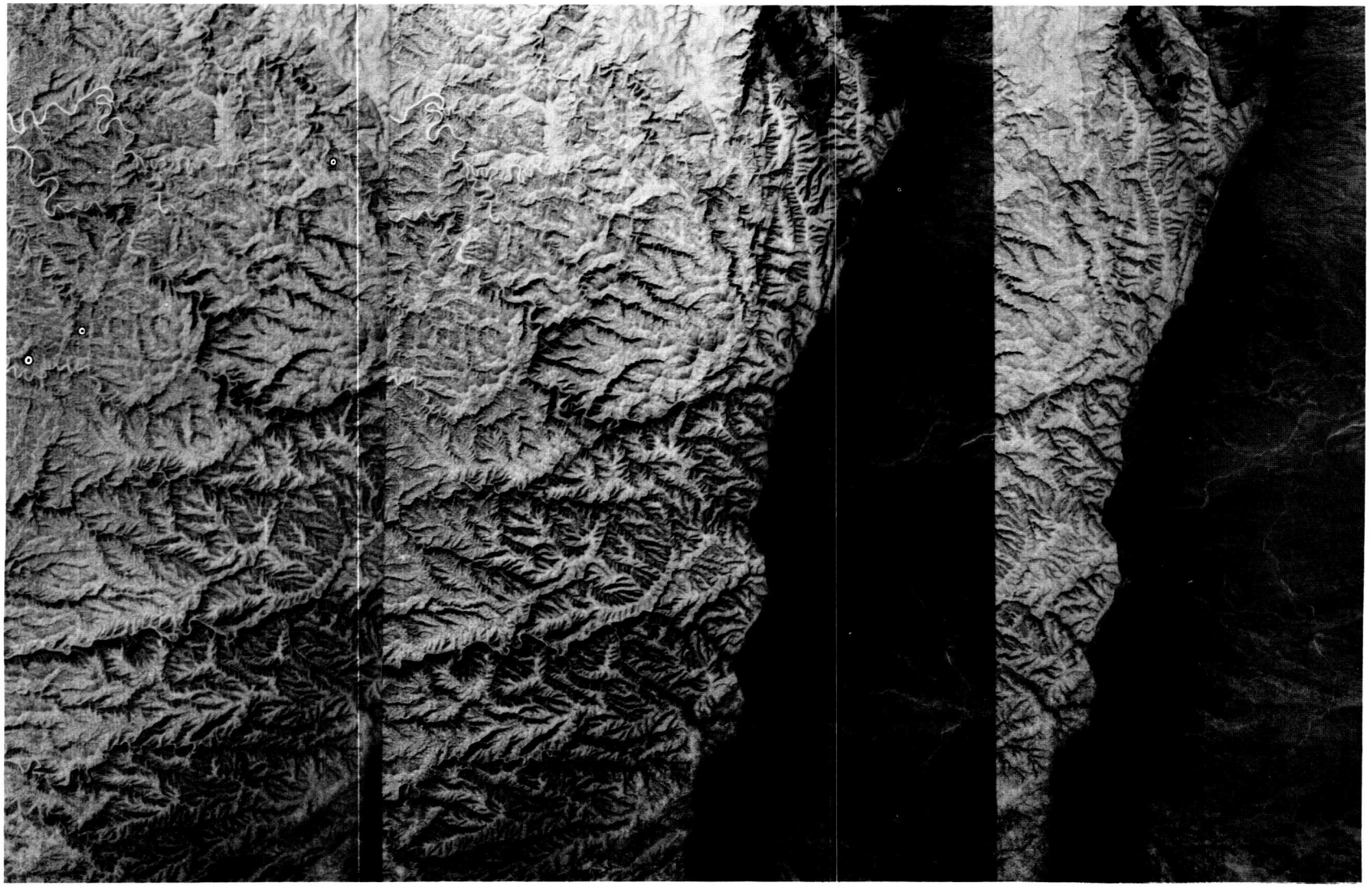
(a) Frame 0819, 3X, 1:250,000. *(b) Frame 0821, 3X, 1:250,000.*

Figure 3-77.- Annular drainage, Tibetan Plateau (stereo). A classic example of annular drainage with outward radial paths was recorded during orbit 46 (GMT 0718:07) from an altitude of 229 km, on type 3414 film. The LFC was operating in 70-percent forward O/L mode, giving a B/H ratio of 0.90. Original scale was 1:750,000.



(a) Frame 2060, 3X, 1:747,000. *(b) Frame 2061, 3X, 1:747,000.*

Figure 3-78.- Death Valley, California (stereo). Centripetal drainage associated with the below-sea-level basin has created extensive and isolated alluvial fans. Recorded during orbit 119 (GMT 1928:54) from an altitude of 227 km, on type 3414 film. The LFC was operating in 60-percent forward O/L mode, giving a B/H ratio of 0.60. Original scale was 1:747,000.

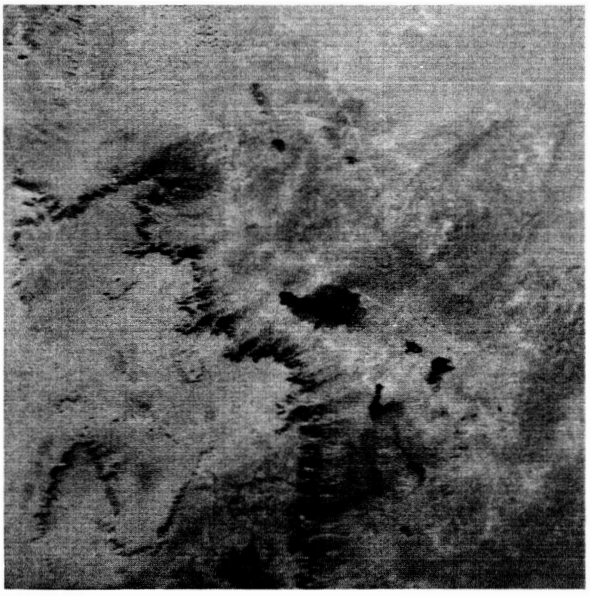


(a) Frame 2291. 2.25X. (b) Frame 2293. 2.25X. (c) Frame 2295. 2.25X.

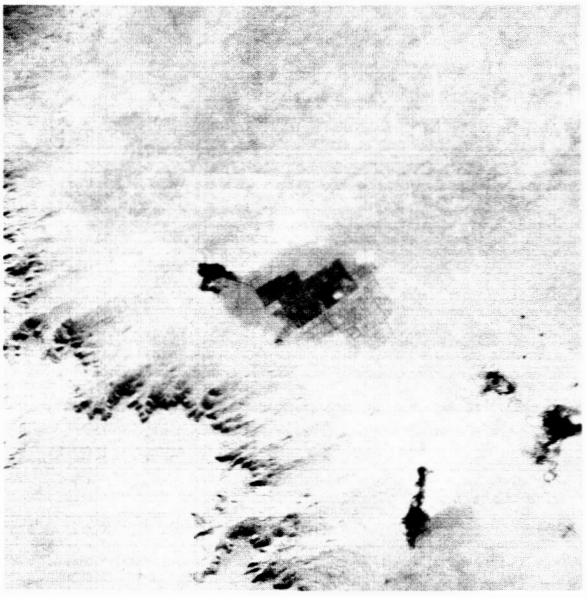
Figure 3-79.- Samhan Range, Oman (stereo triplicate). A striking contrast of terrain slopes showing recent drainage (right) and ancient drainage patterns (left) on either side of this 6,000-ft edifice. Recorded during the final LFC operating period on orbit 120 (GMT 0854:36) from an altitude of 223 km, on type 3414 film. The LFC was operating in 80-percent forward O/L mode with a B/H ratio of 0.60 for frames a and b and 0.60 for frames b and c. Original scale was 1:734,000, and above figure scale is 326,000.



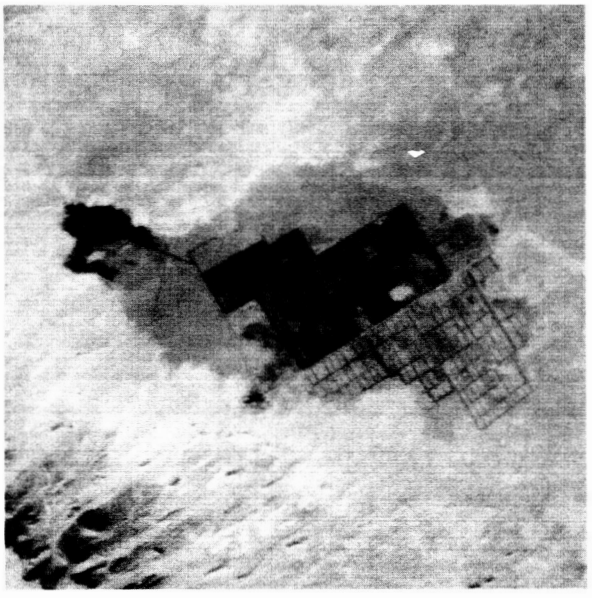
(a) Frame 0079, 1X, 1:1,178,000.



(b) Frame 0079, 2X, 1:589,000.

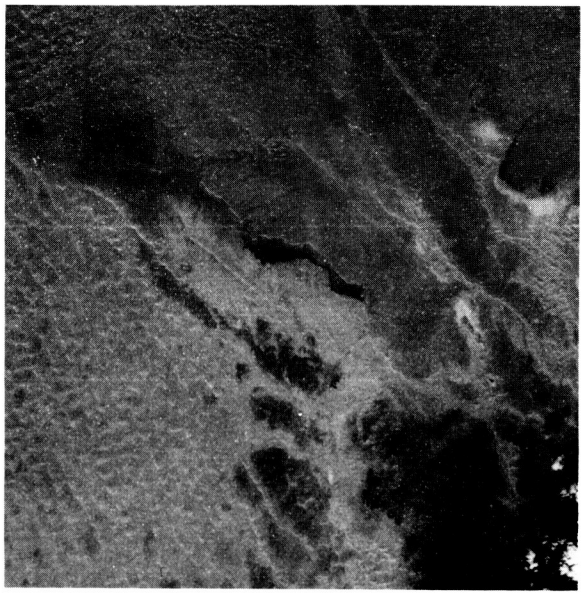


(c) Frame 0079, 4.5X, 1:262,000.

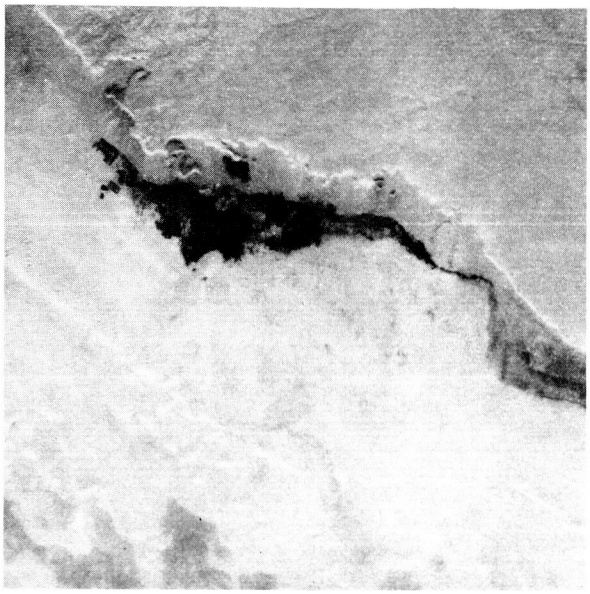


(d) Frame 0079, 10X, 1:117,800.

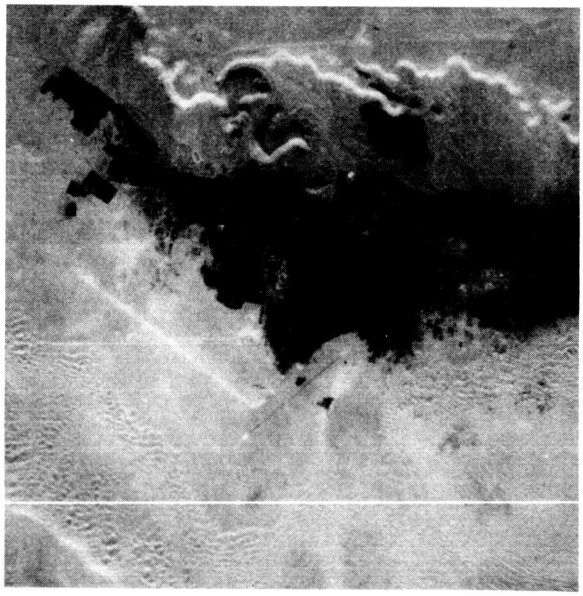
Figure 3-80.- Farafra Oasis in Egypt. LFC photo is from an altitude of 59.23 km during orbit 2 (GMT 279:1307:32), on type 3414 film. Spacecraft nadir coordinates are 27.81° N 28.65° E.



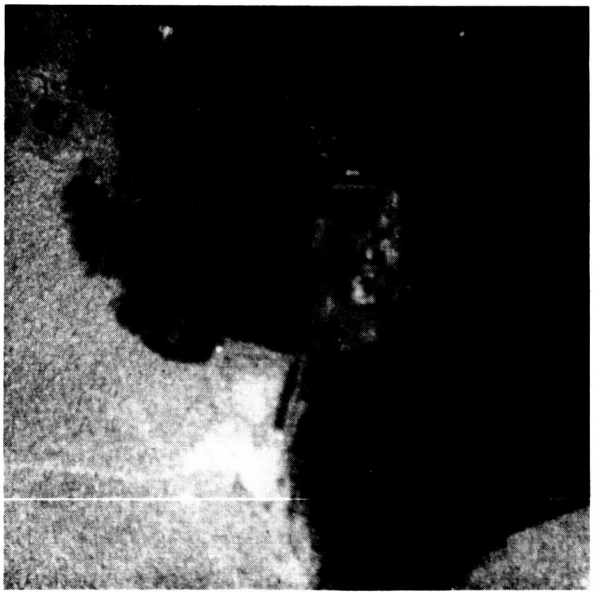
(a) Frame 0130, 1X, 1:1,181,000.



(b) Frame 0130, 4.5X, 1:262,000.

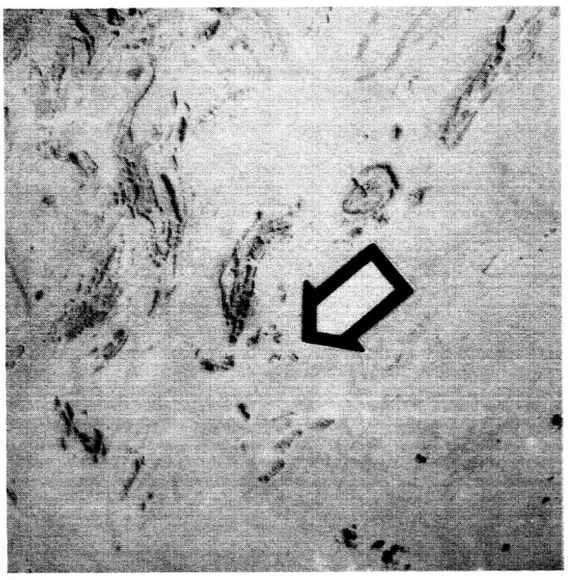


(c) Frame 0130, 10X, 1:118,000.

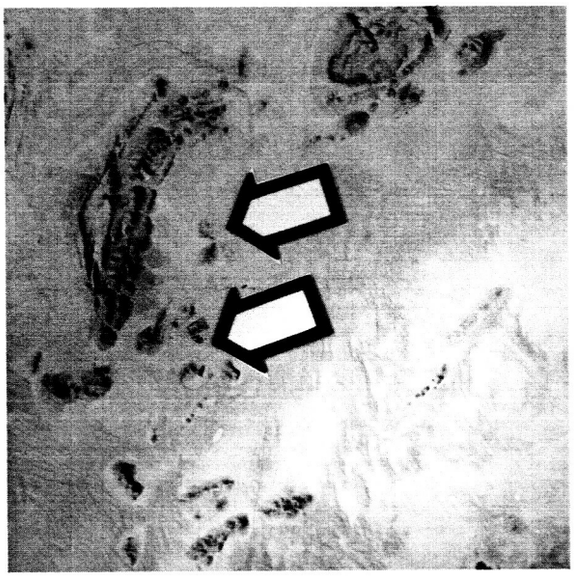


(d) Frame 0130, 35X, 1:33,700.

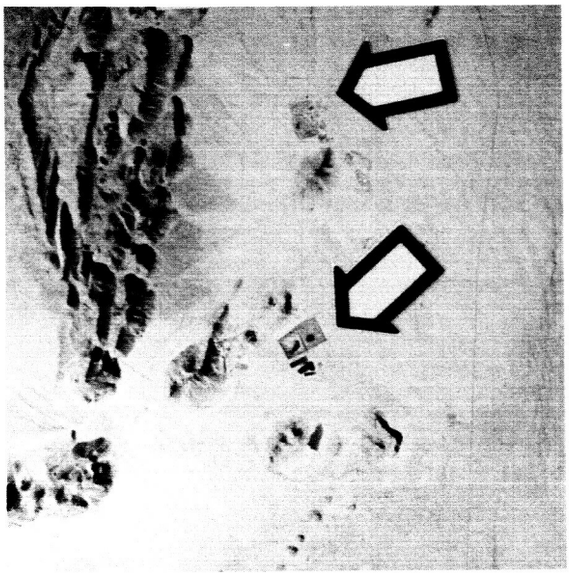
Figure 3-81.- El Golea Oasis, Algeria, on the edge of the Grand Erg Occidental. LFC photography from an altitude of 360.12 km during orbit 3 (GMT 279:1437:59), on type 3414 film. Spacecraft nadir coordinates are 31.27° N 2.54° E.



(a) Frame 1923, 1X, 1:748,000.



(b) Frame 1923, 2X, 1:374,000.



(c) Frame 1923, 4.5X, 1:166,000.



(d) Frame 1923, 10X, 1:74,800.

Figure 3-82.- Aggeneys, Republic of South Africa. Aggeneys is a center of copper mining activity in an otherwise barren area. LFC photo is from an altitude of 228.17 km during orbit 99 (GMT 285:1410:59), on type 3414 film. Spacecraft nadir coordinates are 29.57° S 19.63° E.

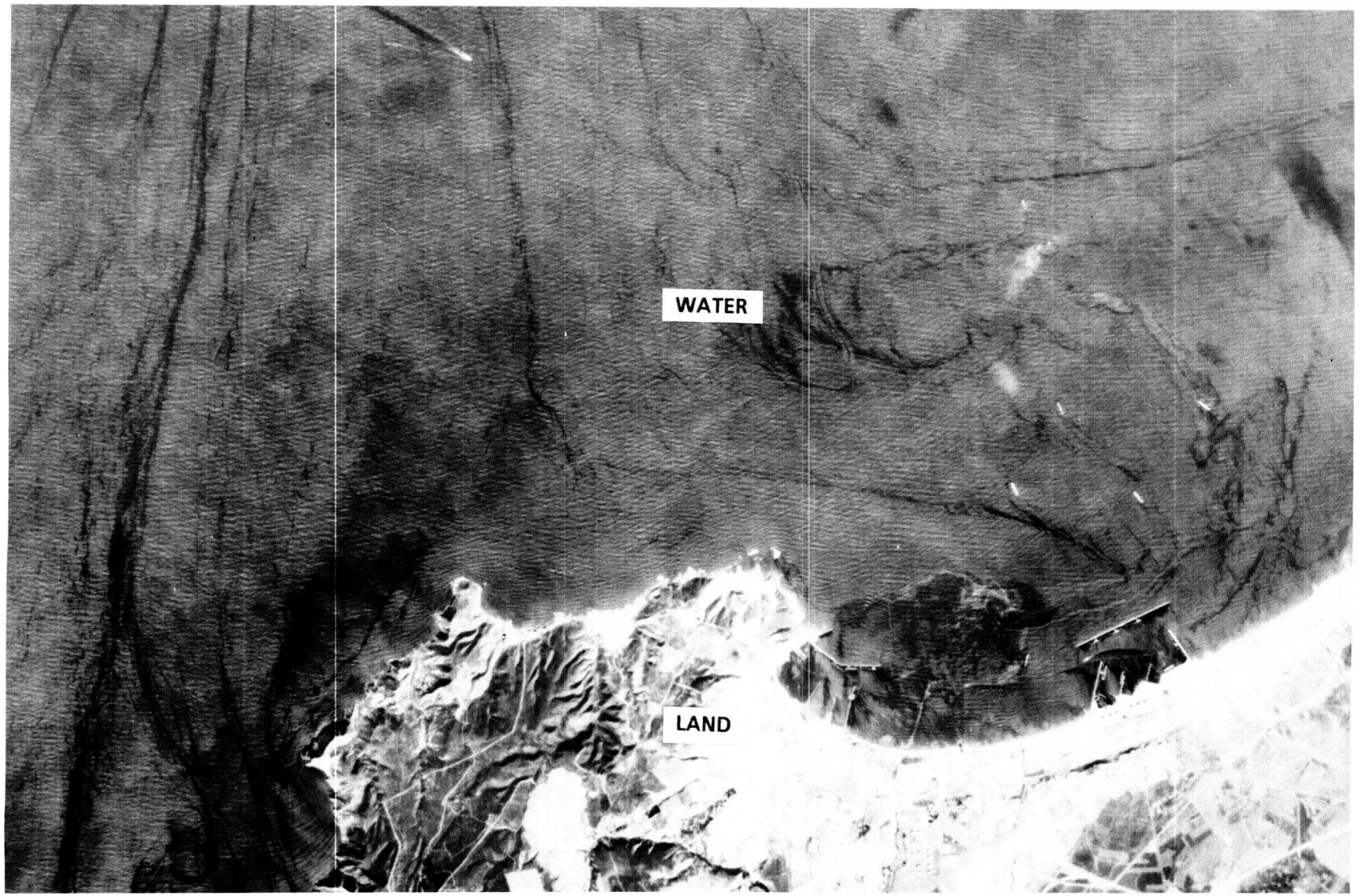


Figure 3-83.- Ocean surface detail in the Golfe d'Arzew at Port aux Poules, Algeria. LFC frame 1357, acquired during orbit 66 (GMT 283:1256:54) from an altitude of 231.64 km, on type 3414 film. Spacecraft nadir coordinates are 36.56° N 0.00° E. Original scale was 1:760,000, and above is shown at 8X, or a scale of 1:95,000.

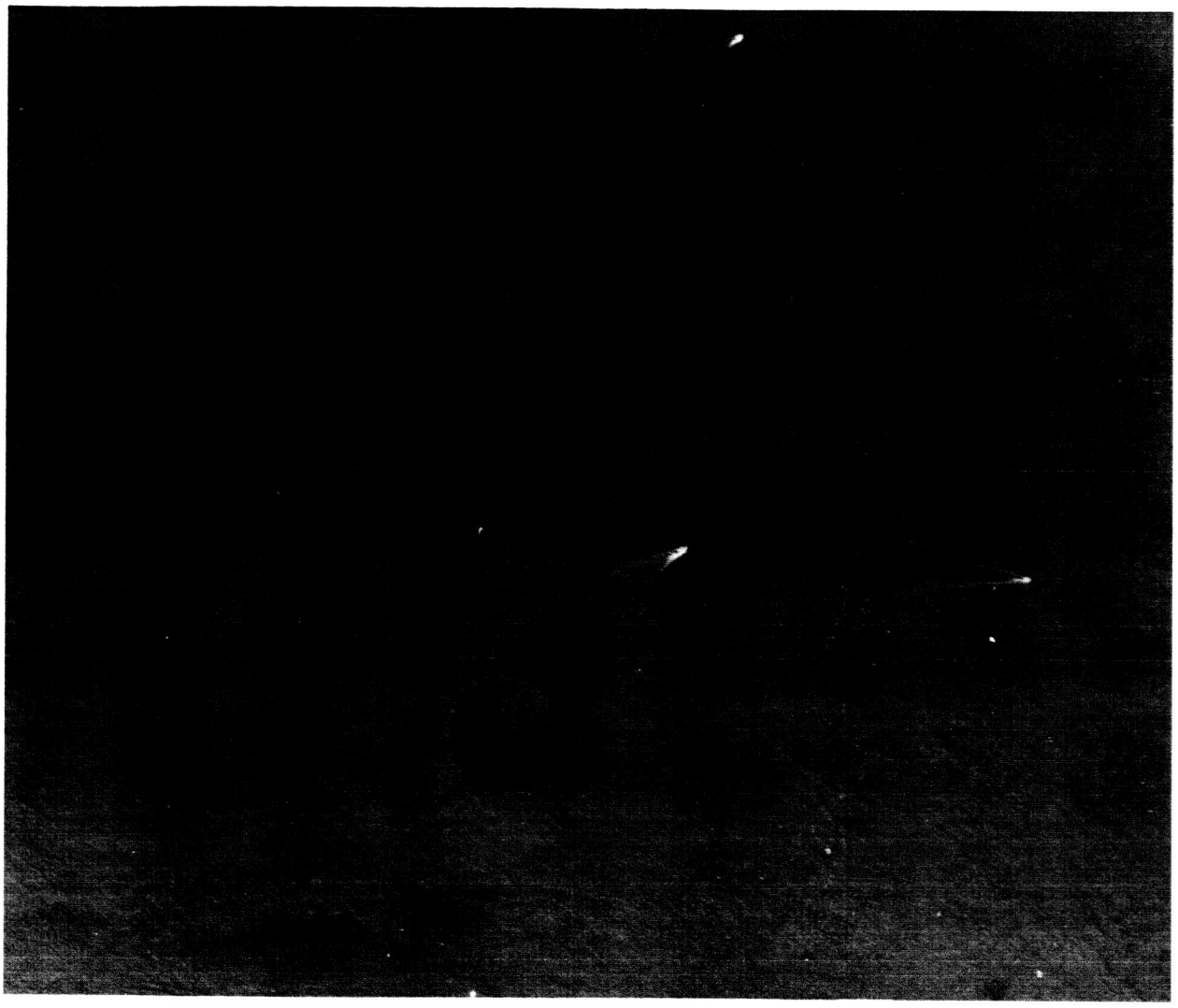
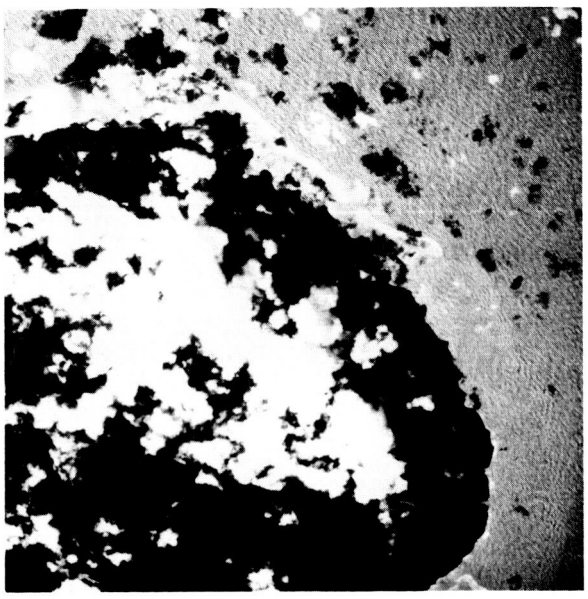
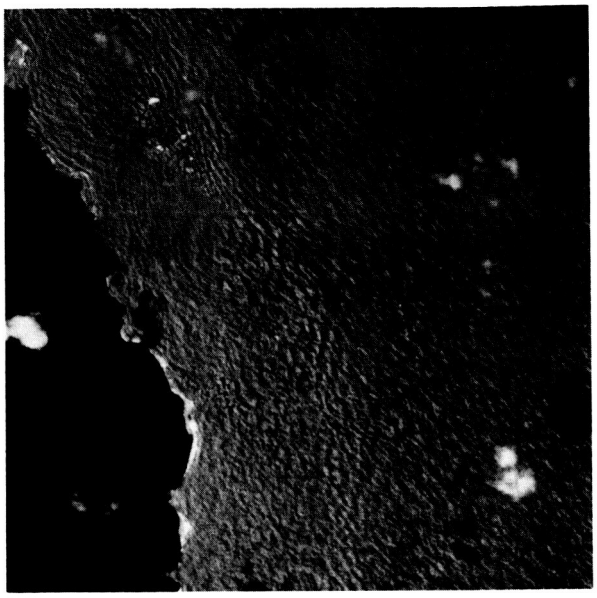


Figure 3-84.- A ship in the Ionian Sea completes an apparent collision avoidance maneuver by execution of a 1.5-km diameter circle. LFC photo is from an altitude of 232.18 km during orbit 65 (GMT 283:1127:23), with an original scale of 1:762,000, on type 3414 film. Spacecraft nadir coordinates are 37.55° N 21.52° E (frame 1296, shown at 8X, 1:95,200).

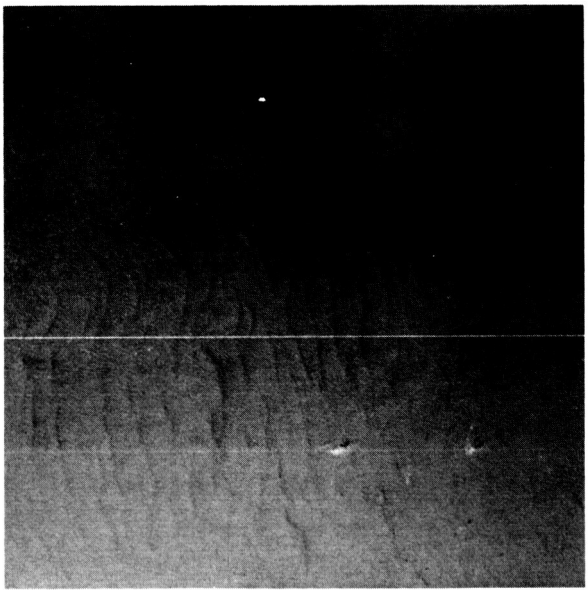


(a) Frame 2114, 4.5X, 1:164,000.

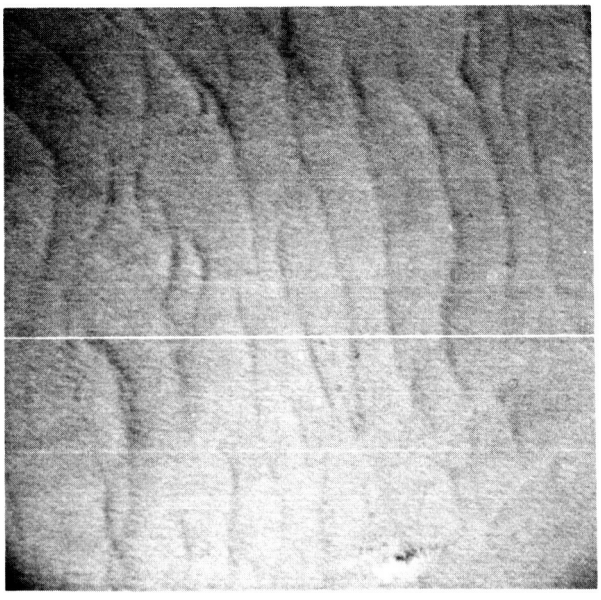


(b) Frame 2114, 10X, 1:73,000.

Figure 3-85.- The island of Tahiti. Captured on the edge of the LFC frame and highlighted by sun glint to bring out the pattern of diffraction waves. LFC photo is from an altitude of 225.00 km during orbit 122 (GMT 287:0011:47), with an original scale of 1:738,000, on type 3414 film.

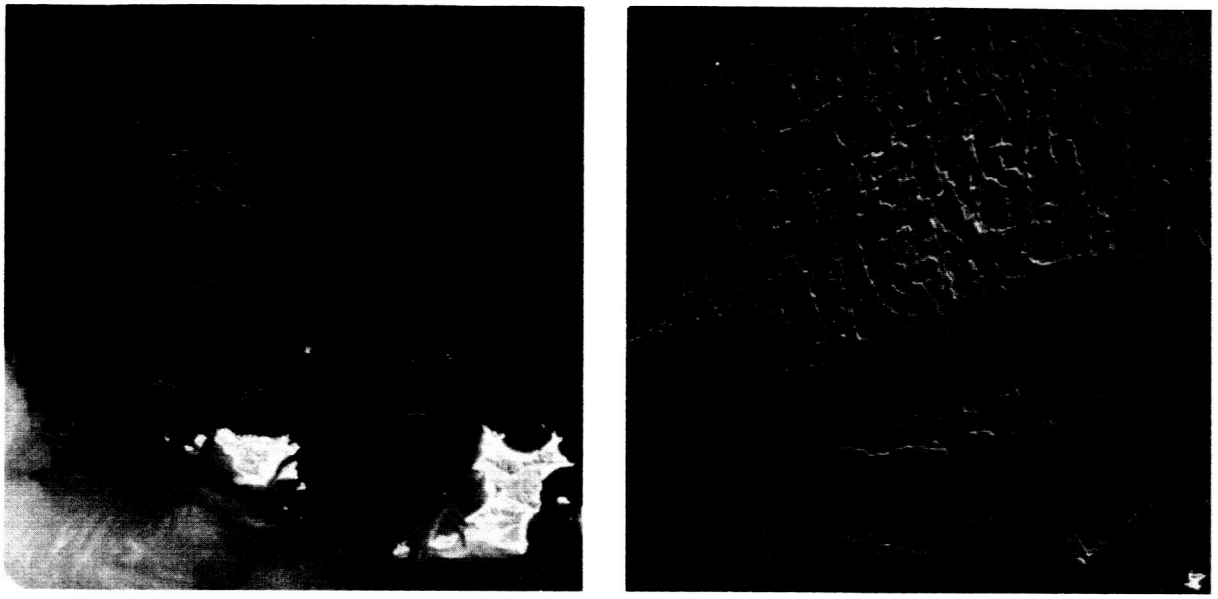


(a) Frame 2007, 2X, 1:369,000.



(b) Frame 2007, 4.5X, 1:164,000.

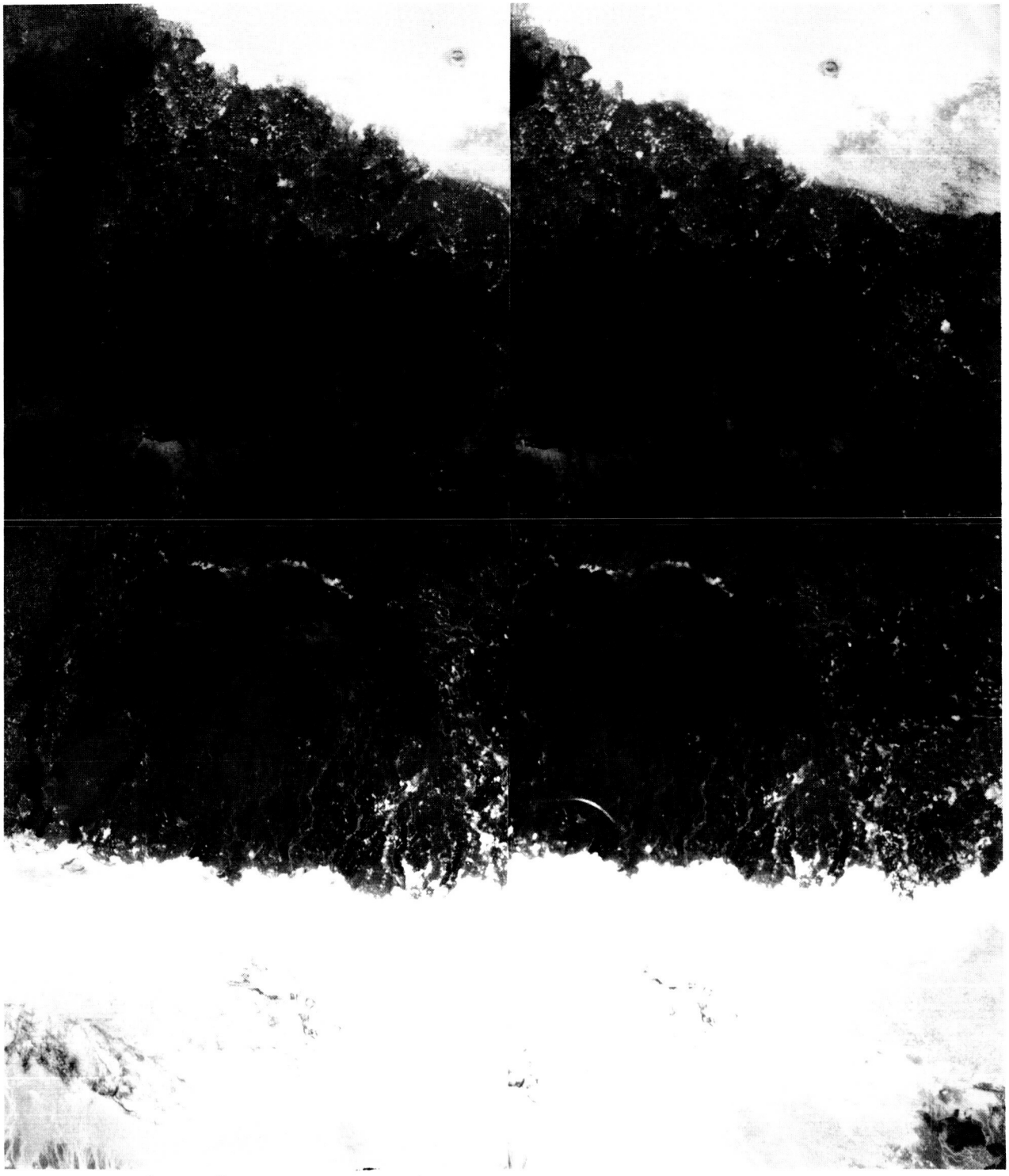
Figure 3-86.- Internal waves in the Indian Ocean off the northwest coast of western Australia. LFC photo is from an altitude of 225.03 km during orbit 110 (GMT 286:0625:07), with an original scale of 1:738,000, on type 3414 film.



(a) Frame 1494, 2X, 1:374,000.

(b) Frame 1494, 4.5X, 1:166,000.

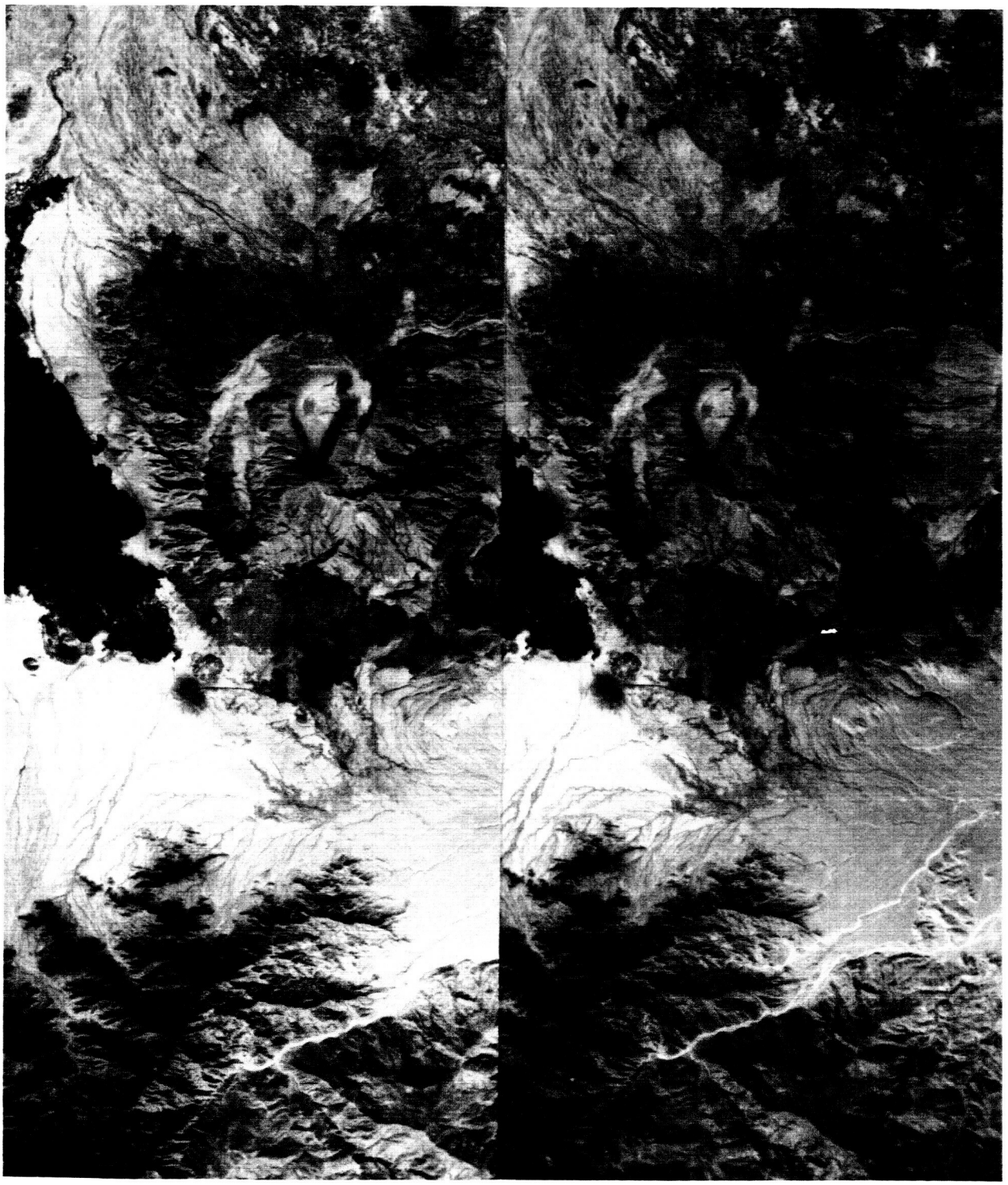
Figure 3-87.- Plankton blooming in the Coral Sea off the eastern coast of Queensland, Australia. LFC photo is from an altitude of 227.85 km during orbit 77 (GMT 284:0532:43), with an original scale of 1:748,000, on type 3414 film.



(a) Frame 1328, 2.7X, 1:275,000.

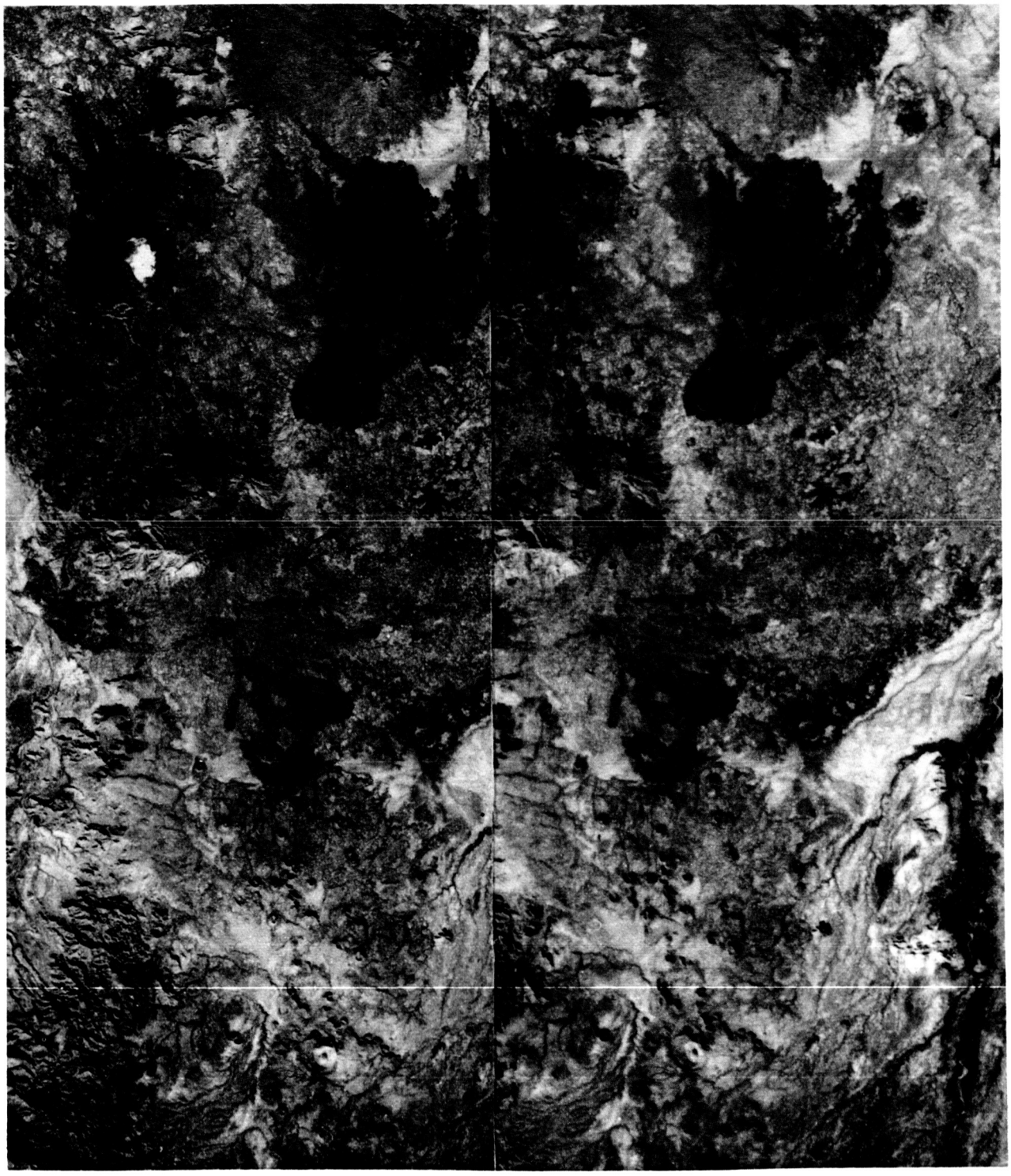
(b) Frame 4107, 2.7X, 1:275,000.

Figure 3-88.- Erta Ale volcanic complex, Ethiopia (stereo). The floor of the Afar depression is heavily marked with old and recent lava flows in this below-sea-level sump. Recorded orbit 65 (GMT 1134:57), altitude 226 km, type 3414 film. The LFC was operating in 70-percent forward O/L mode, giving a B/H ratio of 0.90. Original scale was 1:742,000.



(a) Frame 1328, 4X, 1:185,000. *(b) Frame 1330, 4X, 1:185,000.*

Figure 3-89.- Erta Ale volcanic complex, Ethiopia (stereo). A large caldera with collapsed rim is fringed with numerous vents and recent lava flow. Recorded orbit 65 (GMT 1134:57), altitude 226 km, type 3414 film. The LFC was operating in 70-percent forward O/L mode, giving a B/H ratio of 0.90. Original scale was 1:742,000.



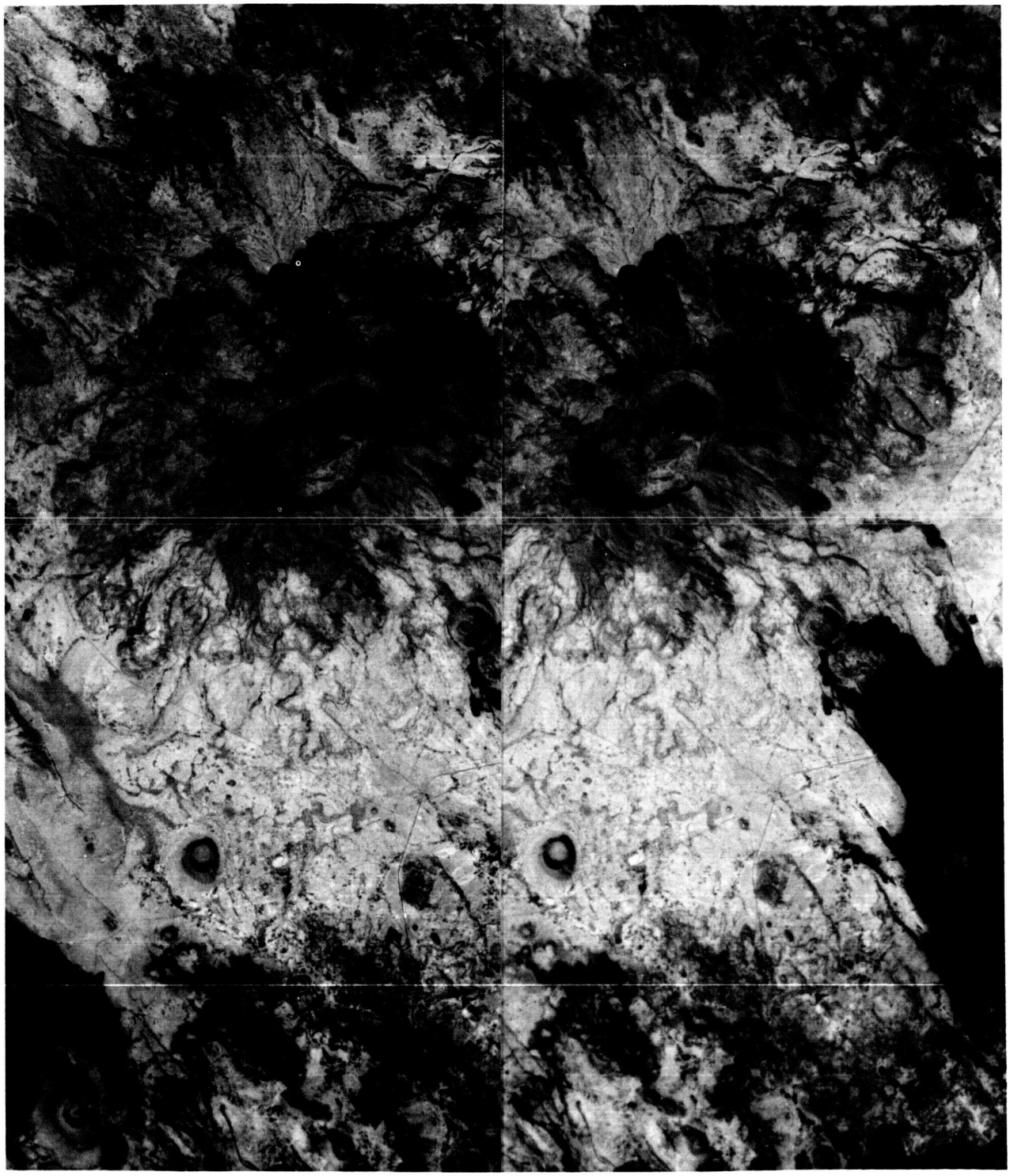
(a) Frame 0098, 4.5X, 1:260,000. *(b) Frame 0102, 4.5X, 1:260,000.*

Figure 3-90.- Volcanic vents, K'oboa, Ethiopia (stereo). A massive volcanic vent field within a heavily faulted plain, recorded orbit 2 (GMT 1312:33), altitude 356 km, type 3414 film. The LFC was operating in 80-percent forward O/L mode, giving a B/H ratio of 1.20. Original scale was 1:1,168,000.



(a) Frame 0101, 7.2X, 1:162,000. *(b) Frame 0103, 7.2X, 1:162,000.*

Figure 3-91.- Active volcano at Gewane, Ethiopia (stereo). Large caldera with old and recent lava flows, recorded orbit 2 (GMT 1313:01), altitude 356 km, type 3414 film. The LFC was operating in 80-percent forward O/L mode, giving a B/H ratio of 0.60. Original scale was 1:1,168,000.



(a) Frame 1871, 5X, 1:146,000. *(b) Frame 1872, 5X, 1:146,000.*

Figure 3-92.- Bola Selullse volcano, Ethiopia (stereo). Active volcano with a very large caldera; note included lake and numerous large vents. Recorded orbit 97 (GMT 1101:57), altitude 223 km, type 3414 film. LFC in 60-percent forward O/L mode, B/H ratio 0.60. Original scale 1:731.000.

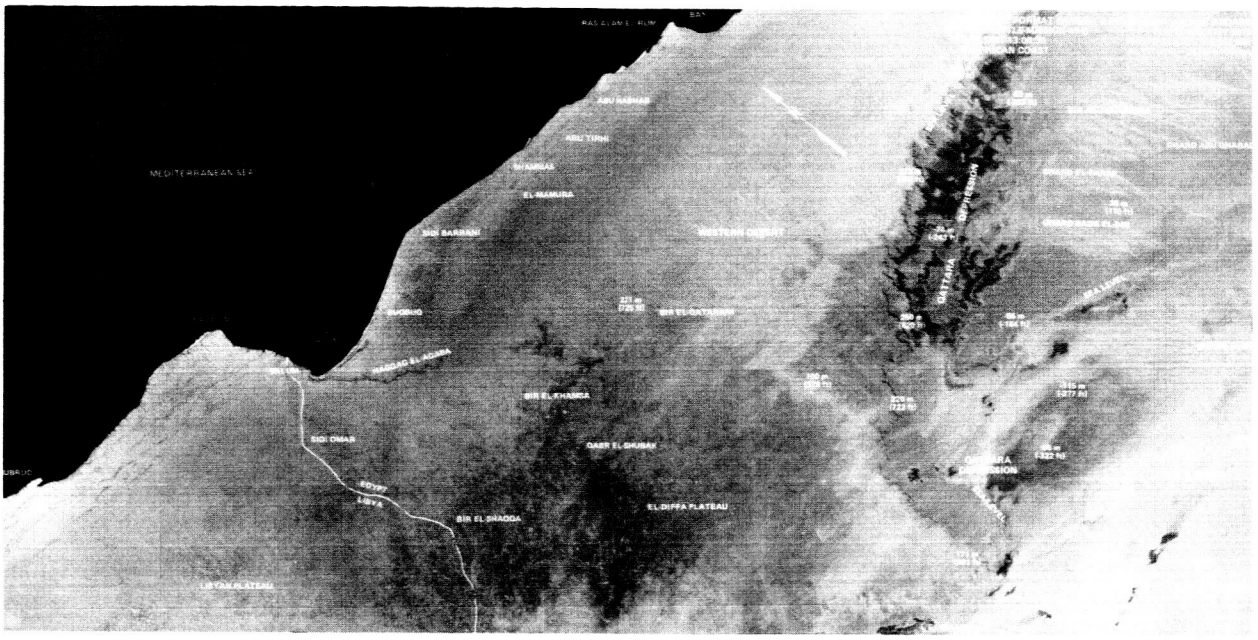


Figure 3-93.- Interface of the Mediterranean Sea and the African continent at the Libya and Egypt boundary. Photo shows the limited features of the vast sand seas in this region. LFC frame 0075, from altitude 359.56 km, orbit 2 (GMT 1306:35). Area covered is 145,400 sq km.

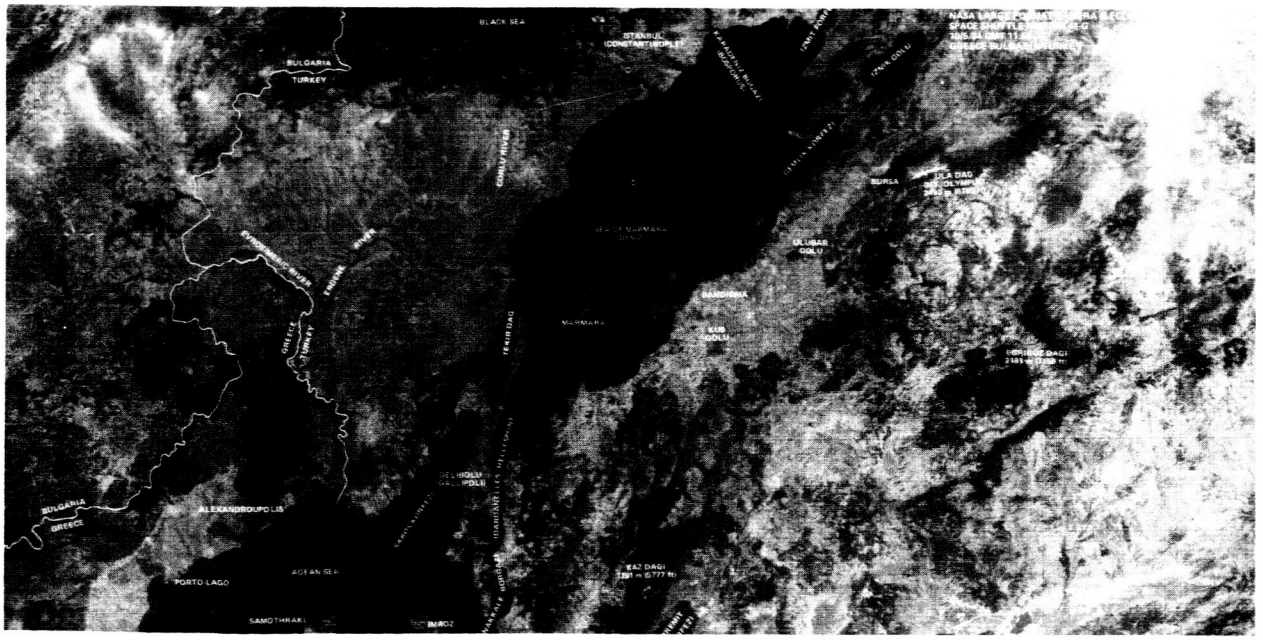


Figure 3-94.- The world of Homer, with historic waterways and other geographic landmarks which have had many names during recorded history. Photo depicts current boundaries of Greece, Bulgaria, and Turkey. LFC frame 0217, from altitude 362.91 km (GMT 1156:37), orbit 17. Area covered is 148,200 sq km.

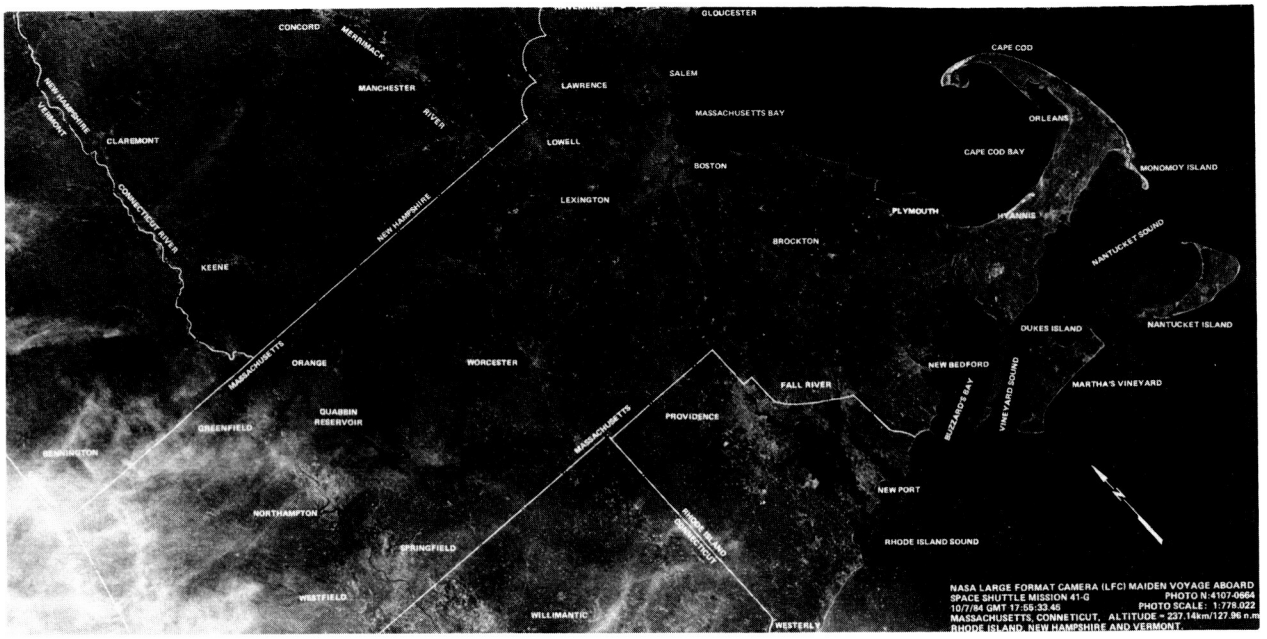


Figure 3-95.- The New England area. New Hampshire, Vermont, Rhode Island, Massachusetts, Connecticut, and a small part of New York (lower left under high, thin clouds) can be seen. LFC frame 0664, from altitude 231.26 km, orbit 37 (GMT 1755:33). Area covered is 60,100 sq km.

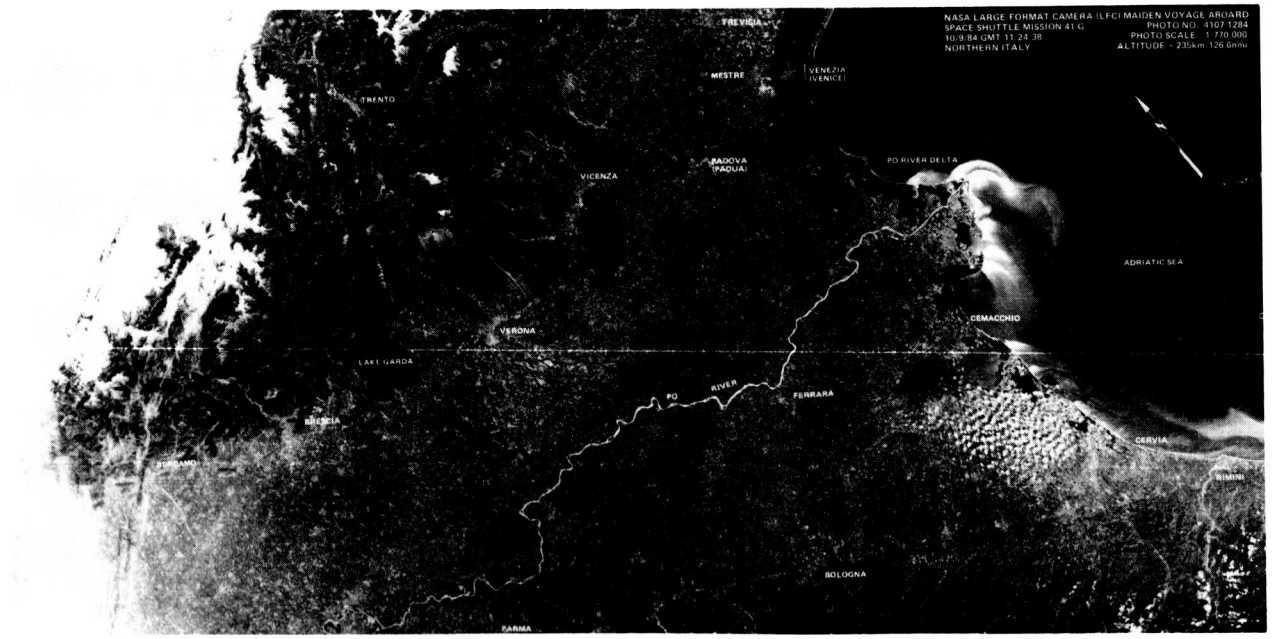


Figure 3-96.- The Po River Valley, northern Italy. Includes foothills of the Italian Alps (higher elevations and Switzerland are under heavy clouds, left) and Venice (upper center). Note striking display of sediment patterns at the Po River Delta as it empties into the Adriatic Sea. LFC frame 1284, from altitude 234.67 km, orbit 65 (GMT 1124.38). Area covered is 62,000 sq km.

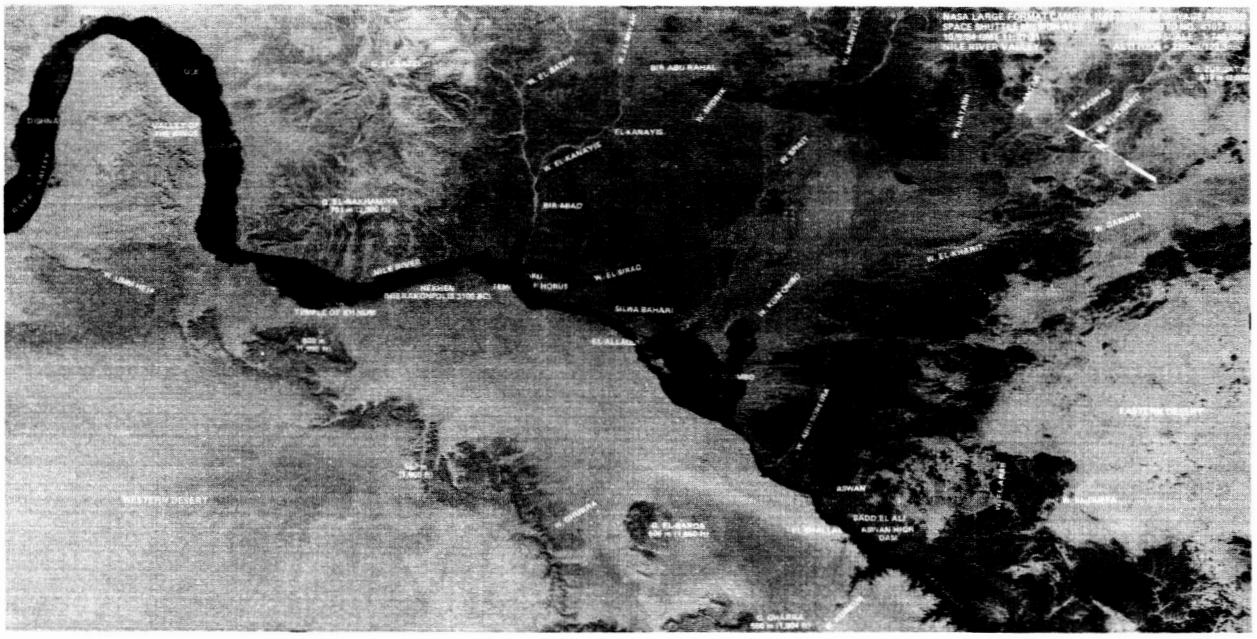


Figure 3-97.- The Nile River Valley. Having supported mankind for thousands of years, this fertile valley serves as a barrier to the western and eastern deserts. Note the Aswan Dams (high and low) and Lake Nasser at lower left. Frame 1314, from altitude of 228.45 km, orbit 65 (GMT 1131:11). Area covered is 58,700 sq km.

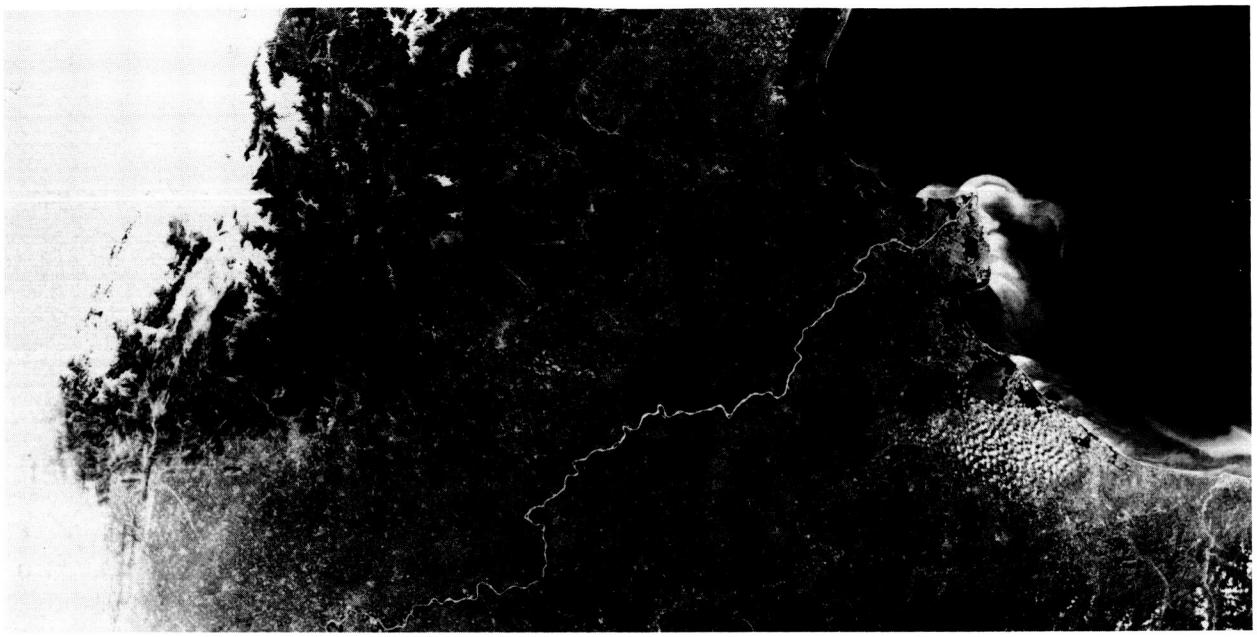


Figure 3-98.- The Po River Valley and Po River Delta, northern Italy. Silt and sediment enter the Adriatic Sea. Frame 1284, acquired orbit 65, (GMT 283:1124:38), altitude 234.67 km, type 3414 film, original scale 1:770,000 (shown at 1:2,199,000). Area covered is 27,500 sq km. Spacecraft nadir coordinates are 45.16° N 11.47° E.

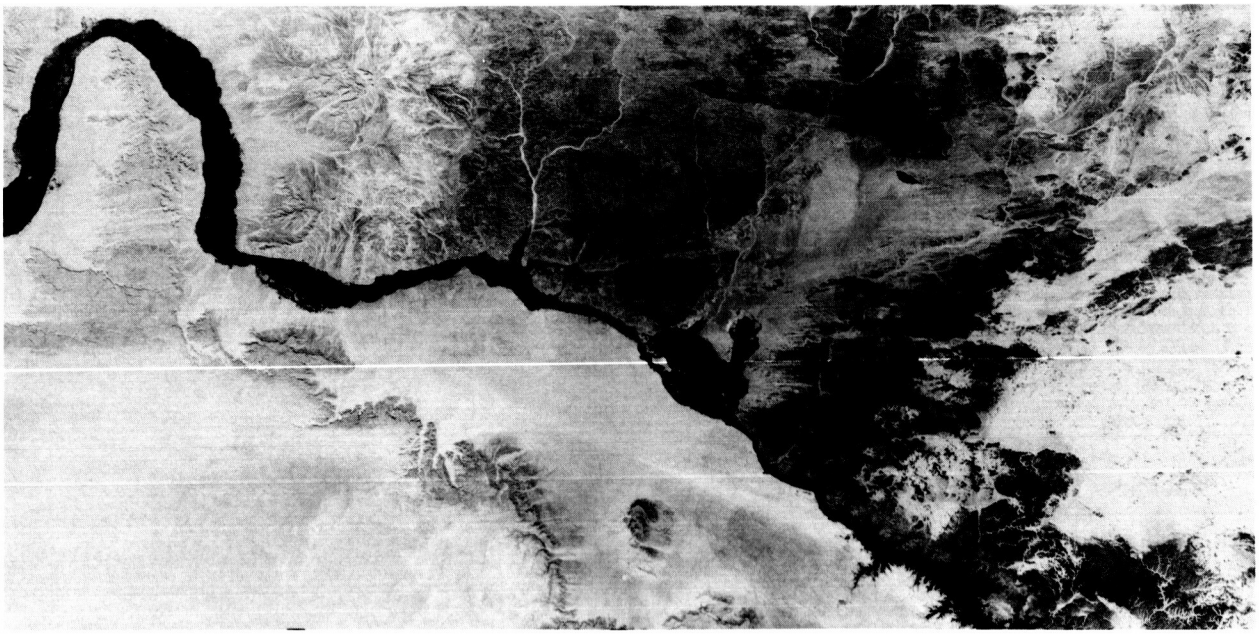
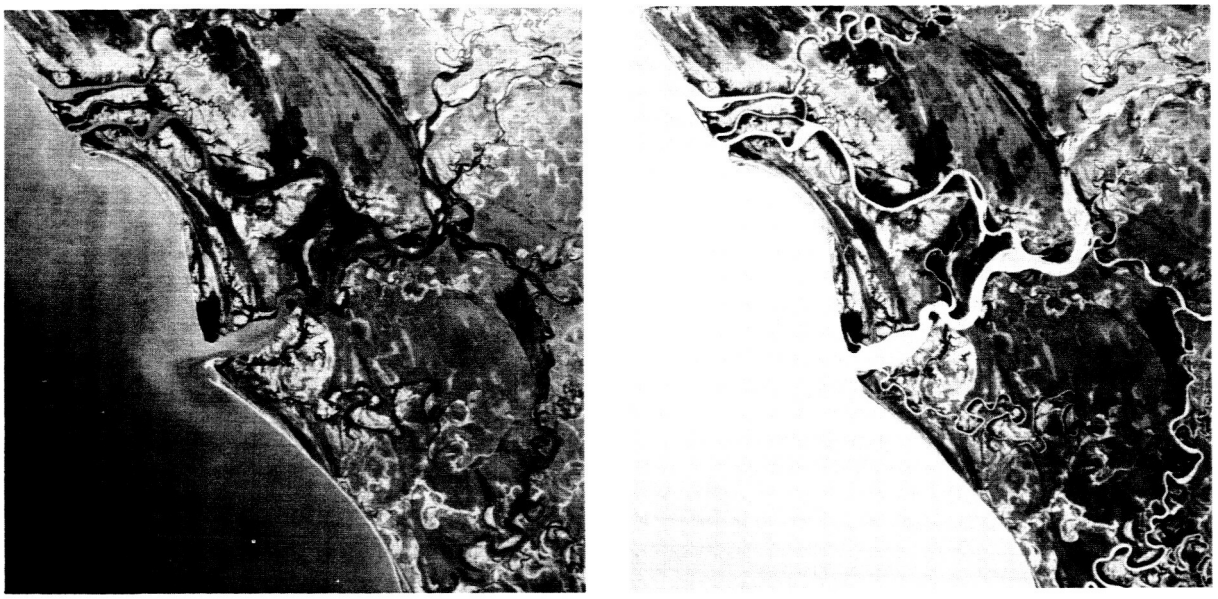


Figure 3-99.- The Nile River Valley, Aswan Dam, and a portion of Lake Nasser in Egypt. This area has relied on moisture and annual sediment deposits for thousands of years to support a major agricultural economy. Frame 1314, acquired orbit 65 (GMT 283:1131:31), altitude 228.45 km, type 3414 film, original scale 1:748,000 (shown at 1:2,141,000). Area covered is 26,100 sq km. Spacecraft nadir coordinates are 24.67° N 32.99° E.



(a) Frame 2129, 2X, 1:368,000. *(b) Frame 2130, 2X, 1:368,000.*

Figure 3-100.- Archer Bay on the Gulf of Carpentaria, Queensland, Australia. The two successive frames utilize sun glint to define the water level line of these estuaries in a remote area of the continent. LFC photography acquired orbit 125 (GMT 287:0437:26), altitude 224.32 km, type 3414 film. Original scale is 1:736,000. Spacecraft nadir coordinates are 14.55° S 141.89° E.

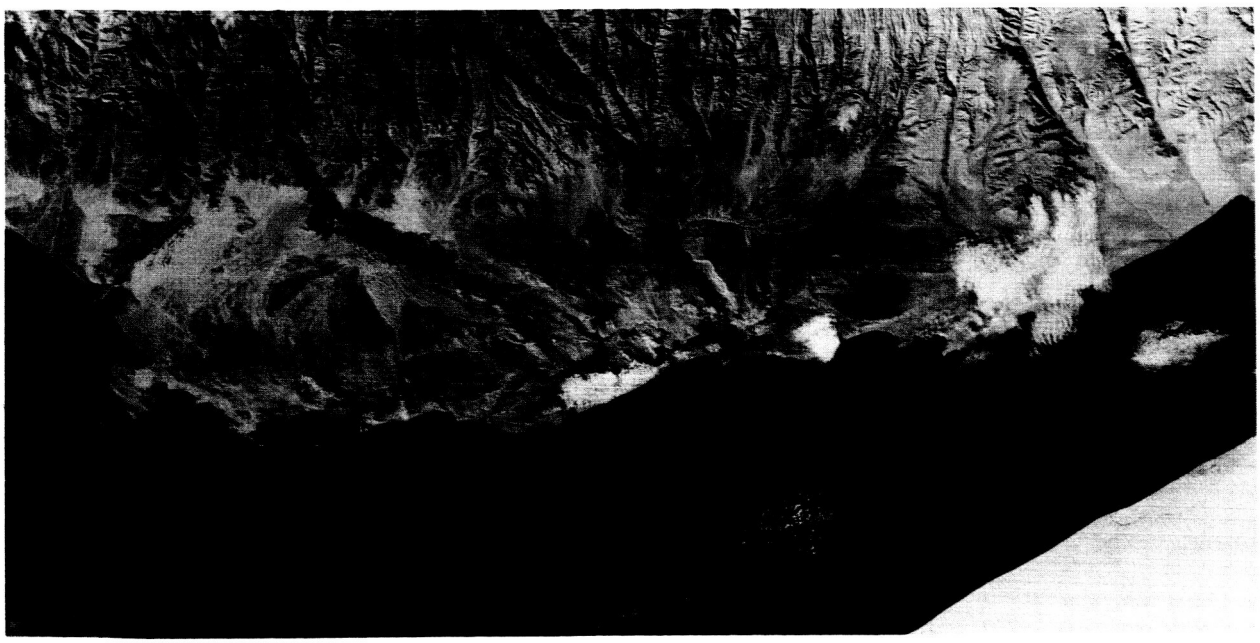
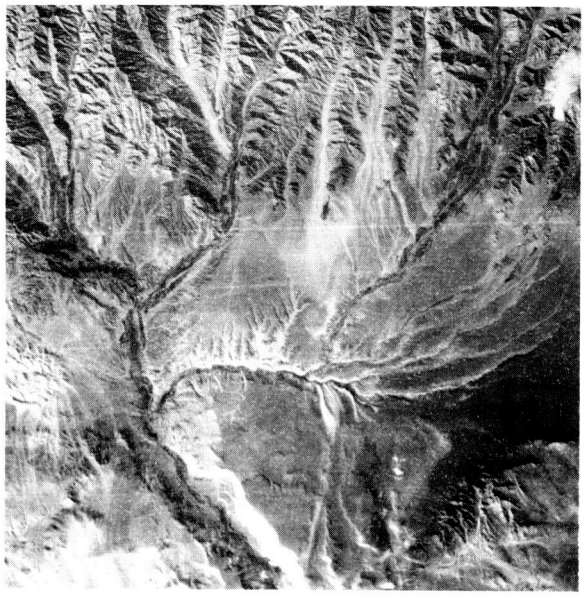
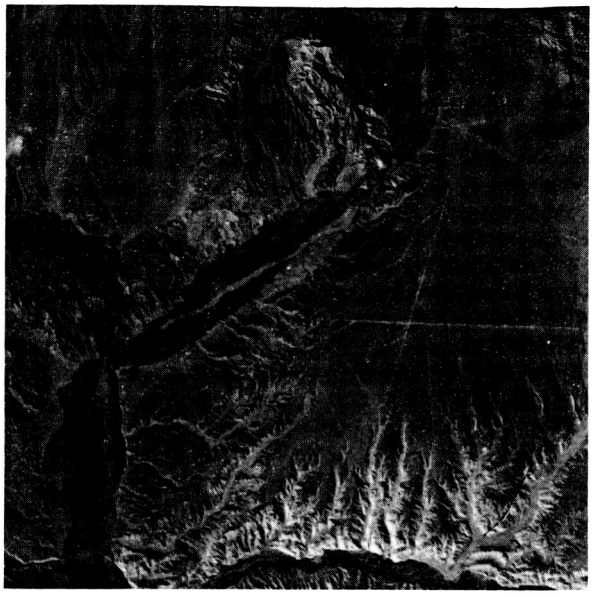


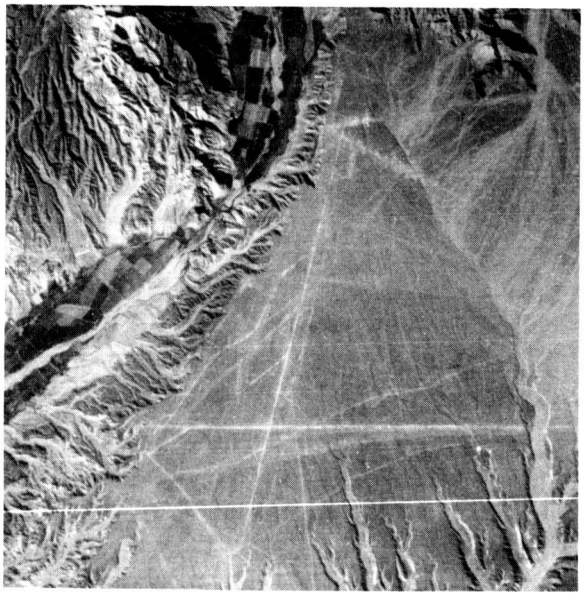
Figure 3-101.- The western coast of Peru. The Peruvian Andes mountains, Pisco, Ica, Palpa, Nazca, San Juan, Yauca, and Chaula can be seen, along with the Pampa da Huayuri, Sechura Desert, and the Nazca Lines. LFC frame 0768, from altitude 223.04 km (GMT 2110:47). Area within the photograph is 55,965 sq km.



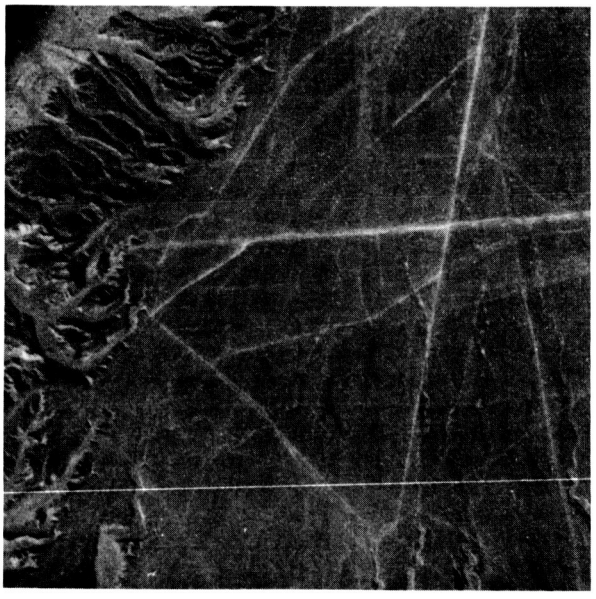
(a) Frame 0769, 1X.



(b) Frame 0769, 3X.



(c) Frame 0769, 4.5X.



(d) Frame 0769, 10X.

Figure 3-102.- Increasing magnification of the pampa floor, showing detail of the Nazca Lines.

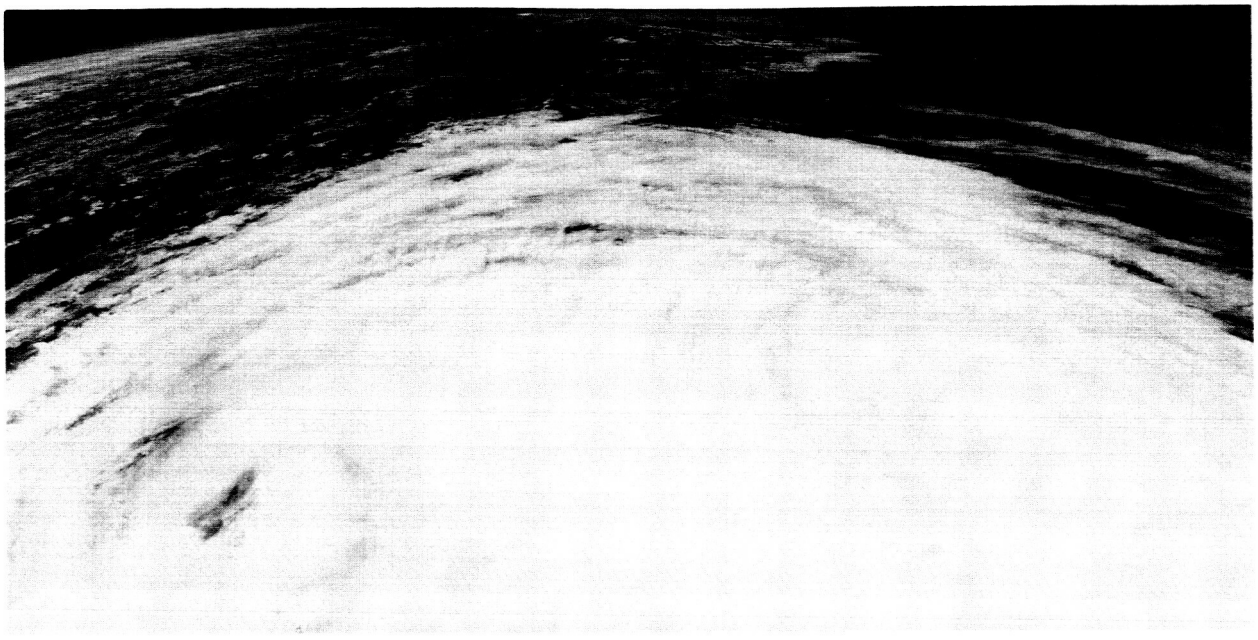


Figure 3-103.- Hurricane Josephine, photographed off the eastern U.S. coast. Spacecraft has left wing rolled up 55.73°, and line of site is to the southwest. In this instance, flight direction is from right to left. LFC frame 2030, acquired orbit 117 (GMT 286:1631:18), altitude 227.46 km, type 3414 film. Spacecraft nadir coordinates are 35.63° N 70.87° W.

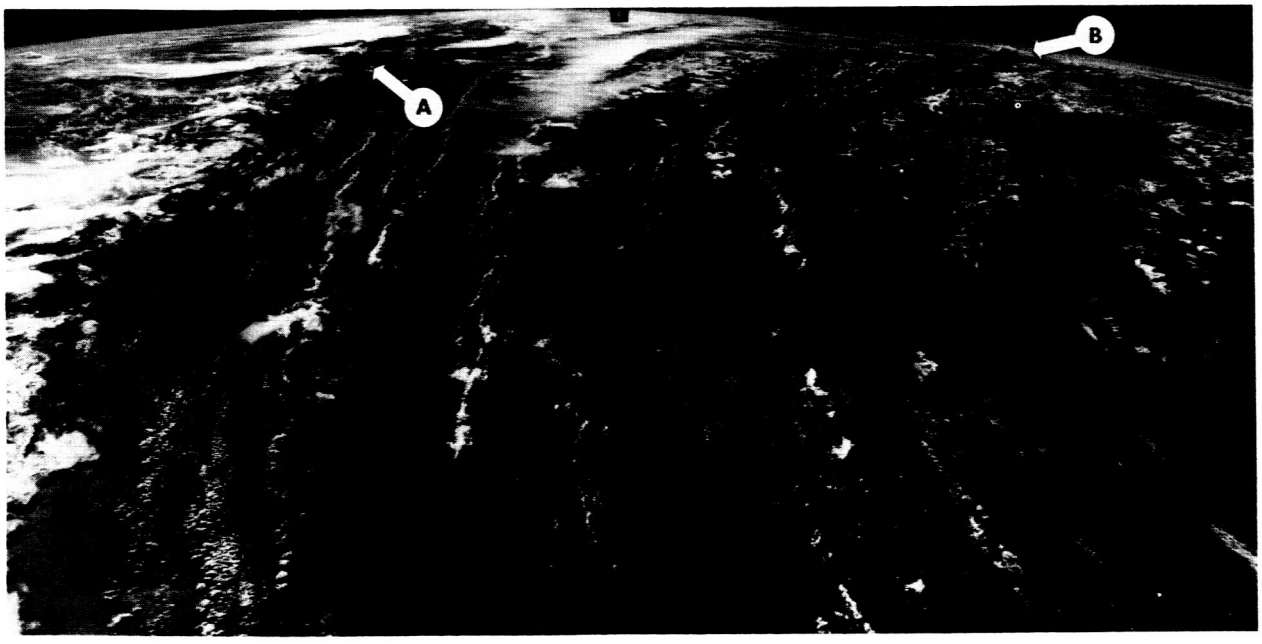
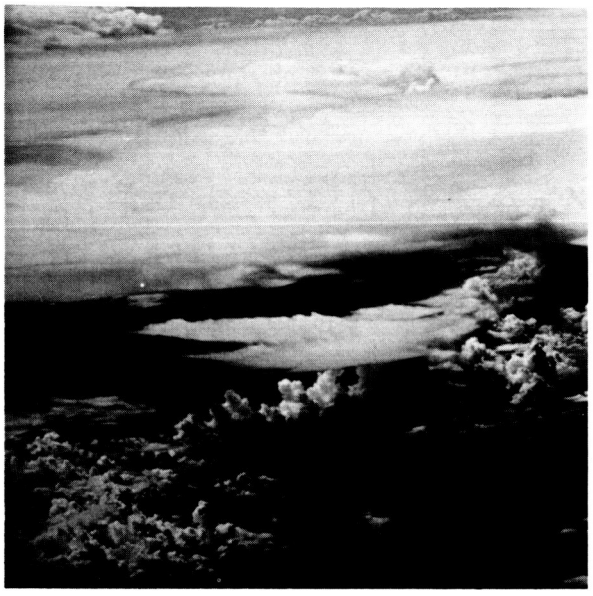


Figure 3-104.- Weather cells on the fringe of Hurricane Josephine. Photographed off the eastern U.S. coast. Spacecraft has left wing rolled up 55.26°, and line of site is to the southwest. In this instance, flight direction is from right to left. LFC frame 2036, orbit 117, altitude 226.17 km (GMT 286:1632:54), type 3414 film. Spacecraft nadir coordinates are 30.71° N 66.27° W.

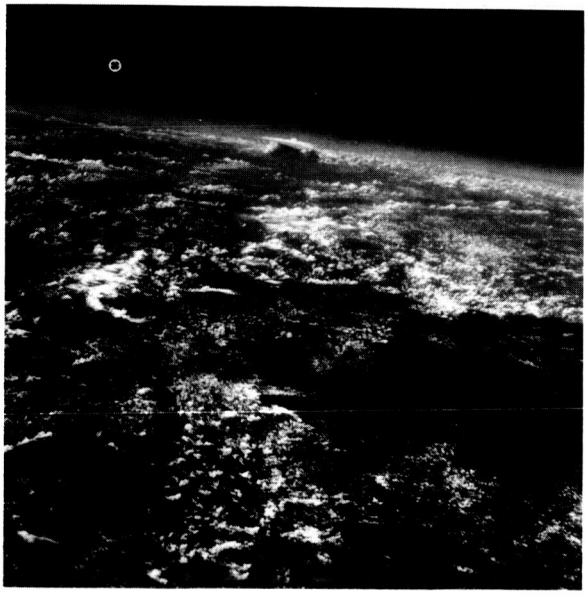


(a) Frame 2036, 1X, 1:3,077,000.



(b) Frame 2036, 4.5X, 1:684,000.

Figure 3-105.- Cloud A as photographed from a slant range of approximately 930 km during orbit 117. Crest of top anvil is at an altitude of approximately 15 to 16 km, with underlying major thunderhead extending from 0.8 to 9.0 km above the ocean surface. Anvil width is approximately 34 km (21 statute miles).



(a) Frame 2036, 1X, 1:4,864,000.



(b) Frame 2036, 4.5X, 1:1,081,000.

Figure 3-106.- Cloud B as photographed from a slant range of approximately 1,482 km during orbit 117. Anvil topknot is at an altitude of approximately 18 km, and anvil width is approximately 38 km (24 statute miles).

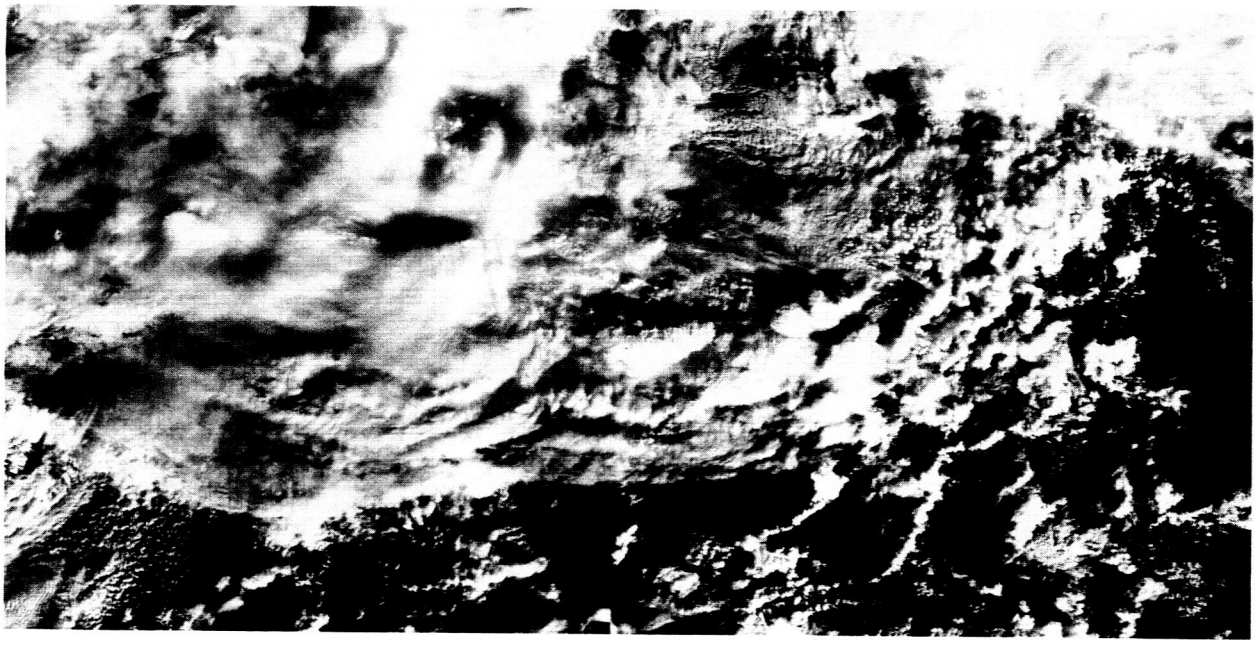


Figure 3-107.- Cloud formations over the Bering Sea at about the Near Islands of the Aleutians. Low sun elevation emphasizes both cloud structure and elevations. Frame 0302, acquired orbit 23 (GMT 280:2050:12), altitude 269.34 km, type 3414 film. Original scale 1:884,000 (shown at 1:2,526,000). Area covered is 36,300 sq km. Spacecraft nadir coordinates are 53.19° N 165.32° E.

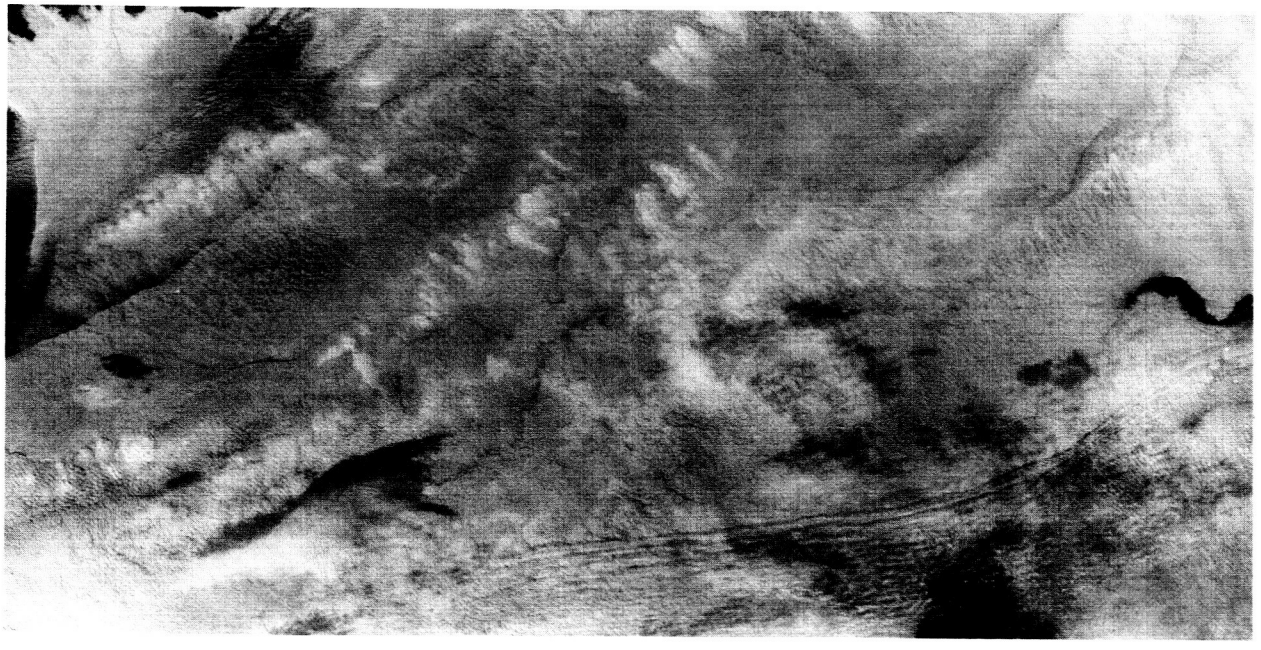


Figure 3-108.- Imagery acquired over the Pacific Ocean just off the coast of southern Peru. Complex frontal systems can be seen moving onshore. LFC frame 0773, orbit 39 (GMT 281:2111:31), altitude 223.49 km, type 3414 film. Original scale 1:733,000 (shown at 1:2,095,000). Area covered is 25,000 sq km, Spacecraft nadir coordinates are 17.21° S 73.96° W.

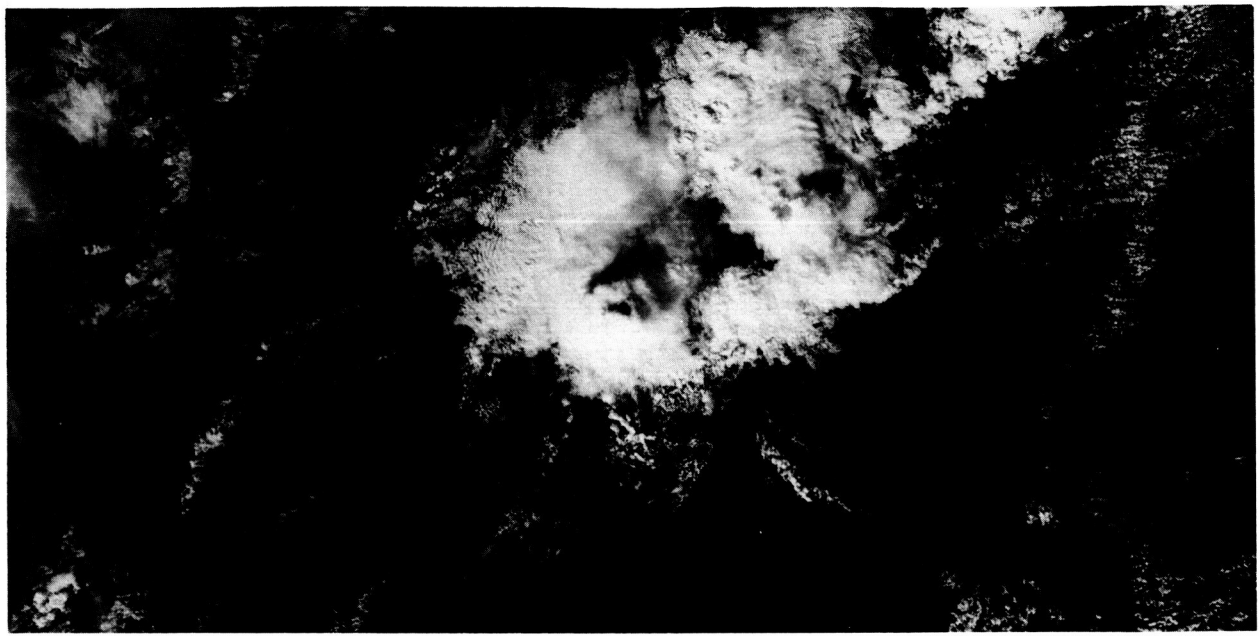


Figure 3-109.- A tropical disturbance developing in the area of the Sawu Sea. Frame 0872, acquired orbit 46 (GMT 282:0731), altitude 222.49 km, on type 3414 film. Original scale 1:730,000 (shown at 1:2,085,000). Area covered is 24,700 sq km. Spacecraft nadir coordinates are 9.41° S 123.12° E.

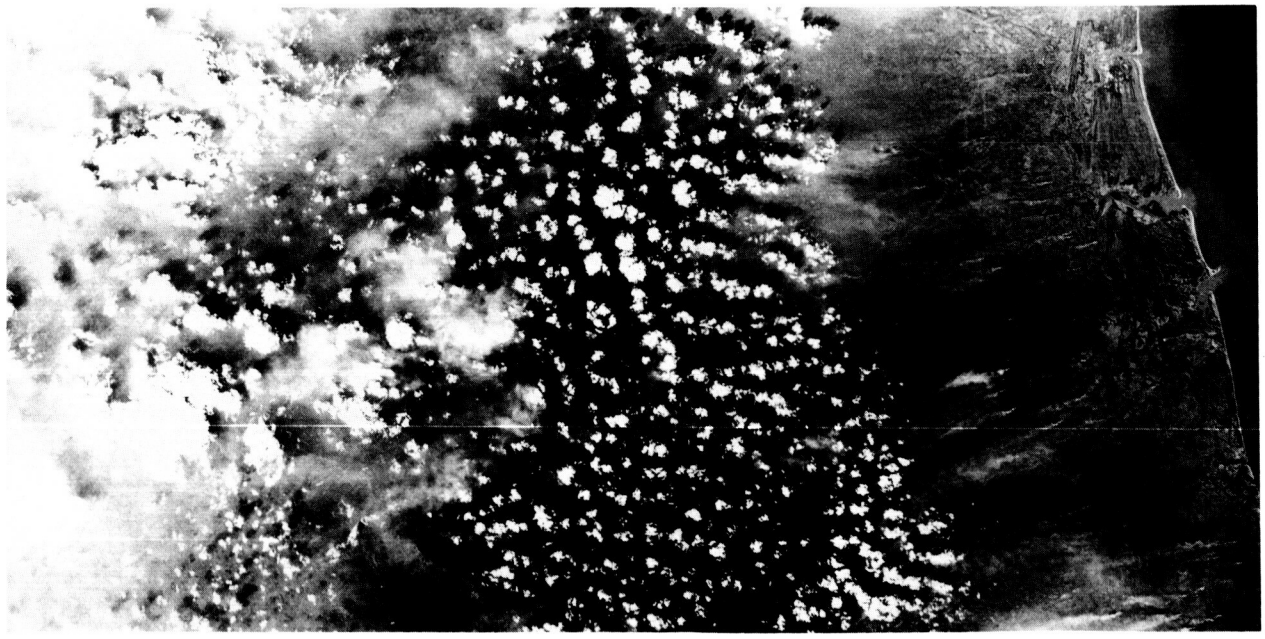
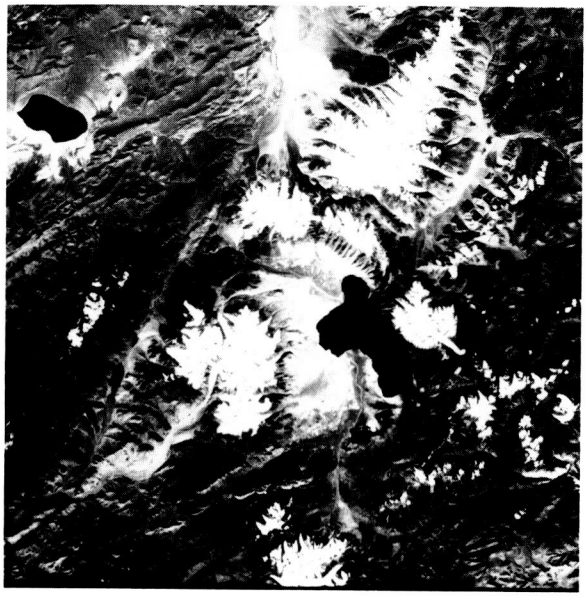


Figure 3-110.- Major thunderstorms in the making over the southeastern coast of Africa at Quelimane, Mozambique. Smoke plumes from burning fields indicate the direction of strong winds offshore, where ocean moisture forms clouds which increase in size and severity as they move inland. Frame 1429, orbit 66 (GMT 283:1312), altitude 226.57 km, type 3414 film. Original scale 1:743,000 (shown at 1:2,124,000). Area covered is 25,700 sq km. Spacecraft nadir coordinates are 17.18° S 36.02° E.



Figure 3-111.- Glaciers and Paleolithic lakes in the Tibetan Plateau. Frame 0164, recorded orbit 15 (GMT 280:0855:07), altitude 361.83 km, type 3414 film. Original scale was 1:1,187,000 (shown at 1:3,391,000). Area covered is 147,000 sq km. Spacecraft nadir coordinates are 35.86° N 79.33° E.



(a) Frame 0164, 1X, 1:1,187,000.



(b) Frame 0164, 3X, 1:396,000.



(c) Frame 0164, 4.5X, 1:264,000.



(d) Frame 0164, 10X, 1:118,700.

Figure 3-112.- Paleolithic lake in the Tibetan Plateau. This imagery reveals some of the lake's former grandeur through its terraces formed by progressive dropping and freezing of its levels over thousands of years. LFC photography acquired orbit 15 (GMT 280:0855:22), altitude 361.65 km, type 3414 film. Original scale 1:1,187,000. Spacecraft nadir coordinates are 35.13° N 80.07° E.



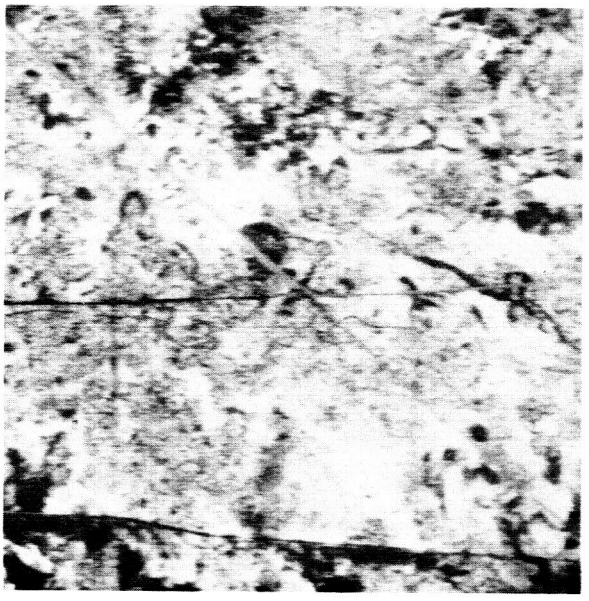
(a) Frame 0163, 10X, 1:118,000. *(b) Frame 0166, 10X, 1:118,000.*

Figure 3-113.- Karatax Shan glaciers in Tibet (stereo). Rising 23,890 ft above the plateau, glaciers on the southeastern slopes of Karatax Shan demonstrate the Paleolithic past of these massive ice rivers. Recorded orbit 15 (GMT 0855:37) from altitude 361 km, on type 3414 film. LFC was operating in 80-percent forward O/L mode, giving a B/H ratio of 0.90. Original scale was 1:1,185,000.



(a) Frame 0163, 2.5X, 1:474,000. *(b) Frame 0167, 2.5X, 1:474,000.*

Figure 3-114.- Glacial basins in Pamzal area, China (stereo). Northwest of Mt. Everest in the Tibetan Plateau are a number of glaciers and landlocked glacial lakes. Recorded orbit 15 (GMT 0855:37) from altitude 361 km, on type 3414 film. The LFC was operating in 80-percent forward O/L mode, giving a B/H ratio of 1.20. Original scale was 1:1,185,000.



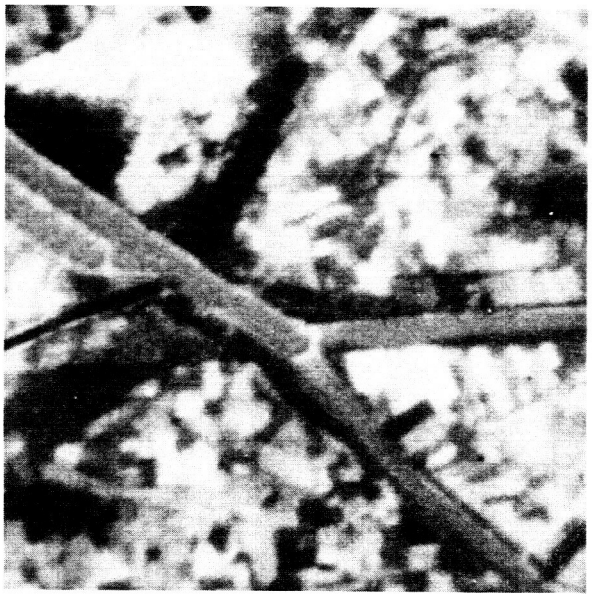
(a) Frame 0543, 4.5X, 1:191,000.



(b) Frame 0544, 4.5X, 1:191,000.

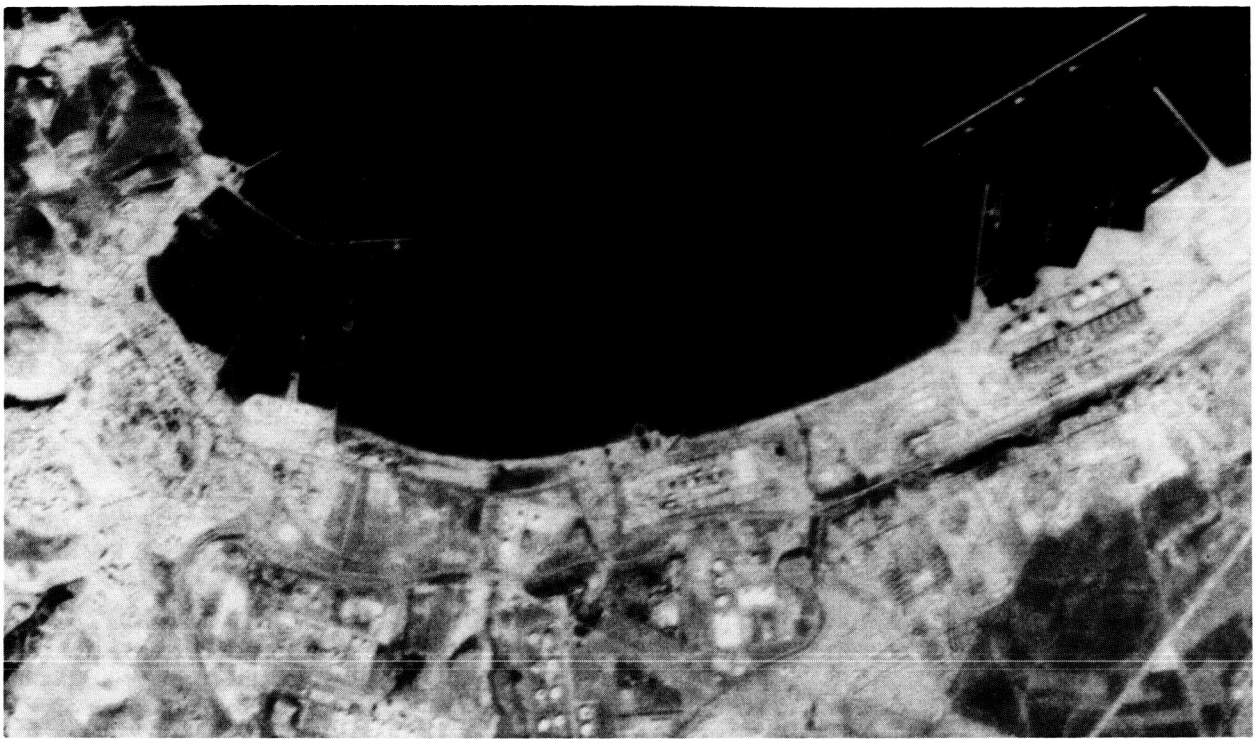


(c) Frame 0543, 35X, 1:24,600.

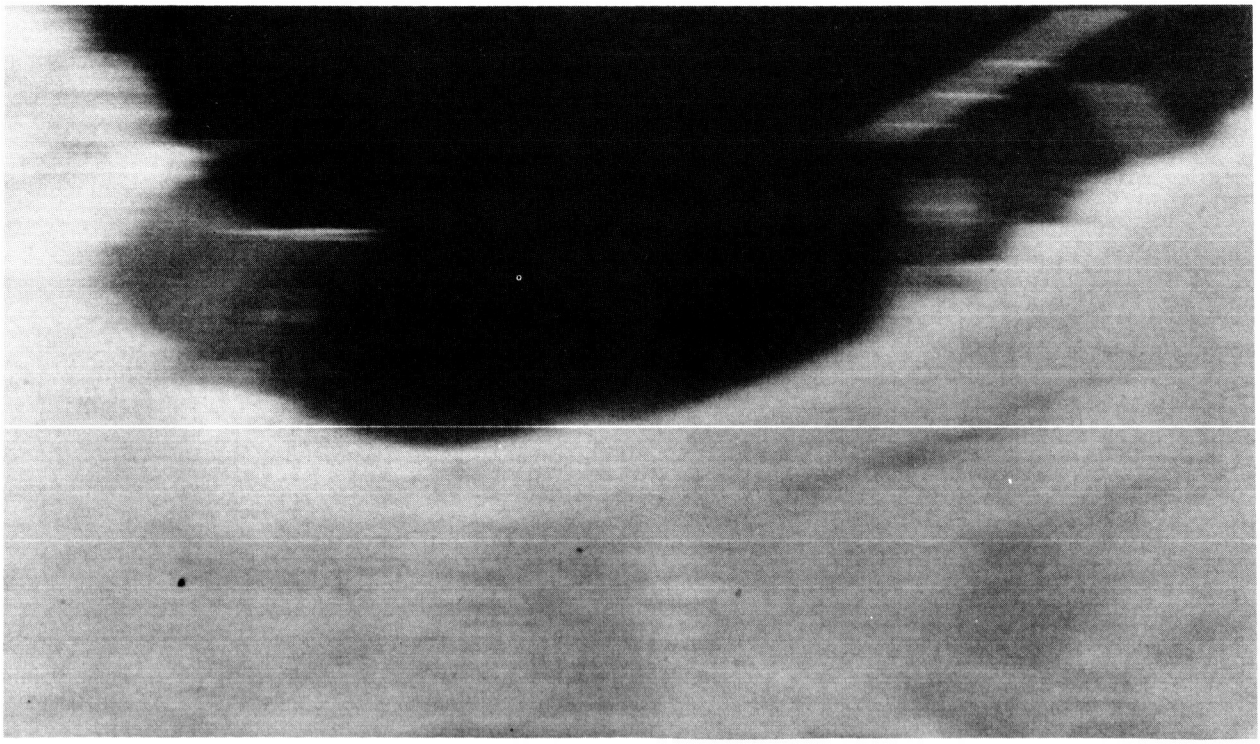


(d) Frame 0544, 35X, 1:24,600.

Figure 3-115.- Smeared and normal LFC imagery. Smeared imagery (a and c) due to inhibited FMC delay command at 23.5 msec exposure, and normal imagery (b and d) with the FMC delay command issued, also at 23.5 msec command. The area photographed is the Ganges River plain near Budaun, Uttar, in northern India, and the spacecraft altitude is 262.6 km.



(a) Frame 0123, 21X, 1:56,000.



(b) Frame 0124, 21X, 1:56,000.

Figure 3-116.- AEC mode acquisitions. Imagery shows the Mediterranean Sea, the Golfo d'Arzew, and Port aux Poules, Algeria. The altitude was 361.3 km, and the original scale was 1:1,185,000.

4. FILM SENSITOMETRY

Section 4 contains the film sensitometry data compiled by the flight film processing laboratory (Precision Photo Laboratory, Dayton, Ohio). It is presented in raw data form for reference of data users and future mission planning groups. The data has been organized into two categories, as follows:

1. Premission/postmission film sensitometry for all earth-viewing flight films: This information is included in table 4-1. The definitions listed below apply to the data in this table.

   - Freezer: Exposed premission (stored at Precision Photo Laboratory)
     Exposed postmission (stock stored at Precision Photo Laboratory)
   - Tube: Exposed premission (flown on STS 41-G)
     Exposed postmission (stock flown on STS 41-G)
   - Ambient: Exposed premission (stored at Precision Photo Laboratory)
     Exposed postmission (stock stored at Precision Photo Laboratory)
   - Control: Exposed postmission (stock stored at Precision Photo Laboratory)

   Within each film type, the emulsion numbers for all films are identical.

2. Flight film processing sensitometry: This information is included in table 4-2. The definitions listed below apply to the data in this table.

   - Head of Roll: End of roll first entering the film processing unit.
   - Tail of Roll: End of roll last out of the film processing unit.

Actual sensitometry measurements and resulting curves are stored in the system documentation files with the LFC.

TABLE 4-1.- LFC FILM SENSITOMETRY DATA SUMMARY, STS 41-G[a]

(a) B&W Film

Film type	Sample identification		Aerial film speed	D-max	Gamma	Base plus fog
3412	Freezer:	Pre	31.00	2.72	1.37	0.23
		Post	31.70	2.70	1.33	0.23
	Tube:	Pre	27.62	2.81	1.57	0.23
		Post	31.71	2.68	1.29	0.22
	Ambient:	Pre	26.36	2.83	1.54	0.24
		Post	30.30	2.72	1.40	0.23
	Control:	Post	28.90	2.63	1.33	0.22
3414	Freezer:	Pre	6.90	2.70	2.01	0.12
		Post	7.75	2.72	1.77	0.12
	Tube:	Pre	6.75	2.68	1.92	0.12
		Post	7.57	2.71	1.87	0.12
	Ambient:	Pre	6.75	2.70	1.97	0.13
		Post	7.93	2.72	1.87	0.13
	Control:	Post	7.23	2.69	1.87	0.13

[a] All sensitometry samples were processed along with appropriate flight film rolls.

TABLE 4-1.- LFC FILM SENSITOMETRY DATA SUMMARY, STS 41-G

(b) Color Film

Film type	Sample identification		D-max			Base plus fog		
			Red	Green	Blue	Red	Green	Blue
SO-131	Freezer:	Pre	3.07	3.37	2.52	0.10	0.12	0.13
		Post	3.14	3.36	2.52	0.10	0.12	0.13
	Tube:	Pre	3.07	3.34	2.48	0.11	0.12	0.14
		Post	3.09	3.36	2.46	0.10	0.13	0.14
	Ambient:	Pre	3.11	3.35	2.46	0.11	0.13	0.14
		Post	3.15	3.37	2.47	0.10	0.13	0.14
	Control:	Post	3.13	3.35	2.45	0.10	0.13	0.14
SO-242	Freezer:	Pre	2.96	2.98	2.57	0.07	0.12	0.13
		Post	2.95	2.94	2.57	0.07	0.12	0.13
	Tube:	Pre	2.99	3.00	2.52	0.07	0.12	0.13
		Post	2.99	2.94	2.49	0.07	0.12	0.13
	Ambient:	Pre	3.02	3.00	2.50	0.07	0.12	0.13
		Post	2.99	2.94	2.51	0.07	0.12	0.13
	Control:	Post	3.00	2.93	2.46	0.07	0.12	0.14

[a] All sensitometry samples were processed along with appropriate flight film rolls.

TABLE 4-2.- LFC FLIGHT FILM PROCESSING
SENSITOMETRY, STS 41-G

Flight roll no.	Processor roll no. (a)	Sensitometry	
		Head of roll	Tail of roll
1	10	Yes	Yes
2[b]	-	No	No
3	8	Yes	Yes
4	7	Yes	Yes
5	6	Yes	Yes
6	5	Yes	Yes
7	4	Yes	Yes
8[c]	-	No	No
9[b]	-	No	No
10	1	Yes	Yes

[a] During master roll breakup at Precision Photo Laboratory, the last section off the flight spool was first into the film processor.

[b] Film was processed at another laboratory for high gamma/ high D-max, since this was nighttime photography (geodesy and stars). Sensitometry curves are not included.

[c] Film was processed at another laboratory to produce dual gamma, low D-max, and higher aerial film speed. Three candidate aim curves are included.

5. LFC BIBLIOGRAPHY AND APPLICABLE DOCUMENTATION

5.1 LFC BIBLIOGRAPHY

Cox, W. J.; Gilligan, P.; and Garney, G.: Geological Analysis of the Durack Range, Western Australia, with LFC Photography. Proceedings of the American Society of Photogrammetry and Remote Sensing, Vol. II, Mar 1987.

Cox, W. J. and Lucas, C.: Spatial and Digital Correlation of Multisensor Data Using the NASA Large Format Camera. Proceedings of Pecora XI Symposium (USGS EROS Data Center, Sioux Falls, S. Dak.), May 1987.

Doyle, F. J.: A Large Format Camera for the Space Shuttle. Photogrammetric Engineering, Vol. 45, 1979, pp. 73-78.

Doyle, F. J.: Film Cameras for Earth Observation From Space. Archives of XV International Congress of Photogrammetry and Remote Sensing, Volumes for Commissions I & IV, Rio de Janeiro, International Society of Photogrammetry, U.S. Geological Survey, Reston, Va., Jun 1984 (in publication).

Federal Mapping Task Force on Mapping, Charting, Geodesy and Surveying. Report to the Office of Management and Budget. Jul 1973, GPO Stock No. 2401-02426.

Fritz, L. W.: Analytical Instruments to Derive Metric Data From the Large Format Camera. Archives of XV International Congress of Photogrammetry and Remote Sensing, Volumes for Commissions I and IV. Rio de Janeiro, International Society of Photogrammetry, U.S. Geological Survey, Reston, Va., Jun 1984 (in publication).

Fritz, L. W. and Malhotra, R. C.: Block Aerotriangulation Capabilities of Large Format Camera Photography. Proceedings of the International Society of Photogrammetry and Remote Sensing, Leipzig, Germany, Sep 4-6, 1987.

Greer, J. D.: An Analysis of Space Shuttle Large Format Camera Coverage of National Forests in the United States. Engineering Field Notes, Vol. 19, Jul-Aug. 1987, pp. 21-35. USDA Forest Service, Washington, D.C.

Greer, J. D.: Can Resource Managers Use Large Format Camera Space Photography in Resource Management? USDA NFAP Occasional Electronic Paper No. 103, Nov 1987, USDA Forest Service, Salt Lake City, Utah.

Greer, J. D.: A Preliminary Report on Imagery Acquired With the Large Format Camera by the Space Shuttle Challenger in October, 1984. USDA NFAP Occasional Electronic Paper No. 102, Apr 1987, USDA Forest Service, Salt Lake City, Utah.

Greer, J. D.: A Review of Space Shuttle Large Format Camera Coverage of Areas in Western China. Remote Sensing of the Environment, 1988 (in Chinese). Illustrated with photographs, drawings, and map. Beijing, Peoples Republic of China.

Greer, J. D.: Shuttle Large Format Camera Cloud Cover Interference Diagrams. Engineering Management Series EM-7140-17, Jul 1988, illustrated. USDA Forest Service Engineering Staff, Washington, D.C.

Greer, J. D.: Space Shuttle Large Format Camera Photography and Resource Management. Proceedings of SPIE - The International Society for Optical Engineering, Airborne Reconnaissance XI, San Diego, Calif., Aug 17-18, 1987.

Greer, J. D.: Space Shuttle Large Format Camera Photography in Resource Management. Engineering Field Notes, Vol. 20, May-Jun 1988, pp. 15-26. Illustrated with photographs. Engineering Technical Information System, USDA Forest Service Engineering Staff, Washington D.C.

Heric, M.: Land Use/Cover Classification of Cairns, Queensland, Australia: A Multispectral Study Involving the Conjunctive Use of the Large Format Camera and the Airborne Imaging Spectrometer. Thesis, University of South Carolina, Columbia, S.C., 1987, and Proceedings of the American Society of Photogrammetry and Remote Sensing, Mar 1987.

Heric, M.; Cox, W. J.; and Gordon, D. K.: Land Cover/Use Classification of Cairns, Queensland, Australia: A Remote Sensing Study Involving Conjunctive Use of the Airborne Imaging Spectrometer, the Large Format Camera, and the Thematic Mapper Simulator. Third Annual Airborne Proceedings, Dr. Gregg Vane, ed. (Jet Propulsion Laboratory, Pasadena, Calif.), Jun 1987.

Hughes, J. G.; Gallagher, J. J.; and Scully-Power, P.: Navy Oceanographer Shuttle Observations. STS 41-G Data Catalog. NUSC TD 7609, Mar 26, 1986, Naval Underwater Systems Center, New London, Conn.

Light, D. L. et al.: Satellite Photogrammetry, Manual of Photogrammetry, 4th ed. American Society of Photogrammetry and Remote Sensing, Falls Church, Va., 1980, pp. 883-977.

Lucas, C.: The Large Format Camera: Novel Analyses of Sensor Applications, Final Report to NASA Marshall Space Flight Center Ala., Aug 12, 1985.

Lucas, C.; Pearson, J.; and Biache, A.: Commercialization of the Large Format Camera. Proceedings of the American Society of Photogrammetry and Remote Sensing, Vol. 4, Mar 16-21, 1986.

Malhotra, R. C.: Potentials of Large Format Camera Photography. Proceedings of the American Society of Photogrammetry and Remote Sensing, Mar 16-23, 1986.

Merkel, R. J.; Salmon, J. J.; and Sims, B. A.: Mission Ephemeris for the Maiden Voyage of the Large Format Camera Aboard the STS 41-G. JSC-20383, Apr 1985.

Mollberg, B. H.: Proposal for the Orbiter Camera Payload System. Nov 29, 1976, NASA Internal Document.

Mollberg, B. H.: Data Management Plan for the Orbiter Camera Payload System (OCPS). JSC-14916, May 18, 1979.

Mollberg, B. H.: Performance Characteristics of the Orbiter Camera Payload System's Large Format Camera (LFC). Proceedings of the Society of Photo-Optical Instrumentation Engineers, Vol. 278, 1981, pp. 66-72.

Mollberg, B. H.: Orbiter Camera Payload System and the Large Format Camera. Proceedings of XIV International Congress of Photogrammetry and Remote Sensing, Volume Commission I, Hamburg, FRG, International Society of Photogrammetry, U.S. Geological Survey, Reston, Va., Jun 1980.

Mollberg, B. H.: Large Format Camera Interagency Working Group Co-Investigator Target Summary. JSC-19975, Jun 1, 1984.

Mollberg, B. H. and Schardt, B. B.: The Orbiter Camera Payload System's Large Format Camera and Attitude Reference System. Progress in Astronautics and Aeronautics, Monitoring Earth's Ocean, Land, and Atmosphere from Space - Sensors, Systems, and Applications, Vol. 97. American Institute of Aeronautics and Astronautics, Inc., 1985, pp. 684-709.

Newton, L. and Derenyi, E.: Control Extension Utilizing Large Format Camera Imagery. Proceedings of the American Society of Photogrammetry and Remote Sensing, Mar 16-23, 1986.

Norton, C. L.; Mollberg, B. H.; and Schroeder, M.: The MC and LFC Cameras, Progress in Imaging Sensors. Proceedings of Commission I of the International Society of Photogrammetry and Remote Sensing Symposium. Stuttgart, FRG, Sep 1-5, 1986, pp. 601-605.

Ondrejka, R. J. and El-Baz, F.: Earth Photography by the Large Format Camera. Proceedings of 12th International Symposium of Remote Sensing of Earth, Manila, the Philippines. ERIM, Univ. of Michigan, Ann Arbor, Mich., Apr 1978, Vol. I, pp. 702-718.

Ondrejka, R. J.: Earth Orbital Photography With the Large Format Camera. Proceedings of Technical Exchange Week, Panama City, Panama. Defense Mapping Agency, Washington, D.C., May 1979, pp. 93-107.

Ondrejka, R. J. and Wood, G. A.: Snapshots From a Window of the World. Optical Spectra, Vol. 14, Issue 12, Dec 1980, pp. 53-56.

Ondrejka, R. J.: Cartographic and Thematic Mapping Potential and Procedures for the Large Format Camera. Archives of XV International Congress of Photogrammetry and Remote Sensing, Volume for Commission I, Rio de Janeiro, International Society of Photogrammetry and Remote Sensing. U.S. Geological Survey, Reston, Va., June 1984.

OSTA-3 Experiments. JSC-19942, NASA/Johnson Space Center, Aug 1984.
Proceedings of a Joint DFVLR-ESA Metric Camera Workshop. Guyenne, T. D. and Hunt, J. J., editors. Oberpfaffenhofen, Germany, Feb 11-13, 1985, ESA SP-209.

Remote Sensing of the Earth From Space: A Program in Crisis. Space Applications Board, National Research Council. Washington, D.C.: National Academy Press, 1985.

Schroeder, M.: The Metric Camera Experiment on the First Spacelab Flight. Acta Astronautics, Vol. 11, No. 1, pp. 73-80, 1984.

Schroeder, M.: Flight Performance of the Spacelab Metric Camera Experiment. Proceedings of IGARSS '84 Symposium, Strasbourg, Aug 27-30, 1984. (Ref. ESA SP-215)

Schroeder, M.: Spacelab Metric Camera Experiments. IAF Congress, Lausanne, Switzerland, Oct 1984.

Scully-Power, P.: Navy Oceanographer Shuttle Observations STS 41-G. NUSC TD 7611, Mar 26, 1986, Naval Underwater Systems Center, New London, Conn.

Short, N. M. and Blair, R. W., Jr.: Geomorphology From Space, A Global Overview of Regional Landforms. NASA SP-486, 1986.

Slater, P. N. et al.: Photographic Systems for Remote Sensing. Manual of Remote Sensing, 2nd ed. American Society of Photogrammetry and Remote Sensing, Falls Church, Va., 1983, pp. 231-291.

Snow, J. W. and Tomilson, E. M.: Cloud Population Measurements Using Photographs Taken From the Space Shuttle. Sixth Symposium on Meteorological Observations and Instrumentation, New Orleans, La., Jan 12-15, 1987.

Taranik, J. V.: Advanced Aerospace Remote Sensing Systems for Global Resource Applications. Proceedings of XV International Symposium on Remote Sensing of the Environment. ERIM, Univ. of Michigan, Ann Arbor, Mich., May 1981.

Togliatti, G. and Moriondo, A.: Analysis of the Metric Camera B&W Images Over Italy. Proceedings of IGARS '84 Symposium, Strasbourg, Aug 27-30, 1984 (Ref. ESA SP-215).

Wood, G. A.: Mission Planning Parameters for the Space Shuttle Large Format Camera. Proceedings of 45th Meeting of American Society of Photogrammetry, Vol. II, Mar 1979, pp. 540-550.

Wood, G. A.: Environmental Factors in the Design of the Large Format Camera. Report of Commission I, Working Group 3, Archives of XIV International Congress of Photogrammetry and Remote Sensing, Volume for Commission I, Hamburg, FRG, International Society of Photogrammetry, U.S. Geological Survey, Reston, Va., Jun 1980.

5.2 LFC APPLICABLE DOCUMENTATION

Document No.	Document Description	Issue Date
JSC-14083	Payload Implementation Plan (PIP): LFC-1	01/83
JSC-14083-1	PIP Payload Data Package Annex 1	
JSC-14083-2	PIP Annex 2	
JSC-14083-3	PIP Annex 3	
JSC-14083-4	PIP Annex 4	
JSC-14083-5	PIP Annex 5	
JSC-14083-6	PIP Annex 6	
JSC-14083-7	PIP Annex 7	
JSC-14083-8	PIP Annex 8	
JSC-14083-9-I	PIP Annex 9, Part I	
JSC-14083-9-II	PIP Annex 9, Part II	
JSC 17920	Statement of Work for LFC Payload Integration (LFC, SOW) Basic	01/82
JSC-17921	QA Plan for LFC Payload Integration (LFC, QAP, QA) Basic	11/82
JSC-17922	Safety Plan for the LFC Payload Integration Engineering Effort	05/83
JSC-18301	End Item Specification for LFC Payload Integration (LFC, EIS) Basic	05/83
JSC-18326	Configuration Management Plan for the LFC Payload Integration (LFC, CMP) Basic	10/82
JSC-18354-1	Ground Integration Requirements Document (GIRD) for the LFC-1 Payload Integration (LFC, LFC-1, GIRD, GIRD-1) Basic	04/83
JSC-18354-2	GIRD for the LFC-2 Payload Integration (LFC, LFC-2, GIRD, GIRD-2) Basic	12/83
JSC-18616	Safety Assessment Report for LFC Payload Integration (LFC, SAR) Basic	09/82
JSC-18617	Fracture Control Plan for LFC Payload Integration (LFC, Fracture Control) Basic	11/82
JSC-18800	Weight and Balance Log for the LFC Payload (LFC, Mass Properties) Basic	Current
JSC-18801	Design and Performance Specification (LFC, PSU, Specification)	02/83

Document No.	Document Description	Issue Date
JSC-18802	Certification Plan and Requirements (LFC, PSU, Certification)	01/84
JSC-18803	Procedures for Installation and Test (17 Procedures)	02/83
JSC-18844	Materials Usage Report for LFC Payload Integration	03/83
JSC-18987	Cargo Systems Manual: LFC, STS 41-D	03/84
JSC-18987	Cargo Systems Manual: LFC, STS 41-G	08/84
JSC-19046	LFC/ORS/MPESS Static Structure (LFC, Structural Certification)	06/83
JSC-19241	FDF: Payload Operations Checklist, STS 41-D (STS 41-D, Checklist, OAST/LFC/GAS) Final	05/84
JSC-19270	Certification Plan and Requirements (LFC, Payload Certification)	01/84
JSC-19318	Acceptance Test Procedure for Power Supply Unit (LFC, PSU, ATP) Final	10/83
JSC-19348	Electromagnetic Compatibility Assessment Report for the LFC Payload (LFC, EMI, EMI/EMC Report) Final	10/83
JSC-19601	Certification Report for the LFC (LFC Payload Certification)	05/84
JSC-19954	Fracture Control Plan for the LFC Support Structure-Tilt (LSS-T, Fracture Control)	06/84
JSC-19965	Flight Data File, Crew Activity Plan, STS 41-G	09/84
JSC-20055	Safety Assessment Report for the LFC/Orbital Refueling System Payload	08/84
JSC-20346	STS 41-G Mission Evaluation Report, OSTA-3 (STS 41-G, Mission Report) Final	01/85
ICD-A-14083	Orbiter/LFC-1 Cargo Interfaces (ICD, LFC, LFC-1) IRN 2	05/83

Document No.	Document Description	Issue Date
ICD-A-14083-001	Orbiter/LFC-2 Cargo Interfaces (ICD, LFC, LFC-2, ORS) IRN 4	12/83
ICD-B-14083	MPESS/LFC Interfaces (ICD, LFC, LFC-1) Basic	03/83
ICD-B-14083-01	Integration of the LFC Into the LFC Payload	02/83
ICD-B-18417	LFC-2/ORS Interfaces (ICD, ORS, LFC-2) Revision A	05/84
SLD-47-000001-801	OCPS Functional ICD, Revision C	10-03-78
SLD-47-000001-802	OCPS Mechanical ICD, Revision D	10-03-78
SLD-47-000001-803	OCPS Electrical ICD, Revision D	10-03-78
SLD-47-000001-804	OCPS Environmental ICD, Revision C	10-03-78
SLD-47-000001-805	OCPS LFC Film Spool ICD (Cancelled)	10-03-78
SLD-47-000001-806	OCPS LFC Installation (Cancelled)	10-03-78
SLD-47-000001-808	OCPS Gas Supply Assembly	01-28-81
SLD-47-000001-901	OCPS BTE and Ground Handling Equipment, Revision D	10-03-78
SLD-47-000001-902	OCPS Launch and Recovery Facilities, Revision C	10-03-78

APPENDIX A
SYSTEM PERFORMANCE TESTING

APPENDIX A
SYSTEM PERFORMANCE TESTING

The LFC was designed to be an instrument which would be capable of superior spatial resolution in the visible spectrum (and to some extent the near infrared spectra), would have minimum geometric distortion for precision cartographic applications, and would provide the photogeologist with wide-area stereoscopic imagery for mineral and fossil fuel exploration. Technical criteria and parameters were established for both optical performance and system dynamic (operating) performance. These parameters and their degree of attainment will be described later as a summation of all the testing which was accomplished. First, however, it is desirable to highlight certain key test points in the program.

A.1 LENS RESOLUTION AND DISTORTION TESTING

Lens level testing was performed on the completed lens cone assembly to verify the spatial resolution and radial distortion characteristics. These tests were conducted on a test fixture containing an array of 11 collimators, the focal lengths of which are 61 cm (24 in.), as shown in figure A-1. It may be noted that this array was not a full array of the 114 collimators which would be required to fill adequately the LFC's defined format. Rather, of the 11 collimators, 7 were positioned orthogonally to the other 4, the lens was rotated to discrete positions, and multiple exposures were made until the proper number of field positions was recorded on film. The minimum number of lens index positions required to accomplish this is 16; and, thus, 16 film exposures are required.

A special vacuum platen film holder was used rather than the LFC film magazine. In this case, the film platen was an optically flat, glass slab, overcoated with an opaque blocking agent to serve as a light mask, which has along-track and across-track (23 x 47) intersections surrounded by the 12 fiducials within the lens focal frame. These machine-generated intersections were printed by strobing the back side of the glass platen, thus causing them to print through the base of the test film. These intersections

are at 1-cm intervals and were used to determine the residual film errors during mensuration of point images for lens distortion analysis.

Each collimator is supplied with film targets as shown in figure A-2 with $\sqrt[12]{2}$ bars of such contrast that their target object contrast (TOC) ratio at the LFC lens entrance pupil is 2:1 (low contrast). Within their formation, these same film targets contained a symmetrical target dot which was used as the reference point for measuring radial image displacement or distortion. At each collimator focal plane, this target dot was subject to precise positioning and alignment through the use of a phototheodolite (see figure A-2), ensuring that all collimators converged to a point at the LFC lens nodal point. The film images produced by the phototheodolite were used for mensurating the exact radial field position of each target dot.

Once all 11 collimator target positions had been properly aligned and documented, photography was begun. Throughout the development program for the LFC, Kodak type 3414 film was used as the standard for all optical and performance testing and was the only material used for distortion determinations. Other film types, however, considered as candidates for Orbiter missions, were tested for spatial resolution characteristics. These films are listed in table A-1.

TABLE A-1.- LFC TEST AND FLIGHT FILMS

Kodak film type	Film description	TOC
3414	High definition aerial	2:1
		1000:1
3412	Panatomic-X Aerocon II	2:1
SO-131	High Definition Aerochrome infrared (IR)	2:1
SO-242	Aerial color	2:1

When the task for the phototheodolite had been completed, the large index table was rotated to bring the LFC lens cone assembly (see figure A-3) into

position for photography. The LFC lens, like the phototheodolite, was on a smaller index table so that it could be rotated to acquire the required 16 semidiagonal target arrays illustrated in figures A-4 and A-5. The angular rotation of the semidiagonals, originating at the center of the image format, and the angular field position, also originating from the format center, are summarized in table A-2.

TABLE A-2.- SEMIDIAGONAL AND TARGET PLACEMENT

Semidiagonal rotation, deg		Target field position, deg	
1 = 0.0	9 = 180.0	1 = 39	9 = 12.0
2 = 26.6	10 = 206.6	2 = 36.5	10 = 7.0
3 = 45.0	11 = 225.0	3 = 34.0	11 = 2.0
4 = 63.4	12 = 243.4	4 = 31.5	
5 = 90.0	13 = 270.0	5 = 29.0	
6 = 116.6	14 = 296.6	6 = 26.5	
7 = 135.0	15 = 315.0	7 = 22.0	
8 = 153.4	16 = 333.4	8 = 17.0	

All resolution and distortion testing was conducted under ambient laboratory conditions. Temperature was maintained at 21° ± 0.5° C (70° ± 1° F), and pressure was 746 torr (mm/Hg). Under flight conditions, the LFC internal pressure is maintained through its self-contained GPCA at 2 psig. Thus, in the vacuum environment of space, the pressure is maintained at 2 psia. All laboratory ambient pressure testing required defocus of collimators to compensate for the space environment induced change in operating pressure.

A.2 LENS/FOCAL PLANE CHARACTERISTICS TESTING

Additional information on lens characteristics was derived during the period following lens final assembly through testing to determine spectral transmission of the lens (with the permanently installed antivignetting filter in place), relative illumination at the focal plane, and internal light scatter or veiling glare under conditions of full-field illumination.

These tests were conducted using both standard optical laboratory test equipment and unique test fixtures.

An example of a unique test fixture is the one used to determine the principal point of autocollimation (PPA) and its position relative to the intersections of both the primary and secondary fiducials (see figure 1-16). The sheer size and weight of the LFC lens cone assembly made it necessary to customize test equipment to accomplish many optical test procedures. The intersection of the primary fiducials establishes the primary center of format, and the secondary fiducials intersection represents the secondary center for format. The specification for the coincidence of points of both the primary and secondary format centers, the PPA, and the principal point of symmetry (PPS) was that all must fall within a circle of 30 μm diameter, as shown in figure A-6.

A.3 LFC FLIGHT SIMULATION TEST

As the final and ultimate test of the LFC in the full-up flight configuration, the LFC was "flown" on a simulated orbital mission in the thermal vacuum test chamber shown in figure A-7. During this test sequence the chamber pressure was maintained at a pressure of 5.6×10^{-5} torr for a period of several days, and the chamber walls were thermally cycled over the extremes of temperatures which might be experienced during a typical space flight. During a series of such tests, the LFC accumulated a total of 492 hr of vacuum exposure. This is equivalent to 20.5 days. When the ARS/SCA was added to the OCPS configuration 2 years later, both the LFC and the ARS were subjected to an additional thermal vacuum test during which the LFC accumulated an additional 255 hours (10.5 days) of thermal vacuum exposure.

In addition to verifying the environmental stability and control of the LFC and its operability in the vacuum environment, system dynamic resolution performance was also verified. To accomplish this, an externally located and controlled collimator projects images of moving targets into the chamber through a viewing port, simulating the orbital velocities that will be encountered during flight. Three remotely controlled mirrors which were

within the chamber and mounted directly in front of the LFC lens, were used alternately to place these targets at -35°, +9.5°, and +35° field positions along the LFC velocity vector.

Target drive velocities were adjusted to simulate angular velocities of 0.011, 0.026, and 0.041 rad/sec. These represent the midpoint and high and low FMC capabilities of the LFC, which are equivalent to orbital altitudes ranging from 185 to 700 km (100 to 375 n. mi.). Then, keeping the collimator targets stationary and disabling the LFC's FMC drive, the collimator was progressively defocused on either side of the optimum focus setting to derive a thorough focus test to verify proper focus of the LFC.

A.4 LFC LABORATORY PERFORMANCE RESULTS

The results of the various operational and performance tests conducted during the course of the LFC development program are summarized briefly in this section.

A.4.1 FOCUS SETTING

During thermal vacuum testing and stationary target photography (as described above), critical focus position for the LFC film magazine vacuum platen was established for the simulated space environment. This was accomplished by using fine adjustment devices which are built into the film platen support structure. Proof of the position recovery was verified many times by resetting the focus followed by optical retest. The accuracy (or repeatability) of position recovery is to approximately 38 μm (0.0015 in.).

A.4.2 VEILING GLARE

The veiling glare, or internal reflection, of both the LFC and SCA lenses was measured as being 7.7 percent. The specification requirement for veiling glare in both lenses was 8 percent or less.

A.4.3 RELATIVE ILLUMINATION

In table A-3, the relative illumination at the LFC focal plane is given for three discrete spectral regions. In the specification it was stated that this would vary by no more than ±10 percent across the film format.

TABLE A-3.- RELATIVE ILLUMINATION

Field angle, deg	Relative illumination, percent		
	580 nm wavelength	650 nm wavelength	720 nm wavelength
-35	103	100	101
-25	99	98	100
-10	94	93	94
0	100	100	100
10	97	97	97
25	100	98	100
35	106	102	106

A.4.4 LENS T-NUMBER

The LFC lens T-numbers were calculated for lenses with various field angles over the 580- to 720-nm spectral range and other spectral bands generic to the two LFC spectral filters for use with candidate flight-film combinations. The specification stated that the T-number be equal to or greater than T-14 (table A-4).

A.4.5 SPECTRAL TRANSMITTANCE

The on-axis spectral transmittance for the LFC lens, with antivignetting filter in place, is shown in table A-5.

A.4.6 SYSTEM RESOLUTION - STATIC

Bar targets ($\sqrt[12]{2}$) which produced a TOC ratio of 2:1 at the entrance pupil of the LFC optics were used for all resolution determination testing. Area

TABLE A-4.- CALCULATED T-NUMBER

Field angle, deg	Transmittance, percent	Relative illumination, percent	T-no.
-35	19.75	1.013	13.5
-25	19.31	.99	13.7
-10	18.27	.937	14.0
0	19.5	1.000	13.6
10	18.92	.97	13.8
25	19.36	.993	13.6
35	20.42	1.047	13.3
Spectral range			
415-720 nm			13.7
505-720 nm			13.6
515-880 nm			13.6

TABLE A-5.- SPECTRAL TRANSMITTANCE

Unfiltered		Haze filter	
nm	Transmittance, percent	nm	Transmittance, percent
350	9.6		
400	2.1		
500	18.4	580	19.2
600	22.3	620	19.4
700	23.0	660	19.4
800	21.1	700	19.9
900	17.5	720	19.4
1000	17.1		

weighted average resolution (AWAR) using 3414 film was specified at not less than 80 line pairs per millimeter (lp/mm) for the full format (9 by 18 in.) and not less than 88 lp/mm for the central square (9 by 9 in.). Minimum acceptable levels for averages of the four format corners were set at 50 lp/mm for the full format and 79 lp/mm for the central square. Detailed data collected for the four flight films have been plotted as shown in figure A-8. Tabular listings for these data are included in table A-6.

TABLE A-6.- LFC AVERAGE RADIAL AND TANGENTIAL RESOLUTION (lp/mm)

Film type	TOC	Corners, in.		AWAR, in.	
		9 x 9	9 x 18	9 x 9	9 x 18
3414	2:1	91	62	90	89
	1000:1	114	103	138	125
3412	2:1	66	49	59	57
SO-131	2:1	38	34	41	39
SO-242	2:1	48	48	58	54

A.4.7 SYSTEM RESOLUTION - DYNAMIC

Because the LFC employs a mechanism for translating the film platen to correct for image smear due to spacecraft forward velocities, a criterion was established to verify adequacy of design over the full range of FMC operation. The specification allows up to 10-percent degradation for FMC error. The error, as measured in testing, was less than 10 percent.

A.4.8 PRINCIPAL POINT OF AUTOCOLLIMATION

The definition for the primary center of format for the LFC is that point at the intersection of two lines connecting the center forward and center aft fiducials and the two center fiducials on the format sides (see figure 1-16). The secondary center of format is that point of intersection of two lines connecting opposing corner fiducials of the central 9- by 9-in. square. Lines at each intersection must be orthogonal to within ±1 min of arc. The coordinates for both the primary and secondary centers of format, the PPA and

the PPS, were required to fall within a circle with a diameter of 0.030 mm. Actual placement is illustrated in figure A-6.

A.4.9 GEOMETRIC DISTORTION

Radial distortion was specified for the full format (9 by 18 in.) and for the central square (9 by 9 in.). For the full format, radial distortion was limited to an envelope of ±25 μm; and, for the central square, the specific envelope was ±10 μm. The radial distortion for the LFC lens with a calibrated focal length of 30.5731 cm (12.037 in.) at ambient laboratory conditions is presented in figure A-9.

A.5 FOCUS VERIFICATION

Since the LFC lens internal pressure (2 psig) was to be approximately 1/7th atm during orbital operation, the lens was defocused to compensate for the change in refractive index of the rarefied gas surrounding the lens elements. This shift in focus is due to the density changes of the enveloping gas and is linear with these pressure changes. The shift in position of the focal plane is easily calculated.

The term "defocus" is relative to the pressure of 1 atm and amounts to a redefinition of the focal plane for any given pressure. Following completion of lens assembly, the focal plane was located using the laboratory collimator array (see figure A-1) under ambient laboratory conditions. This data became the reference focal plane for defocus (or refocus), and a nomograph was generated for proper focus setting under pressure variations (see figure A-10).

This linear function was verified before flight during stellar calibration of the LFC lens at a mountaintop observatory whose elevation was 2,752 m, or 9,030 ft (figures A-11 and A-12). The LFC lens was defocused by the nomogram for the pressure at this altitude, and the earth's moon was imaged on high resolution film (type 3412) at multiple field positions. The change in focal plane position was accomplished by repositioning the film platen in the film magazine for the pressure at the 2,752-m altitude, or 10.5 psia plus 2 psig

(for LFC internal pressure), for a total of 12.5 psia. The net movement of the platen toward the lens was 0.193 mm (0.0076 in.). A qualitative analysis was then made of the imagery of the visual image evaluation (VIE) technique using lunar features to approximate a quantitative value. This worked extremely well and was, of course, later verified by the extremely high resolution imagery obtained during the STS 41-G flight.

A.6 LENS DISTORTION VERIFICATION

Upon completion of the LFC focus verification testing at the Cloudcroft facility and upon arrival of the "dark of the moon," NOAA's National Ocean Service personnel conducted stellar calibration of the LFC. They used the same nomograph (shown in figure A-10) to set the focal plane of the LFC vacuum film holder back. During this test sequence, the LFC optical axis was perpendicular to the earth, and several sets of four-exposure sequences were made of star trails. Each exposure sequence required rotating the LFC lens 90° from the previous sequence. The distortion results from each of these four primary exposures were extremely consistent, resulting in 1-σ error envelopes of ± 0.8 µm at the extremities of the format with the systematic distortions of the greater part of the format determined well under ± 0.1 µm. This result is very significant and implies great reliability in the use of these values in flight imagery analyses. Results of these stellar image analyses are shown in figures A-13 and A-14. It is suggested that only this data be used where lens distortion inputs are required for precise image applications. Additional data on the fiducial and reseau calibrations is included in the full text of the NOAA/NOS Report of Calibration by Stellar Methods, Calibration No. 654-182, prepared by the Photogrammetry Branch, Charting and Geodetic Services. A copy of this report is stored in the system documentation files with the LFC.

COLLIMATOR NUMBER	FIELD POSITION	TARGET ZONE NO.
①	39.0°	1
②	34.0°	3
③	29.0°	5
④	2.0°	11
⑤	26.5°	6
⑥	31.5°	4
⑦	36.5°	2
⑧	7.0°	10
⑨	12.0°	9
⑩	17.0°	8
⑪	22.0°	7

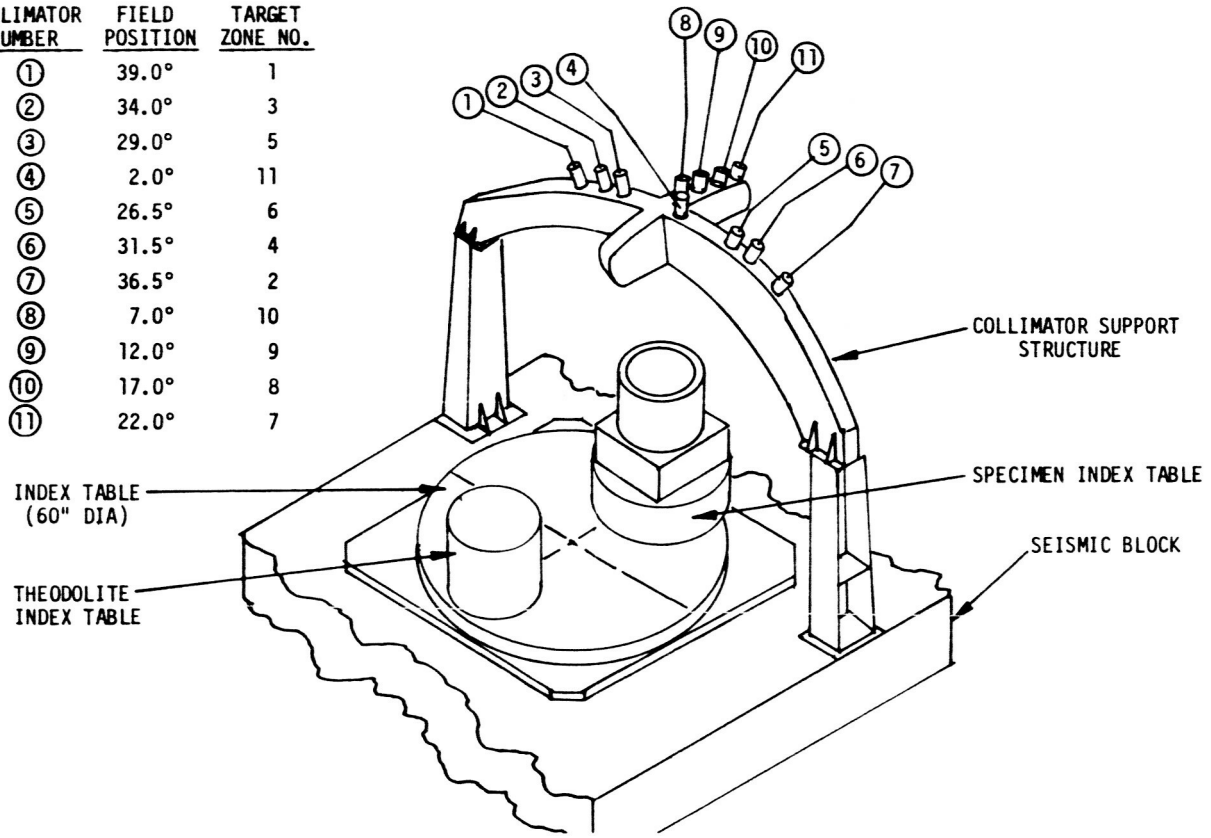


Figure A-1.- LFC image resolution and distortion test fixture.

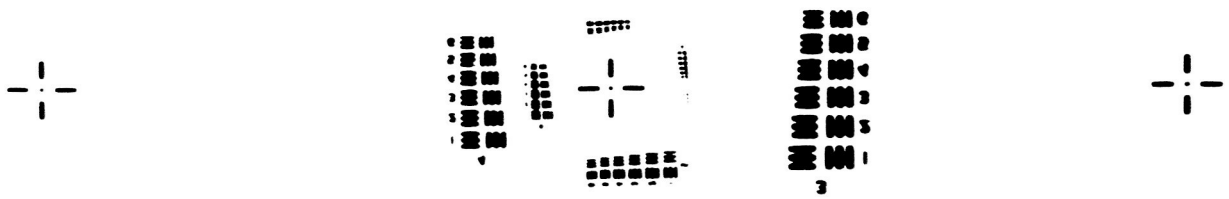


Figure A-2.-Collimator film target design for photo resolution and lens distortion testing.

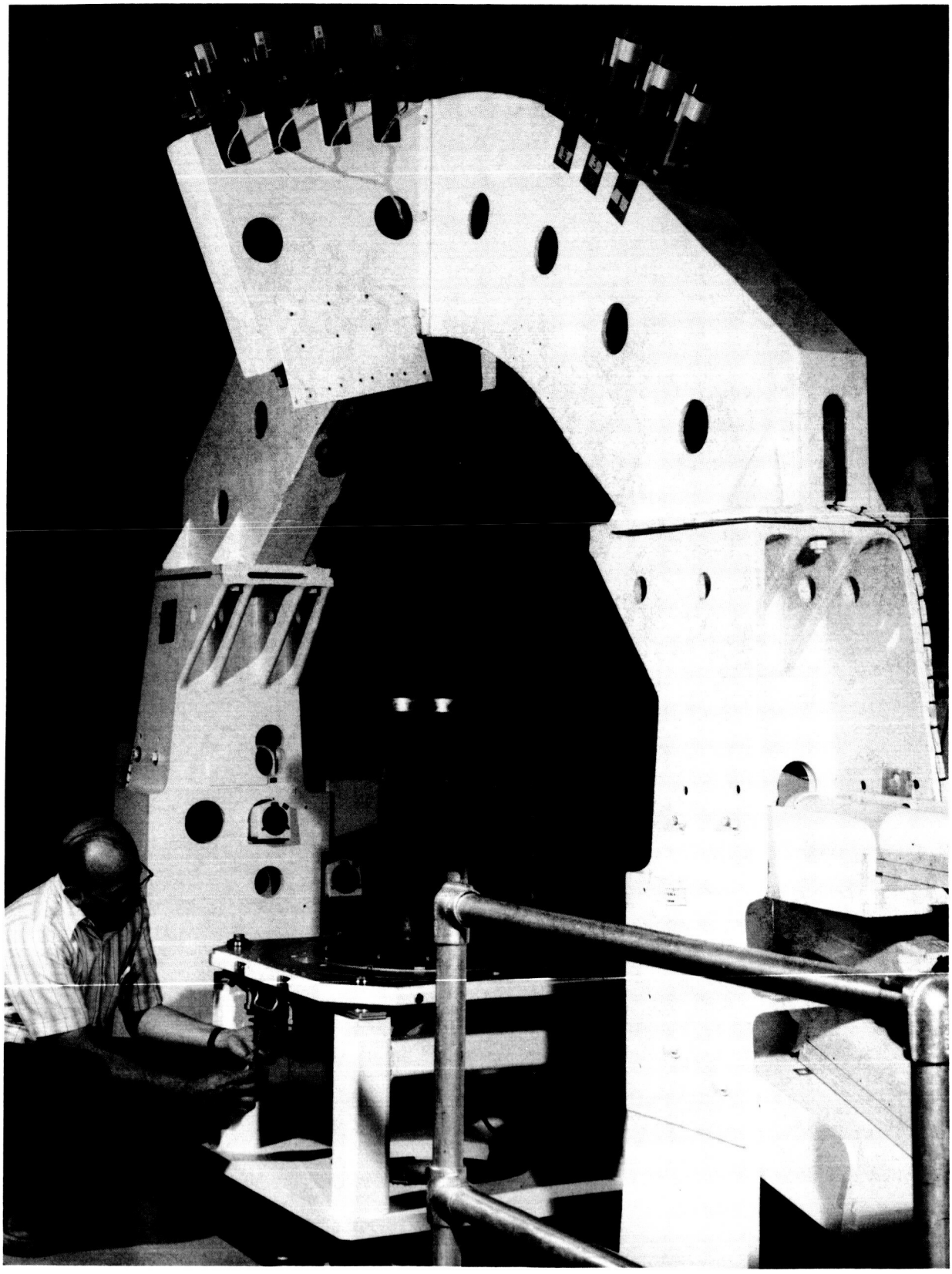


Figure A-3.- LFC resolution and distortion test fixture. (NASA photo S80-26250.)

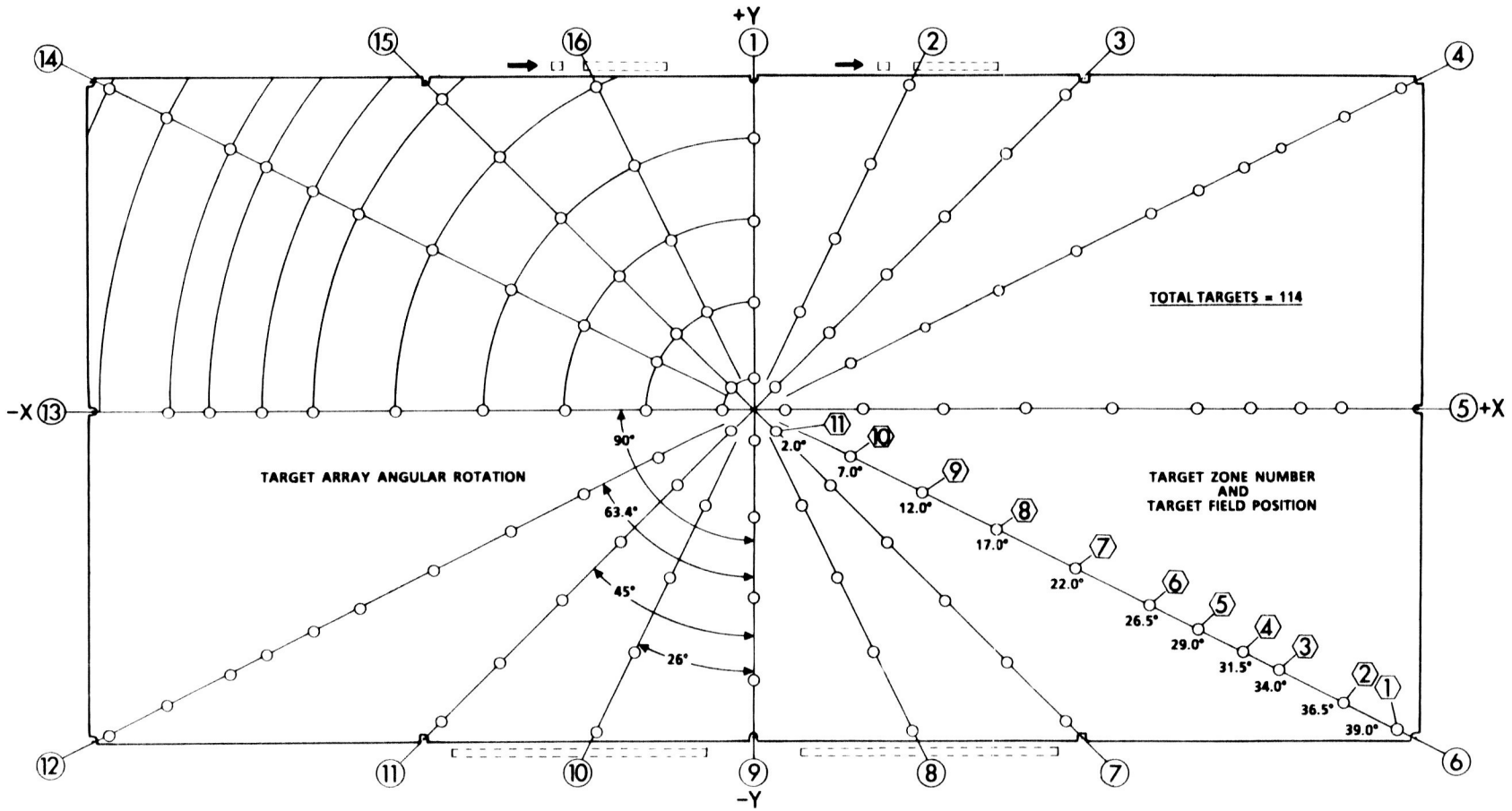


Figure A-4.- LFC semidiagonal and target placement reference.

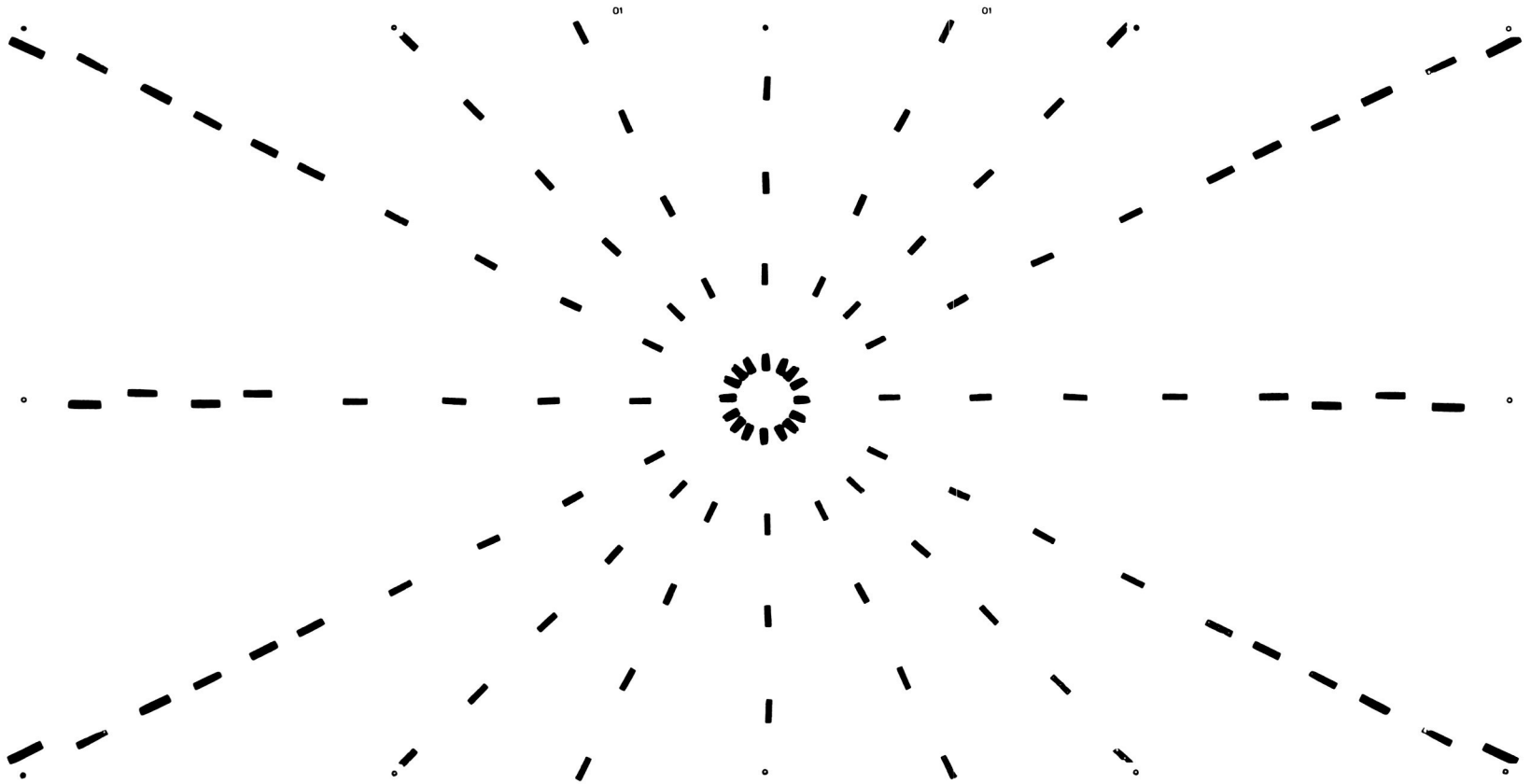


Figure A-5.- Actual imagery from a resolution test sequence, showing relative target array placement.

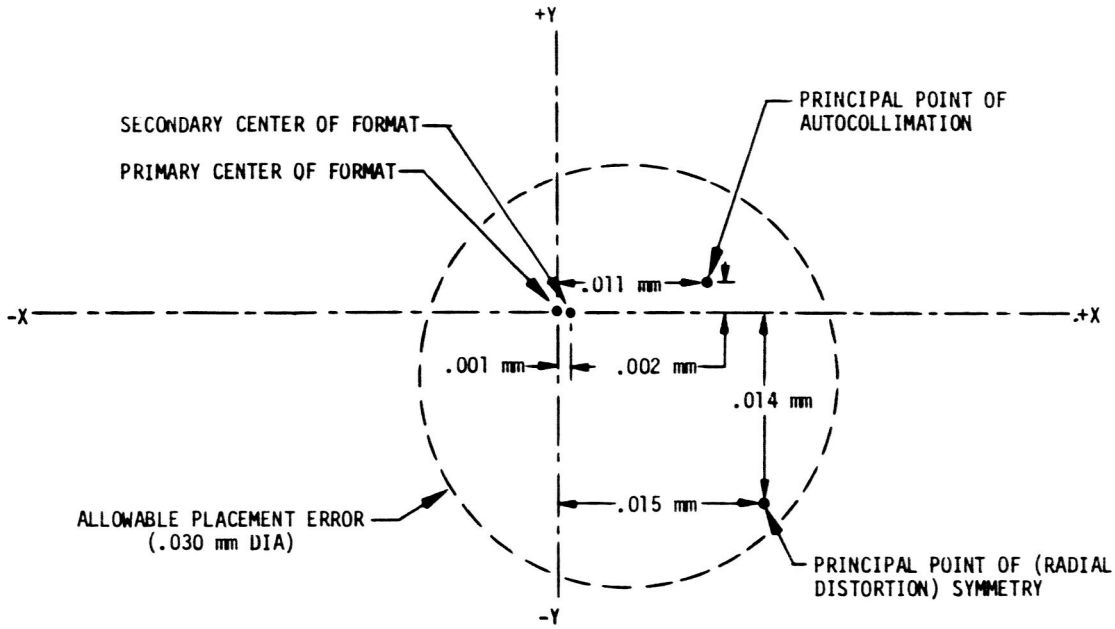


Figure A-6.- Coordinates for the geometric centers of the LFC cartographic lens assembly, serial number (S/N) 001.

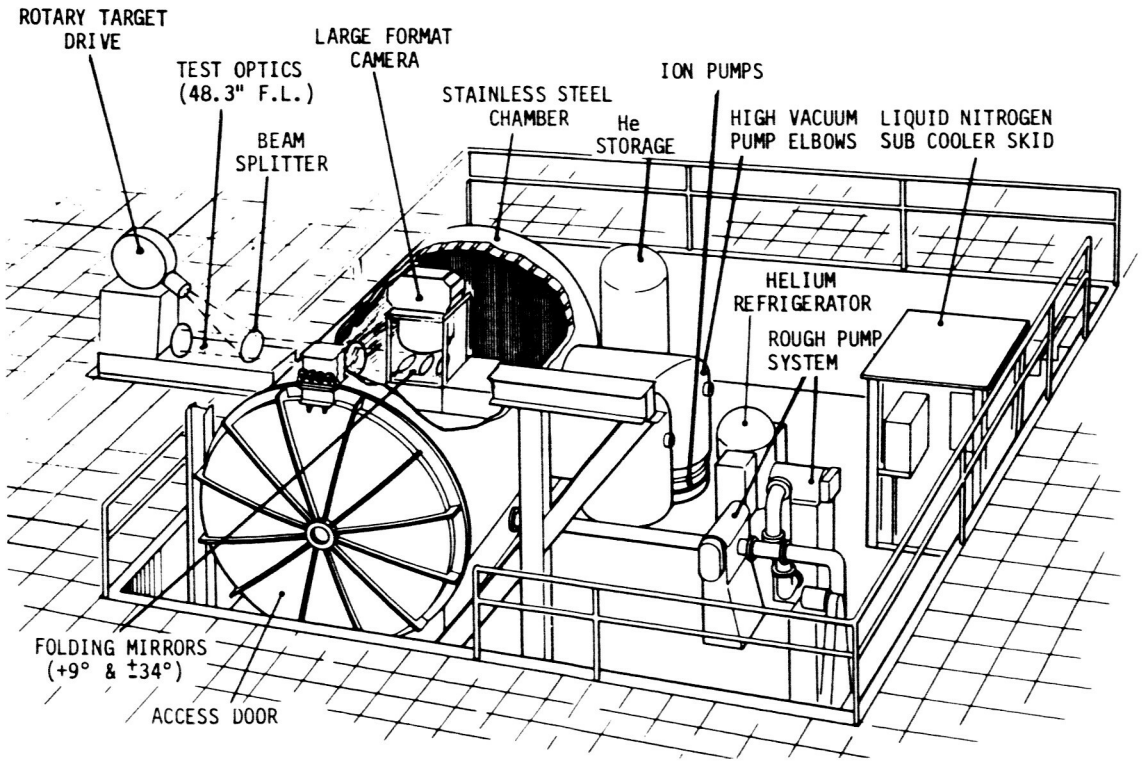


Figure A-7.- Thermal vacuum and dynamic resolution test chamber.

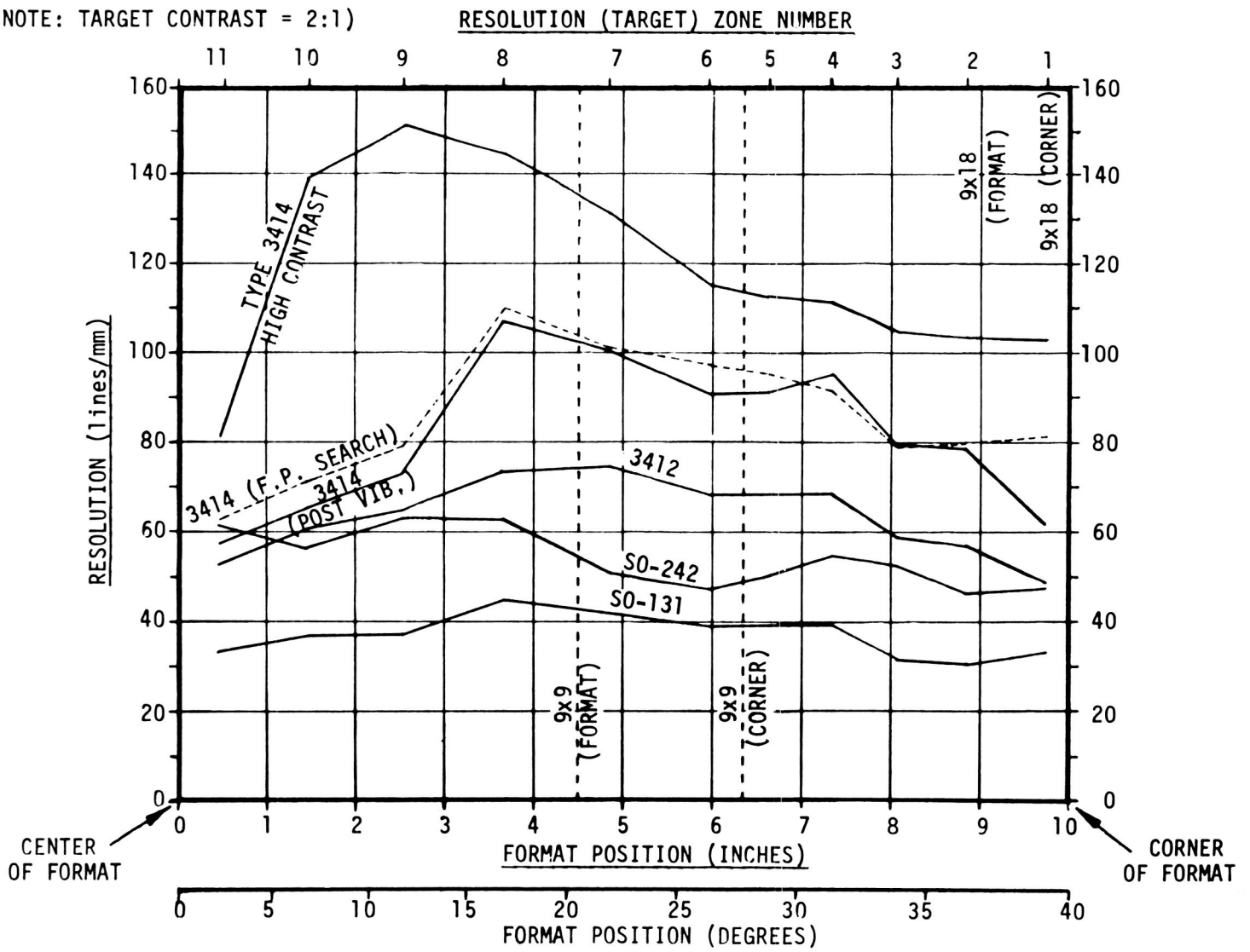


Figure A-8.- Static resolution of the LFC lens assembly. Plotted as a function of field position using the center of the frame format at the point of origin.

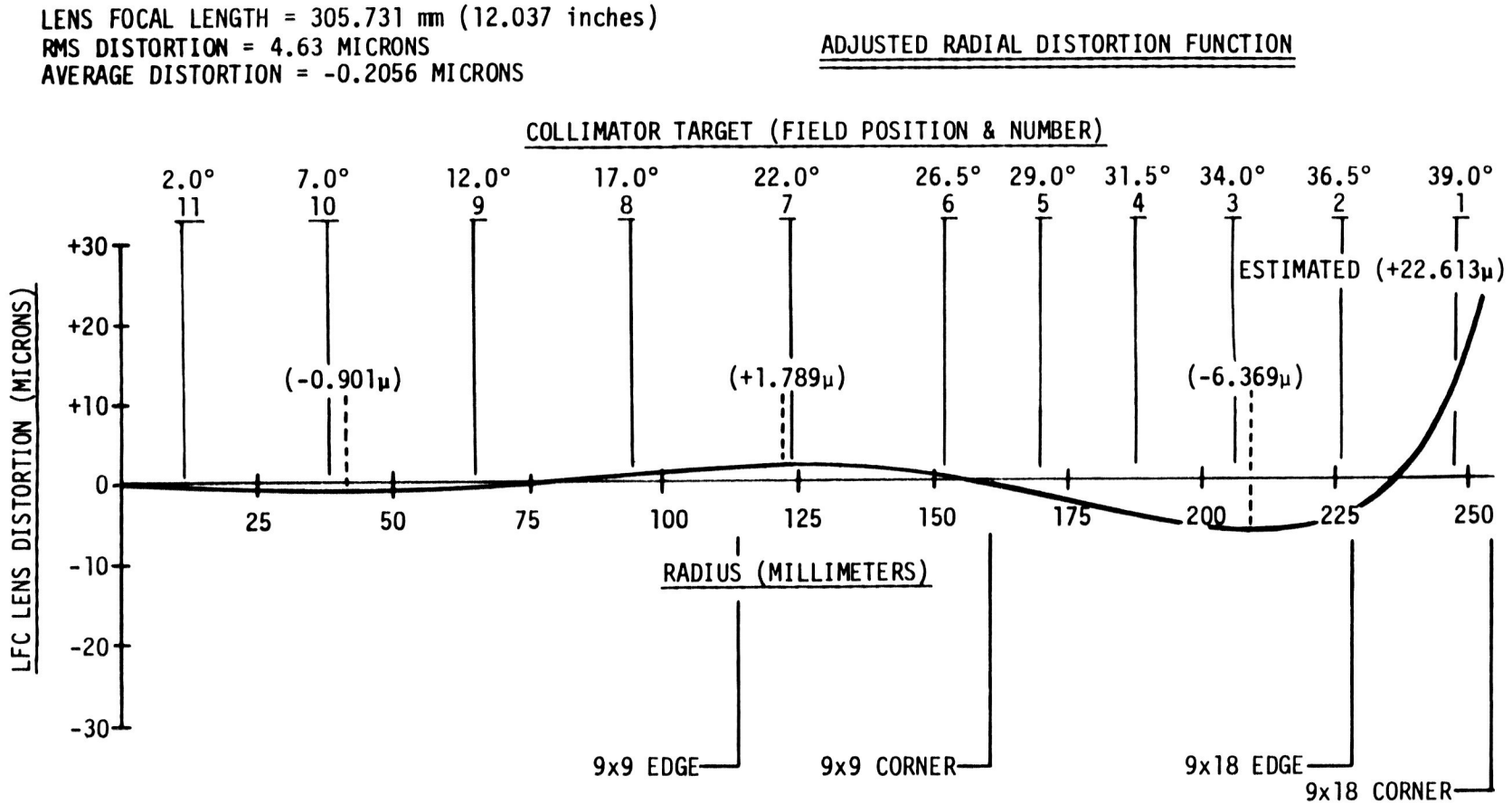


Figure A-9.- Subassembly-level geometric distortion characteristics for the LFC lens cell, as performed on the laboratory collimator array.

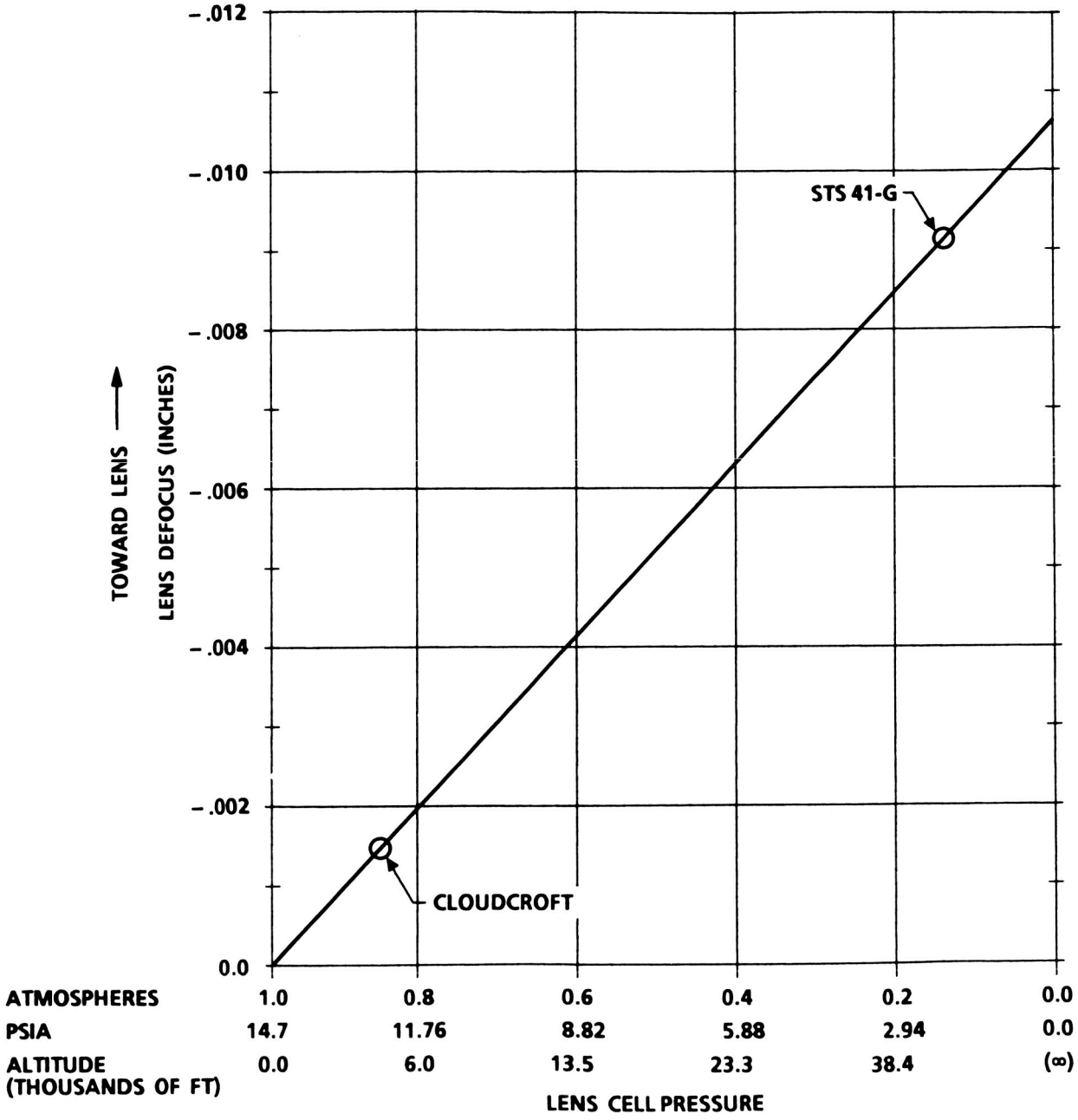


Figure A-10.- Nomograph for system focus shift as a function of pressure variations surrounding the lens cell.

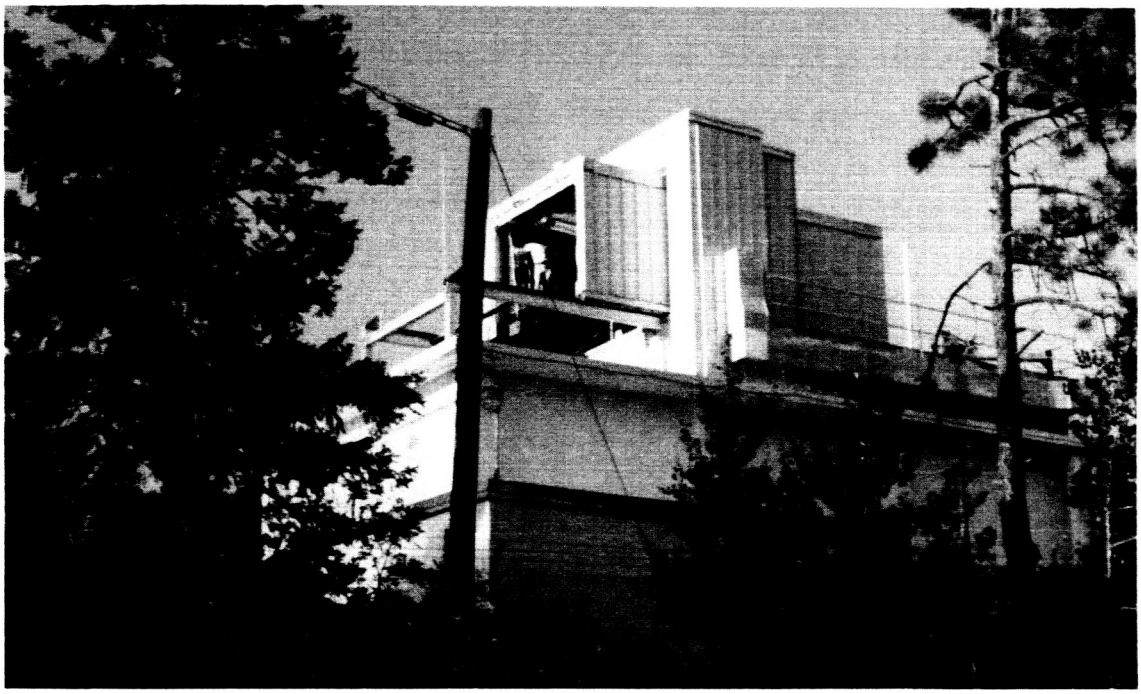


Figure A-11.- NOAA National Ocean Service's Metric Camera calibration facility located at Cloudcroft, New Mexico. (NASA photo S82-36037.)

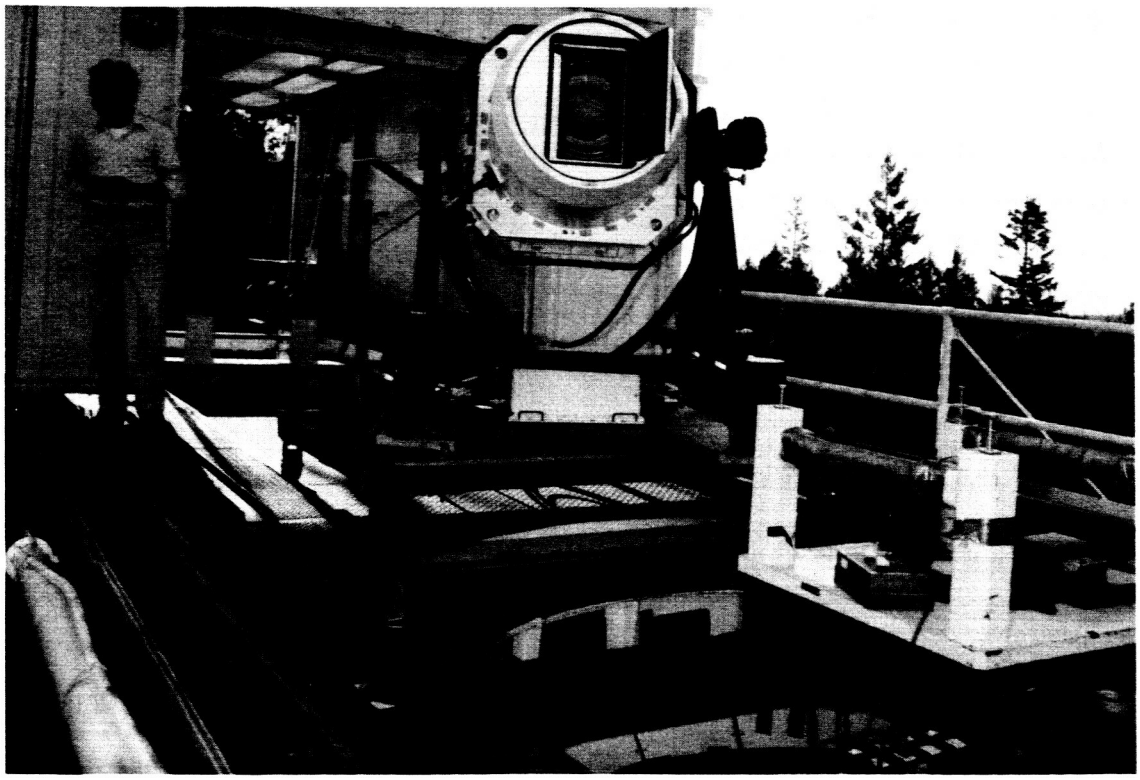


Figure A-12.- LFC in position at the NOAA facility at Cloudcroft. Camera team await darkness and the rise of the moon in preparation for multiple exposures of the lunar disc at various field positions throughout the image format (NASA photo S82-36045).

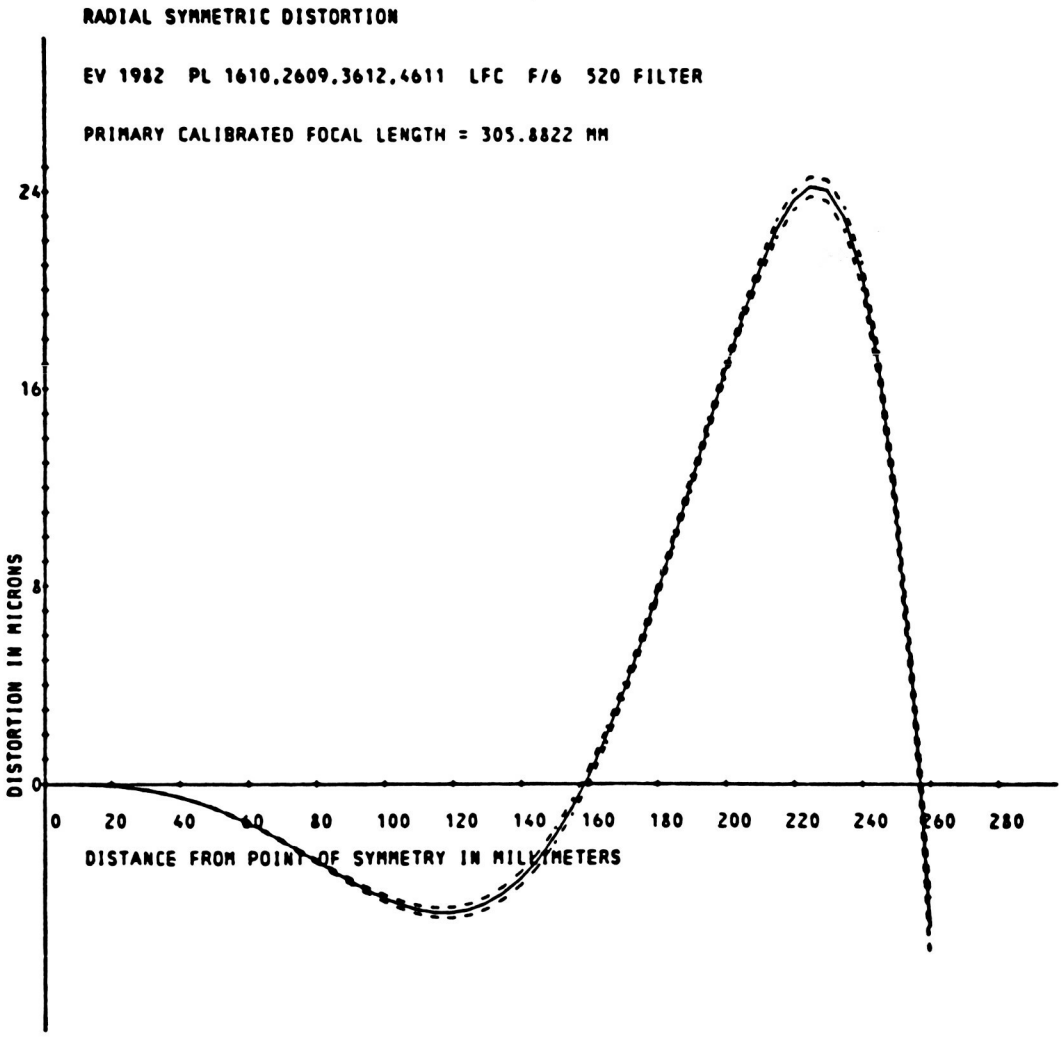


Figure A-13.- LFC radial symmetric distortion. (NOAA calibration number 654-182, July 1982.)

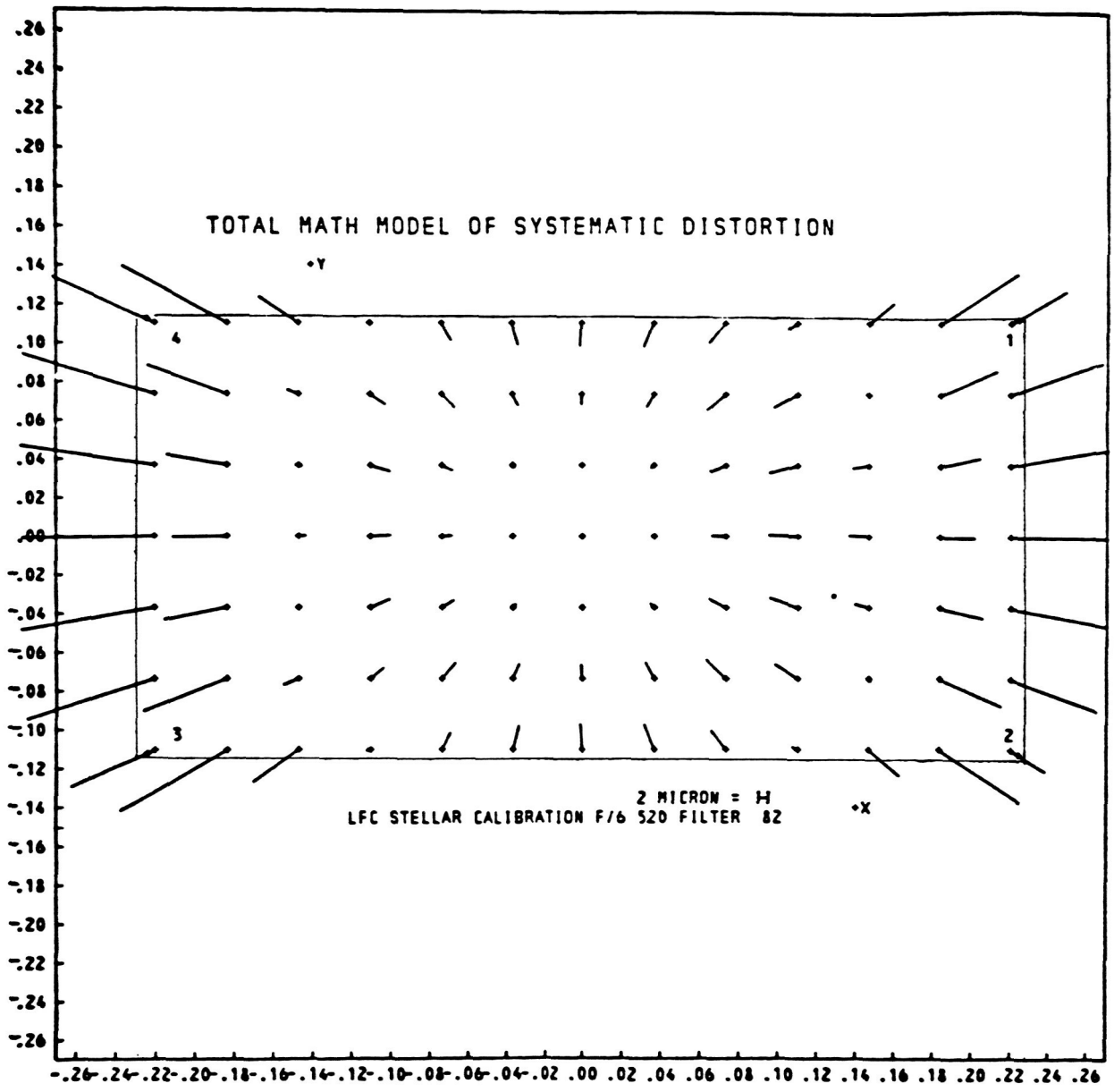


Figure A-14.- Total math model for LFC systematic distortion. (NOAA calibration number 654-182, July 1982.)

APPENDIX B
LFC GROUND COVERAGE MAPS

LARGE FORMAT CAMERA (LFC) PHOTOGRAPHIC FOOTPRINTS

A PHYSIOGRAPHIC ATLAS OF LARGE FORMAT CAMERA (LFC) PHOTOGRAPHY ACQUIRED DURING THE LFC MAIDEN VOYAGE

Aboard the Challenger
STS 41-G Mission,
October 5 through 13, 1984

LFC GROUND COVERAGE MAPS

The LFC acquired partial coverage of the following countries, nations, and regions of the earth on 79 data passes during the 132 orbits of the planet which occurred October 5 through 13, 1984, on the STS 41-G mission.

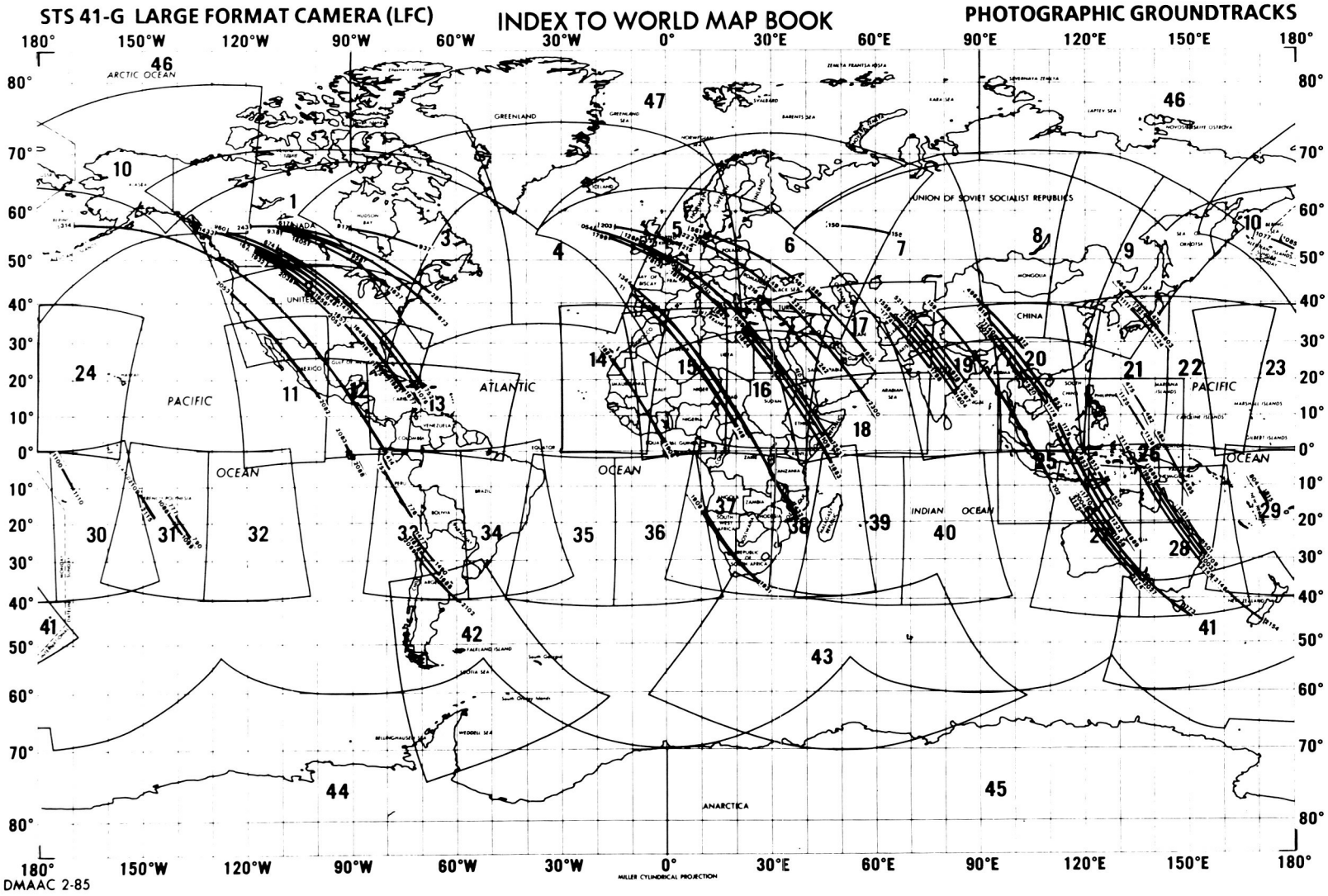
NORTH AMERICA	CENTRAL AMERICA	SOUTH AMERICA	CARIBBEAN
Alaska Peninsula	Costa Rica	Argentina	Bahamas
Aleutian Islands	El Salvador	Chile	Cuba
Canada (6 Prov.)	Guatemala	Ecuador	Dominican Rep.
Mexico	Honduras	Galapagos Isles	Haiti
USA (32 States)		Peru	Jamaica

EUROPE		MIDDLE EAST	
Belgium	Ireland	Afghanistan	Lebanon
Bulgaria	Italy	Armenia	Oman
Czechoslovakia	Netherlands	Crete	Pakistan
Crimea	Poland	Cyprus	Qatar
Denmark	Portugal	Georgia	Saudi Arabia
East Germany	Spain	Iran	Syria
England	Switzerland	Iraq	Turkey
France	Ukraina	Israel	
Greece	West Germany	Jordan	

ASIA		OCEANIA	
Bangladesch	Malaysia	Borneo	Phoenix Islands
Burma	Nepal	Celebes	Solomon Islands
Cambodia	Thailand	French Polynesia	Sonsorol Islands
China	Tibet	Java	Sumatra
India	USSR	Palau Islands	Sunda Islands
Japan	Viet Nam	Papua, New Guinea	Tokalau Islands
Laos			

AUSTRALIA	AFRICA		
New South Wales	Algeria	Ivory Coast	Rep. So. Africa
Northern Territory	Cameroon	Libya	Somalia
Queensland	Canary Islands	Malawi	Sudan
South Australia	Cent. African Rep.	Mali	Tanzania
Tasmania	Chad	Mauritania	Upper Volta
Victoria	Djibouti	Morocco	Western Africa
Western Australia	Egypt	Mozambique	Zaire
New Zealand	Ethiopia	Namibia	Zambia
		Ghana	Niger

NOTE: Use the above information with caution. During the STS 41-G mission, cloud cover was extremely heavy over North America and Europe. The LFC imagery contains cloud cover ranging from 0 to 100 percent. Refer to the LFC 41-G Mission Ephemeris (JSC-20383) for individual site conditions at time of photography.


STS 41-G LARGE FORMAT CAMERA (LFC)
INDEX TO WORLD MAP BOOK
PHOTOGRAPHIC GROUNDTRACKS
ARCTIC OCEAN
GREENLAND
UNION OF SOVIET SOCIALIST REPUBLICS
CHINA
PACIFIC
ATLANTIC
OCEAN
INDIAN OCEAN
ANARCTICA
DMAAC 2-85
MILLER CYLINDRICAL PROJECTION

NOTES

1. The LFC ground coverage was plotted on 1:10,000,000 scale maps. Pertinent maps have been subsequently reduced for this printing.

2. The following maps (pages) from the original atlas have been intentionally omitted from this publication, since there was no LFC coverage of their content:

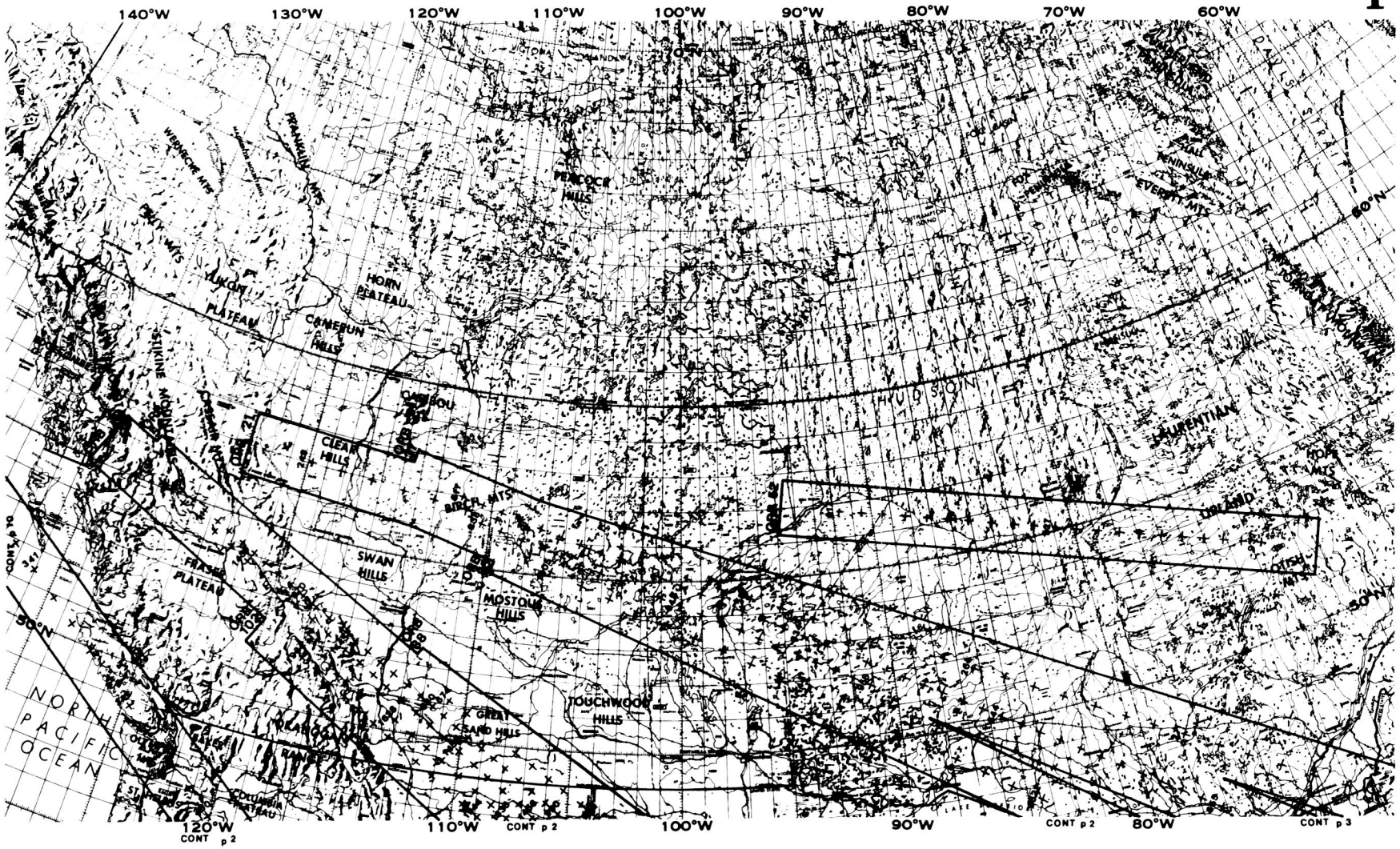
4	24	35
8	25	36
22	32	39
23	34	40

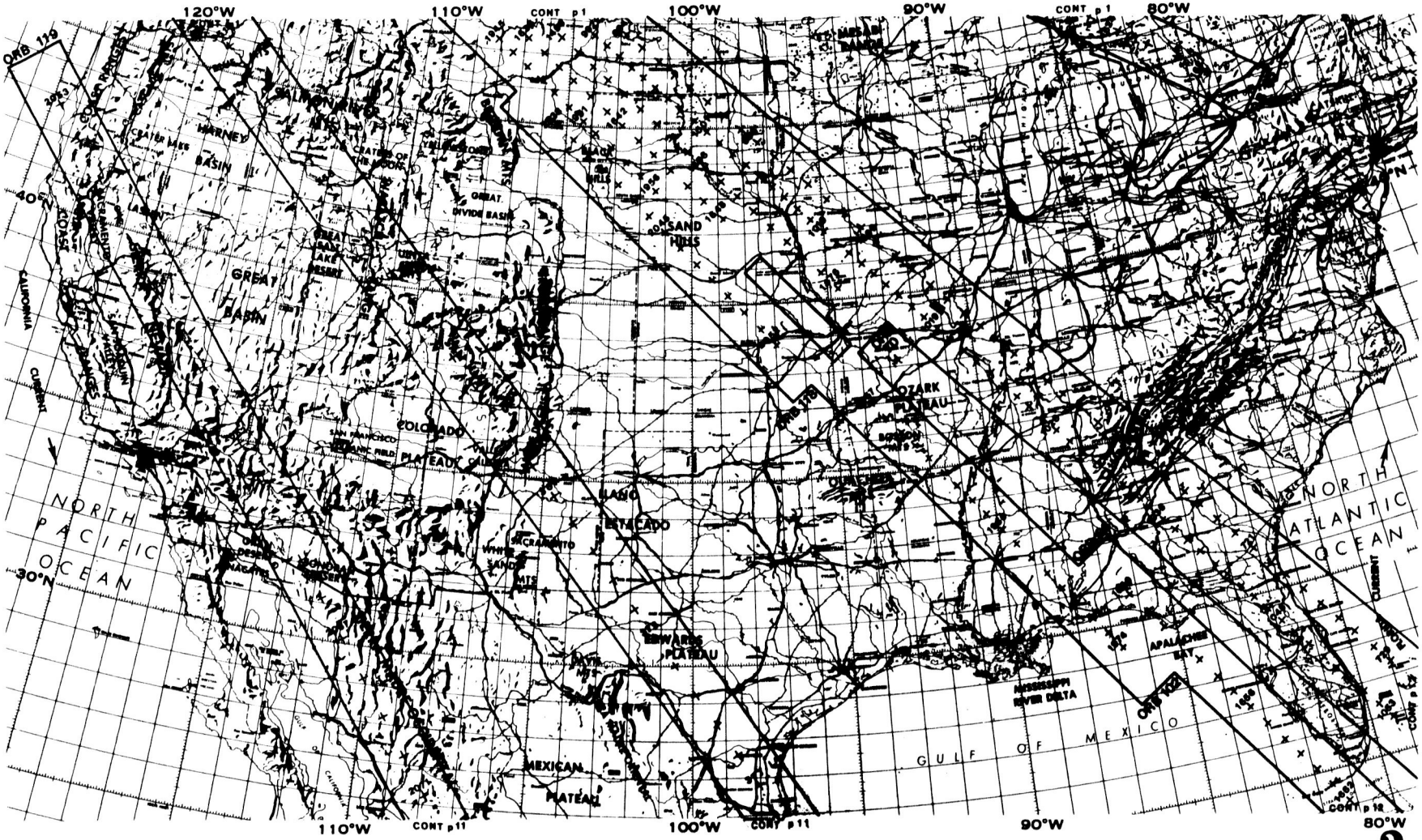
3. The nadir point (LFC center of format) for each frame of photography has been indicated by the placement of the symbol "+". At appropriate intervals, the LFC frame number has been placed above the symbol in order to give a periodic reference for identification of desired frames. Counting forward or backward from this point will numerically identify any desired frame falling between numbered frames.

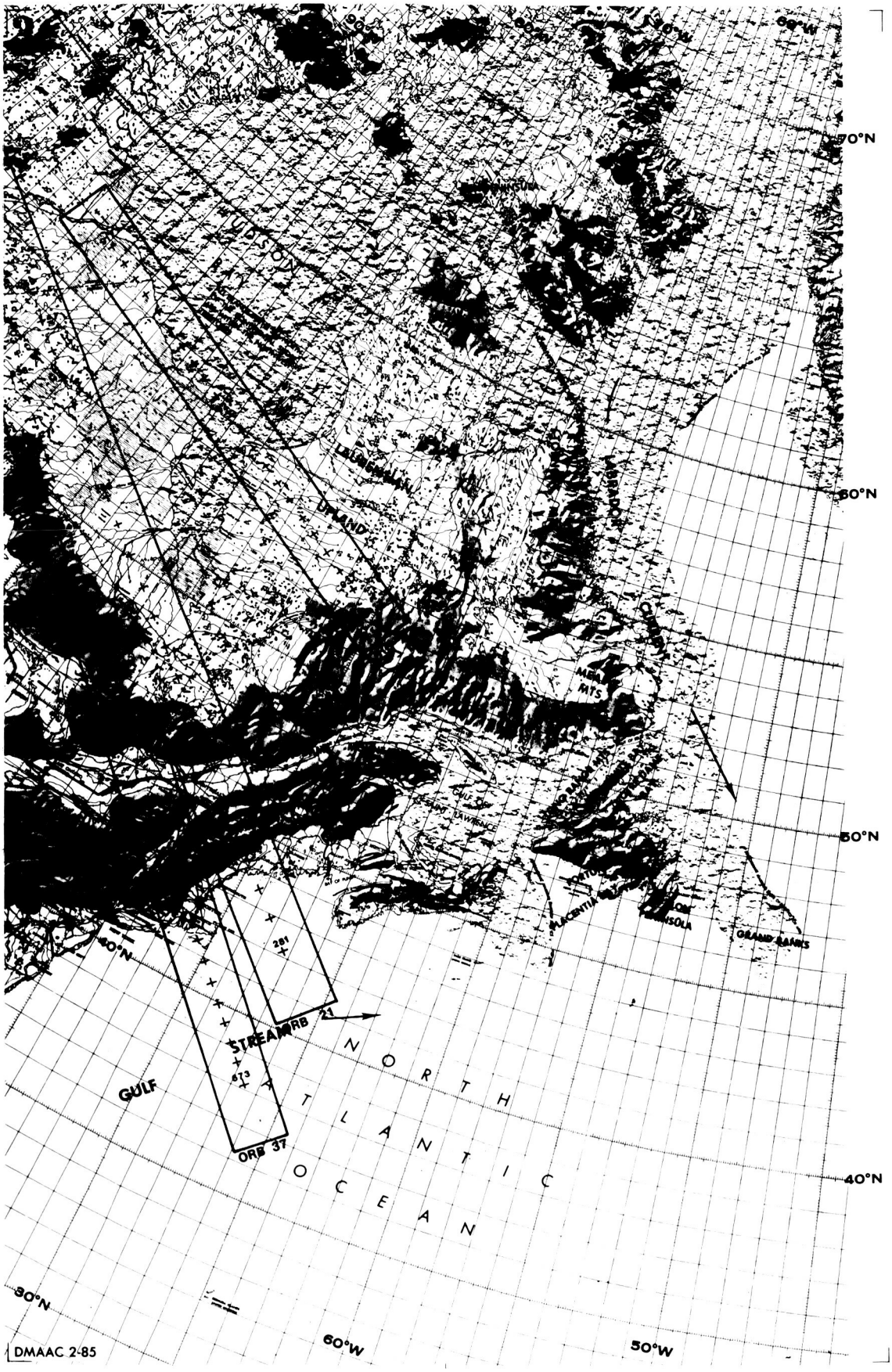
Example: 0932
+

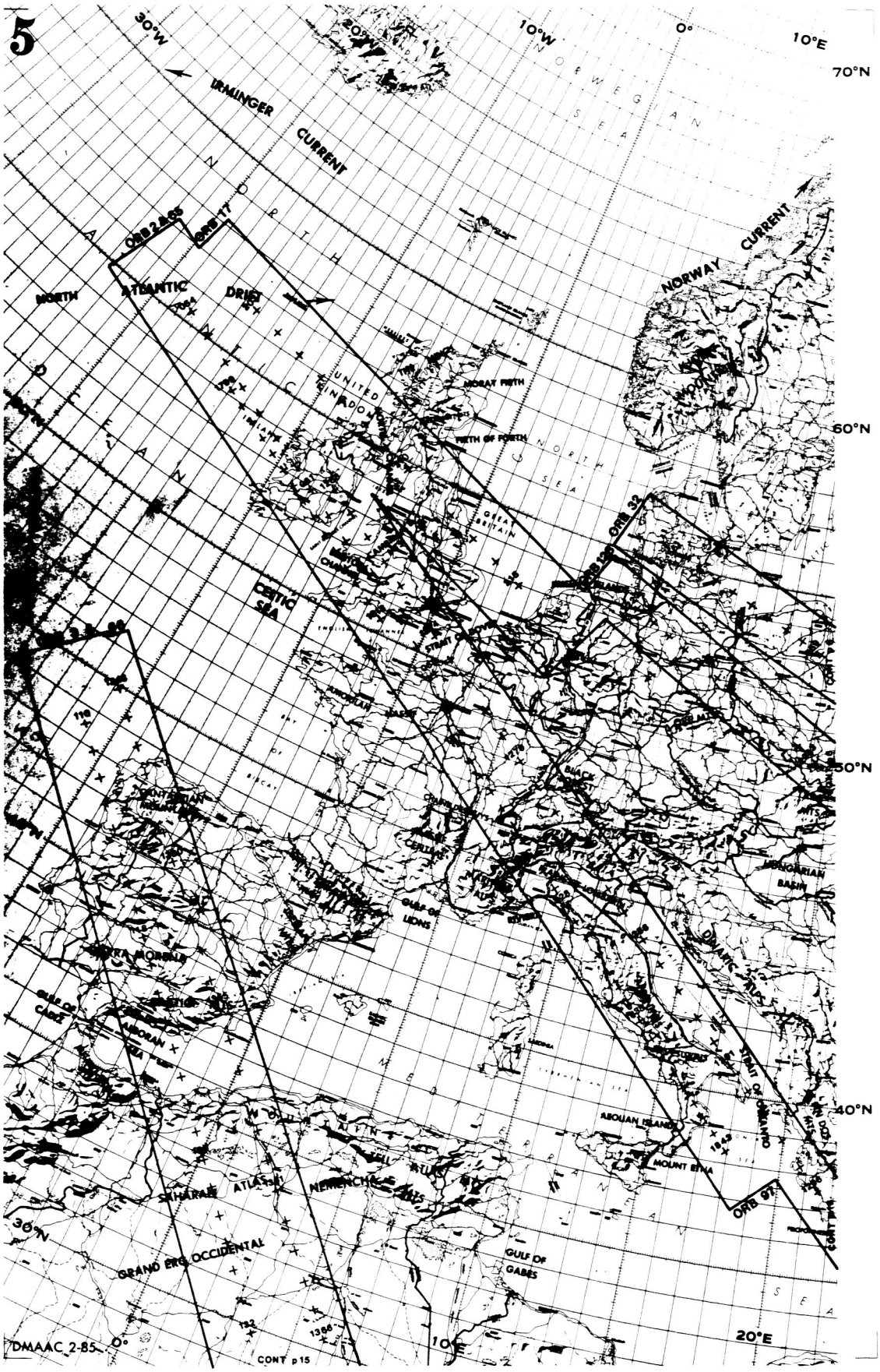
4. In all cases, the direction of flight is from the upper to lower portion of the map when the map is positioned for reading (e.g., always from a northerly to southerly direction).

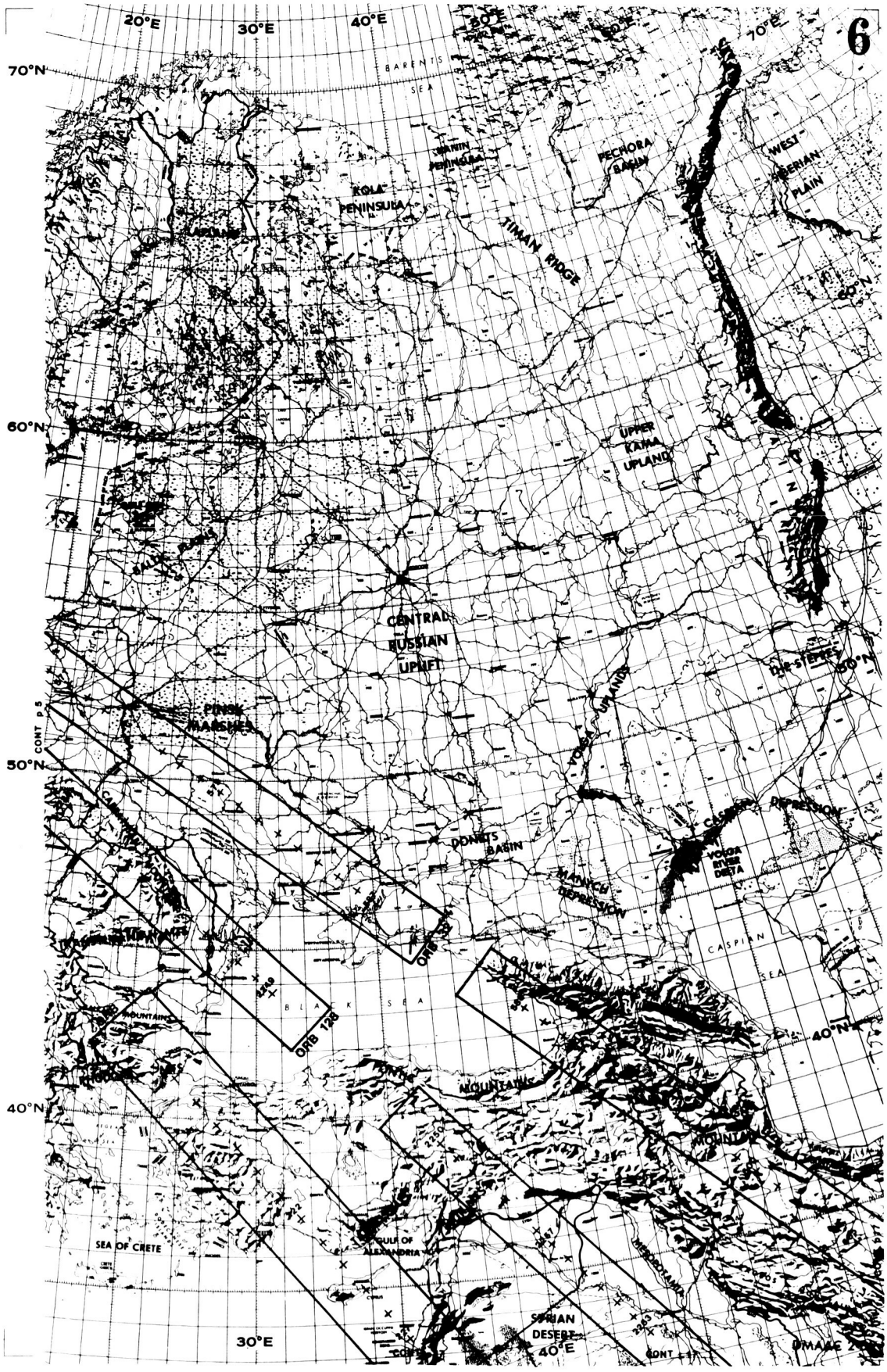
5. The orbit number of the acquisition is also shown for each LFC data pass. In many instances a given data pass is continued from one map to another. Accordingly, the reviewer must note this when he uses the world map index sheet facing this page.

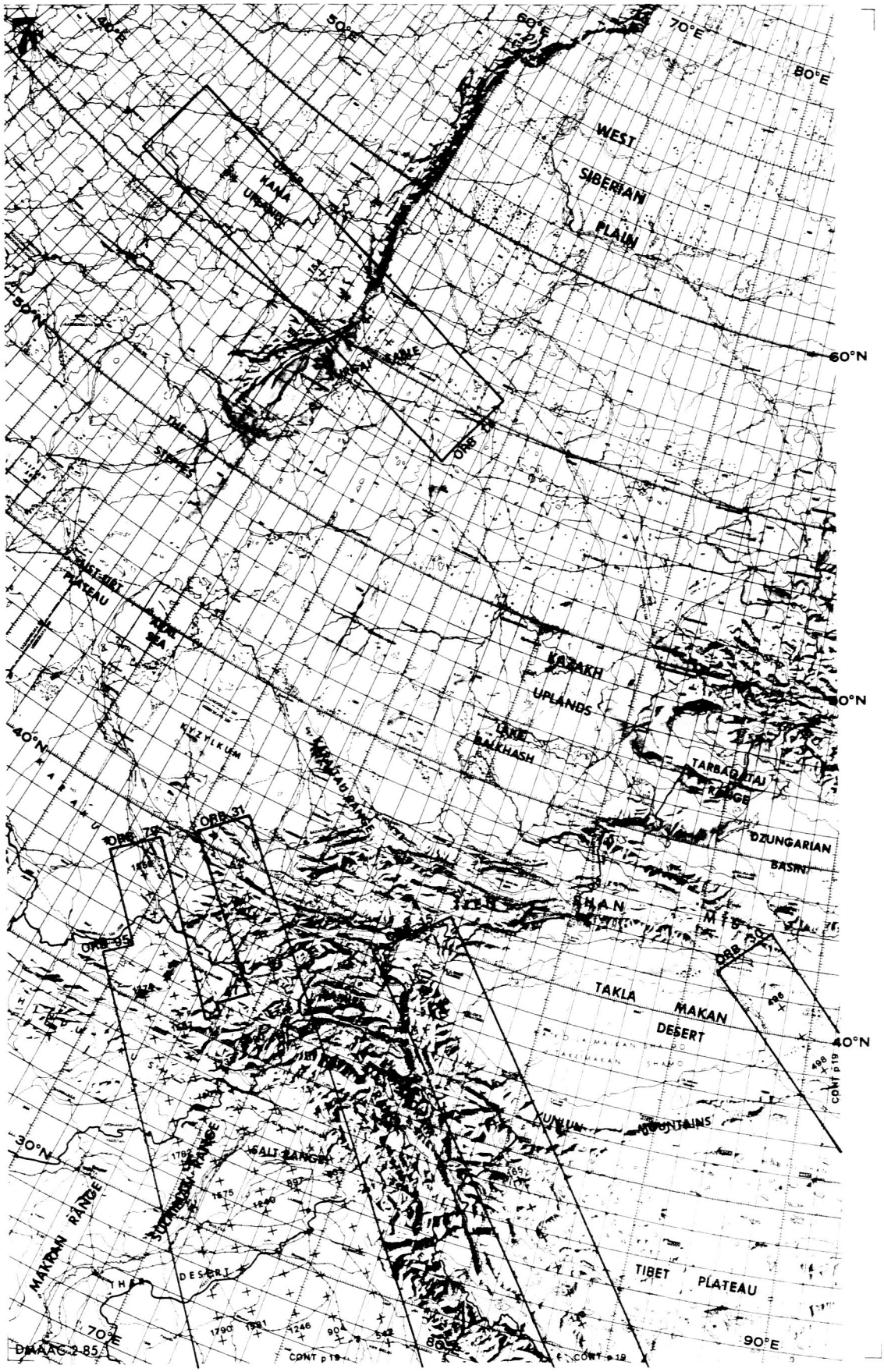

140°W
130°W
120°W
110°W
100°W
90°W
80°W
70°W
60°W
70°N
60°N
50°N
90°N
MACKENZIE MTS
FRANKLIN MTS
PEACOCK HILLS
PRATT MTS
YUKON PLATEAU
HORN PLATEAU
CAMERON HILLS
OTHER BOU
CLEAR HILLS
SILKINE MOUNTAINS
HUDSON
LAURENTIAN
BIRCH MTS
SWAN HILLS
MOSTOUS HILLS
FRASER PLATEAU
NORTH PACIFIC OCEAN
GREAT SAND HILLS
TOUCHWOOD HILLS
CONT p 2
CONT p 2
CONT p 2
CONT p 3

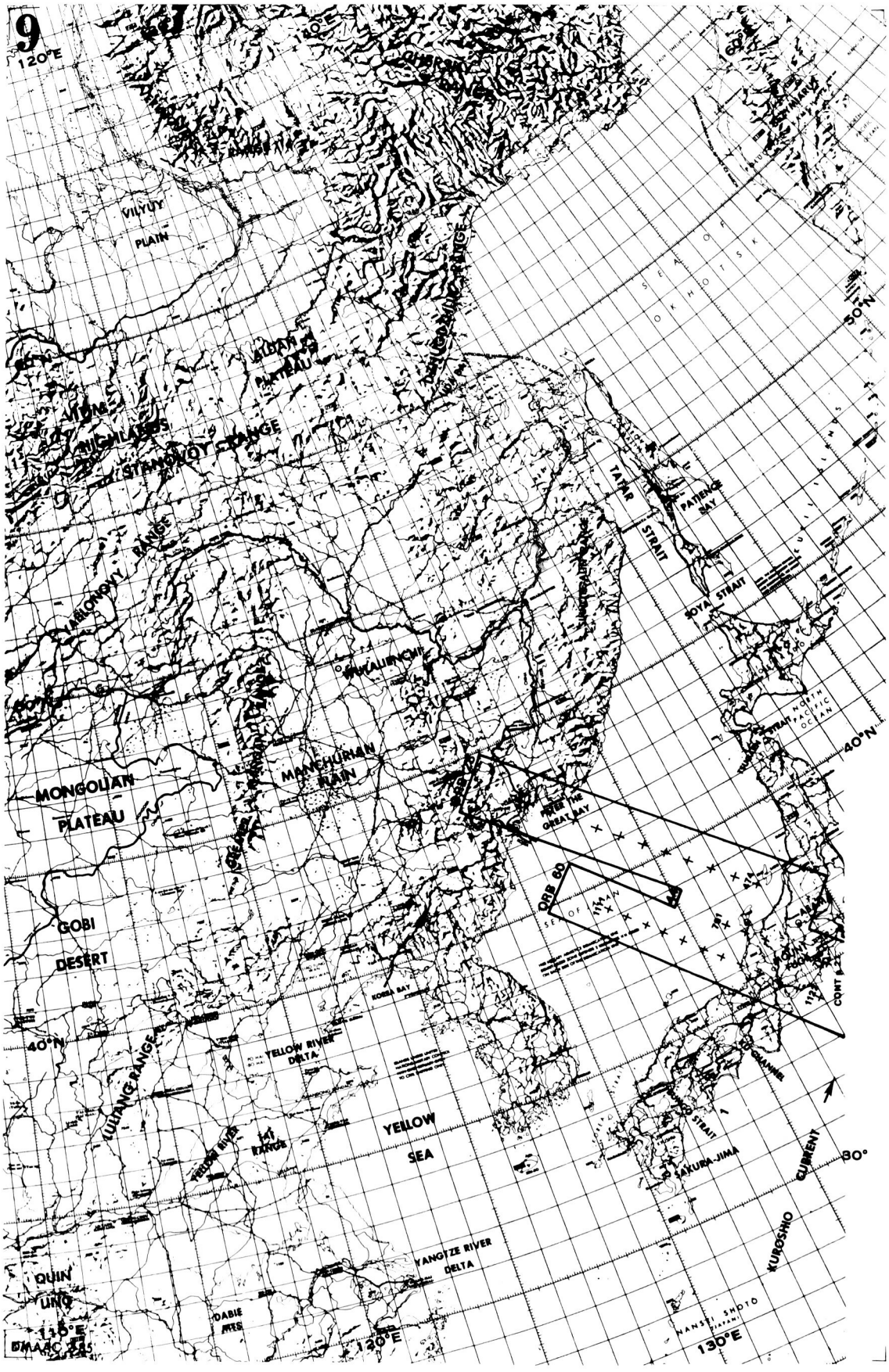

120°W
110°W
CONT p1
100°W
90°W
CONT p1
80°W
ORB 139
40°N
30°N
CALIFORNIA CURRENT
NORTH PACIFIC OCEAN
NORTH ATLANTIC OCEAN
GULF OF MEXICO
GREAT BASIN
COLORADO PLATEAU
OZARK PLATEAU
EDWARDS PLATEAU
MEXICAN PLATEAU
APALACHICOLA BAY
MISSISSIPPI RIVER DELTA
110°W
CONT p11
100°W
CONT p11
90°W
80°W
CONT p12

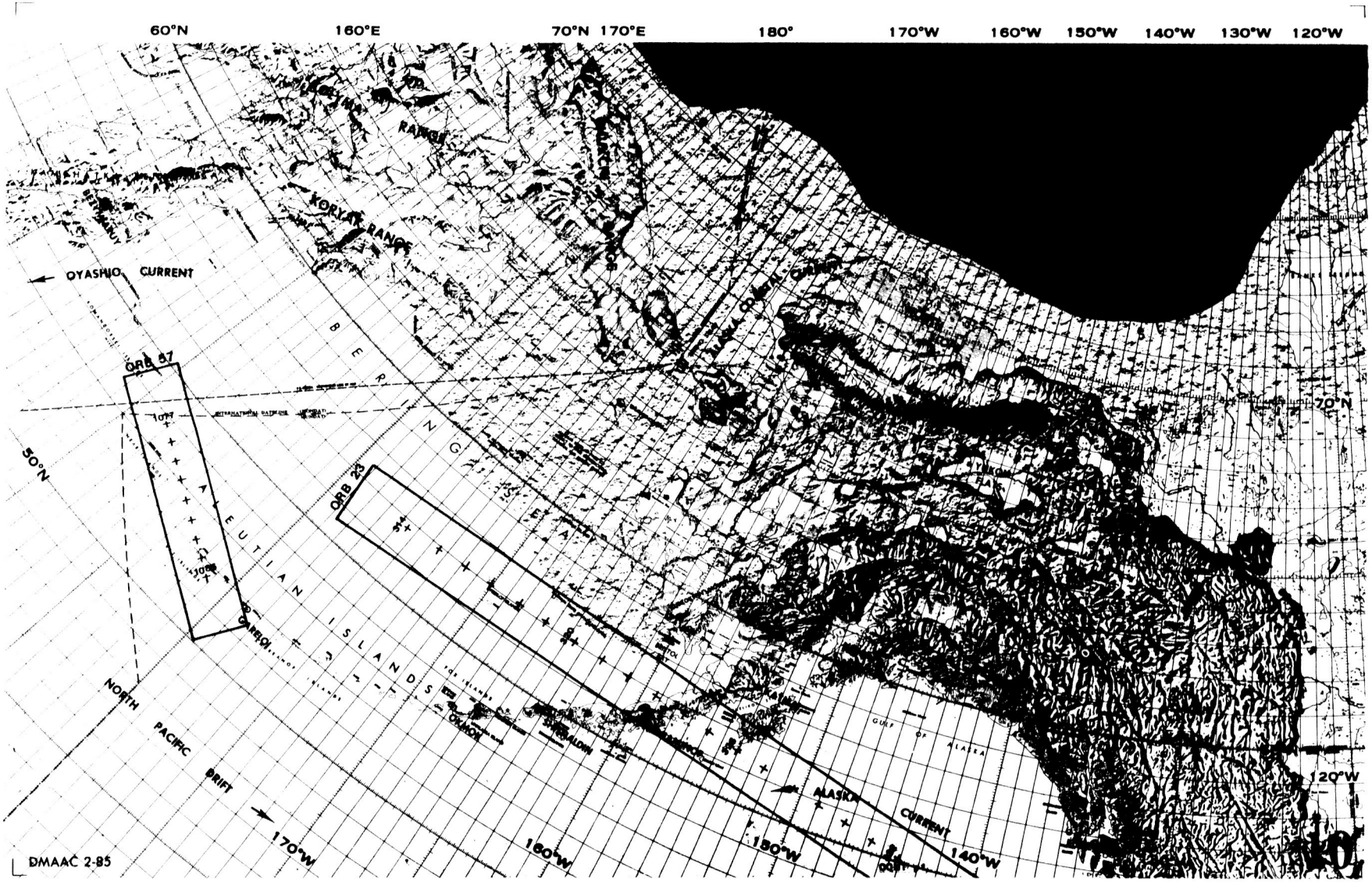

70°N
60°N
50°N
40°N
90°W
80°W
70°W
60°W
50°W
LABRADOR
UPLAND
GULF OF ST LAWRENCE
MEAL MTS
PLACENTIA
AVALON PENINSULA
GRAND BANKS
281
ORB 21
STREAM
673
ORB 37
GULF
NORTH ATLANTIC OCEAN
DMAAC 2-85

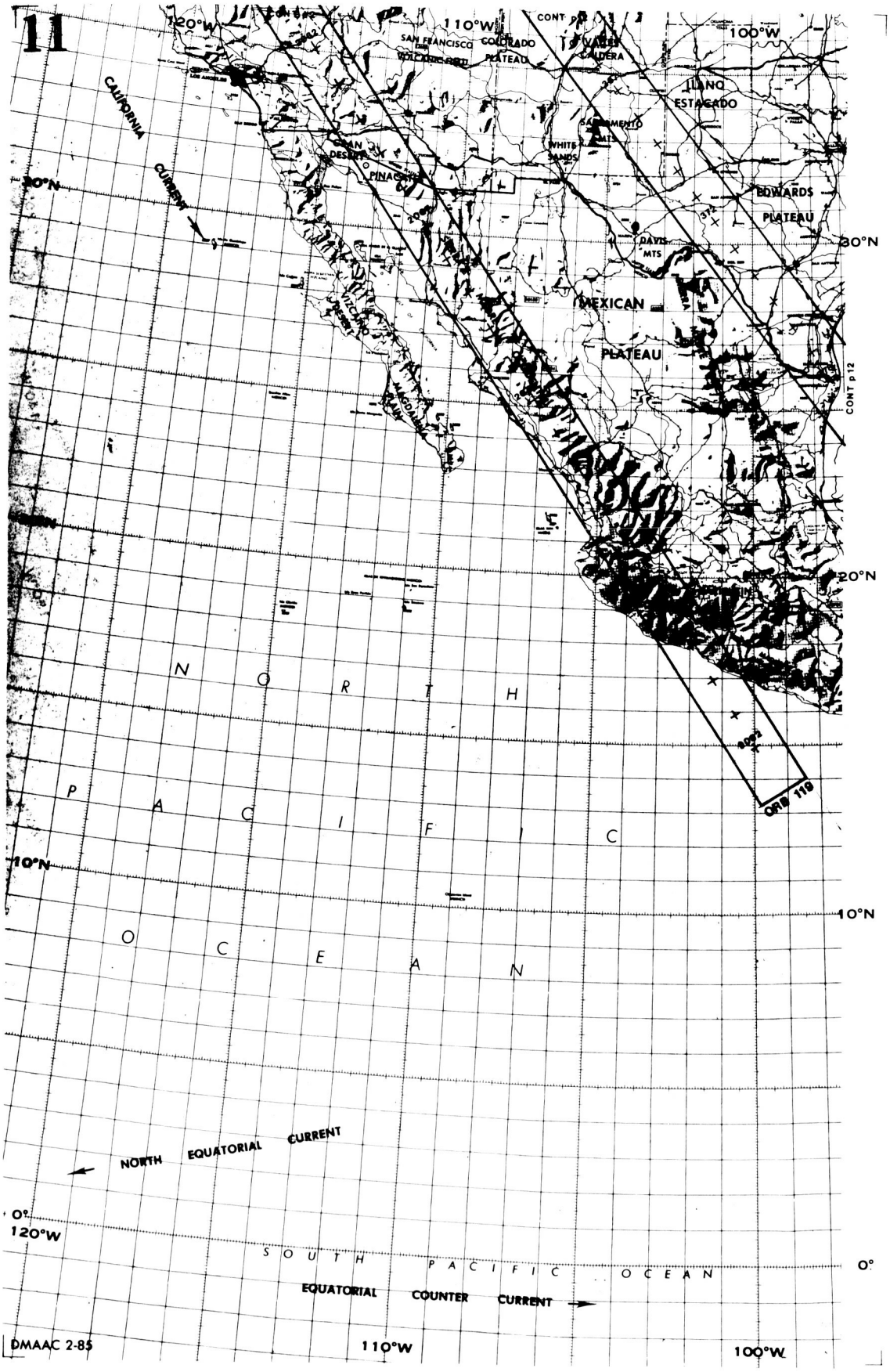

5
30°W
20°W
10°W
0°
10°E
20°E
70°N
60°N
50°N
40°N
30°N
IRMINGER CURRENT
NORWAY CURRENT
NORTH ATLANTIC DRIFT
NORTH ATLANTIC DRIFT
NORWEGIAN SEA
NORTH SEA
ICELAND
UNITED KINGDOM
NORAY FIRTH
FIRTH OF FORTH
GREAT BRITAIN
ORB 2.65
ORB 17
ORB 32
ORB 97
CELTIC SEA
BISCAYAN
GULF OF LIONS
LIGURIAN SEA
TYRRHENIAN SEA
BALEARIC ISLANDS
ALBORAN SEA
ALGERIAN BASIN
STRAIT OF GIBRALTAR
ABOUAN ISLANDS
MOUNT ERVA
SAHARA
ATLAS MTS
GRAND ERG OCCIDENTAL
GULF OF GABES
DMAAC 2-85
CONT p15

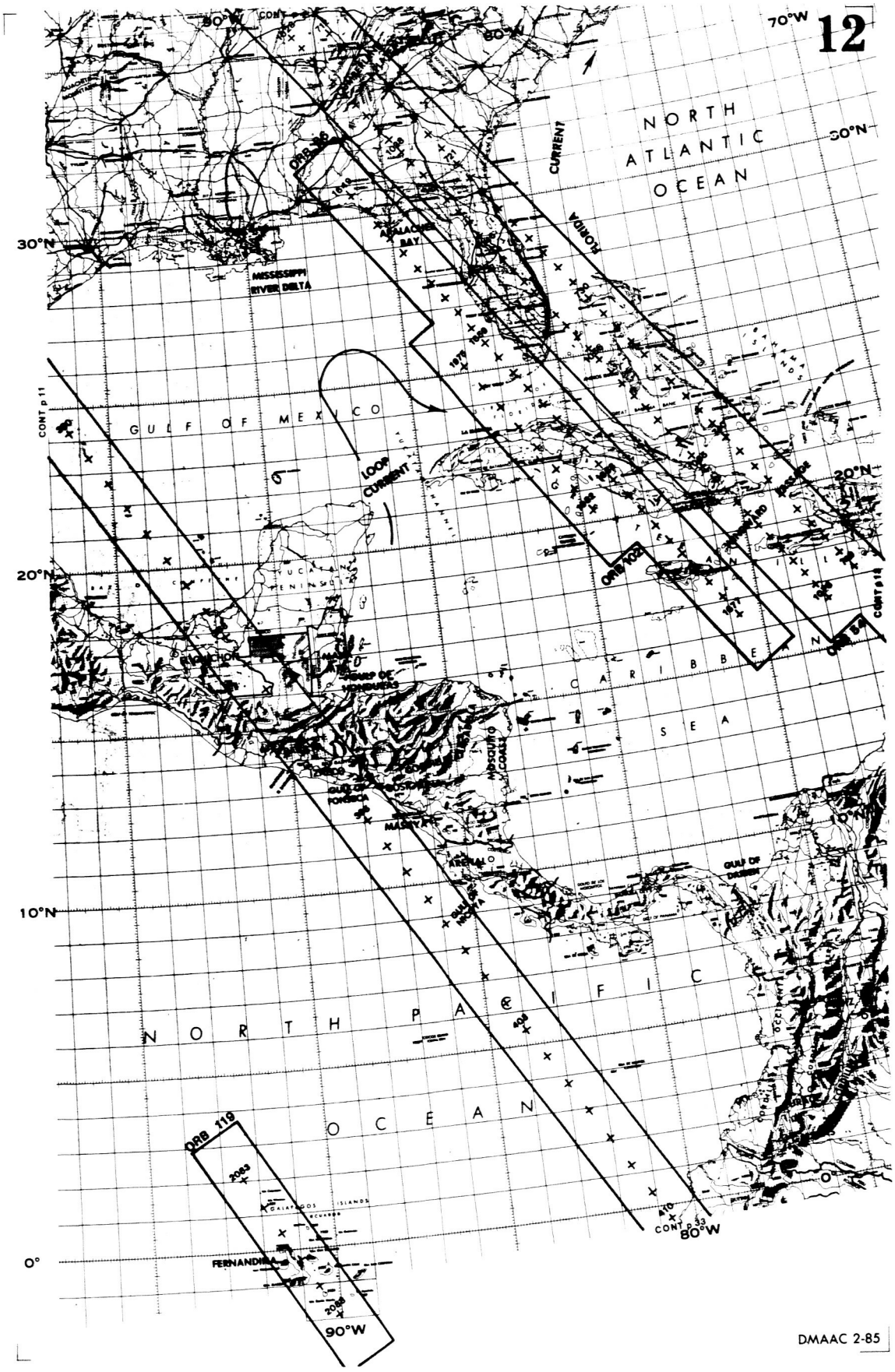

6
20°E
30°E
40°E
50°E
70°E
70°N
60°N
50°N
40°N
30°E
40°E
BARENTS SEA
KOLA PENINSULA
TIMAN RIDGE
PECHORA BASIN
WEST SIBERIAN PLAIN
URAL MTS
UPPER KAMA UPLAND
CENTRAL RUSSIAN UPLIFT
PRIPYAT MARSHES
VOLGA UPLANDS
DNIESTER
DONETS BASIN
MANYCH DEPRESSION
CASPIAN DEPRESSION
VOLGA RIVER DELTA
CASPIAN SEA
BLACK SEA
ORB 128
ORB 129
SEA OF CRETE
GULF OF ALEXANDRIA
SYRIAN DESERT
CONT p 5
CONT p 7

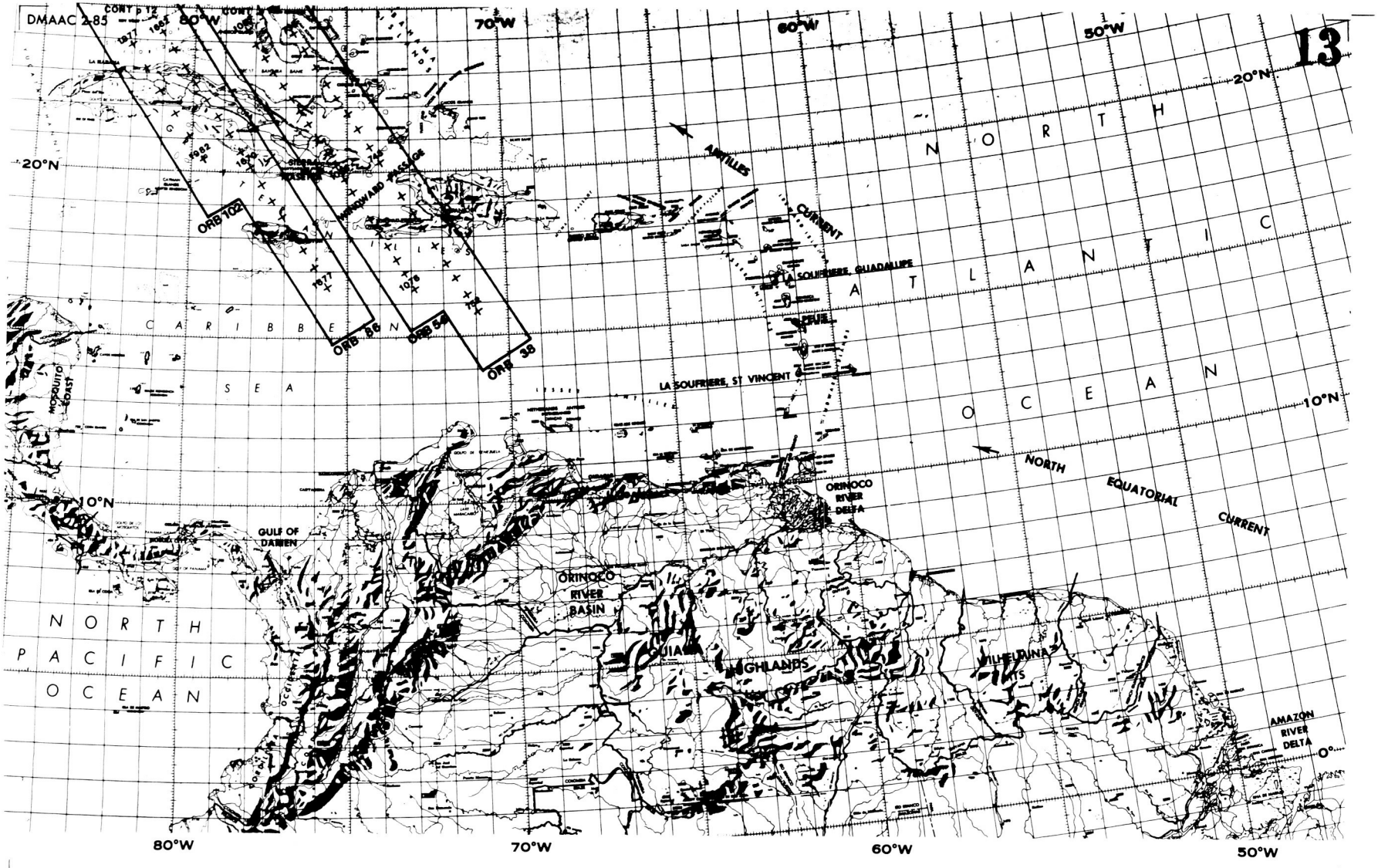

50°E
60°E
70°E
80°E
WEST
SIBERIAN
PLAIN
60°N
50°N
ORB
KAZAKH
UPLANDS
LAKE
BALKHASH
40°N
KYZYLKUM
KARATAU RANGE
TARBAGATAI
RANGE
DZUNGARIAN
BASIN
TIAN
SHAN
Mts
ORB 79
ORB 31
ORB 85
ORB
TAKLA
MAKAN
DESERT
CONT p 19
KUNLUN
MOUNTAINS
30°N
SALT RANGE
SULAIMAN RANGE
MAKRAN RANGE
DESERT
TIBET
PLATEAU
70°E
90°E
DMAAC-2-85
CONT p 19
CONT p 19

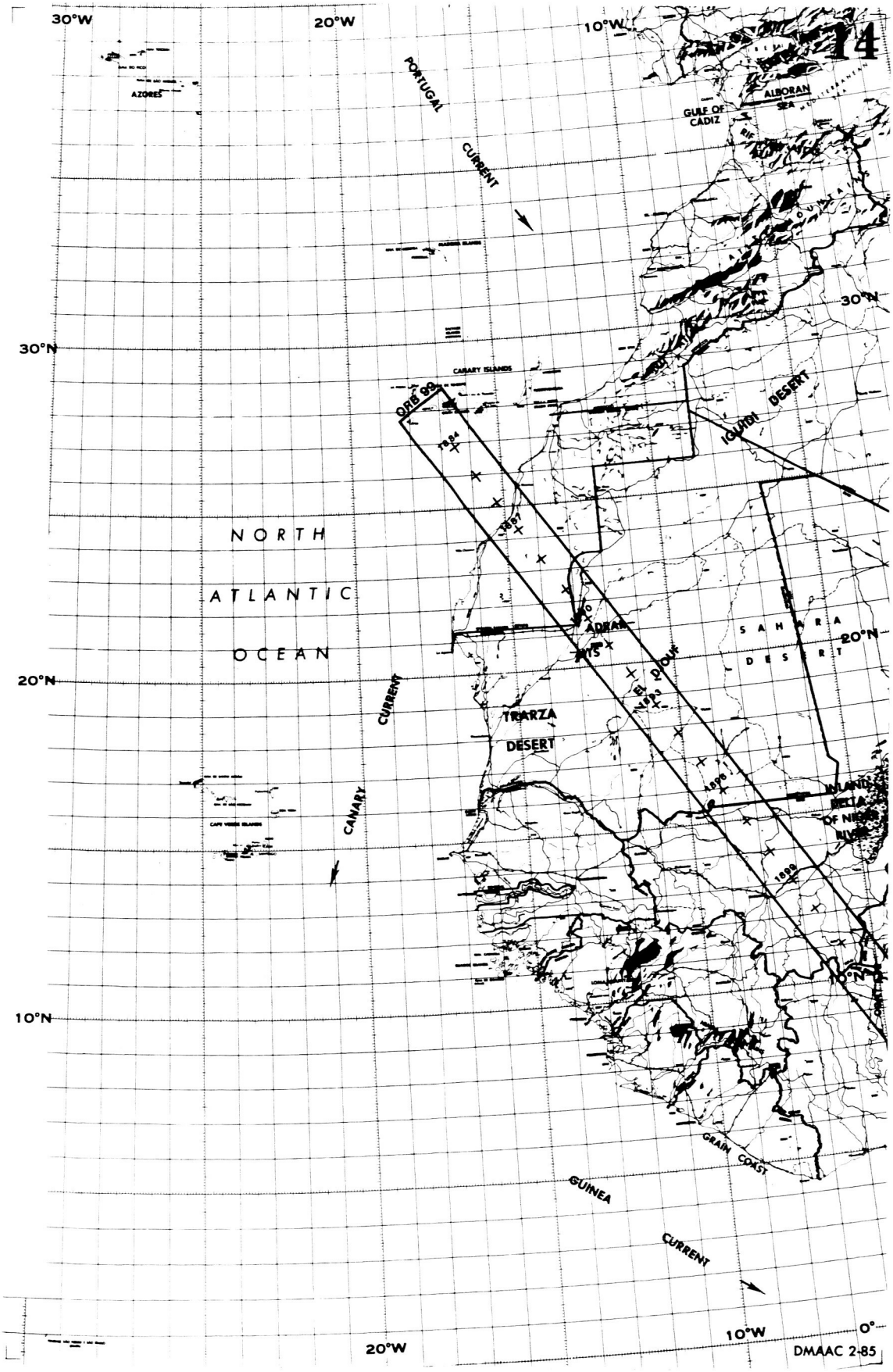

9
120°E
VILYUY
PLAIN
ALDAN
PLATEAU
STANOVOY RANGE
CHERSKIY RANGE
SEA OF OKHOTSK
50°N
TATAR STRAIT
PATIENCE BAY
SOYA STRAIT
SAKHALIN
MANCHURIAN PLAIN
MONGOLIAN PLATEAU
PETER THE GREAT BAY
NORTH PACIFIC OCEAN
40°N
GOBI DESERT
KOREA BAY
YELLOW RIVER DELTA
KUNLUN RANGE
YELLOW SEA
SAKURA-JIMA
KUROSHIO CURRENT
30°
YANGTZE RIVER DELTA
NANSEI SHOTO
130°E
110°E

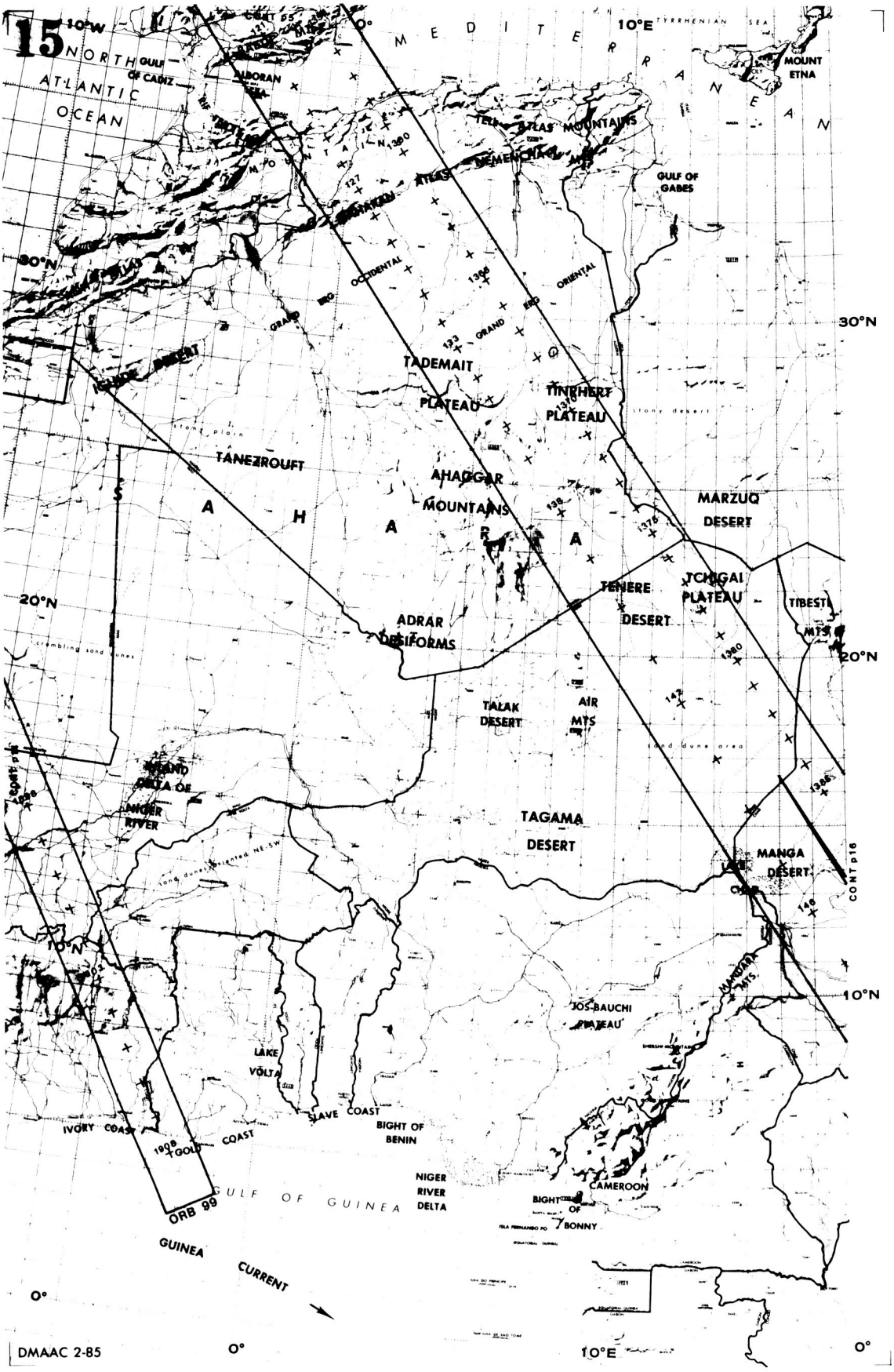

60°N
160°E
70°N 170°E
180°
170°W
160°W
150°W
140°W
130°W
120°W
70°N
50°N
120°W
OYASHIO CURRENT
KORYAK RANGE
ANADYR RANGE
BERING SEA
ALEUTIAN ISLANDS
NORTH PACIFIC DRIFT
ALASKA CURRENT
GULF OF ALASKA
ORB 57
ORB 23
170°W
160°W
150°W
140°W
DMAAC 2-85

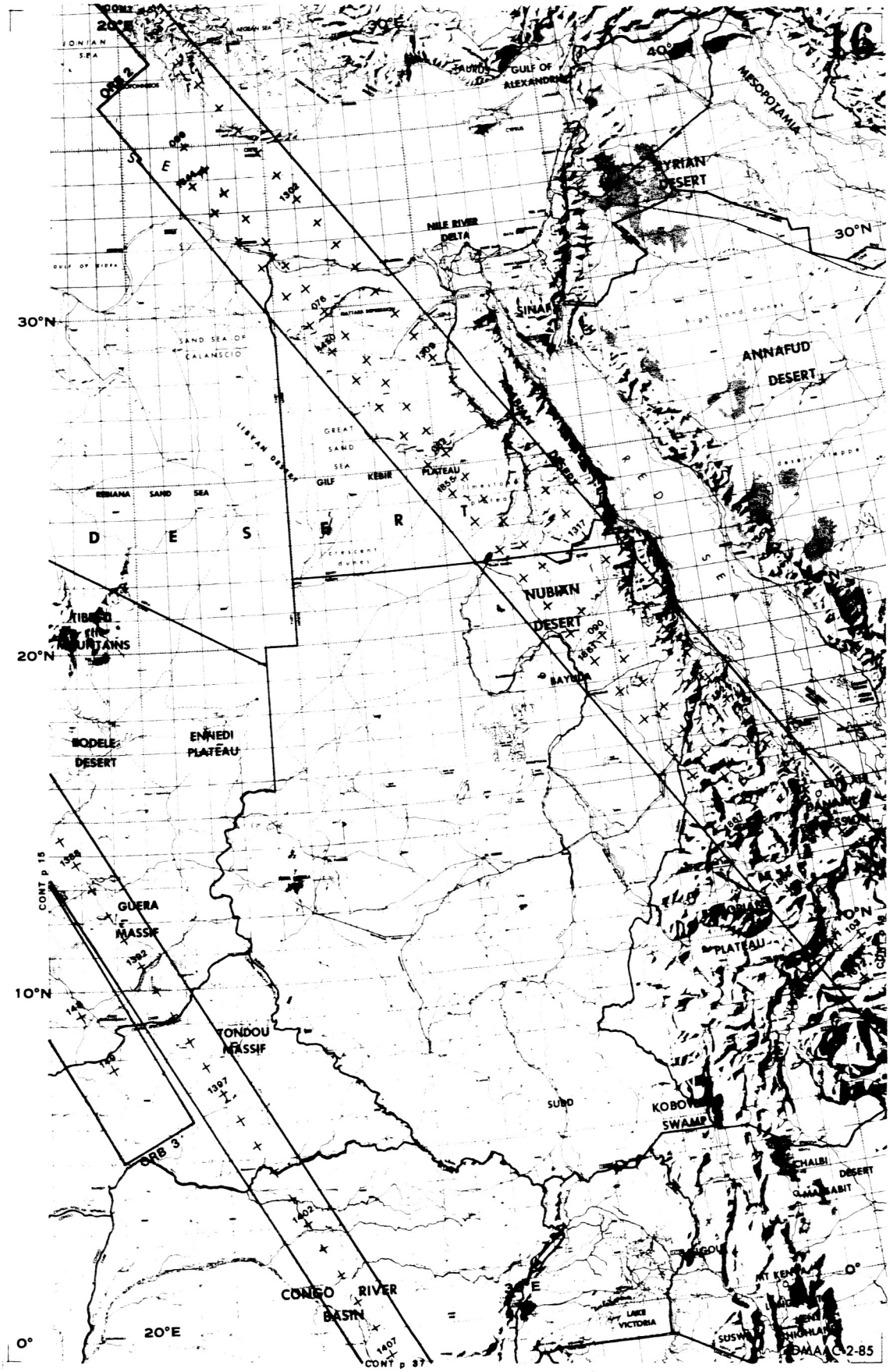

11
120°W
110°W
100°W
CONT p10
SAN FRANCISCO VOLCANIC FIELD
COLORADO PLATEAU
VALLES CALDERA
LLANO ESTACADO
CALIFORNIA CURRENT
SAN DESERTO
PINACATE
CARRIZOZO MTS
WHITE SANDS
BOWARDS PLATEAU
DAVIS MTS
MEXICAN PLATEAU
VIZCAINO DESERT
MAGDALENA PLAIN
CONT p12
30°N
20°N
10°N
0°
N O R T H
P A C I F I C
O C E A N
ORB 119
NORTH EQUATORIAL CURRENT
SOUTH PACIFIC OCEAN
EQUATORIAL COUNTER CURRENT
DMAAC 2-85

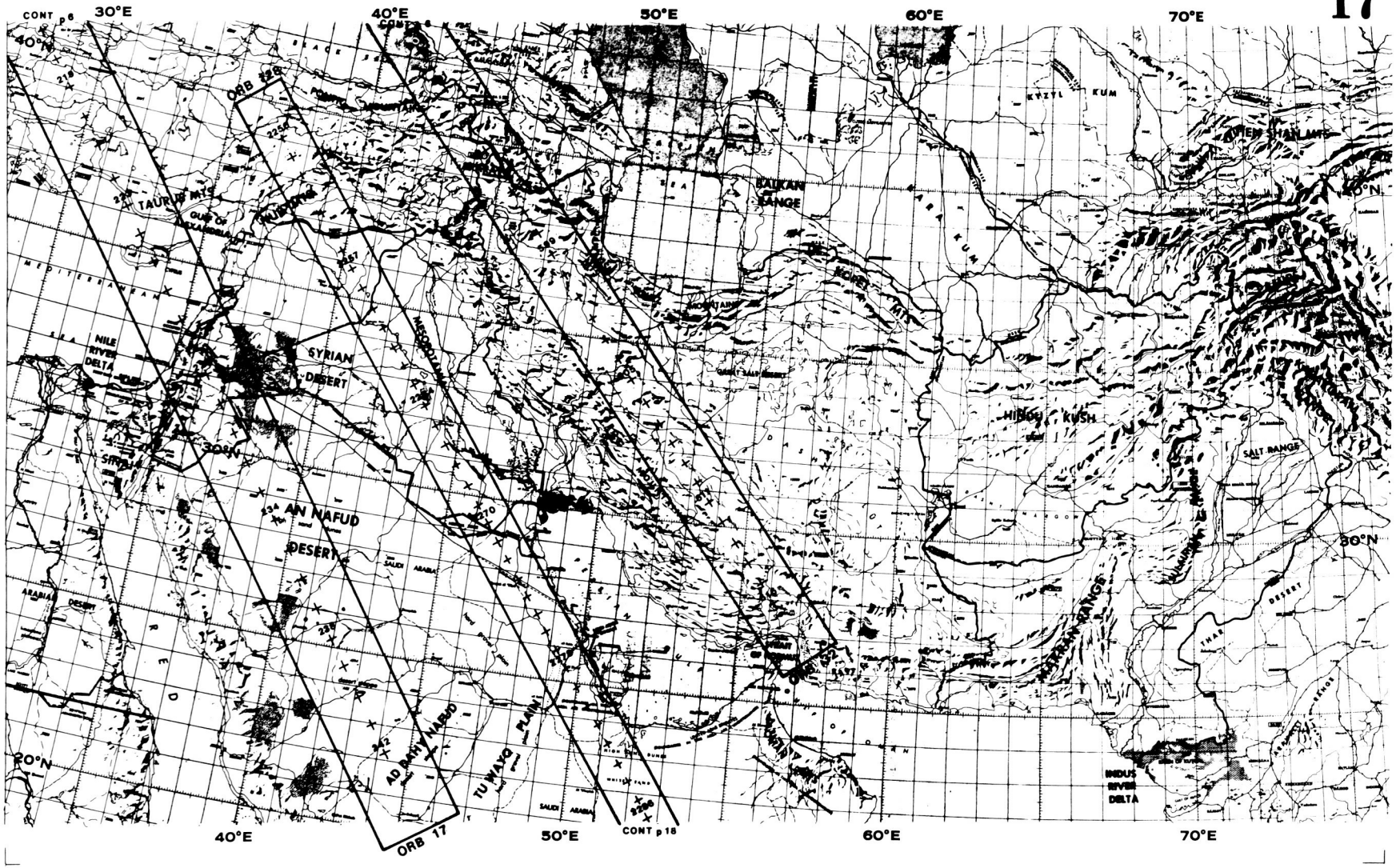

12
70°W
80°W
90°W
30°N
20°N
10°N
0°
NORTH ATLANTIC OCEAN
GULF OF MEXICO
CARIBBEAN SEA
NORTH PACIFIC OCEAN
LOOP CURRENT
FLORIDA CURRENT
MISSISSIPPI RIVER DELTA
APALACHEE BAY
YUCATAN PENINSULA
ORB 103
ORB 119
FERNANDINA
CONT p 11
CONT p 33
DMAAC 2-85

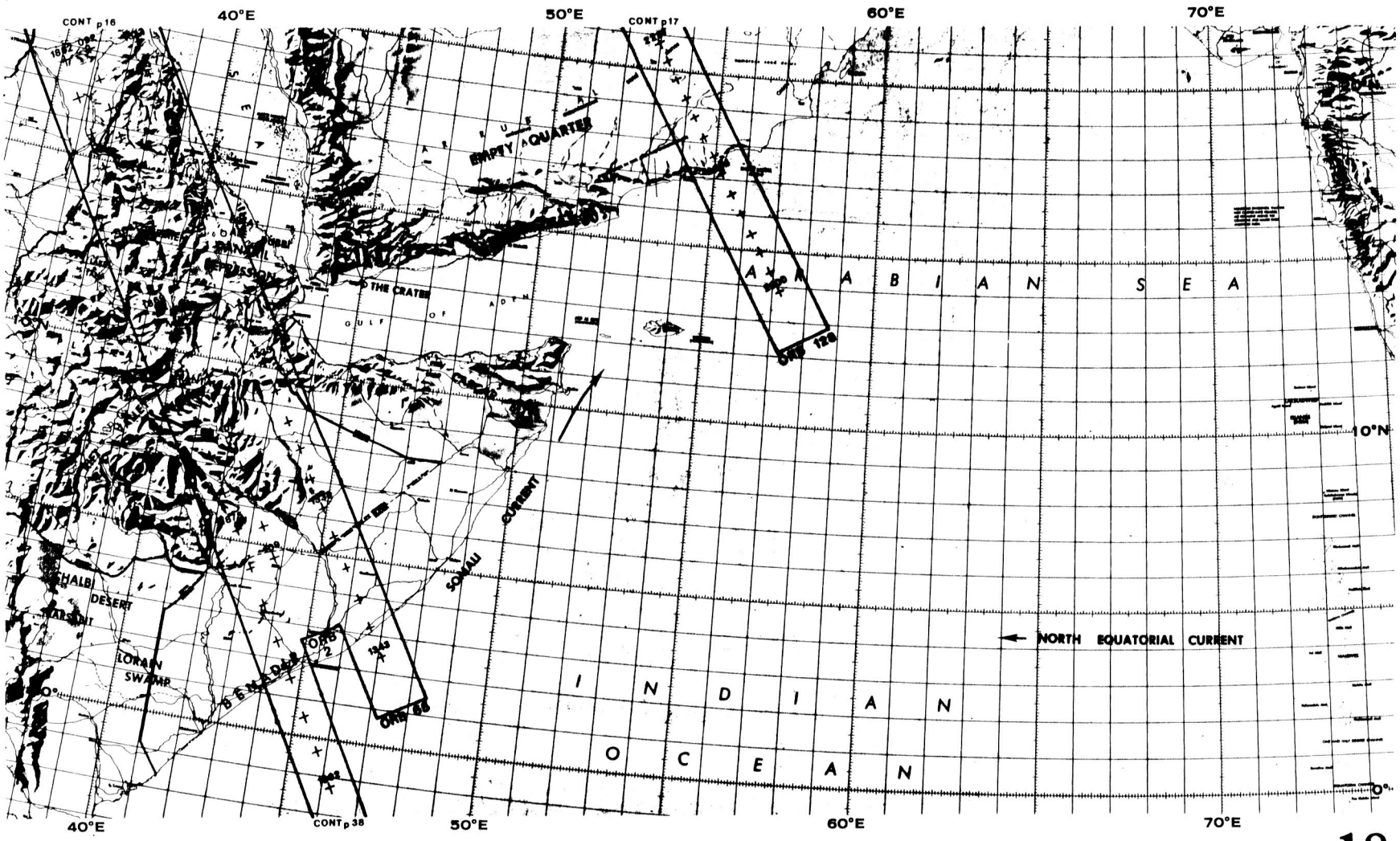

DMAAC 2-85
13
80°W
70°W
60°W
50°W
20°N
10°N
0°
ORB 102
ORB 86
ORB 54
ORB 38
CONT D 12
CONT D 13
NORTHWARD PASSAGE
ANTILLES CURRENT
SOUFRIERE, GUADALUPE
LA SOUFRIERE, ST VINCENT
NORTH EQUATORIAL CURRENT
ORINOCO RIVER DELTA
ORINOCO RIVER BASIN
GULF OF DARIEN
MOSQUITO COAST
AMAZON RIVER DELTA
GUIANA HIGHLANDS
WILHELMINA MTS
CARIBBEAN SEA
NORTH PACIFIC OCEAN
NORTH ATLANTIC OCEAN


14
30°W
20°W
10°W
AZORES
PORTUGAL
CURRENT
GULF OF CADIZ
ALBORAN SEA
30°N
CANARY ISLANDS
ORB 98
IGUIDI DESERT
NORTH
ATLANTIC
OCEAN
ADRAR
SAHARA
DESERT
20°N
EL DJOUF
TRARZA
DESERT
CANARY
CURRENT
CAPE VERDE ISLANDS
INLAND DELTA OF NIGER RIVER
10°N
GRAIN COAST
GUINEA
CURRENT
0°
DMAAC 2-85


15
10°W
NORTH ATLANTIC OCEAN
GULF OF CADIZ
ALBORAN SEA
ATLAS MOUNTAINS
MEMENCHA
GULF OF GABES
MEDITERRANEAN
TYRRHENIAN SEA
MOUNT ETNA
10°E
0°
30°N
20°N
10°N
TADEMAIT PLATEAU
TINRHERT PLATEAU
TANEZROUFT
AHAGGAR MOUNTAINS
SAHARA
MARZUQ DESERT
TENERE DESERT
TCHIGAI PLATEAU
TIBESTI MTS
ADRAR DEGIFORMS
TALAK DESERT
AIR MTS
TAGAMA DESERT
MANGA DESERT
CONT p16
GRAND DELTA DE L'ANGER RIVER
JOS-BAUCHI PLATEAU
MANDARA MTS
LAKE VOLTA
IVORY COAST
GOLD COAST
SLAVE COAST
BIGHT OF BENIN
NIGER RIVER DELTA
CAMEROON
BIGHT OF BONNY
GULF OF GUINEA
ORB 99
GUINEA CURRENT
DMAAC 2-85

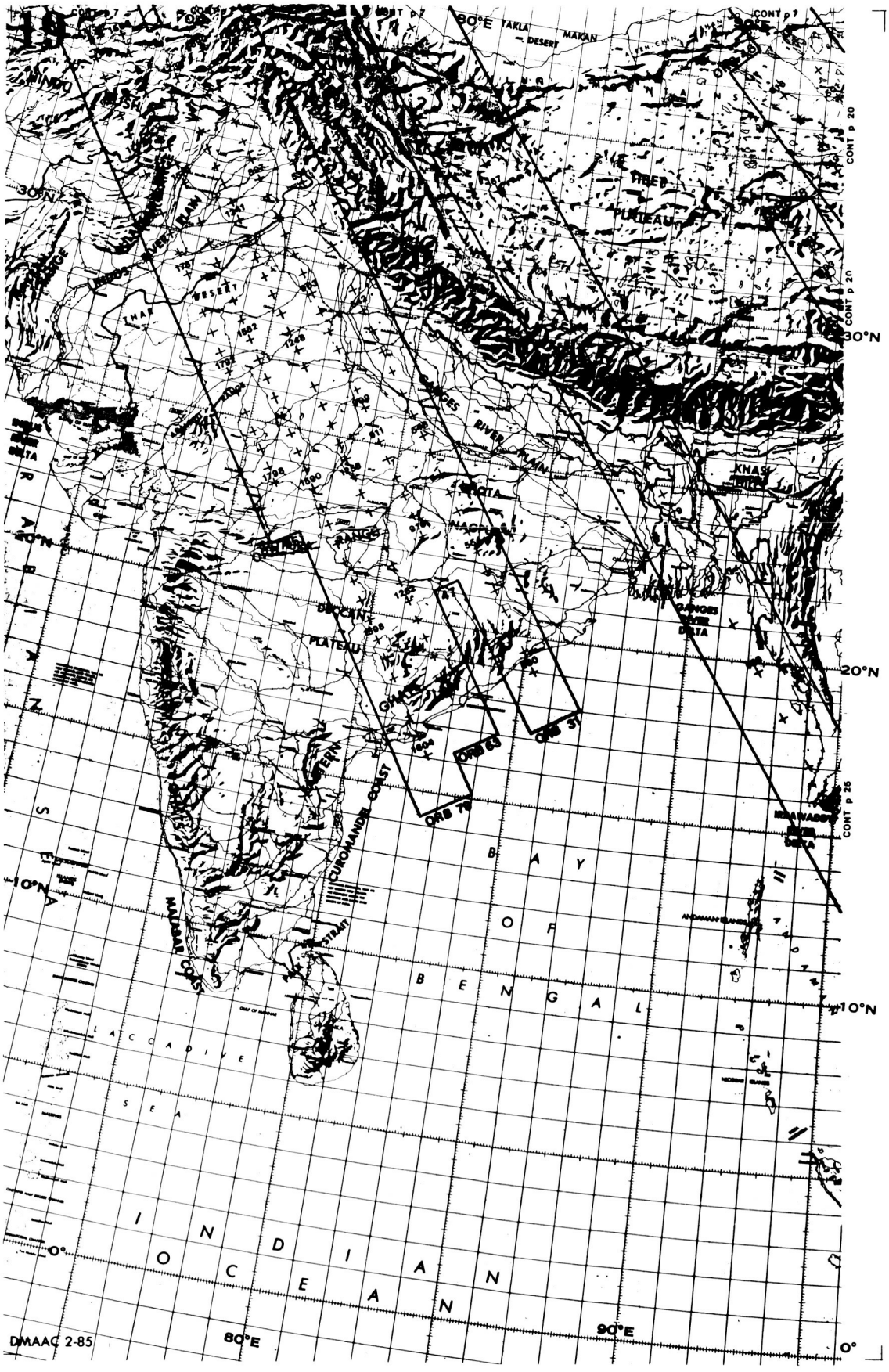

20°E
30°E
40°
GULF OF ALEXANDRIA
MESOPOTAMIA
SYRIAN DESERT
NILE RIVER DELTA
30°N
SINAI
ANNAFUD DESERT
SAND SEA OF CALANSCIO
GREAT SAND SEA
GILF KEBIR PLATEAU
LIBYAN DESERT
EGYPTIAN DESERT
D E S E R T
NUBIAN DESERT
BAYUDA
TIBESTI MOUNTAINS
BODELE DESERT
ENNEDI PLATEAU
GUERA MASSIF
TONDOU MASSIF
SUDD
KOBO SWAMP
CHALBI DESERT
ORB 3
CONGO RIVER BASIN
LAKE VICTORIA
20°N
10°N
0°
CONT p 15
CONT p 37
DMAAC 2-85

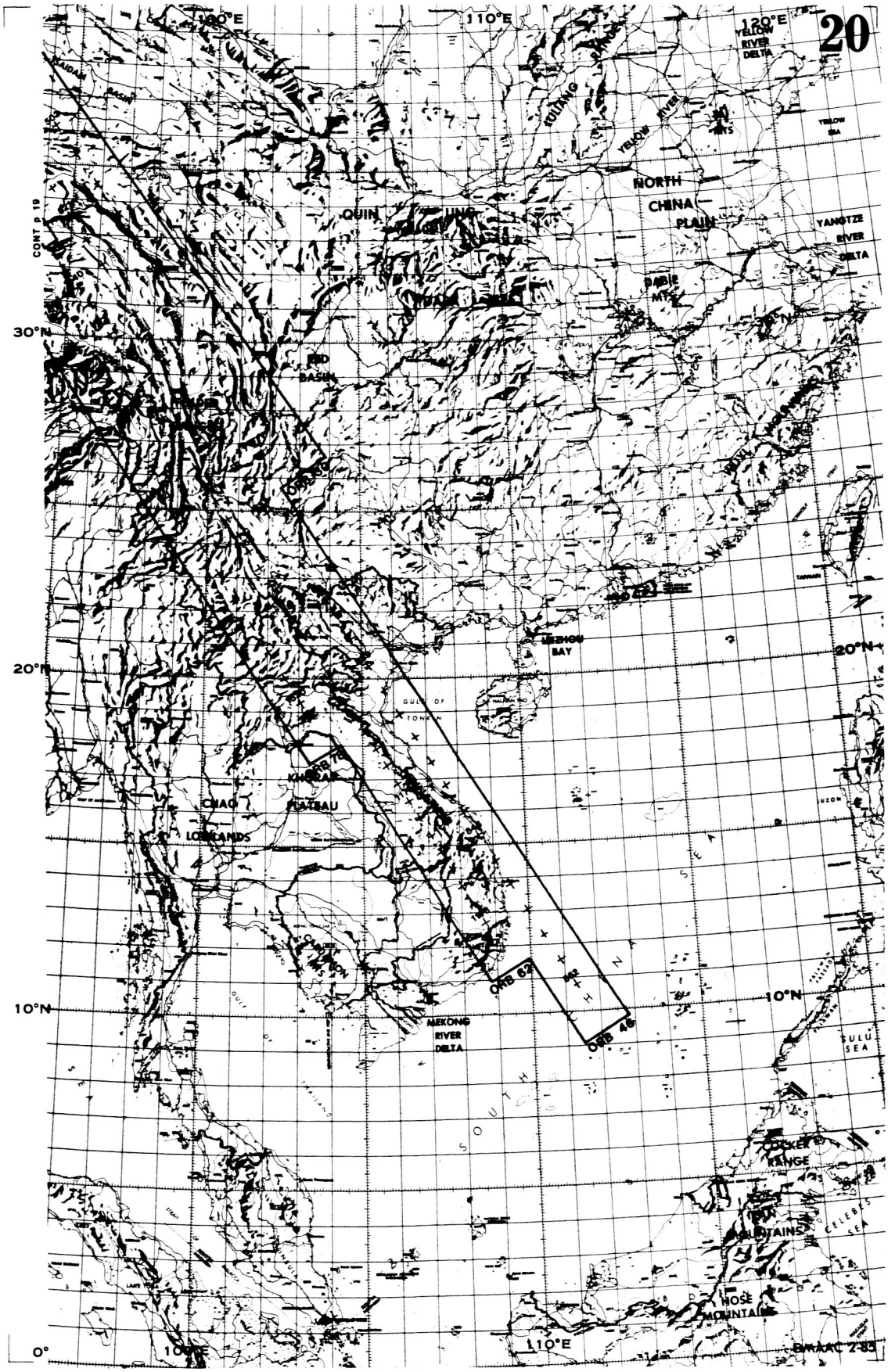

CONT p6
30°E
40°E
50°E
60°E
70°E
40°N
30°N
20°N
ORB 16
ORB 17
TAURUS MTS
GULF OF ALEXANDRETTA
MEDITERRANEAN SEA
NILE RIVER DELTA
SYRIAN DESERT
AN NAFUD DESERT
ARABIAN DESERT
RED SEA
AD DAHNA DESERT
TUWAYQ PLAIN
CASPIAN SEA
KARA KUM
KYZYL KUM
KOPET DAG MTS
ELBURZ MTS
ALBORZ MTS
KAVIR DESERT
DASHT-E LUT
HINDU KUSH
SALT RANGE
SULAIMAN RANGE
THAR DESERT
INDUS RIVER DELTA
CONT p18

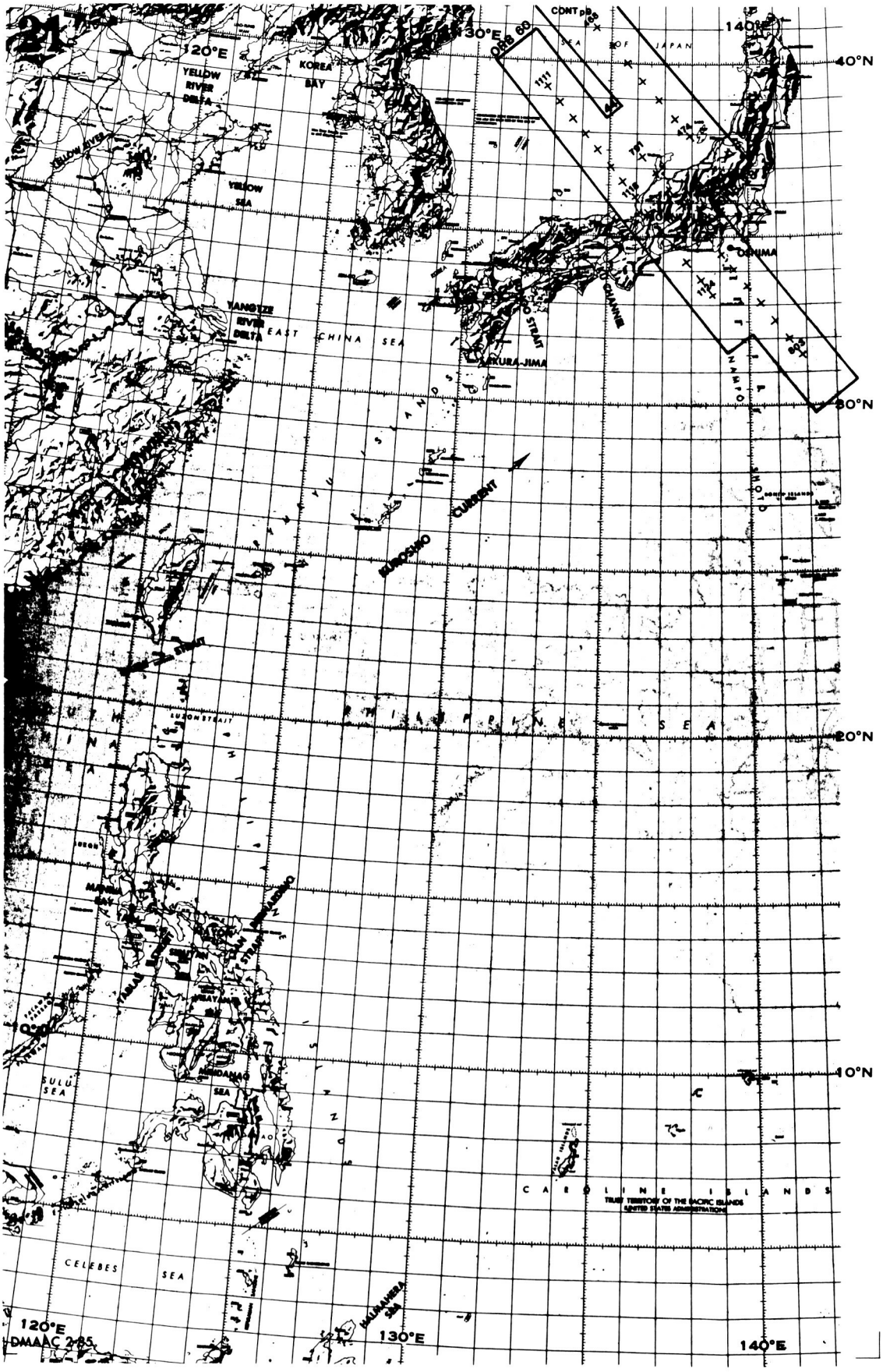

CONT p16
40°E
50°E
CONT p17
60°E
70°E
EMPTY QUARTER
THE CRATER
GULF OF ADEN
ARABIAN SEA
ORB 120
10°N
SOMALI CURRENT
HALBI DESERT
LORAIN SWAMP
BERT DAM
ORB 2
ORB 66
NORTH EQUATORIAL CURRENT
INDIAN OCEAN
0°
CONT p38
40°E
50°E
60°E
70°E

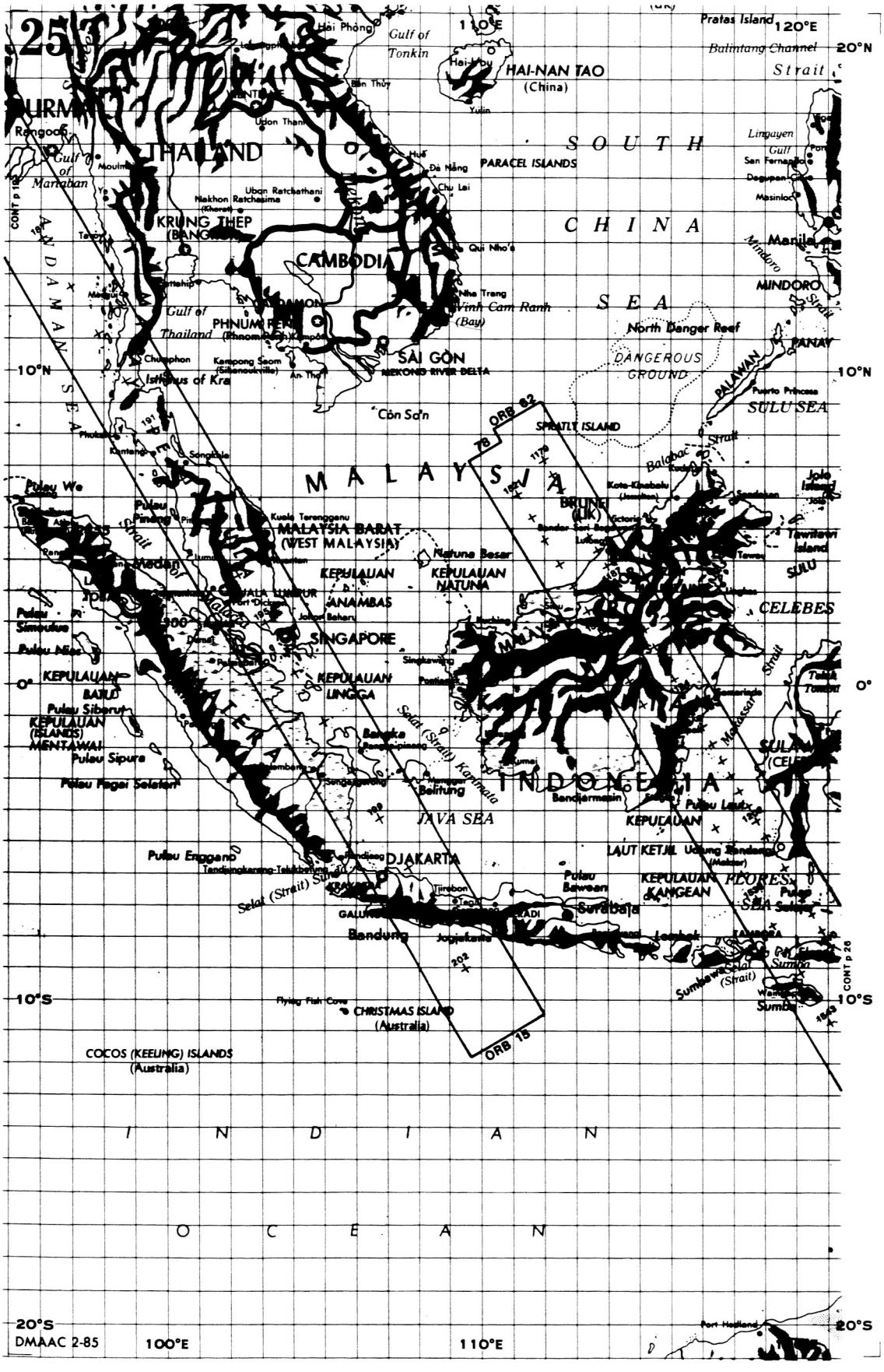
DMAAC 2-85

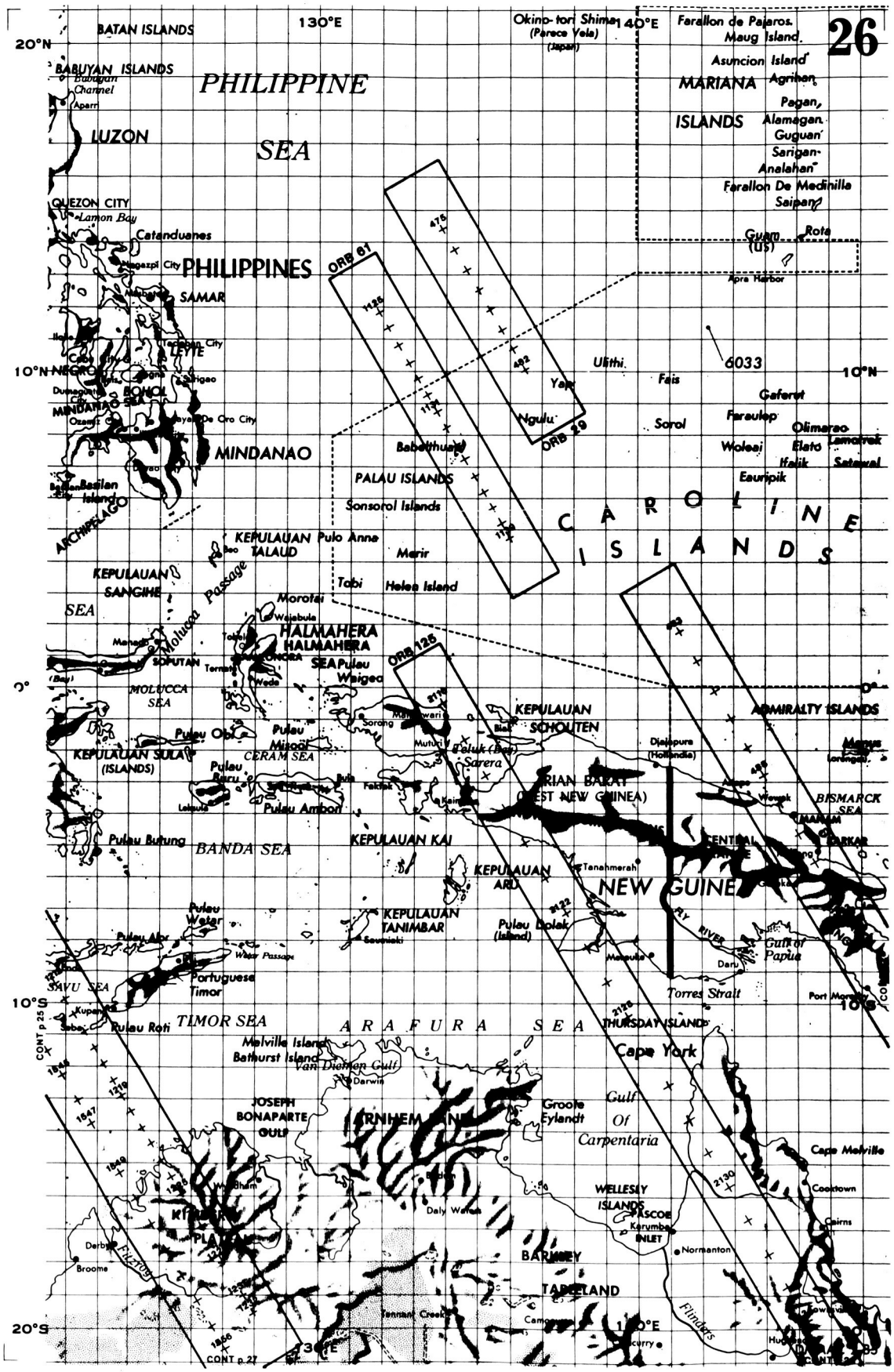
18

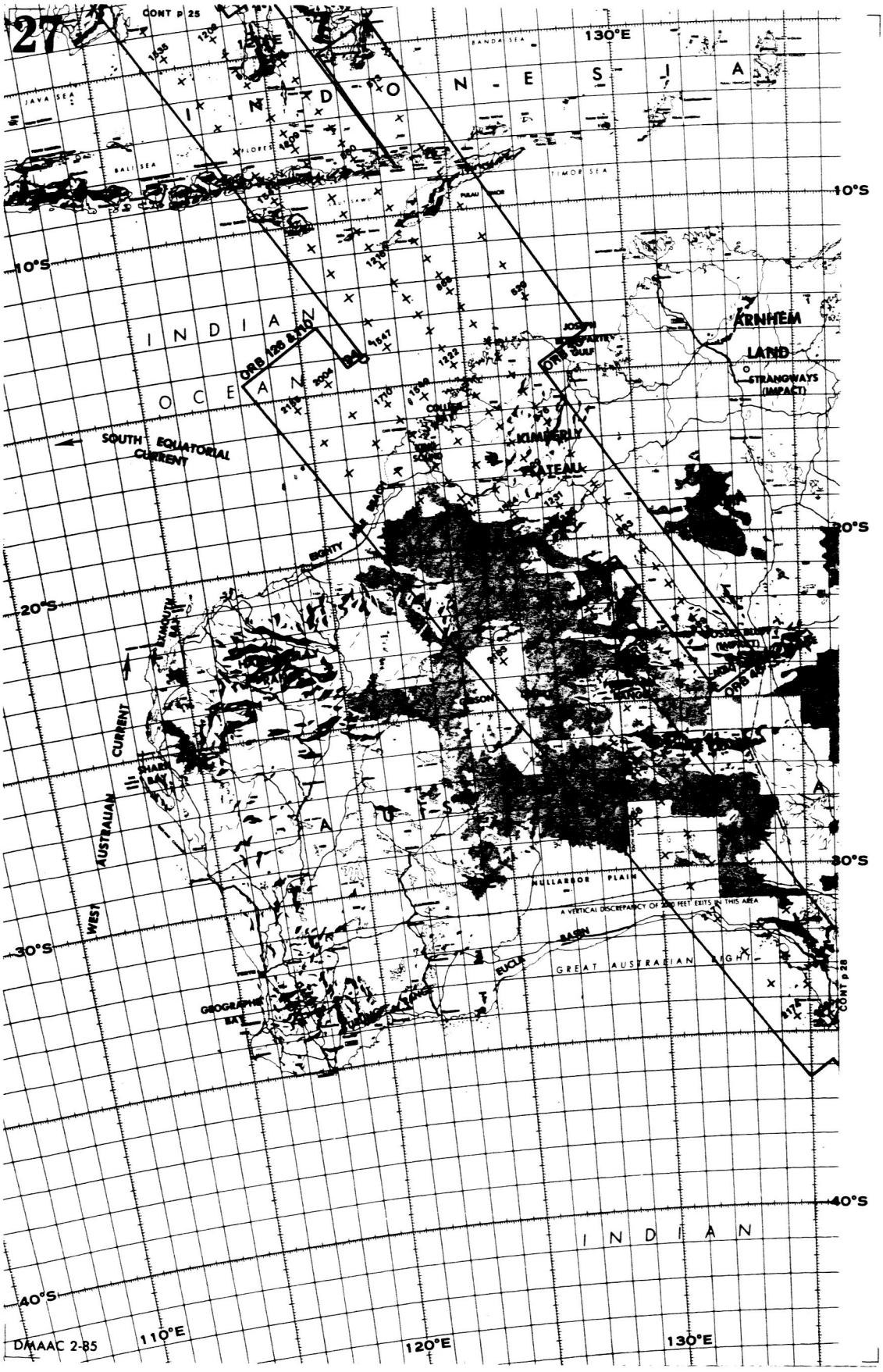

80°E
TAKLA MAKAN DESERT
TIBET PLATEAU
THAR DESERT
INDUS RIVER PLAIN
GANGES RIVER PLAIN
KHASI HILLS
ARAVALLI RANGE
DECCAN PLATEAU
EASTERN GHATS
COROMANDEL COAST
MALABAR COAST
PALK STRAIT
GODAVARI RIVER DELTA
KRISHNA RIVER DELTA
ANDAMAN ISLANDS
BAY OF BENGAL
LACCADIVE SEA
INDIAN OCEAN
ORB 79
ORB 63
ORB 31
CONT p 20
CONT p 25
30°N
20°N
10°N
0°
80°E
90°E
DMAAC 2-85

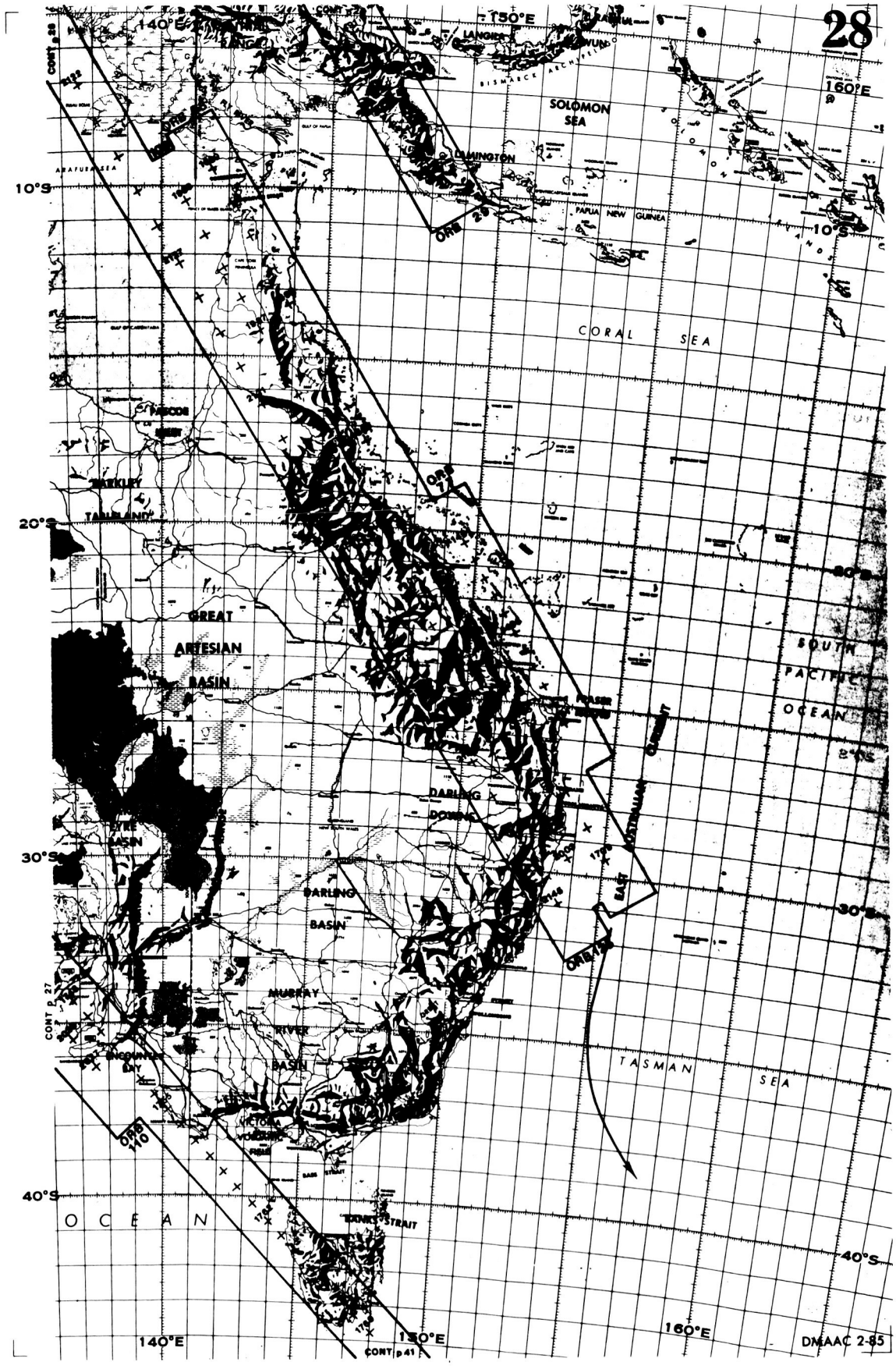

20
100°E
110°E
120°E
30°N
20°N
10°N
0°
CONT P 19
QUIN LING
NORTH CHINA PLAIN
YELLOW RIVER DELTA
YELLOW RIVER
YELLOW SEA
YANGTZE RIVER DELTA
PAIRIE MTS
RED BASIN
HAINAN
TONKIN BAY
GULF OF TONKIN
KHORAT PLATEAU
CHAO PHRAYA LOWLANDS
MEKONG RIVER DELTA
ORB 62
ORB 46
SOUTH CHINA SEA
LUZON
SULU SEA
CROKER RANGE
CELEBES SEA
HOSE MOUNTAINS
BMAAC 2-83

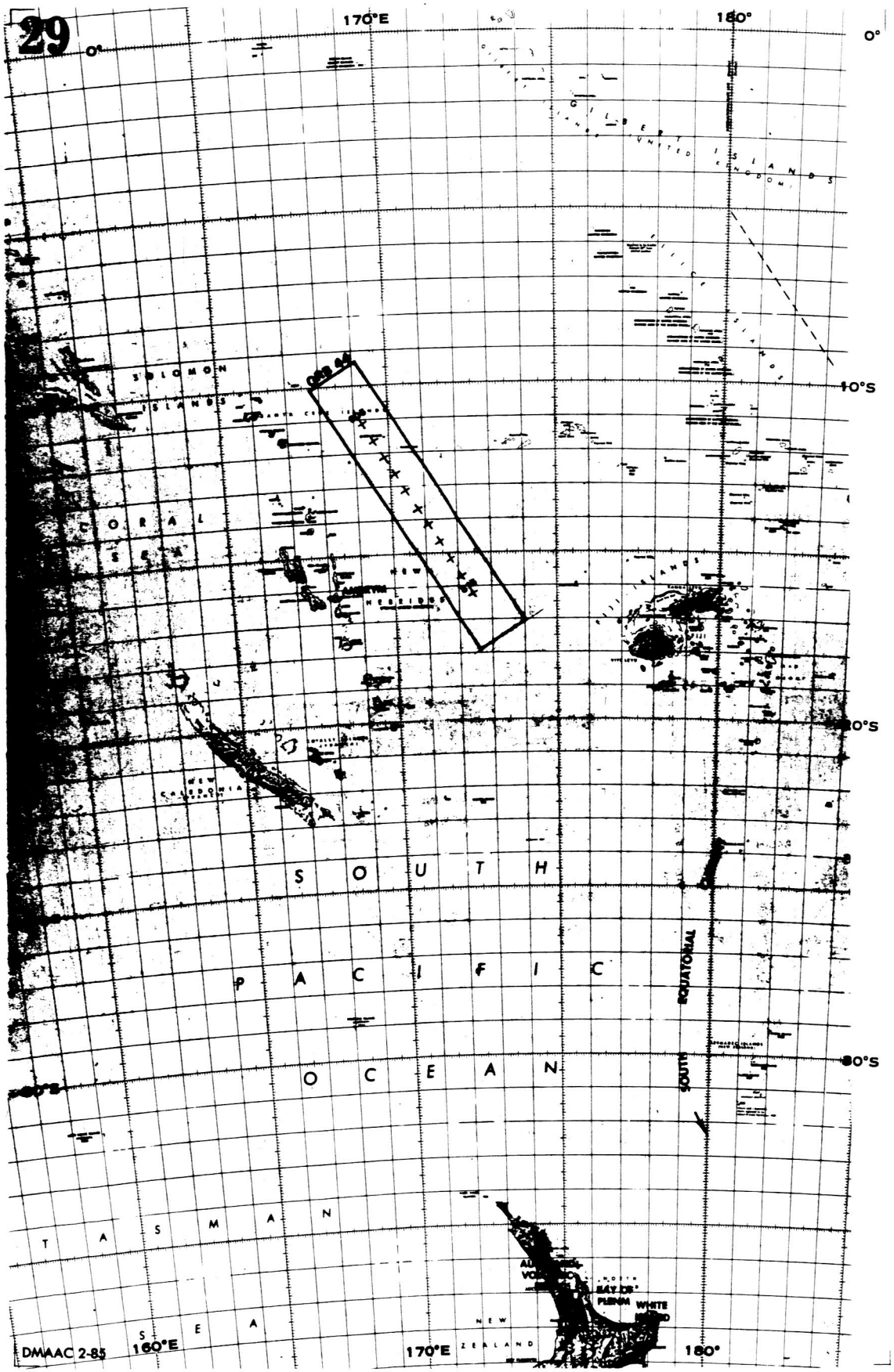

120°E
130°E
140°E
40°N
30°N
20°N
10°N
KOREA BAY
YELLOW RIVER DELTA
YELLOW SEA
YANGTZE RIVER DELTA
EAST CHINA SEA
SEA OF JAPAN
KUROSHIO CURRENT
PHILIPPINE SEA
LUZON STRAIT
SULU SEA
CELEBES SEA
MINDANAO SEA
CAROLINE ISLANDS
TRUST TERRITORY OF THE PACIFIC ISLANDS
UNITED STATES ADMINISTRATION
DMAAC 2385

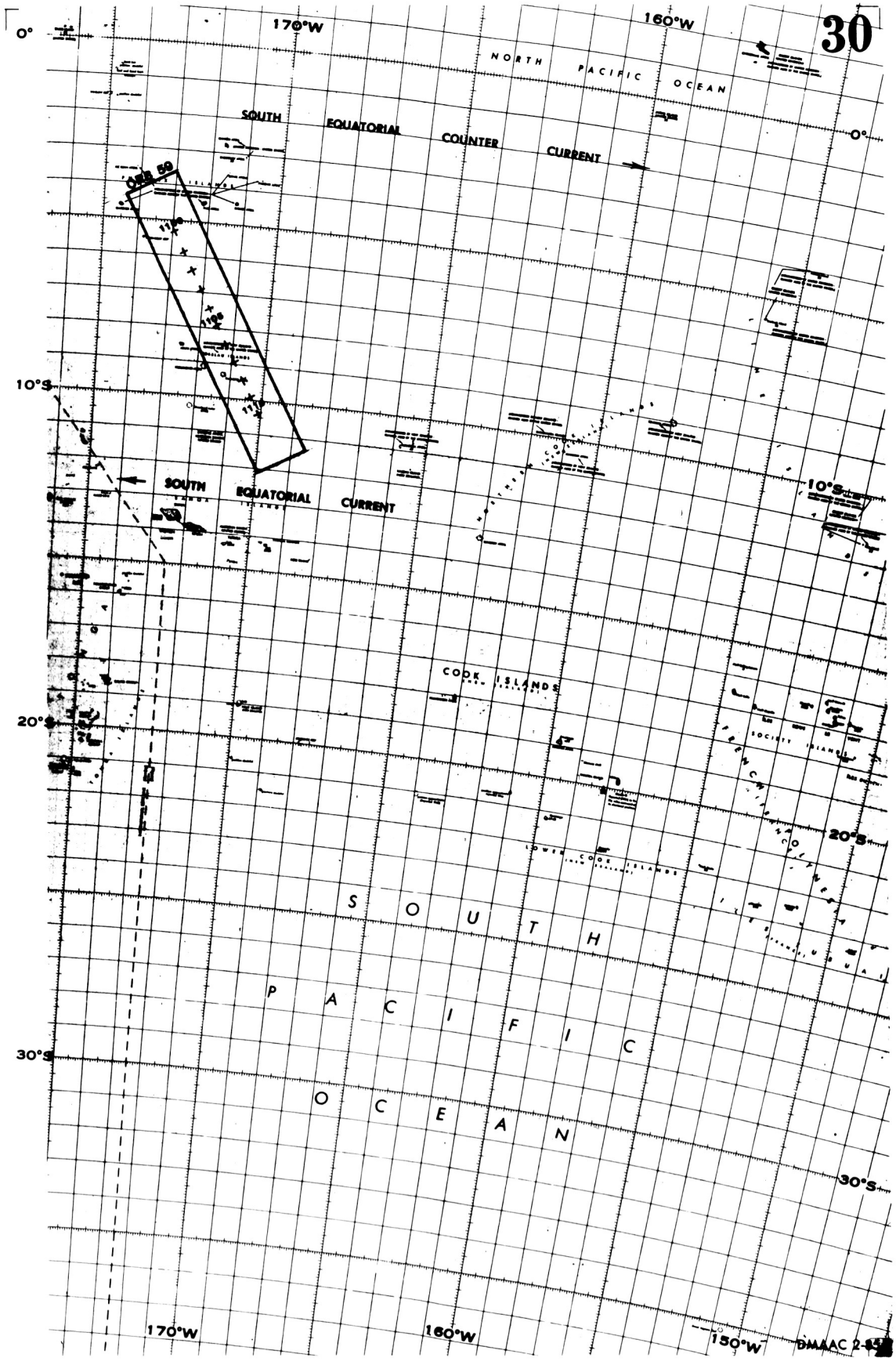

25
Hải Phòng
Gulf of Tonkin
110°E
Pratas Island
120°E
Balintang Channel
20°N
Strait
HAI-NAN TAO (China)
Hai-k'ou
Yulin
BURMA
Rangoon
THAILAND
Gulf of Martaban
Udon Thani
Huế
Đà Nẵng
PARACEL ISLANDS
SOUTH CHINA SEA
Limayen Gulf
San Fernando
Masinloc
Ubon Ratchathani
Nakhon Ratchasima (Khorat)
Chu Lai
KRUNG THEP (BANGKOK)
CAMBODIA
Qui Nho'n
Manila
Mindoro Strait
MINDORO
Nha Trang
Vinh Cam Ranh (Bay)
Gulf of Thailand
PHNUM PENH
North Danger Reef
PANAY
DANGEROUS GROUND
SAI GON
MEKONG RIVER DELTA
10°N
Chumphon
Kampong Saom (Sihanoukville)
An Thoi
Isthmus of Kra
PALAWAN
Puerto Princesa
SULU SEA
Côn Sơn
ORB 82
SPRATLY ISLAND
Balabac Strait
MALAYSIA
BRUNEI (LIK)
Kota Kinabalu (Jesselton)
Sandakan
Jolo Island
Jolo
Pulau We
Kuala Terengganu
MALAYSIA BARAT (WEST MALAYSIA)
Tawitawi Island
Tawitawi
SULU
Natuna Besar
KEPULAUAN NATUNA
KEPULAUAN ANAMBAS
KUALA LUMPUR
Port Dickson
Johore Baharu
Pulau Simeulue
SINGAPORE
CELEBES
Pulau Nias
KEPULAUAN LINGGA
Strait
Tolitoli
Tomini
0°
KEPULAUAN BATU
Pulau Siberut
KEPULAUAN (ISLANDS) MENTAWAI
Pulau Sipura
Belaroka
Selat (Strait) Karimata
Pulau Pagai Selatan
Belitung
Bandjermasin
Pulau Laut
KEPULAUAN
JAVA SEA
Pulau Enggano
Tandjungkarang-Telukbetung
DJAKARTA
LAUT KETJIL
Udjung Pandang (Makasar)
KEPULAUAN KANGEAN
FLORES SEA
Pulau Bawean
Surabaja
Selat (Strait) Sunda
Bandung
Jogjakarta
Lombok
Sumbawa
Selat (Strait)
Sumba
10°S
Flying Fish Cove
CHRISTMAS ISLAND (Australia)
ORB 75
COCOS (KEELING) ISLANDS (Australia)
INDIAN OCEAN
20°S
Port Hedland
DMAAC 2-85
100°E
110°E
CONT P 18
CONT P 26

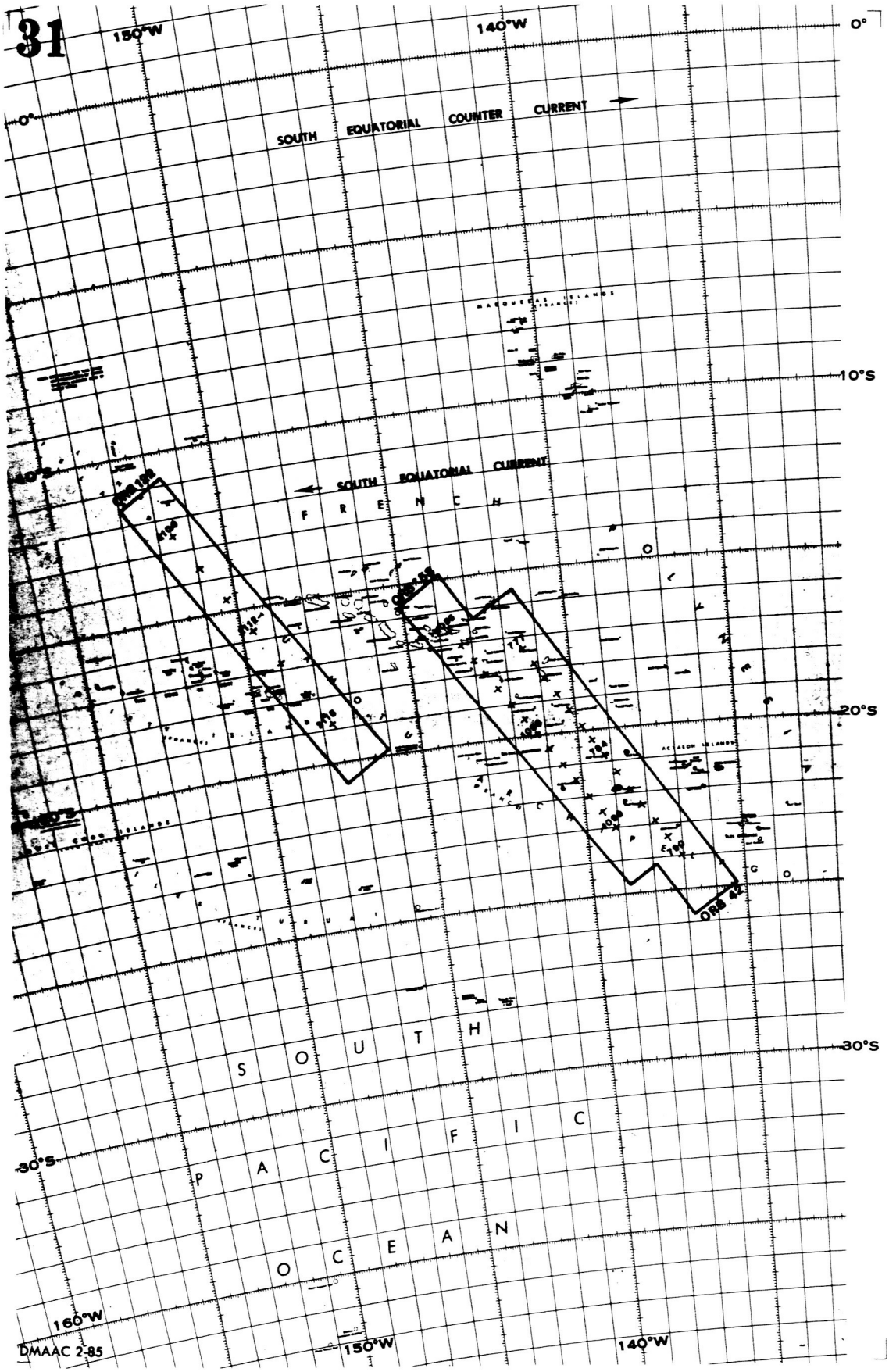

26
BATAN ISLANDS
BABUYAN ISLANDS
Babuyan Channel
LUZON
PHILIPPINE SEA
QUEZON CITY
Lamon Bay
Catanduanes
PHILIPPINES
SAMAR
LEYTE
NEGROS
BOHOL SEA
MINDANAO
Basilan Island
ARCHIPELAGO
KEPULAUAN TALAUD
Pulo Anne
Merir
PALAU ISLANDS
Sonsorol Islands
KEPULAUAN SANGIHE
SEA
Morotai
Tabi
Helen Island
Moluccas Passage
HALMAHERA
SOFUTAN
MOLUCCA SEA
Pulau Obi
KEPULAUAN SULA (ISLANDS)
Pulau Mangole
CERAM SEA
Pulau Buru
Pulau Ambon
Pulau Butung
BANDA SEA
KEPULAUAN KAI
KEPULAUAN TANIMBAR
Pulau Wetar
Pulau Alor
Wetar Passage
Portuguese Timor
SAWU SEA
Kupang
Pulau Roti
TIMOR SEA
ARAFURA SEA
Melville Island
Bathurst Island
Van Diemen Gulf
Darwin
JOSEPH BONAPARTE GULF
ARNHEM LAND
KIMBERLEY
PLATEAU
Derby
Broome
FITZROY
Wyndham
Daly Waters
Tennant Creek
Groote Eylandt
Gulf Of Carpentaria
WELLESLEY ISLANDS
MASCOE
Karumba
INLET
Normanton
BARKLEY
TABLELAND
Cape York
THURSDAY ISLAND
Torres Strait
Gulf of Papua
Port Moresby
Cooktown
Cairns
Flinders
Curry
Hughenden
Townsville
Mackay
Rockhampton
Gladstone
Brisbane
Sydney
Canberra
Melbourne
Adelaide
Perth
Darwin
Alice Springs
Tanahmerah
NEW GUINEA
KEPULAUAN SCHOUTEN
Biak
Sarera
Waigeo
Pulau Waigeo
Sorong
Mutuni
Djajapura (Hollandia)
Wewak
ADMIRALTY ISLANDS
Manus
BISMARCK SEA
Pulau Dolak (Island)
Merauke
Daru
Fly River
Okino-tori Shima (Parece Vela) (Japan)
Farallon de Pajaros, Maug Island
Asuncion Island
Agrihan
MARIANA ISLANDS
Pagan
Alamagan
Guguan
Sarigan
Anatahan
Farallon De Medinilla
Saipan
Guam (US)
Rota
Apra Harbor
6033
Ulithi
Fais
Yap
Ngulu
Sorol
Faraulep
Olimarao
Woleai
Elato
Lamotrek
Ifalik
Satawal
Eauripik
CAROLINE ISLANDS
ORB 81
ORB 89
ORB 125
CONT p. 25
CONT p. 27
130°E
140°E
150°E
160°E
170°E
20°N
10°N
0°
10°S
20°S

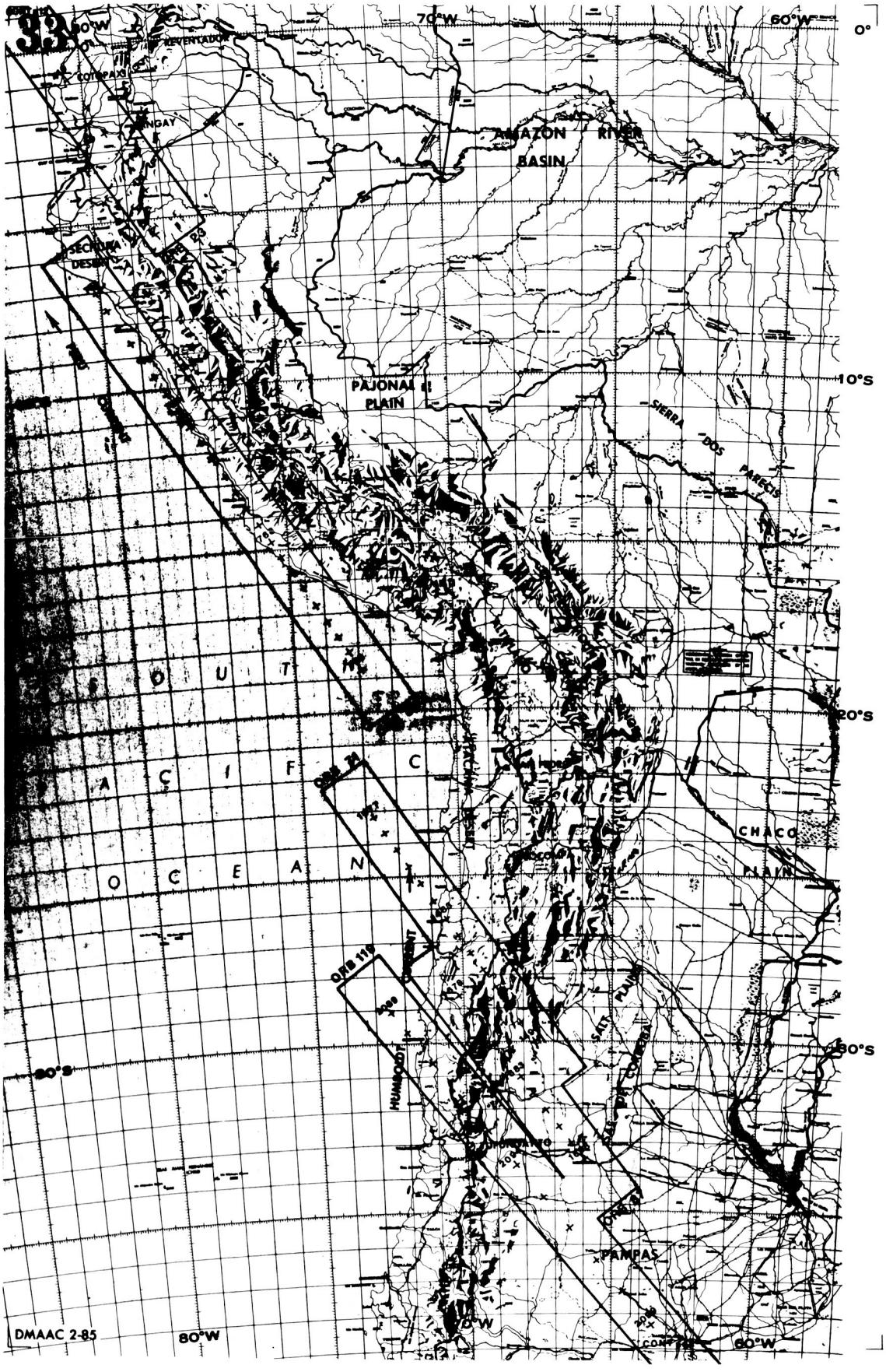

27
CONT P 25
130°E
INDONESIA
JAVA SEA
BALI SEA
BANDA SEA
TIMOR SEA
10°S
INDIAN OCEAN
ORB 128 & 130
ORB 129
ARNHEM LAND
STRANGWAYS (IMPACT)
KIMBERLY PLATEAU
SOUTH EQUATORIAL CURRENT
EXMOUTH BAY
SHARK BAY
AUSTRALIAN WEST CURRENT
NULLARBOR PLAIN
A VERTICAL DISCREPANCY OF 200 FEET EXITS IN THIS AREA
GREAT AUSTRALIAN BIGHT
EUCLA BASIN
GEOGRAPHE BAY
CONT P 28
20°S
30°S
40°S
INDIAN
110°E
120°E
130°E
DMAAC 2-85

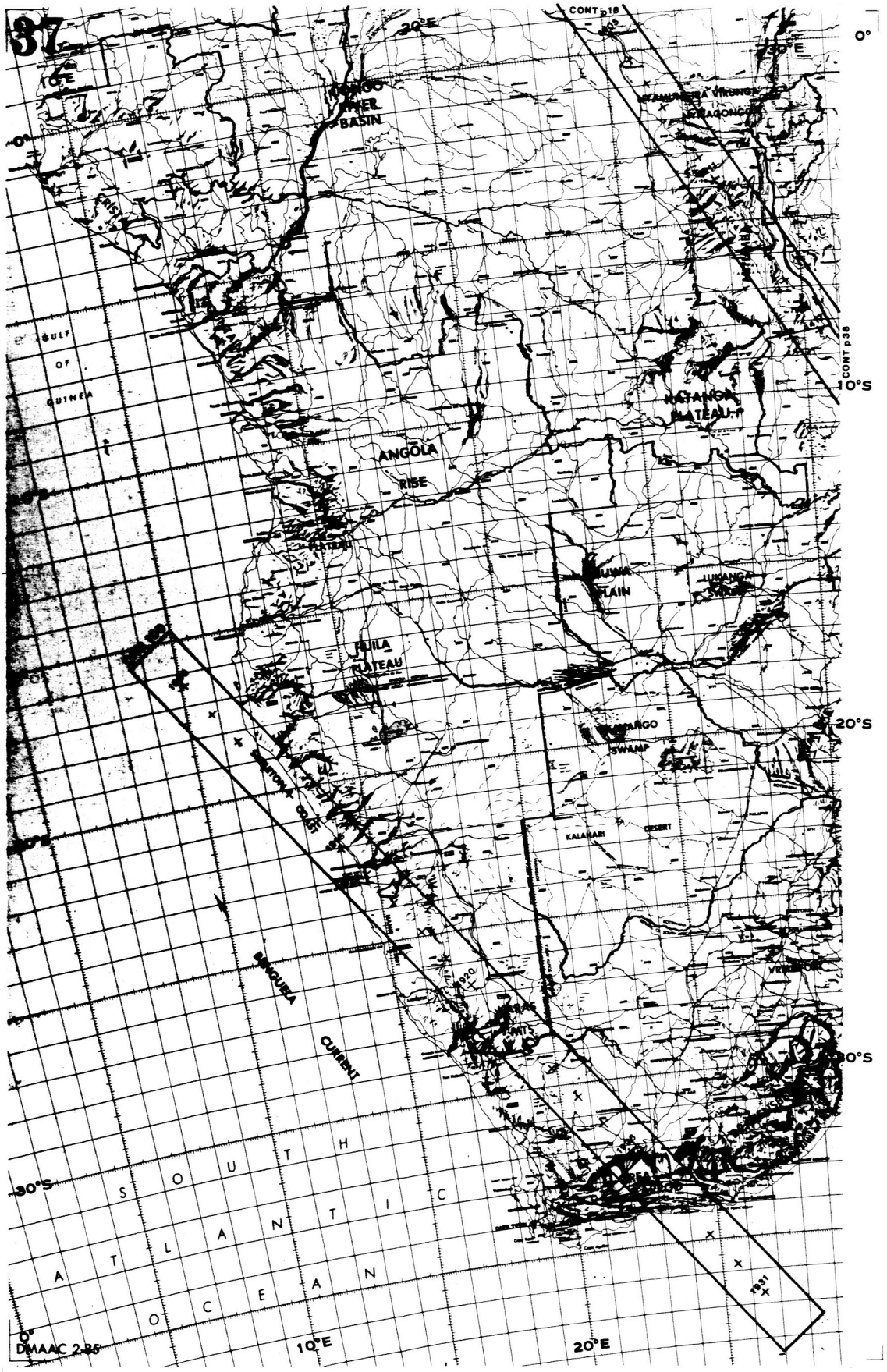

28
140°E
150°E
160°E
10°S
20°S
30°S
40°S
SOLOMON SEA
LAMINGTON
PAPUA NEW GUINEA
CORAL SEA
GREAT ARTESIAN BASIN
DARLING BASIN
MURRAY RIVER BASIN
TASMAN SEA
SOUTH PACIFIC OCEAN
OCEAN
ORB 1
ORB 2
ORB 110
ORBIT
EAST AUSTRALIAN CURRENT
BASS STRAIT
CONT p.27
CONT p.41
DMAAC 2-85

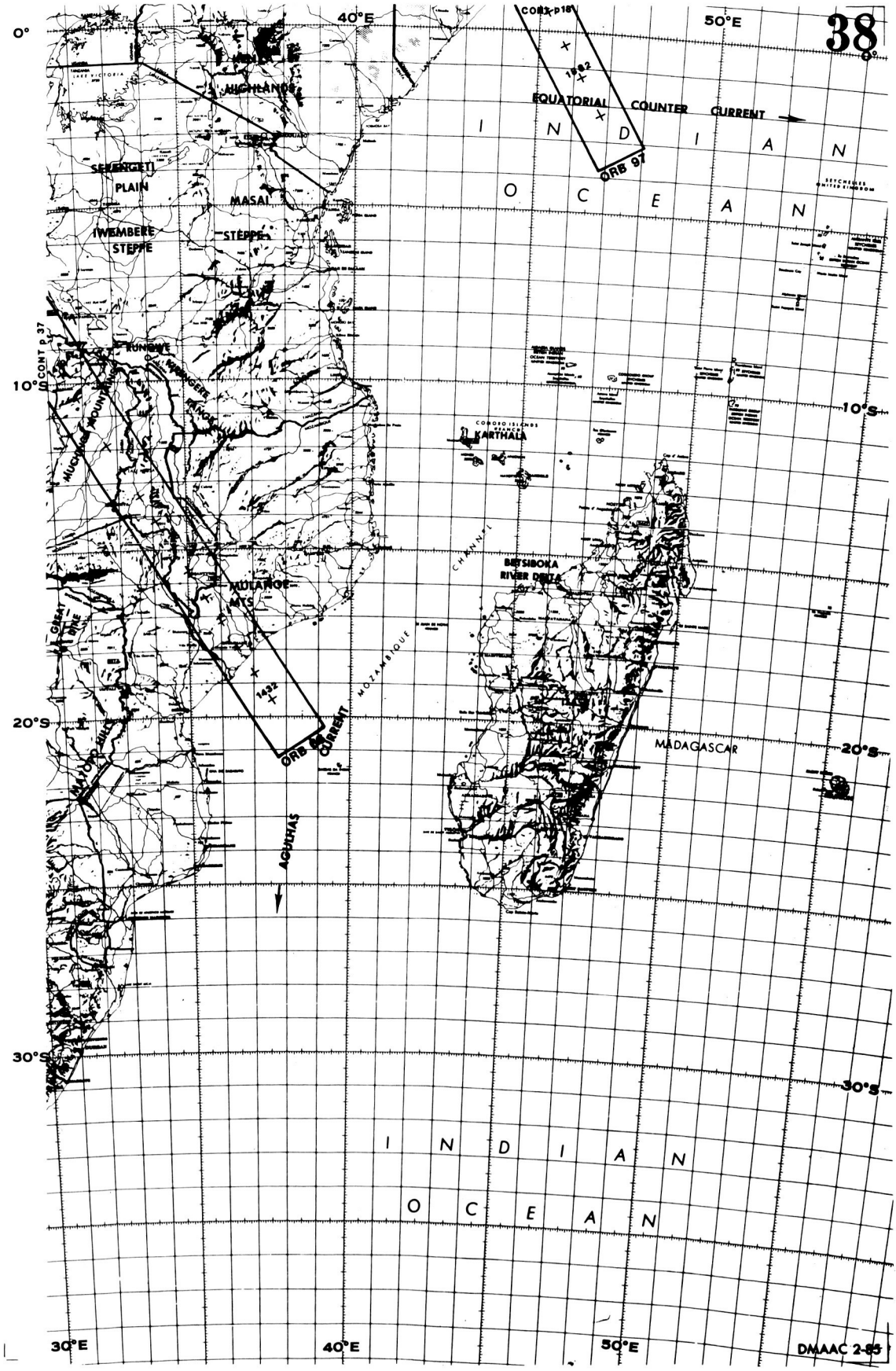

29
170°E
180°
0°
10°S
20°S
30°S
160°E
170°E
180°
SOLOMON ISLANDS
CORAL SEA
NEW CALEDONIA
NEW HEBRIDES
FIJI ISLANDS
GILBERT AND ELLICE ISLANDS
SOUTH EQUATORIAL
SOUTH PACIFIC OCEAN
TASMAN SEA
NEW ZEALAND
DMAAC 2-85

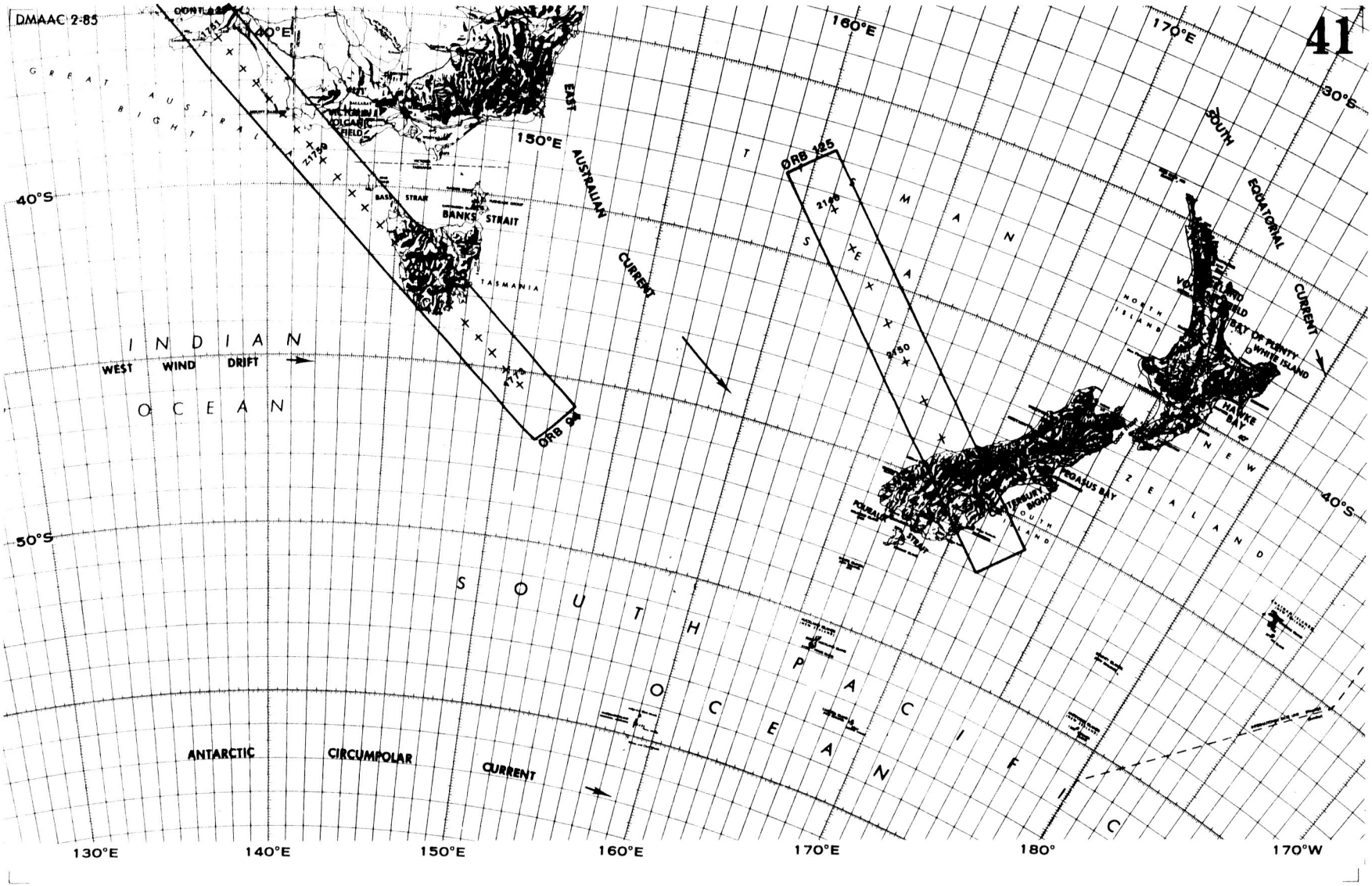

30
0°
170°W
160°W
NORTH PACIFIC OCEAN
SOUTH EQUATORIAL COUNTER CURRENT
0°
10°S
SOUTH EQUATORIAL CURRENT
10°S
COOK ISLANDS
20°S
20°S
SOUTH PACIFIC OCEAN
30°S
30°S
170°W
160°W
150°W
DMAAC 2-85

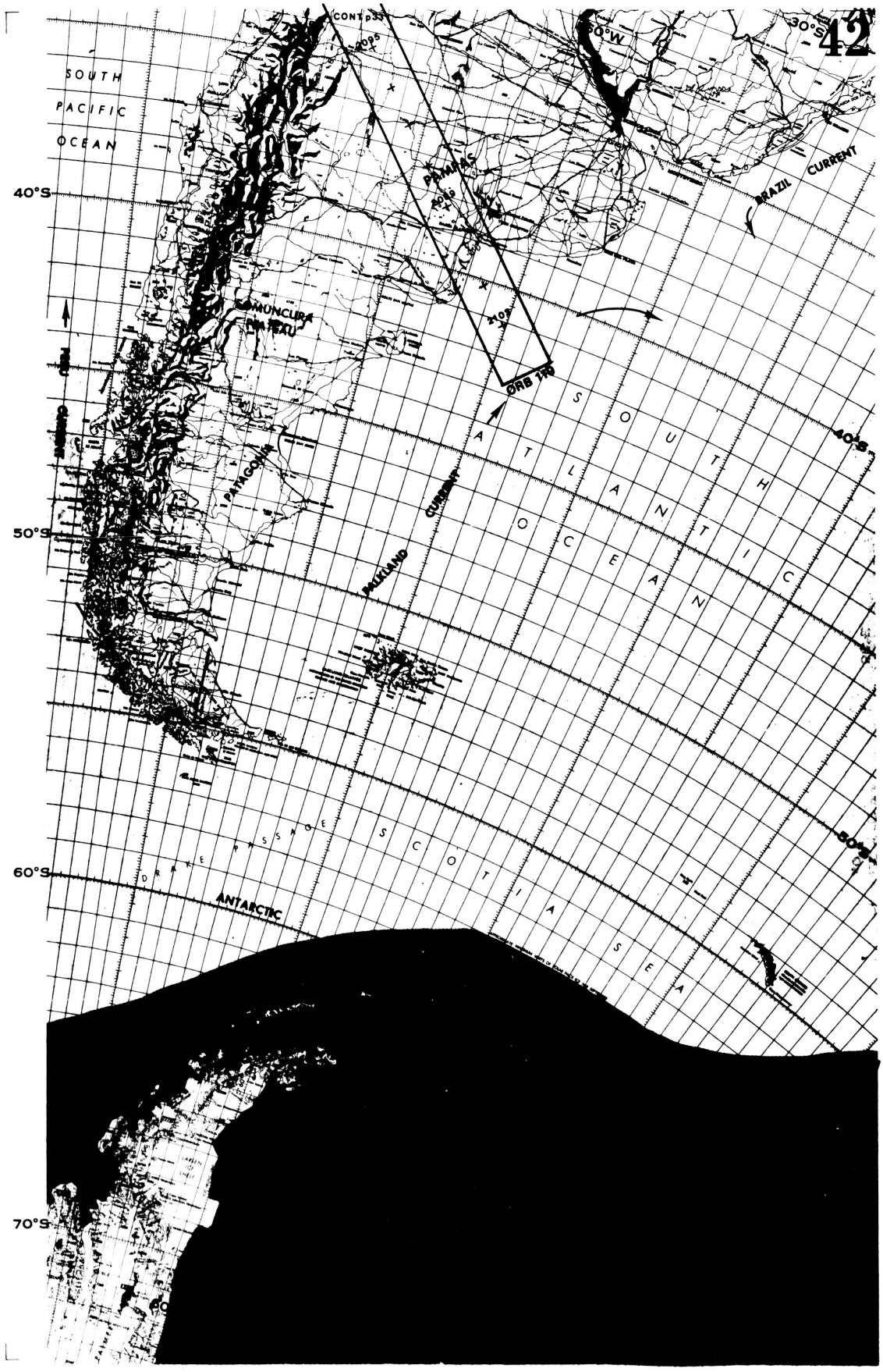

31
150°W
140°W
0°
SOUTH EQUATORIAL COUNTER CURRENT
10°S
SOUTH EQUATORIAL CURRENT
F R E N C H
20°S
S O U T H
P A C I F I C
O C E A N
30°S
160°W
150°W
140°W
DMAAC 2-85


33F
70°W
60°W
0°
10°S
20°S
30°S
80°W
AMAZON RIVER BASIN
PAJONAL II PLAIN
SIERRA DOS PAREDES
CHACO PLAIN
PAMPAS
QUITO
DMAAC 2-85


37
CONT p18
0°
10°E
20°E
30°E
CONGO RIVER BASIN
MTAMBARRA VIRUNGA
KIRAGONGO
CONT p36
10°S
GULF OF GUINEA
KATANGA PLATEAU
ANGOLA RISE
PLATEAU
LUIMA PLAIN
LUKANGA SWAMP
HUILA PLATEAU
20°S
BENGUELA CURRENT
KALAHARI DESERT
30°S
SOUTH ATLANTIC OCEAN
DMAAC 2.86
10°E
20°E


38
0°
40°E
50°E
CONT p 18
EQUATORIAL COUNTER CURRENT
ORB 97
I N D I A N
O C E A N
HIGHLANDS
SERENGETI PLAIN
MASAI STEPPE
IWEMBERE STEPPE
CONT p 37
RUNGWE
KIPENGERE RANGE
MUCHINGA MOUNTAINS
10°S
COMORO ISLANDS
KARTHALA
CHANNEL
BETSIBOKA RIVER DELTA
MULANJE MTS
GREAT RIFT
MOZAMBIQUE
MADAGASCAR
20°S
ORB 143
AGULHAS
30°S
I N D I A N
O C E A N
30°E
40°E
50°E
DMAAC 2-85


DMAAC 2-85
41
GREAT AUSTRALIAN BIGHT
40°E
150°E
160°E
170°E
30°S
40°S
50°S
EAST AUSTRALIAN CURRENT
BASS STRAIT
BANKS STRAIT
TASMANIA
ORB 125
ORB 24
INDIAN OCEAN
WEST WIND DRIFT
SOUTH EQUATORIAL CURRENT
NORTH ISLAND
SOUTH ISLAND
BAY OF PLENTY
WHITE ISLAND
HAWKE BAY
POAUA BAY
NEW ZEALAND
SOUTH PACIFIC OCEAN
ANTARCTIC CIRCUMPOLAR CURRENT
130°E
140°E
150°E
160°E
170°E
180°
170°W


42
CONT p33
SOUTH
PACIFIC
OCEAN
40°S
50°S
60°S
70°S
50°W
30°S
BRAZIL
CURRENT
PANAMA
ORB 210
ORB 190
MUNCURA
PATAGONIA
FALKLAND
CURRENT
SOUTH
ATLANTIC
OCEAN
SCOTIA
SEA
DRAKE PASSAGE
ANTARCTIC